SEISMIC SITE RESPONSE OF 1-D INHOMOGENEOUS GROUND WITH CONTINUOUS VARIATION OF SOIL PROPERTIES
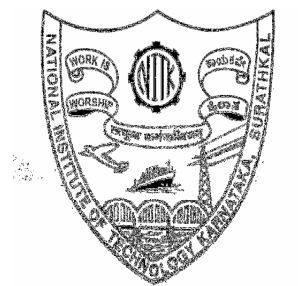
Thesis

Submitted in partial fulfillment of the requirements for the degree of

DOCTOR OF PHILOSOPHY

by

K. V. VIJAYENDRA

DEPARTMENT OF CIVIL ENGINEERING
NATIONAL INSTITUTE OF TECHNOLOGY KARNATAKA
SURATHKAL, MANGALORE – 575025

FEBRUARY 2016

D E C L A R A T I O N
By the Ph.D. Research Scholar

I hereby declare that the Research Thesis entitled **Seismic Site Response of 1-D Inhomogeneous Ground with Continuous Variation of Soil Properties** which is being submitted to the **National Institute of Technology Karnataka, Surathkal** in partial fulfillment of the requirements for the award of the **Degree of Doctor of Philosophy in Civil Engineering,** is *a bonafide report of the research work* carried out by me. The material contained in this Research Synopsis has not been submitted to any University or Institution for the award of any degree.

Register no.: CV08P03, K. V. VIJAYENDRA
Department of Civil Engineering

Place: NITK-Surathkal

Date: 29th February, 2016

<u>CERTIFICATE</u>

This is to certify that the research thesis entitled **Seismic Site Response of 1-D Inhomogeneous Ground with Continuous Variation of Soil Properties** submitted by **K. V. VIJAYENDRA** (Register Number: CV08P03) as the record of research work carried by him, is *accepted as the Research Thesis submission* in partial fulfillment of the requirements for the award of degree of **Doctor of Philosophy**.

Dr. S. K. PRASAD
Professor
Dept. of Civil Engineering
S.J.C.E., Mysore
(Research Supervisor)

Dr. SITARAM NAYAK
Professor
Dept. of Civil Engineering
NITK, Surathkal
(Research Supervisor)

Professor and Head of the Department
Department of Civil Engineering
Chairman, DRPC

ACKNOWLEDGEMENT

ABSTRACT

The main objective of this thesis is to enhance the scope and response estimation ability of routine one dimensional (1D) seismic response analysis in frequency domain using equivalent linear (EQL) method. This is the popularly used method of analysis in engineering practice. For this purpose a computer program is developed incorporating the scheme to accommodate the objectives of this research work.

In order to meet the solution procedure employed in the routine analysis, the soil deposits exhibiting continuous inhomogeneity are also being idealised as layered systems. The analytical results obtained for continuously inhomogeneous soil deposits have demonstrated that the layered idealisation of such soil deposits would result in contradictory response quantities. Secondly, the major limitation of the EQL method is inconsistent estimation of response at high frequency and in the resonant frequency region. This may be attributed to the use of single valued strain in all the frequency ranges during the iterations of EQL scheme of analysis. Both these drawbacks of the popularly used computer programs have been addressed and modifications are implemented in the computer program developed as part of this research work.

The numerical procedure developed and implemented in the computer program is capable of handling all possible cases of idealisation of soil deposit. Two modifications have been proposed to routine EQL analysis scheme; one with respect to computation of effective strain in the iterative process and secondly, frequency dependent damping model is formulated to overcome inconsistencies in predicted response at certain frequency ranges. The results are compared with both analytical solutions and observed data of geotechnical downhole array sites of Japan and USA. Finally an alternative method is proposed to estimate the fundamental period of the layered deposit by approximating it with linearly varying shear wave velocity profile.

The outcome of this research work is expected to enhance the predictive capabilities of the most commonly used site response analysis procedure and contribute in the direction of improving the seismic site response analysis in engineering practice.

Keywords: Seismic site response, Equivalent linear analysis, Frequency dependent analysis, Fundamental period of layered deposits.

CONTENTS

LIST OF FIGURES

LIST OF TABLES

NOMENCLATURE

a	Inhomogeneity parameter
a_{max}	Maximum acceleration
$\bar{a}$	Inhomogeneity parameter
A_I	Amplitude of incident wave
A_R	Amplitude of reflected wave
A_T	Amplitude of transmitted wave
c_i	Damping coefficient
$[C]$	Viscous damping matrix
E	Transmitted wave component
E_I	Wave energy components of incident wave
E_T	Wave energy components of transmitted wave
E_R	Wave energy components of reflected wave
F	Reflected wave component
g	Acceleration due to gravity $\left(m/s^2 \right)$
G	Shear modulus
G_0	Shear modulus at free surface
G^*	Complex shear modulus
$\bar{G}$	Imaginary component of complex shear modulus
G_{max}	Low strain shear modulus
H	Total thickness of the soil deposit
H_i	Thickness of the ith layer

i	Imaginary number $(i = \sqrt{-1})$
$J_v(\bullet)$.	Bessel' function of first kind of order v
k	Complex wave number given by $k^2 = \dfrac{\omega^2 \rho}{(1+2i\zeta)G} = \dfrac{\omega^2 \rho}{G^*}$
k_i	Stiffness coefficient of the ith layer
$[K]$	Assembled stiffness matrix
m_i	Mass coefficient of the ith layer
MMI	Modified Mercali intensity
M_w	Moment magnitude of the earthquake
$[M]$	Assembled mass matrix
r	Correlation regression coefficient
R	Ratio of effective strain to maximum strain
T	Fundamental period of the soil deposit
t	Time in seconds
u	Shear displacement in horizontal direction
$\dot{u}$	Velocity in horizontal direction
$\ddot{u}$	Acceleration in horizontal direction
$U(z)$	Amplitudes of displacement
v_{si}	Shear wave velocity at i^{th} layer
v_{s0}	Shear wave value at the free surface
v_{sH}	Shear wave velocity at the base of the soil deposit
v_{sr}	Shear wave velocity of bedrock
v_s^*	$v_s^* = v_s \sqrt{1+2i\zeta}$

$Y_\nu(\bullet)$	Bessel' function of second kind of order ν
z	Spatial co-ordinate along the depth
α	Impedance ratio between top and the bottom layer $\alpha = \dfrac{v_{s(i)}\rho_i}{v_{s(i+1)}\rho_{i+1}}$
α_b	Impedance ratio between base of the deposit and bedrock $\alpha_b = \dfrac{v_{sH}\rho_s}{v_{sr}\rho_r}$
γ	Shear strain
$\dot{\gamma}$	Rate of shear strain
η	Viscosity coefficient
$\mu\left(= v_{sH}/v_{s0}\right)$	Ratio of shear wave velocity at the base to that of at the surface
σ_I	Stress amplitude of incident wave
σ_T	Stress amplitude of transmitted wave
σ_R	Stress amplitude of reflected wave
ρ_r	Density of the bedrock
ρ_i or γ_i	Mass density or unit weight at i^{th} layer
τ_i & τ_{max}	Shear stress of the ith layer and maximum shear stress
$T(z)$	Amplitudes of shear stress
Λ	Inhomogeneity parameter
ω	Excitation frequency, Rad/s
ξ	Transformed depth coordinate, function of z
ζ	Viscous damping ratio in %

CHAPTER 1

INTRODUCTION

1.1   GENERAL

It is well established that earthquake waves will amplify near the surface as they propagate through the earth mantle and crust after originating from the deep faults. The evaluation of amplification characteristics of the waves is a very important field of study in earthquake geotechnical engineering. Free-field response of the earth surface due to earthquakes is an important parameter to be established in ascertaining the dynamic loads for earthquake resistant design of structures. Thus seismic site response analysis is primarily performed in order to estimate the seismic motion at the free surface of the soil deposit for a given input seismic motion within the deposit or to transfer the free surface motion of soil deposit to the surface of the outcropping bedrock.

Many aftermath survey reports of damages during mild to severe seismic events have revealed that the type of structure, the type of material used and construction practices are vital factors influencing the severity of damage [Borcherdt and Gibbs (1976); Berrill (1977); Bertero (1989) and others]. Nevertheless the dynamic response of the structure is primarily controlled by the closeness of its natural frequency to the predominant frequency of the input earthquake motion. In turn, the predominant frequency of earthquake wave near the surface depends on the characteristics of soil deposit above the bed rock and the level of strain experienced by ground during the earthquake because the seismic wave characteristics are affected as the wave propagates through soil deposit.

Thus, it is important to assess the local site effects on the seismic response of built environment, particularly in urban areas. Hence, microzonation of the urban areas becomes imperative for mitigation of earthquake risks. The reliable evaluation of response of the near surface soil deposit under expected earthquake input motion at

bedrock level is the key problem in seismic microzonation. Well documented fallout studies of data pertaining to strong earthquakes have clearly revealed that the main reason for high intensity site specific seismic motion is the soft soil condition. 1985 Michoacan earthquake of Mexico, 1989 Loma Prieta earthquake, 1994 Northridge earthquake of USA, 1995 Kobe earthquake of Japan, 1999 Kocaeli earthquake of Turkey, 2001 Bhuj earthquake of India and many other events in the recent past are glaring examples of site amplification causing catastrophic damage to structures during earthquakes.

1.2   BACKGROUND AND MOTIVATION

There are several methods available for evaluating seismic response of soil deposits essentially differing in use of numerical techniques and modeling of soil stress-strain behavior. Principally they may be classified as linear, equivalent linear (EQL) and nonlinear methods. Further, the analysis can be one, two or three dimensional. Among these, EQL method based on the solution of wave equation using multiple reflection theory with one or two dimensional idealization is the most popular method. The reason for its popularity is its simplicity, particularly in evaluation of soil parameters used in the analysis. On the other hand, nonlinear method is based on lumped mass idealization of layered soil deposit with equation of motion being integrated in time domain unlike the EQL approach which is based on continuous solution of wave equation in frequency domain. Although in time domain approach the nonlinear behaviour of the soil can be considered more realistically, the main problem is that, it requires several input parameters that are tedious to evaluate. The solution of wave equation using multiple reflection theory in frequency domain has distinct advantages such as deconvolution that is, the bed rock acceleration time history can be computed using the input motion at the surface or at any other intermediate layer.

The most widely used computer program based on equivalent linear method is SHAKE [Schanbel et al. (1972)] and its subsequent versions e.g., SHAKE91 [Idriss and Sun (1992)]. In the recent past, several other computer programs similar to SHAKE are available such as EERA [Bardet et al. (2000)], DYNEQ [Yoshida et al. (2002)], DEEPSOIL [Hashash (2011)], STRATA [Kottke and Rajthe (2008)] etc.,

These programs can compute the dynamic response of horizontally layered soil deposit due to vertically propagating and horizontally polarized (SH-wave) shear waves. These programs are developed based on multiple reflection theory of waves in frequency domain. The nonlinearity is modeled by defining the curves of strain dependent shear modulus and damping. The stiffness degradation of the soil due to the increase in strain is accomplished by comparing the computed strains with generalized strain dependent modulus reduction curves.

Time domain approaches are capable of directly incorporating nonlinear and time varying behavior of the soil. Also, while the analysis is carried out, they preserve the time history of dynamic response quantities which are transient in nature rather than harmonic as it is treated in the frequency domain. On the other hand, in the time domain approach it is impossible to implement the concept of multiple reflection theory which is an exact solution of the wave equation. Using the multiple reflection theory approach, the incident and reflected waves can be separated, input wave can be specified at any point in the half space and incident and reflected wave components can be extracted at any desired location. Most often this aspect is an important requirement in engineering practice. Even though time domain approach is recommended for truly nonlinear analysis, EQL approach based on multiple reflection theory continues to sustain its importance and popularity in the geotechnical earthquake engineering practice. Recently, appreciable research advancements have been achieved in numerical procedures, computational methods, constitutive modeling and measurement of soil properties (both in field and laboratory) that are appropriate for seismic site characterisation procedures. In spite of these developments, according to a survey conducted and reported by Kramer and Paulsen (2004) for large number of practicing engineers throughout the globe, equivalent linear one-dimensional analysis is still the most popular choice for analysis because of its simplicity, convenience in providing input data and easy interpretation of results.

In some instances non-homogeneity of the surface deposit may be due to continuous variation of stiffness and density rather than distinctly layered formation. Recognizing this fact, many investigators have attempted to treat the prevailing condition of non-homogeneity and computed the dynamic response of the deposit subjected to

harmonic base excitation. Among these, important contributions are from Gazetas (1982), Davis (1995), Towhata (1996), Roviths et al. (2011), Vrettos (2013) etc. From the review of these studies it can be concluded that, there is scope and need for improving the routine SHAKE method of analysis for predicting seismic ground response. These analytical studies are dealt to give amplification for the limited cases without considering nonlinear behavior and variation of density along the depth of the soil deposit. Also these analytical studies assume that inhomogeneous surface deposit is overlying a homogeneous elastic half-space or rigid base rock. However, in reality these assumptions are seldom valid.

The analytical and numerical studies, reported in literature, have pointed out that main drawback of the routine one-dimensional modeling of the ground arises out of the assumption of perfectly horizontal layers of varying depths. This assumption leads to unrealistic and contrasting impedance ratio between adjacent layers. In turn, this may result in poor simulation of ground response. Hence, there is a need for overcoming this lacuna by modeling the ground profile with continuous variation of soil properties, particularly shear wave velocity, which introduces a smooth transition zone at layer interfaces instead of abrupt variation.

Although many of the researchers disagree with the effect of loading frequency on the dynamic soil properties, in the recent past, some studies have observed that effect of loading frequency on the soil stiffness and damping is significant. Consequential effect of loading frequency / strain rate on damping ratio is yet to be ascertained clearly. Rix (2004), through experimental study, reaffirmed the general trend of effect of frequency on damping suggested by Shibuya et al. (1995). Even though effect loading frequency on soil properties is debatable, in order to improve the accuracy of response prediction of EQL method, especially in the high frequency range, it may be appropriate to incorporate frequency effects into the analysis procedure.

Equivalent linear method utilizes effective strain (γ_{eff}) to update soil properties after every iteration and these updated shear moduli and damping values are employed in the next iteration. Throughout a particular iteration, these values remain constant. There is no technically rational procedure available to convert the resulting maximum

strain (γ_{max}) to effective strain $\left(\gamma_{eff}\right)$. In their computer program SHAKE91, Idriss and Sun (1992) computed effective strain as $\gamma_{eff} = R\gamma_{max}$ where R is an empirical parameter which depends on magnitude of the earthquake (M) as $R = (M-1)/10$, while Schnabel et al. (1972) recommended a value of 0.55 to 0.65 for R in their program SHAKE. It is observed that single value of parameter R is not capable of reproducing the entire response history at complete range of frequencies. Several other methods for computing R have been proposed. However, they are aimed at altering R depending on excitation frequency instead of acceleration or strain amplitude [Sugito et al. (1994), Yoshida et al. (2002), Kausel and Assimaki (2002) etc.]. Hence, evolving a rational procedure to compute effective strain based on acceleration or strain amplitudes of the corresponding iteration is imperative.

Several post earthquake geotechnical studies have clearly demonstrated that intensity of structural damages and its distribution are closely dependent on dynamic characteristics of the underlying soil deposit i.e., its modal characteristics. Hence, reliable assessment of fundamental period of the soil deposit is an important requirement in seismic site characterisation particularly in the process of microzonation of urban areas. Since shear wave velocity and fundamental period are directly interrelated, many empirical relationships have been proposed to compute average shear wave velocity as an equivalent substitute to complex shear wave velocity profile of inhomogeneous layered deposit. Summary and relative comparison of all empirical methods available till then is given in the paper by Dobry et al. (1976). The order of error in fundamental period computed from these empirical methods could be significantly large in some cases where large velocity gradient exists between layers of the deposit. Hence, evolving an alternative method for evaluation of fundamental period of the deposit, as accurately as possible, is extremely important.

1.3   SCOPE AND OBJECTIVES OF THE WORK

The focus of this study is to improve the prediction capabilities of total stress one dimensional seismic site response analysis using frequency domain equivalent linear approach. The improvements suggested in order to achieve this broad objective are

based on documented limitations of this approach in the literature. Although some modifications are suggested previously, addressing issues related to discrepancies in predicted and observed responses at certain frequency ranges, very few attempts have been made to deal with some of the uncertainties and ambiguities in one dimensional frequency domain site response analysis using equivalent linear approach. The improvements and modifications suggested in this study are believed to enhance the scope of application of equivalent linear one dimensional site response analysis in frequency domain in engineering practice. In the first phase of this study, a computer program SRISD (**S**eismic **R**esponse of **I**nhomogeneous **S**oil **D**eposits) is developed and tested to obtain one dimensional seismic response of inhomogeneous soil deposit with continuous variation in soil properties along the depth. In the next phase, modified method to compute effective strain and consideration of frequency effect are incorporated in equivalent linear analysis. Lastly, an alternative method for estimating fundamental period of layered soil deposit is proposed. For this purpose, variability in shear wave velocity profile along the depth is approximated with continuous variation.

The objectives of the present research work are as follows:

➢ To develop an algorithm and computer program based on the numerical procedure adopted to solve one-dimensional wave equation in frequency domain with nonlinearity of the soil being modeled using equivalent linear approach.

➢ To introduce an option in the computer program to consider continuous variation in soil properties along the depth of the one-dimensional soil profile with different types of inhomogeneity functions.

➢ To provide a refined method to compute effective strain for updating strain dependent shear modulus and damping properties of the soil deposit in successive iterations

➢ To incorporate an option for considering frequency dependent soil properties in equivalent linear approach.

➢ To test and validate computer program by comparing its results, for benchmark problems cited in literature, with results of existing computer programs and closed form solutions

➢ To validate the efficiency of the procedure adopted by comparing the results with response quantities measured during actual earthquakes.

➢ To identify the effects of plasticity index and characteristics of input motion on the dynamic response of soil deposit by performing parametric study

➢ To propose an alternative method to estimate fundamental period of layered soil deposits by idealizing the deposit with an equivalent continuous shear wave velocity profile

1.4   METHODOLOGY

Based on the objectives listed above, following methodology is adopted

• Transform governing equation of motion for one dimensional vertical propagation of waves in continuously inhomogeneous soil deposit into a set of ordinary differential equations.

• Numerically integrate the equations obtained previously using fourth order Runge-Kutta scheme.

• Employ EQL approach incorporating an alternative method to compute effective strain based on intensity of maximum acceleration computed in the preceding iteration and carry out iterations till convergence of shear strain at all nodal points. Implement these procedures in a computer program coded in FORTRAN

• Incorporate different input provisions in the computer program which include details of soil profile with different options for prescribing the shear wave velocity or shear modulus and density as continuous function of depth apart from routine layered configuration.

• Prescribe strain dependent shear modulus and damping properties choosing appropriate curve from a suite of curves available in the built in library or site specific data.

• In order to overcome frequency response discrepancies of equivalent linear analysis, additional damping shall be introduced near the fundamental frequency and damping will be decreased in the high frequency range beyond the first few

7

modes of response. This scheme is envisaged to reduce and enhance the response respectively near resonant frequency and high frequency ranges. Additional damping is attributed to radiation damping due to the energy dissipation in the underlying half-space of the deposit. For this purpose, approximate expression relating radiation damping with modal frequencies shall be used.

- Prescribe input motion at any depth in the form of acceleration time history. The strain, stress, acceleration time histories and amplification ratio between any two depths can be obtained as output at desired depths of the deposit. The variation of peak acceleration, maximum shear strain and maximum shear stress along the depth of the deposit are the default outputs.

- Validate the computer program with the results of the analytical studies reported in literature [for e.g., Gazetas (1982), Towhata (1996), Davis (2004), Rovithis et al. (2011), etc.] and measured field data of vertical geotechnical arrays. The shear wave velocity profile and earthquake data recorded and documented at California Strong Motion Instrumentation Program (CSMIP) and Kiban-Kyoshin network (KiK-net) websites are utilized for this purpose.

- Estimate the fundamental period of the layered soil deposit by approximating the layered shear wave velocity profile with an equivalent linear variation. For this purpose closed form exact analytical solution shall be used to compute the fundamental period of linearly varying shear wave velocity profile.

- Efficiency of the proposed vis-à-vis other available methods to estimate fundamental period shall be verified by comparing their results with values computed from recorded earthquake accelerograms of instrumented geotechnical downhole arrays.

1.5   SCHEME OF PRESENTATION

The entire work is presented in seven chapters. Brief introduction is presented in the first chapter. This includes the importance of the present work, problem statement and list of objectives of the present work. The second chapter describes the seismic response analysis of horizontally layered soil deposit. Various numerical techniques

available for seismic ground response are discussed. Results obtained from frequency domain equivalent linear and time domain nonlinear methods of analyses are compared. Parametric studies carried out to investigate the effect of characteristics of input motion and soil properties on the computed response are presented. The limitations of equivalent linear analysis in frequency domain are highlighted.

In chapter three, significance of idealizing the soil deposit with continuous variation in soil properties is brought out. The uncertainties associated with characterisation of soil deposit as layered deposit and its effects on the computed response are demonstrated through example analysis. The analytical solutions obtained for different kinds of inhomogeneity functions have been reviewed and scope of some of these solutions is extended for additional boundary conditions. Results of the parametric study carried out with regard to effect of inhomogeneity parameters on amplification characteristics are presented. This chapter is concluded with example analyses wherein the improvement in response prediction by approximating the layered profile by means of a continuously varying shear wave velocity profile is demonstrated.

The fourth chapter focuses on the development of numerical scheme for seismic response analysis of continuously inhomogeneous ground. The general features of the computer program SRISD developed as part of this study have been discussed. The results of the analysis using SRISD are validated by comparing with that of SHAKE91 analysis and those from closed form analytical solutions presented in the previous chapter.

The fifth chapter gives the details of two newly proposed improvements to routine equivalent linear analysis. Firstly, a rational method to compute effective strain required to update soil properties in equivalent linear approach is presented. Besides, a new method for frequency dependent equivalent linear analysis is developed. The implementation of these proposals in the framework of SRISD is discussed. Finally, a case study is presented to validate the salient features of the present research work.

An alternate approach for estimating the fundamental period of layered soil deposit is proposed in chapter six. For this purpose layered shear wave velocity profile is approximated with a linearly varying continuous shear wave velocity profile. Efficiency and accuracy of the proposed method is established by comparing its results with other simplified methods, exact solutions and those computed using observed field data. Conclusions and scope for future work are presented in the last chapter. The computer programs used for analytical results of chapters two and three are coded in MATLAB®. These programs are listed in Appendix-I. In Appendix-II details about the computer program SRISD is presented. The description and preparation of input data file along with output of the program is explained using an example analysis.

CHAPTER 2

ANALYSIS OF INHOMOGENEOUS SOIL DEPOSITS – HORIZONTALLY LAYERED PROFILE

2.1 INTRODUCTION

In this chapter the importance of evaluating the dynamic response of the ground during earthquakes and the aspects of seismic wave propagation through layered soil deposit are discussed. Validating facts related to simplification of complex wave phenomena into one dimensional idealisation are elaborated. Theory for one dimensional wave equation and well established solution using the concept of multiple reflection theory applied to one dimensional wave propagation in layered soil deposit is discussed. Various numerical techniques that are available in the literature for the purpose of evaluating the seismic ground response using one dimensional wave equation are reviewed. Finally, some of the deficiencies of equivalent linear analyses in frequency domain against nonlinear analysis in time domain are highlighted using an example. In this preliminary comparative study shear wave velocity profile idealisation, frequency and amplitude characteristics of the input motion are considered as parameters.

The theory of wave propagation deals with the problem of defining the transmission of energy that is released and spreading due to localized disturbance (source) in a medium. The seismic wave propagation through the earth medium is basically a three dimensional problem. Seismic waves originating from the focus propagate in all directions and characteristics of these waves are altered with respect to time and space.

The variations in wave characteristics as the wave propagates in the medium are significantly influenced by source geometry, type of disturbance, path of its propagation, geology of the ground, etc. Basically the seismic waves are classified into body waves and surface waves. The surface waves are generated due to total reflection of the body waves at the free ground surface.

The body waves are classified into primary or longitudinal wave (P-wave) and secondary or transverse wave (S-wave). P-wave propagates generating vibrations parallel to the direction of propagation and S-wave propagates generating vibration normal to the direction of propagation. S-wave component contributing to horizontal oscillations is called SH-wave while that contributing to vertical oscillations is called SV-wave. As a result of complex discontinuities in the earth media the body waves are phenomenally modified due to reflection, refraction, scattering, diffraction, attenuation, amplification, and other propagation related mechanisms [Newmark (1968); Newmark and Rosenblueth (1971); Okamoto (1984)].

2.2   SEISMIC GROUND RESPONSE ANALYSIS

2.2.1   General

The evaluation of ground surface motion due to an earthquake is associated with the solution of the problem of wave propagation. The solution procedure can be clearly distinguished into two fields of study. Firstly, modeling of surface ground motion that includes complete process of wave propagation from mechanism of fault rupture to generation of surface waves dealing with large geometrical domain, basically concerned with the field of study of seismology. The other is related to soil dynamics or earthquake geotechnical engineering in which the response of the subsoil above the bedrock due to propagation of waves are studied to evaluate the surface motion for an input motion prescribed at bedrock. The latter case is justified by the assumption that the earthquake motion at the assumed bedrock level can be defined as a function of distance from the source of disturbance and source mechanism; thereby complexity of the problem is greatly reduced.

From the engineer's point of view, it is essential to obtain accurate and complete site specific ground motion response quantities for reliable soil-structure interaction analysis and designing the structures for future earthquakes. Both engineers and seismologists have accepted that site specific ground motion, due to strong motion seismic events, is greatly affected by the response of the surface soil deposit above the bedrock [Seed and Idriss (1969), Chin and Aki (1991), Beresnev and Wen (1996) and

Field et al. (1997)]. In general, the problem of seismic ground response analysis may be defined as determination of temporal and spatial variation in all response quantities of a soil deposit due to observed or estimated input motion prescribed at a control point within the soil deposit [Lysmer (1978)].

2.2.2 Factors Affecting Ground Response Analysis

In reality, the procedure for exact characterization of strong earthquake motion involves considering all the factors which greatly influence the surface ground motion. According to Ferritto et al. (1999), these factors include seismological factors comprising intensity, frequency characteristics and duration of input motion (Bedrock motion); Geological factors such as soil type, profile of the soil deposit, underlying bedrock type, geologic structure and its profile (topography, basin effects etc.); Geotechnical factors consisting of low strain elastic properties of the soil, damping characteristics of the soil, stiffness degradation behavior of the soils due to cyclic load, natural period of the soil deposit, impedance ratio between the bedrock and overlying soil stratum and stress-strain relationship for soil and finally regarding analytical and numerical procedure which appropriately considers the dimensionality of the problem, soil nonlinearity and continuous or discrete modeling.

It is essential to recognize the fact that seismological factors affecting ground response analysis include large spatial domain compared to geotechnical factors which are usually confined to a relatively small scale. Generally, the outcome of seismicity estimation of a site is presented as the peak acceleration expected for a given return period that usually corresponds to the shaking at a rock outcrop. This site-specific data, typically comprising of anticipated acceleration time history of the rock outcrop, is used as input motion at the bedrock and propagation of waves through soil media is modeled. Then site effects have to be evaluated considering geotechnical parameters such as soil type, deposit thickness, stiffness and damping properties as a function of intensity of the bedrock motion. There are many empirical, simple and complex procedures available to compute site-specific dynamic soil response. The site-specific seismic ground response analysis is primarily aimed at characterisation of modification in the frequency and amplitude of the seismic wave

13

as it propagates through surface soil deposit. More elaborative three dimensional models using methods based on finite element, finite difference, boundary element, etc. are available for seismic ground response analysis [Frankel and Vidale (1992), Frankel (1993), Zeng and Anderson (1996)]. Joyner and Boore (1988) have given extensive review of the works related to site amplification studies.

2.3   JUSTIFICATION FOR ONE DIMENSIONAL ANALYSIS

Usually, considering the limitations and complexities involved, the three dimensional seismic wave propagation problems are often idealized as two or one dimensional problems. The limitations and complexities in three dimensional analysis are; defining the seismic bedrock motion considering all seismological factors including source mechanism and path effects, modeling anisotropic and inelastic stress-strain behavior of soil (constitutive modeling), ascertaining the parameters of the constitutive model through in-situ or laboratory procedures and implementing all these with a numerical procedure which is computationally economical and accurate. Research is still going on to address many aspects of these issues decisively, hence engineers are yet to be satisfied with capabilities and accuracy of the procedure involved in three dimensional modeling.

For any seismic event the distance of wave propagation is often great compared with the dimensions of the source. Therefore, according to Newmark and Rosenblueth (1971), at points sufficiently distant from the source of a disturbance the waves may be regarded as plane waves. Also by modeling the source of fault rupture as a line of relatively large length, it can be assumed that all the waves are propagating parallel to a plane. Thus, according to Roësset (1977), for the situations stated above, the seismic wave propagation problems may be treated as two dimensional. In two dimensional analysis, lateral extent of the soil deposit can be taken into account as finite [Joyner (1975), Marsh (1992)].

The investigation of many acceleration records of earthquakes suggests that wave refraction from edge boundaries, focusing and scattering of waves, alteration to type of waves, etc. that are associated with two and three dimensional effects are important

14

[Tucker and King (1984), Bard and Bouchon (1985) and others]. Where these effects are significant, calculations assuming one-dimensional wave propagation models fail to simulate the observed results [King and Tucker (1984)]. In spite of employing 2D or 3D analysis, according to Boore (2004), in some cases discrepancy between predicted and observed spectral ratios is not negligible, although the results from two and three dimensional analysis can predict the overall trend of the observed response spectra. Despite tremendous additional effort put into spatial modeling, modeling the constitutive behavior and computational procedures, these kinds of differences exists. Even with refinement of geotechnical model to better match the observed characteristics of ground motion the predictions were systematically different than the observations over a wide range of frequencies [Scherbaum et al. (1994)].
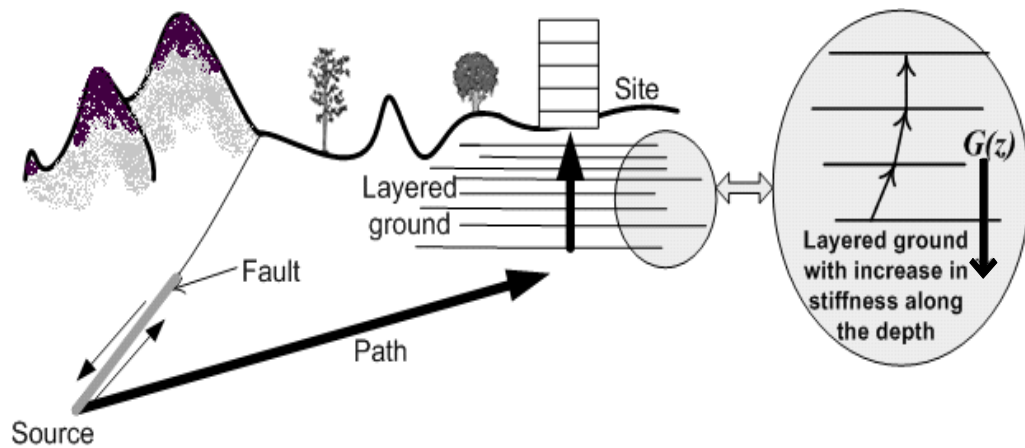
Figure 2.1: Waves propagate almost vertically near the surface due to refraction at horizontal layer boundaries [Modified from Kramer (1996)]

There are many studies available in the literature comparing the ground response estimates using 1D, 2D and 3D analyses [Joyner and Boore (1988), Boore (2004) Bielak et al. (2000), Semblat (2011)]. On the other hand Dickenson et al. (1991), Seed et al. (1994) and Dobry et al. (1994) have shown that the one-dimensional model provided a good approximation to the observed site response in the Loma Prieta earthquake, especially for the case of soft clay sites.

As a further simplification with respect to dimensionality of the problem, the problem is reduced to one dimension by assuming that the seismic surface motion of the soil

15

deposit is primarily due to the upward propagation of shear waves from underlying bedrock. Observational studies carried out using seismograms obtained at several stations in Japan and elsewhere have confirmed that the angle of incidence is less than five degrees near the surface of the deposit [Salt (1974)]. Also these studies have indicated that incident angle of shear wave at the surface layer becomes almost vertical irrespective of epicentral distance. Thus, as a consequence of Snell's law, use of vertically incident waves as the excitation can be justified because, body waves tend to become vertical as they travel upwards as shown in Figure 2.1. This is true if the ground surface, the rock surface and the boundaries between different soil surfaces are nearly horizontal. Otherwise, two/three dimensional analysis is indispensable [Idriss and Seed (1968)].

2.4   GOVERNING EQUATION OF MOTION FOR WAVE PROPAGATION

Consider homogeneous soil deposit overlying rigid bedrock subjected to an input seismic motion at its base. The balance of forces on an infinitesimal soil element of depth dz is shown in the Figure 2.2. Here τ is the shear stress, ρ is the density, u is the displacement in the horizontal direction (x-axis) and $\ddot{u}$ is the resulting horizontal acceleration due to change in shear stress in that direction. The wave propagation is considered in the z-direction alone.

Considering the inertia force of the element, equilibrium in the horizontal direction can be stated as

$$-\rho \ddot{u} dz - \tau + \left(\tau + \frac{\partial \tau}{\partial z} dz \right) = 0 \tag{2.1}$$

That is,

$$\rho \ddot{u} = \rho \frac{\partial^2 u}{\partial t^2} = \frac{\partial \tau}{\partial z} \tag{2.2}$$

Eq. (2.2) is the equation for one dimensional ground response analysis. If the soil stress-strain behaviour is assumed to be represented by Kelvin-Voigt model [Tsai and

Housner (1970); Kramer (1996)], then the shear stress τ is related to shear strain and rate of shear strain as,

$$\tau = G\gamma + \eta\dot{\gamma} \tag{2.3}$$

Here, strain is $\gamma = \dfrac{\partial u(z,t)}{\partial z}$ strain rate is $\dot{\gamma} = \dfrac{\partial^2 u(z,t)}{\partial z \partial t}$, G is the shear modulus and η is the viscosity coefficient. Substituting for τ in Eq. (2.2),

$$\rho\frac{\partial^2 u}{\partial t^2} = \frac{\partial \tau}{\partial z} = G\frac{\partial^2 u}{\partial z^2} + \eta\frac{\partial^3 u}{\partial z^2 \partial t} \tag{2.4}$$
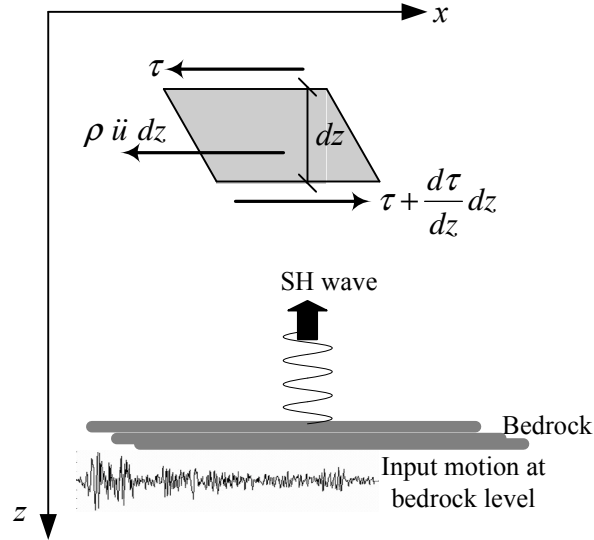
Figure 2.2: Equilibrium of forces acting on an infinitesimal element

Introducing complex shear modulus, G^* as $G^* = (1 + 2i\zeta)G$ where, ζ is the frequency dependent viscous damping ratio and $i = \sqrt{-1}$. ζ is related to η as $\zeta = \dfrac{\omega\eta}{2G}$ [Kramer (1996)], where ω is the loading frequency. Thus the stress-strain relation may be expressed as

$$\tau = G^*\gamma = (1 + 2i\zeta)G\gamma \tag{2.5}$$

By substituting Eq. (2.5) to Eq. (2.2),

$$\rho \frac{\partial^2 u}{\partial t^2} = G^* \frac{\partial \gamma}{\partial z} = G^* \frac{\partial^2 u}{\partial z^2} \tag{2.6}$$

Since $u(z,t)$ is a function of both space and time, by separation of variables the horizontal displacement $u(z,t)$ can be expressed as,

$$u(z,t) = u_1(z)u_2(t) = U(z)e^{i\omega t} \tag{2.7}$$

Expressing the complex wave number k, as $k^2 = \dfrac{\omega^2 \rho}{(1+2i\zeta)G} = \dfrac{\omega^2 \rho}{G^*}$ and substituting Eq. (2.7) into Eq. (2.6) yields an ordinary differential equation as

$$\frac{d^2 U(z)}{dz^2} + k^2 U(z) = 0 \tag{2.8}$$

The solution of the equation may be expressed as

$$U(z) = Ee^{ikz} + Fe^{-ikz} \tag{2.9}$$

Hence the horizontal displacement is given by Eq. (2.7) as,

$$u(z) = Ue^{i\omega t} = Ee^{i(kz+\omega t)} + Fe^{-i(kz-\omega t)} \tag{2.10}$$

Here E and F are complex constant, which can be determined by boundary conditions. Physically E represents the transmitted wave (upwards) and F represents reflected wave (downwards) at each of the layer interfaces.

2.5   OVERVIEW OF MATHEMATICAL METHODS

2.5.1   Theory of multiple reflections – Frequency domain analysis

The analytical solution to the general problem of transmission of elastic waves through distinctly stratified horizontal layers of linearly elastic material was dealt by Thomson (1935) and Haskel (1953). Later this approach, well known as theory of multiple reflections of waves, is extended to geophysical problem associated with

transmission of seismic waves in stratified geologic medium by Haskel (1960). For the problems related to wave propagation in soil deposits consisting of multiple horizontal homogeneous layers, the solution given in the previous section for single layer can be extended using multi-reflection theory [Roësset and Whitman (1969), Tsai and Housner (1970), Schnabel et al. (1972), Cherry (1974), Roësset (1977), Erdik (1987) and others]. Figure 2.3 shows the model for a horizontally multi-layered soil deposit. The coordinate z is defined independently for each layer measuring from the top. That is, for the ith layer, z_i ranges from 0 to H_i which is the thickness of the ith layer. The density ρ_i, maximum shear modulus (low strain) G_i or maximum shear wave velocity v_{si} and damping factor ζ_i are assumed to be constant within each layer. By accounting for boundary conditions, the theory of multiple reflections gives the total response at all layers by summing the closed form solution of each layer. The boundary conditions are

i. The shear stress at ground surface is zero $\Rightarrow$ $\tau(z_1 = 0, t) = \tau_0 = 0$

ii. The displacement is continuous at the interface of boundary layers
$\Rightarrow$ $u_m(z_m = H_m, t) = u_{m+1}(z_{m+1} = 0, t)$

iii. The shear stress is continuous at the interface of boundary layers
$\Rightarrow$ $\tau_m(z_m = H_m, t) = \tau_{m+1}(z_{m+1} = 0, t)$

These boundary conditions will yield $2n$-1 equations to evaluate $2n$ unknowns those are corresponding to $E_1, E_2, E_3, ...E_n$ and $F_1, F_2, F_3............F_n$ which are the amplitudes of the upward and downward wave components in each of the layers respectively. Hence we can obtain all the wave amplitudes when one of the amplitude is given at an arbitrary layer as an input motion.

The displacement in the mth layer is obtained using Eq. (2.10) as,

$$u_m(z_m, t) = (E_m e^{ik_m z_m} + F_m e^{-ik_m z_m}) e^{i\omega t} \qquad (2.11)$$
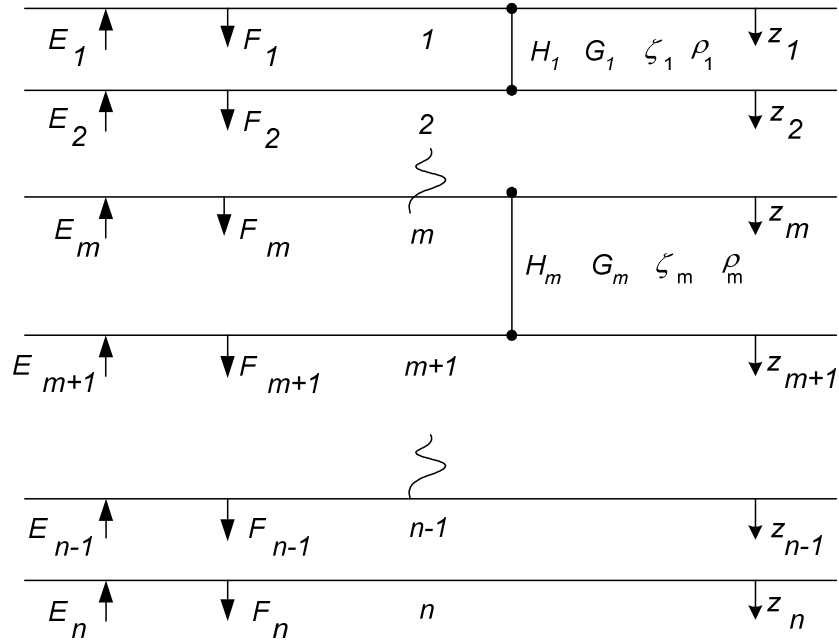
Figure 2.3: Model ground representing layered soil deposit

The shear stress in the layer is,

$$\tau_m = G_m^* \gamma_m(z_m, t) = iG_m^* k_m (E_m e^{ik_m z_m} - F_m e^{-ik_m z_m}) e^{i\omega t} \tag{2.12}$$

If the displacement and shear stress at the top and bottom of the mth layer are $u_m^{(t)}(0,t)$, $\tau_m^{(t)}(0,t)$ and $u_m^{(b)}(H_m,t)$, $\tau_m^{(b)}(H_m,t)$ respectively, then from Eq. (2.11) and Eq. (2.12) we have,

$$
\begin{aligned}
u_m^{(t)} &= (E_m + F_m)e^{i\omega t} \\
\tau_m^{(t)} &= iG_m^* k_m (E_m - F_m)e^{i\omega t}
\end{aligned}
\tag{2.13}
$$

$$
\begin{aligned}
u_m^{(b)} &= (E_m e^{ik_m H_m} + F_m e^{-ik_m H_m})e^{i\omega t} \\
\tau_m^{(b)} &= iG_m^* k_m (E_m e^{ik_m H_m} - F_m e^{-ik_m H_m})e^{i\omega t}
\end{aligned}
\tag{2.14}
$$

i.e.,

$$
\begin{Bmatrix} u_m^{(t)} \\ \tau_m^{(t)} \end{Bmatrix} = \begin{bmatrix} 1 & 1 \\ iG_m^* k_m & -iG_m^* k_m \end{bmatrix} \begin{Bmatrix} E_m \\ F_m \end{Bmatrix} e^{i\omega t}
\tag{2.15}
$$

$$\begin{Bmatrix} u_m^{(b)} \\ \tau_m^{(b)} \end{Bmatrix} = \begin{bmatrix} e^{ik_m H_m} & e^{-ik_m H_m} \\ iG_m^* k_m e^{ik_m H_m} & -iG_m^* k_m e^{-ik_m H_m} \end{bmatrix} \begin{Bmatrix} E_m \\ F_m \end{Bmatrix} e^{i\omega t} \qquad (2.16)$$

Eliminating E_m and F_m from the above equation yields,

$$\begin{Bmatrix} u_m^{(b)} \\ \tau_m^{(b)} \end{Bmatrix} = \begin{bmatrix} \cos(k_m H_m) & \dfrac{\sin(k_m H_m)}{G_m^* k_m} \\ -G_m^* k_m \sin(k_m H_m) & \cos(k_m H_m) \end{bmatrix} \begin{Bmatrix} u_m^{(t)} \\ \tau_m^{(t)} \end{Bmatrix} \qquad (2.17)$$

Based on the boundary condition, continuity of displacement and shear stresses at the layer boundary interfaces, we get the following results for m and $m+1$ layer

$$\begin{Bmatrix} u_m^{(b)} \\ \tau_m^{(b)} \end{Bmatrix} = \begin{Bmatrix} u_{m+1}^{(t)} \\ \tau_{m+1}^{(t)} \end{Bmatrix} \qquad (2.18)$$

Combining, Eq. (2.17) and Eq. (2.18), displacement and shear stresses at the top of successive layers are related as following

$$\begin{Bmatrix} u_{m+1}^{(t)} \\ \tau_{m+1}^{(t)} \end{Bmatrix} = \begin{bmatrix} \cos(k_m H_m) & \dfrac{\sin(k_m H_m)}{G_m^* k_m} \\ -G_m^* k_m \sin(k_m H_m) & \cos(k_m H_m) \end{bmatrix} \begin{Bmatrix} u_m^{(t)} \\ \tau_m^{(t)} \end{Bmatrix} \qquad (2.19)$$

The Haskel-Thomson transfer matrix $\overline{A}_m$ for the mth layer relating the displacements and stresses of successive layers in terms of layer properties may be defined as,

$$\begin{bmatrix} \overline{A}_m \end{bmatrix} = \begin{bmatrix} \cos(k_m H_m) & \dfrac{\sin(k_m H_m)}{G_m^* k_m} \\ -G_m^* k_m \sin(k_m H_m) & \cos(k_m H_m) \end{bmatrix} \qquad (2.20)$$

By recursively applying the relation to other layers from layer ($m+1$) to the top of the surface layer, we obtain,

$$\begin{Bmatrix} u_{m+1} \\ \tau_{m+1} \end{Bmatrix} = \begin{bmatrix} \overline{A}_m \end{bmatrix} \begin{bmatrix} \overline{A}_{m-1} \end{bmatrix} \begin{bmatrix} \overline{A}_{m-2} \end{bmatrix} \ldots\ldots\ldots \begin{bmatrix} \overline{A}_2 \end{bmatrix} \begin{bmatrix} \overline{A}_1 \end{bmatrix} \begin{Bmatrix} u_0 \\ \tau_0 \end{Bmatrix} \qquad (2.21)$$

For a deposit of total thickness H and consisting of n layers, the displacement and stresses at the base and surface of the deposit can be established as,

$$\left\{ \begin{matrix} u_H \\ \tau_H \end{matrix} \right\} = \left[\bar{A}_{n-1} \right] \left[\bar{A}_{n-2} \right] \left[\bar{A}_{n-3} \right] \ldots\ldots\ldots\ldots \left[\bar{A}_2 \right] \left[\bar{A}_1 \right] \left\{ \begin{matrix} u_0 \\ \tau_0 \end{matrix} \right\}$$

i.e., $\left\{ \begin{matrix} u_H \\ \tau_H \end{matrix} \right\} = \left[\begin{matrix} \bar{A}_{11} & \bar{A}_{12} \\ \bar{A}_{21} & \bar{A}_{22} \end{matrix} \right] \left\{ \begin{matrix} u_0 \\ \tau_0 \end{matrix} \right\}$

(2.22)

where,

$$\left[\begin{matrix} \bar{A}_{11} & \bar{A}_{12} \\ \bar{A}_{21} & \bar{A}_{22} \end{matrix} \right] = \left[\bar{A} \right] = \left[\bar{A}_{n-1} \right] \left[\bar{A}_{n-2} \right] \left[\bar{A}_{n-3} \right] \ldots\ldots\ldots\ldots \left[\bar{A}_2 \right] \left[\bar{A}_1 \right] \qquad (2.23)$$

$\left[\bar{A} \right]$ is the transformation matrix between layers 1 and n. By using the Eq. (2.22), we can obtain the displacement for all layers, when amplitude at base or at an arbitrary layer is given. The most useful aspect of multiple reflection theory is that deconvolution is possible, that is from the observed acceleration record at the surface we can obtain corresponding bedrock acceleration time history. For this purpose we use the boundary condition that the shear stress at the ground surface is zero, i.e. $\tau_0 = 0$ in Eq. (2.22). Most of the computer programs such as, SHAKE [Schnabel et al. (1972)], EERA [Bardet et al. (2000)] etc., for site response analysis based on theory multiple reflections of waves have been developed using an alternative form of amplification transfer function. Haskel-Thomson transformation matrix is derived by incorporating reflected and transmitted wave amplitudes in successive layer interfaces [Cherry (1974); Roësset (1977)]. Using the boundary conditions of continuity of stress and displacement at the interface of m and m+1 layers, the transformation matrix is given by,

$$\left\{ \begin{matrix} E_{m+1} \\ F_{m+1} \end{matrix} \right\} = \left[\begin{matrix} \frac{1}{2}(1+\alpha_m)e^{ik_m H_m} & \frac{1}{2}(1-\alpha_m)e^{-ik_m H_m} \\ \frac{1}{2}(1-\alpha_m)e^{ik_m H_m} & \frac{1}{2}(1+\alpha_m)e^{-ik_m H_m} \end{matrix} \right] \left\{ \begin{matrix} E_m \\ F_m \end{matrix} \right\} \qquad (2.24)$$

22

where α_m is called impedance ratio. It is defined as $\alpha_m = \dfrac{G_m^* k_m}{G_{m+1}^* k_{m+1}}$. Thus, in this case, Haskel-Thomson transfer matrix $\tilde{A}_m$ relating the amplitudes of successive layers in terms of layer properties may be defined as,

$$\tilde{A}_m = \begin{bmatrix} \dfrac{1}{2}(1+\alpha_m)e^{ik_m H_m} & \dfrac{1}{2}(1-\alpha_m)e^{-ik_m H_m} \\ \dfrac{1}{2}(1-\alpha_m)e^{ik_m H_m} & \dfrac{1}{2}(1+\alpha_m)e^{-ik_m H_m} \end{bmatrix} \tag{2.25}$$

The transfer matrix relates the amplitudes of upward and downward propagating waves between layer m and layer $(m+1)$. By recursively applying the relation to other layers from layer n to the surface layer, we obtain,

$$\begin{Bmatrix} E_n \\ F_n \end{Bmatrix} = \begin{bmatrix} \tilde{A}_{n-1} \end{bmatrix}\begin{bmatrix} \tilde{A}_{n-2} \end{bmatrix}\begin{bmatrix} \tilde{A}_{n-3} \end{bmatrix}\ldots\ldots\ldots\begin{bmatrix} \tilde{A}_2 \end{bmatrix}\begin{bmatrix} \tilde{A}_1 \end{bmatrix}\begin{Bmatrix} E_1 \\ F_1 \end{Bmatrix}$$

i.e., $\begin{Bmatrix} E_n \\ F_n \end{Bmatrix} = \begin{bmatrix} \tilde{A}_{11} & \tilde{A}_{12} \\ \tilde{A}_{21} & \tilde{A}_{22} \end{bmatrix}\begin{Bmatrix} E_1 \\ F_1 \end{Bmatrix} = \begin{bmatrix} \tilde{A} \end{bmatrix}\begin{Bmatrix} E_1 \\ F_1 \end{Bmatrix}$ \hfill (2.26)

where, $\begin{bmatrix} \tilde{A} \end{bmatrix}$ is the transformation matrix between layers 1 and n. By using the Eq. (2.26), along with the stress free boundary condition at the surface, we can obtain the amplitude of displacement for all layers when amplitude at base or at an arbitrary layer is given. Let u_i and u_j be the displacements at the top of the ith and j^{th} layers respectively. From Eq. (2.10) we have,

$$u_i(z_i = 0, t) = (E_i + F_i)e^{i\omega t} \tag{2.27}$$

$$u_j(z_j = 0, t) = (E_j + F_j)e^{i\omega t} \tag{2.28}$$

Therefore displacement ratio between i^{th} and j^{th} layers is,

$$\frac{u_i(z_i = 0, t)}{u_j(z_j = 0, t)} = \frac{(E_i + F_i)e^{i\omega t}}{(E_j + F_j)e^{i\omega t}} = \frac{(E_i + F_i)}{(E_j + F_j)} = T_{i/j}(\omega) \tag{2.29}$$

where $T_{i/j}(\omega)$ is the transfer function (function of frequency) between i^{th} and j^{th} layers. The transfer function $T_{i/j}(\omega)$ defined in Eq. (2.29) for displacements is valid as well for velocity and acceleration. The absolute value of the transfer function $\left(\left|T_{i/j}(\omega)\right|\right)$ is defined as the amplification ratio between the corresponding layers. Since the transfer function does not contain the amplitude F_1 at the ground surface, by assuming E_1, we can calculate E and F at all the other layers from Eq. (2.26). Then the transfer function between any two arbitrary layers may be calculated. When the amplitude of a response quantity is given at i^{th} layer, the corresponding response quantity at the jth layer is calculated from Eq. (2.29) using $\left(\left|T_{i/j}(\omega)\right|\right)$. Since the transfer function is a function of frequency, the frequency of the harmonic wave influences the magnitude of the transfer function.

However the input motion, such as earthquake accelerogram, is a random function of time. It consists of several harmonic components of different frequencies. Therefore, it is essential to decompose the given wave form into harmonic waves in order to extend this method in seismic analysis. Usually Fast Fourier Transform (FFT) is used to divide the random accelerogram into its harmonic components. The response quantities thus obtained using this frequency domain approach, are recomposed into time histories using inverse Fourier transform (IFFT). Schnabel et al. (1972) used this procedure of evaluating the ground response in their most popular computer program SHAKE. SHAKE91 [Idriss and Sun (1992)] is the later version of SHAKE.

Recently, many other computer programs are developed implementing this procedure. EERA [Bardet et al. (2000)] which is spread sheet version of SHAKE91, STRATA [Kottke and Rajthe (2008)], DEEPSOIL [Hashash (2011)] are some of them which are available as freeware programs and are very much popular equally among researchers and practicing engineers. In this work either EERA and/or DEEPSOIL are used for various parametric analyses in frequency domain as well as for the purpose of comparative studies. The frequency domain equivalent linear analyses carried out using other programs are synonymously referred to as SHAKE analysis throughout this thesis.

2.5.2 Time domain analysis - Lumped parameters idealisation

When nonlinear effect is significant and the problem is essentially two or three dimensional, a discrete model of the soil profile (finite differences or finite elements) and true nonlinear analysis in time domain is the recommended procedure. For such models, the resulting wave propagation equations are solved numerically in the time domain using direct integration schemes. Equation of motion is integrated using explicit or implicit direct integration scheme.
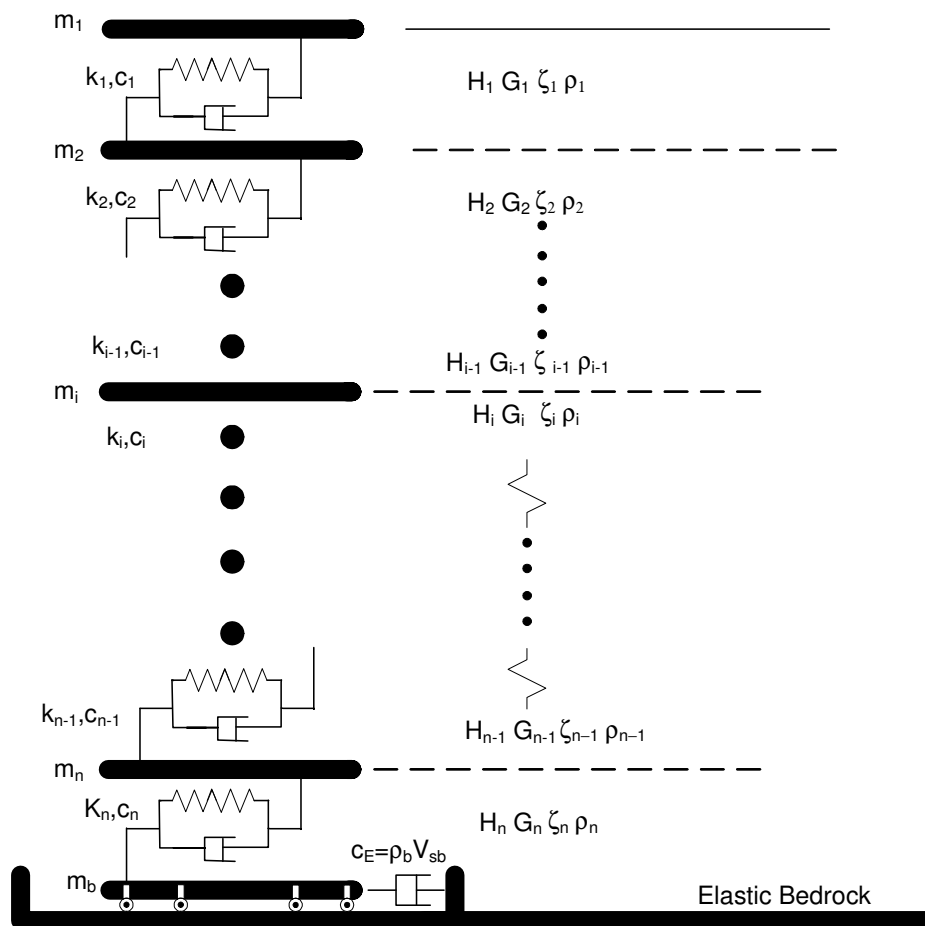
Figure 2.4: Lumped parameters model of the soil deposit [Modified from Hashash and Park (2001)]

The main advantage of time domain analysis is that the cyclic stress-strain behavior of soil can be incorporated conveniently by using an appropriate constitutive law. Also the analysis can be carried out both in terms of total stresses and in terms of effective

stresses. In case of effective stress analysis, the pore pressure generation and dissipation during the earthquake is directly taken into account in the formulation.

When a soil deposit is assumed to be made up of horizontal layers with distinctly different mechanical properties and subjected to vertically propagating shear waves, it may be analyzed by modeling it as one dimensional as in the theory of multiple reflections of waves. However in time domain approach, soil deposit is spatially discretised either using continuum model or using discrete lumped mass approach. In the latter approach, each layer of the soil deposit is replaced by a lumped mass connected with spring and dashpot to represent its elastic and energy dissipating properties. One dimensional analysis in time domain using lumped mass approach is employed for the purpose of comparison and validation of results of the present research work.

A simple mechanical model of the soil deposit as shown in Figure 2.4 is representing a semi-infinite medium with a unit width and an infinite length for which the equation of motion of multi-degrees of freedom may be formulated using basic theory of vibration [Clough and Penzien (1993); Chopra (1995)].

The mass of each soil layer is assumed to be concentrated at a point due to equal contribution from the adjacent layers. That is, the lumped mass corresponding to any layer is obtained by lumping half the mass of each of the two consecutive layers at their common boundary with lumped mass corresponding to first layer being, $m_1 = \rho_1 H_1 / 2$. In general, lumped mass of ith soil layer is,

$$m_i = \frac{\rho_{i-1} H_{i-1} + \rho_i H_i}{2}, \qquad i = 2, 3, \ldots \ldots n \qquad (2.30)$$

Here ρ_i and H_i are mass density and thickness of the ith layer respectively. The stiffness coefficients for linear elastic material may be expressed for i^{th} soil layer may be expressed as $k_i = G_i / H_i$, where G_i is the average shear modulus of the soil of ith layer. The viscous damping coefficient c_i is similarly expressed for each of the layer based on appropriate viscous damping coefficient at small strain level [Hashash and

Park (2002)]. Thus the equation of motion for discrete model can be expressed in terms of assembled matrices as [Clough and Penzien (1993)],

$$[M]\{\ddot{u}\} + [C]\{\dot{u}\} + [K]\{u\} = -[M][I]\ddot{u}_b \qquad (2.31)$$

Here, $[M]$ is the assembled mass matrix, $[K]$ is the assembled stiffness matrix and $[C]$ is the assembled viscous damping matrix. Displacement, velocity and acceleration vectors relatively with respect to bedrock in the horizontal direction are respectively represented by $\{u\}, \{\dot{u}\}\ \&\ \{\ddot{u}\}$. The acceleration time history $\ddot{u}_b(t)$, is the prescribed input motion at the base of the deposit. The order of mass, stiffness and damping matrices depend on number of layers employed to model the soil deposit. The mass matrix is diagonal while stiffness and damping matrices are symmetric tri-diagonal. The equation of motion (Eq. 2.31) can be solved by using direct numerical integration techniques such as Newmark-β or Wilson-θ or any other unconditionally stable methods [Bathe and Wilson (1987)]. The absolute response quantities of any soil layer may be computed, for example absolute acceleration of the ith layer is $\ddot{u}_i + \ddot{u}_b$. At every time step the computed strains are used along with the material constitutive model to compute shear stress and to update the stiffness matrix.

This approach has been employed by many researchers and among them the earliest attempt was by Idriss and Seed (1967, 1968). They used lumped parameters to represent inertia, stiffness and damping properties of the continuously inhomogeneous deposit. In their study the deposit is assumed to be overlying rigid bedrock. Later many computer codes have been developed, e.g., MASH [Martin and Seed (1978)], DMOD [Matsovic (1993)], TESS [Pyke (2000)], DEEPSOIL [Hashash and Park (2001); Hashas et al. (2011)], DESRA [Finn et al. (1977)], etc., with several modifications and improvements in this approach of discrete lumped parameter idealisation to estimate the response the surface soil deposit. Particularly these improvements are aimed at modeling nonlinear stress strain behavior of soil. Also to prescribe input motion at the base of the deposit with appropriately modeling the soil and rock interface to account for underlying elastic half-space characteristics.

Apart from modeling the inertia, stiffness and damping properties of the soil deposit with discrete lumped parameters, continuum discretization is also employed in site response analysis. Usually, finite difference, finite element method, boundary element method, etc. are the numerical procedures which have been used in the solution formulation. The details of these methods and their implementation in site response analysis are elaborated elsewhere [Kramer (1996), Bardet and Tobita (2001), Stewart and Kwok (2008), Hashash et al. (2010), Semblat (2011), etc.].

The main concern in use of all the methods of analyses discussed above is about modeling the damping characteristics of the soil deposit. Frequency independent hysteretic damping model employed in frequency domain equivalent linear analysis is deficient of physical explanation [Ching and Glaser (2001)]. On the other hand, many studies have concluded that Rayleigh damping formulation used in time domain analysis is ambiguous because it is based on principle of orthogonality of mode shapes [Chang et al. (2000); Park and Hashash (2004)]. Even though efficient methods for modeling the energy dissipation characteristics of soil have been proposed, they are not popular because their implementation is rather mathematically complex [Inaudi and Kelly (1995); Inaudi and Markis (1996)].

2.6   AMPLIFICATION OF SURFACE RESPONSE

2.6.1   Amplification functions

In solving the problem of site response for prescribed motion at the base of the soil column, it is essential to satisfy the appropriate boundary conditions particularly at the interfacial boundary of bedrock and soil column. Contrasting rigidity across the soil-bedrock boundary controls the magnitude of energy dissipation within the soil column.

Hence it is important to consider the finite rigidity of the underlying medium. Joyner and Chen (1975) formulated a solution procedure by considering the bedrock as elastic. There are two practical situations, causing main difference in how the input motion is prescribed. In the first case the input motion is prescribed as control motion

at the rock outcropping ($2E_r$) and compute free soil surface ($2E_1$) and/or within (bedrock) $E_r + F_r$ response of the deposit, referred to as deconvolution. Secondly, input motion is prescribed as control motion within the deposit often at the interface of soil base and top of bedrock. In the latter case, the responses are computed at surface and/or at any point within the deposit. Most often the recorded motions are available at the outcropping rock surface and are used to estimate the bedrock motion $E_r + F_r$ in a nearby site.
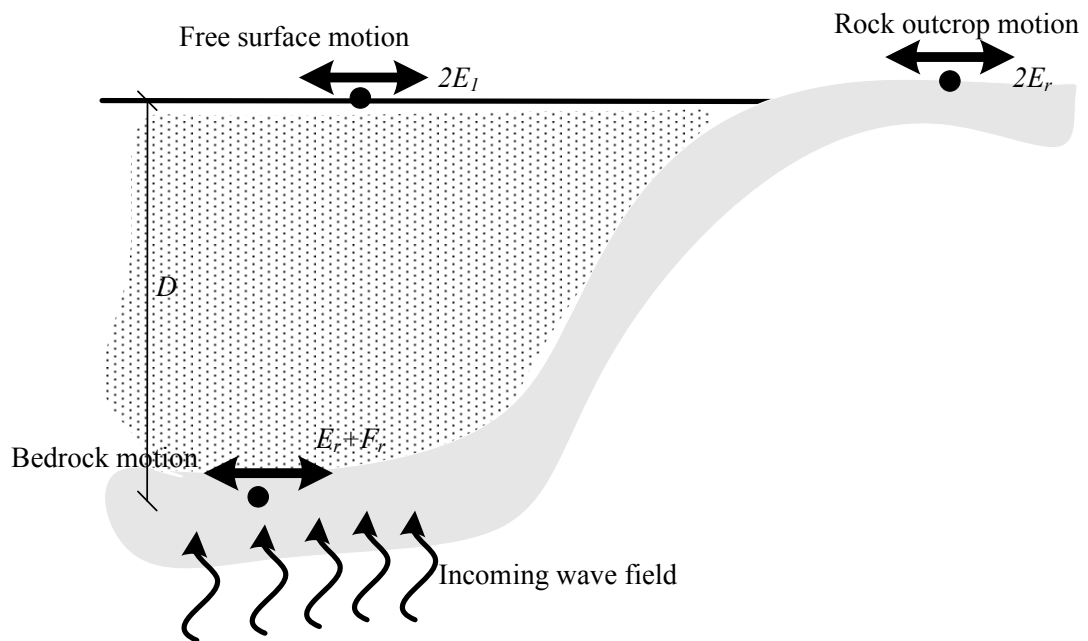
Figure 2.5: Terminology related to amplification of surface motion with respect to input bedrock motion

The modification to amplitude and frequency characteristics of the wave as it propagates through the soil deposit is often represented by amplification function defined as the ratio of frequency response at the surface of the deposit to input motion at its base. Amplification function is dependent on the elastic property of the bedrock on which the soil deposit is based. Often the expression for amplification function is obtained for two situations depicted in Figure 2.5. Firstly for the case in which bedrock is assumed to be rigid that is amplification function (Amp_1) is obtained disregarding the elastic and damping properties of the bedrock. Thus Amp_1 is the ratio of response at the free surface (at $z = 0$) of the deposit to input motion at the soil and

bedrock interface (at $z = D$), that corresponds to absolute value of the transfer function between surface and base of the deposit, i.e.,

$$Amp_1(\omega) = \left| T_{surface/base} \right| = \left| \frac{u_0}{u_H} \right| \tag{2.32}$$

In terms of Eq. (2.26) noting that because of stress free $(\tau_0 = 0)$ boundary condition at the surface (i.e., $F_1 = E_1$) and using the elements of the transformation matrix for displacement amplitudes between surface and base we get,

$$Amp_1(\omega) = \left| \frac{2E_1}{E_n + F_n} \right| = \left| \frac{2}{\tilde{A}_{11} + \tilde{A}_{21}} \right| \tag{2.33}$$

The other terminology for amplification function is Amp_2, associated with the case in which the bedrock is considered to be elastic. This also corresponds to ratio of free surface motion at the top of the soil deposit to rock outcrop motion, therefore Amp_2 may expressed as,

$$Amp_2 = \left| \frac{2E_1}{2E_r} \right| = \left| \frac{2E_1}{2E_{n+1}} \right| = \left| \frac{1}{\tilde{A}_{11}} \right| \tag{2.34}$$

The amplification ratio, Amp_2 represents the ratio of the amplitude of free surface motion to that of outcropping motion which is representing surface motion in the absence of soil deposit [Roësset (1977); Towhata (2008)]. The maximum value of these amplification functions for the case of homogeneous soil deposit of depth H, damping ratio ζ and shear velocity v_s is given by Roësset (1977) as,

$$\left. \begin{array}{l} \left(Amp_1\right)_{max} = \dfrac{v_s}{\omega_i H \zeta} \\[4mm] \left(Amp_2\right)_{max} = \dfrac{v_s}{\alpha v_s + \omega_i H \zeta} \end{array} \right\} \tag{2.35}$$

In the above equation impedance ratio $\alpha = v_s \rho_s / v_{sr} \rho_r$, where v_s and v_{sr} are the shear wave velocities in soil and rock respectively while ρ_s and ρ_r are their respective densities. Natural frequency corresponding to i^{th} mode is given by, $\omega_i = \dfrac{(2i-1)\pi v_s}{2H}$.

Relationships for the amplification functions Amp_1 and Amp_2 derived using the transformation matrix involving displacement and shear stresses is as follows.

Using the boundary condition, zero shear stress at the surface $(\tau_0 = 0)$ in Eq. (2.22) we get following results,

$$\left.\begin{array}{l} u_H = \overline{A}_{11} u_0 \\ \tau_H = \overline{A}_{21} u_0 \end{array}\right\} \tag{2.36}$$

Therefore, from Eq. (2.32) and Eq. (2.36) we get,

$$Amp_1(\omega) = \left|\frac{u_0}{u_H}\right| = \left|\frac{1}{\overline{A}_{11}}\right| \tag{2.37}$$

The displacement and shear stress at the top of elastic bedrock is obtained using Eq. (2.11) and Eq. (2.12) as,

$$\left.\begin{array}{l} u_r(0,t) = (E_r + F_r)e^{i\omega t} \\ \tau_r(0,t) = iG_r^* k_r (E_r - F_r)e^{i\omega t} \end{array}\right\} \tag{2.38}$$

E_r and F_r are transmitted and reflected wave amplitudes in the rock. G_r^* and k_r are complex shear modulus and wave number of the elastic half-space respectively. Eliminating F_r from Eq. (2.38) and satisfying the condition of continuity of displacement and stresses at the soil-bedrock interface i.e., $u_H = u_r$ and $\tau_H = \tau_r$ by using Eq. (2.36) yields the following relationship,

$$iG_r^* k_r u_H + \tau_H = 2iG_r^* k_r E_r e^{i\omega t} \tag{2.39}$$

31

Substituting Eq. (2.36) in Eq. (2.39) and noting that the shear stress vanishes at the free surface, surface displacement is given as $u_0 = 2E_1 e^{i\omega t}$. Therefore we get Amp_2 as,

$$Amp_2 = \left| \frac{2E_1}{2E_r} \right| = \frac{iG_r^* k_r}{iG_r^* k_r \bar{A}_{11} + \bar{A}_{21}} \qquad (2.40)$$

It can be verified that for the rigid bedrock condition, wherein G_r^* tends to infinity, then Eq. (2.40) reduces to case of amplification function Amp_1 given in Eq. (2.37).

2.6.2 Effect of soil and bedrock impedances

In order to emphasize the effect of impedance ratio at the soil and bedrock interface on the amplification of response, parametric analysis is carried out using a hypothetical soil deposit of total thickness $50.0m$ and constant unit weight equal to $18.5\ kN/m^3$. Shear modulus of the deposit is considered to be linearly proportional to depth, which results in shear wave velocity to be proportional to square root of depth. The depth dependent shear wave velocity $(v_s(z))$ has the form, $v_s(z) = v_{s0}(1 + az)^{0.5}$ in which v_{s0} shear wave value at the free surface and a is the inhomogeneity parameter which controls the rate of variation of $v_s(z)$.

Firstly, the deposit is assumed as homogeneous with shear wave velocity 200 m/s which is the average value of the inhomogeneous shear wave velocity profile. The deposit is divided into 25 layers, each of $2.0m$ thick that result in layer fundamental frequency of 25 Hz. In the second case the deposit is divided into 30 non-uniform layers to approximate actual continuous velocity variation. The layer discretization conforms to minimum fundamental frequency of each of the layer is 25 Hz, except bottom most layer. The resulting impedance ratio of between successive layers varies between 0.85 and 1.0. Figure 2.6 shows the shear wave velocity profiles of both cases considered in this parametric study along with variation of impedance ratio between the layers. The amplification of input motion at bedrock level to free-surface motion is computed for both rigid and elastic bedrock cases. For the latter case, the amplification is computed by varying the impedance ratio $(1/\alpha)$ between base of the

deposit and elastic bedrock. The values of $1/\alpha\left(=v_{sr}\rho_r/v_s\rho_s\right)$ considered in this analysis are 1, 2, 4 and 16.

The amplification ratios for rigid and flexible bedrock cases, respectively Amp_1 and Amp_2, are computed from Eq. (2.37 and 2.40). Figure 2.7a shows surface to bedrock frequency dependent amplification for the case of homogeneous deposit. In Figure 2.7b the peak amplification values of Figure 2.7a and corresponding frequencies are plotted. Figures 2.8a and 2.8b respectively show amplification and peak values of the amplification plots for the case of inhomogeneous soil deposit.
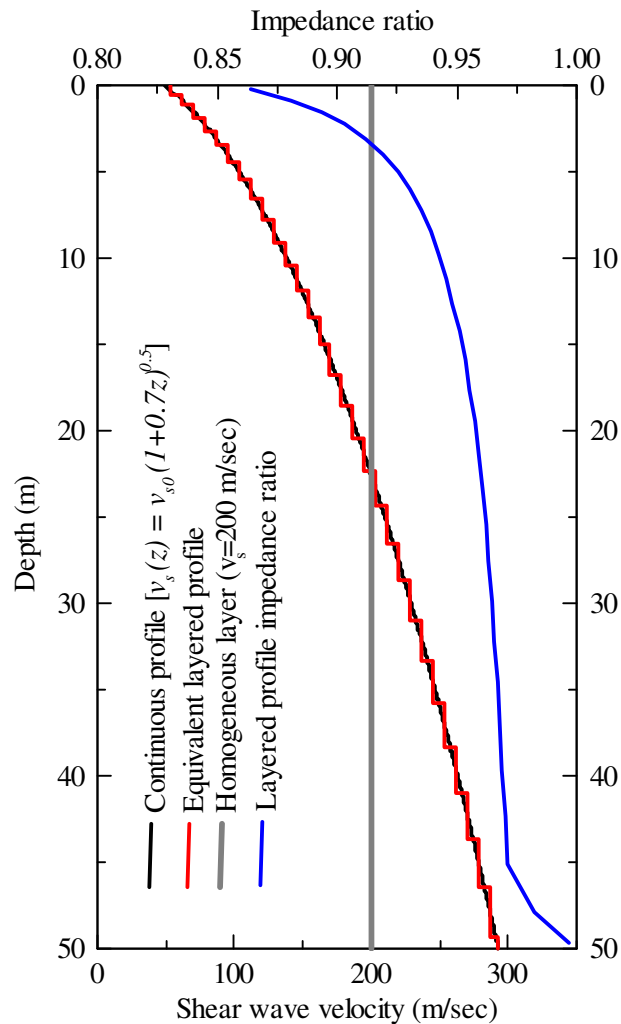
Figure 2.6: Shear wave velocity profiles considered for the parametric study on free-surface to bedrock amplification. Grey and red lines represent the velocity profile of the equivalent homogeneous and layered inhomogeneous deposits.
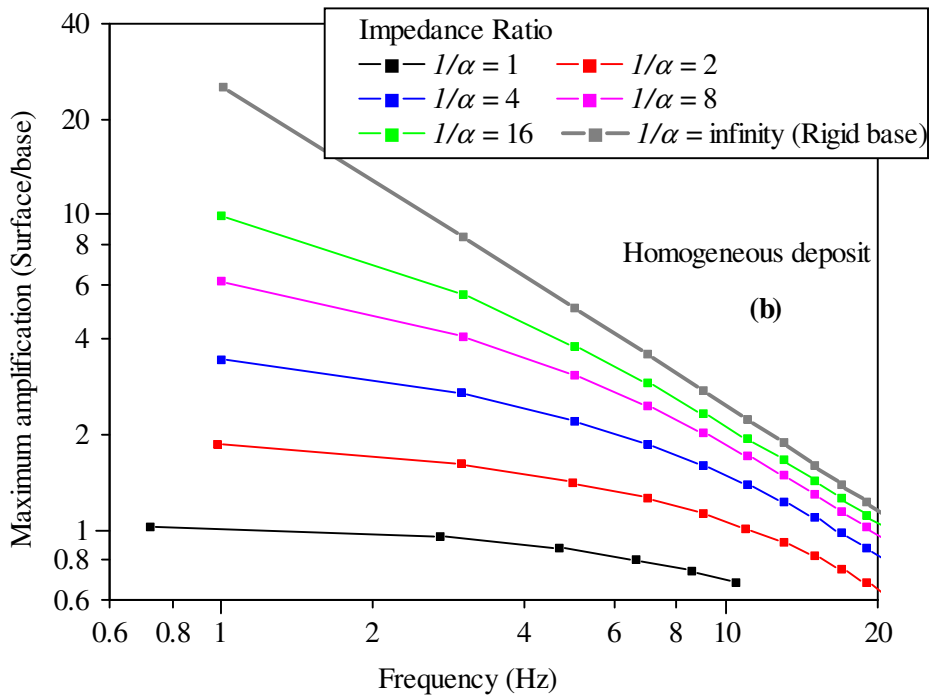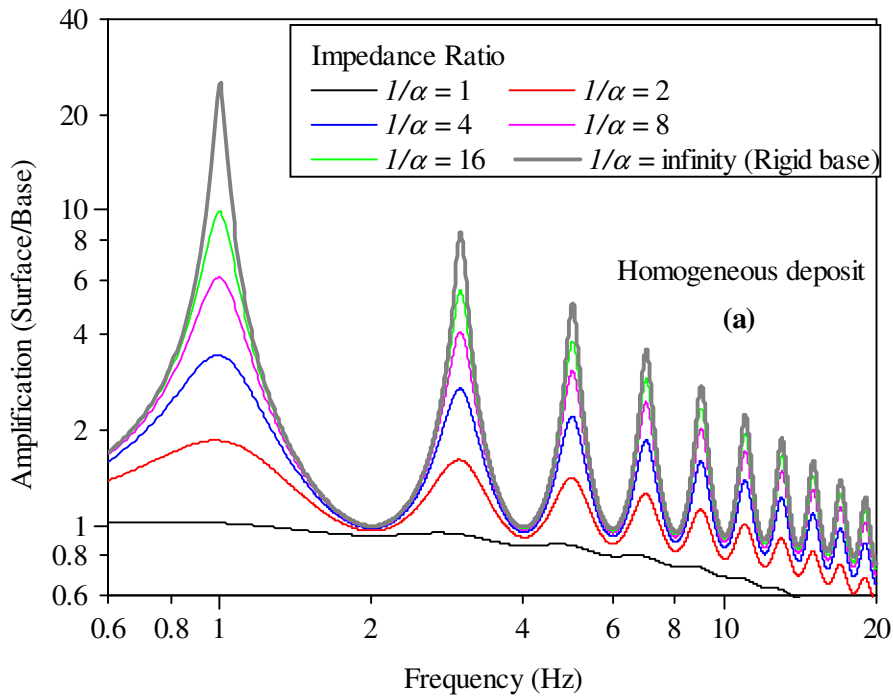
Figure 2.7: Amplification of motion between free-surface and bedrock for the case of a homogeneous deposit (a) frequency dependent amplification (b) variation of maximum amplification at modal frequencies
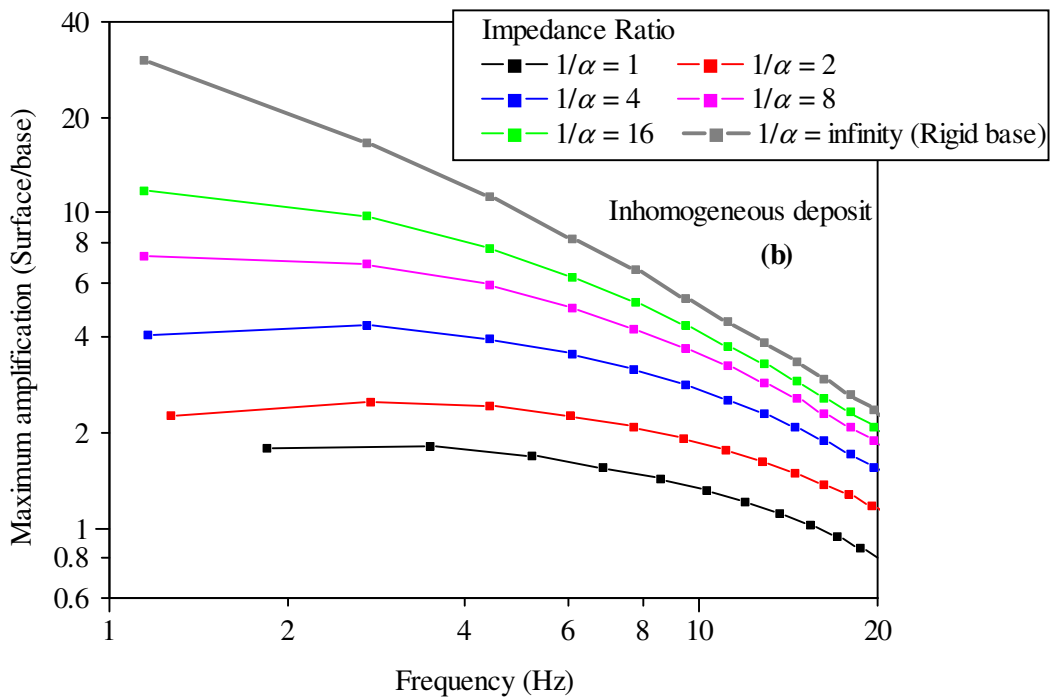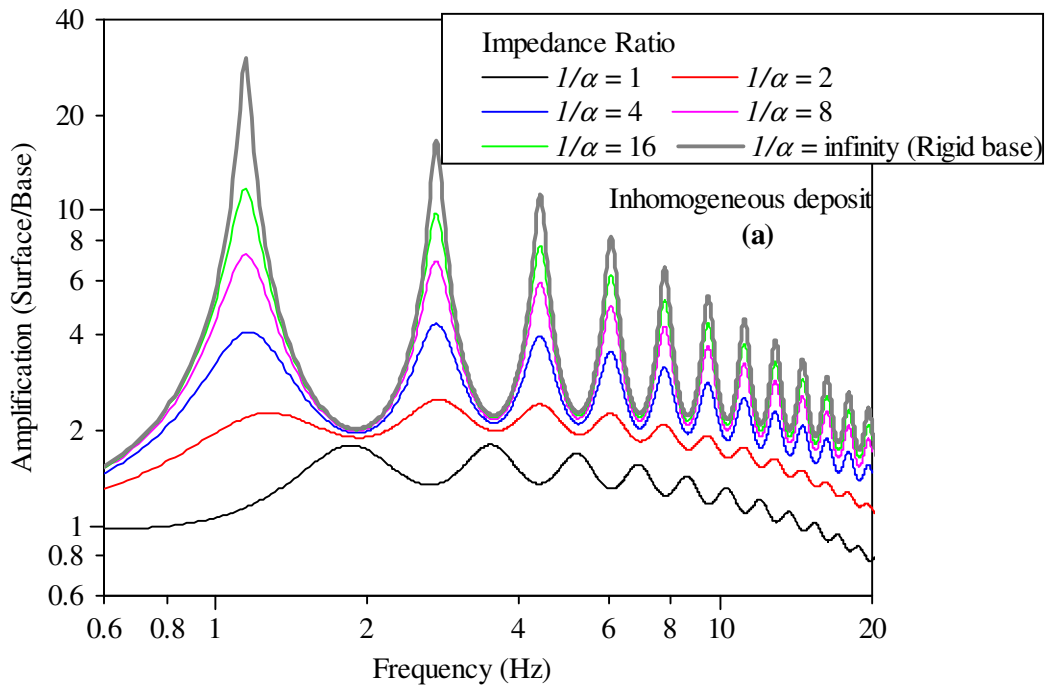
Figure 2.8: Amplification of motion between free-surface and bedrock for the case of an inhomogeneous deposit (a) frequency dependent amplification (b) variation of amplification at modal frequencies

Figures 2.7a and 2.8a demonstrate that amplification tends to its maximum value at the frequencies corresponding to modal frequencies of the deposit. In addition, these figures reveal the well established facts of wave propagation in layered soil deposit

such as, rigid bedrock idealisation leads to larger amplification than for the deposit overlying a flexible base; impedance ratio at the soil and bedrock interface has significant influence of the amplification characteristics; the peaks of amplification ratio reduce with frequencies and almost converge to same value at high frequencies for different impedance ratios. The average fundamental period of both the deposits considered here is 1.0 sec (natural frequency = 1 *Hz*) and damping ratio of 2.5% is used for the both the deposits.

As it can seen in Figure 2.6 the inhomogeneous deposit is relatively soft near the surface and stiff towards the base compared to homogeneous deposit. Effect of this velocity gradient on the amplification trends is evident from Figure 2.7b and 2.8b. The modal frequencies almost unaltered, particularly after first mode, due to contrasting impedance ratio. Whereas, there is a clear shift in the fundamental frequency to lower value when $1/\alpha = 1$ compared to that for $1/\alpha > 1$ in case of homogeneous deposit.

On the other hand, in case of inhomogeneous deposit there is an increase in fundamental frequency when $1/\alpha = 1$ compared to higher values of $1/\alpha$. In both the deposits fundamental and higher frequencies do not alter with increase in $1/\alpha$. Though the natural frequencies of individual layers is same (i.e. 25 *Hz*) in both the cases, higher frequency responses are filtered more effectively in case of homogeneous deposit than in inhomogeneous deposit. This phenomenon, probably, can be attributed to comparatively stiff layers near the base of the inhomogeneous deposit. In case of the homogeneous deposit, for $\alpha = 1$, the peaks of the amplification ratio are less than one for all frequencies above fundamental frequency and appears to be much flatter compared to that of inhomogeneous deposit. Whereas in case of inhomogeneous deposit the amplification is greater than one up to about 15 *Hz* which corresponds to well above fundamental frequency of the deposit.

The above study necessitates the need for clear understanding that is required in specifying the point of control for input motion and prescribing bedrock properties. In frequency domain analysis this is not an issue of concern because input motion can be specified at any point inside the deposit (often termed as within motion) or at free

surface (outcropping motion). On the other hand in time domain approach always there is ambiguity associated with specifying input motion and prescribing the properties of the bedrock. Whenever the input motion is specified as within motion, it is prescribed at the base of the deposit with bedrock being considered as rigid. For specifying the motion at outcropping rock surface the elastic properties of the rock is considered. However, many still opt to convert outcrop motion to within motion using linear frequency domain approach and specify that converted motion at the base of the deposit with rigid bedrock idealisation. For e.g., Visone et al. (2010) employed this procedure to analyze one dimensional soil deposit using time domain finite element approach in their comparative study. This kind of unsophisticated practice is still in vogue among many practicing engineers in spite of clear guidelines set out in this regard by others [e.g. Kowk et al. (2007), Hashash et al. (2010), etc.]. In general, boundary condition at the base of the deposit can be modeled to accommodate transmission waves back into half-space by considering elastic properties of the bedrock or can be idealised as totally reflecting boundary by considering the bedrock as rigid. Both these have large implication on the predicted surface response for an input motion at the base of the deposit. Hence, it is important to give primary attention to appropriately model the soil deposit and accordingly specify the input motion. In this regard, Kowk et al. (2007) proposed following guidelines based on detailed parametric investigation. If the input motion is an outcrop motion, then this motion is applied at the base of the deposit with elastic bedrock boundary condition. If the input motion required to be used is a within motion, usually vertical array record at some depth, then the base motion is applied using rigid bedrock boundary condition.

2.7 METHODS OF MODELING STRAIN DEPENDENT SOIL PROPERTIES

Apart from modeling of wave propagation model used in seismic site response analyses, amplitude and frequency content of computed motions are primarily controlled by the dynamic properties such as shear modulus and material damping of the soil deposit. Laboratory tests on soils have revealed that pronounced nonlinear

behaviour under shear loading conditions is manifested depending upon the type of soil, initial confining pressure, rate and magnitude of loading, etc. If nonlinear behaviour of earth materials observed in laboratory is applicable to in-situ soil properties subject to earthquake loading, then site response calculations must accommodate these strain dependencies as nonlinear constitutive relations. Seed and Idriss (1970) and Hardin and Drnevich (1972a) are some of the earliest research efforts to give the trend of this observable fact through the curves depicting decrease in shear modulus and increase in material damping with increasing shear strain. Subsequently many developments have taken place in characterizing the soil behaviour for dynamic analysis. In general nonlinear and equivalent-linear are the two approaches used to model strain dependent soil response.

2.7.1 Equivalent linear Method

Seed and Idriss (1970) formulated and proposed an equivalent linear characterization of dynamic soil properties to model nonlinear behavior of soil and implemented in the most widely used computer program SHAKE [Schnabel et al. (1972)]. In equivalent-linear method, the nonlinear variation of soil shear moduli and damping are modeled as a function of shear strain. The hysteretic stress-strain behavior of soils under symmetrical cyclic loading is represented by an equivalent modulus and equivalent damping ratio. The equivalent modulus is corresponding to the secant modulus through the endpoints of the hysteresis loop and equivalent-linear damping ratio is proportional to the energy loss from a single cycle of shear deformation. An iterative procedure, based on linear dynamic analysis, is performed to find the shear modulii and damping ratios corresponding to the computed shear strains.

The equivalent linear analysis procedure is depicted in Figure 2.9 and flowchart to implement it in seismic site response analysis is shown in Figure 2.10. As shown in these figures, initial estimates of the dynamic shear modulus, corresponding to low strain shear modulii (G_{max}), and damping ratios are assigned to each of the layer for the first iteration. For the second and subsequent iterations, shear modulus and damping ratio values corresponding to an effective strain (γ_{eff}) are determined.

Effective strains for all the layers are calculated as a fraction of the maximum strain obtained from the previous iteration. These effective shear strains are assumed to be constant within each of the soil sub-layers for the entire duration of the excitation.
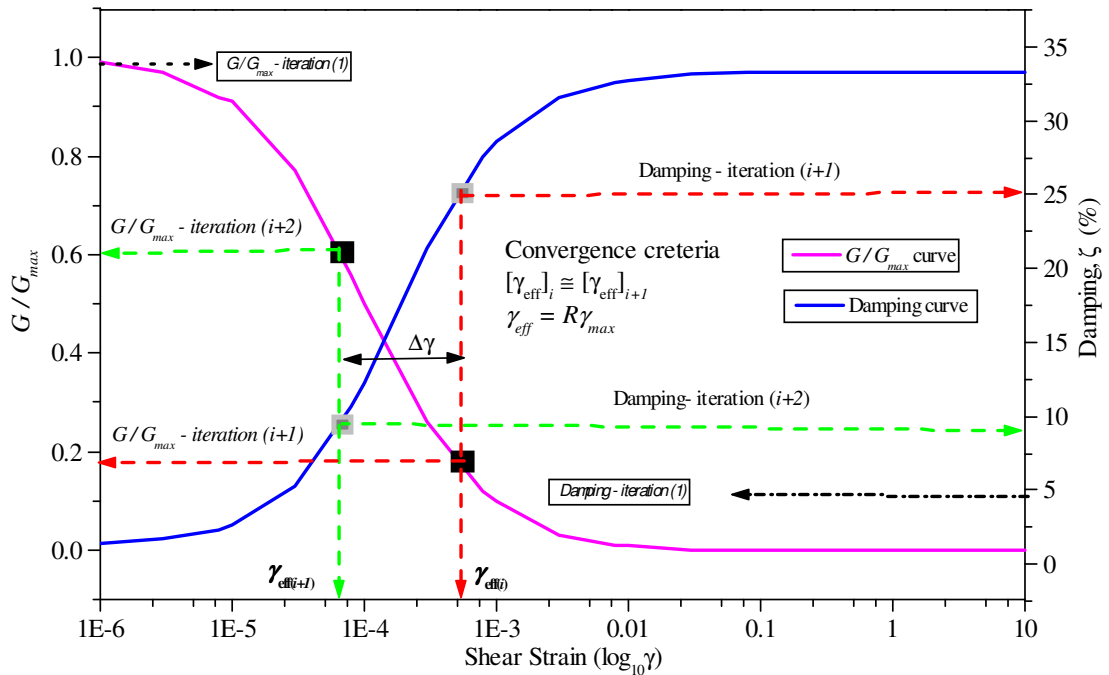
Figure 2.9: Iterative procedure for equivalent linear analysis

The ratio of equivalent effective shear strain to the calculated maximum strain is specified as an input data (R) and the same value of R is used for all sub-layers. Idriss and Sun (1992) proposed an empirical formula to compute the ratio, as $R = (M-1)/10$ where M is the magnitude of the earthquake corresponding to input motion. The effective strains thus computed at the mid-depth of each of the soil layer from the previous iteration are used to obtain new values of strain-dependent modulus and damping ratio for the subsequent iteration as shown in Figures 2.9 and 2.10. The linear response calculation is repeated, new effective strains evaluated, and iterations performed until the changes in properties are below some tolerable limit (i.e., $\Delta\gamma$ is negligible). Generally five to eight iterations are sufficient to achieve convergence. For the purpose of illustration, a set of strain dependent shear modulus $\left(G/G_{max}\right)$ and damping $\left(\zeta \text{ in } \%\right)$ curves for sand proposed by Seed and Idriss (1970) is shown in Figure 2.11.
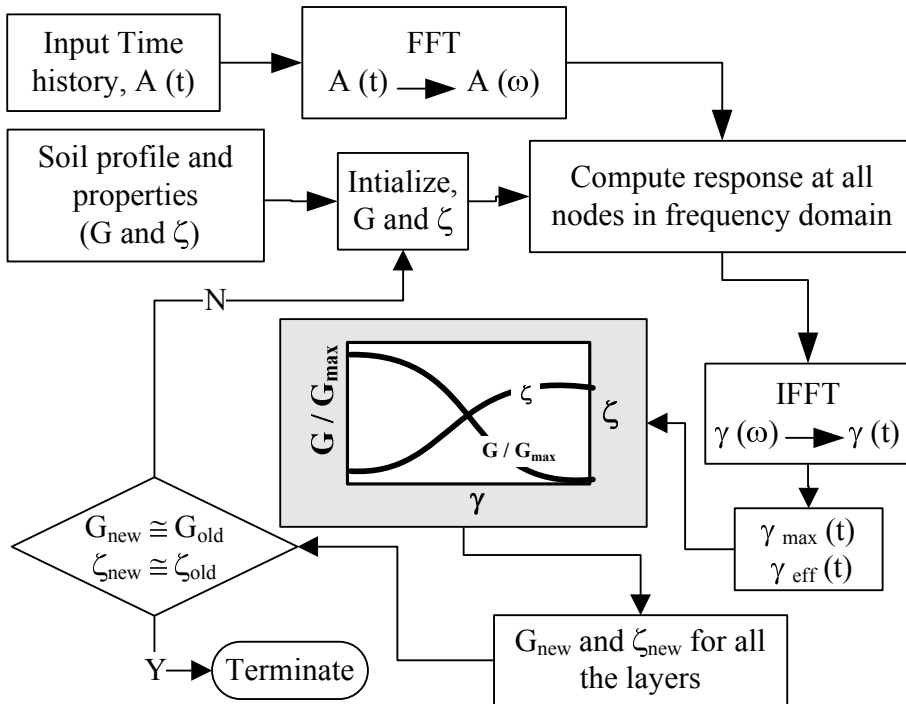
Figure 2.10: Flowchart for equivalent linear method implementation to account for strain dependency of shear modulus and damping in seismic response analysis in frequency domain.
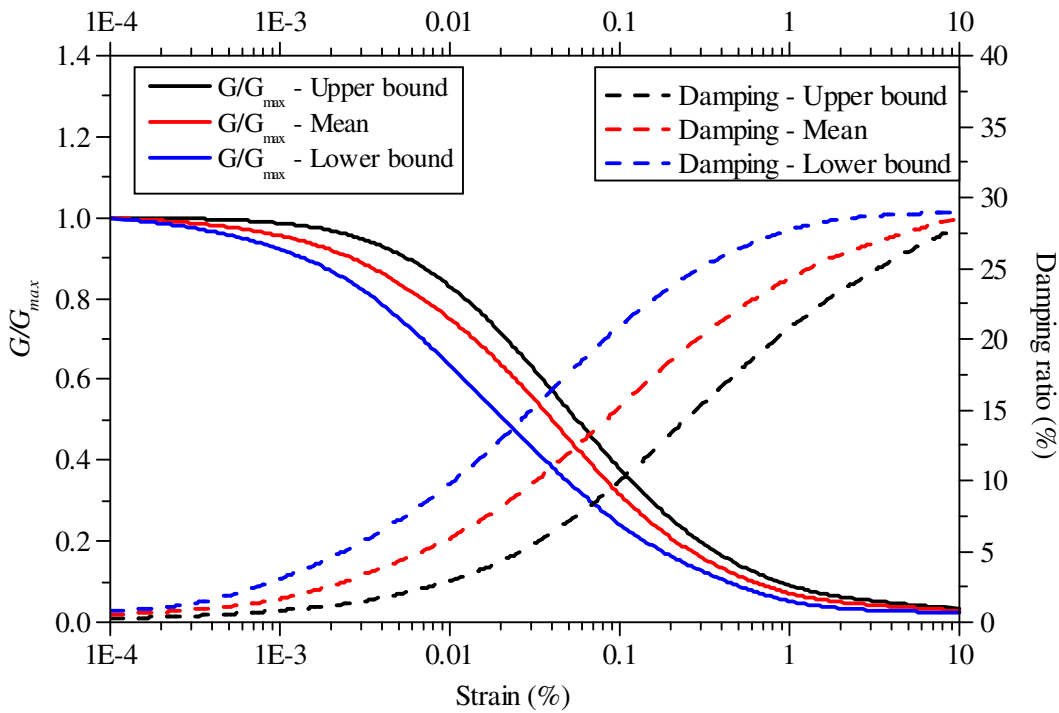
Figure 2.11: Strain dependent shear modulii and damping curves for sand [Seed and Idriss (1970)]

The equivalent linear method of analysis has been found to provide acceptable results for many engineering applications. However, a number of limitations of equivalent linear method have been noted in the literature [Yu et al. (1993), Sugito (1995), Kausel and Assimaki (2002), Yoshida et al. (2002), etc.]. The inherent limitations of this formulation is that, the effective uniform shear strain compatible frequency independent soil properties for each of the layer are assumed to be same for entire duration of shaking i.e., all hysteresis loops are symmetric about origin of the stress-strain plot. Hence permanent plastic deformations are not modeled. Any site response analysis program which employs equivalent linear approach, is capable of total stress analysis only. Hence it does not perform analysis wherein the stiffness of the soil is modified at each iteration to account for generated excess pore water pressures i.e., progressive loss of strength and large displacements resulting as a consequence of excess pore water pressure are neglected. Equivalent linear approach does not consider the maximum shear strength of the soil as one of the parameters. Hence there is a possibility that, the computed shear stresses may exceed the dynamic shear strength of the soil particularly when soft soil deposit is subjected to bedrock input motion of high level acceleration. This aspect can result in over prediction of peak ground acceleration, particularly the high frequency components.

In spite of these limitations, numerous validation studies have demonstrated the accuracy of the one dimensional equivalent linear method to model the dynamic response of various soil profiles for which ground surface and representative rock input motions are available [Seed et al. (1994); Dobry et al. (1994)].

2.7.2   Nonlinear method

The seismic site response analysis using nonlinear models is accomplished in time domain using explicit or implicit direct integration of equation of motion at desirable time steps. Usually, if the methods track the exact form of stress-strain relationship, then they are referred to as nonlinear methods. A variety of nonlinear soil models are used, they have been primarily developed from laboratory test results. They range from relatively simple cyclic stress-strain relationships such as Ramberg-Osgood model [Streeter et al. (1974)], elasto-plastic model [Richart (1975)], Iwan-type model

[Joyner and Chen (1975); Taylor and Larkin (1978); Bardet and Tobita (2001)], the hyperbolic model [Hardin and Drnevich (1972b)], Martin-Devidenkov model [Martin and Seed (1978, 1982)] etc. to advanced constitutive models incorporating yield surfaces, hardening laws, and flow rules. Critical assessment of these models may be found in Finn (1988).

Much attention has been given to plasticity theory for development of constitutive models of soil response to cyclic loading. Elastic-plastic models of soil behaviour under cyclic loading based on multi-yield or boundary surface kinematic hardening plasticity theory are accepted as suitable means of obtaining plastic modulus progressively. Pande and Zienkiewicz (1982) give general description of the developments made in elastic-plastic constitutive modeling. Available elastic-plastic constitutive models are complex and incorporate many calibrating parameters which are impossible to directly measure in field or laboratory. Nonlinear methods can be formulated in terms of effective stresses to allow modeling of the generation and dissipation of excess pore pressure during and after earthquake shaking. In case of nonlinear effective stress models coupled equations are used to treat two phase soil system (soil and water phases). Studies on validation of the elastic-plastic models suggest that the accuracy of predicted response is strongly path dependent [Finn (1999)]. Hence use of data from static tests for calibrating the elastic-plastic model parameters may not be adequate for reliable seismic response analysis i.e., these parameters must be evolved from appropriate cyclic shear tests. As it is very difficult to obtain undisturbed samples of loose sand in the field, parameters evaluated from laboratory tests on these samples are unreliable. Hence it is difficult to characterize the volume change characteristics which controls pore-water pressure development in saturated loose sands.

Nonlinear models of cyclic behaviour essentially consist of a backbone curve and rules that describe unloading and reloading behavior, pore-pressure generation, and shear modulus degradation. Modulus reduction curves coupled with the small strain modulus (G_{max}) can be used to construct backbone curves. Unload-reload rules are usually simulated using Masing's rule [Hardin and Drnevich (1972b)]. This rule is

empirically devised in the sense it is based on geometrical manipulation of stress-strain plot by translation of origin and expansion of vertical and horizontal axes to model the unloading and reloading curves, starting from every reversal point of a hysteresis loop.

Above mentioned nonlinear models have certain limitations and advantages in describing the response of soils to the cyclic loads produced due to earthquakes. When the advantages provided by the fully nonlinear soil response programs is weighed against the cost of laboratory testing programs required to obtain modeling parameters of the constitutive relation, the conclusion is not encouraging to use these methods for practice. In their review study pertaining to computer programs for seismic site response analysis, Dickenson et al. (1998) noted that, one dimensional nonlinear analysis program DESRA-2C [Lee and Finn (1991)] is capable of conducting effective stress analysis with redistribution and dissipation of pore water pressure, but the constitutive relationships utilized in DESRA-2C require 18 material constants for each soil layer. Similarly, another popular program SUMDES [Arulanandan et al. (2000)] which incorporates plasticity model based on critical state soil mechanics requires as many as twenty soil parameters for each layer. Hence it becomes very difficult and expensive to scrutiny the performance of these sophisticated models through parametric studies, which is an essential exercise to be performed before using it for practical field problems. With the advent of significant development in laboratory testing facilities, sophisticated constitutive relationships can be developed merely by curve fitting process as mentioned by Ishihara (1996), *"……there is no nonlinear model of any kind established on a sound physical basis"*.

In the recent years, researchers are strongly advocating nonlinear method of analysis for predicting seismic site response. Their concern basically originated from observed laboratory test data which consistently show that stress-strain relationship of soils is nonlinear and hysteretic. The nonlinear soil response during strong earthquakes is also observed from field data [Beresnev and Wen (1996)]. The characteristic of the nonlinearity of site effects is to cause the difference in the amplification factor between rock and soil site to decrease as the excitation strength increases. However, the question of how far laboratory studies reflect the field behaviour remains to be

answered. Main reason for this is attributed to sample disturbance and stress relief, which are inevitable to some degree when sampler is inserted into the ground and sample is extracted from the sampler.

2.8   OVERVIEW OF COMPUTER PROGRAMS FOR SITE RESPONSE ANALYSIS

Circumstances under which geotechnical engineers have to work particularly, in the field of soil dynamics, are changing rapidly since last five decades. This is primarily because of development in the field of computer technology and duly cost of computing has been reduced drastically. Research that has taken place in understanding the behaviour of soils under cyclic loading, though not without ambiguities and uncertainties, has resulted in the development of several constitutive models. As a consequence of these, considerable number of computer programs has been developed particularly for estimating ground response under seismic loading. Basically what differentiates these programs are, the numerical schemes used in the solution of wave equation, the dimensionality of the problem that can be handled, the constitutive models for stress-strain behaviour and finally type of analysis i.e., total or effective stress analysis. The requirements of the practicing engineers are also changing in terms of simplicity in preparation of input files, intended use of these programs, more reliable outputs for variety of applications, etc.

Varieties of computer programs that can be used to predict the dynamic response of soil deposits are available. The level of sophistication of numerical and analytical methods used in these programs varies considerably. Some of the simple programs require just strain dependent modulus and damping curves whereas more complex programs require multitude of soil parameters for each soil layer in the model [Lade (2005)]. In addition, the computer programs that have been developed for modeling dynamic soil response rely on various simplifications and assumptions in order to solve equations for wave propagation through soils. The variety of analysis procedures for dynamic soil response ranges from relatively simple linear-elastic total stress soil models to sophisticate and fully nonlinear effective stress techniques.

It is more than four decades since the first computer program SHAKE [Schnabel et al. (1972)] was published and is sustaining its popularity even today in some or the other form. This computer program uses theory of multiple reflections of waves with equivalent-linear modeling of soil behaviour to compute the response of a one-dimensional, horizontally layered visco-elastic system subjected to vertically propagating shear waves. Exact continuum solution to the wave equation is adopted with Fast Fourier Transform (FFT) algorithm to transform the transient motions of earthquake into harmonic waves. The success of SHAKE in explaining the response of horizontal layered ground during earthquakes led to the computer programs QUAD-4 [Idriss et al. (1973)], LUSH [Lysmer et al. (1974)] and FLUSH [Lysmer et al. (1975)] which are generalized extensions of one dimensional equivalent linear model to two and three dimensions.

In the recent past several computer programs similar to SHAKE are available such as EERA [Bardet et al. (2000)], WESHAKE [US Army Corps of Engineers], ProShake [EduPro Civil Systems, Inc.] etc. Essentially all these programs enhance the computing features particularly with respect to input and output of the program otherwise the technical qualifications are same as SHAKE. Equivalent linear approach with multiple reflection theory is coded for site response analysis considering frequency effects in DYNEQ [Yoshida et al. (2002)] details of which are discussed in chapter six. Silva and Lee (1987) and Schneider et al. (1993) developed an alternative solution procedure in which, control motions are represented with power spectral density functions instead of time histories. The bedrock power spectrum is propagated through a one-dimensional soil profile as explained in Silva (1976) and probabilistic estimates of peak time-domain values of shear strain or acceleration from the power spectrum is obtained using random vibration theory. The computer program RASCAL [Silva and Lee (1987)] is developed using this procedure such that the error resulting from transformation of time domain to frequency domain and vice versa as opted in SHAKE is eliminated. Kottke and Rathje (2008) developed the computer program STRATA to compute seismic response of one dimensional soil deposit using equivalent linear approach similar to SHAKE. In addition, STRATA

has an option to carry out analysis based on random vibration theory (RVT) in which input motion can be provided in terms of Fourier amplitude spectra.

CHARSOIL [Streeter et al. (1974)] is one of the earliest computer programs which implemented the truly nonlinear approach for evaluation of ground motion. Ramberg-Osgood representation of the stress-strain behaviour of soil is incorporated into the equation of motion and solved the equations by method of characteristics [Papadakis et al. (1974); Streeter et al. (1998); Douglas et al. (2003)]. Freeware NERA [Bardet and Tobita (2001)] is the code available for nonlinear seismic response analysis of layered ground. This program is based on finite difference approach for solution of equation motion and utilizes Iwan – Mroz model [Joyner and Chen (1975)] to represent soil behaviour. DESRA-2 [Lee and Finn (1978)] and its later version DESRA-2C [Lee and Finn (1991)] is the computer program developed for nonlinear ground response analysis including effective stress formulation. This program is developed based on lumped mass MDOF system idealization of the soil deposit. The equation motion is integrated directly using Newmark-β algorithm [Bathe and Wilson (1987)]. The stress-strain behaviour of the soil is represented by the hyperbolic skeleton curve and Masing criterion is used to define loading and unloading behaviour. Procedure for modeling nonlinear cyclic behavior of soil, effective stress formulation and their implementation in ground response analysis is detailed in Ishihara and Towhata (1982). Summary about subsequent developments in the generations of computer programs and comparative study with regard to these programs can be found in Liao et al. (2002), Suwal et al. (2014), Bolisetti et al. (2014), etc. Detailed technical evaluation and review about most popularly used site response analysis computer programs with regard to merits and demerits, limitations, along with modus operandi of their usage are given by Kwok et al. (2007), Stewart and Kwok (2008) and Matasovic and Hashash (2012).

An interesting survey report about usage of computer programs in ground response analyses is prepared by Kramer and Paulsen (2004). This survey report is an attempt to access the popularity of site response analysis methods and computer codes used in geotechnical engineering practice. This report clearly indicates that one dimensional equivalent method of analysis is the most popular among practicing engineers and

consultants over the other methods used for ground response analyses. The difficulty in reliable estimation of the calibrating parameters of nonlinear material models and effort involved in obtaining other physical characteristics of the soil required for these methods have made the professionals to abstain from using these techniques in routine site response analysis. Hence computer programs developed using equivalent linear analysis in frequency domain continue to be popular among researchers and practicing engineers for general purpose seismic site characterisation applications such as validation of advanced method of analysis and large scale microzonation studies [e.g., Ansal et al. (2001); Pitilakis (2004); Sitharam and Anbazhagan (2008), Ansal et al. (2010) and others].

2.9   COMPARISON   BETWEEN   EQUIVALENT   LINEAR   AND NONLINEAR METHODS

In the literature, number studies have been conducted to compare the response of the soil deposits using both equivalent linear and truly nonlinear methods. Among them the most important studies reported by Constantopoulos et al. (1973), Joyner and Chen (1975), Finn et al. (1977), Finn (1978), Yu et al. (1993) etc. are frequently cited in the literature for the purpose of comparison. Yu et al. (1993) recognized the existence of specific ranges where nonlinear and linear responses will differ and predicted these ranges from simple qualitative reasoning as well as from quantitative analysis. In the low frequency range difference is hardly noticeable because the wavelength is long; waves are not greatly affected by the subsurface strata. As most of the energy is concentrated in the intermediate frequency range, the attenuation of strong motion by hysteretic damping reduces the amplitude relative to weak motion. Hence they observed that there is a decrease in spectral amplitudes in case of nonlinear method compared to linear analysis. They have concluded that, transition from low frequency to intermediate frequency range occurs well below the spectral corner frequency and also depends on thickness of soil deposit.

Finn et al. (1977) have investigated the validity of the equivalent linear method for determining the effect of stress-strain nonlinearity of soil deposit on its dynamic response by analyzing the response of level site of dry sand deposit of 61 *m* thickness.

Sinusoidal base motion of wide range of frequencies of acceleration amplitude of 0.065g is considered as an input motion. The results are very similar except around frequency of 1 Hz, where equivalent linear method using SHAKE shows a tendency toward higher resonant peak.

Finn et al. (1978) compared the acceleration response spectra (5% damping) of ground motions, for a shallow cohesionless soil deposit of about 15 m thickness, obtained using SHAKE, DESRA and CHARSOIL. The soil profile used for the response analyses is shown in Figure 2.12a. The soil is a uniform deposit of saturated sand with water table being located at a depth of 1.5 m. The distribution of the low strain shear modulus along the depth of the deposit is shown. The input motion at the base of the deposit used was derived from first 10 seconds record of N-S acceleration component of the 1940 El Centro earthquake scaled to 0.1g. Stress-strain curves were set almost identical between the hyperbolic model used in DESRA and the Ramberg-Osgood model used in CHARSOIL which correspond to strain dependent modulus and damping curves employed in the equivalent linear approach of SHAKE. The acceleration response spectra thus computed is compared in Figure 2.12c. All the methods show strong response around a period of 0.5 sec, but SHAKE shows much stronger response.

It may be noted that, in case of SHAKE, there is an increase of about 40% in the maximum amplification of the pseudo-acceleration above the values computed by CHARSOIL and DESRA. It should be noted that the predominant period of input motion and the fundamental period of the soil deposit considered for the analysis almost match. This stronger response is also reflected in the magnitudes of computed maximum shear stresses at various depths in the sand deposit as shown in Figure 2.12b.

Several comparative studies have reported this tendency of increased response around resonance in the analysis based on equivalent linear method. If the fundamental period of the site, as determined by the strain compatible elastic stiffness after the final iteration, is close to the predominant period of the input motion then resonance occurs. This tendency is often termed as pseudo-resonance because it is primarily the

function of the method adopted i.e., equivalent linear analysis in which analysis is carried out with constant set of soil properties throughout the duration of motion. Hence there is time for resonant response to buildup. In case of nonlinear approach, as the soil stiffness properties are altered at every time step according to the current state of strain, there is no scope for pseudo-resonance to buildup. The equivalent linear method overestimates the dynamic response quantities due to pseudo-resonance as shown in Figures 2.12.

However Yoshida et al. (2002), while proposing frequency dependent equivalent linear approach, has ruled out pseudo-resonance effect as the cause for overestimated response quantities rather with an altogether different argument which is explained in chapter five of this report. Apart from the problem of pseudo-resonance, it has been observed that the equivalent linear approach underestimates the amplification at high frequencies. This shortcoming of equivalent linear method has been confirmed by many comparative studies involving field data as well as theoretical studies based on nonlinear approaches [Beresnev and Wen (1996); Yu et al. (1993)].

Very recently more rigorous comparative analysis between equivalent linear and truly nonlinear analysis is carried out and reported by Yoshida (2014). In his study, different soil profile configurations from more than 200 sites and about 11 strong motion earthquake data were employed for relative evaluation of site response analysis procedures. The main conclusions drawn in this elaborate comparative study quantitatively confirmed many of the earlier reported limitations of the equivalent linear approach. The response quantities that were used for comparisons include peak values of acceleration (PGA), velocity (PGV) and displacement (PGD) apart from their respective response time histories. Also response spectra and Fourier spectra of surface responses were used for further assessment. Yoshida (2014) finally concluded that the PGA is overestimated on an average by about 41% while PGV and PGD are underestimated by about 6% and 20% respectively by EQL approach compared to nonlinear total stress analysis. However, averages of different spectral quantities obtained using EQL approach satisfactorily agree with that of truly nonlinear time domain analysis.

49
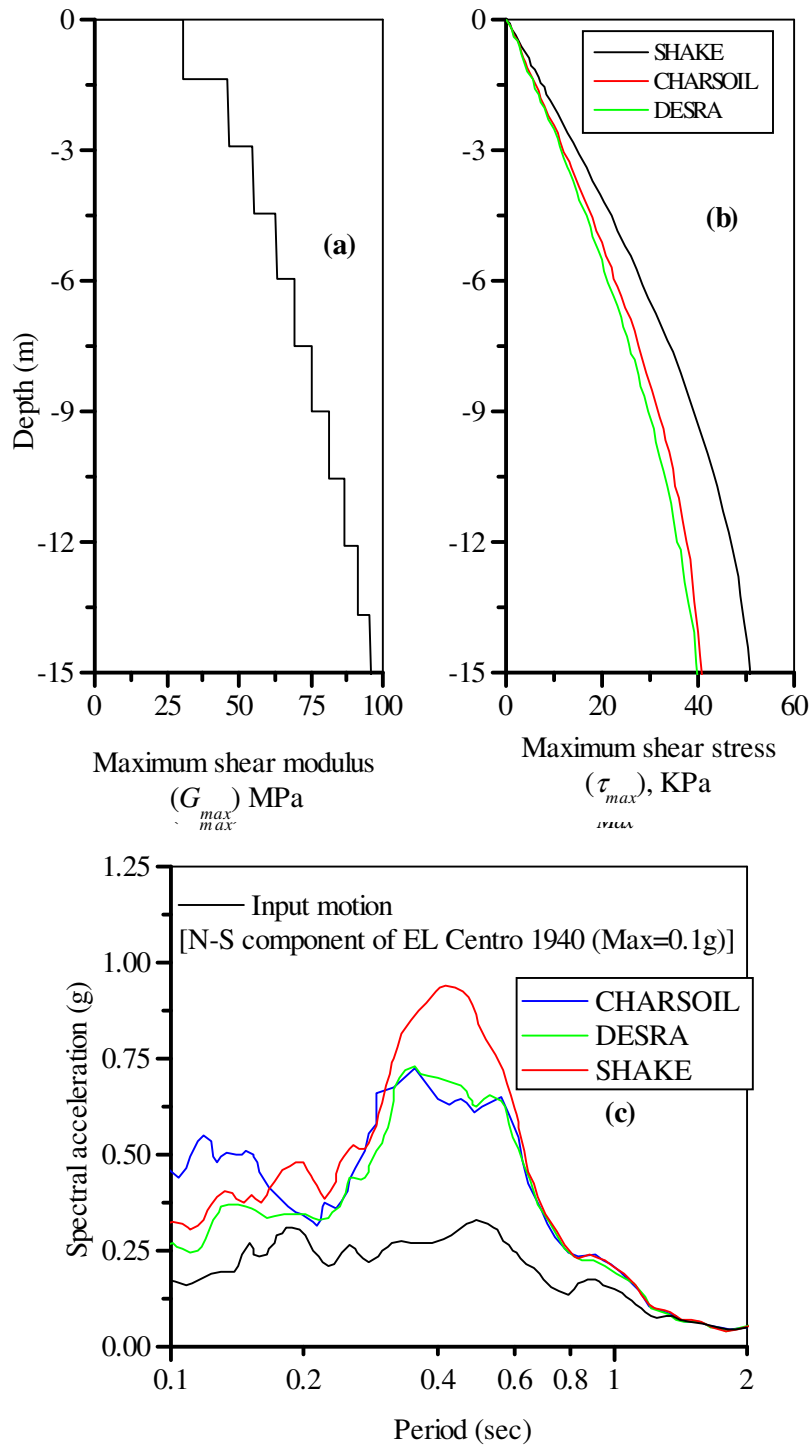
Figure 2.12: Comparison between responses computed using equivalent linear and nonlinear analysis [Finn et al. (1978)]. (a) Shear modulus profile of the soil deposit used in comparative study (b) Maximum shear stress variation along the depth computed using total stress analyses of SHAKE, DESRA and CHARSOIL (c) Acceleration response spectra computed using total stress analyses of SHAKE, DESRA and CHARSOIL

50

2.10 COMPARATIVE STUDY OF FREQUENCY AND TIME DOMAIN ANALYSIS

In this study an example analysis is carried out to verify the conclusions reported with regard to deficiencies of equivalent linear method of analysis as against nonlinear time domain analysis. For this purpose inhomogeneous and equivalent homogeneous soil deposits shown in Figure 2.6 is considered here again.

2.10.1 Input motions

In order to study the influence of frequency characteristics input acceleration time history on the computed response, two accelerograms with distinctly different frequency characteristics are selected. These accelerograms correspond to recorded data of Loma-Prieta earthquake of 1989 and Northridge earthquake of 1994. Details of these records are shown in Table 2.1 and acceleration time histories are shown in Figure 2.13. The Fourier amplitude spectra and spectral acceleration plot of these two input motions EQ1 and EQ2 are shown in Figure 2.14a and 2.14b respectively. Apart from studying effect of frequency characteristics of input motion, to study effect of intensity of shaking on the predicted response, the EQ1 and EQ2 are scaled to $0.1g$ and $0.4g$ respectively. Form these figures it is evident that the input motion EQ1 has energy concentrated over wide range of frequencies compared to that of input motion EQ2. On the other hand, significant duration of intensive shaking in EQ2 is comparatively larger than that in EQ1.

Table 2.1: Details of the input motions used for the comparative analyses

Eq. ID	Event	Station (Code)	Maximum acceleration	Predominant period[*] (s)	Significant duration*(s)
EQ1	Loma-Prieta (1989)	Gilroy #1– Gavilan College (CSMIP 47006)	$0.357g$	0.40	5.00
EQ2	Northridge (1994)	Lake Hughes #12A (CSMIP 24607)	$0.257g$	0.22	9.80
EQ3	Kobe (1995)	Port Island (PI) array recorded at the depth -83m	0.665	0.36	8.01
* - Ground motion parameters are obtained from SeismoSignal (Ver. 4.0)					
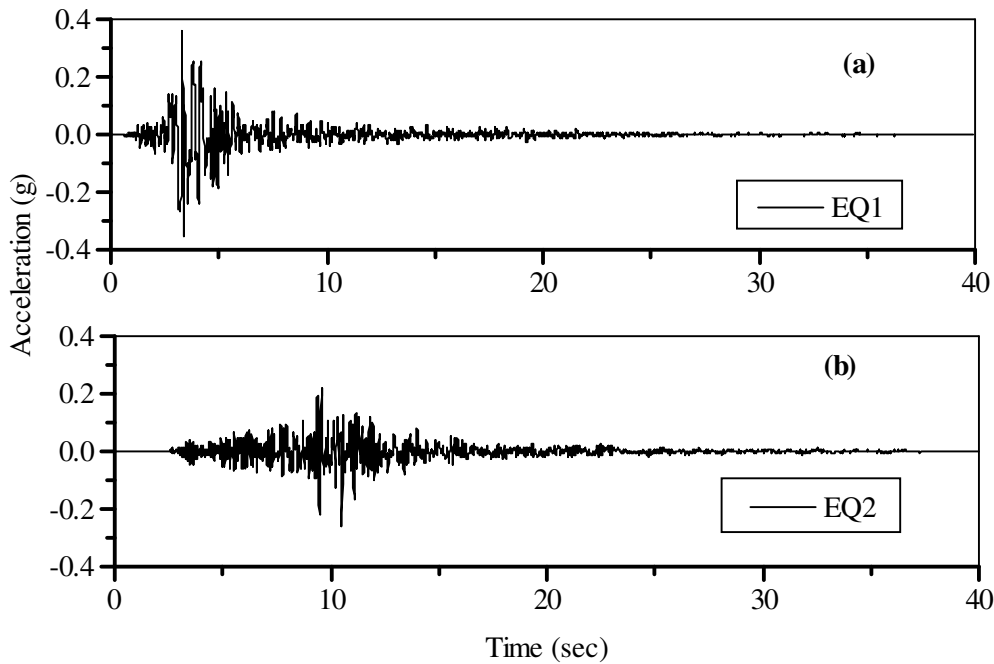
Figure 2.13: Input ground motions used for the analysis (a) EQ1 and (b) EQ2
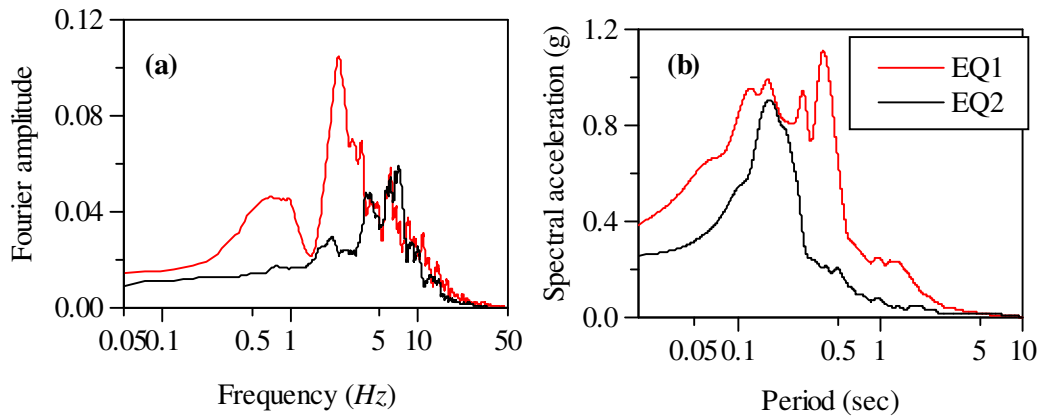
Figure 2.14: Spectral characteristics of input ground motions EQ1 and EQ2 Smoothened Fourier spectra (b) Acceleration response spectra (Damping = 5%)

Equivalent linear analysis is carried out using EERA program and for nonlinear analysis in time domain DEEPSOIL is employed. DEEPSOIL has option for both equivalent linear analysis and time domain nonlinear analysis. Hence, for the sake of convenience, in this study, for some of the analyses DEEPSOIL is used even for equivalent linear analysis. For equivalent linear analysis the shear strain dependent modulus and damping properties is modeled using the mean curves proposed for sand by Seed and Idriss (1970). These curves are shown in Figure 2.11. The comparative study is carried out only for the case of input motion specified at the base of the deposit overlying rigid bedrock.

2.10.2 Linear analysis

In order to assess the efficiency of multiple reflection theory of waves implemented in frequency domain analysis against time domain analysis, linear analysis is carried out keeping the shear modulus and damping constant. The constant damping ratio used in this analysis is 2.5% and unit weight of the soil is taken to be 18.50 kN/m^3. Linear analysis in frequency domain is carried out using EERA code and for time domain analysis DEEPSOIL soil is employed. The analysis is performed for homogeneous deposit having constant shear wave velocity of 200 m/sec. As explained earlier, the 50m thick homogeneous deposit is discretised into 25 uniform layers such that fundamental frequency of these individual layers is set to 25 Hz. For the purpose of comparing linear frequency and time domain results, the results from the linear analyses are presented in terms of variation in computed peak acceleration along the depth, acceleration time history response at the surface of the deposit and response spectra of the surface acceleration response. However, the amplification result is already presented in Figure 2.7 for the rigid bedrock case which clearly depicts the modal frequencies of the deposit.
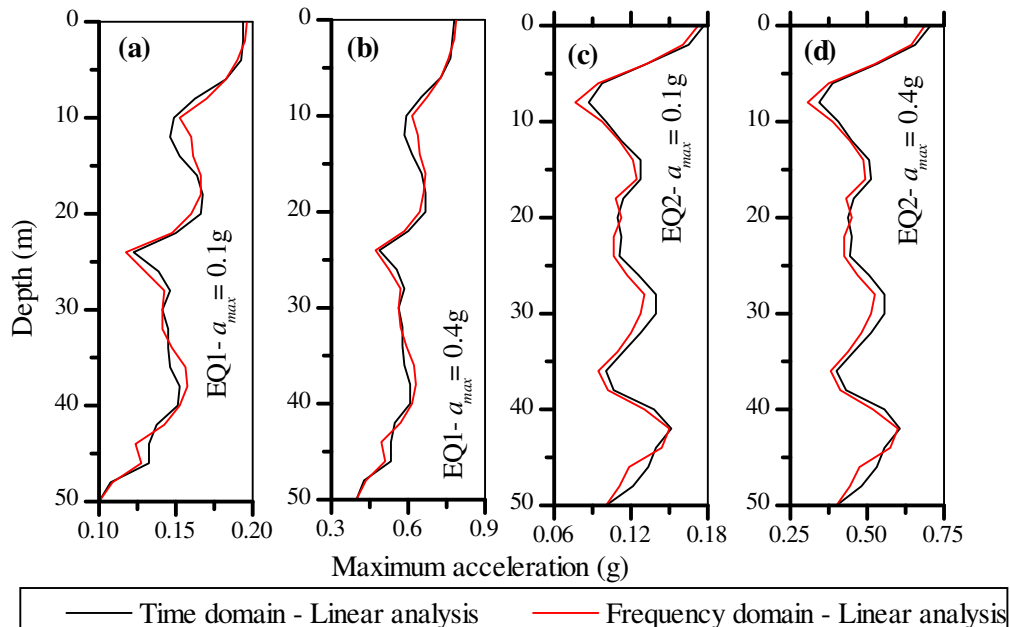
Figure 2.15: Comparison of maximum acceleration profile along the depth computed from frequency and time domain analysis. (a) Input motion EQ1 (Scaled to a_{max}=0.1g); (b) Input motion EQ1 (Scaled to a_{max}=0.4g); (c) Input motion EQ2 (Scaled to a_{max}=0.1g); (d) Input motion EQ2 (Scaled to a_{max} = 0.4g)

The maximum acceleration profile obtained from both, frequency domain and time domain analyses, are presented in Figure 2.15. The comparisons are shown for the cases of EQ1 and EQ2 input motions scaled to 0.1g and 0.4g respectively in Figures 2.15 (a), (b), (c) and (d) respectively. The maximum accelerations computed along the depth from these two analyses for all the cases considered are in good agreement with negligibly small differences.
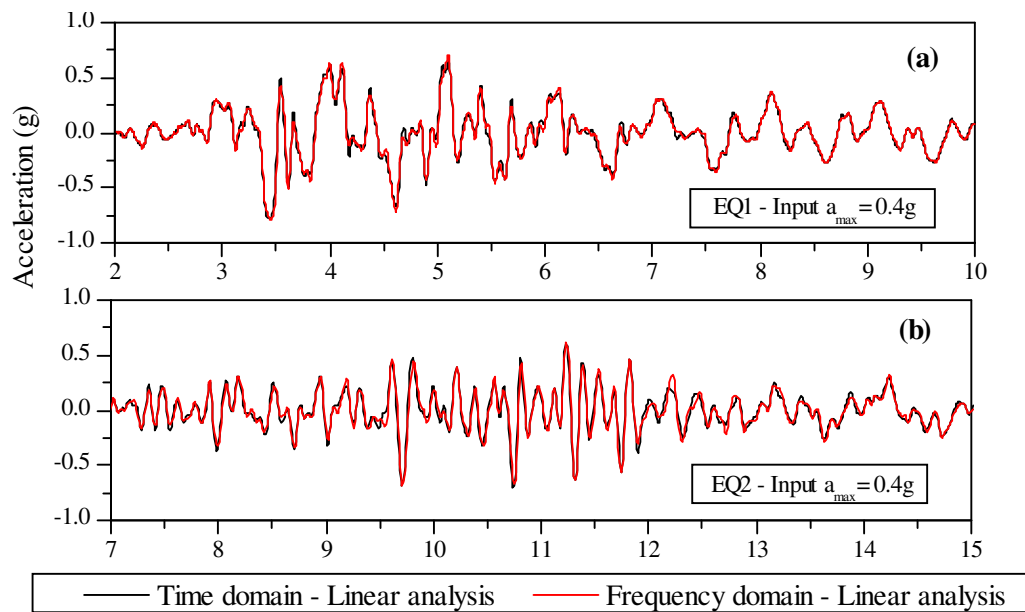
Figure 2.16: Comparison of surface acceleration response from frequency and time domain analysis. (a) Input motion EQ1 (Scaled to a_{max}=0.4g); (b) Input motion EQ2 (Scaled to a_{max}=0.4g)

In Figures 2.16 (a) and (b) acceleration time history responses computed for the cases of EQ1 and EQ2 input motions respectively are presented for strong motion portion time window. The result presented Figure 2.16 corresponds to input motions EQ1 and EQ2 that are scaled to maximum of 0.4g. Figures 2.17 (a), (b), (c) and (d) compare response spectra of estimated surface acceleration time histories under input motion cases EQ1 (a_{max} =0.1g), EQ1 (a_{max} =0.4g), EQ2 (a_{max} =0.1g) and EQ2 (a_{max} = 0.4g) respectively. The time history responses and their response spectra results are satisfactorily comparable in both the cases of analyses under moderate to high intensity input motions with different frequency characteristics. Both these figures confirm the adequacy of frequency domain analysis as compared to time domain analysis for linear site response analysis of layered soil deposits.
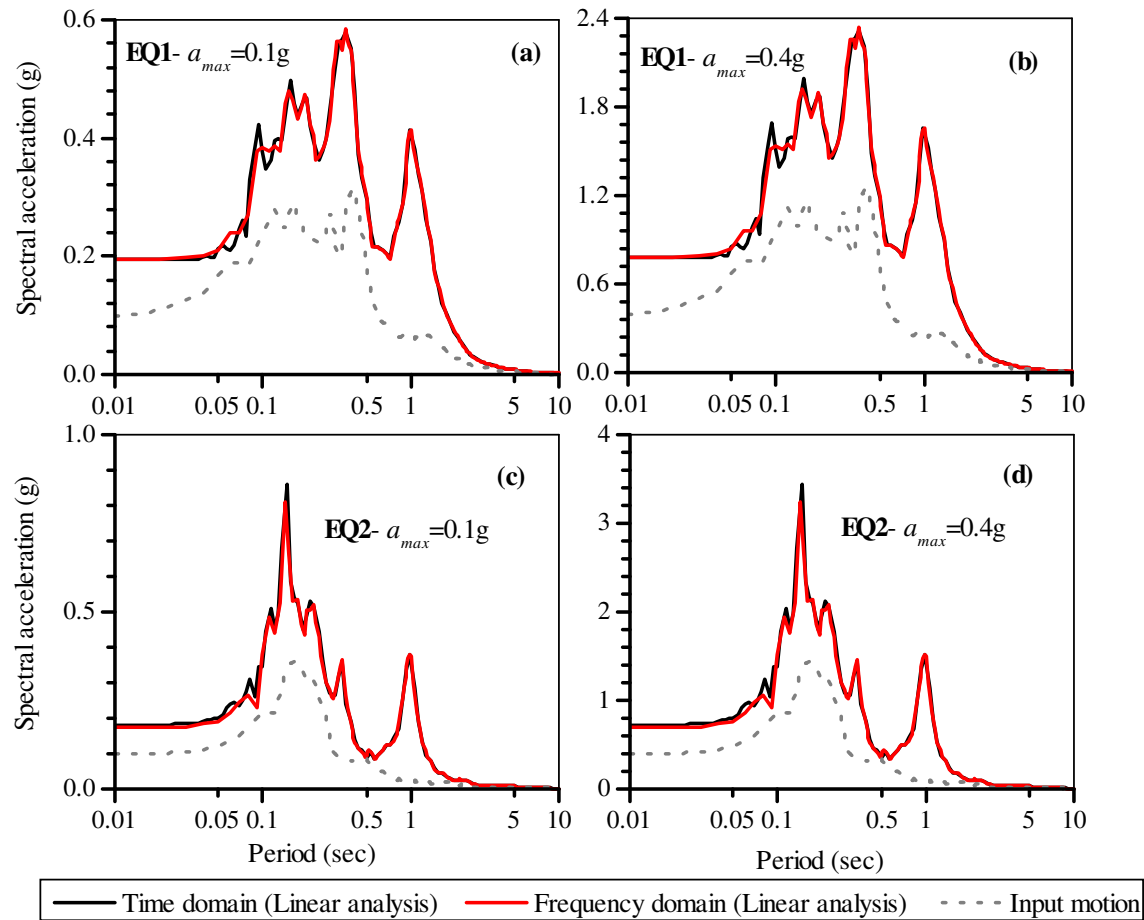
Figure 2.17: Comparison of acceleration response spectrum (5% damping) of surface acceleration records computed from frequency and time domain analysis. (a) Input motion EQ1 (a_{max}=0.1g); (b) Input motion EQ1 (a_{max}=0.4g); (c) Input motion EQ2 (a_{max}=0.1g); (d) Input motion EQ2 (a_{max} = 0.4g).

Nevertheless, it is should be noted that there are small differences in the results of frequency domain and time domain methods of analysis. The reasons for differences, though negligibly small, may be attributed to inherent deficiencies of frequency domain analysis. Primarily, the error associated with transform of input time history signal to sum of harmonic signals of distinct amplitudes and frequencies having phase differences using Fourier transformation.

These harmonic signals with distinct frequencies are used as input motions to get steady response of the deposit. The steady state responses to these harmonic excitations are also of the same frequency as that of input signal with obvious phase difference depending on damping. That is, the computed response is free of transient components of the response associated with other modal frequencies of the deposit. In time domain analysis the computed response includes the contribution of transient response components of other modes [Sarma (1994)] which may contribute to the small difference in computed responses from these methods of analyses.

The predominant periods of the input motions are 0.4 sec and 0.16 sec for EQ1 and EQ2 motions respectively (Table 2.1). The response spectrum of computed surface motion in both the cases clearly demonstrates that, the response of the deposit reaches its peak at predominant periods of the input motions. Apart from this the response spectrum has another distinct peak at the fundamental period of the soil deposit (1.0 sec) in all the cases presented in Figure 2.17. Also over all shape of the response spectrum in case of linear response appears to be scaled up drift of the input motion spectrum except at the fundamental period of the soil deposit.

The ratio of computed surface peak ground acceleration (PGA) to maximum (a_{max}) of EQ1 and EQ2 input motions is found to be about 2 and 1.7 respectively for both the cases of $a_{max} = 0.1g$ and $a_{max} = 0.4g$. That is the soil deposit has comparatively higher amplified response under EQ1 than due to input motion EQ2. However it is interesting to

note that response spectrum for EQ2 input motion has larger peak values than that for EQ1 input motion though computed PGA of the surface response is the other way.

Most important observation of the linear response analysis is that, there are no visible peaks in the response spectrum of the computed response surface motion under EQ1 excitation between predominant period of the input motion and the fundamental period of the soil deposit. Whereas in case of EQ2 excitation there are two small peaks in the response spectrum trends within this range of periods. These intermediate peaks which are distinct characteristics of the spectrum for EQ2 case coincide with the third (1/5 sec) and second (1/3 sec) modal periods of the deposit. This observation holds good for both frequency domain and time domain analyses. In conclusion it may be stated that characteristics of the input motion will greatly influence the response of the deposit particularly at resonant frequencies.

2.10.3 Equivalent linear and nonlinear analysis

Equivalent linear (EQL) approach is used in frequency domain analysis to approximate nonlinear cyclic behavior of soil. On the other hand in time domain analysis it is possible to exactly simulate the experimentally observed dynamic behavior of soil. The direct integration scheme employed to solve uncoupled equation of motion in time domain analysis can track strain dependent modulus degradation and hysteretic damping of the soil response under cyclic loading at every step of time increment. The comparative analysis carried out here aims to reaffirm adverse implications of EQL analysis on the computed results of seismic site response analysis which are reported in the literature to advocate true nonlinear analysis. Here too, the homogeneous and inhomogeneous soil deposit configurations (Figure 2.6) used in the previous section are considered. The strain dependent shear modulus and damping properties of the soil corresponding to average curves of sand proposed by Seed and Idriss (1970), shown in Figure 2.11, is adopted for both EQL and nonlinear analysis. In this comparative study DEEPSOIL program is employed to carry out analyses. The R value equal to 0.5 is used to calculate effective strain in the iterations of equivalent linear analysis.
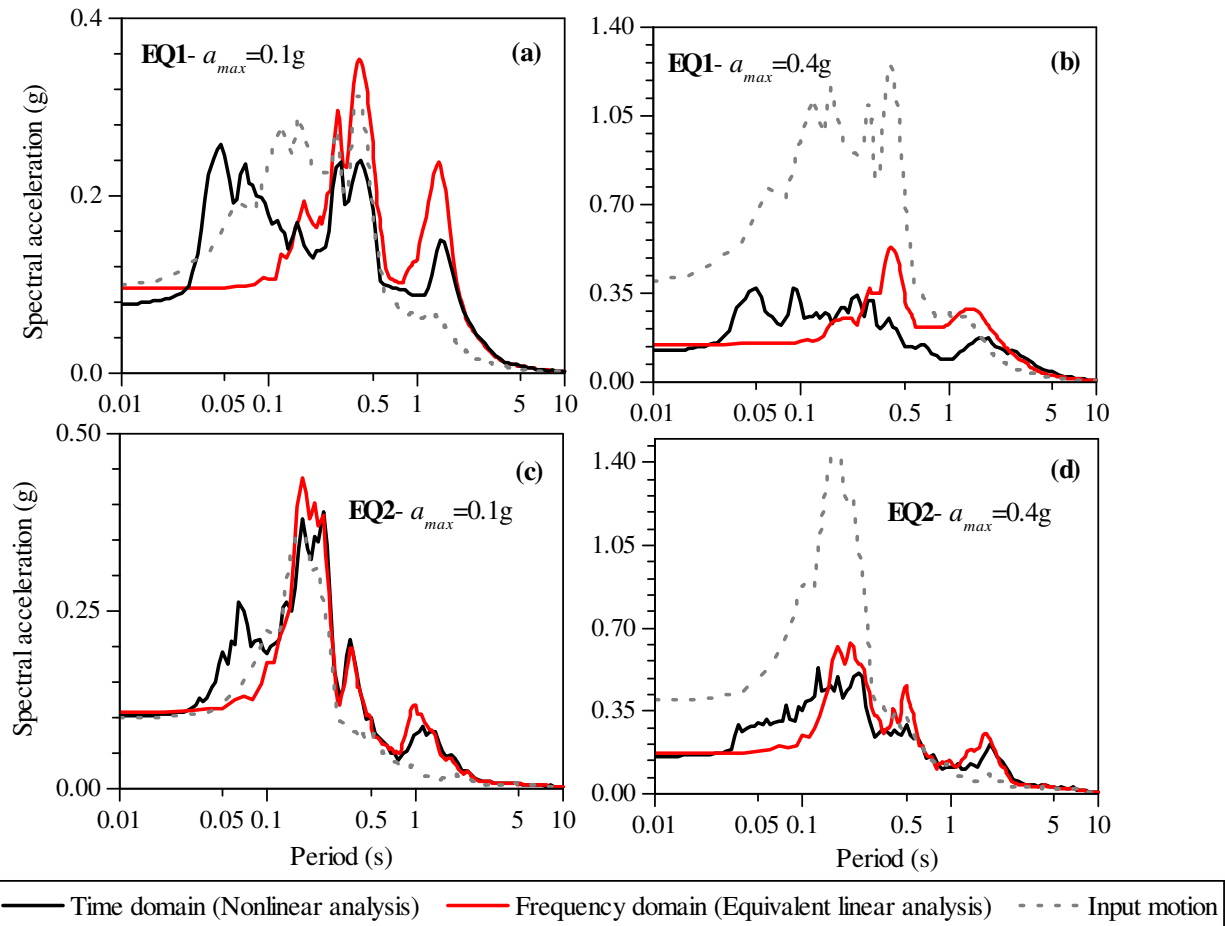
Figure 2.18: Comparison of acceleration response spectrum (5% damping) of surface acceleration records computed using EQL and nonlinear analysis (Homogeneous deposit) (a) Input motion EQ1 (a_{max}=0.1g); (b) Input motion EQ1 (a_{max}=0.4g); (c) Input motion EQ2 (a_{max}=0.1g); (d) Input motion EQ2 (a_{max} = 0.4g).
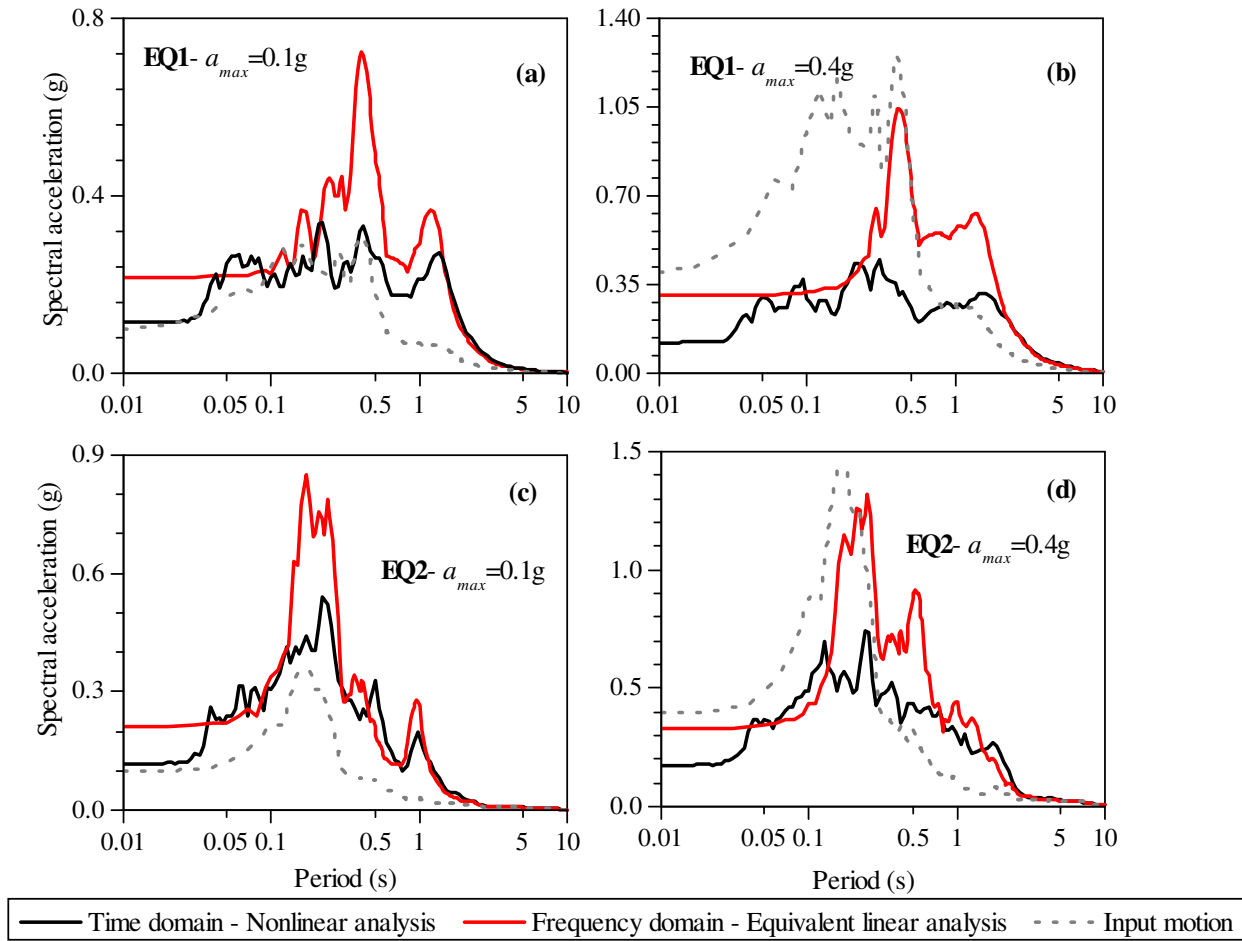
Figure 2.19: Comparison of acceleration response spectrum (5% damping) of surface acceleration records computed using EQL and nonlinear analysis (Inhomogeneous deposit) (a) Input motion EQ1 (a_{max}=0.1g); (b) Input motion EQ1 (a_{max}=0.4g); (c) Input motion EQ2 (a_{max}=0.1g); (d) Input motion EQ2 (a_{max} = 0.4g).
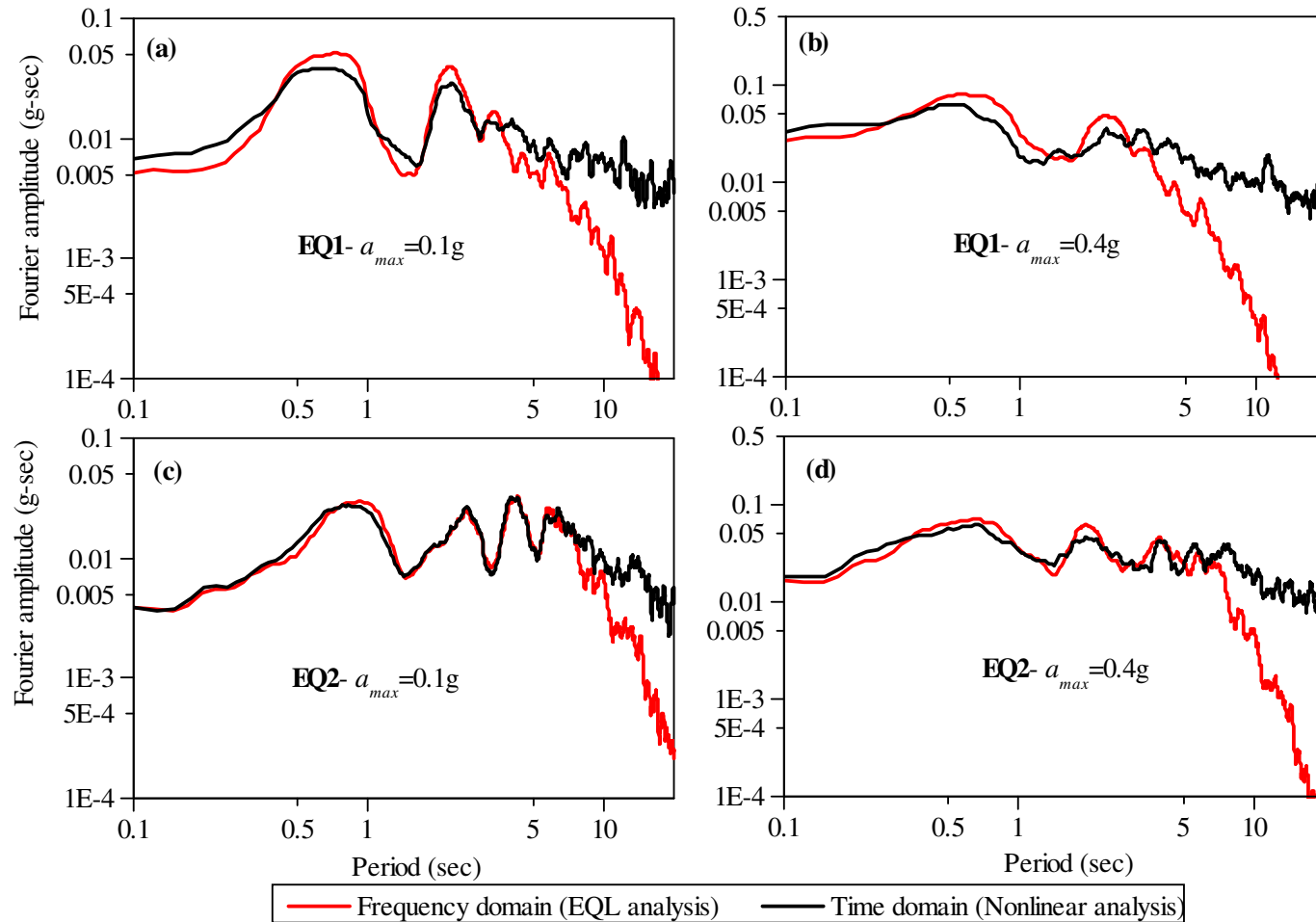
Figure 2.20: Comparison of Fourier spectrum of surface acceleration records computed using EQL and nonlinear analysis (Homogeneous deposit) (a) Input motion EQ1 (a_{max}=0.1g); (b) Input motion EQ1 (a_{max}=0.4g); (c) Input motion EQ2 (a_{max}=0.1g); (d) Input motion EQ2 (a_{max} = 0.4g).
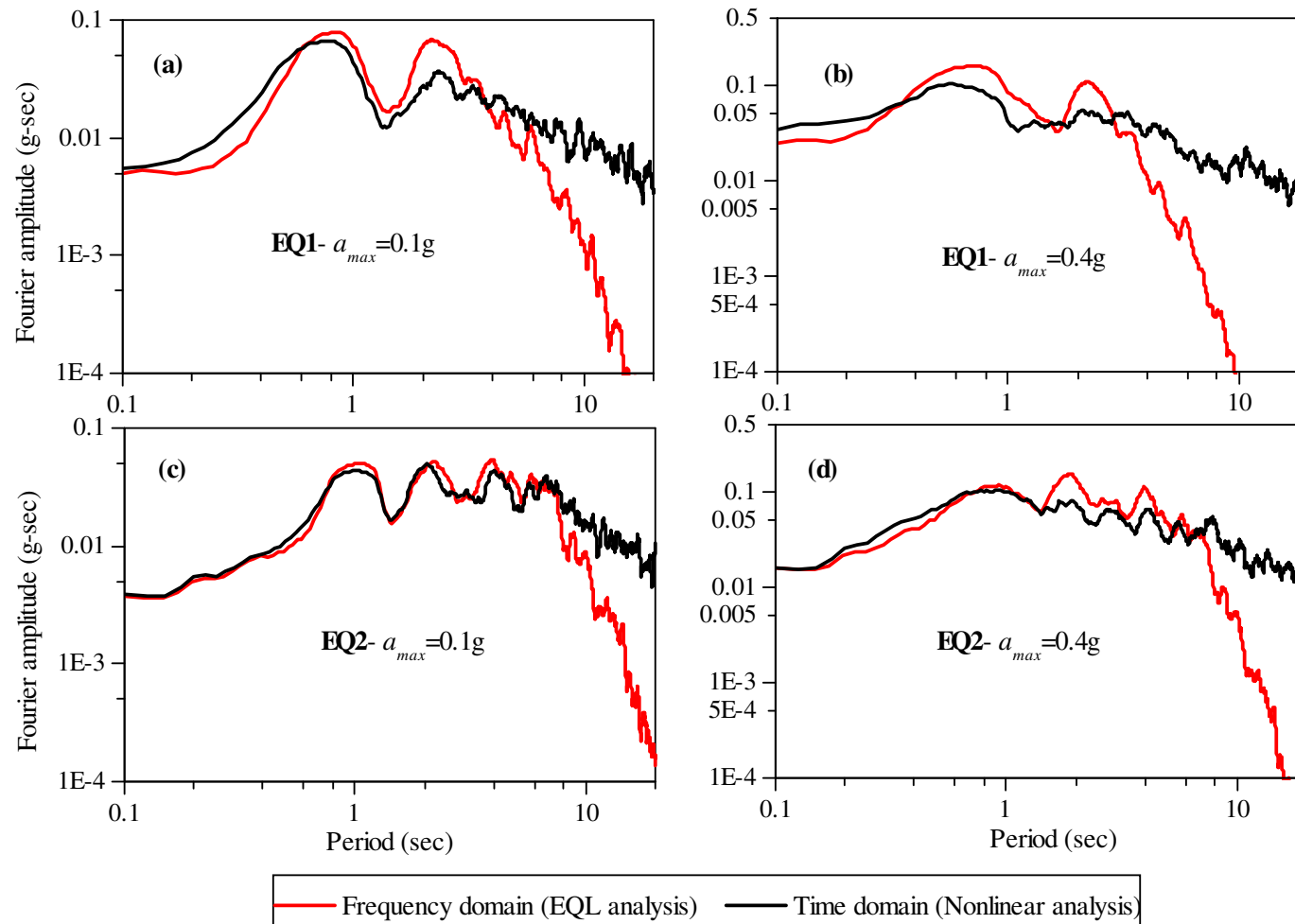
Figure 2.21: Comparison of Fourier spectrum of surface acceleration records computed using EQL and nonlinear analysis (Inhomogeneous deposit) (a) Input motion EQ1 (a_{max}=0.1g); (b) Input motion EQ1 (a_{max}=0.4g); (c) Input motion EQ2 (a_{max}=0.1g); (d) Input motion EQ2 (a_{max} = 0.4g).

2.10.3.1 Homogeneous soil deposit

Figures 2.18a and 2.18b present the comparison of results of surface acceleration response spectra for EQL and nonlinear analysis for EQ1 input motion scaled to $0.1g$ and $0.4g$ respectively. Figures 2.18c and 2.18d present these results for the case of EQ2 input motion scaled to $0.1g$ and $0.4g$ respectively. All the observations made in case of linear analysis of homogeneous deposit with respect to general trends of the response spectrum of computed surface motion are equally valid for EQL and nonlinear analyses. In general, it should be noted that the nonlinearity of the soil has resulted in attenuation of input motion as the waves propagate to surface in all the cases shown in Figure 2.18 except for the case of EQ2 input motion of $a_{max} = 0.1g$. Also, attenuation is observed to be large for $a_{max} = 0.4g$ compared to $a_{max} = 0.1g$, it can be concluded that the nonlinear response will result in decreased peak response with increase in intensity of input motion. The EQL approach has overestimated spectral accelerations at all frequencies including and above fundamental frequency of the soil deposit compared to nonlinear approach. The spectral values of the surface response of the homogeneous deposit under EQ2 excitation having $a_{max} = 0.1g$ obtained using EQL method closely agrees with that of nonlinear method.

Apart from decreased amplitudes, shift in modal periods to higher values is evident in all the cases signifying stiffness degradation due to strain softening behaviour of the deposit. Comparing shift in modal periods for input motions with $a_{max} = 0.1g$ and $a_{max} = 0.4g$ it can be concluded that modal periods get longer as the intensity of input motion increases. At frequencies above predominant frequency of the input motion, EQL method has yielded suppressed response compared to nonlinear approach. As mentioned earlier, this aspect of under prediction of response at higher frequencies by EQL approach has been reported by many studies [e.g., Finn (1977, 1978); Yu et al. (1993) etc.]. Compared to linear analysis, EQL analysis shows up with almost same trend but nonlinear analysis does not have dominant peaks at frequencies other than fundamental frequency.

In all the cases there appears to be a unique frequency range at which the spectral values computed for the response obtained by EQL analysis are lower than that for nonlinear analysis. The frequency at which the response spectrum of EQL analysis crosses response spectrum of nonlinear analysis is close to about 7 *Hz* (at period ≈ 0.14 sec) for all the four cases considered in Figure 2.18. Above this frequency limit the response spectrum becomes horizontal, that represents constant spectral values almost independent of period. This observation leads to the conclusion that the response computed at higher frequencies using EQL analysis is independent of characteristics of the input motion. That is it mainly depends on the mechanical and geometrical properties of the soil deposit and the model used to represent strain dependent behaviour of the soil.

2.10.3.2 Inhomogeneous soil deposit

In Figure 2.19 the comparison between the response spectra of computed surface acceleration response using EQL and nonlinear analyses are presented. The shear wave velocity profile of the soil deposit considered in this analysis is shown in Figure 2.6. The average shear velocity of the deposit is equal to 200 *m/sec* which is equal to shear wave velocity of the homogeneous deposit considered previously. All the four cases presented in Figure 2.19 have higher spectral values when compared to respective response spectra of homogeneous deposit. Obviously this is due to presence of relatively soft layers close to surface of the deposit than that of homogeneous soil deposit. Though higher response is evident, it should be noted that the shape of response spectra have not been altered much in case of inhomogeneous deposit compared to response spectra of the homogeneous deposit. In this case also the response spectra in the almost same short period region has constant trend as in the homogeneous deposit case. However it is interesting to note that the spectral values in the short period range less than about 0.1 *sec* pertaining to EQL analysis is over estimated compared to nonlinear analysis. That is generalized conclusions from some of the earlier studies (for e.g. Figure 2.12) regarding under estimation of spectral values in high frequency range may not be valid for all cases.

To understand this discrepancy in high frequency spectral values for homogeneous and inhomogeneous deposit, Fourier amplitude spectrum of the estimated surface acceleration response using EQL and nonlinear analysis are compared. Figure 2.20 and Figure 2.21 show the smoothened Fourier spectra of the responses obtained for homogeneous and inhomogeneous deposits respectively. Notably, in these figures the EQL analysis shows lower high frequency response than that of nonlinear analysis in a consistent manner for both homogeneous and inhomogeneous soil deposits when compared to nonlinear analysis. The frequency range at which this deviating trend of EQL approach is observed is uniquely consistent for given input motion irrespective of its scaled peak acceleration magnitude of $a_{max} = 0.1g$ and $a_{max} = 0.4g$. However, for EQ1 motion the frequency corresponding to lower EQL response is about 5 Hz, while for EQ2 it is about 10 Hz.

Amplification ratio of the responses between surface and input motions are plotted for homogeneous and inhomogeneous deposit cases in Figure 2.22 and Figure 2.23 respectively. The amplification of surface motion is independent of input motion characteristics in case of linear response. However, equivalent linear analyses results evidently show the effect of shear modulus and damping properties on amplification transfer function.
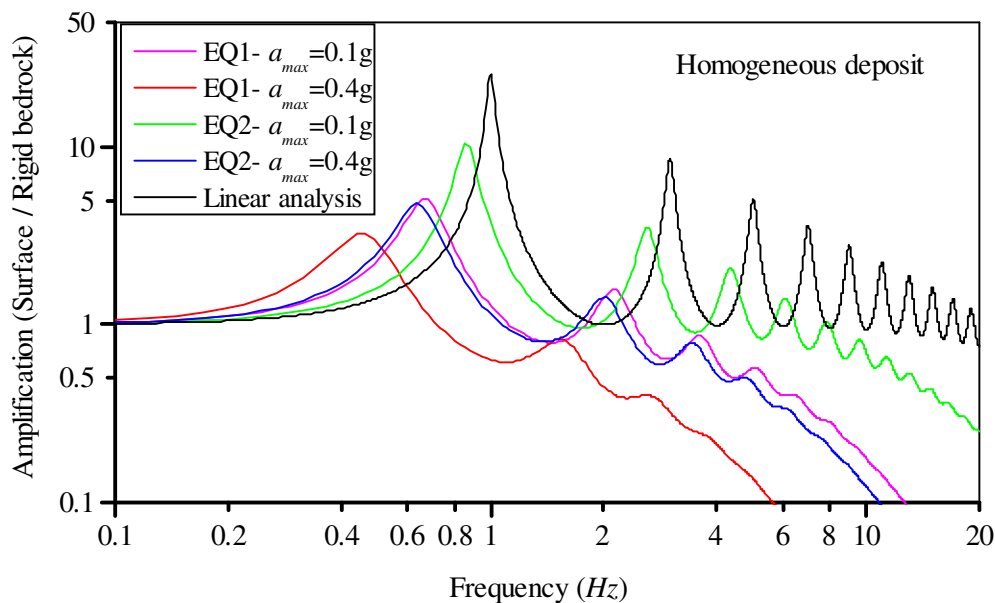
Figure 2.22: Amplification ratio for homogeneous deposit computed for the response obtained using equivalent linear analysis

64
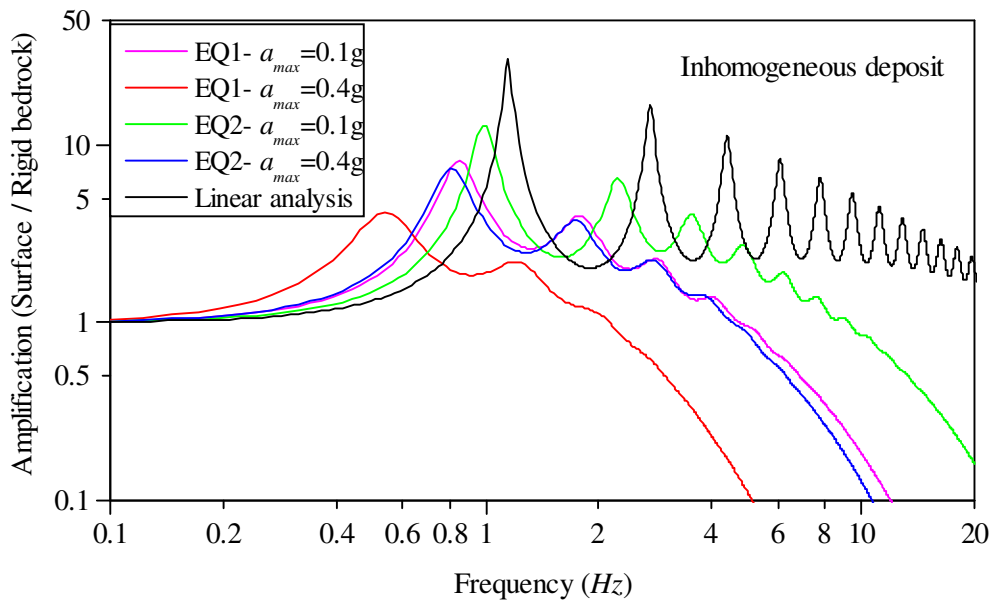
Figure 2.23: Amplification ratio for inhomogeneous deposit computed for the response obtained using equivalent linear analysis

For all the four cases of input motions the amplification of motion at the surface clearly signifies the effect of input motion characteristics. The amplification decreases with increase in intensity of input motion. The amplification ratio in case of EQ2 input motion is significantly higher compared to the case of EQ1. This brings out the effect of frequency characteristics of the input motion on amplification as it was evident in response spectrum representation also. It is also interesting to note that, the amplification of deposit under EQ2 input motion with $a_{max} = 0.4g$ almost follow the amplification under EQ1 with $a_{max} = 0.1g$. Since the strain dependent properties incorporated in EQL analysis are same for both input motion cases, EQ1 must have resulted in stronger strain response in near surface layers compared to EQ2 motion. Shift of peaks to lower frequencies with increased intensity of motion indicate that the modal frequencies of the deposit decrease as input motion is stronger. Also, the high frequency response diminishes with increase in intensity of input motion.

The diminishing high frequency response in EQL analysis in frequency domain compared to nonlinear analysis in time domain can be attributed mainly to use of constant values of damping and shear modulus throughout a particular iteration for all frequencies. High frequency response is associated with small strain magnitude and

strain level associated with low frequency response is significantly high. However, in case EQL analysis constant values of modulus and damping corresponding to effective strain is used; this in turn overestimates low frequency range response and underestimates high frequency response. Also, there are reasons inherent to nonlinear analysis in time domain that can significantly contribute to high frequency response [Sarma (1994); Joyner and Chen (1975)].

2.11 EFFECT OF STRAIN DEPENDENT SHEAR MODULUS AND DAMPING ON SITE RESPONSE

This study is primarily intended to illustrate the effect of plasticity index, one of the many soil properties which are of concern to prepare input data for EQL analysis. The objective of considering the change in plasticity index values is to show the effect of change in shape of shear modulus and damping curves with strain level on the site response. There are several soil models available to simulate strain dependent soil properties, particularly shear modulus and damping. These soil models are typically expressed in terms of strain versus G/G_{max} and ζ curves depending on type of soil (for ex. clay, sand, gravel etc.) and in-situ state of soil (confining pressure, relative density, OCR, age, etc.). Hence making an ideal choice regarding representation of strain dependent soil properties for EQL analysis is important and at the same time a difficult decision one has to make. This parametric study is an attempt to understand the consequential effect of improper representation of strain dependent soil properties on the computed response.

The computed site response using EQL approach significantly depends on shear modulus and damping ratio properties employed in the analysis. In order to comprehend this, as an exemplar study, the effect of plasticity on the response of the soil deposit under seismic excitation is considered. For this purpose, a 60 m deep homogeneous clay deposit is considered. The constant shear wave velocity of the deposit is considered to be 200 *m/s* while its unit weight is assumed to19 *kN/m^3*. The shear wave velocity and unit weight of the bedrock are taken as 1500 *m/s* and 22 *kN/m^3* respectively. The plasticity of the soil deposit is varied with the same values as that of Vucetic and Dobry (1991) curves, shown in Figure 2.24 and Figure 2.25, such

that actual values of shear modulus and damping are taken without interpolation. The equivalent linear analysis is carried out using computer program STRATA [Kottke and Rathje (2008)].
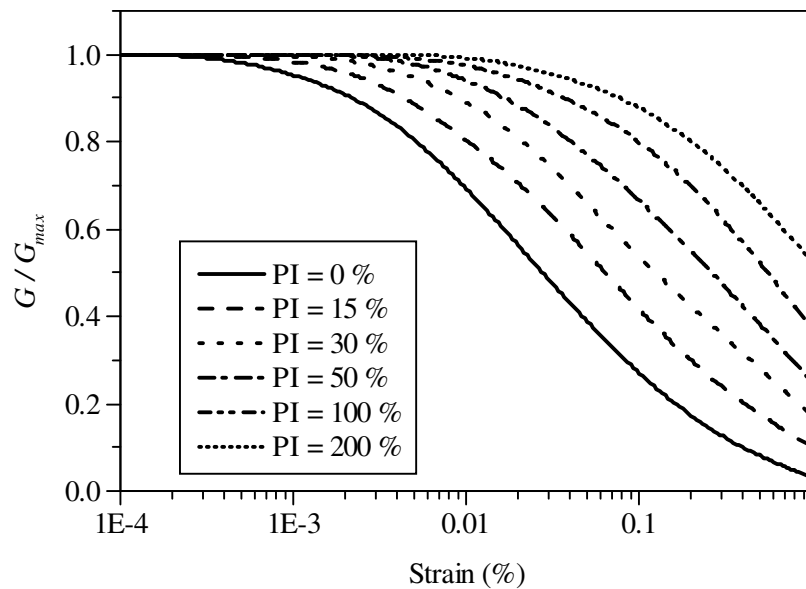
Figure 2.24: Strain dependent G/G_{max} curves [Vucetic and Dobry (1991)]
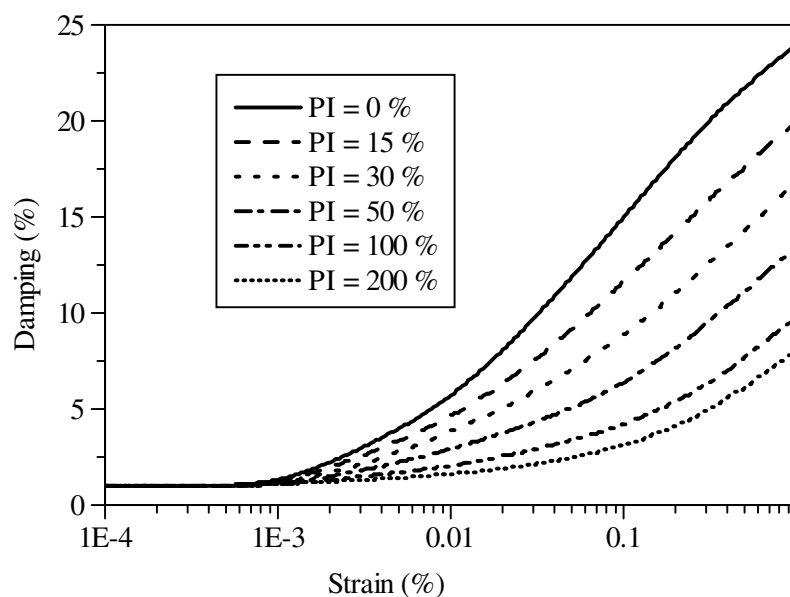
Figure 2.25: Strain dependent Damping curves [Vucetic and Dobry (1991)]

Apart from studying the effect of plasticity index on the response, the other objective of this parametric study is to understand the effect of characteristics of input earthquake motion on the nonlinear response of the soil deposit. It is well established

that the stiffness degradation with respect to induced shear strain is primarily controlled by its magnitude. However, strain level induced under cyclic loading is a function of several other factors apart from intensity of shaking. Influences of some of these additional factors are not yet quantified conclusively. Among these, influence of frequency and number of cycles of excitation are not well understood. In case of seismic excitation wherein frequency and number cycles of loading scenario are very much complex compared to nature of loading usually employed in a laboratory test. Hence there are several studies which made efforts to simulate strain dependent shear modulus and damping properties of soil directly from downhole array records of strong and weak earthquake events in order to verify and/or validate observations made in controlled laboratory tests [Kokusho et. al. (1992), Elgamal et. al. (1995), Zeghal et. al. (1995), Davis and Berrill (1998), etc.]. In the process, possible refinements were proposed to improve the soil constitutive models to simulate stiffness degradation upon cyclic loading [Zhou and Gong (2001); Li and Assimaki (2010); Drosos et al. (2012)]. Nevertheless, directly incorporating these recommendations in EQL method of analysis is impossible because the soil nonlinearity under cyclic loading is approximated by secant modulus corresponding to effective (or average) strain. However, new generation of strain dependent shear modulus and damping curves have been proposed incorporating influence of number of cycles and frequency of loading which can be used conveniently in equivalent linear analysis procedure, for example, Darendeli (2001). The details of such empirical relations particularly of those which are used in this research work to model strain dependent shear modulus degradation and damping ratio are detailed in chapter four of this thesis.

Two earthquake motions are considered as input motions at bedrock level; outcrop motion recorded at Gilroy site during 1989 Loma Prieta earthquake, i.e. the same input motion one (EQ1) used in the earlier analysis (Figure 2.13a) and the other one, designated as EQ3, corresponds to *within* motion accelerogram recorded at the depth of 83.0m of Port Island downhole array during 1995 Kobe earthquake is shown in Figure 2.26. Predominant period, maximum acceleration and significant duration of the EQ3 record are also tabulated in Table 2.1 along with respective details of EQ1.
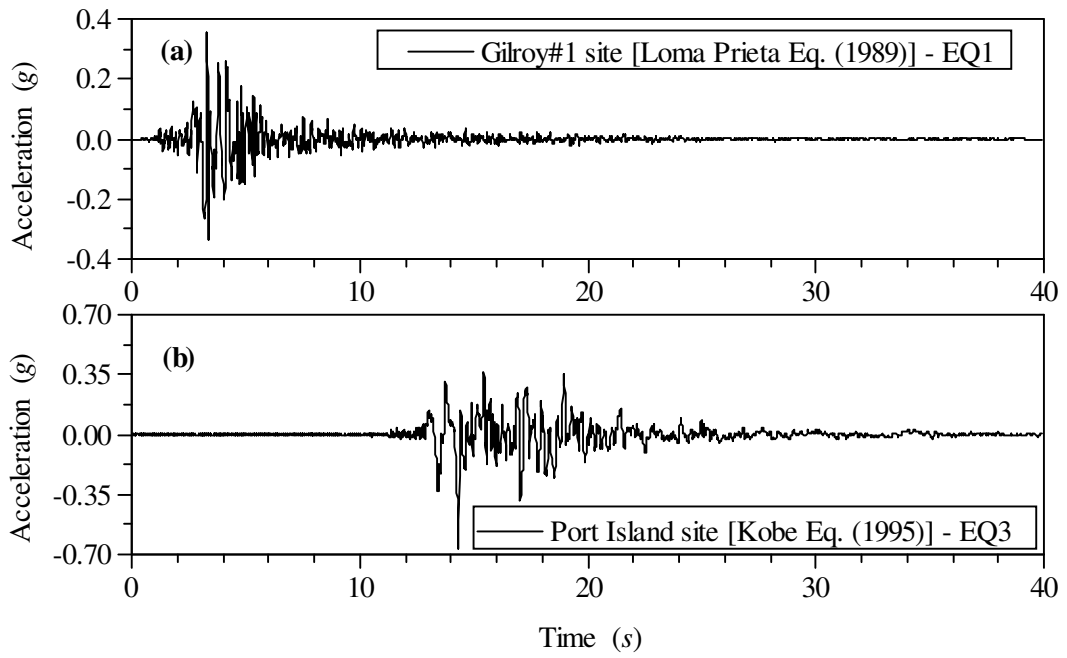
Figure 2.26: Input motions used in the analyses; (a) EQ1; (b) EQ3
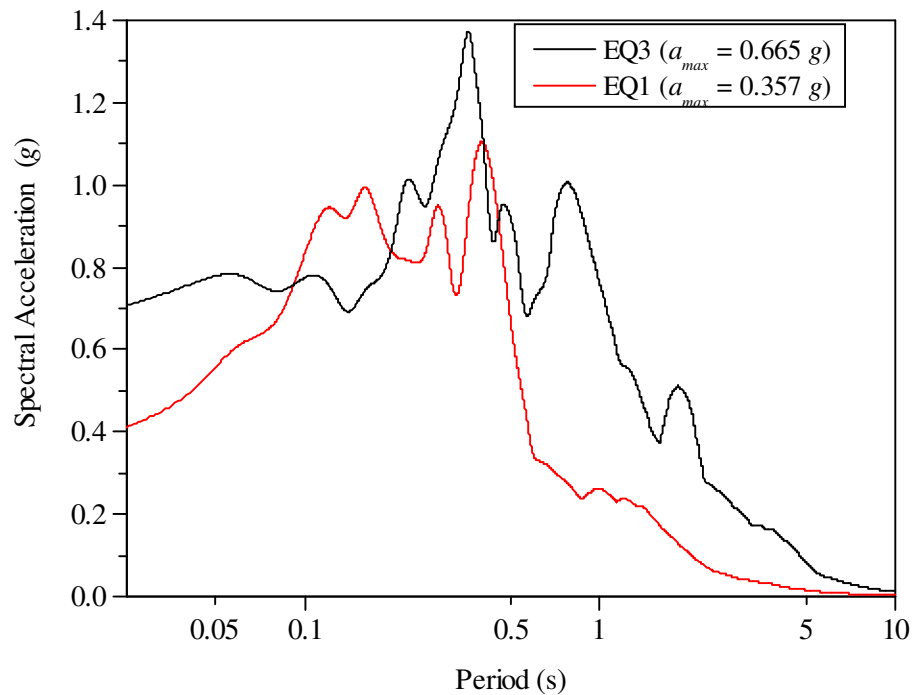
Figure 2.27: Response spectra of the input motions EQ3 and EQ1 used in the analysis; Kobe earthquake record $\left(\text{EQ3 - } a_{max} = 0.665\,g \right)$ and Loma- Prieta earthquake record $\left(\text{EQ1 - } a_{max} = 0.357\,g \right)$.

In order to compare their spectral characteristics, the response spectra of these two motions are shown in Figure 2.27. The two input motions considered for the analysis were recorded in different geological conditions and their characteristics are distinctly different as can be observed from their accelerograms. The peak accelerations recorded in the above mentioned cases are about $0.36g$ and $0.66g$ respectively for Loma Prieta (EQ1) and Kobe (EQ3) earthquakes. The response spectrum presented in Figure 2.27 clearly shows the difference in frequency characteristics of these two earthquakes. The EQ3 motion exhibits high spectral amplitudes in the low frequency range while EQ1 record has relatively large spectral amplitudes in the high frequency ranges. However, the predominant period of these earthquakes motions are relatively very close and is about $0.4s$.

Apart from analyzing the deposit under recorded acceleration levels, analyses are also carried out for the case of input motion corresponding to low level of shaking. For this purpose both the accelerograms were normalized to give same peaks of about 0.007g. This particular parametric analysis may be helpful in capturing the effect of frequency and predominant period of the input earthquake motion. Since intensity of shaking is low, the induced strain level should be moderately low. Hence influence of frequency content and predominant period of the input motion may dominantly influence the building up of strain which in turn can influence shear modulus and damping ratio depending upon the duration of shaking. Significant duration of shaking of EQ1 and EQ3 motions are 5 and 8 seconds respectively and they are markedly different. In order to ascertain effect of level of shaking and plasticity indices of the soil on the computed response, both strong and weak motions are considered as input motions assuming different values of PI for the deposit soil.

Figure 2.28 shows the computed peak acceleration profile for the cases of scaled down input motions with varying plasticity indices of the deposit. For low level of shaking there is always amplification of surface motion irrespective of plasticity index of the deposit. Also in case of low level of shaking there is localized amplification at 36 m depth in case of Loma Prieta input motion for all values of plasticity indices. Overall trend of the computed peak acceleration profiles for the cases of input motions EQ1 and EQ3 are distinctly different.
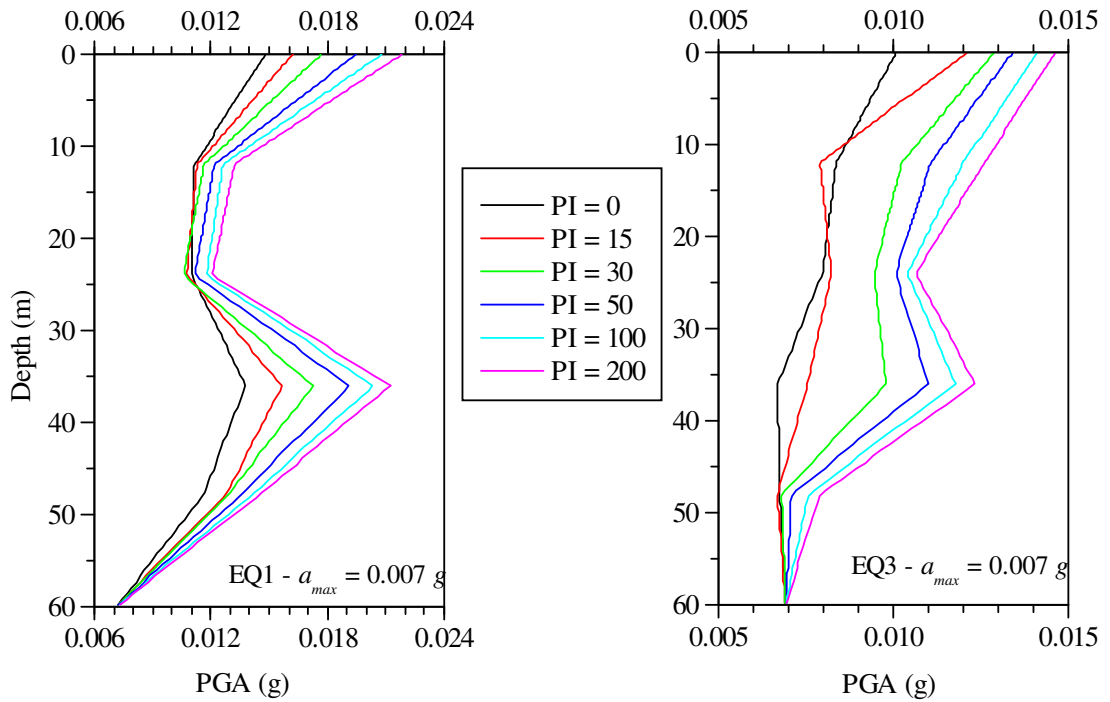
Figure 2.28: Peak acceleration profile computed for input motions EQ1 and EQ3 scaled to $a_{max} = 0.007\,g$ for different plasticity index values
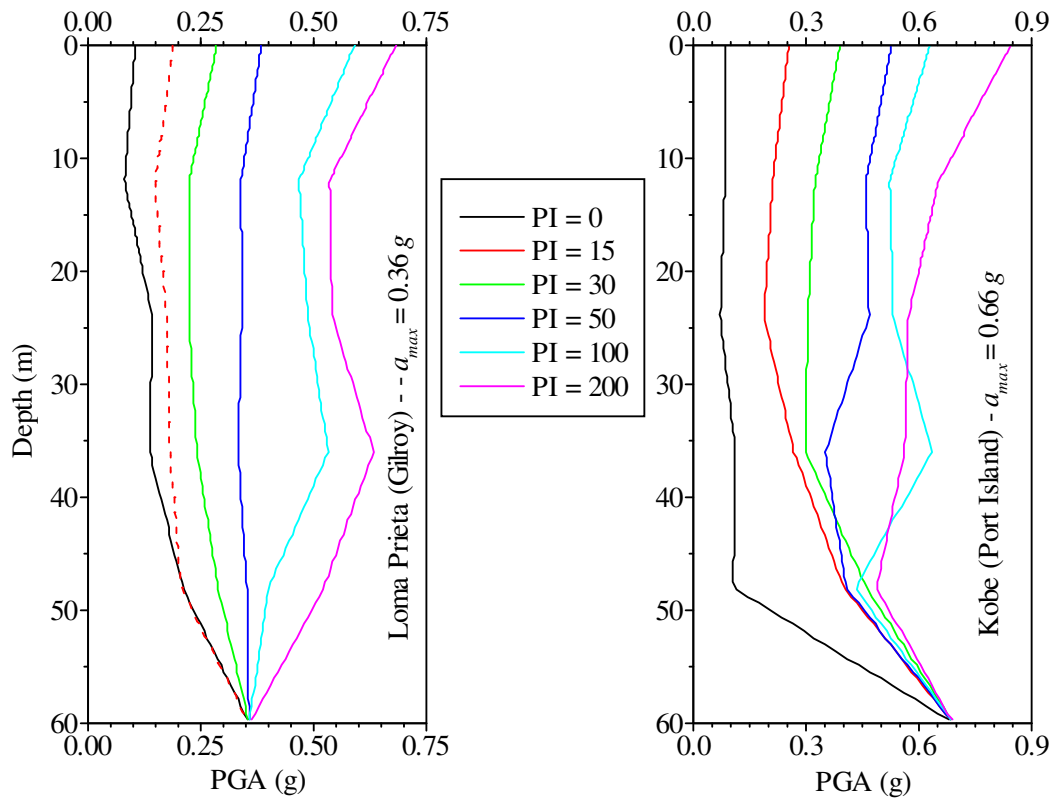
Figure 2.29: Peak acceleration profile due to relatively strong input motions EQ1$\left(a_{max} = 0.36\,g\right)$ and EQ3$\left(a_{max} = 0.66\,g\right)$ for different plasticity index values

For all values of PI, the peak acceleration profile due to EQ1 input motion exhibits almost similar variation along the depth including for the case of PI = 0 which corresponds to cohesionless soil. While for EQ3 input motion the peak acceleration profiles clearly exhibit their dependency on PI value used for the soil. For plasticity index ranging from 0 to 15 %, the amplification at 36 m depth is relatively low in case of Kobe earthquake input motion. This aspect evidently demonstrates that, the frequency characteristics of earthquake input motion and plasticity index of the deposit both have direct influence on the amplification and deamplification of waves at different depths of the deposit.

Figure 2.29 shows computed maximum acceleration profiles under excitation of EQ1 and EQ3 input motions with different maximum levels of acceleration. The maximum acceleration of EQ1 input motion is 0.36g while that of EQ3 is 0.66g. Under the excitation of these higher level of shaking there is significantly more deamplification in peak acceleration response in case of Kobe earthquake (EQ3) compared to Loma Prieta earthquake (EQ1). This tendency vanishes as the plasticity index of the soil increases beyond PI = 50% for the case of EQ1 input motion and this trend of deamplification of input motion at the surface persists for all values plasticity indices used in this analysis with an exception for PI = 200 % in case of EQ3 input motion.

Apart from comparison of maximum accelerations computed at the surface, it is interesting to note that the predicted maximum acceleration response along the depth of the soil deposit is entirely different for the strong input motion compared to that of weak input motion. For PI < 50%, the motion is attenuated at all the depths of the soil deposit. When PI > 50%, maximum accelerations are more than peak ($a_{max} = 0.36g$) of the Loma Prieta (EQ1) input motion throughout the entire depth. But in case of Kobe (EQ3) input motion the waves are attenuated at all depths for all cases of plasticity indices except for the case of PI equal to 200 %. The ratio of peak values of surface to bedrock acceleration is about 2.5 and 1.2 for Loma Prieta and Kobe input motions respectively for the case of PI = 200%.

72
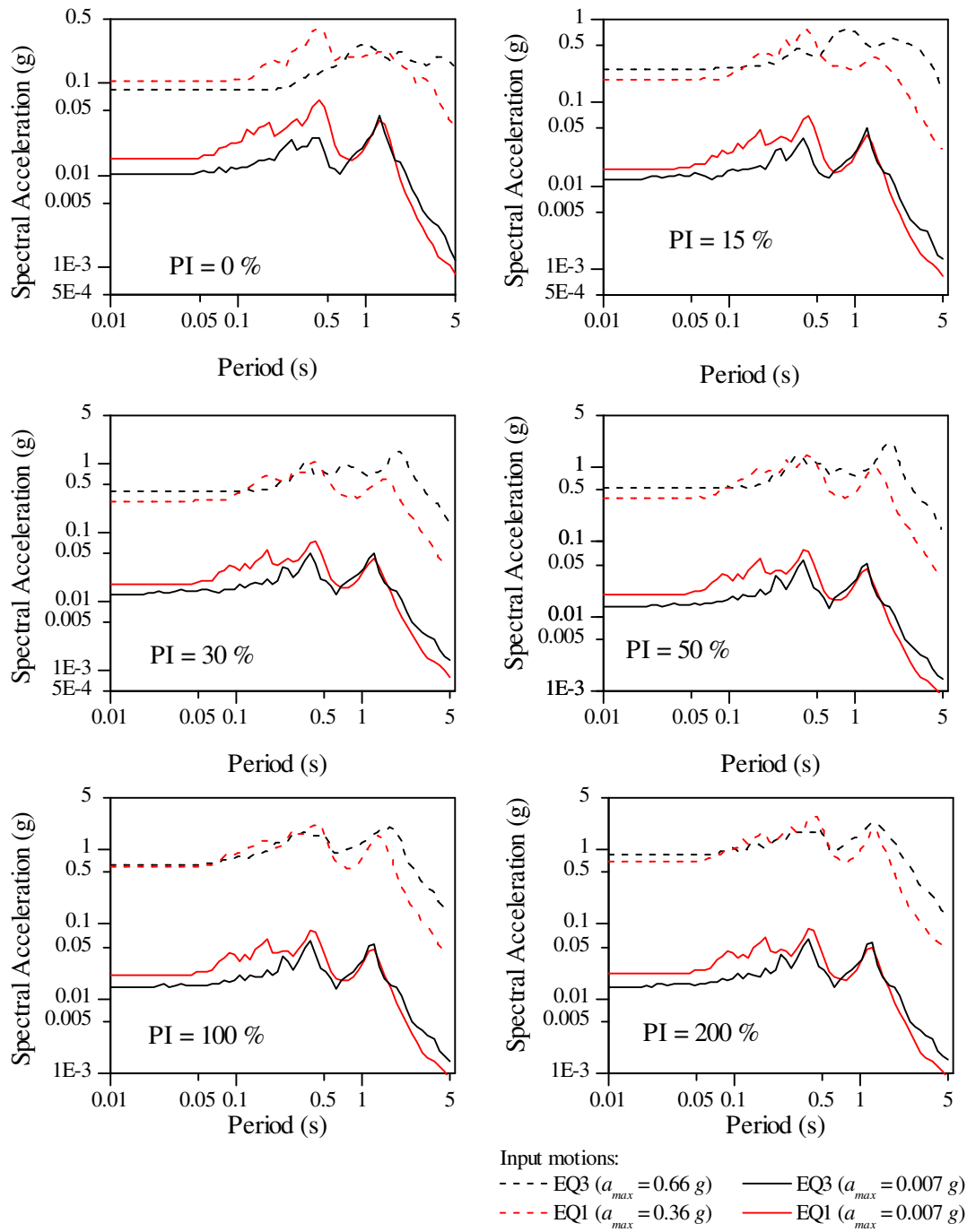
Figure 2.30: Comparison of response spectrum of computed surface motion of a homogeneous deposit using EQL analysis for different values of plasticity index.

The response spectra of the computed surface acceleration time histories are shown in Figure 2.30 for all the cases of plasticity indices under both EQ1 and EQ3 input motions with and without scaling down acceleration time histories. Spectral acceleration values of the predicted surface motions for weak input motions are

almost identical irrespective of plasticity of the soil. However, EQ1 input motion has yielded marginally higher spectral accelerations compared to EQ3 input motion. This difference is noticeably higher for PI=0. While in case of strong input motion the effect of plasticity index on the computed surface response is evident particularly when plasticity index increases in the range of 0 to 50%. Response spectra of the surface motion for PI = 100% and PI = 200% is almost indistinguishable. With the exception of PI = 0%, for all other cases the difference in spectral values in the period range less than about 1.0s is negligible for EQ1 and EQ3 input motions though the characteristics of these input motions are distinctly different. But for the period range greater than 1.0s the response due to EQ3 input motion has resulted in higher spectral values than that of EQ1 motion for all values of plasticity indices. Obviously, higher response at lower frequency ranges may be attributed to larger amplitudes of EQ3 accelerogram compared to EQ1 input motion. It should be noted that, though the predominant period of both the input motions are less than 1s (Figure 2.27), the spectral accelerations of EQ3 input motion in the low frequency range (< 1Hz) is significantly larger than that of EQ1 motion.

Figure 2.31 shows amplification of input motion as waves traverse from bedrock to surface. The amplification transfer functions between surface and bedrock demonstrate that the frequencies corresponding to peaks are almost coinciding for both the cases of normalized (0.007g) Loma Prieta and Kobe input motions. However under the excitation of strong input motion, there is significant difference in amplification values also in shifting of modal frequencies towards lower values. These plots of amplification transfer functions clearly indicate that as the intensity of shaking increases generally amplification decreases. Also, shifting of modal frequencies towards lower values with increase in intensity of shaking is evident from these figures. It is interesting to note that as the plasticity index increases there is increase in amplification ratio. This increase in amplification is more pronounced as intensity of shaking deceases. More interestingly, as plasticity index increases again we can observe the shifting of modal frequencies towards higher values and convergence to frequencies that corresponding to low intensity shaking.
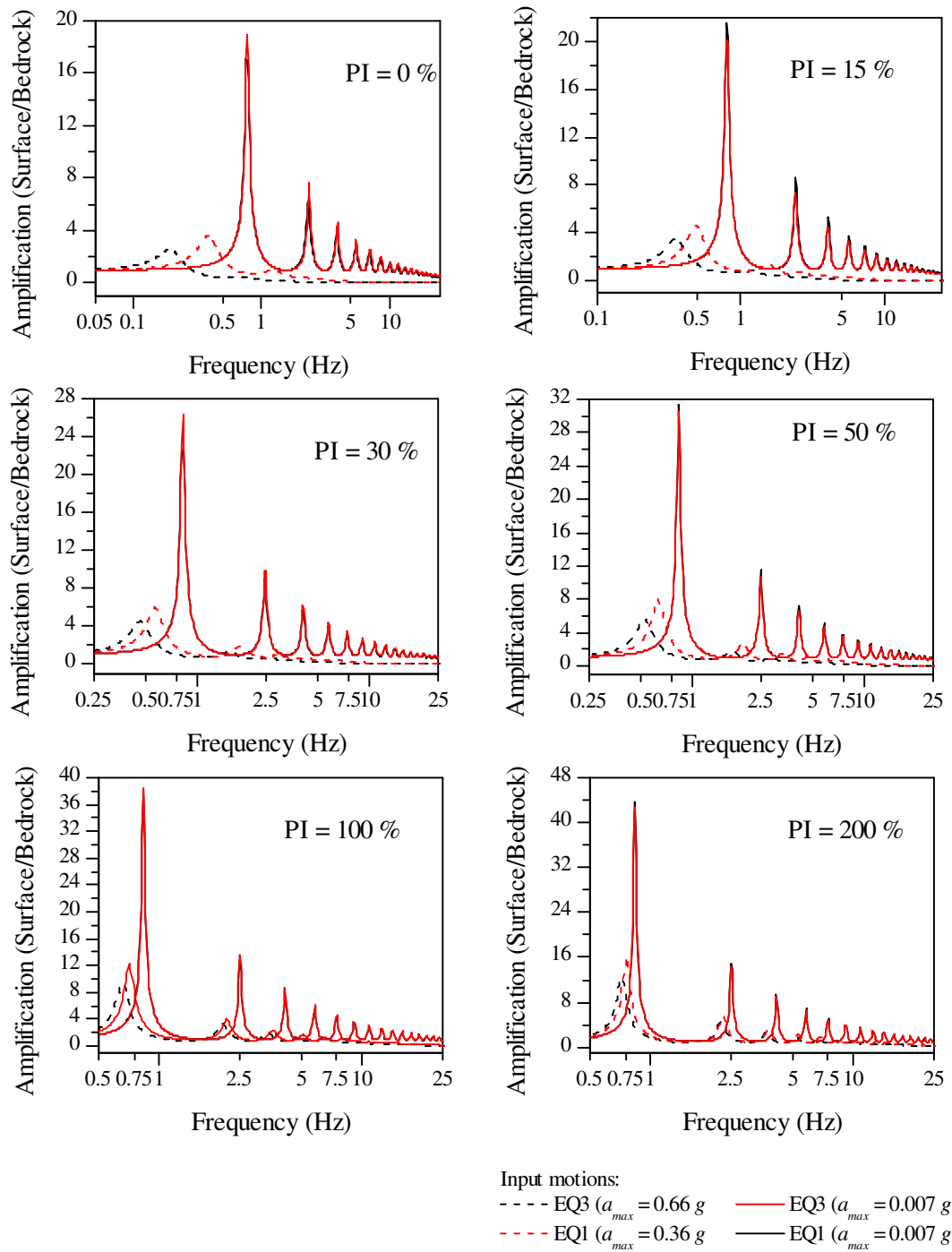
Figure 2.31: Comparison of amplification transfer function between surface and base of the homogeneous deposit for weak and strong input motions using EQL analysis for different values of plasticity index.

2.12 SUMMARY

In this chapter various methods available to estimate seismic site response are reviewed with the main objective of appraising their relative merits and demerits particularly for general purpose applications in engineering practice. In order to capture nature of deviations in predicted responses using frequency domain linear and equivalent linear analyses relative to time domain linear and nonlinear analyses, comparative study is carried out by using input motions of varying amplitude and frequency content. In order to recognize the importance of accurate characterization of shear wave velocity both inhomogeneous and equivalent homogeneous deposits are considered for the parametric studies. Finally, a parametric study is performed in which the effect of selection of curves used to model strain dependent stiffness degradation and damping properties of the soil deposit on computed response is established by considering plasticity index as a parameter. Outcome of these review and parametric studies are summarized as follows,

In view of nature of geological process leading to formation of soil deposit and physics of wave propagation, one-dimensional formulation is justifiable. One-dimensional analysis is dominantly popular among engineers because of its simplicity. Moreover, the result of one dimensional analysis particularly using multiple reflection theory is successfully validated with field observations by many researchers. However, under many circumstances the computed responses, even using complex numerical procedures and two or three dimensional modeling, fail to simulate the observed behaviour.

Numerical procedures enumerated in this chapter have their own advantages and disadvantages particularly with respect to accuracy and computational effort involved. Therefore more than numerical procedure used, the important aspects which probably can improve results are precise evaluation of geometrical and mechanical characteristics particularly proper idealization of inherent inhomogeneity soil deposit along its depth.

Equivalent linear technique is used in order to account for nonlinear behaviour of soil deposit under strong seismic excitation. Equivalent linear analysis makes use of strain dependent shear modulus and damping curves to update these properties in an iterative manner. In most of the situations, seismic site response analysis is accomplished by employing generic curves developed for such purposes and readily available in literature. However, experience and engineering judgment are key factors for making appropriate selection of such average curves depending upon site conditions, most often, assessed based on fewer and routine geotechnical investigations.

Popularity of computer programs implementing equivalent linear method is evident primarily because of its ease in implementation and interpretation of results as compared to true non-linear analysis. Obviously non-linear time domain method has ability to simulate dynamic response of ground because at every time step mechanical properties of soil are updated. However complexities involved in obtaining the realistic parameters of non-linear models makes it unpopular in routine engineering practice. Hence there is always scope for improvement of equivalent linear method with clear understanding of its inefficiencies and lacunae.

The comparative study is carried out using one dimensional frequency domain and time domain linear analyses for low amplitude input motions with distinctly different frequency characteristics. The results obtained from both these methods of analyses are in good agreement. The response spectra of the computed surface accelerogram clearly revealed the effect of frequency content of the input motion on the estimated peak response. The input motion with wide range of frequency content (EQ2 motion) tends to excite soil deposit significantly at the frequencies corresponding to its higher modes. Thus it is important to consider frequency content of the input motion as well as modal frequencies of the soil deposit in frequency dependent damping formulation to control discrepancies in the response at resonant frequencies.

The comparative study carried out with respect to equivalent linear and nonlinear approaches for relative high amplitude input motions has brought out some of the limitations of equivalent linear analysis. Primarily, the outcome of this study confirms

well established limitations of equivalent linear analysis, i.e., it underestimates high frequency response compared to nonlinear analysis and also it results in overestimation of response at fundamental frequency of the deposit. Both these discrepancies are probably related to the main drawback of the equivalent linear analysis: the use of constant values of shear modulus and damping throughout a particular iteration at all frequencies. Results presented herein indicate that the frequency range at which underestimation of response sets off appears to be consistently associated with the frequency content of the input motion and modal characteristics of the soil deposit.

Based on the parametric study reported here, broadly following observations can be made. The response of the soil deposit excited by means of two input motions with distinctly different frequency characteristics but normalized to same relatively low maximum acceleration is equally sensitive to spectral characteristics of the input motion and plasticity index of the soil. However, the maximum acceleration profile appears to be having almost identical kind of variation with different magnitudes of maximum accelerations depending on plasticity index. Though large difference is observed in computed peak surface acceleration for different PI values, the response spectra of these surface motions appears to be having negligible difference in spectral amplitudes of the response spectrum.

Another important issue of concern with respect to equivalent linear analysis is computation of effective strain which is required to allocate strain dependent soil properties compatible with induced strain level for the succeeding iteration. The procedure which is implemented for this purpose in popular site response analysis computer programs is indistinct because the effective strain is calculated as the product of maximum strain and constant value (R) which remains same throughout the analysis at all layers of the soil deposit irrespective of intensity of shaking induced at that layer. The guideline recommended to obtain R value, based on magnitude of the earthquake, is ambiguous. Hence, an alternative rational procedure is proposed in Chapter 5.

CHAPTER 3

ANALYSIS OF CONTINUOUSLY INHOMOGENEOUS SOIL DEPOSITS – ANALYTICAL STUDIES

3.1   INTRODUCTION

The earthquake waves originating from source of disturbance located inside the earth's crust propagate through geological medium before reaching the surface. The geometrical and mechanical characteristics of soil deposit near the surface have greater influence on wave characteristics than other factors associated with an earthquake. Recognizing this fact, particularly geotechnical engineers have considered the problem of predicting the surface motion due to input motion at the bedrock level as one of the major tasks in the field of study of soil dynamics. As has been discussed in the previous chapter, most popular method of modeling the ground is approximating it as stack of uniform visco-elastic layers of infinite lateral extent. Then seismic response analysis of the soil deposit is carried out due to incident shear wave at the bedrock level and propagating vertically through the surface layers. Thus the problem of site response analysis is essentially treated as one-dimensional. In this chapter some of the analytical studies in which the soil deposit is modeled as continuously inhomogeneous instead of discrete layers of uniform properties are reviewed. Basically all these studies consider shear modulus and/or shear wave velocity to vary continuously assuming all other properties (for e.g. density, damping, etc.) to remain constant with depth.

In order to meet the requirement of the popular methods of ground response analysis procedures, it is essential to model the inhomogeneous surface deposit as a layered system. Hence, whatever be the method of geophysical investigation adopted, finally the data has to be interpreted so as to yield appropriate layered system. In many instances even though the soil deposit exhibits almost continuous variation of stiffness/shear wave velocity along the depth, it is customarily interpreted as layered deposit for the sake of accommodating it in the analysis procedure. This tendency to

idealize surface deposit as layered system in spite of deposit exhibiting continuous variation of stiffness and density properties may have serious shortcoming on the accuracy of results of ground response analysis. Hence, this chapter attempts to study the appropriateness of approximating the deposit with continuous variation of shear modulus compared to layered idealisation. Modeling the surface deposit with continuous variation in soil properties may overcome the problem of pseudo resonance conditions that prevail due to trapping of waves and the reverberations inside the layers with contrasting impedances at their boundaries. The comparison is made between the computed responses of the deposit with both, layered and its approximated continuous idealizations.

Natural soil deposits are inherently inhomogeneous and anisotropic. Therefore the soil properties significantly vary in all the directions at every point along the depth. The distribution of these soil properties at a site depends on heterogeneity of constituent materials, geological history and its incessant alteration by nature. Among several other reasons, most importantly, the inhomogeneity of soil is the consequence of variation of its mechanical and physical properties [Lambe and Whitman (1979); Wood (2004); Schevenels et al. (2007)]. Inhomogeneity of the soil deposit is the outcome of several causes; its genesis, mode of sedimentation process, stress history and in-situ state of stress, microstructures and mineral composition, etc. Usually the soil properties vary gradually along the depth of sedimentary soil deposits and these variations are primarily influenced by the mode, material type and rate of sediment deposition. Inhomogeneity in case of residual soil deposits can be manifested due to gradual process of weathering, fluctuations in ground water table, temperature variation, and other environmental conditions. Ageing is also an important time factor for inducing significant alterations to engineering properties of the soil [Schmertmann (1991)]. Thus, it is clear that, irrespective of the method of formation both natural and man made soil deposits usually tend to exhibit continuous variation of soil properties and deformation characteristics with depth.

Inherent variability of soil properties along the depth is evident in most of the natural soil deposits. Attempts have been made to satisfactorily model this inherent variability through statistical analysis. Primarily, these studies are intended to model both

variability of properties due to heterogeneity and inconsistency in testing procedures adopted to measure respective soil properties [Terzaghi (1955), Krahn and Fredlund (1983), Phoon and Kulhawy (1999), Sojka et al. (2001)]. It is well established that shear modulus at any depth of natural soil deposit is dependent on in-situ confining stress and over consolidation ratio which are functions of depth [Gibson (1974), Hardin and Richart (1963), Gazetas (1981) and others]. Residual soil is also found to exhibit continuous variation with regard to its shear modulus and damping properties along the depth. Macari and Hoyos (1996) have reported that the variation of these properties for a particular residual soil deposit considered in their study can be approximated by an equation of linear trend. They found that at any depth z, in terms of their magnitudes at the surface $(z=0)$, the shear modulus and damping may be represented by $G(z) = G_{(z=0)}(1+0.15z)$ and by $\zeta(z) = \zeta_{(z=0)}(1-0.2z)$ respectively. Even in case of soil deposits apparently exhibiting layered profile, in some instances, the properties are observed to be varying gradually at the layer interfaces signifying presence of smooth transition zone between the layers [Davis (1994, 1995); Pyke et al. (2007)].

3.2   DISCREPANCIES IN LAYERED DEPOSIT CHARACTERISATION

As earthquake waves propagate through soil media, their amplification or attenuation is mainly dependent on shear wave velocity and geometrical characteristics of soil deposit overlying the bedrock. Many kinds of field tests are available in practice to quantify these characteristics. Some of these procedures can directly measure the shear wave velocities at different depths of the soil profile, while in other cases it is obtained employing empirical methods in an indirect manner. Also there are sophisticated methods of field tests available such as, SASW, Suspension P-S logging, downhole methods etc., in which continuous profiling of shear wave velocities across the depth of the soil deposit is possible. However these methods seem to be expensive and they aren't considered as part of routine geotechnical investigation. In this regard, the results of penetration tests such as SPT, SCPT, etc., are more popularly employed to assess shear wave characteristics of soil deposits using well established empirical relationships [Ohta and Goto (1978); Mayne and Rix (1995); Kokusho and Yoshida

(1997); Vijayendra and Prasad (2001); Andrus et al. (2007); Wair et al (2012) and others]

Geophysical field tests for determination of shear wave velocity of soil deposit are classified into invasive and non-invasive methods. Boreholes are necessary in the former method and test is carried out on the surface without making boreholes in the latter case. These methods are essentially associated with propagation of body and surface waves respectively. Cross hole, down hole and suspension P-S logging methods of investigations are the techniques for which boreholes are necessary. Most popular method among the non-invasive methods is Spectral Analysis of Surface waves (SASW) wherein test is conducted from the top surface of the soil deposit. Good account of these methods with respect to their advantages, limitations and latest developments are given by Lo Presti, et al. (2004), Boore (2006) and references cited therein.

Results of invasive method of field tests like down hole or cross hole or suspension logging procedures, are obtained in terms of depth versus travel-time curves for the arrival of shear waves at the receiver of the borehole. These are then used in conjunction with bore log details which consists of information about layered structure of the soil deposit to interpret average shear wave velocity of each of these layers.

Towhata (1996), with an example, clearly demonstrated this aspect of interpreting the down hole survey test data to yield layered velocity structure though the soil deposit exhibits continuous variation of stiffness properties. To substantiate his argument, he considered travel time-depth data of a downhole survey at Shin-Ohta site in Japan. If layered structure exists then travel time versus depth plot must consist of as many piecewise linear segments as the number of layers with distinct shear wave velocity present in the deposit. The slope of these linear segments would yield shear wave velocity of each of these layers. Even though travel time-depth plot exhibits nonlinear continuous variation indicating the continuous variation of shear wave velocity with depth, as is done routinely, it is approximated with piecewise linear segments to get approximate average shear wave velocity of idealized layered deposit.

Thus giving an accurate description of velocity structure (P and S waves) of the soil deposit formation overlying bedrock is inherently difficult because of peculiarities associated with wave motion in complex geological media. The procedure involved in interpretation of data obtained from any of these field tests requires expertise and thorough experience in analyzing the data. Many times it appears that these interpretations are subjective [Boore (2003); Brown et al. (2002)]. Also it is interesting to note that, results interpreted for a particular site from data obtained using different field tests often do not agree and some times differ to a large extent. In order to illustrate this aspect, data reported by Boore et al. (2003) is employed. They have reported the data pertaining to shear wave velocity profile for La Cienega site, USA using surface to borehole and suspension P-S logging methods. Suspension P-S logging data have been interpreted to fit complex layering system using the results of surface to borehole velocity logging results as a guideline. Interpreted shear wave velocity structure thus obtained from these analyses are shown in Figure 3.1 along with actual field data of suspension logging method. This figure clearly demonstrates the inconsistency of final result or judgment involved in interpretations of the results.
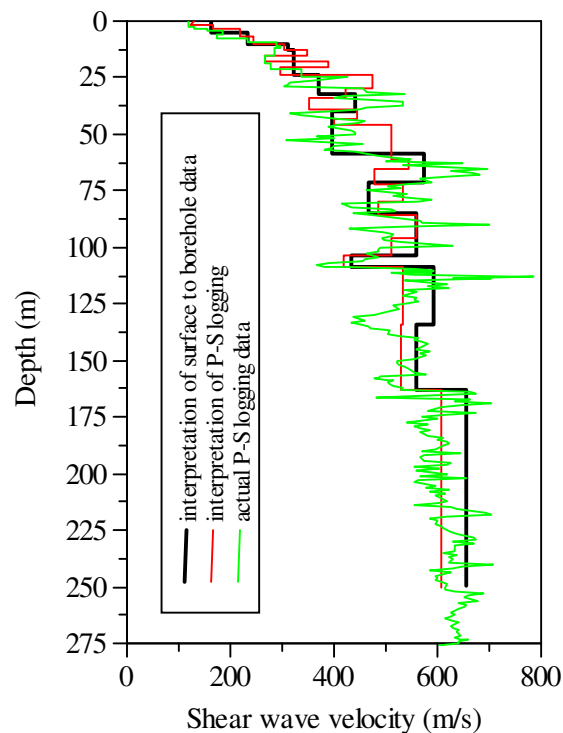
Figure 3.1: Comparison of shear wave velocity profiles interpreted from data obtained from different field tests at La Cienega site USA [Boore et al. (2003)].

3.3   PHYSICAL IMPLICATIONS OF LAYERED IDEALIZATIONS

The product of shear wave velocity, density of a layer and the cosine of the angle of incidence is termed as impedance of that layer. In case of horizontally layered soil deposits subjected to disturbance of vertically propagating body waves the incidence angle is considered to be zero.

If v_{s1} and v_{s2} are the shear velocities of two successive layers with ρ_1 and ρ_2 as their corresponding densities, then the impedance contrast between these layers is quantified by the ratio of their impedances as, $\rho_1 v_{s1} / \rho_2 v_{s2}$. Impedance contrast is mainly responsible for phenomenon of trapping of seismic waves within the layer leading to change in wave characteristics including magnitude of amplification of ground motions.
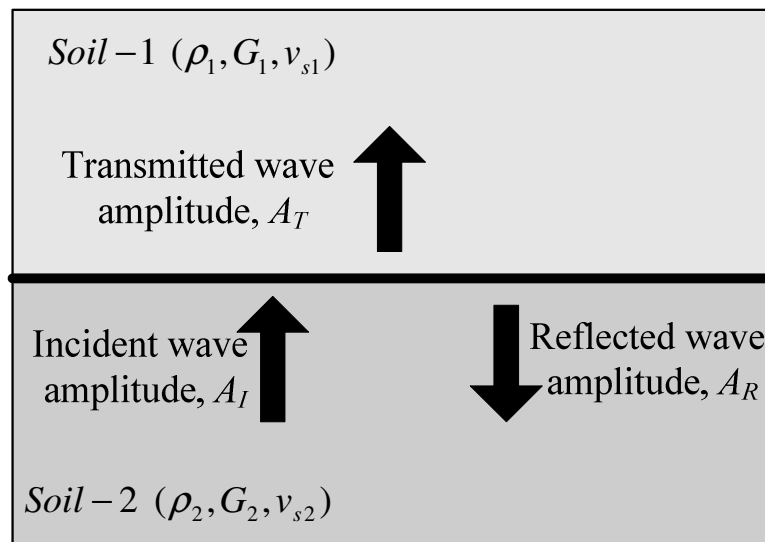
Figure 3.2: Phenomenon of wave propagation at the layer interface

Figure 3.2 shows soil deposit of two layers with distinct shear wave velocity and density properties. As waves propagating in the upward direction reach the interface of these two layers, part of the wave energy is transmitted and the remaining is reflected back as indicated the Figure 3.2. The amplitudes of incident, transmitted and reflected waves are respectively represented by A_I, A_T and A_R [Kramer (1996)]. These are related to one another in case of vertically propagating wave as,

84

$$A_T = \frac{2}{1+\alpha} A_I$$
$$A_R = \frac{1-\alpha}{1+\alpha} A_I$$

<div align="right">(3.1)</div>

Here $\alpha = \rho_1 v_{s1} / \rho_2 v_{s2}$ is the impedance ratio between the two the layers. From Eq. (3.1) it is clear that, amplitude of incident wave is partially transmitted to overlying layer depending upon impedance contrast of the adjacent layers.

The energy transmitted across the boundary is also dependent on the impedance ratio between the layers at that boundary interface. Transmitted and reflected energy components across a boundary are proportional to square of the corresponding wave amplitudes [Towhata (2008)]. Thus the transmitted and reflected wave energies expressed as their ratio with respect to incident wave energy are given by,

$$E_T = \frac{4\alpha}{(1+\alpha)^2} E_I$$
$$E_R = \frac{(1-\alpha)^2}{(1+\alpha)^2} E_I$$

<div align="right">(3.2)</div>

In the above equations E_I, E_T and E_R respectively represent incident, transmitted and reflected wave energy components. In the field of study of laminated composites the reflected component of the energy is also termed as impedance mismatch and is considered to be effective means to represent mismatch in impedance across the layer boundaries [for e.g. Chen and Chandra (2004)]. Similarly, the transmitted and reflected stress amplitudes across the interfaces of layers with contrasting impedances are represented using following relationships [Kramer (1996)].

$$\sigma_T = \frac{2\alpha}{1+\alpha} \sigma_I$$
$$\sigma_R = \frac{\alpha-1}{1+\alpha} \sigma_I$$

<div align="right">(3.3)</div>

In order to understand the effect of contrasting impedances of layers on wave amplitudes, the ratio of amplitudes of reflected waves to that of transmitted waves at

an interface of two layers is plotted against impedance ratio in Figure 3.3. Also ratio of reflected to transmitted magnitudes of energy and stress are plotted in the same figure. This figure clearly indicates that, the nature and magnitude of amplitudes of transmitted and reflected waves at an interface is affected by impedance ratio. When $\alpha < 1$, displacement amplitude of the reflected wave is less than one and approaches 0.5 as impedance ratio approaches zero which corresponds to absence of top layer. Therefore when waves arrive at a free surface, the amplitude of transmitted wave becomes twice that of incident wave. For the case of impedance ratio far greater than one, wave reflection is dominant compared to its transmitted counterpart and no wave is transmitted if the overlying layer is infinitely rigid (i.e., $A_T \to 0$ as, $\alpha \to \infty$). Hence incident wave will be reflected back completely. For $\alpha < 1$, almost all incident wave energy has to be dissipated in the top layer while significantly large magnitude of energy is reflected as the top layer is relatively stiffer than the bottom layer. Consequential effect of these features of energy transmission across the boundary of layers with contrasting impedances is reproduced in magnitude of stress transmitted to top layer. In case of ratio of reflected and transmitted stress amplitudes, as the impedance ratio decreases, the stress response transmitted to top layer decreases and tends to zero as the wave reaches free surface.
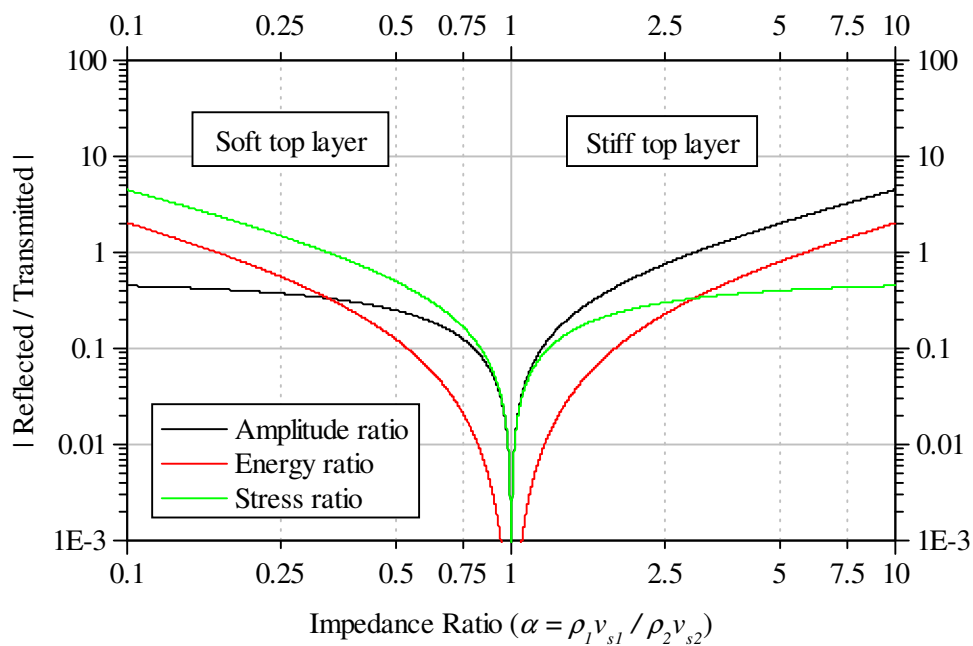
Figure 3.3: Influence of impedance ratio on transmitted and reflected waves

More importantly, it should be noted that all the wave energy is transmitted completely without any reflection as the impedance ratio tends one ($\alpha \rightarrow 1$), that is, ratio of reflected to transmitted wave amplitude tends to zero. The impedance ratio at any location of the deposit tends to one when the shear wave velocity and density properties of the soil exhibit continuous variation along its entire depth. If the ground which is continuously heterogeneous in reality is approximated with an equivalent layered idealisation, then superficially contrasting impedances between the layers is induced in the analysis. This kind of layered approximation of continuously inhomogeneous soil deposit may in turn affect the computed responses significantly.
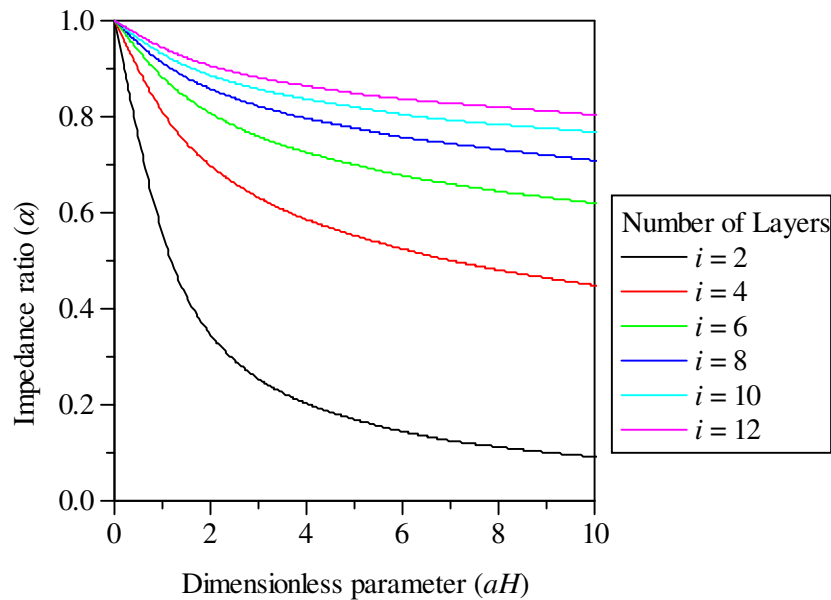
Figure 3.4: Effect of equivalent layered idealisation of continuously inhomogeneous soil deposit on impedance ratio.

Figure 3.4 demonstrates the effect of idealizing a linearly distributed shear wave velocity profile into an equivalent layered deposit. The linearly varying shear wave velocity profile as a function of depth (z), may be expressed in terms of surface shear wave velocity, v_{s0} and inhomogeneity parameter, a as $v_s(z) = v_{s0}(1 + az)$. Thus $a = 0$ corresponds to homogeneous layer and as a increases shear wave velocity variation becomes steeper. In Figure 3.4, the resulting impedance ratio between the layers of the idealised layered profile is plotted against dimensionless parameter aH where H is the total depth of the profile. The layer depths are calculated to yield

constant impedance ratio across all the intended number of layer boundaries. For a given value of a, as the number of layers employed to approximate the actual profile decreases the impedance ratio between the layers will shift further away from one indicating more contrasting impedances between the layers. Whatever may be the number of layers used in approximation of continuously inhomogeneous deposit , there always exist some difference in the impedances across adjacent layers. By comparing the trends of the curves of 8, 10 and 12 layers, it is evident that there is no appreciable advantage by simply increasing the number of layers beyond certain limit because reduction of difference in impedances between layers is not substantial for any degree of inhomogeneity.

As a consequence of modeling the ground as a layered medium, apart from changes in the amplitude of transmitted and reflected waves, there is also a possibility of trapping transmitted waves inside a layer when there is sharp change in impedance ratio between the layers of relatively greater depths. That is along with difference in layer impedances, depth of the layers also matters in wave propagation. When wave length is longer or shorter than the depth of the layer, then the pseudo resonance state may prevail in that layer. This kind of situation leads to localized resonance condition due to the reverberation of trapped waves. This may result in, depending on magnitude of damping associated with that layer, high amplification of ground motions in a certain frequency range. Hence, apart from impedance ratio, other mechanical and geometrical properties of the layered system will greatly affect wave transmission mechanism.

Thus the effect of layered idealisation on the ground response is evident. Hence, seismic ground response analysis may yield erroneous results in case the surface deposit is modeled as layered ground when its stiffness and density characteristics are being continuously varying with depth. Usually in practice, this kind of factitious method of modeling the deposit is followed in order to meet the requirement of the popularly adopted method of analysis like one employed in computer program SHAKE. While using such methods of analysis, uniform shear wave velocity values for each of the layer must be judiciously assigned in order to avoid fictitious amplification of waves transmitted through those layers leading to trapping of waves

resulting in prevalence of pseudo resonance conditions. In such instances, where surface deposit shows continuous variation of soil stiffness and density properties, it is important to model it appropriately with closely stacked thin layers or more preferable develop the physical and mathematical model to account for prevailing actual continuous variation of deposit characteristics.

Recognizing the fact that, in some instances inhomogeneity of the surface deposit may be due to continuous variation of stiffness and density rather than distinctly layered formation, many investigators have attempted to treat the prevailing condition of inhomogeneity and computed the dynamic response of the deposit subjected to harmonic base excitation [Ambraseys (1959), Idriss and Seed (1968), Schreyer (1977), Dobry et al. (1976), etc.]. Some of these analytical studies considered vanishing shear modulus or shear wave velocity near the surface. However more often non-zero stiffness at the surface is evident in reality. Some of these studies have attempted to address this problem with rigorous analytical solutions by modeling the variation of stiffness and/or shear wave velocity with different inhomogeneity parameters. Among these, foremost contributions in the recent past include Gazetas (1982), Dakoulas and Gazetas (1985), Towhata (1996), Zhao (1996), Travasarou and Gazetas (2004), Rovithis et al (2011), Vrettos (2013) and many others.

3.4   SOIL DEPOSIT WITH CONTINUOUS VARIATION OF STIFFNESS ALONG THE DEPTH

The wave equation for one-dimensional transverse vibration due to shear wave propagation in a soil deposit with constant density, ρ and shear modulus, $G(z)$ varying continuously along the depth is given by

$$\frac{\partial^2 u}{\partial t^2} = \frac{1}{\rho} \frac{\partial}{\partial z}\left(G(z) \frac{\partial u}{\partial z} \right) \tag{3.4}$$

Here, $u(z,t)$ represent the horizontal displacement at depth z and time t. Noting that, $v_s^2 = G/\rho$, in terms of shear wave velocity, the above equation may be expressed as,

$$\frac{\partial^2 u}{\partial t^2} = \frac{\partial}{\partial z}\left([v_s(z)]^2 \frac{\partial u}{\partial z}\right)$$ (3.5)

Many researchers have treated the problem of computing amplification of ground motion in a soil deposit with shear wave velocity increasing with depth. The general trend of depth dependent function defining continuous variation of shear wave velocity profile is given by

$$v_s(z) = v_{s0}(1+az)^n$$ (3.6)

Here, v_{s0} is shear wave velocity at $z = 0$ (surface), a is positive constant representing rate of heterogeneity and n is a positive power in the range $0 < n \leq 1$. Correspondingly, linear variation of shear wave velocity is obtained by setting $n = 1$. In fact, the above equation is a general form of the particular cases considered earlier by several researchers. For the case of constant density, either of the two forms of equation of motion i.e., Eq. (3.4) or Eq. (3.5) can be employed to model the continuously inhomogeneous trend in terms shear modulus or shear wave velocity respectively. In case of geotechnical investigation surveys to profile small strain shear modulus using seismic refraction or cross-hole techniques, propagation path of the signal is generally assumed to be a straight line in order to calculate travel time of the signal. This may result in discrepancies in computed results [Woods (1978)]. In recognition of this tendency, geophysicists use different forms of depth dependent velocity functions as prerequisite in geophysical investigations to apply correction to computed travel time data. Some of these popularly employed body wave velocity functions, including the trend given in Eq. (3.6), representing continuous inhomogeneity of the earth are presented in Kaufman (1953), Hŕyeiw (1989) and others. One of the earliest studies with regard to dynamic response analysis of continuously inhomogeneous soil deposits is by Ambraseys (1959). He considered the case in which the shear modulus is assumed to be linearly varying with depth. This corresponds to the case $n = 0.5$ in Eq. (3.6). Later Toki and Cherry (1972 and 1974) considered a more general case of depth dependent shear modulus variation of the form $G(z) = \Lambda(G_0 + z)^m$ in which Λ is the proportionality constant, G_0 is the shear modulus at $z = 0$ (surface) and for $m < 1$.

They studied the effect of degree of inhomogeneity on the variations of acceleration and strain responses along the depth of continuously inhomogeneous deposits. Schreyer (1977) obtained the solution for the free vibration response characteristics of the deposit having shear wave velocity profile varying according to Eq. (3.6) for the case of $n = 2$ and for various values of (include both $a < 0$ & $a > 0$) heterogeneity factors. Forced vibration response study carried out for the case of exponentially decaying forcing function applied at the surface of the deposit, Schreyer (1977) has shown that the soil layer response along its depth is sensitive to both a and the rate of exponential decay of the forcing function. Compiling the results of the above study, expressions to compute natural frequencies and corresponding mode shapes are presented by Gazetas (1982). For this purpose, soil deposits having continuous variation of shear wave velocity profile as given by Eq. (3.6) with various values of n (=0.25, 0.5, 2/3 and 1.0) are considered.

3.4.1 Soil deposit with linearly varying shear wave velocity profile $(n = 1)$

If shear wave velocity is assumed to be varying linearly as shown in Fig. 3.5, then

$$v_s(z) = v_{s0} + \bar{a}z \tag{3.7}$$

v_{s0} is the non-zero shear wave velocity at surface ($z = 0$) and $\bar{a}$ is the constant defining rate of change of v_s with depth. Comparing Eq. (3.6) and Eq. (3.7), it is evident that the parameter $\bar{a}$ of Eq. (3.7) is represented by $\bar{a} = av_{s0}$. Substituting Eq. (3.7) in Eq. (3.5) and noting that ρ is assumed to be constant, results in,

$$\frac{\partial^2 u}{\partial t^2} = \frac{\partial}{\partial z}\left[(v_{s0} + \bar{a}z)^2 \frac{\partial u}{\partial z}\right] \tag{3.8}$$

Assuming the solution of the wave equation as, $u(z,t) = U(z)\exp(i\omega t)$ and substituting in Eq. (3.8) we get,

$$\frac{d^2 U}{dz^2} + \frac{2\bar{a}}{(v_{s0} + \bar{a}z)}\frac{dU}{dz} + \frac{\omega^2}{(v_{s0} + \bar{a}z)^2}U = 0 \tag{3.9}$$

91

Consider a transformation of $x = \dfrac{\omega}{\bar{a}} \ln(v_{s0} + \bar{a}z)$ and substituting in Eq. (3.9) yields an equation with constant coefficients as,

$$\frac{d^2 U}{dx^2} + \left(\frac{\bar{a}}{\omega}\right)\frac{dU}{dx} + U = 0 \tag{3.10}$$
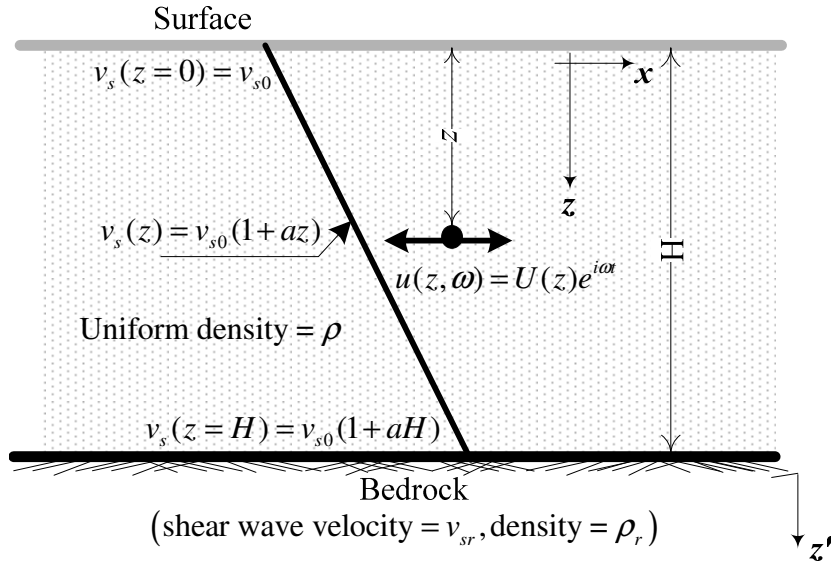
Figure 3.5: Soil deposit with linearly varying shear wave velocity profile

Thus the solution of Eq. (3.10) is obtained as,

$$U(x) = A_1 e^{\left(-\frac{\bar{a}}{2\omega} + \sqrt{\left(\frac{\bar{a}}{2\omega}\right)^2 - 1}\right)x} + A_2 e^{\left(-\frac{\bar{a}}{2\omega} - \sqrt{\left(\frac{\bar{a}}{2\omega}\right)^2 - 1}\right)x} \tag{3.11}$$

Substituting back for x, as $x = \dfrac{\omega}{\bar{a}} \ln(v_{s0} + \bar{a}z)$ and further simplification yields the solution of Eq. (3.9),

$$U(z) = \frac{1}{\sqrt{(v_{s0} + \bar{a}z)}} \left\{ A_1 e^{i\sqrt{\left(\omega/\bar{a}\right)^2 - (0.5)^2}\, \ln(v_{s0} + \bar{a}z)} + A_2 e^{-i\sqrt{\left(\omega/\bar{a}\right)^2 - (0.5)^2}\, \ln(v_{s0} + \bar{a}z)} \right\} \tag{3.12}$$

The expression for shear stress amplitude is obtained by noting that, $\tau(z) = G(z)\dfrac{\partial U(z)}{\partial z}$ i.e,

$$\tau(z) = \bar{a}\rho\sqrt{v_s}\left\{A_1\left(i\kappa - 0.5\right)e^{i\kappa\ln(v_S)} - A_2\left(i\kappa + 0.5\right)e^{-i\kappa\ln(v_S)}\right\} \qquad (3.13)$$

where, $\kappa = \left[\left(\dfrac{\omega}{\bar{a}}\right)^2 - \dfrac{1}{4}\right]^{0.5}$, $i = \sqrt{-1}$, A_1 and A_2 are constants. Using the boundary condition, shear stress vanishes at the surface in Eq. (3.13), we get,

$$A_2 = A_1\exp\left[i2\kappa\ln(v_{s0})\right]\dfrac{i\kappa - 0.5}{i\kappa + 0.5} \qquad (3.14)$$

Therefore, response at the surface, $U(0) = U(z = 0)$ may be expressed as,

$$U(0) = \dfrac{i2\kappa}{\sqrt{v_{s0}}}C \qquad (3.15)$$

where, C is a new constant, $C = \dfrac{A_1\exp[i\kappa\ln(v_{s0})]}{i\kappa + 0.5}$. The response at the base $U(H) = U(z = H)$ of the deposit is given by

$$U(H) = \dfrac{iC}{\sqrt{v_{sH}}}\left[\sin(\kappa\ln\mu) + 2\kappa\cos(\kappa\ln\mu)\right] \qquad (3.16)$$

where, the ratio of shear wave velocity at the base to that at the surface is $\mu\left(= v_{sH}/v_{s0}\right)$. Also at the base the shear stress is given by,

$$\tau(z = H) = \tau(H) = -C\bar{a}\rho\left(\dfrac{\omega}{\bar{a}}\right)^2\sqrt{v_{sH}}\left[2i\sin(\kappa\ln\mu)\right] \qquad (3.17)$$

If z' is the depth coordinate measured downwards from the top of bedrock then the displacement and shear stress for $z' \geq 0.0$ is given by,

$$U(z') = A_1'e^{i\omega z'/v_{sr}} + A_2'e^{-i\omega z'/v_{sr}} \qquad (3.18)$$

$$\tau(z') = \rho_r v_{sr}^2\dfrac{\partial U(z')}{\partial z'} = i\rho_r\omega v_{sr}\left\{A_1'e^{i\omega z'/v_{sr}} - A_2'e^{-i\omega z'/v_{sr}}\right\} \qquad (3.19)$$

where, v_{sr} and ρ_r are shear wave velocity and density of the bedrock. A_1' and A_2' are constants. In case of elastic bedrock, compatibility of displacements and stresses at the soil and bedrock interface yields,

$$\tau(z=H) = \tau^t(z'=0) \Rightarrow 2C\bar{a}\rho\left(\frac{\omega}{a}\right)^2 \sqrt{v_{sH}}[2\sin(\kappa\ln\mu)] = \rho_r\omega v_{sr}\left(A_1' - A_2'\right) \quad (3.20a)$$

$$U(z=H) = U'(z'=0) \Rightarrow \frac{iC}{\sqrt{v_{sH}}}\left[\sin(\kappa\ln\mu) + 2\kappa\cos(\kappa\ln\mu)\right] = A_1' + A_2' \quad (3.20b)$$

These boundary conditions imply,

$$2A' = \frac{iC}{\sqrt{v_{sH}}}\left[\sin(\kappa\ln\mu)\left\{\frac{2i\omega}{a}\alpha_b + 1\right\} + 2\kappa\cos(\kappa\ln\mu)\right] \quad (3.21)$$

where $\alpha_b = \rho v_{sH} / \rho_r v_{sr}$ is the impedance ratio at the base of the soil deposit with respect to underlying bedrock. Amplification ratio between input motion and surface motion for rigid bedrock condition (within motion) is obtained by using Eq. (3.15) and Eq. (3.16) as,

$$Amp_{(1)} = \frac{U_0(z=0)}{U_H(z=H)} = \frac{2\kappa\sqrt{\mu}}{\left[\sin(\kappa\ln\mu) + 2\kappa\cos(\kappa\ln\mu)\right]} \quad (3.22)$$

While amplification of surface response with respect to outcrop motion (elastic bedrock) is obtained from Eq. (3.15) and Eq. (3.21)

$$Amp_{(2)} = \frac{U(z=0)}{2A_1'} = \frac{2\kappa\sqrt{\mu}}{\left[\sin(\kappa\ln\mu)\left\{\frac{2i\omega}{a}\alpha_b + 1\right\} + 2\kappa\cos(\kappa\ln\mu)\right]} \quad (3.23)$$

Here $Amp_{(1)}$ and $Amp_{(2)}$ are used to represent same terminologies of amplification ratio as used in the previous chapter. These results are also obtained in slightly different form by Gazetas (1982), Lojelo and Sano (1988) and Zhao (1996). The results obtained above are corresponding to the undamped case. To include viscous damping into analysis, the shear wave velocity v_s in the equation may simply be

replaced with $v_s = v_s\sqrt{1+2i\zeta}$ where ζ is the damping ratio corresponding to viscous damping. .

For the purpose of demonstrating the effect of surface shear wave velocity on amplification in ground motion for the case of continuously inhomogeneous deposit, amplification results for a 40 m thick deposit of constant density and linearly varying shear wave velocity profile i.e., $v_s(z) = v_{s0}(1+az)$ is considered. Figure 3.6 shows the amplifications computed from Eq. 3.22 ($Amp_{(1)}$) for two deposits with identical rate of heterogeneity ($a = 0.2$) but with different v_{s0} values. That is, in both the cases the shear wave velocity ratio $(\mu = v_{sH}/v_{s0} = 7)$ between base and surface of the deposit is kept the same. The underlying bedrock is considered to be rigid. Hence, irrespective of shear wave velocity distribution, for given values of μ and a the magnitude of peak amplification is same. However, modal natural frequencies are affected, because average shear wave velocity corresponding to $v_{s0} = 40m/s$ and $80m/s$ cases considered are 160 m/s and 320 m/s respectively. The results presented above are obtained for damping value, $\zeta = 2.5\%$.
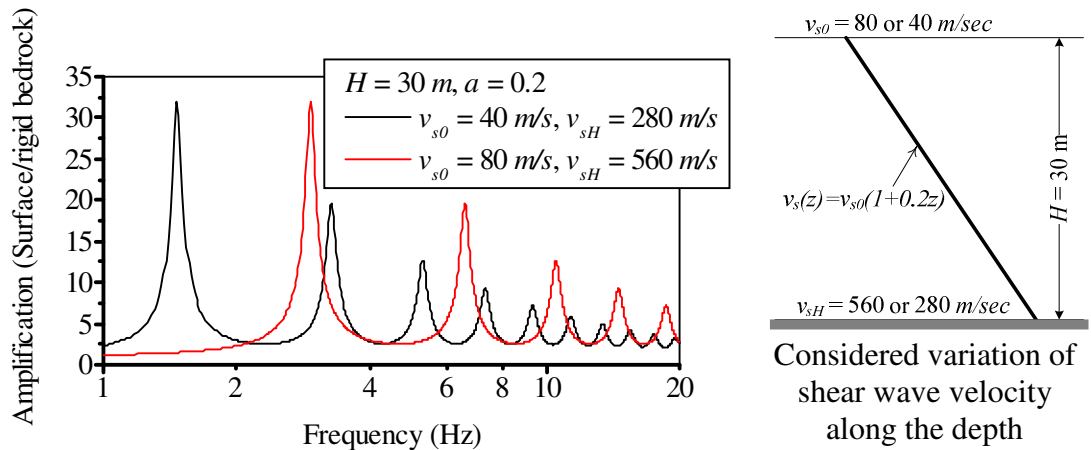
Figure 3.6: Amplification characteristics for the deposit of linearly increasing shear wave velocity profile with different surface shear wave velocities.

For the same deposit shown in Figure 3.6, with $v_{s0} = 80$ $m/\sec$ but varying a values, results in a change in surface deposit/bedrock impedance ratio. For the values of

$a = 0.1,\ 0.2,\ 0.5\,\&\,0.75$ the amplification computed from Eq. (3.22) is plotted in Figure 3.7. This figure clearly demonstrates the effect of rate of heterogeneity on amplification characteristics. Obviously, the mean shear velocity of the deposit increases with increase in value of a for the given magnitude of shear wave velocity at the surface. Hence, the fundamental frequency of the deposit increases with increase in the value of a.
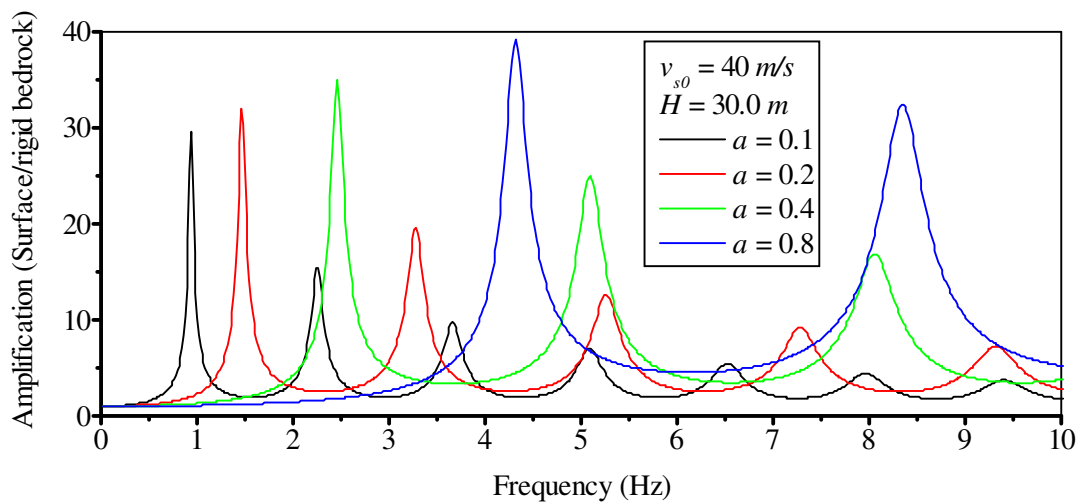
Figure 3.7: Amplification characteristics for the deposit of linearly increasing shear wave velocity profile with different rates of heterogeneities.
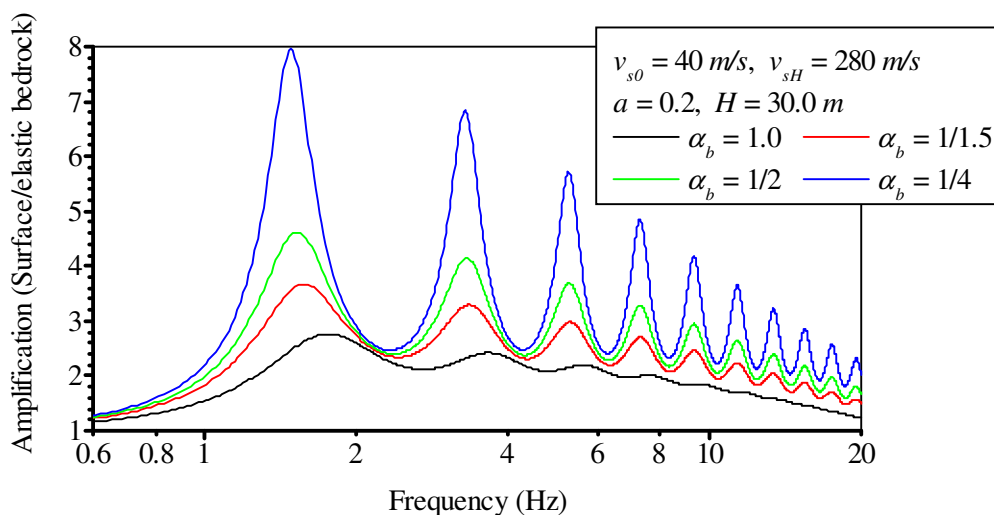
Figure 3.8: Amplification characteristics for the deposit of linearly increasing shear wave velocity profile overlying elastic bedrock with different impedances.

In order to study the effect of impedance ratio between base of the deposit and elastic bedrock, the amplification of surface motion is computed for 30 m thick deposit of

96

$v_{s0} = 40 \; m/s$ and $v_{sH} = 280 \; m/s$. The bedrock shear wave velocity is varied to give impedance ratio of $1/\alpha_b = 1$, 1.5, 2.0 and 4.0 between base of the soil deposit and bedrock.
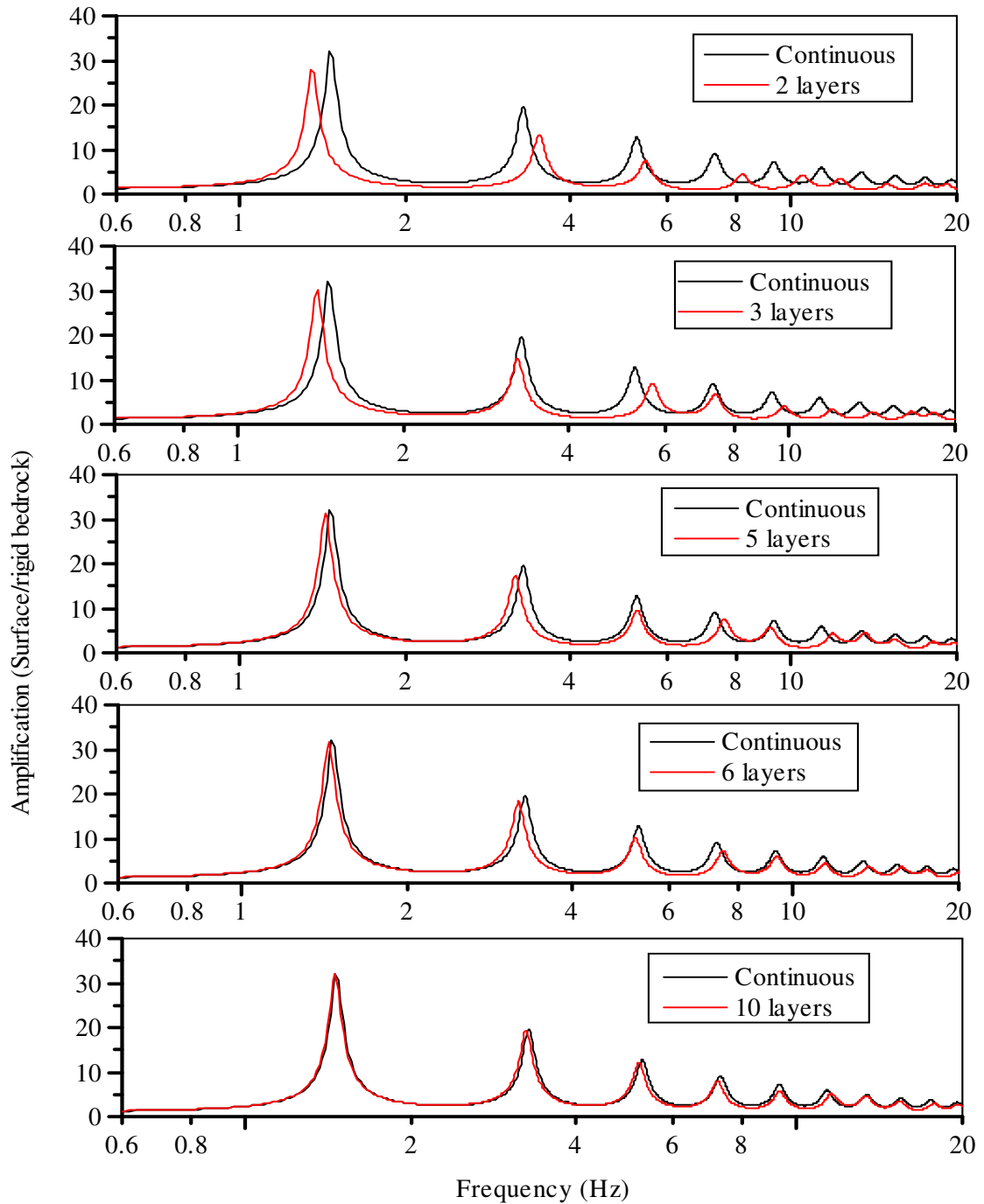
Figure 3.9: Amplification characteristics for the deposit of linearly increasing shear wave velocity profile and approximated layered profile.

Figure 3.8 presents these results obtained using Eq. (3.23), from which it can be concluded that, as the impedance ratio decreases (i.e., as the bedrock become stiffer) the peak amplification increases, also troughs get shifted upwards. Hence the flexibility of the bedrock results in increase in radiation damping. These results are obtained for the damping ratio of $\zeta = 2.5\%$. Effect of impedance ratio on modal frequencies of the deposit is almost negligible. However there is noticeable increase in fundamental frequency of the deposit as bedrock becomes more flexible which is significant for the case of $\alpha_b = 1$. More important observation to be noted is that the attenuation at troughs of the amplification function decrease at high frequencies with decrease in α_b value.

Figure 3.9 demonstrates the effect of idealizing an inhomogeneous deposit with an equivalent layered profile. For this purpose various configurations of layered profiles are considered as substitutes for the linearly distributed shear wave velocity profile. The thickness of layers for each of these different configurations is calculated keeping the impedance ratio constant between successive layers. Therefore as the number of discrete layers employed to approximate continuous variation of shear wave velocity increases the impedance ratio between layers approach one. However, as demonstrated earlier impedance ratio never becomes one irrespective any number of layers that are used. From this figure it is clear that when 10 layers are used to represent actual profile the amplification almost converges to exact analytical solution, however this is valid for the type and degree of inhomogeneity considered here. Also as the number of layers decreases the impedance contrast is increased between the layers which in turn significantly affect the high frequency response with underestimation of peak values.

3.4.2 Continuous variation of shear wave velocity with $n < 1$ and $n > 1$ $(n \neq 1)$

In the study presented above only the case of soil deposits with shear wave velocity varying linearly along the depth is considered. In order to study the effect of variation of shear wave velocity as a nonlinear function of depth of the deposit on amplification characteristics of the surface motion, some of the recent literature in this regard has

98

been reviewed. These studies mainly differ in type and kind of depth dependent function, defining the variation of shear wave velocity or shear modulus of the soil deposit, considered for the analysis. These studies cover most of the real situations of continuously inhomogeneous ground encountered in practice. Most important among these studies include Towhata (1996), Hadid and Afra (2000), Afra and Pecker (2002), Davis and Hunt (1994), Davis (1995), Rovithis et al. (2011) and Vrettos (2013). These analytical studies may be considered as general in the sense; the results are presented for arbitrary values of the parameters that define the degree of inhomogeneity unlike the study presented in the previous section wherein the solutions were obtained for particular case of inhomogeneity parameters.

Towhata (1996) observed that routine analysis with treatment of inhomogeneity of the soil deposit using approximated layered idealisation with distinct uniform layer properties resulted in contradictory response values. That is, the peak ground acceleration values computed from routine analysis yielded lower values for relatively soft deposits when compared with that obtained for stiffer soil deposits. Hence, Towhata (1996) dealt the case of continuous variation of shear modulus property in a manner described by the following relation,

$$G(z) = \Lambda(z + z_0)^m \tag{3.24}$$

Here Λ is a constant parameter which controls the magnitude of the shear modulus of $G(z)$, while the parameter z_0 governs the rate of inhomogeneity and the power m stands for type of inhomogeneity which is a function physical and mechanical characteristics of the soil deposit.

In fact one can establish equivalence between Eq. (3.6) and Eq. (3.24) by virtue of the relationship $v_s(z) = \left(G(z)/\rho\right)^{0.5}$ where ρ is assumed to be constant. The relationship between the parameters of Equations (3.6) and (3.24) are $v_{s0} = \sqrt{\Lambda z_0^m / \rho}$, $n = m/2$ and $a = z_0^{-1}$. However, most importantly, the limitation of Eq. (3.6) is $v_{s0} \neq 0$. Hence it is convenient to use Eq. (3.24) whenever it is required to consider $v_{s0} = 0$ or low shear wave velocity value near the surface. Towhata (1996) presented the relationship for

displacement as a function of depth and results presented are limited to amplification of surface motion with respect to outcropping rock motion for undamped case. The amplification functions derived based on the procedure of Towhata (1996) are presented below. Herein, this particular study is extended to include amplification with respect to rigid bedrock motion and damped response. Relationships for both the amplification functions, $Amp_{(1)}$ and $Amp_{(2)}$, are derived and presented. Figure 3.10 shows the inhomogeneous soil deposit considered in the analysis.
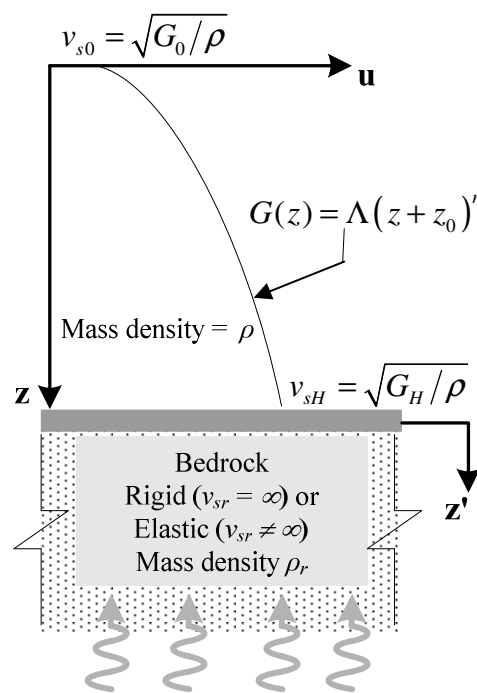
Figure 3.10: Details of the continuously inhomogeneous soil deposit considered in the analysis

Substituting Eq. (3.24) in Eq. (3.4) and assuming mass density of the soil deposit as constant we get,

$$\rho \frac{\partial^2 u}{\partial t^2} = \frac{\partial}{\partial z}\left\{\Lambda(z_0 + z)^m \frac{\partial u}{\partial z}\right\} \tag{3.25}$$

Seeking harmonic solution of the equation, the displacement and shear stress in horizontal direction may be expressed as

$$u(z,t) = U(z)e^{i\omega t} \tag{3.26}$$

$$\tau(z,t) = T(z)e^{i\omega t} \tag{3.27}$$

Amplitudes of displacement and shear stress $U(z)$ and $T(z)$ respectively are related as,

$$T(z) = G(z)\frac{\partial U(z)}{\partial z} \tag{3.28}$$

Finally, Equations (3.25), (3.26), (3.27) and (3.28) yields [Towhata (1996)],

$$(z_0 + z)^m \frac{d^2T}{dz^2} + \frac{\rho\omega^2}{A}T = 0 \tag{3.29}$$

The solution of this equation in terms Bessel's functions is given by Towhata (1996) for the cases $0 < m < 2$, $m = 2$ and $m > 2$. However, for $m = 2$ that corresponds to the shear wave velocity profile with linear variation, the amplification results have been presented earlier (Section 3.4.1). In the analysis carried out by Towhata (1996) the bedrock underlying the soil deposit is considered to be elastic and the amplification results presented therein was limited to $v_{sr} = v_{sH}$. Also the results presented by Towhata (1996) were limited to undamped response of the deposit. For the purpose of carrying out more general parametric study including effect of variation of impedance at the interface of soil and bedrock the essential amplification functions have been derived including effect of damping in the following sections.

3.4.2.1 Case 1: *0 < m < 2*

The solution of Eq. (3.29) for shear stress and displacement are,

$$\left.\begin{aligned} T(z) &= (z_0 + z)^{0.5}\left\{A_1 J_\nu(\xi) + A_2 Y_\nu(\xi)\right\} \\[2em] U(z) &= \frac{-(z_0 + z)^{-0.5}}{\rho\omega^2}\left[\left\{A_1 J_\nu(\xi) + A_2 Y_\nu(\xi)\right\} - \frac{2-m}{2}\xi\left\{A_1 J_{\nu+1}(\xi) + A_2 Y_{\nu+1}(\xi)\right\}\right] \end{aligned}\right\} \tag{3.30}$$

Here A_1 and A_2 are constants. Bessel functions of first and second kinds of order v are respectively represented by $J_v(\bullet)$ and $Y_v(\bullet)$. The order of the Bessel function, v and transformed depth coordinate, ξ are given by the following

$$
\left.\begin{aligned}
v &= 1/(2-m) \\
\xi &= 2v\sqrt{\rho\omega^2/\Lambda}\,(z_0+z)^{\left(1-\frac{m}{2}\right)}
\end{aligned}\right\}
\tag{3.31}
$$

Using the boundary condition, at $z = 0$ shear stress is zero in Eq. (3.30), the expression for displacement amplitude is obtained as,

$$
U(z) = \frac{A_3(z_0+z)^{-0.5}}{\rho\omega^2} \times \left[Y_v(\xi_0)\left\{ J_v(\xi) - \frac{2-m}{2}\xi J_{v+1}(\xi) \right\} \right.
$$
$$
\left. - J_v(\xi_0)\left\{ Y_v(\xi) - \frac{2-m}{2}\xi Y_{v+1}(\xi) \right\} \right]
\tag{3.32}
$$

Here A_3 is a new constant given by $A_3 = \dfrac{A_2}{J_v(\xi_0)}$ and ξ_0 is the value of ξ at $z = 0$.

Therefore displacement amplitude at $z = 0$ and at $z = H$ are obtained using Eq. (3.32)

$$
U(0) = \frac{A_3(m-2)}{\pi\rho\omega^2\sqrt{z_0}}
\tag{3.33}
$$

$$
U(H) = \frac{A_3(z_0+H)^{-0.5}}{\rho\omega^2}\left[Y_v(\xi_0)\left\{ J_v(\xi_H) - \frac{2-m}{2}\xi_H J_{v+1}(\xi_H) \right\} \right.
$$
$$
\left. - J_v(\xi_0)\left\{ Y_v(\xi_H) - \frac{2-m}{2}\xi_H Y_{v+1}(\xi_H) \right\} \right]
\tag{3.34}
$$

The shear stress amplitude at $z = H$ obtained from Eq. (3.30) is,

$$
\mathrm{T}(H) = A_3(z_0+H)^{0.5}\left\{ -Y_v(\xi_0)J_v(\xi_H) + J_v(\xi_0)Y_v(\xi_H) \right\}
\tag{3.35}
$$

ξ_H is the value of ξ at $z = H$. Assuming bedrock underlying the soil deposit as rigid (within motion) the amplification of input motion with respect to ground surface motion is given by ratio of U_0 and U_H i.e.,

102

$$Amp_{(1)} = \frac{U_0(z=0)}{U_H(z=H)} = \sqrt{\frac{(z_0+H)}{z_0}} \frac{m-2}{\pi} \times$$

$$\left[Y_\nu(\xi_0) \left\{ J_\nu(\xi_H) - \frac{2-m}{2} \xi_H J_{\nu+1}(\xi_H) \right\} \right. \qquad (3.36)$$

$$\left. - J_\nu(\xi_0) \left\{ Y_\nu(\xi_H) - \frac{2-m}{2} \xi_H Y_{\nu+1}(\xi_H) \right\} \right]^{-1}$$

For the case of elastic bedrock (outcrop motion), if the z' is the depth coordinate measured from the top of bedrock (Figure 3.10) then the displacement and shear stress for $z' \geq 0.0$ is given by Eq. (3.18) and Eq. (3.19) respectively. Satisfying the boundary condition with respect to continuity of displacement and shear stress at soil and bedrock interface, we get,

$$Amp_{(2)} = \frac{U_0}{2A_1'} = \frac{m-2}{\pi\rho\omega^2\sqrt{z_0}} \times$$

$$\left(\frac{1}{\rho\omega^2\sqrt{z_0+H}} \left[Y_\nu(\xi_0) \left\{ J_\nu(\xi_H) - \frac{2-m}{2} \xi_H J_{\nu+1}(\xi_H) \right\} \right. \right.$$

$$\left. - J_\nu(\xi_0) \left\{ Y_\nu(\xi_H) - \frac{2-m}{2} \xi_H Y_{\nu+1}(\xi_H) \right\} \right] \qquad (3.37)$$

$$\left. + \frac{\sqrt{z_0+H}}{i\omega\rho_r v_{sr}} \left[Y_\nu(\xi_H) J_\nu(\xi_0) - Y_\nu(\xi_0) J_\nu(\xi_H) \right] \right)^{-1}$$

Gazetas (1982) dealt this case ($0 < m < 2$) adopting the depth dependent shear wave velocity function in the form given by Eq. (3.6) and presented results for limited cases of n values. While Rovithis et al. (2011) presented the results for the more general case in the sense that for $0 < n \leq 1$. However they extended their study to deposit consisting of two layers with continuously inhomogeneous top layer being overlying a homogeneous deposit. This particular case will be discussed later in this chapter. The amplification function given by them is limited to ratio between motions at surface and rigid bedrock at the base.

3.4.2.2 Case 2: _m >2_

Following the same procedure as dealt above the displacement amplitude along the depth of the deposit is obtained for $m > 2$ as,

$$U(z) = \frac{A_3}{\sqrt{\Lambda\rho}\omega(z_0 + z)^{0.5(m-1)}}\left[Y_{-\nu}(-\xi_0)J_{1-\nu}(-\xi) - J_{-\nu}(-\xi_0)Y_{1-\nu}(-\xi)\right] \qquad (3.38)$$

Above equation is used to compute surface ($z = 0$) and base ($z = H$) displacement as

$$U(0) = \frac{A_3(m-2)}{\pi\rho\omega^2\sqrt{z_0}} \qquad (3.39)$$

$$U(H) = U(z) = \frac{A_3}{\sqrt{\Lambda\rho}\omega z_0^{0.5(m-1)}}\left[Y_{-\nu}(-\xi_0)J_{1-\nu}(-\xi_H) - J_{-\nu}(-\xi_0)Y_{1-\nu}(-\xi_H)\right](3.40)$$

Amplification ratio for the case $m > 2$ can be obtained for input motion prescribed at the top of rigid bedrock as

$$Amp_{(1)} = \frac{m-2}{\pi\omega}\sqrt{\frac{\Lambda(z_0 + H)^{m-1}}{\rho z_0}}\left[Y_{-\nu}(-\xi_0)J_{1-\nu}(-\xi_H) - J_{-\nu}(-\xi_0)Y_{1-\nu}(-\xi_H)\right]^{-1}(3.41)$$

The amplification of input motion prescribed at the top of outcropping rock surface with respect to surface motion of the soil deposit is given by

$$Amp_{(2)} = \frac{m-2}{\pi\rho\omega^2\sqrt{z_0}} \times$$

$$\left(\frac{1}{\sqrt{\Lambda\omega^2\rho(z_0 + H)^{m-1}}}\left[Y_{-\nu}(-\xi_0)J_{1-\nu}(-\xi_H) - J_{-\nu}(-\xi_0)Y_{1-\nu}(-\xi_H)\right]\right.$$

$$\left.+ \frac{\sqrt{(z_0 + H)}}{i\omega\rho_r v_{sr}}\left[J_{-\nu}(-\xi_0)Y_{-\nu}(-\xi_H) - Y_{-\nu}(-\xi_0)J_{-\nu}(-\xi_H)\right]\right)^{-1}$$

(3.42)

The amplification functions presented above are limited to undamped response only. As explained earlier in section 3.4.1, in order to account for equivalent viscous damping of the soil the complex shear modulus (G^*) or complex shear wave velocity (v_s^*) can be substituted for G and v_s respectively [Kramer (1996)]. That is, for the case of viscous damping, $G^* = G(1+2i\zeta)$ or $v_s^* = v_s\sqrt{1+2i\zeta}$ where ζ is equivalent viscous damping ratio.

3.4.3 Mode shapes

3.4.3.1 Case 1: $0 < m < 2$

Natural frequencies of the continuously inhomogeneous deposit having shear modulus distribution given by Eq. (3.24), for the case of $0 < m < 2$, can be extracted using Eq. 3.34. Imposing the condition of zero displacement at the base under the state of free vibration we get the characteristic equation,

$$Y_v(\xi_0)\left\{J_v(\xi_H)-\frac{2-m}{2}\xi_H J_{v+1}(\xi_H)\right\}-J_v(\xi_0)\left\{Y_v(\xi_H)-\frac{2-m}{2}\xi_H Y_{v+1}(\xi_H)\right\}=0 \quad (3.43)$$

Solving the above equation we get the ith root $\xi_H^{(i)}$ which in turn yields corresponding natural frequency ω_i of the soil deposit as,

$$\omega_i = \frac{\xi_H^{(i)}(2-m)}{2(z_0+H)}v_{sH} \quad (3.44)$$

The corresponding free vibration displacement function $\left(U^{(i)}(z)\right)$ along the depth is obtained by substituting Eq. 3.44 in Eq. 3.32. Normalizing this depth dependent displacement with respect to surface displacement results in dimensionless mode shape, $\Phi^{(i)}(z)$ as follows,

$$\Phi^{(i)}(z) = \frac{\pi}{(m-2)}\sqrt{\frac{z_0}{z_0+z}}\times\left[Y_v\left(\xi_0^{(i)}\right)\left\{J_v\left(\xi^{(i)}\right)-\frac{2-m}{2}\xi^{(i)}J_{v+1}\left(\xi^{(i)}\right)\right\}\right.$$
$$\left.-J_v\left(\xi_0^{(i)}\right)\left\{Y_v\left(\xi^{(i)}\right)-\frac{2-m}{2}\xi^{(i)}Y_{v+1}\left(\xi^{(i)}\right)\right\}\right] \quad (3.45)$$

3.4.3.2 Case 2: *m >2*

The characteristic equation for the case of $m > 2$, is obtained using Eq. 3.40, as

$$Y_{-\nu}\left(-\xi_0\right)J_{1-\nu}\left(-\xi_H\right)-J_{-\nu}\left(-\xi_0\right)Y_{1-\nu}\left(-\xi_H\right)=0 \tag{3.46}$$

After solving the above equation for $\xi_H^{(i)}$, the corresponding frequencies can be calculated using Eq. (3.44). Finally the mode shape corresponding to that particular modal frequency is obtained using Eq. (3.44) and Eq. (3.38) as follows,

$$\Phi^{(i)}(z)=\frac{\pi\omega}{m-2}\sqrt{\frac{\rho z_0}{\Lambda\left(z_0+H\right)^{m-1}}}\times$$
$$\left[Y_{-\nu}\left(-\xi_0^{(i)}\right)J_{1-\nu}\left(-\xi^{(i)}\right)-J_{-\nu}\left(-\xi_0^{(i)}\right)Y_{1-\nu}\left(-\xi^{(i)}\right)\right] \tag{3.47}$$

3.4.4 Parametric study on effect of inhomogeneity parameters

To compute amplification for different degrees of inhomogeneities of the soil deposit with respect to both rigid and elastic bedrock cases using Equations (3.36, 3.37, 3.41 and 3.42) MATLAB® code is developed. Using this program some of the the examples of the parametric study presented in Towhata (1996) are reproduced. In the first case the deposit 30.0 *m* thick with surface shear wave velocity v_{s0}, equal to 100 *m/s* is considered. For this relatively stiff deposit overlying elastic base, the amplification function ($Amp_{(2)}$) is obtained for $m=1$ and $m=4$ with impedance ratio of one between base of the deposit and bedrock (i.e. $v_{sr}=v_{sH}=300 \ m/s$). While in the second case, $v_{s0}=10 \ m/s$ with $v_{sr}=v_{sH}=300 \ m/s$ are used to represent the deposit which is relatively soft near the surface. The results presented in Figure 3.11 are for undamped case with base to bedrock impedance ratio of one. The shear wave velocity profiles corresponding to all the four cases considered here are also shown. This figure clearly demonstrates the effect of type and degree of inhomogeneity on the stiffness of the deposit near the surface. As the value of exponent of the shear wave velocity or shear modulus variation function increases, the profile characterizes

reduction in stiffness near surface, hence greatly affects the surface amplification of base input motion.
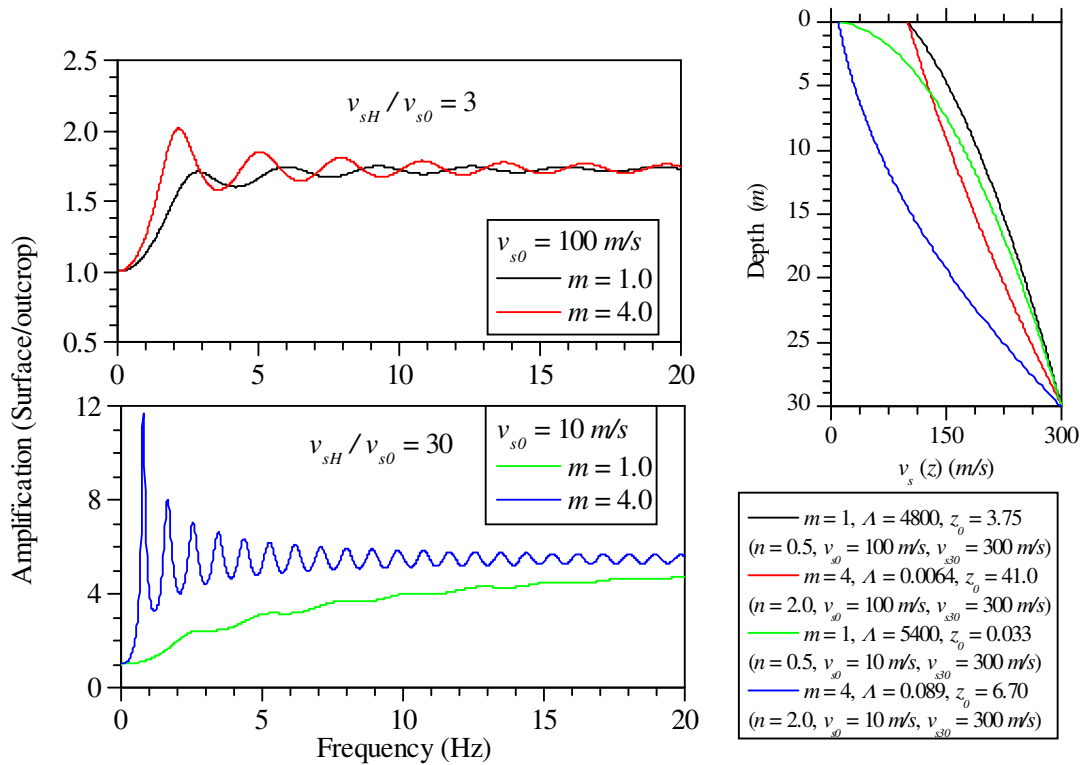
Figure 3.11: Amplification of inhomogeneous soil deposit for different values of m and v_{s0}. Results reproduced for the examples taken from Towhata (1996)

In the first case ($v_{s0} = 100 \ m/s$) the effect of variation in the value of m is almost insignificant. Particularly at high frequencies the amplification converges to a constant value of about 1.7 irrespective of type of inhomogeneity. In case of relatively soft deposit ($v_{s0} = 10 \ m/s$) there appears to be significant effect of type of inhomogeneity. In case of $m = 4$ the surface motion is amplified manifold in the lower frequency range compared to $m = 1$ and in the high frequency range the amplification converges to constant value of about 5.5. Hence it can be concluded that in the lower frequency range the amplification depends on type of inhomogeneity.

It is interesting to note that, the amplification is almost converging to a unique value for both the cases with different values of m in the high frequency range. In fact it can be shown that both Eq. (3.37) and Eq. (3.42) converge to $\sqrt{v_{sH}/v_{s0}}$ for all values

of m and for large values of ω. In the first case $\sqrt{v_{sH}/v_{s0}} = \sqrt{3}$ and in the second case $\sqrt{v_{sH}/v_{s0}} = \sqrt{30}$ which are close to the values in the Figure 3.11 at high frequency ranges. In order investigate this aspect the amplification at surface are computed for different values of m.
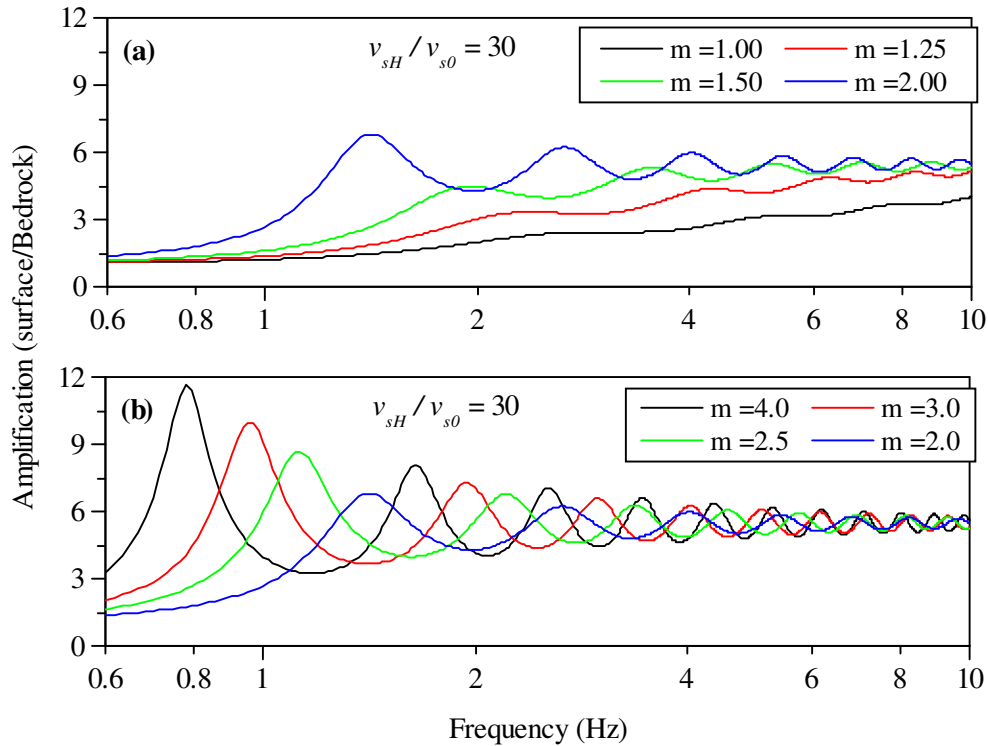
Figure 3.12: Amplification of inhomogeneous soil deposit for $v_{sH}/v_{s0} = 30$ and different values of m

Figure 3.12(a) and 3.12(b) show the effect of m on amplification function for $m \leq 2$ and $m \geq 2$ respectively. All the curves shown in these figures are obtained for $v_{s0} = 10 \ m/s$ and $v_{sr} = v_{sH} = 300 \ m/s$. As stated above, it is evident that high frequency range amplification is almost same (of about $\sqrt{v_{sH}/v_{s0}}$) for all values of m. However for the case of $m \leq 2$ the convergence to this unique value is at much higher values of frequencies compared to $m \geq 2$. Also for the case of $m \geq 2$, right from first peak the amplification function is oscillating about the value equal to $\sqrt{v_{sH}/v_{s0}}$ while for $m < 2$ this happens at higher mode peaks. Further, Figure 3.13(a) presents the

108

amplification trends for different values of ratio of base to surface shear wave velocities v_{sH}/v_{s0} (μ) with $m=1$ and $H=30$ m.

Table 3.1: Fundamental frequencies of the soil deposit considered for parametric study presented in Figure 3.13.

v_{sH}/v_{s0}	Case (a) $v_{s0}=10$ m/s		Case (b) $v_{s0}=100$ m/s	
(μ)	v_{sH}	Frequency (Hz)	v_{sH}	Frequency (Hz)
30	300	1.916	3000	19.16
20	200	1.278	2000	12.78
15	150	0.960	1500	9.60
10	100	0.643	1000	6.43
5	50	0.328	500	3.28
2	20	0.143	200	1.43
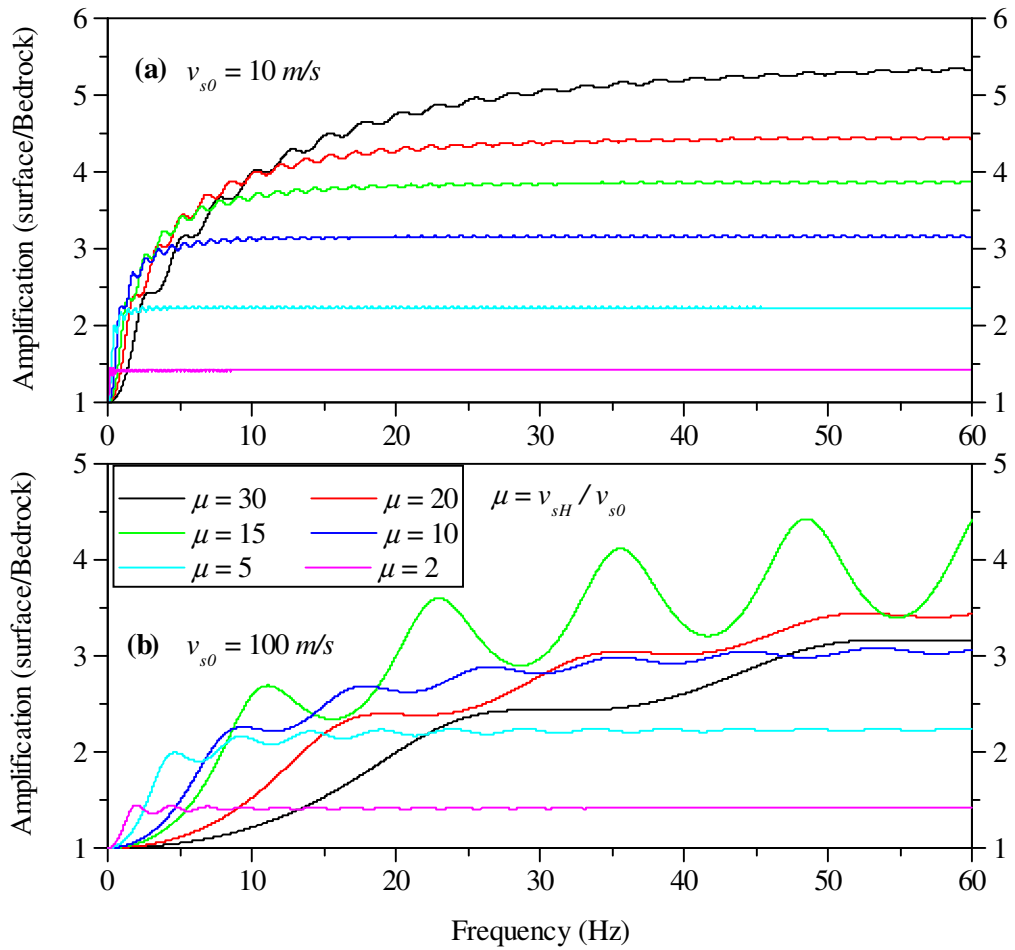
Figure 3.13: Amplification of inhomogeneous soil deposit for $m=1$ and different values of $\mu(v_{sH}/v_{s0})$; (a) $v_{s0}=10$ m/s (b) $v_{s0}=100$ m/s.

Two cases of surface shear wave velocities $v_{s0} = 10 \ m/s$ and $v_{s0} = 100 \ m/s$ have been considered for this parametric study. Figure 3.13(a) presents the results for $v_{s0} = 10 \ m/s$ while Figure 3.13(b) presents the results for $v_{s0} = 100 \ m/s$. The fundamental frequencies of the soil deposit with different inhomogeneity parameters considered here are calculated using the characteristic Eq. (3.43). These frequencies are presented in Table 3.1. For given values of μ and m the frequency is directly proportional to v_{s0} or v_{sH} . Thus increase in v_{s0} or v_{sH} proportionately increases the fundamental frequency. Thus, ten folds increase in both v_{s0} and v_{sH} in Case (b) compared to Case (a) has resulted in proportionate increase in fundamental frequency of the respective soil deposit. Obviously, frequencies corresponding to higher modes are also shifted in the same manner.

For the results presented above the analyses are carried out to obtain amplification function assuming impedance ratio between base of the deposit and bedrock as one. In the following sections results are presented for the cases of varying impedance ratio and also for the case of soil deposit overlying rigid bedrock. The shear wave velocity ratio between base and surface of the soil deposit (v_{sH} / v_{s0}) and exponent value m (or n) control the trend of the continuous variation of shear modulus (or shear wave velocity) profile. As v_{sH} / v_{s0} increases the deposit represent larger inhomogeneity, lower value of m combined with relatively large v_{sH} / v_{s0} values will result in sharp transition of shear wave velocity near the surface.

In order to study the effect of surface shear wave velocity on the response of continuously inhomogeneous deposit overlying rigid bed rock, the analysis is carried out for constant values of $v_{sH} / v_{s0} = 5$ and $m = 0.4 \left(n = 0.20 \right)$ with 5% of damping ratio and varying surface shear wave velocity $\left(v_{s0} \right)$ of the profile. The four different values of surface shear wave velocities considered are 50 *m/s*, 100 *m/s*, 200 *m/s* and 400 *m/s*. The shear wave velocity profiles considered in this parametric study are shown in Figure 3.14a. The amplification transfer function obtained for these cases is shown in Figure 3.14b.
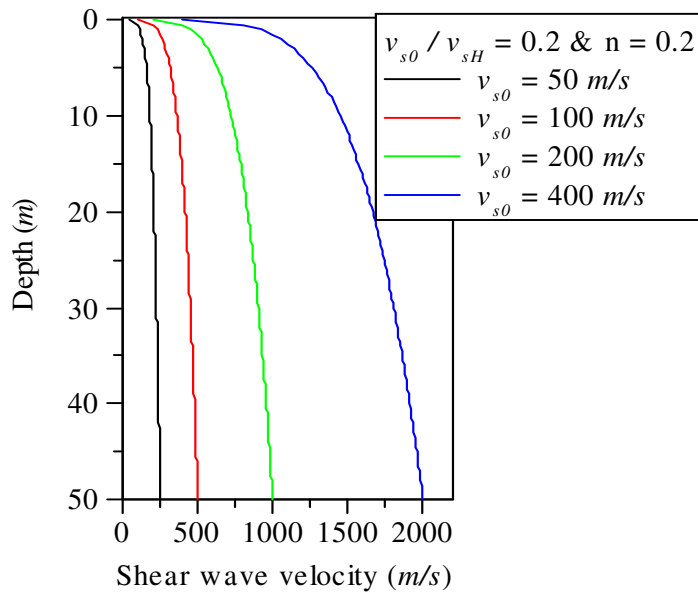
Figure 3.14a: Profiles with continuous variation of shear wave velocity,
$v_{sH} / v_{s0} = 5$ & $m = 0.4 (n = 0.20)$ **for different surface shear wave velocities**
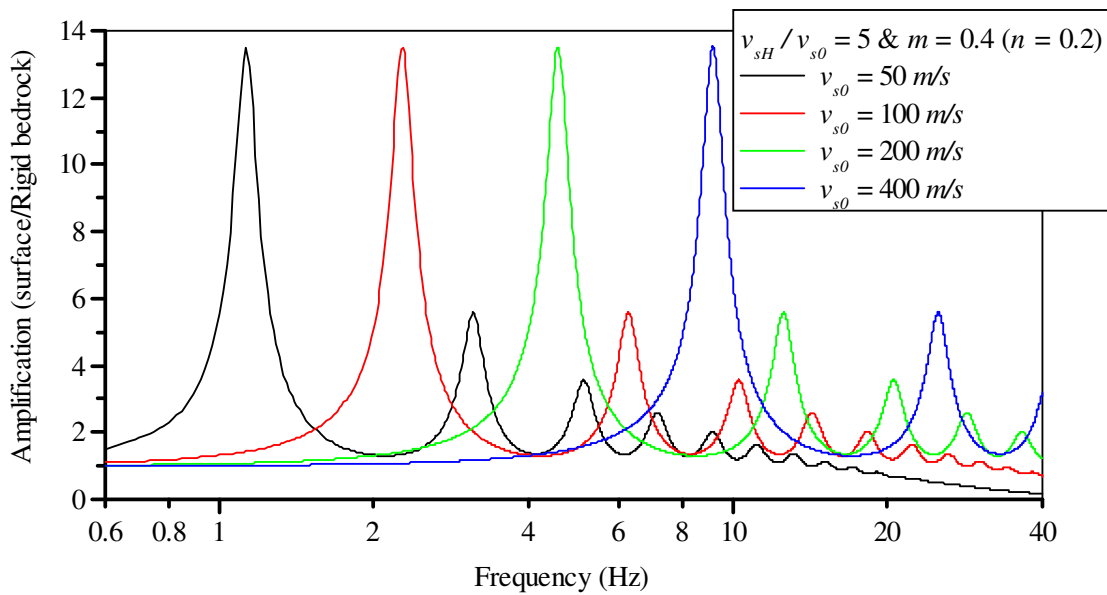
Figure 3.14b: Effect of surface velocity on amplification of inhomogeneous deposit overlying rigid bedrock

It can be observed that for constant values of inhomogeneity parameters i.e., surface to base shear wave velocity ratio and exponent value ($v_{sH} / v_{s0} = 5.0$ & $m = 0.40$) the amplification at all modes remains same irrespective of surface shear wave velocity (v_{s0}) value. However, the variation in periods corresponding to these peak values of amplification transfer function is considerable for different surface shear wave

velocities. That is, the modal frequency characteristic of the deposit is sensitive to surface shear wave velocity of the deposit with all other factors of the inhomogeneous deposit being constant. As v_{s0} increases, the modal frequencies increase while amplifications with respect to these frequencies remain almost unaffected. Also, ratio between successive modal frequencies increase as the soil becomes stiffer as v_{s0} increase. Thus it can be concluded that the amplification characteristics are depend on v_{sH}/v_{s0}, m and v_{s0} in case of an inhomogeneous deposit.

An analysis is also carried out for the values of $m = 0.02$, 0.40, 1.20, 2.0 and 4.0 (i.e. n = 0.01, 0.20, 0.60, 1.0 and 2.0). The values of v_{sH}/v_{s0} considered in this analysis are 1.25, 2.0, 4.0 and 20 with v_{s0} equal to 200 m/s. Figure 3.15 shows the effect of inhomogeneity parameters on the amplification of surface motion due to input motion prescribed at the top of rigid bedrock.

The effect of exponent value, m, of the inhomogeneity function on the amplification peaks is almost insignificant when the velocity ratio is close to one i.e., which correspond to more or less homogeneous deposit. But the amplification peaks are well separated and shifted to higher frequencies as velocity ratio increases because the modal frequencies increase with increase in v_{sH}/v_{s0} value. Thus it can be concluded that, modal characteristics of the deposit is very much sensitive to shear wave velocity ratio v_{sH}/v_{s0} particularly for larger values compared to small values of v_{sH}/v_{s0}.

For $m < 1$ the difference in peak amplification corresponding to fundamental frequency is noticeable for all cases of v_{sH}/v_{s0} considered. On the other hand for $m > 1$ amplification peaks corresponding to fundamental frequency is almost same except for very large value of v_{sH}/v_{s0} in which case the peak amplification is marginally enhanced for $m = 1$. For all the results presented in this figure damping ratio of 5% is used. For the soil deposit on rigid bedrock the effect of inhomogeneity appears to be relatively inconsequential as shown in both Figure 3.14b and Figure 3.15 when compared to deposit on elastic base as evident from Figures 3.11, 3.12 and 3.13.
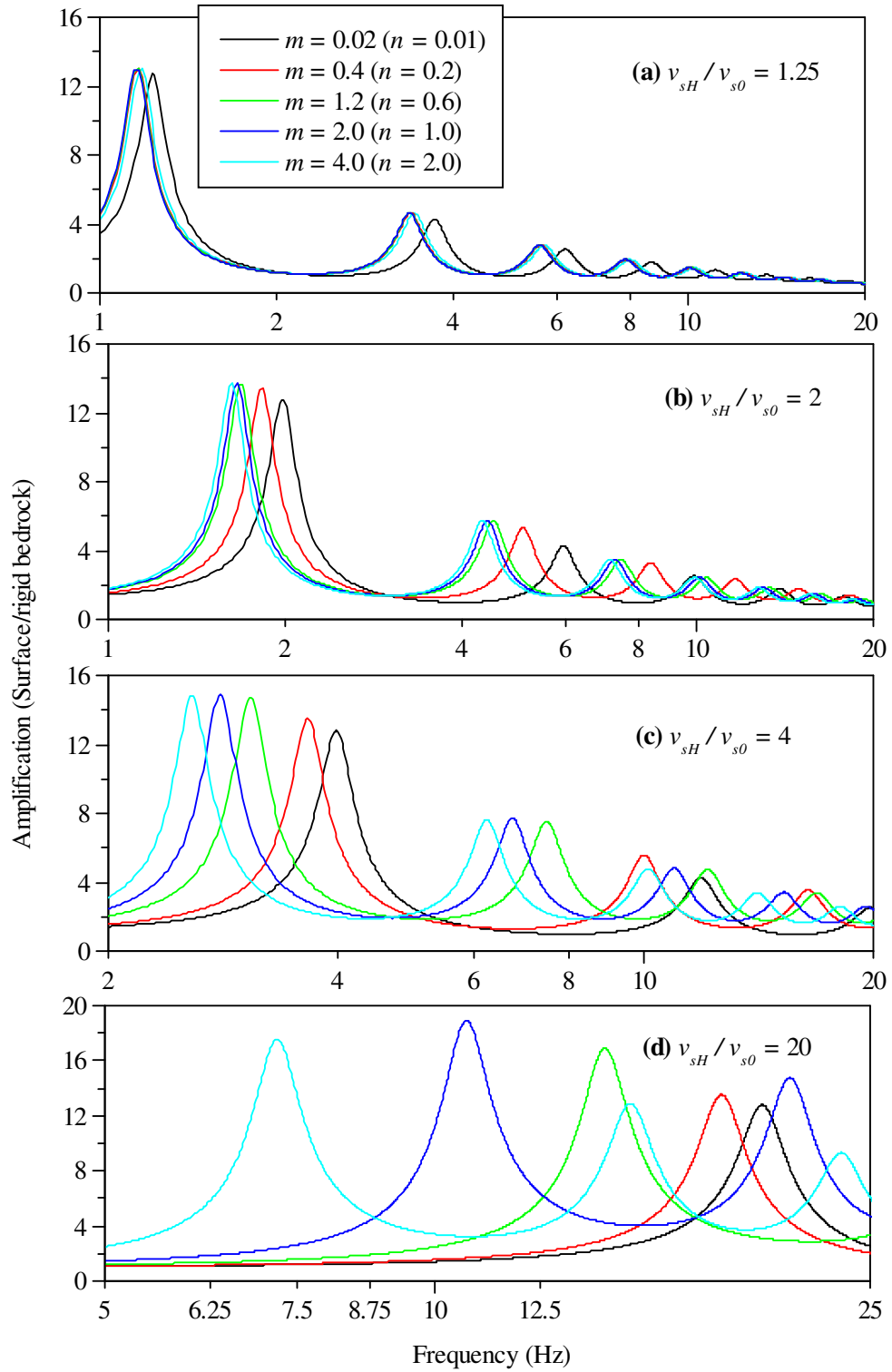
Figure 3.15: Effect of inhomogeneity parameters on amplification of inhomogeneous deposit overlying rigid bedrock.
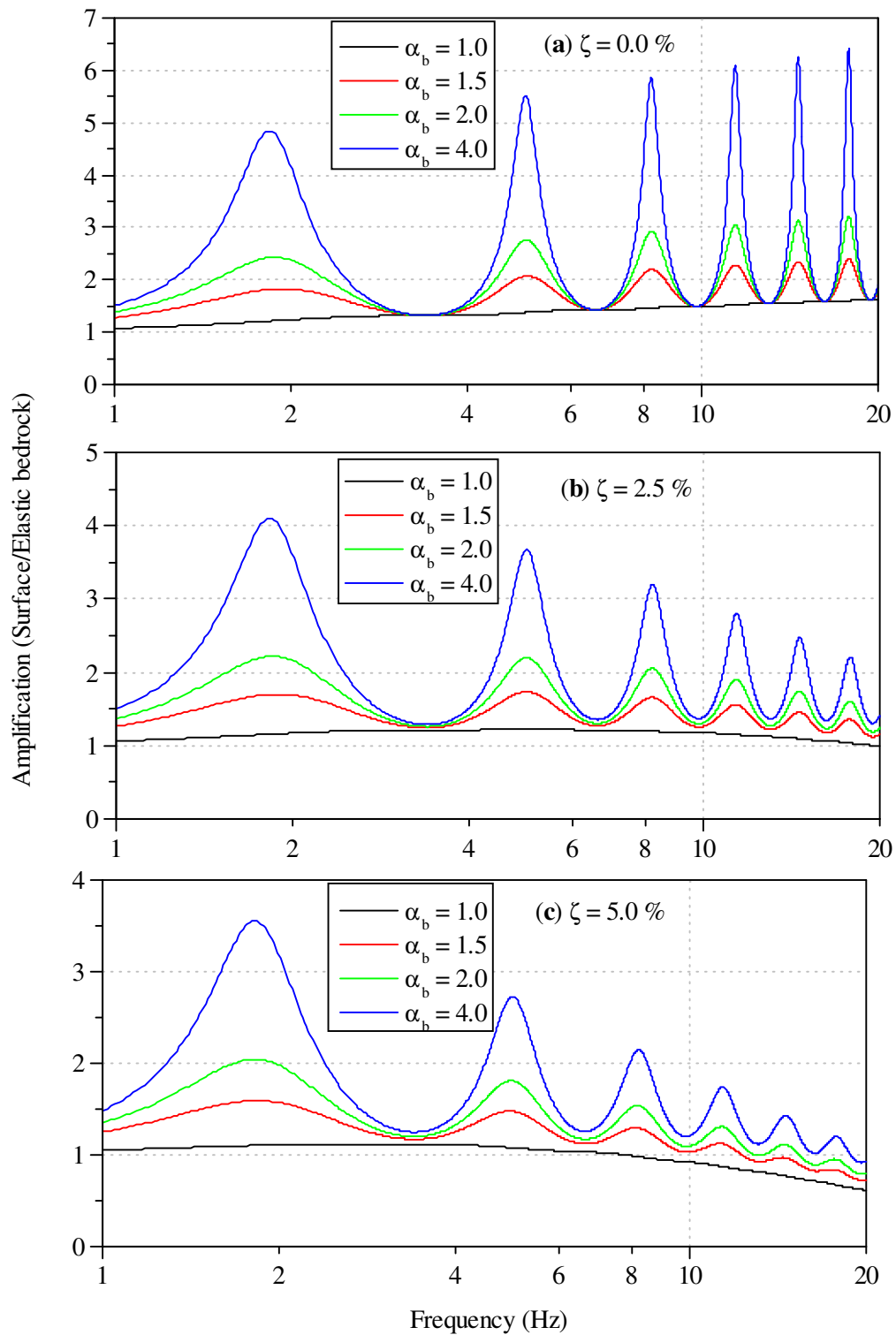
Figure 3.16: Effect of impedance ratio between base of the soil deposit and bedrock on amplification of inhomogeneous deposit overlying elastic bedrock for different damping ratios of the soil ($v_{s0} = 100 m/s, \mu = 4 \& m = 0.4$).

Figure 3.16 shows the effect of contrasting impedances of soil and the elastic bedrock on the amplification characteristics. For an undamped case, the amplification increases with frequency for all values of impedance ratios, α_b at the base with respect to bedrock, as observed earlier. The rate of increase in amplification peak values decreases with increase in frequency and this decrease in rate of increase in peak values appears to be considerable with increase in impedance ratio. On the other hand as the damping ratio increases the peaks of the amplification function monotonically decreases. The decrease in amplification is apparently considerable with increase in impedance ratio.

3.4.5 Effect of inhomogeneity parameters on mode shapes

In an attempt to understand overall effect of inhomogeneity parameters on the response, particularly consequence of low surface shear wave velocity deposits combined with higher degree of inhomogeneity, mode shapes are computed for soil deposits with different inhomogeneity parameters. For this purpose, for two different cases of surface to base shear wave velocity ratios mode shapes are computed using Eq. (3.45) and Eq. (3.47) respectively for the different values of m in the ranges $m < 2$ and $m > 2$. The values of m used in this analysis are 0.5, 1.5, 2.5 and 4.0. The natural frequencies corresponding to first four modes for all the cases considered in this study are computed using the respective characteristic equations of Eq. (3.43) and Eq. (3.46). These modal frequencies are presented in Table 3.2.

Table 3.2: First four modal frequencies of the soil deposits with different inhomogeneity parameters

	$\mu(v_{sH}/v_{s0}) = 2$				$\mu(v_{sH}/v_{s0}) = 20$			
$m \rightarrow$	0.5	1.5	2.5	4.0	0.5	1.5	2.5	4.0
$\omega_1\,(rad/s)$	2.84	2.63	2.57	2.54	28.00	20.04	14.49	11.25
$\omega_2\,(rad/s)$	7.75	7.01	6.87	6.79	74.82	40.90	29.02	23.67
$\omega_3\,(rad/s)$	12.75	11.56	11.31	11.18	121.86	63.82	45.36	36.91
$\omega_4\,(rad/s)$	17.77	16.13	15.79	15.60	168.95	87.49	62.26	50.51
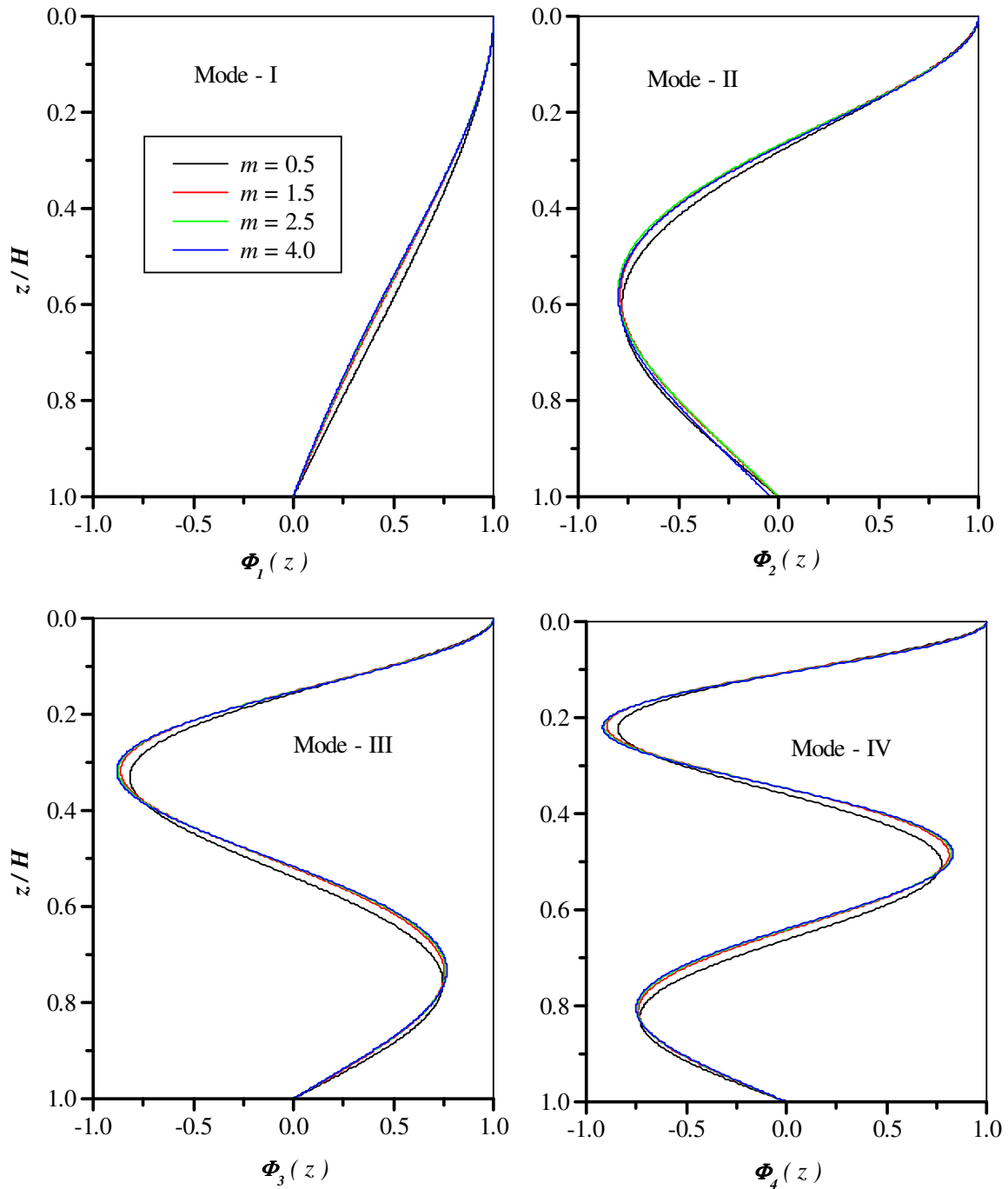
Figure 3.17: Mode shapes for the soil deposit with $\mu\left(v_{sH}/v_{s0}\right)=2$ **for different values of** *m***.**
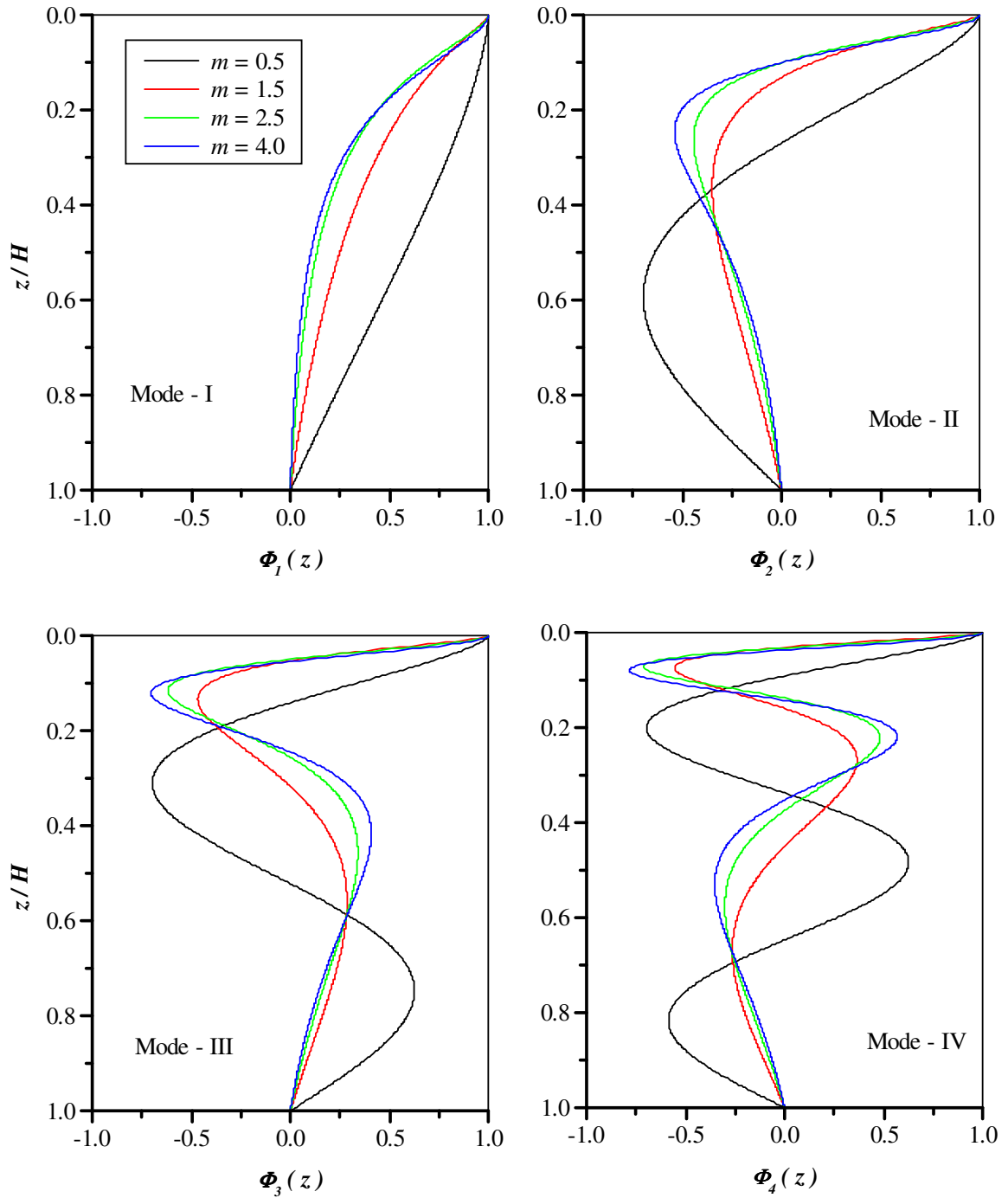
Figure 3.18: Mode shapes for the soil deposit with $\mu\left(v_{sH}/v_{s0}\right) = 20$ **for different values of *m*.**

Figure 3.17 and Figure 3.18 show the mode shapes of the soil deposit with $\mu\left(v_{sH}/v_{s0}\right)=2$ and $\mu\left(v_{sH}/v_{s0}\right)=20$ respectively. First case ($\mu=2.0$) represents a soil deposit which is close to homogeneous deposit while latter one ($\mu=20.0$) represents a case of higher degree of inhomogeneity particularly low surface shear wave velocity. Interestingly, mode shapes of soil deposit with $\mu=2$ are almost tangential to the vertical near the surface. While for the soil deposit with $\mu=20$ the mode shapes become tangential to the horizontal in case of all modes. It is clear from these figures that, the mode shapes are almost comparable to homogeneous deposit for a soil deposit with moderate inhomogeneity and also satisfy zero shear stress boundary condition at the surface [Rovithis et al. (2011)].

The contradictory trend in mode shape near the surface in case of higher degree of inhomogeneity is of particular interest in view of large near surface amplification. As the soil deposit is relatively weaker near the surface more is the deviation from the assumed boundary condition of zero shear strain at the surface. This aspect is well demonstrated by Towhata (1996) with paradoxical results obtained in case of routine layered deposit idealisation. In fact, Travasarou and Gazetas (2004) have shown that the assumption of zero shear strain at the surface for the case of vanishing near surface stiffness will result in underestimation of response quantities when the soil deposit is discretised into homogeneous layers.

3.5 INHOMOGENEOUS DEPOSIT OVERLYING A HOMOGENEOUS LAYER OF FINITE THICKNESS

In the previous sections the analytical solutions presented was limited to a single continuously inhomogeneous layer overlying rigid or elastic bedrock. In this section some of the analytical solutions available in the literature with regard to a continuously inhomogeneous layer overlying a homogeneous layer are discussed. Results presented in Figures 3.11 and 3.12 of previous section are, in fact, pertaining to the configuration of inhomogeneous layer overlying a homogeneous half-space. This configuration is a consequence of assuming impedance ratio one between base of inhomogeneous soil deposit and underlying soil stratum. Afra and Pecker (2002)

considered an inhomogeneous layer at the top of homogeneous half-space. In their study, the shear modulus of the top layer is characterised by continuous function of depth analogous to Eq. (3.24) in which the exponent value was limited to $0 \le m < 2$. Later this solution is extended to include the case of finite thickness homogeneous layer underlying continuously inhomogeneous top layer.

Rovithis et al (2011) and Mylonakis et al. (2013) considered a two layer system in which top layer is characterised as inhomogeneous shear wave velocity profile overlying a homogeneous layer of finite thickness. The inhomogeneity function defining shear wave velocity profile of the top layer is similar to Eq. (3.6). The depth dependent shear wave velocity function considered in their study is given by,

$$v_s(z) = v_{sH} \left[b + \left(\frac{b-1}{H} \right) z \right]^n \tag{3.48}$$

i.e, it is similar to Eq. (3.6) except that $a = (b-1)/bH$. Here the parameter b is related to μ (ratio of base to surface shear wave velocities) as $b = (1/\mu)^{1/n}$.

3.5.1 Amplification of surface motion

Two-layer soil deposit consisting of homogeneous layer underlying an inhomogeneous top layer is shown in Figure 3.19. Total depth of the top layer is H_1 and H_2 is the depth of homogeneous bottom layer. The depth coordinate for the top layer is z_1 ($0 \le z_1 \le H_1$) and that for bottom layer is z_2 ($0 \le z_2 \le H_2$). The mass densities of these two layers are ρ_1 and ρ_2 respectively. The shear wave velocity profile of the top layer $v_{s1}(z_1)$, is defined by the Eq. (3.6) wherein exponent n is limited to less than one ($0 < n < 1$); while for bottom homogeneous layer, overlying rigid bedrock, it is v_{s2}. The amplification function for single inhomogeneous layer having shear wave velocity profile as defined in Eq. (3.6) overlying rigid bedrock has been obtained by Rovithis et al. (2011). Substituting Eq. (3.6) in Eq. (3.5) and following the same procedure that has been presented in the previous sections, the

displacement at any depth z_1 due to input motion at the base of the top inhomogeneous layer is obtained in terms of Bessel functions as,

$$u(z) = \frac{A_1 \left[1 + az_1\right]^{-\nu(1-n)}}{\mu \sqrt{1 + aH_1} Y_{\nu+1}\left(\xi_0^{(1)}\right)} \left\{ J_\nu\left(\xi^{(1)}\right) Y_{\nu+1}\left(\xi_0^{(1)}\right) - Y_\nu\left(\xi^{(1)}\right) J_{\nu+1}\left(\xi_0^{(1)}\right) \right\} \tag{3.49}$$

Here $\xi^{(1)}$ is the transformed depth coordinate,

$$\xi^{(1)} = \frac{\omega}{a v_{s0}(1-n)} \left(1 + az_1\right)^{1-n} \tag{3.50}$$

$\xi_0^{(1)} = \xi^{(1)}$ at $z_1 = 0$, $\nu = \dfrac{2n-1}{2(1-n)}$ $(0 < n < 1)$, $\mu = \dfrac{v_{sH}}{v_{s0}}$ and A_1 is a constant.
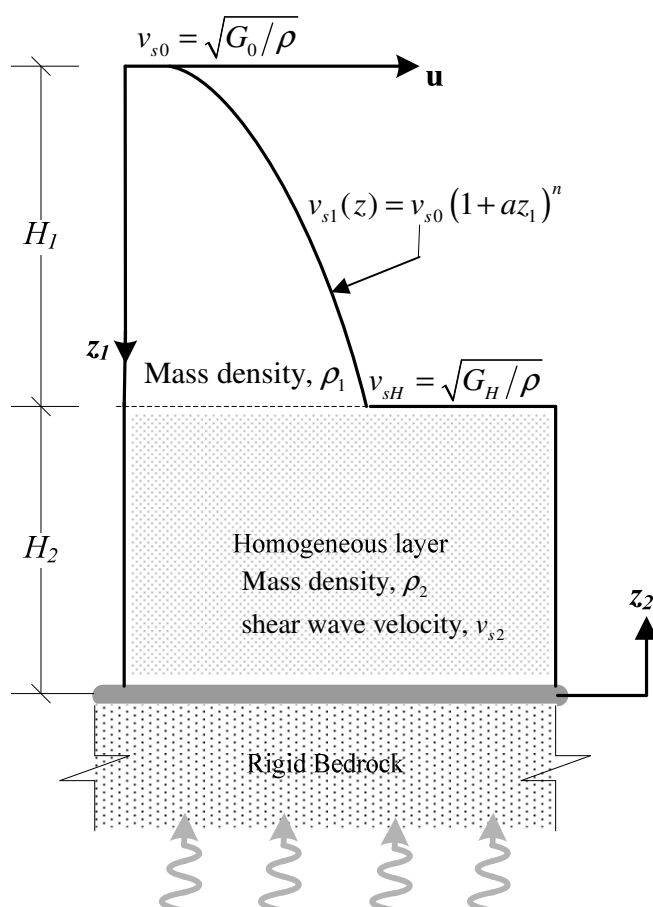
Figure 3.19: Two-layer deposit comprising of an inhomogeneous surface layer followed by a homogeneous layer over a rigid base

The response at the top of the homogeneous layer due to harmonic excitation at it base is given by [Kramer (1996)],

$$u_2(z_1 = H_1 \text{ or } z_2 = H_2) = B_1 \sin\left(\frac{\omega z_2}{v_{s2}}\right) + B_1 \cos\left(\frac{\omega z_2}{v_{s2}}\right) \tag{3.51}$$

Input motion at the bedrock level is, $u_2(z = H_1 + H_2 \text{ or } z_2 = 0) = u_H$ is the boundary condition to be used along with other boundary conditions such as, the displacement is continuous i.e., $u_2(z_2 = H_2) = u_1(z_1 = H_1)$ and $\tau_2(z_2 = H_2) = \tau_1(z_1 = H_1)$ i.e., shear stress is continuous at the layer interface. Employing these boundary conditions along with the boundary conditions at the free surface (i.e., at $z_1 = 0$ enforcing stress free condition) of the deposit the integration constants are evaluated. Finally, amplification at the surface with respect to input motion prescribed at rigid bedrock level is,

$$Amp_{(1)} = \left[\frac{2(1-n)a\rho_2}{\pi\sqrt{1+aH_1}}\right]\frac{1}{[\psi_1(\omega)-\psi_2(\omega)]} \tag{3.52}$$

Here,

$$\psi_1(\omega) = \left(\frac{\omega\rho_2}{v_{sH}}\right)\times\left[J_\nu\left(\xi_H^{(1)}\right)Y_{\nu+1}\left(\xi_0^{(1)}\right)-J_{\nu+1}\left(\xi_0^{(1)}\right)Y_\nu\left(\xi_H^{(1)}\right)\right]\cos\left(\frac{\omega H_2}{v_{s2}}\right)$$

$$\psi_2(\omega) = \left(\frac{\omega\rho_1}{v_{s2}}\right)\times\left[J_{\nu+1}\left(\xi_H^{(1)}\right)Y_{\nu+1}\left(\xi_0^{(1)}\right)-J_{\nu+1}\left(\xi_0^{(1)}\right)Y_{\nu+1}\left(\xi_H^{(1)}\right)\right]\sin\left(\frac{\omega H_2}{v_{s2}}\right)$$

Using Eq. (3.52) we can get the surface amplification of base motion as a function of excitation frequency for the case of soil deposit whose shear wave velocity profile varies as given by Eq. (3.6) and overlies homogeneous layer of constant shear wave velocity. However, as in the previous case, the amplification response is obtained disregarding nonlinear behaviour of soil and density of the soil deposit remains constant with depth. In case bottom layer is inhomogeneous then the above given equations cannot be used. To include viscous damping (damping ratio, ζ) in the analysis, shear wave velocity (v_s) of the layers is replaced with $v_s^* = v_s\sqrt{1+2i\zeta}$.

3.5.2 Parametric study on amplification of two-layer soil deposit

This section deals with the study of amplification characteristics of inhomogeneous layer overlying a homogeneous layer of constant shear wave velocity. The analytical solution to this problem is obtained in the form of amplification transfer function between surface motion and input motion at the top of rigid bedrock underlying the bottom homogeneous layer, and given by Eq. (3.52).
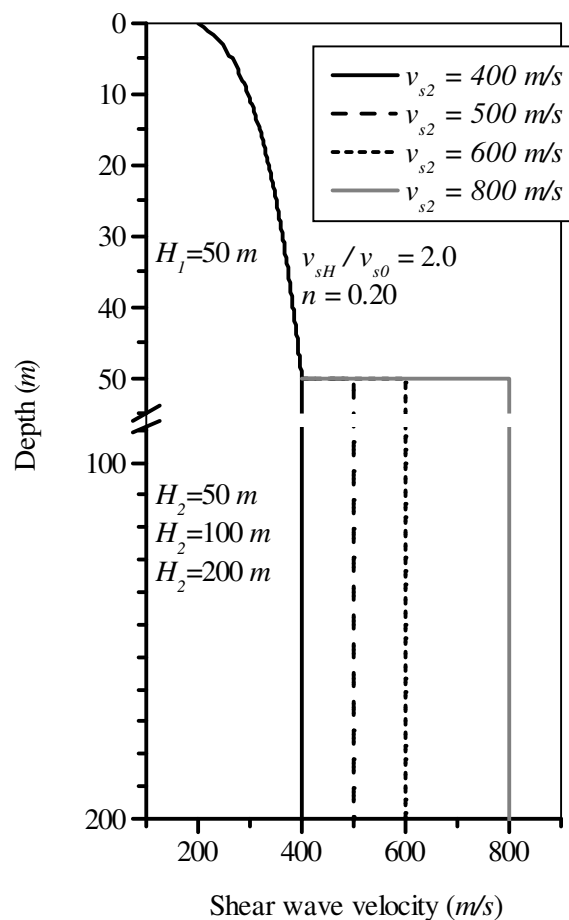
Figure 3.20: Soil Deposit with continuous variation of shear wave velocity, overlying a homogeneous soil deposit of shear wave velocity of different depths.

In order to study the effect of depth and stiffness of the homogeneous layer on amplification of base input motion at the surface of the deposit, these properties of the bottom layer is varied as indicated in Figure 3.20. The inhomogeneity parameters considered are velocity ratio associated with top layer, $v_{sH} / v_{s0} = 2.0$ and exponent $n = 0.20$ of the velocity function. The densities of top and bottom layers are kept

constant at $\rho_1 = \rho_2 = 2000 \; kg/m^3$. The depth of the bottom layer (homogeneous layer) is considered to vary with three cases i.e., $H_2 = 50, 100$ and $200 \; m$ and four shear wave velocity cases i.e., $v_{s2} = 400, \; 500, \; 600$ and $800 \; m/s$ are considered.
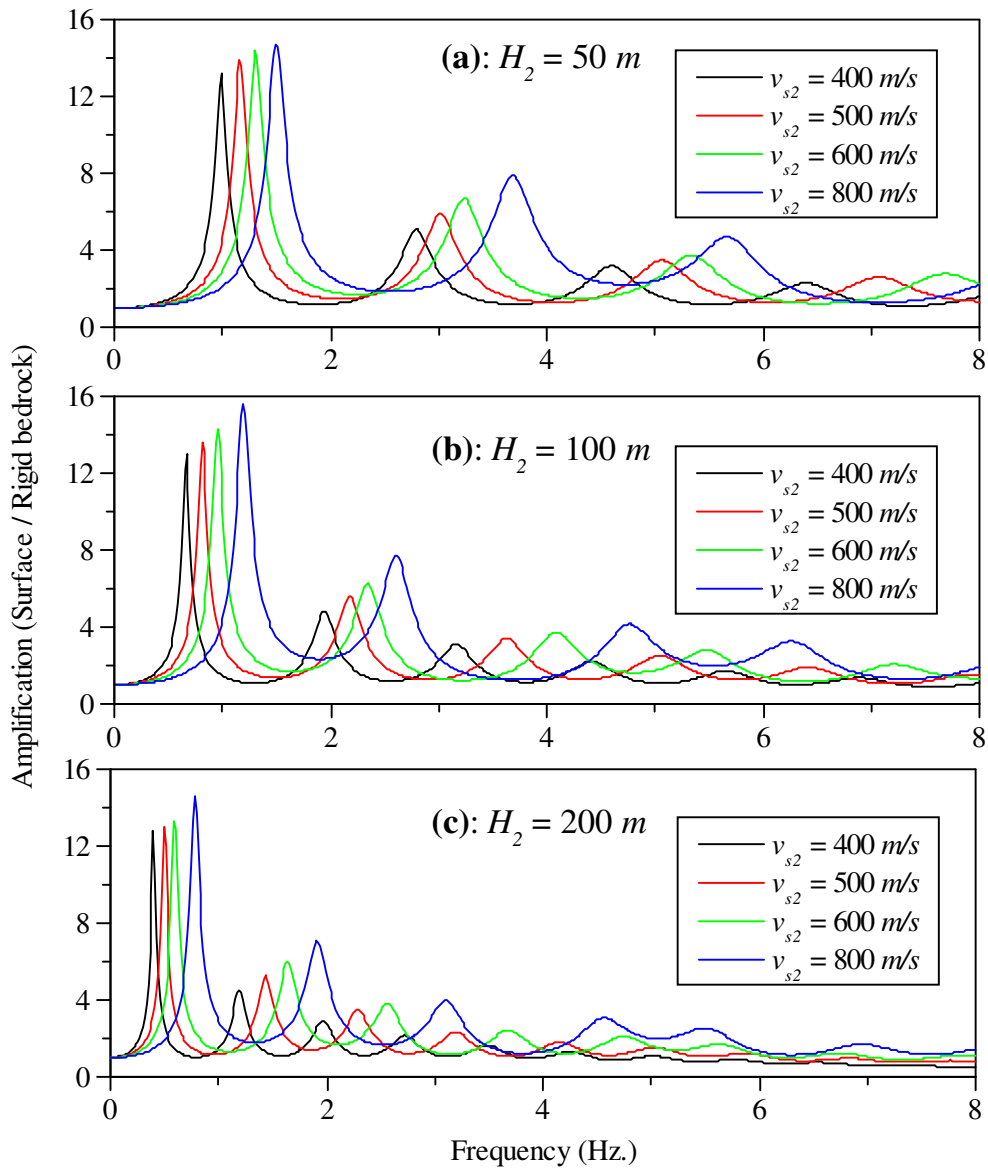
Figure 3.21: Effect of depth and shear wave velocity of homogeneous layer underlying an inhomogeneous layer on amplification ratio and modal frequencies.

The results of this parametric study are shown in Figure 3.21. The frequency dependent amplification characteristics of the inhomogeneous deposit overlying a homogeneous deposit of depths 50 m, 100 m and 200 m for different v_{s2} values are

shown in Figures 3.21a, 3.21b and 3.21c respectively. As it can be observed from these figures, the peak amplifications corresponding to modal frequencies is maximum for the case of $v_{s2} = 800 \; m/s$ when compared to other cases. Hence, it can be concluded that the amplification increases as the stiffness of the bottom layer increases and this increase is significant for impedance ratio $\left(v_{s2}/v_{sH}\right)$ greater than about 2. At lesser values of impedance ratio the increase in amplification is comparatively insignificant particularly as the depth of the bottom layer increase.

It is interesting to note that the effect of depth of homogeneous layer on amplification characteristics appears to be complex phenomenon than the effect of velocity ratio v_{s2}/v_{sH}. Also, comparing the results of depth, H_2 equal to 100 m and 200 m to that of 50 m, particularly at higher frequencies (after two or three modes) the trend of amplification is considerably affected at higher frequencies particularly for stiffer bottom layer i.e., $v_{s2} = 800 \; m/s$. Also, amplification is marginally greater in case of $H_2 = 100m$ compared to $H_2 = 200m$ deposit for all values of v_{s2}.

3.6 AMPLIFICATION OF MULTI-LAYERED SOIL DEPOSIT WITH CONTINUOUSLY INHOMOGENEOUS LAYER PROPERTIES

All the above mentioned studies consider the case of inhomogeneous elastic layer with shear modulus or shear wave velocity varying continuously as a function of depth. The work presented by Davis and Hunt (1994), Davis (1995) and Davis (1994) considered multiple layers with linear variation of shear modulus in each of the layers.

Site response under seismic excitation studies usually employ idealised site models in which homogeneous soil layers are separated by distinctly defined horizontal layer interfaces. The impedance mismatches at these interfaces give rise to wave reflections which strongly affect the calculated free surface response. In order to avoid this inconsistency Davis (1995) extended the concept proposed in the work of Davis and Hunt (1994) to incorporate smoothly varying interfaces between the layers. This was justified by the argument that the interfaces are made up of weathered soil [Macari

and Hoyos (1996)]. The variation is assumed to be linear, thus avoiding superficial impedances at the interface of adjacent layers.

3.6.1 Amplification function for inhomogeneous multiple layers

Employing the Haskell-Thomson transfer matrix approach Davis and Hunt (1994) obtained an analytical solution for SH wave amplification by multiple layers of Gibson soil shown in Figure 3.22. Gibson soil represent elastic or viscoelastic layers with linearly varying shear modulus [Gibson (1974)].
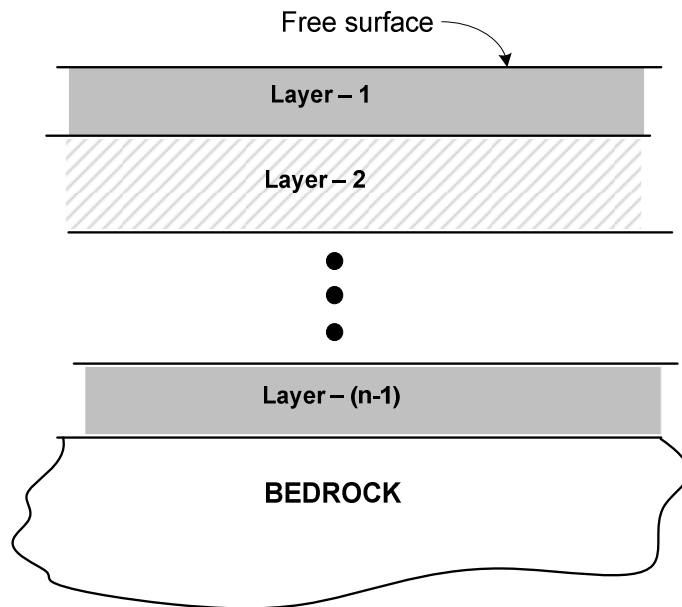
Figure 3.22: Multiple layers of Gibson soil above homogeneous elastic bedrock [Reproduced from Davis (1995)]
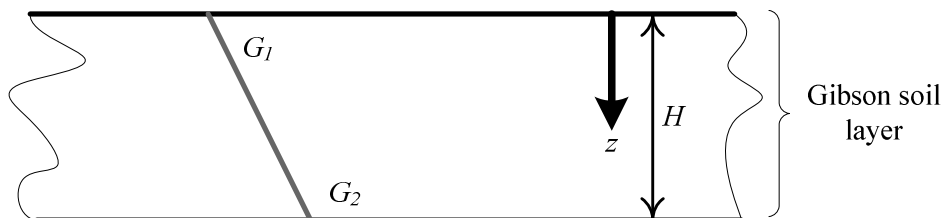
Figure 3.23: Linear variation shear modulus along the depth of individual layer [Reproduced from Davis (1995)]

Consider a single layer of Gibson soil of thickness H shown in Figure 3.23 subjected to vertically propagating SH waves. Let z be the local depth coordinate within the layer and $u(z,t)$ denote horizontal displacement and $\tau(z,t)$ denote shear stress. Subscripts 1 and 2 refer to conditions at the upper and lower surfaces of the layer, respectively. Let ω denote the excitation frequency; ρ the mass density; $G^*(z) = G(z)(1+i\zeta)$, complex shear modulus and ζ, is the hysteretic damping ratio. Suppose G^* is a linear function of z, such that $G^*/\rho = \tilde{a} + \tilde{b}z$, where $\tilde{a}$ and $\tilde{b}$ are complex constants given by $\tilde{a} = v_{s1}^2(1+i\zeta)$ and $\tilde{b} = \dfrac{v_{s2}^2 - v_{s1}^2}{H}(1+i\zeta)$ with v_{s1} and v_{s2} being the corresponding shear wave velocities at top and bottom of the layer.

A transfer matrix is derived for the response at the top of a Gibson soil layer in terms of the response at the base. Multiplying the transfer matrices for each soil layer leads to relations between the free surface response and the bedrock incident wave form. This relation yields the free surface amplification function. This procedure is similar to that which is used in the program SHAKE except that the transfer matrix for each layer is derived assuming it as Gibson layer instead of homogeneous layer idealisation.

Following the same procedure as described in Chapter 2 (Eq. 2.22) the transfer matrix for the ith Gibson layer in terms of particle velocity and shear stress is expressed as,

$$\begin{bmatrix} \dot{u}_2 \\ \tau_2 \end{bmatrix} = \begin{bmatrix} \overline{A}_{11}^{(i)} & \overline{A}_{12}^{(i)} \\ \overline{A}_{21}^{(i)} & \overline{A}_{22}^{(i)} \end{bmatrix} \begin{bmatrix} \dot{u}_1 \\ \tau_1 \end{bmatrix} \tag{3.53}$$

where,

$$\left. \begin{aligned} \overline{A}_{11}^{(i)} &= \frac{\pi\omega\sqrt{\tilde{a}}}{\tilde{b}}\left[-Y_1(\xi_1)J_0(\xi_2) + J_1(\xi_1)Y_0(\xi_2)\right] \\[2mm] \overline{A}_{12}^{(i)} &= \frac{i\pi\omega}{\tilde{a}\tilde{b}}\left[-Y_0(\xi_1)J_0(\xi_2) + J_0(\xi_1)Y_0(\xi_2)\right] \\[2mm] \overline{A}_{21}^{(i)} &= \frac{i\pi\rho\omega\sqrt{\left[\tilde{a}(\tilde{a}+\tilde{b}h)\right]}}{\beta}\left[-Y_1(\xi_1)J_1(\xi_2) + J_1(\xi_1)Y_1(\xi_2)\right] \\[2mm] \overline{A}_{22}^{(i)} &= \frac{\pi\omega\sqrt{\left[\tilde{a}+\tilde{b}h\right]}}{\tilde{b}}\left[-Y_0(\xi_1)J_1(\xi_2) - J_0(\xi_1)Y_1(\xi_2)\right] \end{aligned} \right\} \tag{3.54}$$

Here $J_\nu(\bullet)$ & $Y_\nu(\bullet)$ denote Bessel functions of the first and second kind of order ν, and $\xi_1 = \dfrac{2\omega\sqrt{\tilde{a}}}{\tilde{b}}$ and $\xi_2 = \dfrac{2\omega\sqrt{\tilde{a}+\tilde{b}h}}{\tilde{b}}$. The matrix $\bar{A}$ is the Haskell-Thomson matrix for the layer with linear shear modulus variation. It can be used recursively to find the response of multiple layer deposit. Consider the case with $(n-1)$ layers illustrated in Figure 3.22. The free surface response, $(\dot{u}_0, \tau_0)$, is related to the response at the bedrock interface, $(\dot{u}_n, \tau_n)$, by

$$\begin{bmatrix} \dot{u}_n \\ \tau_n \end{bmatrix} = \begin{bmatrix} \bar{A}^{(n-1)} \end{bmatrix} ... \begin{bmatrix} \bar{A}^{(i)} \end{bmatrix} .. \begin{bmatrix} \bar{A}^{(2)} \end{bmatrix} \begin{bmatrix} \bar{A}^{(1)} \end{bmatrix} \begin{bmatrix} \dot{u}_0 \\ \tau_0 \end{bmatrix} = \begin{bmatrix} \bar{A}_{11} & \bar{A}_{12} \\ \bar{A}_{21} & \bar{A}_{22} \end{bmatrix} \begin{bmatrix} \dot{u}_0 \\ \tau_0 \end{bmatrix} \qquad (3.55)$$

In Equation (3.55), each of the matrices $\bar{A}^{(1)}, \bar{A}^{(2)}, ...$ is the appropriate transfer matrix to each of the layer $i = 1, \ 2, \ ....$ and $\bar{A}$ is the product of all the $\bar{A}^{(i)}$ matrices.

Considering harmonic input motion at the top of the bedrock along with appropriate boundary conditions at the free surface and at the elastic bedrock-soil layer interface, amplification function between surface/bedrock is obtained as,

$$Amp_{(2)} = \frac{\dot{u}_0}{2\dot{u}_n} = \left| \frac{\rho_r v_{sr}}{\bar{A}_{21} + \rho_r v_{sr} \bar{A}_{11}} \right| \qquad (3.56)$$

In the above equation, ρ_r and v_{sr} denote bedrock density and shear wave velocity respectively.

Here an attempt is made to verify the possibility of idealizing the continuously inhomogeneous soil profile with an equivalent layered profile consisting of Gibson layers (i.e., linear variation of shear modulus). For this purpose soil profile of Figure 3.11 is discretised into 10 layers with linear distribution of shear modulus and amplification is computed using Eq. (3.55) and Eq. (3.56). The results obtained from both the analyses are compared in Figure 3.24. The amplification function computed using 10-layer equivalent profile almost exactly compares with that of exact solution. Thus it can be concluded that soil profile exhibiting continuous variation of soil properties can be modeled with an equivalent layered profile consisting of Gibson

layers instead of idealizing it as a homogeneous layered profile as is being made in routine analysis procedure.
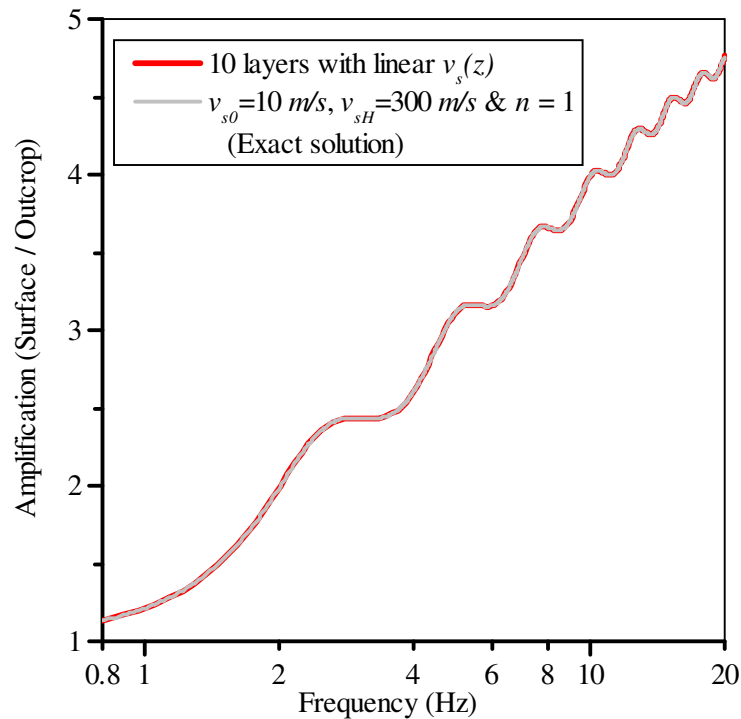
Figure 3.24: Comparison of amplification function computed for an equivalent layered profile consisting of Gibson layers with that of exact solution.

3.6.2 Parametric study on transition Gibson layer at layer interfaces

The effect of contrasting impedances between the adjacent layers at their interfaces is evident. Also natural soil deposits seldom exhibits perfectly layered profile. Despite this fact usually the soil deposit is idealised as layered profile in routine one-dimensional site response analysis. Thus it may be appropriate to introduce a transition layer at the interface in order to achieve smooth transition of impedance between the adjacent layers. This may also help in overcoming pseudo-resonance conditions resulting in spurious high frequency responses. Here a parametric analysis is performed to study the effect of depth of transition layer on the surface motion amplification.

A 30 m depth deposit made up of two layers is considered for the analysis. The depth of each layer is 15 m, the shear wave velocity of the top layer is assumed to be 100

m/s and that of bottom layer is 300 *m/s*. A transition layer at the interface of these two layers is considered. The depth *d*, of this transition layer is varied from 0 to 15 *m*. The effect of introducing transition layer on the amplification of surface motion is presented in Figure 3.25. In this figure, the frequency is normalized with respect to fundamental frequency of the deposit and amplification is presented in terms of its peak values at first five modes. From this figure it can be observed that introducing transition layer at the interface greatly improves the high frequency response without affecting the amplification at the fundamental frequency significantly.
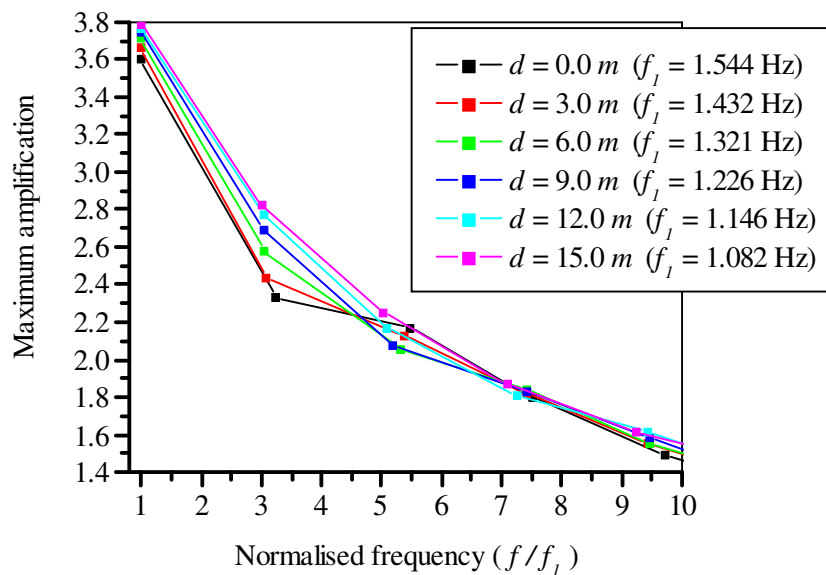
Figure 3.25: Effect of transition layer depth on the amplification of surface motion.

3.7 COMPARISON BETWEEN CONTINUOUSLY INHOMOGENEOUS SOIL DEPOSIT AND ITS LAYERED APPROXIMATION

In Figure 3.9 the amplification result of exact solution obtained for the deposit with linear variation of shear wave velocity along the depth is compared with that obtained for different layered configurations. Obviously, from this figure, it was evident that as number of layers is increased to closely represent the actual velocity profile the amplification seems to approach the exact solution. However it is interesting note that, though the convergence is evident for sufficiently large number layers in the first peak

(i.e. corresponding to first mode of vibration), there are substantial differences in the frequencies and amplification of the higher mode of vibration.

In order to study the effect of arbitrariness and inconsistency in prescribing layered idealisation for a surface deposit which possesses nearly continuous variation of shear wave velocity distribution and uniform density throughout its depth, the deposit of 40m thickness with linear distribution of shear wave velocity is considered here. The shear wave velocity is varying from 80 m/s at the surface to 720 m/s at the base and it is overlying an elastic bedrock having $v_{sr} = 720 \ m/s$. Thus the shear wave velocity function defining the profile is given by $v_s(z) = 80(1 + 0.2z)$. Inconsistency in decision making about depth of each layer is incorporated by varying the thicknesses of each of the layer of equivalent two layer and three layer models to represent 40m thick continuously inhomogeneous deposit. Based on its depth from the surface and its thickness, the average shear wave velocity of each layer is assigned. In equivalent layer system the layer thicknesses H_1 and H_2 are varied resulting in variation of impedance ratios between the top two layers as well as bottom layer and bedrock. Density being constant, the impedance ratio between any two layers is simply the ratio of their shear wave velocities.

Two layer equivalent model of the actual continuous variation is shown in Figure 3.26. The variation of impedance ratio as H_1 and H_2 are varied is plotted with respect to ratio of H_1 and H_2. There seem to be consistency in the trend of variation of impedance ratio at both interfaces i.e., between the top two layers as well as bottom layer and bedrock but obviously no particular relation exists between them. The maximum amplification computed for the ratios of H_1 / H_2 is shown along with corresponding impedance ratio. Though maximum amplification computed for equivalent layered idealisation closely agrees with that of exact value for a particular configuration of two layer thicknesses, it is important to note that frequency at which this amplification is obtained does not match with that of exact solution. Close agreement of maximum amplification of equivalent two layer deposit with that of exact value is incidentally at $H_1 / H_2 = 4.0$.
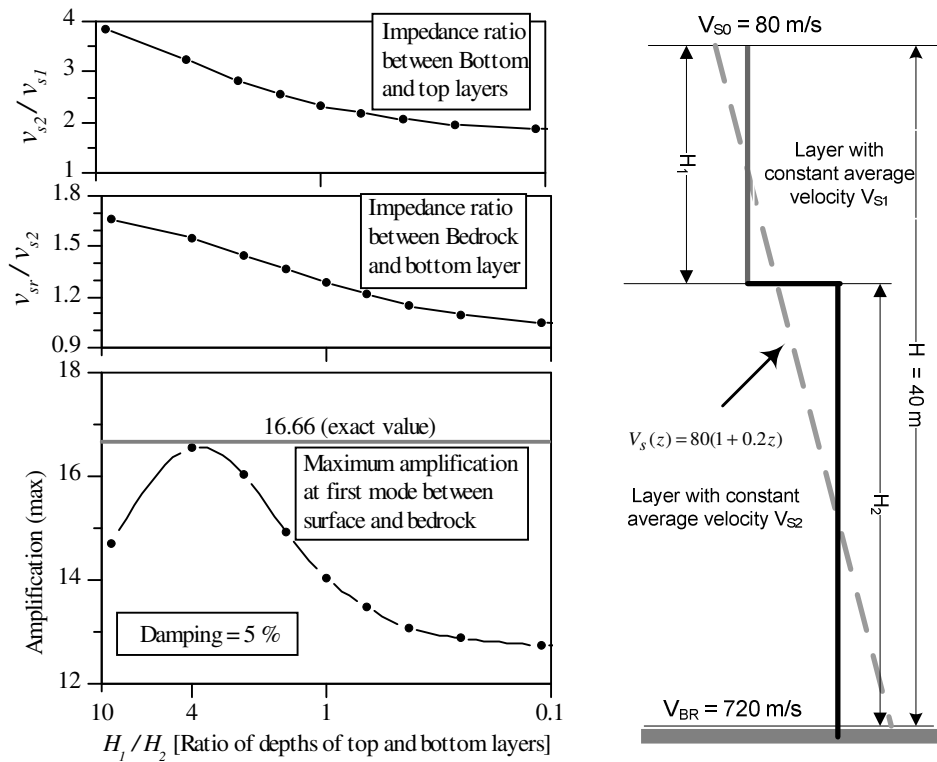
Figure 3.26: Effect of contrasting impedance ratio on amplification characteristics of idealized equivalent two layer system

Further, to demonstrate the implications of inconsistency in layered approximation the same deposit considered in the previous example is approximated with three layers with variation in their depths. In the three layers approximation, depths of top and bottom layers are considered to be of same thickness (i.e., $H_1 = H_3$) while middle layer thickness H_2 is varied such that total thickness of the deposit is $40m$ i.e., $H_2 = 40 - 2H_1$. Three layer equivalent model of the actual continuous variation is shown in Figure 3.27. The variation of impedance ratio as H_2 and H_1 (or H_3) are varied is plotted with respect to ratio of H_2 and H_1 (or H_3). As in the previous case (two layer approximation), there is no particular relation existing with contrasting impedance ratios between any of the two layers and amplification. The maximum amplification computed for ratio of H_2 / H_1 (or H_2 / H_3) is shown along with resulting impedance ratios between top and middle layers, middle and bottom layers

and bottom layer and bedrock. Close agreement of maximum amplification of equivalent two layer deposit is incidentally found to be at $H_2/H_1\left(or\ H_2/H_3\right)=3.0$.
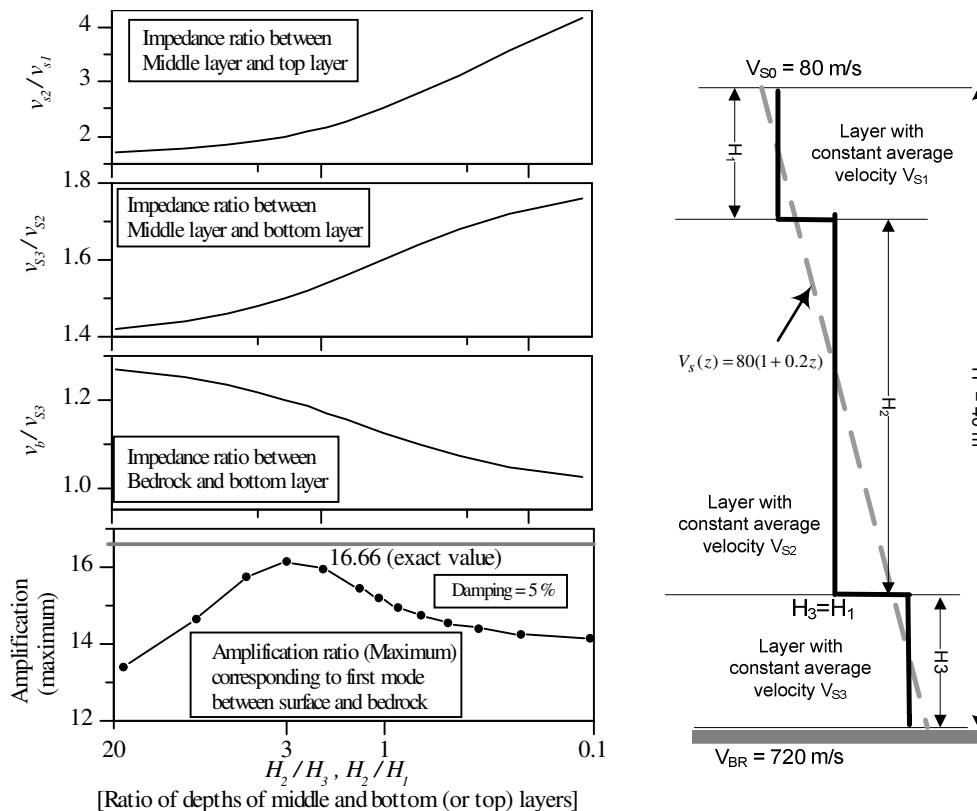
Figure 3.27: Effect of contrasting impedance ratio in idealized three layer system on amplification

Finally, comparison of results pertaining to ground response analysis of continuously inhomogeneous deposit and its layered approximation is made in respect of seismic input motion at the bedrock level. The 40*m* depth deposit considered previously is analysed by idealizing it as 40 layers of 1.0*m* thick and 2 uniform layers of 20*m* thick (Figure 3.28a). For the purpose of comparing effect of layered idealisation of actual continuous variation on the computed response due to input earthquake motion at the base of the deposit. An earthquake motion recorded at Diamond Heights (USA) during 1989 Loma Prieta earthquake is normalized to 0.1*g* peak acceleration and used as input motion.

In both cases of layered deposit idealizations, both linear and equivalent linear analyses were carried out using the program EERA. In order to implement equivalent

linear approach arbitrarily selected average strain dependent shear modulus and damping curves are used in the analysis,. In case of linear analysis, computation is carried out using initial values of shear modulus and damping. The response of the deposit is compared in terms of maximum acceleration computed along the depth of the profile. Figure 3.28b shows the variation of the acceleration response in terms of its maximum values along the depth. Results obtained from equivalent linear analysis (EQL) and linear analysis (L) for ideal 40 layers deposit is compared with those of approximated 2 layers deposit.
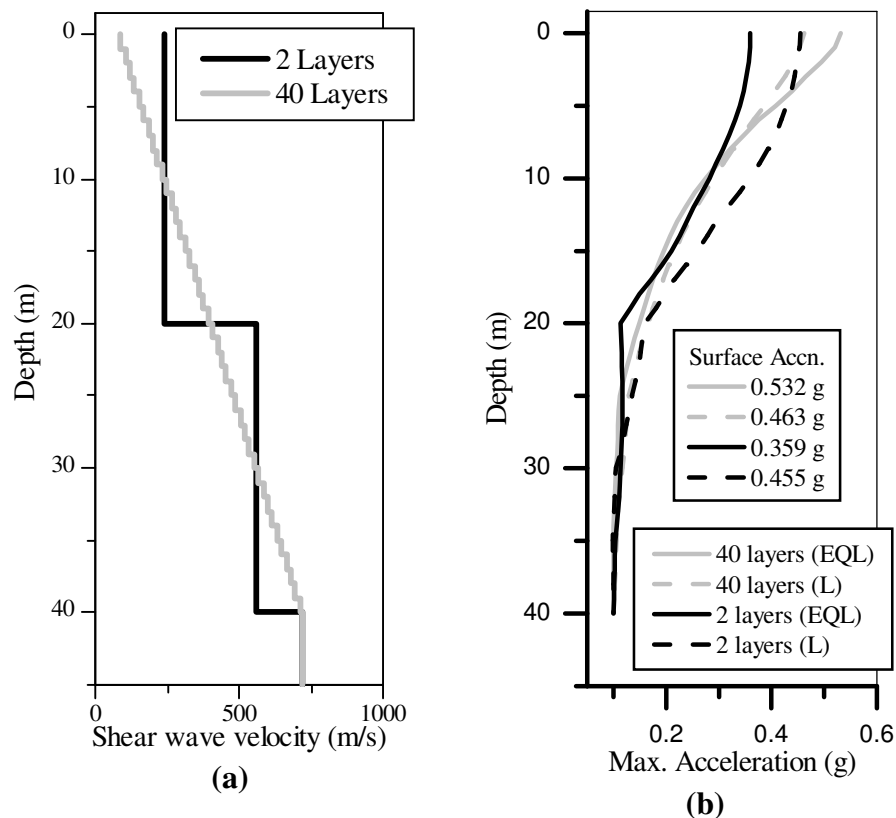
Figure 3.28: (a) 2-layers and 40-layers idealisation (b) Comparison of maximum accelerations computed along the depth

In case of linear analysis both idealisations yield almost similar values of maximum acceleration at the surface. However, for the depths in the range of about 5m and 30m the maximum accelerations are higher for approximated 2 layer deposit when compared to 40 layers deposit. On the other hand, in case of equivalent linear analysis the surface acceleration computed for 2 layer system is grossly underestimated by

about 33 percent when compared to that of 40 layers deposit case. Also, incidentally, in case of 40 layers deposit the difference in variation of maximum accelerations along the depth computed from linear and EQL analyses is not much below 10*m* from the surface. Surprisingly, in contrast to this observation, this kind of phenomenon is not observed in case of linear and EQL analysis of two layered model though same strain dependent stiffness and damping properties are used in the analysis. This needs to be investigated further, with rigorous parametric study, to conclude on effects of contrasting impedance properties on the results of linear and EQL analysis. However, this clearly indicates that inappropriate layered idealisation will have profound effect on the response than the kind of nonlinear model (strain dependent stiffness and damping model) employed.
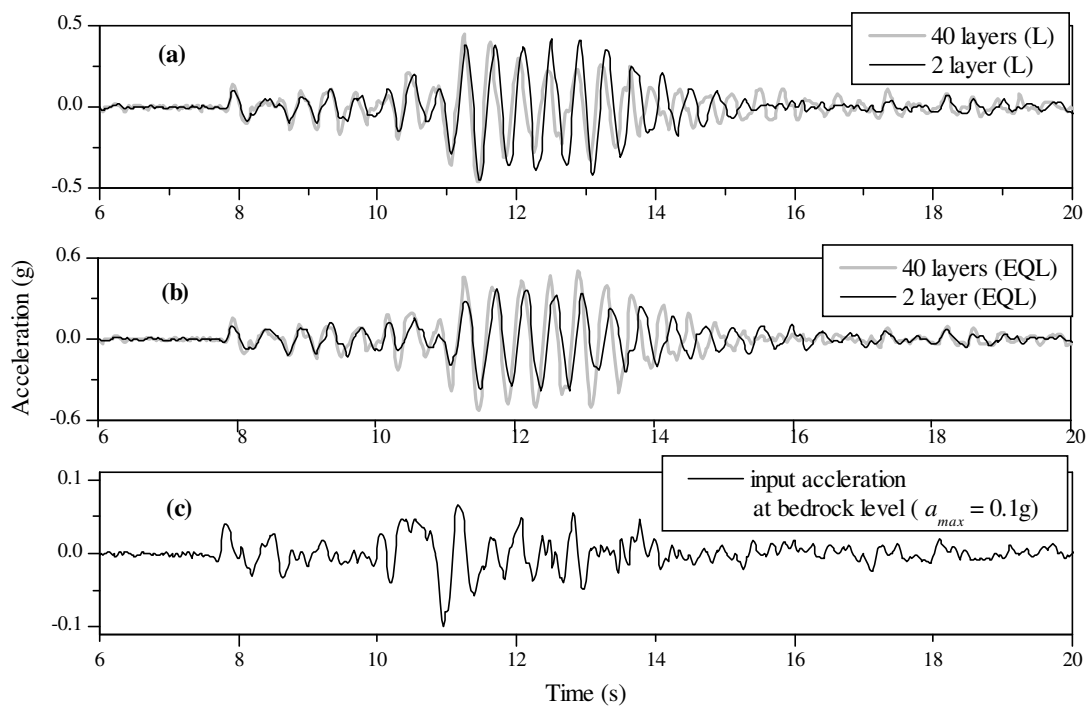
Figure 3.29: Comparison of computed acceleration time histories at the surface for 2-layers and 40-layers models, (a) linear analysis, (b) Equivalent linear analysis and (c) Input ground motion at the bedrock level.

Figure 3.29 compares the acceleration time histories computed at the surface for the cases under consideration i.e., both ideal 40 layer and approximated 2 layer models. These responses are obtained for the same input motion shown at the bottom (Figure 3.29c), which is given at the bedrock level. In case of both linear (Figure 3.29a) and equivalent linear analysis (Figure 3.29b), there are noticeable differences in the

characteristics of the response. Particularly, in case of linear analysis the peak value surface accelerations are almost comparable (0.463g and 0.455g respectively for 40 and 2 layer cases) but their time history characteristics are different. While in EQL analysis the underestimation of maximum response (0.532g and 0.359g respectively for 40 and 2 layer cases) in case of two layered deposit compared to that of continuation variation idealisation is observed. Hence it can be concluded that contrasting layer impedances may result in underestimation of high frequency response.

3.8   COMPARISON USING OBSERVED EARTHQUAKE DATA

As discussed earlier, there are discerning issues with respect to geotechnical investigations and subsequent interpretation of soil profile for the purpose of ground response analysis. These issues result in inconsistent predicted response quantities. In order to overcome these inherent deficiencies in the current practices, which are difficult to quantify, this study proposes to approximate the surface deposit with continuous variation soil properties. In the advent of this conceptually abstract alternative, the approximation of shear wave velocity profile of surface deposit with best fit continuous variation is considered as an initial option. The approximated continuous variation is replicated by closely stacked layers and assigned with appropriate shear wave velocity values and routine analysis of layered deposit used in programs like SHAKE is carried out.

For the purpose of demonstrating the efficacy of the proposed method, data recorded at an instrumented geotechnical array during an earthquake event is considered. For this purpose, geotechnical downhole array established at La-Cienega site of USA is considered. This particular array was installed by the California Strong Motion Instrumentation Program (CSMIP) with the support of California Department of Transportation (Caltrans). La-Cienega downhole array consists of four accelerometers installed at depths 0.0 m, 18.3 m, 100.60 m and 252.0 m. La-Cienega array has recorded many events of different magnitudes and peak accelerations. Among these event recorded on 4th April, 1997 is considered in this study. Shear wave velocity profile of this particular array as interpreted from the data obtained from different

geotechnical investigations is shown in Figure 3.1. Here same data pertaining to PS-logging is reproduced in Figure 3.30. Continuous variation approximation of continuous PS-logging data using power law and corresponding 3-layer approximation is also shown in Figure 3.30. The continuous variation approximation of shear wave velocity along the depth (z) is represented by the equation $v_s(z) = v_{s0} + bz^c$. Nonlinear regression method is used for curve fitting process by setting constraint on non-zero shear wave velocity at surface v_{s0} (=120m/s). The best fit for scattered PS-logging data is obtained with parameters $b = 88.87$ and $c = 0.32$ resulting in correlation coefficient of $r^2 = 0.75$. Shear wave velocities of 120 m/s at the surface and 640 m/s at the bedrock level are kept same for the layered and continuous variation idealisations.
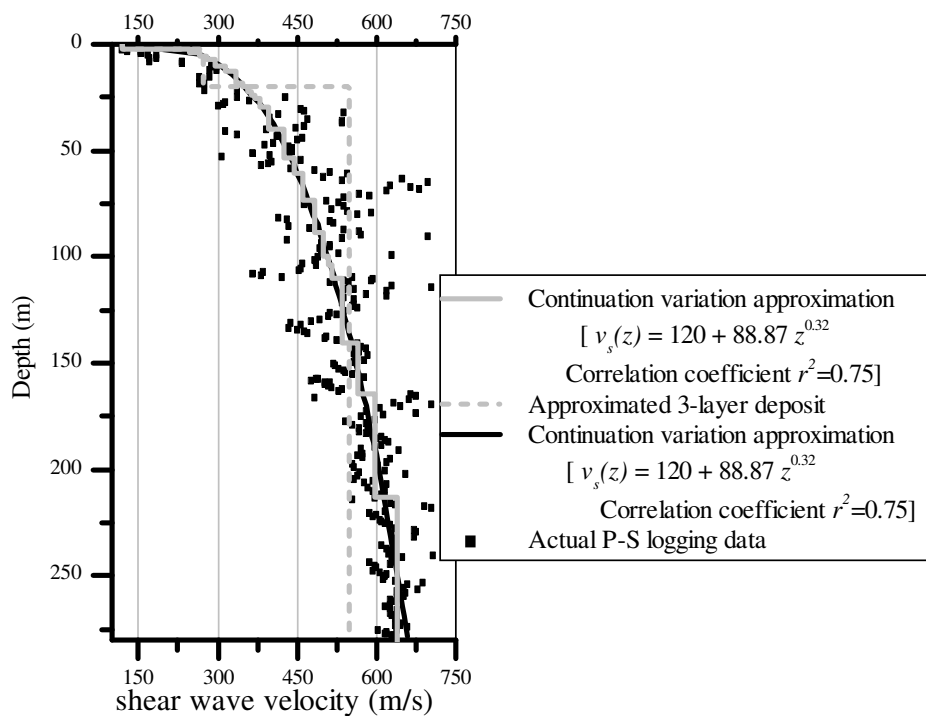
Figure 3.30: PS-logging data of La-Cienega array and corresponding layered and continuous approximation.

The 4th April, 1997 seismic event recorded by this array is one of the of low magnitude $(M_L = 3.3)$ earthquake at an epicentral distance of 6.7km and focal depth of 4.2km. The acceleration time histories recorded during this event, at surface and

100m depth in 360° and 90° component directions, are shown in Figure 3.31. These data are available at California Strong Motion Instrumentation Program (CSMIP) website. The recorded peak accelerations are 0.059g and 0.013g respectively at surface and 100 m depth for 360° component, while corresponding values for 90° component are 0.078g and 0.022g respectively.
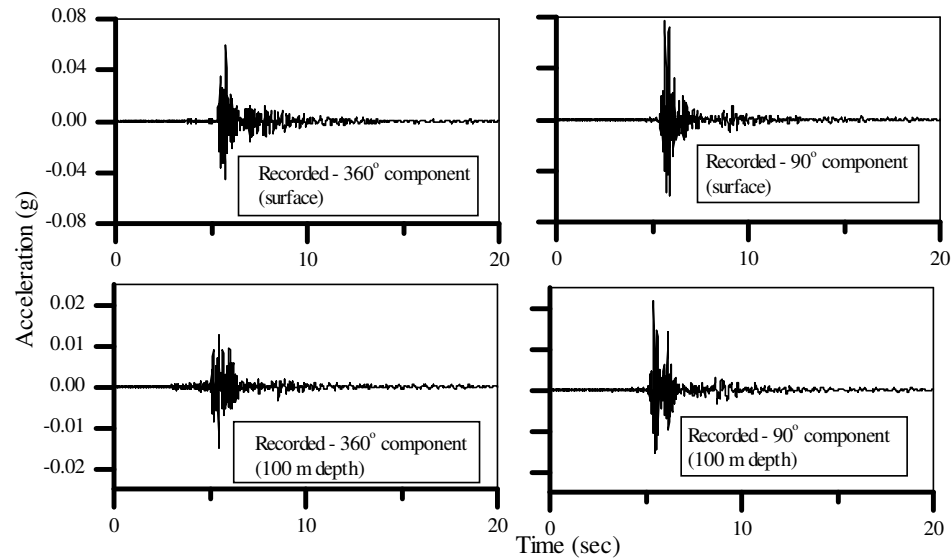
Figure 3.31: Acceleration time history data of 4th April 1997 earthquake recorded at La-Cienega geotechnical array.

The computer program EERA is used to perform ground response analysis. The analysis is carried out to compute response at the top (ground surface) of the idealized surface deposit due to an input motion at the base of the deposit. In order to ascertain the effectiveness of the proposed continuous variation idealisation of shear wave velocity profile of an inhomogeneous deposit, predicted ground surface motions from the analysis is compared with the observed response of the deposit. Also efficiency of the proposed method is verified by comparing its results with that of idealized 3-layer deposit in terms of surface response quantities. For the purpose of preparing the deposit profile data of La-Cienega geotechnical array for EERA program, the continuous variation shown in Figure 3.30 is approximated using 40 layers in order to closely represent the variation trend without significant contrasting impedance ratio between any two adjacent layers. However, the three layer deposit is represented in the input data in the manner as shown in Figure 3.30. Henceforth, in this study, La-

Cienega deposit idealized as 40 layers deposit to closely represent continuous variation of shear wave velocity shall be referred to as LCC and that with 3-layer idealisation as LC3L.

Considering the low magnitude of the earthquake and lower level of peak accelerations of input motion (Figure 3.31) the influence of nonlinear response may be considered to be insignificant. However, nonlinear analysis is carried out using equivalent linear approach of EERA. For this purpose, the nonlinearity of the soil deposit is modeled with strain dependent shear modulus and damping curves shown in Figure 3.32a and 3.32b respectively. Since the La-Cienega deposit is predominantly a clayey soil deposit a typical strain dependent shear modulus [Sun et al. (1988)] and damping [Idriss (1990)] curves of cohesive soil are used. The density of the soil is considered to be constant ($\rho = 2.055$ t/m^3) throughout the depth of the deposit.

Strain v/s G/G_{max}
—— 0.0 to 282.0 m
- - - - $\geq$ 282 m

Strain v/s Damping
—— 0.0 m to 282.0 m
- - - - $\geq$ 282.0 m

(a)

(b)
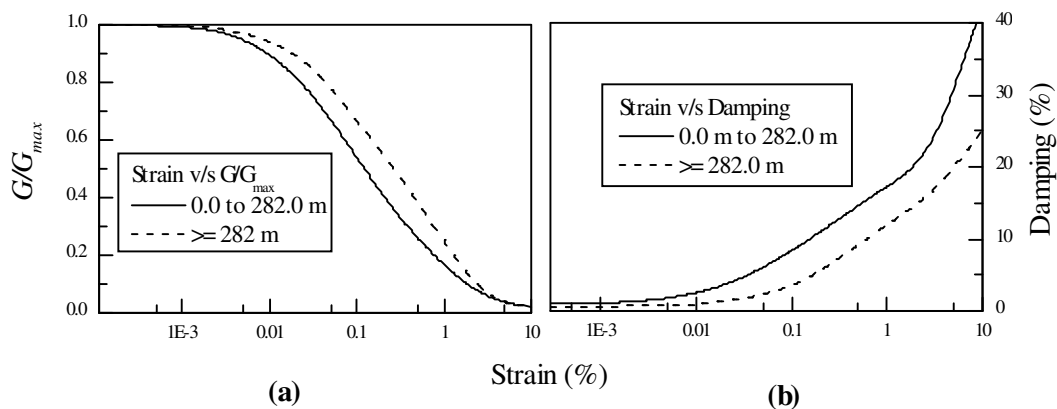
Strain (%)

Figure 3.32: Strain dependent shear modulus and damping curves used in the analysis

In previous sections it was demonstrated that, the ground surface response due to excitation at the base of the deposit is greatly affected by shear wave velocity values at the surface (v_{s0}) and at the base (v_{sH}) of the deposit. Hence, these shear wave velocity values (v_{s0} and v_{sH}) in both the cases (LCC and LC3L) are prescribed with identical values of $v_{s0} = 120 m/s$ and $v_{sH} = 640 m/s$ respectively. Thus two idealized cases LCC and LC3L synonymously represent the important geotechnical characteristics of the deposit except for geometrical characteristics in terms of depths of the layers considered. This factor influences the impedance characteristics of the

deposit as a consequence of variation in average shear wave velocities of these idealized layers.
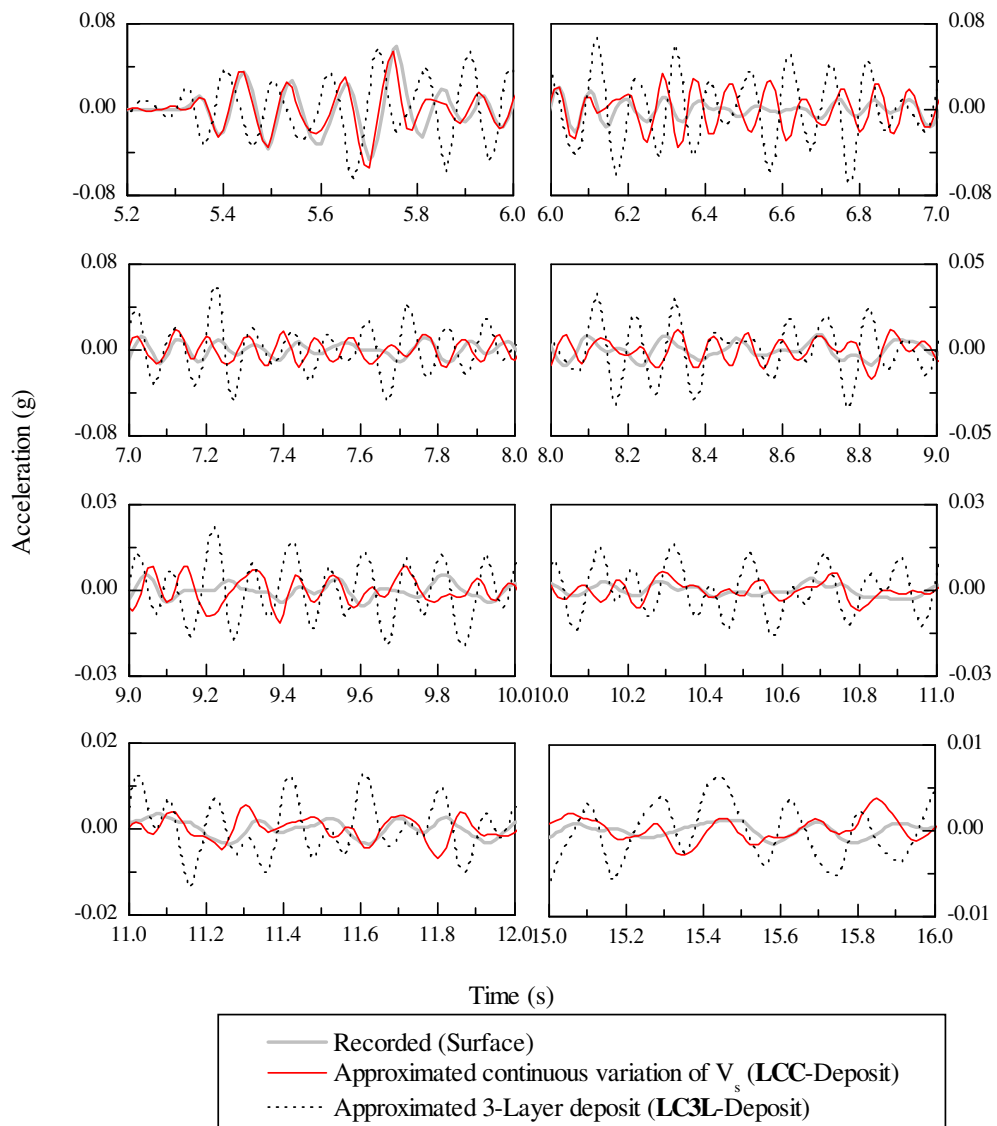
Figure 3.33: Comparison of computed surface acceleration time history in different time windows with corresponding observed record of 360° component.

The earthquake ground response analysis for both (LCC and LC3L) the cases is carried out to predict the surface responses due to prescribed input motion at $100m$ depth. The analysis is performed for both $360°$ and $90°$ components of the recorded earthquake shown in Figure 3.31. Results of these analyses are shown in Figure 3.33 and Figure 3.34 in terms of acceleration time histories at the surface of the deposit. Figure 3.33 gives acceleration time history computed at ground surface for the both

LCC and LC3L cases of soil deposit idealisations due to 360° component input motion. For the purpose of clarity the results are presented in different time windows.
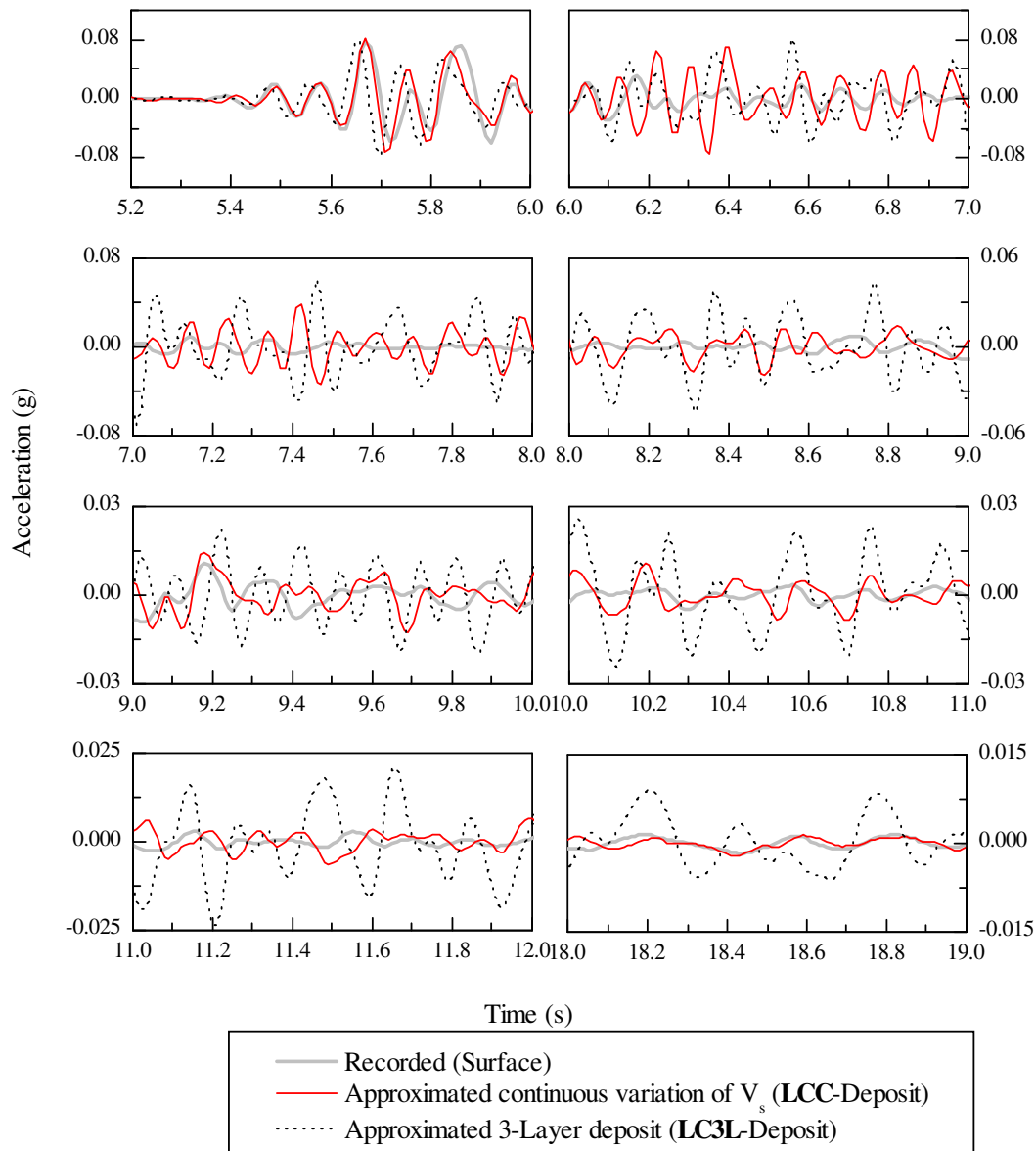
Figure 3.34: Comparison of computed surface acceleration time history in different time windows with corresponding observed record of 90° component.

It is clear from this Figure 3.33 that, the predicted surface response using LCC-deposit has a trend which closely matches with trend of the observed motion in the region of peak acceleration (5.2*s*–6.0*s*) when compared to LC3L deposit case. However, in the region between 6.2 and 9.0 seconds both LCC and LC3L cases over predicts the responses compared to observed record with LCC prediction being closer

to measured record than LC3L prediction. More importantly, after 9.0s the LC3L shows wayward trend with unusual amplification of motion than the recorded data, whereas LCC closely follows the recorded response. These kinds of similar observations can be made with respect to response due to input motion of 90° component as shown in Figure 3.34.

The peak ground accelerations predicted and recorded for various cases are tabulated in Table 3.3. From this table it can be seen that the predicted peak surface accelerations with the deposit of LCC case is more closer to recorded data than the LC3L case for the 360° component input motion. In case of 90° component input motion, LCC deposit yielded exactly the same peak acceleration as that of observed data. In case of LC3L deposit even though the predicted peak values are within the acceptable limits there exists phase difference in the occurrence of peak response.

Table 3.3: Comparison peak acceleration computed using LCC and LC3L idealised deposits with measured data for both the components of the earthquake.

Peak Surface accelerations obtained from	Input motion component of the earthquake	
	360° – Component	90° – Component
Recorded data	**0.059g**	**0.078g**
Computed using LCC-Deposit case	0.055g	0.078g
Computed using LC3L -Deposit case	0.067g	0.083g

In order to verify the objectives of this study further, surface responses computed from both idealisations (LCC and LC3L) are compared using their corresponding response spectra. Response spectra for 5% damping are obtained for computed surface acceleration responses of both the cases of idealisations of the deposit. These response spectra are plotted in Figure 3.35 along with that of acceleration recorded at the surface. Peak spectral accelerations obtained for the surface response of approximated continuous variation coincide well with that of measured response compared to 3-layer idealisation of the deposit. Particularly in case of 360° component input motion, shown in Figure 3.35a, response spectrum of the surface

acceleration predicted from LCC deposit case almost coincides with that of measured record. Whereas, in case of LC3L deposit idealisation, response spectrum show considerably over estimated spectral acceleration ordinates. It is pertinent to note that, despite peak values of predicted surface accelerations mentioned in Table 3.3 have shown appreciable difference with measured values, comparison of spectral values is found to be satisfactory.
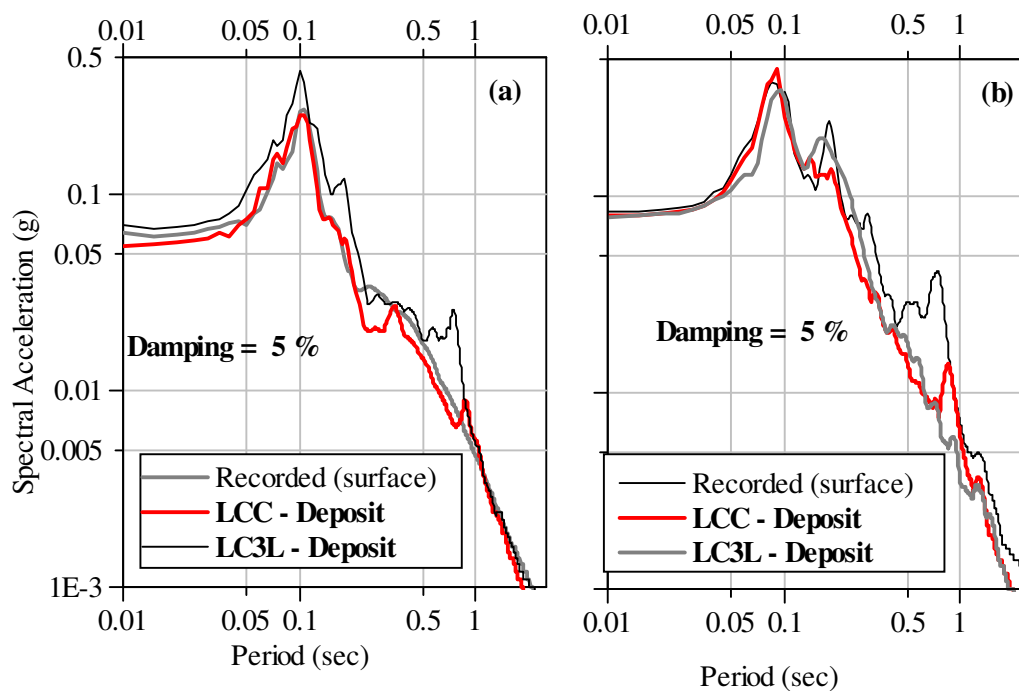
Figure 3.35: Comparison of acceleration response spectra of predicted and observed ground motions at the surface of the deposit for the input motion cases of (a) 360⁰-component and (b) 90⁰-component.

In case of 90⁰-component input motion, shown in Figure 3.35b, there is a marginal difference between spectral values of predicted and measured acceleration reponses. However, comparatively LCC deposit has yielded better results than LC3L deposit when compared with actually measured data. In spite of good agreement with peak value of acceleration in this case (Table 3.3), there are considerable differences in spectral values, particularly in period range of 0.5*s* to 1.0*s*. This observation is apparent for the case of LC3L idealisation in particular.

3.9 FREQUENCY CHARACTERISTICS OF ESTIMATED SURFACE RESPONSE

In the previous chapter, it has been observed that, equivalent linear analysis fails to simulate the measured ground motions at high frequencies and in general the analysis doesn't yield consistent results under weak and strong ground shaking. Many of the researchers have attributed this particular deficiency of equivalent linear approach to frequency dependency of soil properties, i.e., strain rate dependency of shear modulus and damping. The parametric study presented here is an attempt to address the problem by examining the possibility of layer impedances as the cause for poor response simulation at higher frequency ranges.
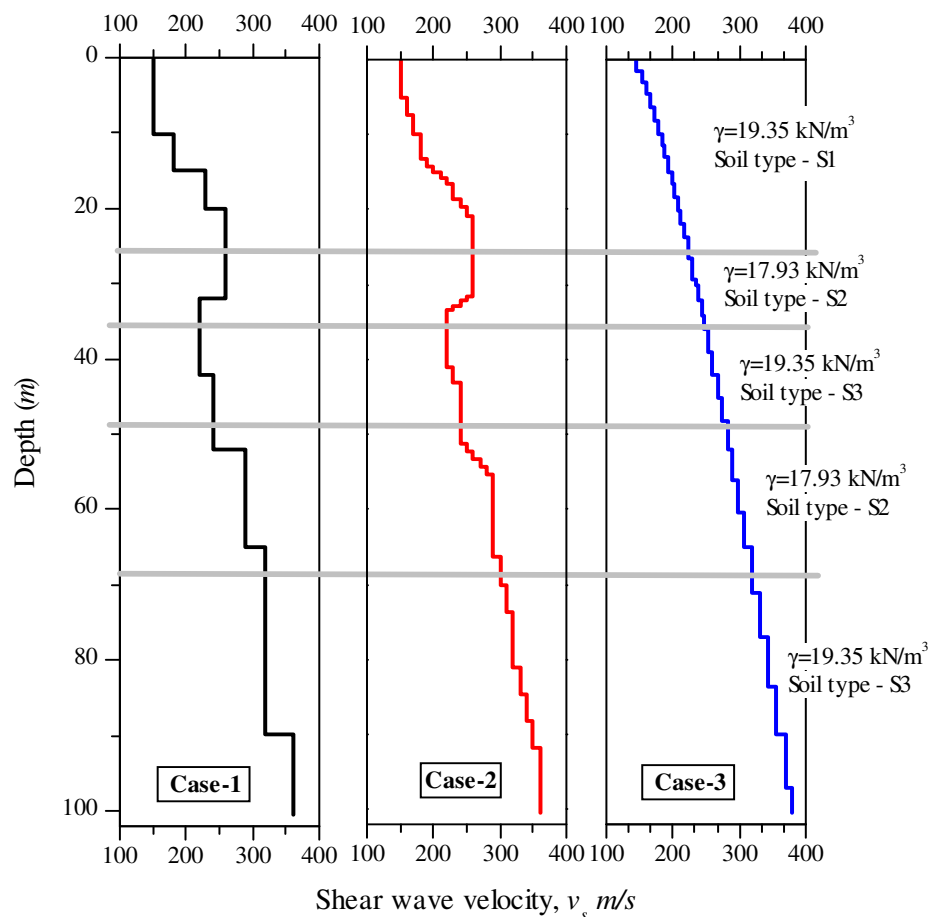
Figure 3.36: Shear wave velocity profiles considered for Case-1, Case-2 and Case-3 analyses

In order to compare the efficiency of the different cases of layer interpretations in simulating the high frequency responses at the surface of the soil deposit, an instrumented geotechnical downhole array at El-Centro Meloland (USA) is considered. This geotechnical array was installed by the California Strong Motion Instrumentation Program (CSMIP) near USA-Mexico border.

The details of El-Centro Meloland geotechnical array are available at the website of Calibration Sites for Validation of Non-Linear Geotechnical Models [Stewart (2002)] sponsored by PEER Lifeline Programs. The information available includes continuous PS logging data and its layered idealisation. Based on these data three distinctly different layered profiles referred to as Case-1, Case-2 and Case-3 are considered. The shear wave velocity profiles corresponding to these cases are shown in Figure 3.36. Site specific strain dependent damping and modulus reduction curves corresponding to soil types S1, S2 and S3 are as shown in Figure 3.37.

Basis for three cases of layer interpretations are as follows,

Case-1: Layered idealisation interpreted in routine manner as usually obtained by engineering judgment based on PS-logging data of the site as available in program website. Totally 15 layers used to define the velocity profile.

Case-2: Layered deposit considered in Case (1) is modified by elimination of sudden velocity gradients at the layer interfaces. This is obtained by assuming smooth linear velocity gradient at layer interfaces extending over an appropriate depth in both of the adjacent layers. Thus 48 layers are employed to model this case.

Case-3: Interpreted layered deposit to match idealised continuous variation of shear wave velocity. Best fit for the PS-logging data is obtained using simple power law equation $V_s(z) = V_{s0} + bz^c$ where, b and c are constants, $V_s(z)$ is the shear wave velocity at depth z measured from surface and V_{s0} is the non-zero surface shear wave velocity. Curve fitting process to approximate the PS-logging data using the above equation results in $v_s(z) = 140 + 11.18z^{0.63}$ with regression coefficient, $r^2 = 0.72$. Using this

144

trend, 35 layers are used to model the shear wave velocity variation across the depth of the soil profile.
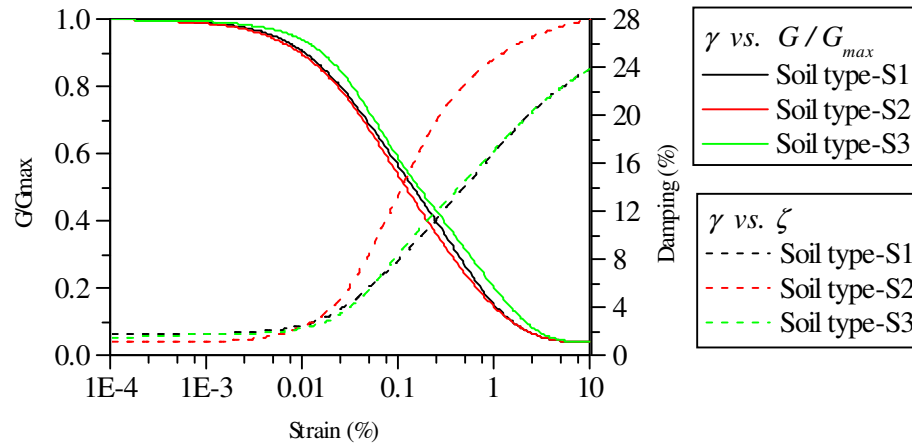
Figure 3.37: Strain dependent soil properties used in the analyses
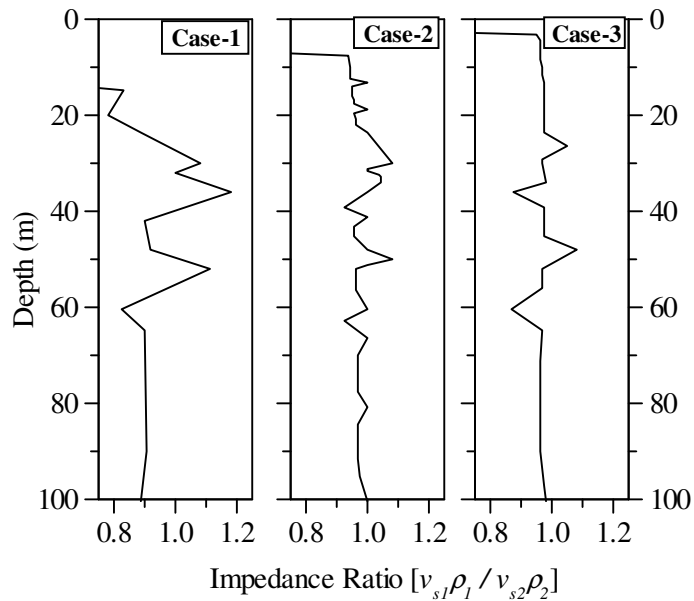
Figure 3.38: Variation of impedance ratio across depth in different cases of layer idealisations.

Figure 3.38 shows the variation of resulting impedance ratios between the layers as a consequence of different cases of layered idealisation of the soil deposit. It must be noted here that impedance contrast is significantly large in Case-1 compared to other two cases. Unlike Case-2, in Case-3 the impedance ratio is almost equal to unity between most of layers except for few layers around mid depth of the deposit.

3.9.1 Earthquake data

El-Centro Meloland geotechnical array is instrumented with accelerometers at depths $0m$, $30m$, $100m$ and $195m$. This array recorded an earthquake event namely Baja California event of Mexico on April 04, 2010. The magnitude of this event is reported to be $M_w=7.2$ at an epicentral distance of about $70km$ (Origin: $64km$ south of Mexico-USA border at a shallow depth of about $10km$). The 270° component of this event recoded maximum acceleration of $0.099g$ at $100m$ depth and $0.191g$ at the surface of this array [Center for Engineering Strong Motion Data (CESMD)]. The recorded data is shown in Figure 3.39.
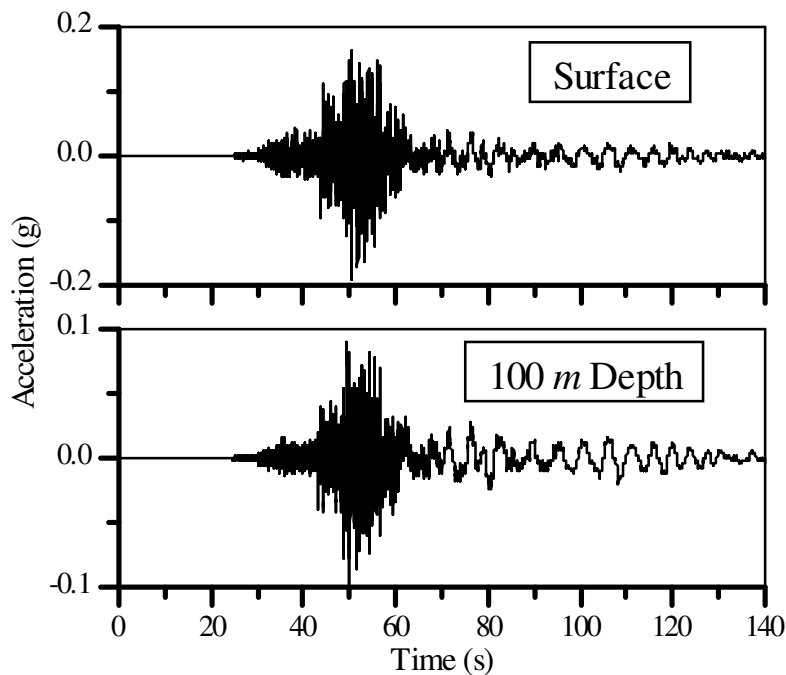
Figure 3.39: Recorded accelerograms at the surface and at 100 *m* depth of El-Centro Meloland geotechnical array during April 04, 2010 earthquake.

3.9.2 Analysis and results

Using EERA equivalent linear analyses is carried out to predict surface motion for all the above cases. Acceleration time history recorded at the depth of 100 *m* (Figure 3.39) is used as input motion at the base of the soil profiles (Figure 3.36) representing 3 cases of layer idealisations considered herein.
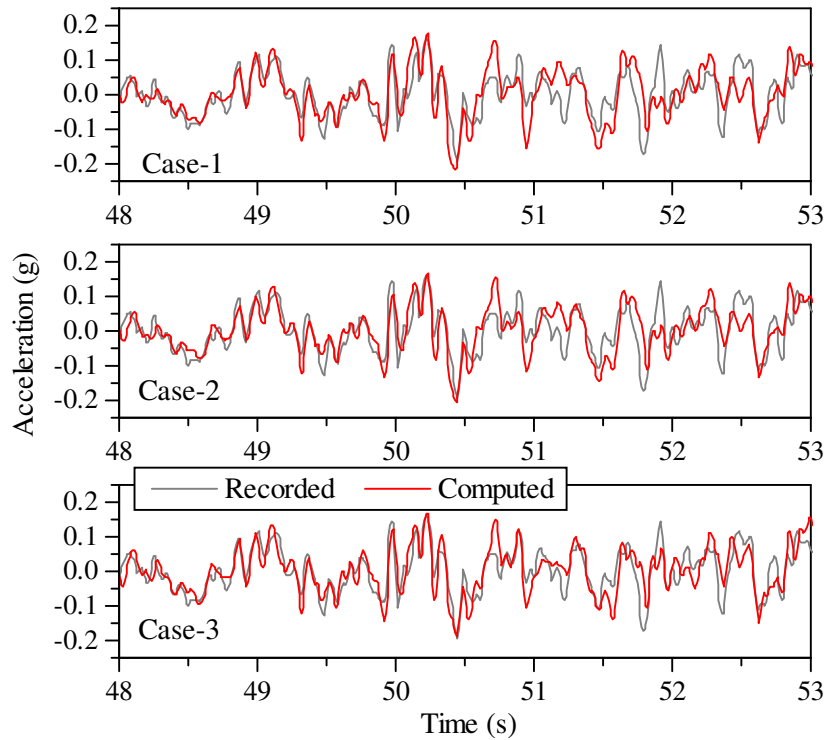
Figure 3.40: Comparison of computed surface responses for the cases considered with recorded accelerogram at the surface

The computed acceleration time histories for all the three cases of analyses are compared with that of measured. The results of these analyses along with measured acceleration record at the surface are presented in Figure 3.40 in the time window of 48 to 53 seconds which represent strong motion phase of the record (time window includes presence of negative and positive maximum accelerations). Computed acceleration time histories of the surface motion are in good agreement with the trend of measured record particularly in the initial phase and attenuating phase (low amplitude signals). However, in the strong motion phase there are noticeable differences in the results of all the three cases of analyses.

The computed maximum accelerations are -0.216g (at time, t = 50.43s), -0.205g (at, t = 50.44s) and -0.189g (at, t = 50.44s) for cases 1, 2 and 3 respectively, while corresponding recorded data is -0.192g (at t = 50.45s). Hence from Figure 3.40., it may be noted that, better prediction of peak acceleration in Case-3 compared to that of Case-1 is evident, though the trend of accelerograms are almost identical for all the cases. Also, many of the peaks of recorded data are better simulated in Case-3 compared to other two cases.

In order to comparatively study the discrepancies in the prediction of responses with different layered idealisations, smoothened Fourier spectra of the responses obtain for each case are plotted. These are compared with that of measured response as illustrated in Figure 3.41.
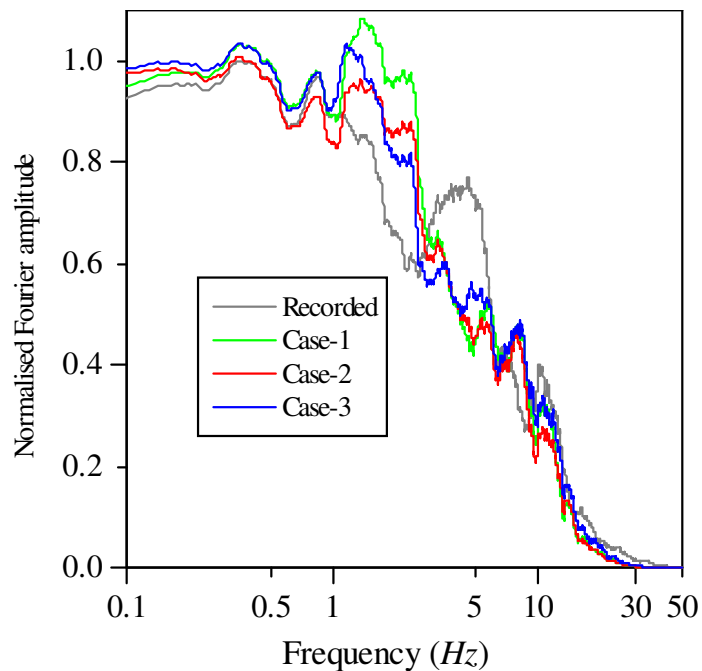
Figure 3.41: Comparison of Fourier spectra of computed surface responses from different cases of shear wave velocity profiles with that of recorded accelerogram at the surface

For the purpose of comparison all the spectra are normalized with respect to peak Fourier amplitude of measured record resulting in unit maximum for the Fourier spectra of recorded data. In the lower frequency ranges (less than 1 *Hz*), spectra of the predicted responses under all the cases are more or less same within acceptable range of differences with respect to spectral values of recorded motion. In this frequency range it is interesting to note that frequency distribution of Fourier amplitudes of Case-2 closely follows the trend of measured data compared to other two cases.

In the intermediate range of frequencies (1 to 10 *Hz.*), Fourier spectra of computed responses for all the three cases are waywardly deviating from spectra of recorded data. Fourier amplitudes are higher in the range of about 1 to 2.5*Hz*, lower in the range of about 2.5 to 5.5 *Hz* and thereafter following closely the spectra of recorded

motion up to 10 *Hz*. In these ranges again we may notice that Case-2 and Case-3 hardly have any noticeable difference between them and show better comparison than Case-1 with the recorded data.
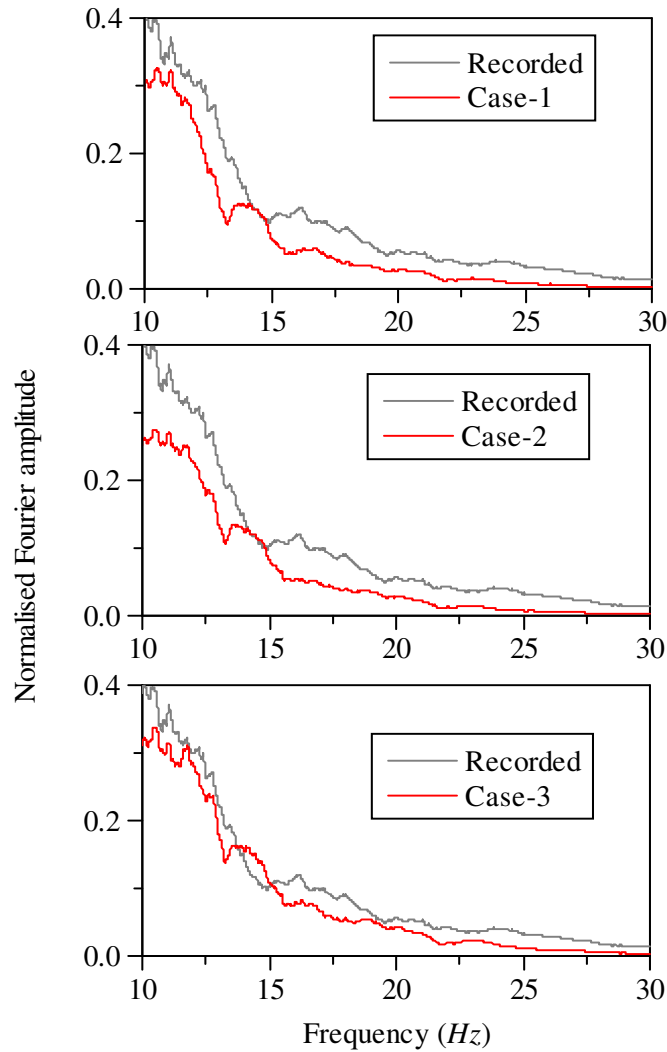
Figure 3.42: Comparison of Fourier spectra of computed surface responses for different cases of shear wave velocity profiles in the frequency range 10 to 30 Hz.

As observed in many of the earlier studies, for e.g., Yoshida et al. (2002), Kausel and Assimaki (2002) etc., in the higher frequency range (>10 *Hz*) all the three cases monotonically underestimate the responses than the actual. Hence an attempt has been made to closely look at the effect of variation in layer impedances on the computed high frequency responses using equivalent linear analysis. In order to understand the clear variations in the results of responses at high frequency range, normalized

Fourier spectra between 10 to 30 *Hz* are plotted separately for all the three cases considered in Figure 3.42 along with spectra of recorded motion.

In Figure 3.42 the comparison clearly indicates that, all layer idealisations considered yield lower amplitude responses in the high frequency region. Even though response computed using Case-2 idealisation observed to be more promising in lower frequency ranges than Case-1, it fails to show better comparison than Case-1 in higher frequency ranges. However, Case-3 idealisation shows remarkably better simulation of high frequency spectral values of observed record. For the purpose of quantitative comparison of predictions alternative plot is presented in Figure 3.43 by taking the ratio of Fourier amplitudes of recorded surface motion to that of each of the cases considered. In this figure horizontal line at unit value is the reference line representing perfect simulation (ratio of recorded motion spectral amplitudes to itself).
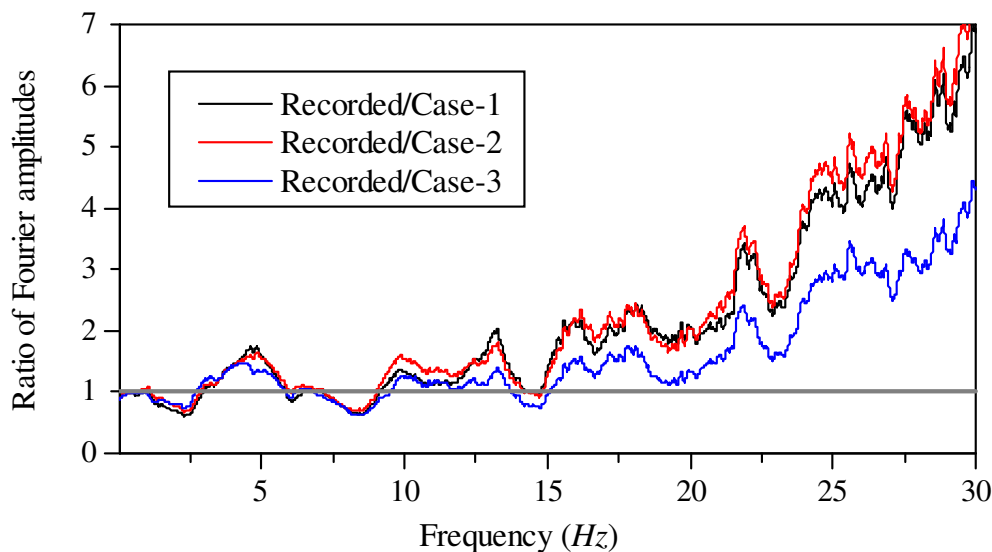
Figure 3.43: Comparison of normalized Fourier amplitude ratio of computed surface responses in the frequency range 1 to 30 *Hz*.

Spectral ratios of Case-1 and Case-2 clearly indicate that between 15 *Hz* and 30 *Hz*, they are underestimated by the magnitude of 2 to 7 times while correspondingly it is only 1 to 3.5 times in Case-3 idealisation. Up to 15 *Hz* all cases show acceptably good simulations and this favorable trend continues up to 20 *Hz* for Case-3. Thus it can be concluded that underestimation of response using equivalent linear analysis in the high frequency region arises mainly due to contrasting impedance ratios between the

adjacent layers. Also different layer idealisations of soil deposit indicate that avoiding sudden velocity gradients at the layer interfaces greatly improve the high frequency simulations. One possible and effective way of achieving this is by idealising the soil deposit using continuously varying shear wave velocity profile (case-3).

3.10 SUMMARY

In this chapter the importance of idealizing the soil deposit as continuously inhomogeneous deposit is highlighted. In view of the process involved with its genesis, influence of environmental, mechanical and other actions are primary reasons for the natural soil deposit to exhibit continuous inhomogeneity. This aspect is well recognized and many studies have attempted to address the problem by seeking analytical solution to response of continuously inhomogeneous deposit and identified the factors which considerably affect the response of such deposits. Also categorically these studies have recognized the fact that eventually the response obtained by modeling such continuously inhomogeneous soil deposits by approximated layered profiles may give inconsistent results. Some of the case studies involving actual observed data have revealed that analysis carried out with routine layered idealisation may result in contradictory response. Literature available in this regard has been reviewed and important results are presented. Also, in this study, an attempt is made to extend the solutions obtained in some of these earlier studies with further derivation to address more general cases. However these analytical studies are limited to linear elastic analysis and only inhomogeneity with respect to variation of shear modulus/shear wave velocity of the soil deposit is considered. The depth inhomogeneity of other soil properties particularly density of the soil deposit is disregarded. Comparative and parametric studies are carried out to identity the effects of approximating the continuously inhomogeneous soil deposits with layered profile idealization on the computed response. Summary of important observations made from these studies is presented below.

The amplification transfer function between surface and base of the deposit is presented for different inhomogeneity functions defining the variation of shear modulus or shear wave velocity along the depth. Starting with a simple case of linear

variation of shear wave velocity along the depth, higher degree inhomogeneity functions representing the continuous variation of stiffness property have been dealt. Analytical results with regard to amplification transfer functions and mode shapes of such inhomogeneous deposits are presented for different inhomogeneity parameters.

Theoretically, the effect of impedance ratio between successive layers on the transmitted and reflected magnitudes of wave amplitude, stress amplitude and wave energy are discussed. As the impedance of the layer decreases wave energy dissipated in that layer increases. Thus wave energy at the surface of a relatively soft layer turns out to be smaller. However, the wave amplitude increases as the impedance of a layer is lower relative to base layer. Since amplification of wave amplitude is sensitive to layer impedances, the importance of appropriate idealization the shear wave velocity profile of the soil deposit is emphasized. For this purpose, variation in impedance ratio across the layers as a consequence of approximating a continuously inhomogeneous deposit with layered profile is parametrically studied. Study carried out for a particular case of inhomogeneity function indicates that the decrease in contrasting impedance ratio tends to be insignificant after certain limiting number of layers used to approximate the continuously varying shear wave velocity profile.

It is observed that as the impedance ratio between inhomogeneous soil deposit and underlying bedrock decreases the maximum amplification increases. More importantly, in case of relatively flexible bedrock, troughs of the amplification transfer function is shifted upwards indicating increase in radiation damping as much of energy is reflected back into flexible half-space. Also it is noted that in case of rigid bedrock underlying an inhomogeneous deposit, irrespective of the degree of inhomogeneity the maximum amplification is unaltered. However, in this instance, the modal frequencies of the deposit are dependent on degree of inhomogeneity. Also shifting of modal frequencies to higher values is evident with increase in shear wave velocity near the surface of the deposit. Both these observations are important in view of the current practice of modeling the bedrock as rigid when input motion is prescribed at the base of the deposit (within motion). This assumption not only leads to overestimation of the responses at resonant frequencies but also affects the spectral characteristics of the computed response.

The analytical study carried out in this chapter also brings about the following important observations,

- As the damping increases the amplification peaks decreases with increase in frequency and rate of decrease is dependent on the impedance ratio between surface layer and bedrock at the base of the deposit.

- The response of continuously inhomogeneous deposits is sensitive to impedance ratio between surface layer and bedrock, inhomogeneity parameters such as ratio of shear wave velocity at the base to that at the surface $\left(v_{sH} / v_{s0} \text{ or } G_H / G_0 \right)$ and degree of inhomogeneity defined by power $(m \text{ or } n)$ of the inhomogeneity function.

- As the ratio v_{sH} / v_{s0} increases (refers to decrease in v_{s0}, i.e., large shear wave velocity gradient near the surface) the modal characteristics are very much sensitive compared to small values of v_{sH} / v_{s0}.

- Similarly, for the values of $m < 1$ the response characteristics are significantly affected compared to large values of m for all values of velocity ratios.

- Trends of the mode shapes corresponding to all the natural modes of vibration of the deposit are significantly different for low and high values of v_{sH} / v_{s0} particularly near the surface of the deposit signifying deviation from the assumptions made regarding surface boundary condition.

Amplification characteristics of waves at the free surface of an inhomogeneous layer overlying a homogeneous layer of finite thickness (instead of half-space) are studied. In particular, the effect of depth of homogeneous bottom layer on amplification at the free surface. As the shear wave velocity of the bottom layer increases the amplification increases because of decrease in impedance ratio between the two layers. Increase in depth of the bottom layer decreases the resonant frequencies but maximum amplification depends on the ratio of depths of top and bottom layer. More importantly, all resonant amplitudes are considerably higher than that obtained for single layer for all values of impedance ratio between base of the deposit and bedrock.

The solution obtained for stack of multiple Gibson layers is used to study the scope for incorporating a transition layer at the interfaces of homogeneous layered system in order to achieve gradual variation in layer impedances at their interfaces. Thereby it is intended to overcome unrealistic effects of contrasting impedances on the amplification characteristics of layered deposits. The parametric study carried out by varying the depth of transition zone with respect to layer thickness indicates that prediction of high frequency response can be improved without affecting much the lower mode responses. Also it is shown that appropriate configuration of Gibson layers can be used effectively to represent continuously inhomogeneous soil deposits instead of approximating them with stack of homogeneous layers.

In order to verify the observations made above, two independent studies are carried out using the profile data of two instrumented geotechnical downhole arrays. The earthquake data recorded at these sites are used to compare the computed response from different shear wave velocity profile idealisations with an objective to investigate the implications of idealizing the deposit with continuous and layered profiles. Firstly, calculated responses for three different layered idealisations were compared with the measured response (La-Cienega site, USA). Results of idealisation with more number of layers indicating continuous variation in soil properties is found to be closer to reality than those with less number of layers.

In the second case study an attempt is made to address the issue of underestimation of high frequency response in equivalent linear analysis. For this propose, analyses are carried out considering three cases of layered idealisations, with distinctly different impedance characteristics, representing the shear wave velocity profile of a soil deposit of El-Centro Meloland geotechnical array site. The computed surface responses are compared with those of actually measured data. The results clearly demonstrate that the high frequency response characteristics are very much sensitive to layer configuration particularly for contrasting impedance ratios between the layers.

CHAPTER 4

ANALYSIS OF CONTINUOUSLY INHOMOGENEOUS SOIL DEPOSITS - COMPUTER PROGRAM **SRISD**

4.1   INTRODUCTION

Characterisation of local site effects for earthquake ground motion is usually performed using one dimensional earthquake ground response analysis. These classes of analyses procedures are often based on the assumption that perfectly horizontally layered soil profile is excited by vertically propagating and horizontally polarized shear waves. In fact, in some instances non-homogeneity of the surface deposit may be due to continuous variation of stiffness and density rather than distinctly layered formation. Review of analytical studies pertaining to amplification characteristics of continuously inhomogeneous soil deposits and outcome of these studies have been presented in the previous chapter. Also, comparative study carried out with regard to modeling continuous inhomogeneity with an equivalent layered profile consisting of sufficiently large number of layers closely representing the trend of continuous variation has revealed distinct advantages in improving the results. Particularly, improvement in high frequency response simulation using equivalent linear procedure was evident compared to routine layered analysis. In view of these studies it can be concluded that, there is scope for improving the standard equivalent linear method of predicting seismic ground response. As these analytical studies have pointed out, main drawback of the routine one-dimensional modeling of the ground arises out of the assumption of uniform horizontal layers of varying depths. This kind of modeling the ground leads to unrealistic and contrasting impedance ratio between adjacent layers. In turn this results in poor simulation of ground response. Hence there is need for overcoming this lacuna by modeling the ground profile with continuous variation of soil properties thus resulting in smooth transition instead of abrupt variation.

In the previous chapter, fallout of performing the analysis based on obscurely modeled layered idealisation when the ground essentially exhibits continuous

variation of soil properties has been brought out. In this chapter numerical analysis and the associated computer program developed for seismic response analysis of 1-D continuously inhomogeneous ground is presented. The details about the computer code **SRISD** (**S**eismic **R**esponse of **I**nhomogeneous **S**oil **D**eposits) along with example analyses for validation and testing of the program are presented.

4.2   NUMERICAL PROCEDURE TO SOLVE 1-D WAVE EQUATION

The procedure described here is similar to the one implemented by Prasad (1996). This procedure was developed essentially for limited application, primarily, to verify experimental data pertaining to model ground prepared using a laminar box. The main objective of the test was to study the deformation characteristics of the homogeneous model ground under harmonic excitation. Thus, in his study the computer code developed was limited to carrying out linear analysis under harmonic excitation. In the present study, the numerical procedure is further modified and extended to develop a general purpose site response analysis computer program which will have all the features and capabilities of any other available computer program based on equivalent linear response analysis. Apart from this broad objective, the envisaged computer program shall include some additional attributes to accommodate the refinements based on the outcome of this research work.

4.2.1   Governing equations

For a soil deposit with continuous variation in shear modulus along the depth (z), wave equation for the upward propagation of shear waves given by Equation (3.4) of previous chapter may be expressed using the usual notations as,

$$\rho \frac{\partial^2 u}{\partial t^2} = \frac{\partial}{\partial z}\left[G^*(z) \frac{\partial u}{\partial z} \right]$$
(4.1)

where G^* is the complex shear modulus, given by,

$$G^* = G(1 + 2i\zeta) = G + i\overline{G}$$
(4.2)

156

Here G $\left(G = \rho v_s^2\right)$ is the shear modulus, $i = \sqrt{-1}$, ζ is the equivalent viscous damping coefficient which is considered to be independent of frequency of excitation and $\bar{G} = 2iG\zeta$. If the excitation is considered to be harmonic, then displacement and shear stress are expressed as functions of space and time as given by Equations (3.26) and (3.27) respectively (Chapter 3). Combining these with Eq. (4.1) yields,

$$G^* \frac{\partial^2 T}{\partial z^2} + \rho \omega^2 T = 0 \tag{4.3}$$

Since shear modulus is complex, the shear stress amplitude, T is also complex. If τ_1 and τ_2 are real and imaginary parts respectively of shear stress amplitude, we have,

$$T = \tau_1 + i\tau_2 \tag{4.4}$$

Therefore, it follows

$$\left.\begin{array}{l} \dfrac{dT}{dz} = \dfrac{d\tau_1}{dz} + i\dfrac{d\tau_2}{dz} = \tau_1' + i\tau_2' \\[3mm] \dfrac{d^2T}{dz^2} = \dfrac{d^2\tau_1}{dz^2} + i\dfrac{d^2\tau_2}{dz^2} = \tau_1'' + i\tau_2'' \end{array}\right\} \tag{4.5}$$

Substituting in (4.3) yields,

$$G\tau_1'' - \bar{G}\tau_2'' + \rho\omega^2\tau_1 + i(\bar{G}\tau_1'' + G\tau_2'' + \rho\omega^2\tau_2) = 0 \tag{4.6}$$

Making both real and imaginary parts equal to zero,

$$G\tau_1'' - \bar{G}\tau_2'' + \rho\omega^2\tau_1 = 0 \tag{4.7}$$

$$\bar{G}\tau_1'' + G\tau_2'' + \rho\omega^2\tau_2 = 0 \tag{4.8}$$

Combining the above equations (4.7) and (4.8), we have,

$$\begin{Bmatrix} \tau_1'' \\ \tau_2'' \end{Bmatrix} = -\rho\omega^2 \begin{bmatrix} G & -\bar{G} \\ \bar{G} & G \end{bmatrix}^{-1} \begin{Bmatrix} \tau_1 \\ \tau_2 \end{Bmatrix} \tag{4.9}$$

This yields,

$$\tau_1'' = \frac{-\rho\omega^2(G\tau_1 + \bar{G}\tau_2)}{G^2 + \bar{G}^2} \tag{4.10}$$

$$\tau_2'' = \frac{\rho\omega^2(\bar{G}\tau_1 - G\tau_2)}{G^2 + \bar{G}^2} \tag{4.11}$$

From Eq. (4.5), we have $\tau_1' = \dfrac{\partial \tau_1}{\partial z}$; $\tau_2' = \dfrac{\partial \tau_2}{\partial z}$; $\tau_1'' = \dfrac{\partial \tau_1'}{\partial z}$ and $\tau_2'' = \dfrac{\partial \tau_2'}{\partial z}$.

Taking $\kappa_1 = \tau_1$; $\kappa_2 = \tau_2$; $\kappa_3 = \tau_1'$ and $\kappa_4 = \tau_2'$, we have,

$$\frac{d\kappa_1}{dz} = \kappa_1' = \kappa_3; \text{ i.e, } \kappa_3 = \frac{\partial \tau_1}{\partial z} = \tau_1' \tag{4.12}$$

$$\frac{d\kappa_2}{dz} = \kappa_2' = \kappa_4; \text{ i.e, } \kappa_4 = \frac{\partial \tau_2}{\partial z} = \tau_2' \tag{4.13}$$

$$\frac{d\kappa_3}{dz} = \kappa_3' = \frac{-\rho\omega^2(G\kappa_1 + \bar{G}\kappa_2)}{G^2 + \bar{G}^2} \tag{4.14}$$

$$\frac{d\kappa_4}{dz} = \kappa_4' = \frac{\rho\omega^2(\bar{G}\kappa_1 - G\kappa_2)}{G^2 + \bar{G}^2} \tag{4.15}$$

Therefore simultaneous equations (4.12) to (4.15) represent a set of four first order ordinary differential equations. Numerical solution of these differential equations is obtained using the Fourth order Runge-Kutta method to give $\kappa_1, \kappa_2, \kappa_3$ and κ_4. Then, shear stress amplitude is given by Eq. 4.4,

$$T = \kappa_1 + i\kappa_2 \tag{4.16}$$

Displacement, shear strain and acceleration amplitudes are obtained using the following,

Displacement; $U(z) = -\dfrac{1}{\rho\omega^2}\dfrac{\partial T}{\partial z} = -\dfrac{1}{\rho\omega^2}(\kappa_3 + i\kappa_4)$ (4.17)

Shear strain; $\dfrac{\partial U}{\partial z} = \dfrac{T}{G^*} = \dfrac{\kappa_1 + i\kappa_2}{G + \bar{\bar{G}}}$ (4.18)

Acceleration; $\ddot{u}(z) = \dfrac{1}{\rho}(\kappa_3 + i\kappa_4)$ (4.19)
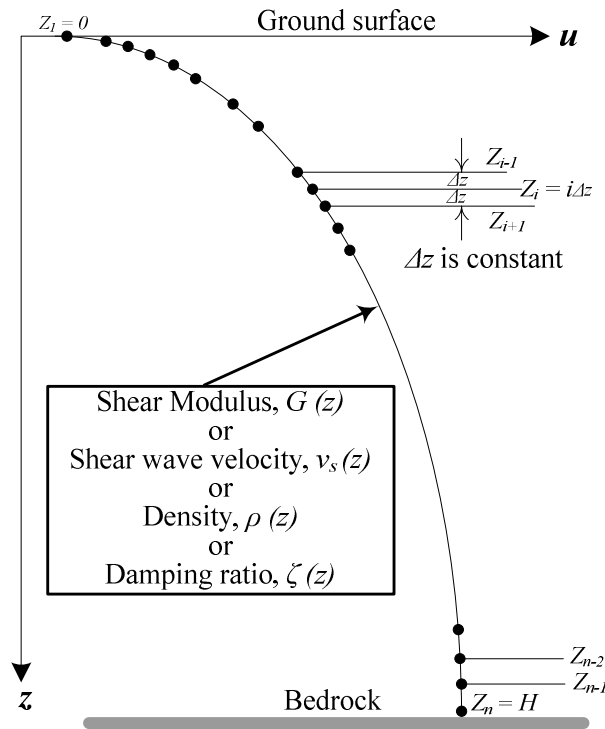
Figure 4.1: One-dimensional soil deposit with continuous variation in soil properties and its discrete idealisation in space

The above set of ordinary differential equations (4.12, 4.13, 4.14 and 4.15) may be expressed in the general form as,

$$
\left.
\begin{aligned}
\frac{d\kappa_1}{dz} &= f_1(z, \kappa_1, \kappa_2, \kappa_3, \kappa_4) \\
\frac{d\kappa_2}{dz} &= f_2(z, \kappa_1, \kappa_2, \kappa_3, \kappa_4) \\
\frac{d\kappa_3}{dz} &= f_3(z, \kappa_1, \kappa_2, \kappa_3, \kappa_4) \\
\frac{d\kappa_4}{dz} &= f_4(z, \kappa_1, \kappa_2, \kappa_3, \kappa_4)
\end{aligned}
\right\}
$$
(4.20)

159

Here f_1, f_2, f_3 and f_4 are the functions of dependent and independent variables representing the derivatives of $\kappa_1, \kappa_2, \kappa_3$ and κ_4 respectively. Assuming that the soil properties such as shear modulus $(G(z))$ or shear wave velocity $(v_s(z))$, density $(\rho(z))$ and damping ratio $(\zeta(z))$ of the deposit is defined at n data points including bed rock at the depths $Z_1, Z_2, Z_3, \ldots\ldots Z_i \ldots\ldots Z_{n-1}, Z_n$ measured from the surface $(Z_1 = 0)$, then between any two data points Z_i and Z_{i+1} the soil properties may be interpolated for any desired variation.

Suppose, the step size for numerical differentiation is Δz, the soil properties are determined for all the nodes $(Z_n / \Delta z)$ using corresponding interpolation function. The discrete idealisation of the deposit for the purpose of implementing numerical procedure is shown schematically in Figure 4.1. Procedure described above can accommodate continuous variation in shear modulus or shear wave velocity, density and damping ratio of the deposit along the depth. The system of first order total differential equations (Equations 4.12 to 4.15) are solved for the values of $\kappa_1, \kappa_2, \kappa_3$ and κ_4.

4.2.2 Fourth order Runge - Kutta scheme

The computer program SRISD is developed to obtain responses using Equations (4.17), (4.18) and (4.19). In order to solve the simultaneous Equations (4.12), (4.13), (4.14) and (4.15) fourth order Runge-Kutta numerical differentiation scheme is used. In this method the truncation error is $(\Delta z)^5$ [Atkinson (1984)] and it is worth noting that the gain in accuracy achieved using higher order method is not much vis-à-vis fourth order scheme, particularly, in view of added computational effort and complexity involved [Ralston and Rabinowitz (1978)]. The following steps illustrate the method of implementation of fourth order Runge-Kutta scheme to solve for $\kappa_1, \kappa_2, \kappa_3$ and κ_4 of Eq. (4.20) at any depth z_i with an interval of Δz (Figure 4.1). In general form, using the values of $\kappa_1, \kappa_2, \kappa_3$ and κ_4 at z_i, that is $\kappa_j^{(i)}$ where $j = 1$ to 4 at z_i, $\kappa_j^{(i+1)}$ may be computed using fourth order Runge-Kutta scheme as,

$$\kappa_j^{(i+1)} = \kappa_j^{(i)} + \frac{1}{6}(q_1^{(j)} + 2q_2^{(j)} + 2q_3^{(j)} + q_4^{(j)})(\Delta z) \tag{4.21}$$

where the coefficients $q_1^{(j)}, q_2^{(j)}, q_3^{(j)}$ are $q_4^{(j)}$ represented by the following relationships,

$$\left.\begin{cases} q_1^{(j)} = f_j\left(z_i, \kappa_1^{(i)}, \kappa_2^{(i)}, \kappa_3^{(i)}, \kappa_4^{(i)}\right) \\[2mm] q_2^{(j)} = f_j\left(z_i + \frac{\Delta z}{2}, \kappa_1^{(i)} + \frac{\Delta z q_1^{(j)}}{2}, \kappa_2^{(i)} + \frac{\Delta z q_1^{(j)}}{2}, \kappa_3^{(i)} + \frac{\Delta z q_1^{(j)}}{2}, \kappa_4^{(i)} + \frac{\Delta z q_1^{(j)}}{2}\right) \\[2mm] q_3^{(j)} = f_j\left(z_i + \frac{\Delta z}{2}, \kappa_1^{(i)} + \frac{\Delta z q_2^{(j)}}{2}, \kappa_2^{(i)} + \frac{\Delta z q_2^{(j)}}{2}, \kappa_3^{(i)} + \frac{\Delta z q_2^{(j)}}{2}, \kappa_4^{(i)} + \frac{\Delta z q_2^{(j)}}{2}\right) \\[2mm] q_4^{(j)} = f_j\left(z_i + \Delta z, \kappa_1^{(i)} + \Delta z q_3^{(j)}, \kappa_2^{(i)} + \Delta z q_3^{(j)}, \kappa_3^{(i)} + \Delta z q_3^{(j)}, \kappa_4^{(i)} + \Delta z q_3^{(j)}\right) \end{cases}\right\} \tag{4.22}$$

The coefficients $q_1^{(j)}, q_2^{(j)}, q_3^{(j)}$ and $q_4^{(j)}$ are computed for all values of j successively at the depth z_i knowing $\kappa_1^{(i)}, \kappa_2^{(i)}, \kappa_3^{(i)}$ and $\kappa_4^{(i)}$ either from the boundary condition (that is at $z = 0$) or from the computations of previous iteration. Then using equation (4.21) $\kappa_1^{(i)}, \kappa_2^{(i)}, \kappa_3^{(i)}$ and $\kappa_4^{(i)}$ are updated to $\kappa_1^{(i+1)}, \kappa_2^{(i+1)}, \kappa_3^{(i+1)}$ and $\kappa_4^{(i+1)}$ respectively. This procedure may be continued for all the nodes that are equally spaced at Δz.

4.2.3 Boundary conditions

In Eq. 4.21, $\kappa_j^{(i+1)}$ for $i = 0$ may be computed using the values of $\kappa_j^{(0)}$ which may be established with the boundary condition at the surface i.e., shear stress $\tau_{(z=0)} = 0$. As a result, from Eq. 4.16 we have $T_{(z=0)} = 0$. Therefore at $z = 0$ we get $\kappa_1 + i\kappa_2 = 0$. Hence, $\kappa_1^{(0)} = 0$ and $\kappa_2^{(0)} = 0$. Assuming that the acceleration is known at the surface, we have $\ddot{u}_{(z=0)} = (\kappa_3 + i\kappa_4)/\rho$ for all time increments. Input acceleration being a real quantity, we get $\kappa_3^{(0)} = \rho \ddot{u}(z = 0, t)$ and $\kappa_4^{(0)} = 0$. Thus at $z = 0$ satisfying the boundary condition of zero shear stress and known acceleration yields,

$$\left.\begin{aligned} \kappa_1^{(0)} &= \kappa_2^{(0)} = \kappa_4^{(0)} = 0 \\[4mm] \kappa_3^{(0)} &= \rho \ddot{u}(z = 0, t) \end{aligned}\right\} \tag{4.23}$$

4.2.4   Frequency domain analysis

The theory and equations developed in the above section are capable of analyzing the ground response due to input steady state harmonic acceleration record. However, general seismic accelerogram is usually transient and defined in time domain at discrete time intervals. Therefore it is necessary to decompose this time history data into its harmonic components and corresponding amplitudes. To accomplish this fast Fourier transformation (FFT) may be adopted. Among several FFT techniques that are available, Cooley and Tukey algorithm is popular. In the present study Sande-Tukey algorithm based on decimation in frequency process is used. Although these two methods differ in type of process they will produce identical final results [Remirez (1985)].

Consider the accelerogram $a(t)$ defined at discrete intervals of time which typically represents the data of an earthquake event of total duration T as follows,

$$a(t) = \begin{cases} a(t) & for \ 0 < t < T \\ 0 & for \ t > T \end{cases} \tag{4.24}$$

The Fourier transform $A(\omega)$ of this function is defined as,

$$A(\omega) = \int_0^T a(t)e^{-i\omega t}dt \tag{4.25}$$

Since the given data is in discrete form the above integral may be replaced by the summation over the time axis of N equal intervals, which correspond to the $N+1$ time coordinates t_n, $n = 0, 1, 2, ...N$, such that $t_{n+1} - t_n = \Delta t$ for all values of $n = 0, 1, 2, ...N-1$, so that,

$$A(k) = \sum_{n=0}^{N-1} a(n)e^{-i\left(\frac{2\pi}{N}\right)nk} \quad , \quad 0 \leq k < N \tag{4.26}$$

Depending on whether the value of k is odd or even the above equation can be expressed as,

$$A(2k) = \sum_{n=0}^{\frac{N}{2}-1} \left[a(n) + a\left(n + \frac{N}{2} \right) \right] W^{n(2k)} \tag{4.27}$$

for even values of k and when k is odd, we have

$$A(2k+1) = \sum_{n=0}^{\frac{N}{2}-1} \left[a(n) - a\left(n + \frac{N}{2} \right) \right] W^{n(2k+1)} \tag{4.28}$$

where $W = e^{-i\left(\frac{2\pi}{N} \right)}$ is complex valued weighting function. From Eq. (4.27) and Eq. (4.28) we get the two sided frequency domain record at discrete frequencies ω_k for $k = 0, 1, 2, \ldots \frac{N}{2} - 1$ at $\Delta\omega = \frac{2\pi}{T}$ from N data points of time domain record. Fourier transform has an inverse that has an almost identical structure to recover discrete time record from its frequency domain data as,

$$a(n) = \frac{1}{N} \sum_{k=0}^{N-1} A(k) e^{i\left(\frac{2\pi}{N} \right) nk} \quad , \quad 0 \le n < N \tag{4.29}$$

the above equation yield the equations,

$$a(2n) = \frac{1}{N} \sum_{k=0}^{\frac{N}{2}-1} \left[A(k) + A\left(k + \frac{N}{2} \right) \right] W^{-k(2n)} \tag{4.30}$$

$$a(2n+1) = \frac{1}{N} \sum_{k=0}^{\frac{N}{2}-1} \left[A(k) - A\left(k + \frac{N}{2} \right) \right] W^{-k(2n+1)} \tag{4.31}$$

Equations (4.30) and (4.31) are the inverse Fourier transforms of $A(\omega)$, in which apart from scaling factor $1/N$ the inverse Fourier transform is just as Eq. (4.27) and Eq. (4.28) with W being replaced by its complex conjugate. Hence, algorithm that computes the Fourier transform can be used, with minor modification, to compute the inverse discrete Fourier transform. It is evident from the equations that, the even and odd parts of the $A(\omega)$ or $a(t)$ can be computed separately using discrete points of

length $N/2$ and this decomposition can be applied recursively thereby reducing the computational effort to enormous extent [Schilling and Harris (2002)]. Thus FFT algorithm requires the condition $N = 2^M$ to be satisfied. In order to meet this condition actual record is appended with required number of zeros at the same time interval. This, adding quiet zone to accelerogram, in fact has got additional advantage because it improves the frequency resolution. In the SRISD computer program, the FFT pseudo-code given by Chapra and Canale (1998) is implemented with modification.

4.3 SOIL PROFILE DATA

Soil profile data consist of geometrical data and material properties. The geometrical data depends on how the soil profile is modeled with respect to soil properties. The soil properties associated with an inhomogeneous deposit in turn depends upon the type of inhomogeneity. The inhomogeneity of the soil deposit is usually modeled using layered idealisation. However, more often available field and laboratory data will generally provide information about the soil properties and its distribution along the depth at discrete points, often at constant interval, to appropriately model as one-dimensional soil deposit. In general the soil deposit can be modeled as continuous profile or discrete data points or layered profile depending on analysis model employed. The numerical procedure described above is modified in spatial discretization of the soil deposit to provide flexibility in modeling as explained in the following sections. Usually, low strain shear modulus or shear wave velocity, density and initial damping ratio of the soil deposit are the essential soil properties for the seismic site response analysis.

4.3.1 Continuous profile

If the soil properties are continuously varying along the depth the data is required to be given in the form of an appropriate function of depth. Most popular power law functions which can be used to model continuous distribution of shear modulus or shear wave velocity along with analytical solutions for the amplification response are discussed in the previous chapter.

For continuously inhomogeneous soil deposits the data is in the form of associated parameters of the function defining its variation. The numerical procedure described above is also compliant for modeling continuous variation of damping and density of the soil deposit. Along with these parameters of the depth function defining the trend of soil properties distribution, appropriate uniform step size for spatial discretization is to be selected (Δz in Figure 4.2a) with due consideration to rate of change of soil properties along the depth in order to ensure accuracy.
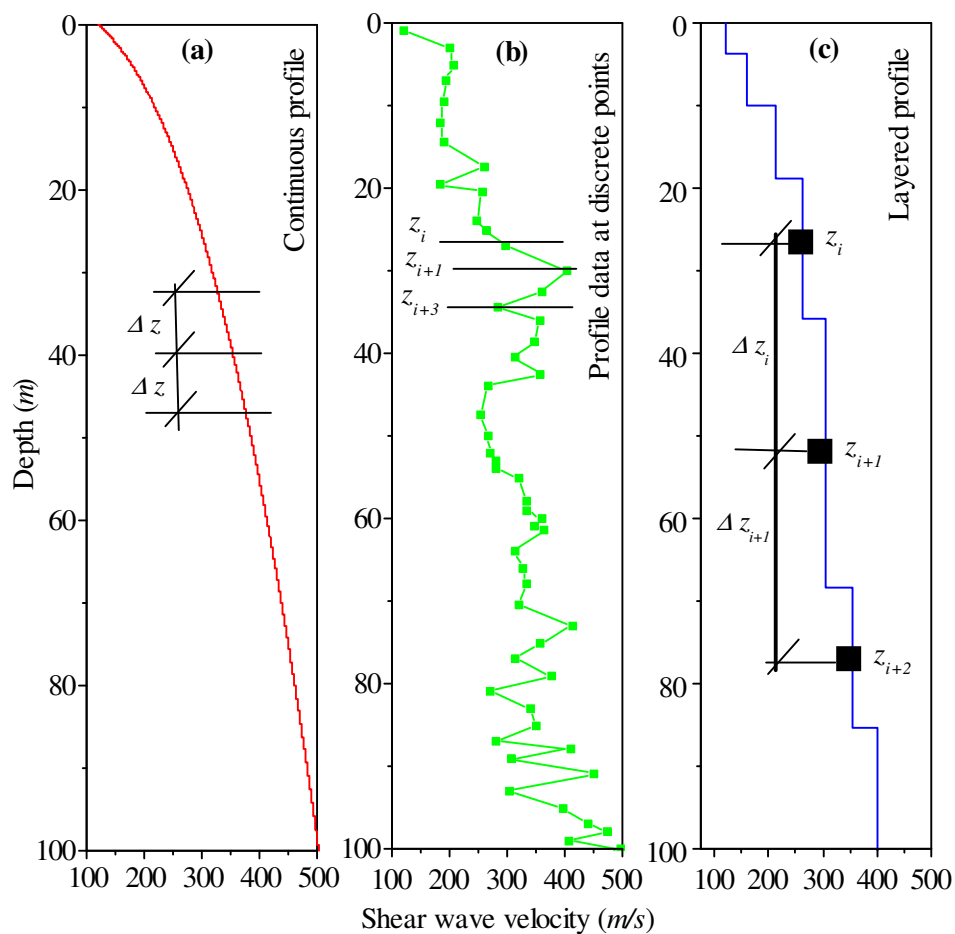
Figure 4.2: Different options for soil profile data and corresponding input data to control step size depending upon the profile configuration; (a) Continuous profile data, (b) Profile data at discrete points and (c) Layered profile data

4.3.2 Profile data at discrete points

In case of continuous profiling techniques such as continuous P-S logging technique, shear wave velocity distribution along the depth is obtained often at equally spaced

discrete points. Usually such information is interpreted to arrive at layered shear wave velocity profile. In the numerical procedure explained above, it is possible to use this raw data of discrete shear wave velocity distribution along the depth for response analysis. For this purpose the values of shear wave velocities or shear modulus and corresponding depths are used as profile input data. That is, $v_{s(i)}$ or G_i is prescribed at corresponding depths z_i for $i = 1, 2, ...n$. In general all the soil properties between these data points are assumed to be linearly distributed and can be obtained by interpolation. The procedure is illustrated in Figure 4.2b.

4.3.3 Layered profile

The numerical procedure using Runge-Kutta method developed for seismic response of continuously inhomogeneous soil deposits can be generalized to carry out analysis of layered profiles. For this purpose, the variable step size for spatial discretization is used. In the procedure developed Δz_i is constant, whereas in case of layered profile Δz_i between two successive layers is the difference in mid-depths of these two layers as shown in Figure 4.2c. At these points the data pertaining to soil properties (shear wave velocity or shear modulus, density and damping ratio) of those layers are to be prescribed. These data are considered to be uniform throughout the depth of that layer.

In classical numerical analysis, the methods which can implement variable step size are called adaptive methods and they are often preferred to improve the speed depending on the solution trend. Here the objective is to accommodate analysis of layered profile within the frame work of the numerical algorithm developed for continuously inhomogeneous profiles. The procedure for numerical implementation of this variable step size discretization along with its effect on stability and accuracy is detailed elsewhere [Schilling and Harris (2002)]. However, the procedure can be easily programmed to adjust step size depending upon thicknesses of adjacent layers such that the process is advanced to mid-reach of every layer. In order to enhance the accuracy of the solution, intermediate data points with appropriate spacing may be considered.

4.4   INPUT MOTION SPECIFICATION

4.4.1   Surface motion

The surface boundary condition used to obtain the initial values of $\kappa_1, \kappa_2, \kappa_3$ and κ_4 at $z = 0$ can be directly used in the response analysis for the case of input motion prescribed at the surface of the soil deposit. Eq. (4.23) gives the values as $\kappa_1^0 = \kappa_2^0 = \kappa_4^0 = 0$ and $\kappa_3^0 = \rho\ddot{u}(z = 0, t)$. Here, $\ddot{u}(t)$ is the acceleration time history for which the responses are calculated at any desired depths.

4.4.2   Base motion

For the case of input motion is to be prescribed at the base of the soil deposit the initial values of $\kappa_1, \kappa_2, \kappa_3$ and κ_4 given in Eq. (4.23) alone is not sufficient. However, the procedure used here is similar to deconvolution of surface motion to obtain base motion but with modification. Almost all popular computer programs developed for equivalent linear analysis of layered deposits the response at surface due to base input motion is obtained using the relative amplification between surface and base and vice versa as detailed earlier (Chapter 2). Herein, instead of using amplification function, shooting method [Schilling and Harris (2002)] is introduced for estimating the surface motion. For any arbitrary surface motion given at the surface, the base motion is estimated and adjusted accordingly to obtained target accelerogram in an iterative manner. For this purpose, the iterative scheme employed to implement equivalent linear method is also simultaneously used for estimation and updating of input accelerogram at the base of the soil deposit ($z = H$). If the input motion is to be given at any intermediate depth ($0 < z_i < H$) other than surface ($z = 0$) or base ($z = H$) the same procedure is used.

4.5   EQUIVALENT LINEAR ANALYSIS

In equivalent-linear method, the nonlinear behaviour of soil is modeled by considering shear modulus and damping as a function of shear strain. The hysteretic stress-strain behavior of soils under cyclic loading is represented by an equivalent

modulus and damping ratio. The equivalent modulus is corresponding to the secant modulus through the endpoints of the hysteresis loop and equivalent-linear damping ratio is proportional to the energy loss from a single cycle of shear deformation. An iterative procedure, based on linear dynamic analysis, is performed to find the shear modulus and damping ratios corresponding to the computed shear strains. The iterative procedure of equivalent linear method (EQL) to update shear modulus and damping consistent with computed effective strain in a particular iteration is previously described in Chapter 2 (Section 2.7.1). As shown in the Figures 2.9 and 2.10, initial estimates of the dynamic shear modulus, corresponding to low strain shear modulus (G_{max}) and damping ratios (ζ) are assigned to each of the nodes for the first iteration.

Thus equivalent linear analysis essentially requires input of shear modulus ratio (G/G_{max}) and damping ratio (ζ) curves expressed as function of strain (γ_{eff}). In case of routine large scale ground response studies usually readily available information with respect to different types of soil are used. Many of the computer codes for e.g., SHAKE [Schnabel et al. (1972)], SHAKE91 [Idriss and Sun (1992)], DEEPSOIL [Hashash (2011)], STRATA [Kottke and Rathje (2008)], EERA [Bardet et al (2000)], etc. have incorporated some of the popular generic curves and they are readily available for the user. For example, such typical data pertaining to clay and sand are presented in Table 4.1. In fact the data given in this table is taken from the computer program STRATA. If the site specific information is available, then G/G_{max} and ζ values at discrete strain data are to be provided by the user. In both the cases linear interpolation is carried out to compute G/G_{max} and ζ at any intermediate strain level. In the following sections data required to be provided in this regard for the computer program SRISD is discussed.

4.5.1 Modeling strain dependent shear modulus and damping properties

In the computer program SRISD the G/G_{max} and ζ versus γ_{eff} curves are approximated by a polynomial function and data is given in the form of coefficients of the polynomial function. This procedure is implemented to overcome linear interpolation

between data points and thereby associated interpolation error is avoided. Firstly, it is demonstrated that many of the generic data curves can be satisfactorily represented by a seventh degree polynomial. Thus G/G_{max} and ζ can be conveniently expressed as a continuous function of effective strain. For some of the popularly used generic strain dependent G/G_{max} and ζ curves, the polynomial coefficients are incorporated in the subroutine. The seventh degree polynomial to represent strain dependent shear modulus and damping ratio is given by,

$$\left.\begin{matrix} \dfrac{G}{G_{max}}(\gamma) \\[2mm] \zeta(\gamma) \end{matrix}\right\} = \sum_{i=0}^{7} B_i \gamma_{eff}^i \qquad (4.32)$$

Here γ_{eff} is the effective strain computed based on computed maximum strain (γ_{max}) in the previous iteration. Coefficients of Eq. (4.32) B_i $(i = 0,1,2,...7)$ are distinctly different curve fitting constants for shear modulus and damping. The procedure of expressing strain dependent modulus degradation and damping in the form Eq. (4.32) is verified for two popularly used curves for clayey soils of different plasticity indices (*PI*) proposed by EPRI (1993) and Vucetic and Dobry (1991). The results of the curve fitting process are tabulated in Tables 4.2 and 4.3. Figures 4.3a and 4.3b show the curves of strain dependent G/G_{max} and ζ respectively obtained using the curve fitting coefficients tabulated in Table 4.2 for the data of EPRI (1993), while Figures 4.4a and 4.4b present these results respectively for the curves proposed by Vucetic and Dobry (1991). In these figures actual data points of respective curves are also plotted. It is clear from these figures that the Eq. (4.32) exactly represents the experimental data. Further this procedure is also validated for the confining pressure dependent curves proposed for cohesionless soil proposed by EPRI (1993). The curve fitting results are tabulated in Table 4.4. Figures 4.5a and 4.5b show the comparison of the actual data and curve fitted to these data using Eq. 4.32. As in the previous case, here too the curves fitted using polynomial function exactly represents the actual data.

Hence it can be concluded that, the polynomial function of appropriate degree can be used to represent the strain dependent shear modulus and damping ratio of the soil. As

stated previously, in the computer program SRISD this method of modeling strain dependent soil properties is adopted in the EQL process. Hence user is required to give the polynomial coefficients of the curve fitted for any specific data. Currently, the program has incorporated many of the popular strain dependent modulus and damping curves which can be selected by specifying appropriate soil type.

Table 4.1: Typical strain dependent shear modulus and damping ratio data used in equivalent linear analysis programs

Clay (PI = 30 %) Vucetic and Dobry (1991)			Sand (depth 50 ft – 120 ft) EPRI (1993)		
Strain (%)	G/G_{max}	Damping (%)	Strain (%)	G/G_{max}	Damping (%)
1.00E-04	1	1	1.00E-04	1	0.57
3.16E-04	1	1	3.16E-04	0.99	0.86
1.00E-03	1	1	1.00E-03	0.96	1.7
3.16E-03	0.98	2.1	3.16E-03	0.88	3.1
1.00E-02	0.9	3.8	1.00E-02	0.74	5.5
3.16E-02	0.75	5.9	3.16E-02	0.52	9.5
1.00E-01	0.53	8.8	1.00E-01	0.29	15.5
3.16E-01	0.35	12.5	3.16E-01	0.15	21.1
1.00E+00	0.17	16.9	1.00E+00	0.06	24.6

Table 4.2: Curve fitting constants for EPRI (1993) data for strain dependent shear modulus and damping ratio as function of plasticity index

PI (%)	10		30		50		70	
	G/G_{max}	ζ (%)	G/G_{max}	ζ (%)	G/G_{max}	ζ (%)	G/G_{max}	ζ (%)
B_0	0.0311	19.9173	0.0736	18.9623	0.1529	17.4294	0.2993	13.6964
B_1	-0.1146	-7.0103	-0.1638	-2.7322	-0.2339	4.1378	-0.3395	7.8039
B_2	-0.1827	-22.351	-0.0477	-24.616	0.1747	-16.0703	0.4468	-6.8748
B_3	-0.5027	-9.2886	-0.527	-18.2789	-0.2501	-15.8412	0.3778	-10.1341
B_4	-0.2664	0.3865	-0.4247	-5.9456	-0.3417	-6.6096	0.0663	-4.8517
B_5	-0.0507	1.0999	-0.1376	-0.9258	-0.14	-1.4526	-0.0178	-1.1233
B_6	-0.0022	0.2604	-0.0206	-0.0558	-0.0249	-0.1655	-0.0073	-0.1243
B_7	0.0002	0.0197	-0.0012	1.23E-04	-0.0017	-0.0077	-0.00067	-0.005

Table 4.3: Curve fitting constants for Vucetic and Dorby (1991) data for strain dependent shear modulus and damping ratio as function of plasticity index

PI (%)	0		15		30		50		100		200	
	G/G_{max}	ζ (%)	G/G_{max}	ζ (%)	G/G_{max}	ζ (%)	G/G_{max}	ζ (%)	G/G_{max}	ζ (%)	G/G_{max}	ζ (%)
B_0	0.03	24.0028	0.1001	20.001	0.1701	16.8998	0.25	13.5005	0.37	9.8008	0.5299	8.1001
B_1	0.0075	8.5138	-0.2162	10.9906	-0.6246	9.9717	-0.4538	6.4271	-0.5848	9.9304	-0.5148	8.4099
B_2	0.5836	9.8422	-0.1256	14.8948	-1.1145	3.9827	-0.0234	-7.5504	-0.0826	7.5563	-0.1091	3.7345
B_3	0.7477	23.321	-0.5119	26.4607	-1.6152	5.1277	0.0192	-11.5965	0.1435	5.613	0.1254	-0.1051
B_4	0.6138	19.1844	-0.4135	20.8089	-1.0575	4.7096	0.0259	-6.4102	0.1181	3.2993	0.1149	-0.8093
B_5	0.2597	7.3975	-0.1474	8.0266	-0.3463	2.1107	0.0226	-1.7072	0.045	1.2034	0.0446	-0.3369
B_6	0.052	1.3832	-0.0255	1.5128	-0.0564	0.4497	0.0068	-0.2112	0.0086	0.2308	0.0086	-0.0593
B_7	0.004	0.1011	-0.0018	0.1113	-0.0037	0.0365	0.000659	-0.0091	0.000654	0.0176	0.000649	-0.004

Table 4.4: Curve fitting constants for EPRI (1993) data for strain dependent shear modulus and damping ratio as a function of confining pressure

$\sigma_0 (kPa)$	0 – 20		20 – 50		50 – 120		120 - 250		250 – 500		500 – 1000	
	G/G_{max}	ζ (%)	G/G_{max}	ζ (%)	G/G_{max}	ζ (%)	G/G_{max}	ζ (%)	G/G_{max}	ζ (%)	G/G_{max}	ζ (%)
B_0	0.0424	27.2203	0.0654	24.6988	0.0914	22.5769	0.1176	20.8966	0.148	19.0629	0.2004	16.46
B_1	-0.1308	11.4236	-0.1815	9.8169	-0.2018	10.1673	-0.2373	11.0627	-0.3043	11.4558	-0.3294	10.3354
B_2	-0.0596	5.1472	-0.1015	-3.2211	0.0121	-4.5242	0.0419	-3.9918	0.0321	-4.1865	0.2104	-8.3465
B_3	-0.2661	12.6187	-0.452	1.5603	-0.3544	-1.404	-0.3413	-2.4417	-0.3261	-4.6421	0.004	-12.488
B_4	-0.1019	10.0609	-0.302	3.7854	-0.295	2.0344	-0.3294	1.1986	-0.3471	-0.5919	-0.1358	-6.299
B_5	0.0044	3.5033	-0.0801	1.6684	-0.0925	1.204	-0.1168	0.9726	-0.1339	0.3695	-0.0683	-1.6288
B_6	0.0068	0.5768	-0.0092	0.3025	-0.0129	0.2438	-0.0187	0.2176	-0.0232	0.1237	-0.0131	-0.2172
B_7	0.000776	0.0370	-0.000344	0.0203	-0.000673	0.0174	-0.0011	0.0165	-0.0015	0.0109	-0.000914	-0.01.19
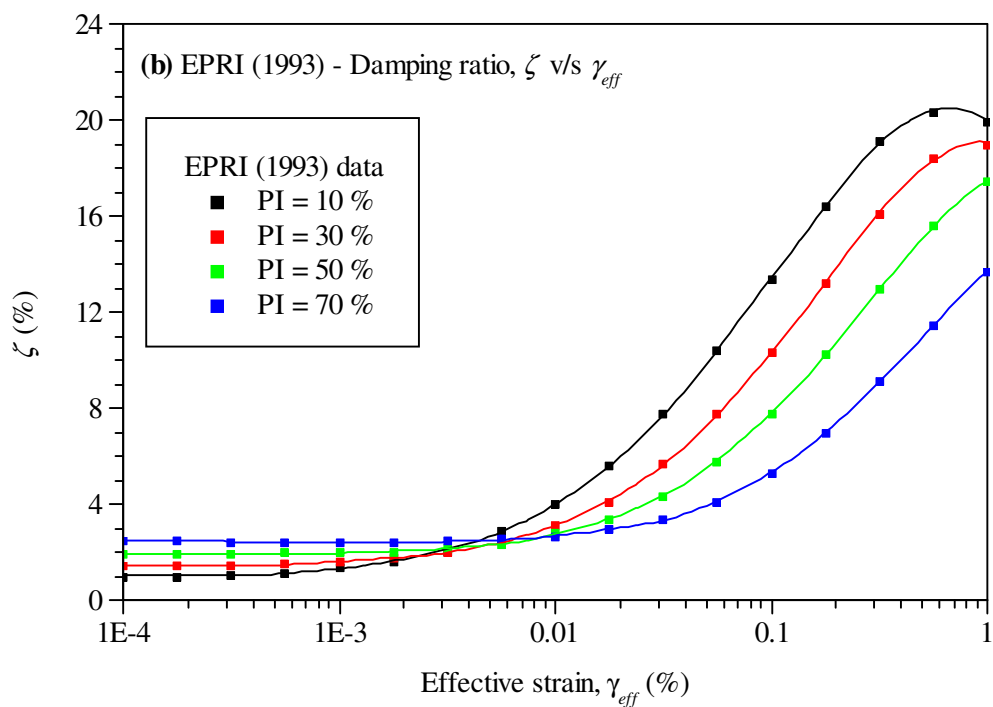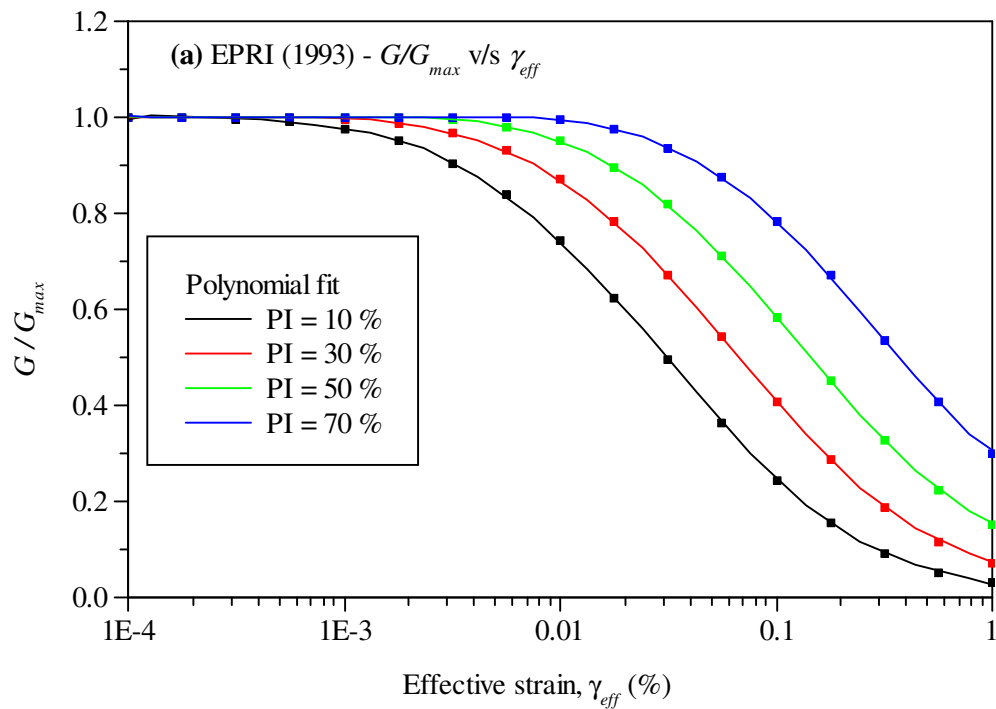
Figure 4.3: Curve fitting for EPRI (1993) data for strain dependent shear modulus and damping ratio as a function of Plasticity Index
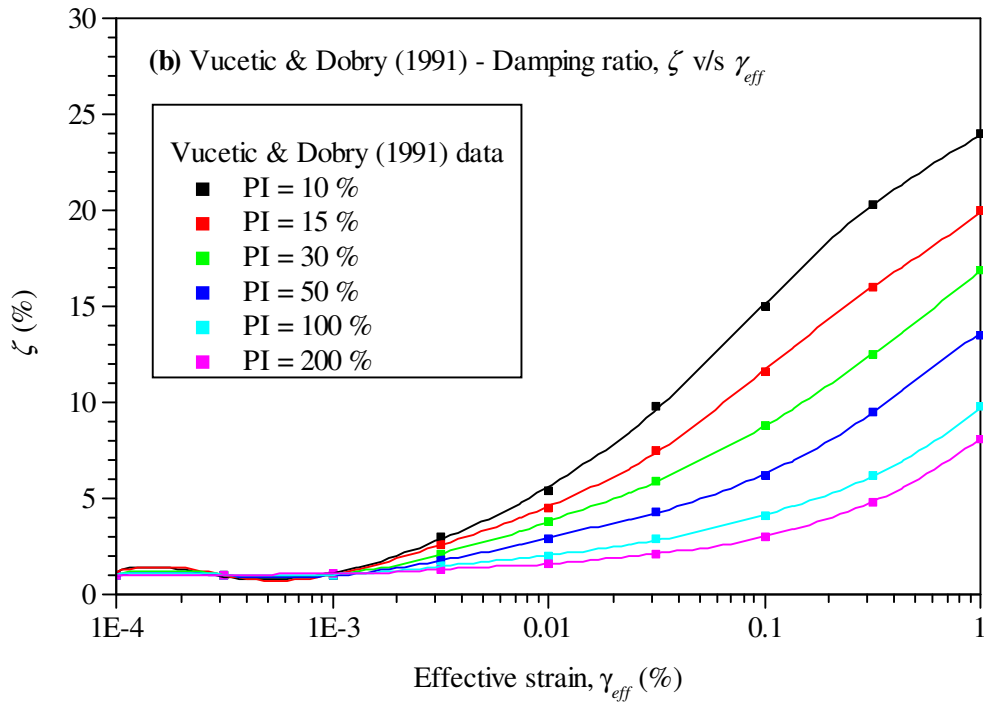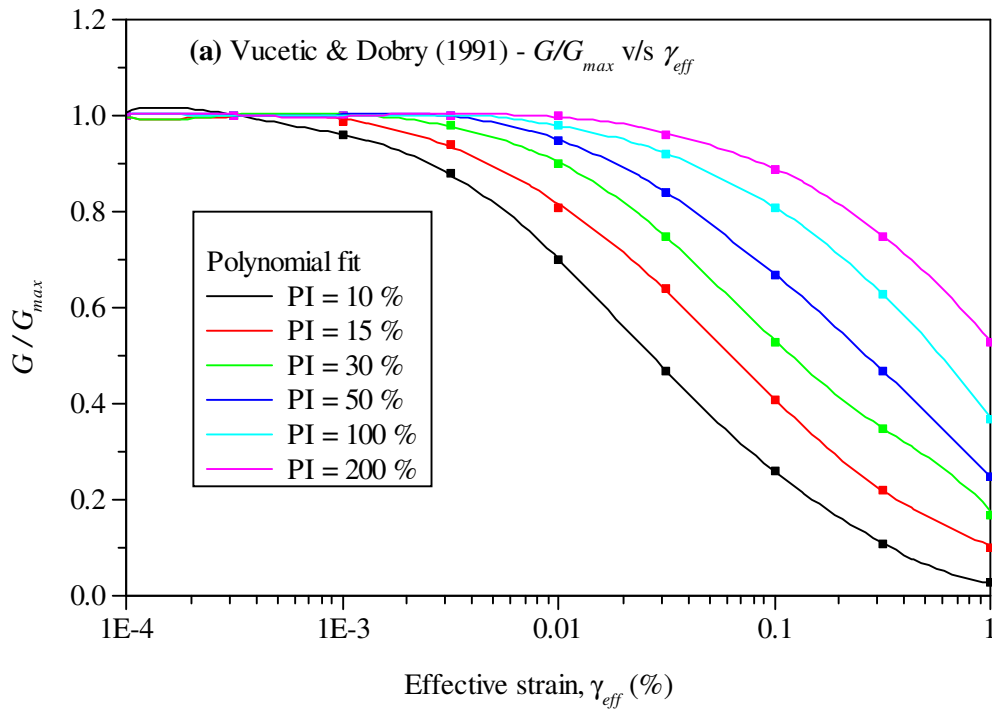
Figure 4.4: Curve fitting for Vuocetic and Dorby (1991) data for strain dependent shear modulus and damping ratio as a function of Plasticity Index
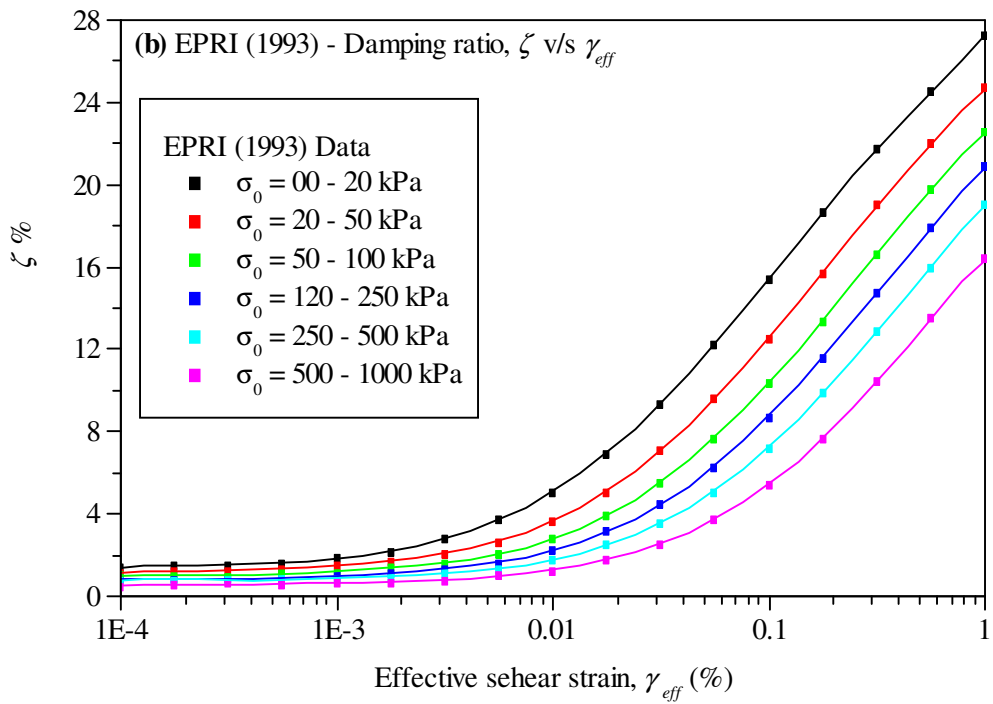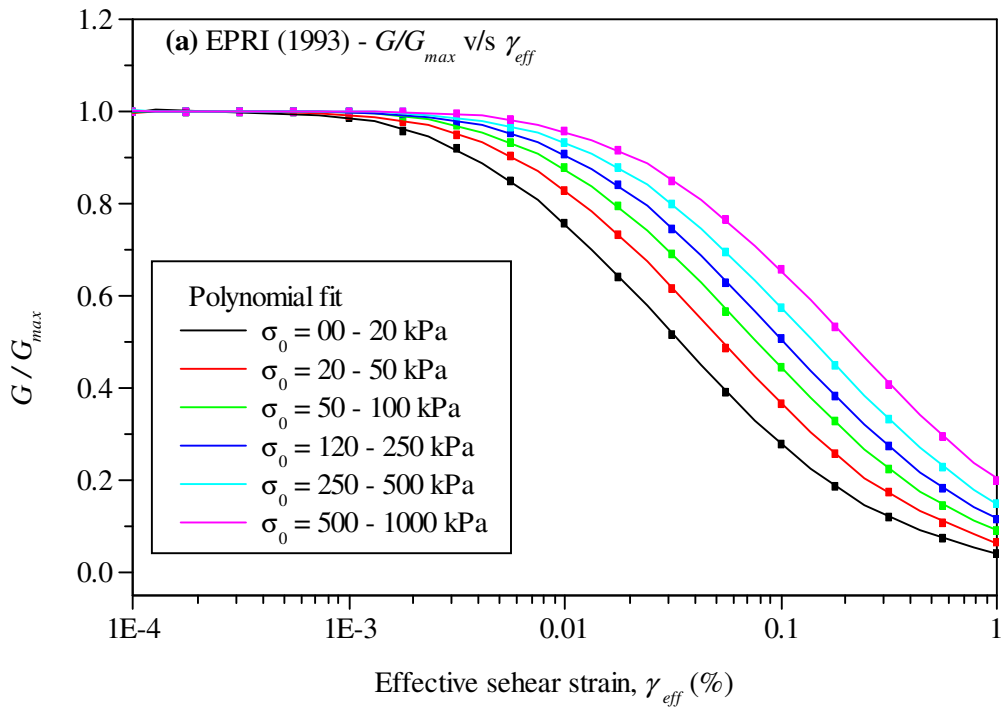
Figure 4.5: Curve fitting for EPRI (1993) data for strain dependent shear modulus and damping ratio as a function of confining pressure

4.5.2 Empirical shear modulus and damping curves

As discussed previously the important input in seismic site response analysis is the dynamic soil properties assigned to each layer. Both, equivalent linear analysis in frequency domain and true nonlinear analysis in time domain, require strain dependent shear modulus reduction curve and damping curve as input assigned to each layer depending on its soil characteristics. Some of the routinely used data to model strain dependent shear modulus and damping are reported in the form of curves and have limitation with respect to general application. However, reliability of computed response has direct bearing on the choice of these curves in the analysis. Basically, these curves have been obtained for the soil from particular region and it is impossible to explicitly include all the other factors which considerably influence shear modulus and damping properties in an experimental setup. It has been categorically reported that shear modulus and damping curves are dependent on several characteristics most importantly soil type, effective confining stress and soil plasticity. To a lesser extent these curves are also found to be sensitive to grain size, number of loading cycles, frequency of loading, degree of saturation, over consolidation ratio (OCR), aging, etc [Hardin and Drnevich (1972a, 1972b); Darendeli (2001)]. The relative importance of these factors as reported and tabulated by Darendeli (2001) is shown in Table 4.5.

But effects of some of these factors are yet to be ascertained conclusively. Therefore use of such generic curves proposed for particular type of soil disregarding all other significantly influencing factors, have posed uncertainty with respect to reliability of computed response because some of these factors may be vital for the problem at hand. Recognizing these many have attempted to incorporate these factors through statistical analysis by considering relatively large data that comprise many of these influential factors. Also, having these curves expressed analytically has added advantage with respect to convenience in computer implementation because interpolation process between experimental strain data points for intermediate strain values can be eliminated. Hardin and Drnevich (1972a) extensively studied the soil parameters that directly affect the strain dependent shear modulus and damping

curves and proposed hyperbolic model [Hardin and Drnevich (1972b)]. Several rigorous attempts have been made in the past, for example Ishibashi and Zhang (1993), Darendeli (2001), Zhang et al. (2005) etc, to express γ_{eff} versus G/G_{max} and ζ curves in the equation form. Usually these empirical equations are developed by statistical analysis of experimental curves. There are several such curves reported in the literature and a good account of such curves is given in Darendeli (2001).

Table 4.5: Relative importance of soil parameters e influencing strain dependent Shear modulus and Damping curves [Darendeli (2001)]

Parameter	Effect on normalized strain dependent G/G_{max} curve	Effect on normalized strain dependent Damping curve
Strain Amplitude	✓✓✓	✓✓✓
Mean Effective Confining Pressure	✓✓✓	✓✓✓
Soil Type and Plasticity	✓✓✓	✓✓✓
Number of Loading Cycles	✓	✓✓✓
Frequency of Loading (above 1 Hz)	✓	✓✓
Over consolidation Ratio	✓	✓
Void Ratio	✓	✓
Degree of Saturation	✓	✓
Grain Characteristics, Size, Shape, Gradation, Mineralogy, soil structure,	✓	✓
✓✓✓ - Very important, ✓✓ - Important, ✓- Less important		

Among these empirical relationships SRISD program has included the models proposed by Ishibashi and Zhang (1993), Darendeli (2001) and Zhang et al, (2005), along with other options, in its subroutine which updates soil properties for the next iteration of EQL process. The equations pertaining to these models are presented in the following sections.

4.5.2.1 Ishibashi and Zhang (1993) equations

Ishibashi and Zhang (1993) developed set of empirical equations incorporating effect of overburden pressure for sands and extended these equations to clays by modifying the associated constants to take account of plasticity index. The strain dependent shear modulus and damping properties are given by,

$$\frac{G}{G_{max}}(\gamma, PI) = K(\gamma, PI)\sigma_m'^{m(\gamma, PI)} \tag{4.33}$$

$$\zeta(\gamma, PI) = \frac{0.333\left(1 + e^{-0.0145(PI)^{1.3}}\right)}{2}\left[0.586\left(\frac{G}{G_{max}}\right)^2 - 1.547\left(\frac{G}{G_{max}}\right) + 1\right] \tag{4.34}$$

The plasticity index (PI) dependent functions $K(\gamma, PI)$ and $m(\gamma, PI)$ are,

$$\left.\begin{array}{l} m(\gamma, PI) = 0.272\left[1 - \tanh\left\{0.4\ln\left(\dfrac{0.000556}{\gamma}\right)\right\}\right]e^{-0.0145(PI)^{1.3}} \\[4mm] K(\gamma, PI) = 0.5\left[1 - \tanh\left\{0.492\ln\left(\dfrac{0.000102 + n(PI)}{\gamma}\right)\right\}\right] \end{array}\right\} \tag{4.35}$$

Here,

$$n(PI) = \begin{cases} 0.0 & \text{for} \quad PI = 0 \\ 3.37\times10^{-6}\,(PI)^{1.404} & \text{for} \quad 0 < PI \le 15 \\ 7.0\times10^{-7}\,(PI)^{1.976} & \text{for} \quad 15 < PI \le 70 \\ 2.7\times10^{-5}\,(PI)^{1.115} & \text{for} \quad PI > 70 \end{cases}$$

4.5.2.2 Darendeli (2001) equations

The modulus degradation and damping equations presented by Darendeli (2001) include, apart from effect of plasticity index and confining pressure, many additional parameters such as significant number of loading cycles, frequency of loading and OCR. The modulus and damping relationships as function of these parameters were obtained by employing statistical analysis on a wide range of experimental data. The shear modulus is given by,

$$\frac{G}{G_{max}}(\gamma) = \frac{1}{1 + \left(\dfrac{\gamma}{\gamma_r}\right)^{0.919}} \tag{4.36}$$

Here reference strain γ_r is,

$$\gamma_r = \left(\frac{\sigma'_m}{p}\right)^{0.3483} \left[0.0352 + \left(0.001 PI \times OCR^{0.3246}\right)\right] \qquad (4.37)$$

Damping is expressed as a function of G/G_{max},

$$\zeta(\gamma) = \zeta_{mas} \left\{ \left(0.6329 - 0.0057 \ln N\right)\left(\frac{G}{G_{max}}\right)^{0.1} \right\} + \zeta_{min} \qquad (4.38)$$

Here,

$$\zeta_{min} = \left(\frac{\sigma'_m}{p}\right)^{-0.2889} \left[0.8005 + \left(0.0129 PI \times OCR^{-0.1069}\right)\right] \times \left(1 + 0.2919 \ln f\right) \qquad (4.39)$$

$$\zeta_{mas} = 1.0215\zeta_{mas1} + 0.594\zeta_{mas1}^2 + 6.152 \times 10^{-5}\zeta_{mas1}^3 \qquad (4.40)$$

In Eq. (4.39) f is the loading frequency in Hz. and ζ_{mas1} of Eq. (4.40) is damping ratio corresponding to Masing hysteretic behaviour and is related to reference strain as,

$$\zeta_{mas1} = \frac{4}{\pi} \left[\frac{\gamma - \gamma_r \ln\left(\frac{\gamma + \gamma_r}{\gamma_r}\right)}{\left(\frac{\gamma^2}{\gamma + \gamma_r}\right)} - 0.5 \right] \qquad (4.41)$$

4.5.2.3 Zhang et al. (2005) equations

Zhang et al (2005) presented $G/G_{max}(\gamma)$ and $\zeta(\gamma)$ equations which incorporated geological age of the soil deposit. The equation for $G/G_{max}(\gamma)$ is same as Eq. (4.36) but the values of curvature parameter β and reference strain (γ_r) are considered to be function of geological age of the soil.

$$\frac{G}{G_{max}}(\gamma) = \frac{1}{1 + \left(\frac{\gamma}{\gamma_r}\right)^{\beta}} \qquad (4.42)$$

The damping is given by,

$$\zeta(\gamma) = 10.6\left(\frac{G}{G_{max}}\right)^2 - 31.6\left(\frac{G}{G_{max}}\right) + \zeta_{min} + 21 \tag{4.43}$$

where,

$$\zeta_{min} = \left(0.008(PI) + 0.82\right) \times \left(\frac{\sigma'_m}{100}\right)^{-\frac{\lambda}{2}} \tag{4.44}$$

Values of α, γ_r and λ are given in Table 4.6 along with corresponding regression coefficients representing fitness of each of the parameter as obtained by Zhang et al (2005, 2008).

Table 4.6: Curve fitting parameters β, γ_r and λ of **Eq. (4.43)** and **Eq. (4.44)** for different geological groups [Zhang et al (2005, 2008)]

Age	β	γ_r	λ
Quaternary soil	$0.021PI + 0.834$ $(r^2 = 0.505)$	$0.0011PI + 0.0749$ $(r^2 = 0.508)$	$0.316e^{(-0.0142PI)}$ $(r^2 = 0.323)$
Tertiary and older soil	$0.0009PI + 1.026$ $(r^2 = 0.015)$	$0.0004PI + 0.0311$ $(r^2 = 0.143)$	$0.316e^{(-0.0110PI)}$ $(r^2 = 0.232)$
Residual / Saprolite soil	$0.043PI + 0.794$ $(r^2 = 0.053)$	$0.0009PI + 0.0385$ $(r^2 = 0.107)$	$0.420e^{(-0.0456PI)}$ $(r^2 = 0.486)$

4.5.2.4 Comparison of Empirical Equations

Figures 4.6a and 4.6b present comparisons between the strain dependent shear modulus degradation curves as function of plasticity index proposed by Vucetic and Dobry (1991) with that estimated using empirical equations proposed by Zhang et al. (2005) and Darendeli (2001) respectively. Figures 4.7a and 4.7b compare strain dependent damping curves proposed by Vucetic and Dobry (1991) with Zhang et al (2005) and Darendeli (2001) curves respectively. The analytical curves closely simulate the experimental curves within strain limit of about 0.1% while beyond this, differences are significant. Moreover, as the plasticity index increases the difference

increases appreciably with Vucetic and Dobry (1991) curves displaying more stiffer behaviour. In case of damping curves the analytical curves of both Zhang et al. (2005) and Darendeli (2001) tend to show higher damping compared to Vucetic and Dobry (1991) curves with increase in plasticity index particularly beyond the strain level of 0.1%. Zhang et al (2005) shear modulus and damping curves almost converges to unique value at high strain range.
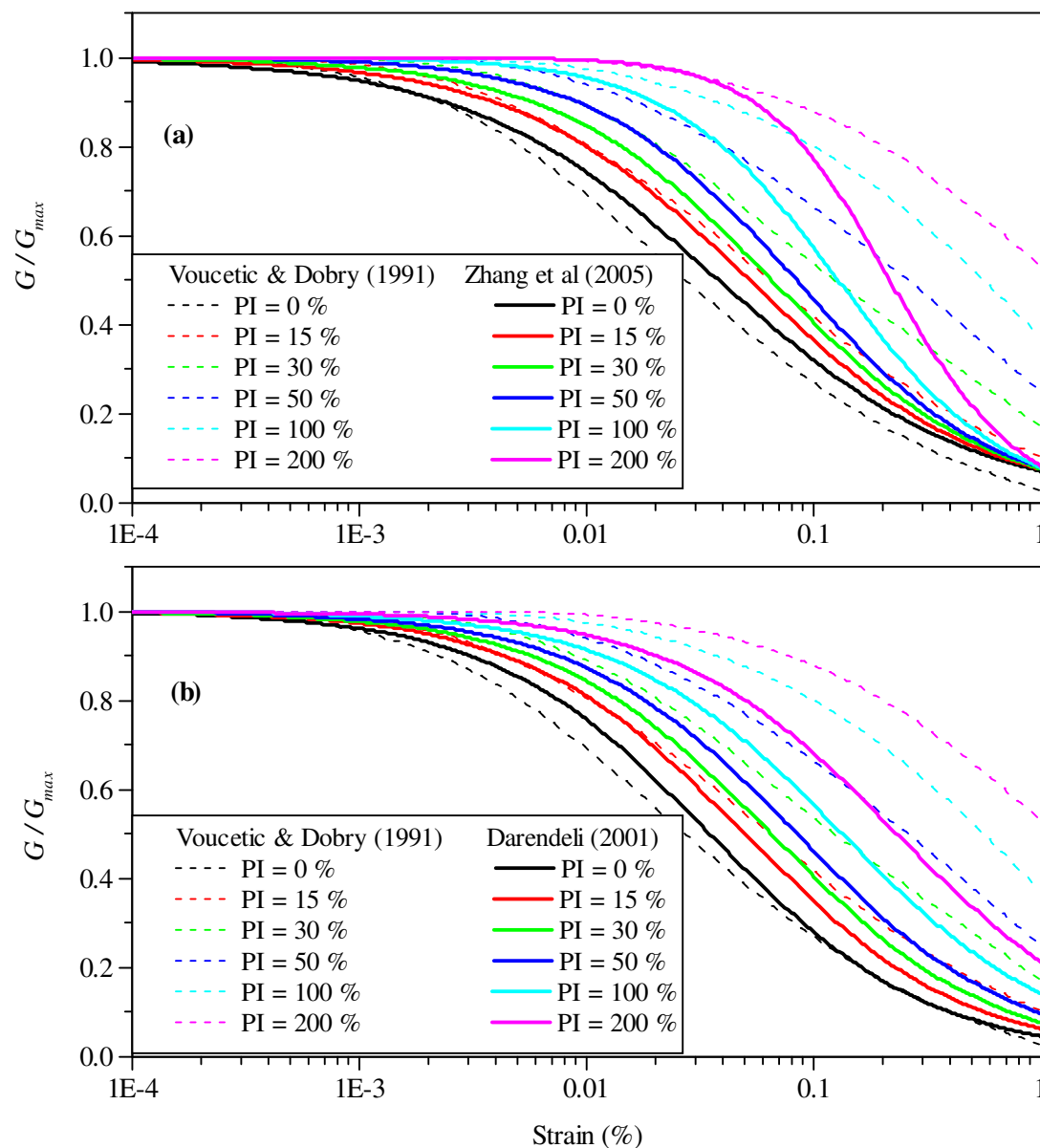
Figure 4.6: Strain dependent shear modulus degradation curves as a function of plasticity index (for $\sigma'_m = 100\ kPa$). Comparison of γ vs G_{max} curves proposed by Vucetic and Dobry (1991) with (a) Curves proposed by Zhang et al (2005), (b) Darendeli (2001).
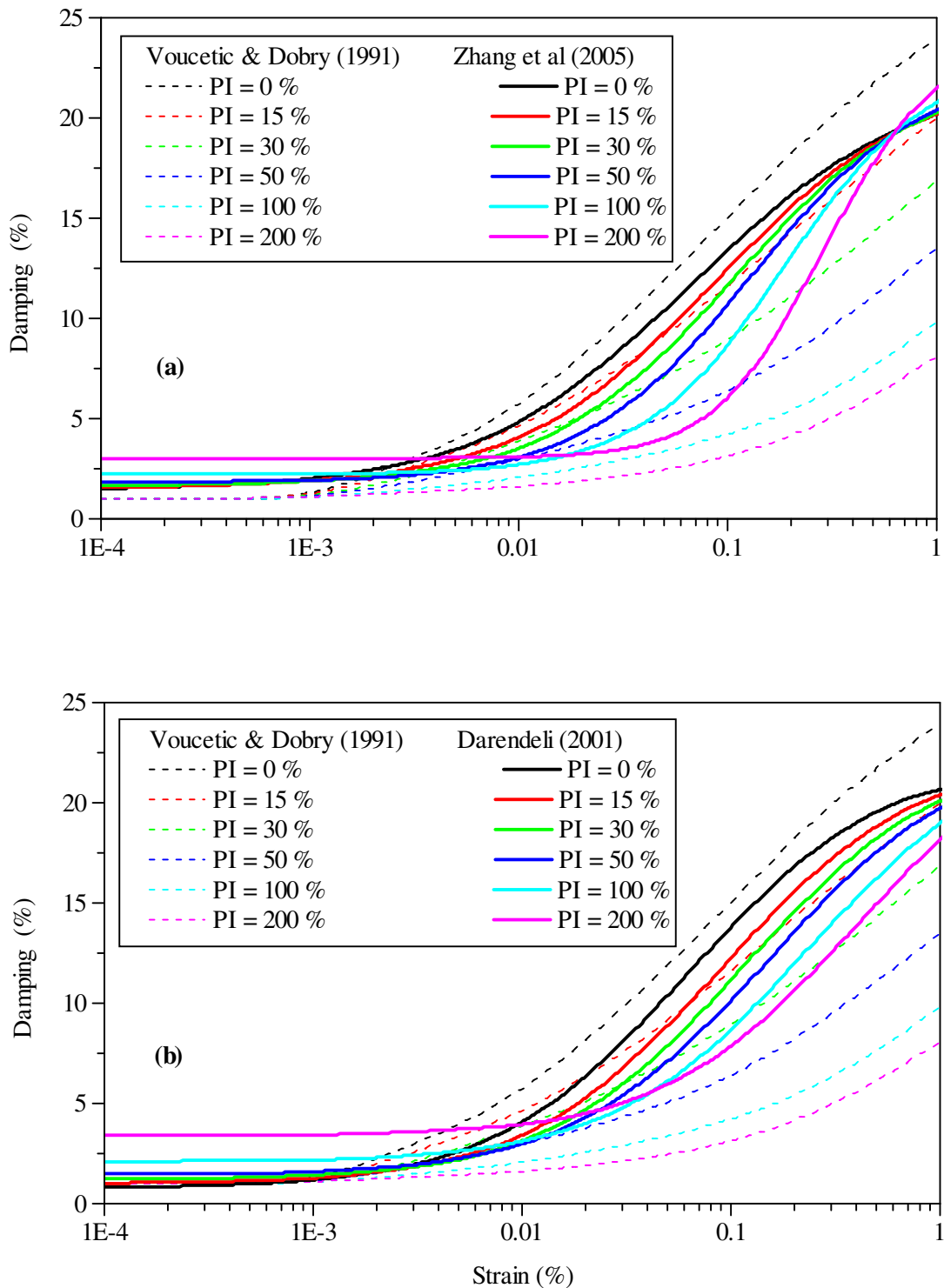
Figure 4.7: Strain dependent damping ratio curves as a function of plasticity index (for $\sigma'_m = 100$ _kPa_). Comparison of γ vs G_{max} curves proposed by Vucetic and Dobry (1991) with (a) Curves proposed by Zhang et al (2005), (b) Darendeli (2001).

4.6 GENERAL DESCRIPTION OF COMPUTER PROGRAM SRISD

The computer program SRISD, coded in FORTRAN, is capable of analyzing for response of inhomogeneous soil deposits under seismic excitation. The program is having same features as that of popular program SHAKE91 with regard to input and output features. However, several additional features have been incorporated into the program in order to fulfill the objectives of this research work. The main part of the program implements the numerical solution of the wave equation obtained using Runge-Kutta scheme.

4.6.1 Outline of the program

The input to program SRISD is dependent on the type of modeling adopted to characterize the soil profile as discussed earlier in Section 4.3. Input motion data consists of time history of the acceleration record along with depth at which it is to be prescribed. Fourier transform of this input motion is obtained and is used to get the response of the deposit at all the desired depths of the deposit using the solution procedure explained earlier in Section 4.2. The time histories of strain at all the nodes of the deposits are computed and effective strains at these nodes are calculated to update soil properties using the respective shear modulus and damping curves. Updated soil properties are employed in the successive iteration of the equivalent linear procedure as explained in Section 4.5. Finally, after convergence of strain is achieved at all the nodes the control exits from the main body of the program to prepare required results as output.

4.6.2 Input soil profile data

Three options given for defining the shear wave velocity or shear modulus profile of the inhomogeneous soil deposit are as follows,

4.6.2.1 Layered profile

This is the option which is used in most of the popular programs (SHAKE, SHAKE91, DEEPSOIL, EERA, STRATA, etc.) for seismic site response analysis, in which layer

information such as thickness, unit weight, low strain shear wave velocity or shear modulus and initial value of soil damping are to be provided. For the case of equivalent linear analysis, the input data regarding type of strain dependent shear modulus and damping curves are to be specified for each of the layers.

4.6.2.2 Continuously inhomogeneous deposit

In this case the shear wave velocity or shear modulus profile of deposit is defined using depth dependent function. For this purpose currently SRISD includes several options to choose from. These options comprise of all the forms of depth dependent G and v_s functions discussed in the previous chapter. Depending on the type of inhomogeneity function selected to model the profile, related parameters are to be given as input. Even the damping and density properties of the soil deposit can be considered to continuously varying along the depth. As in the previous case, the type of shear modulus and damping model need to be specified. Also, currently SRISD is provided with the option of modelling soil deposits consisting of two continuously inhomogeneous layers with different degree of inhomogeneities.

4.6.2.3 Soil profile defined using discrete data points

If the shear wave velocity data along the depth of the deposit is obtained using continuous PS logging field test then using this option such raw data can be used to compute response of the deposit. Again, as in the previous case, data pertaining to density, initial damping and type of soil are required to be specified at each of the shear wave velocity data points. The shear wave velocity, density and damping are assumed to vary linearly at all the nodes between the data points. In this case, as in layered profile case the shear modulus and damping properties of the soil are updated only at these discrete data points and linear interpolation is carried out to obtain updated soil properties at nodes between primary nodes.

4.6.3 Earthquake data

The data required with regard to input motion are time history of the input acceleration record, the time interval between acceleration data points and total

number of acceleration data points. Additionally, maximum cut-off frequency to filter out high frequency components of the input motion may be given. Also, depth at which the input motion is prescribed shall be specified.

4.6.4 Equivalent linear analysis data

The data pertaining to strain dependent shear modulus and damping curve for each of the soil modeling may be selected from the suite of curves for which pertinent data is built into SRISD material library. These include several generic curves such as those proposed by EPRI (1993), Vucetic and Dobry (1991), Seed and Idriss (1970) and others. The data of these curves are expressed in equation form using polynomial function (Eq. 4.32) and coefficients of this function are used as data to specify the curve (for ex., Tables 4.3, 4.4 & 4.5). Also, the equations (in Section 4.6.2) proposed by Ishibashi and Zhang (1993), Darendeli (2001) and Zhang et al. (2005) have been incorporated into the material library of the program SRISD. The ratio of effective strain to maximum strain (R) is to be specified to carry out EQL process. However supplementary options with regard to selection of R value are provided and more discussion about these improvements to routine EQL approach is detailed in the next chapter (Chapter 5). The additional feature which is unique to SRISD compared to other available programs is that the damping and shear modulus curves can be selected independent of each other and keep either of these soil properties constant with the other being iteratively updated. This option has been accommodated for the purpose of making parametric study on effect of these properties individually on the response of continuously inhomogeneous soil deposits.

4.7   TESTING OF PROGRAM

The computer program SRISD is coded to perform equivalent linear site response analysis in the frequency domain with acceleration time history as input motion. Primary difference between other programs available for this purpose and SRISD is that, it can model the soil deposit properties as continuously varying with depth. However it can also perform analysis with regular layer idealisation as it is being treated in other programs. Herein program is tested for reliability of its output by

comparing it with that of other programs. As an example of this testing process one of the analyses carried out is presented here. The output for the problem under consideration is compared with results obtained using SHAKE91 program [Idriss and Sun (1992)]. Also, results obtained from SRISD are compared with exact analytical solutions presented in the previous chapter.

4.7.1   Problem statement

For the purpose of testing SRISD program, the soil deposit considered here is the one which is used as demonstration example in the manuals of the computer programs SHAKE91 and EERA. The analysis is carried out for validating SRISD output with respect to that of SHAKE analysis. The soil deposit considered for this study is shown in Figure 4.8. The soil deposit considered is of 45.7 m depth and consisting of sand and clay layers overlying bedrock of shear wave velocity 1219.2 *m/s*. The soil deposit is discretised into 17 layers. The shear wave velocities of these layers vary in the range of 275 *m/s* to 550 *m/s*. The unit weight is of constant value of 19.66 kN/m^3 up to a depth of about 20 *m* and 20.45 kN/m^3 for the remaining depth up to bedrock (which has a unit weight of 22.02 kN/m^3).

The curves proposed by Sun et al., (1988) and Seed and Idriss (1970) are used to model strain dependent modulus reduction property of clay and sand respectively. The strain dependent damping for both sand and clay are represented by lower range curve recommended for sand by Seed and Idriss (1970). The curves representing strain dependent soil and bedrock properties that are adopted in the analysis are shown in Figure 4.9. Following the procedure described in Section 4.5.1, the input data for these curves were obtained for EQL analysis using SRISD.

The input data file for SRISD essentially consists of soil profile data and input earthquake motion. For sake of convenience soil profile input data is almost kept in the same format as that of SHAKE91. However, the input fields are format free unlike formatted fields of SHAKE program.

The input motion for SRISD is to be given in a separate file. The input acceleration time history considered in the example analysis is the one corresponding to Loma-

Prieta (USA) earthquake of 1989 recorded at Diamond Heights. The peak acceleration of the record is 0.1129 *g*. The remaining part of the input file for SRISD consists of various options for output specification. These options include acceleration, strain and stress time histories at different depths, amplification ratio as a function of frequency between any two layers, maximum response quantities etc. All these desired output options are instructed to the program through format free fields. For equivalent linear analysis, the value of *R* used in SRISD and SHAKE91 analyses is 0.5. The convergence of maximum strain in all the 17 layers was achieved after 8 iterations. In case of SRISD analysis variable step sizes are used for discretization along the depth of the deposit as explained earlier to simulate SHAKE91 analysis. When layered analysis option is selected in SRISD the program computes distance between mid-depth of successive layers and assigns these step sizes (Δz_i) at corresponding depths.
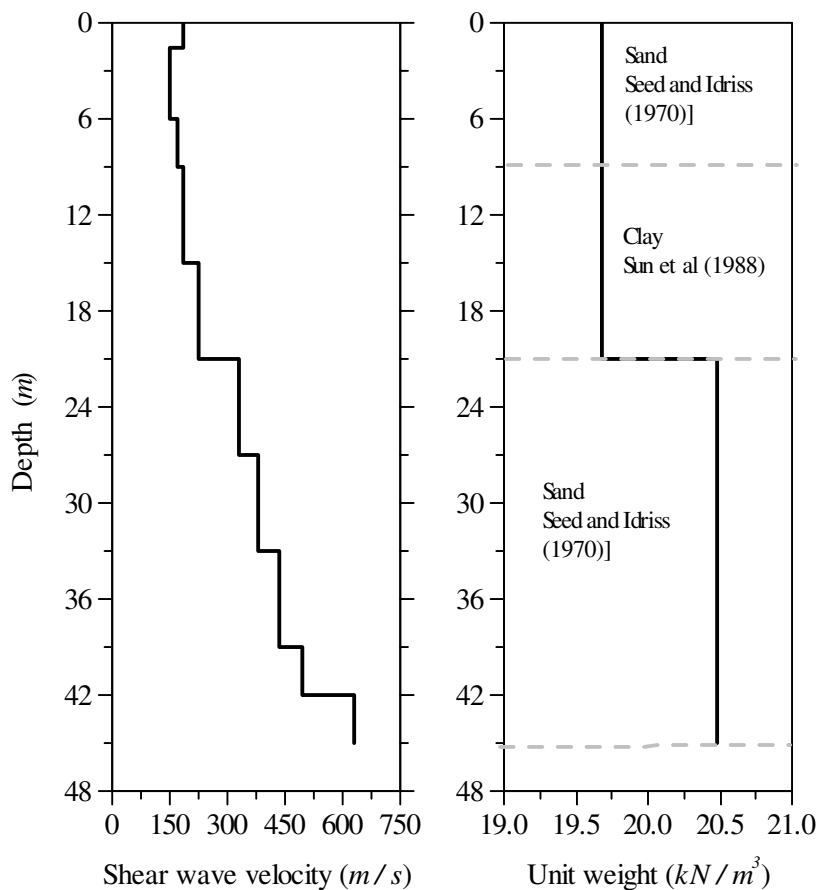
Figure 4.8: The shear wave velocity and unit weight profiles of layered soil deposit considered for example problem to validate SRISD output.

186
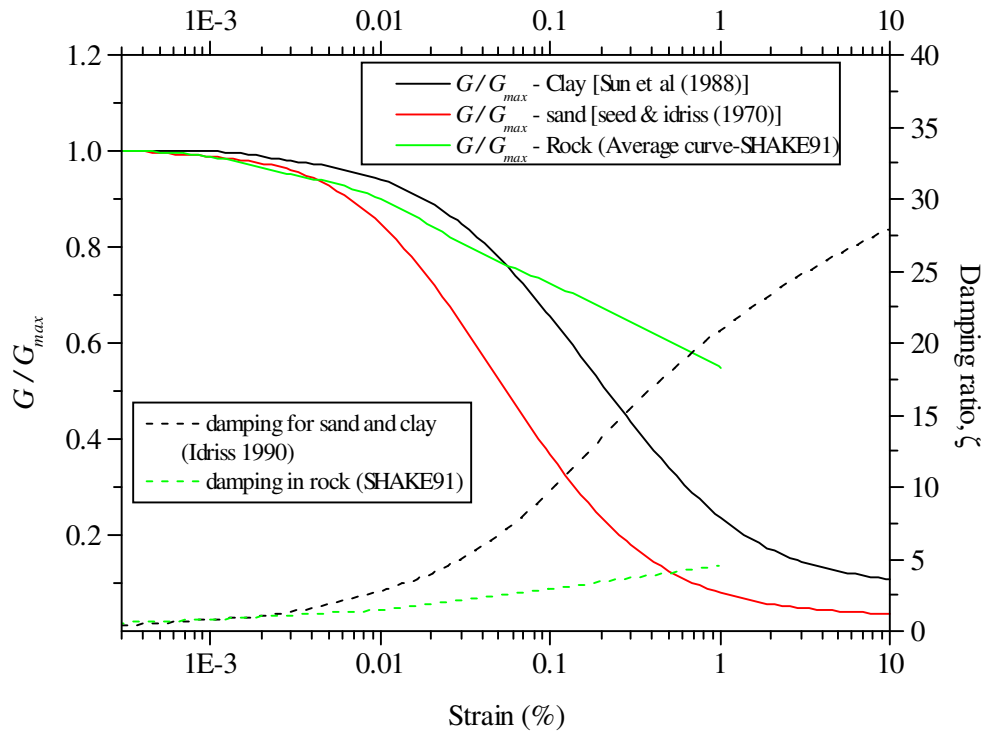
Figure 4.9: Stain dependent soil and bedrock properties used in the example analysis.
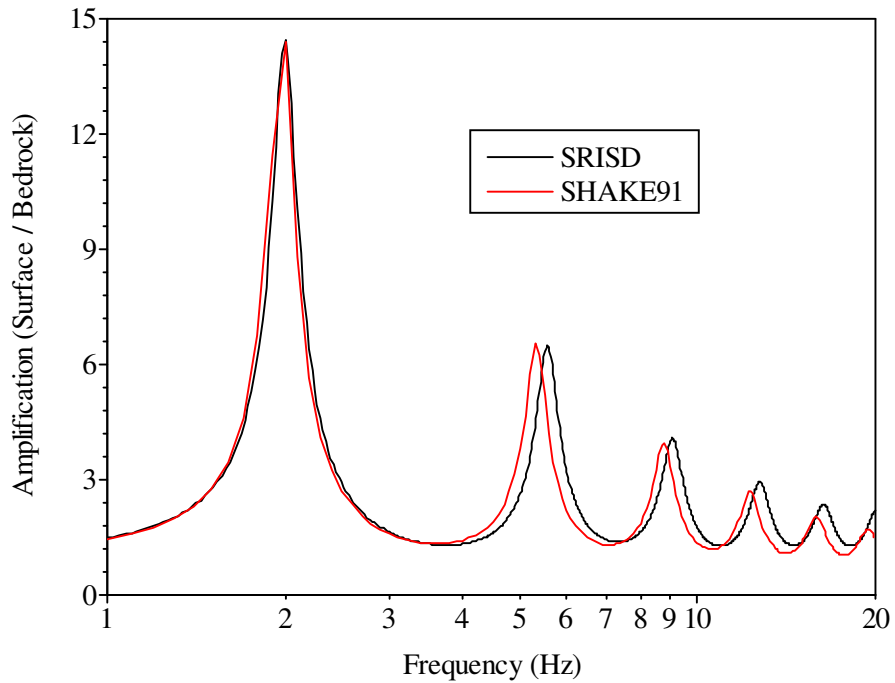
Figure 4.10: Comparison of amplification ratio between surface layer and bedrock motions computed from SHAKE91 and SRISD for the example profile shown in Figure 4.8.
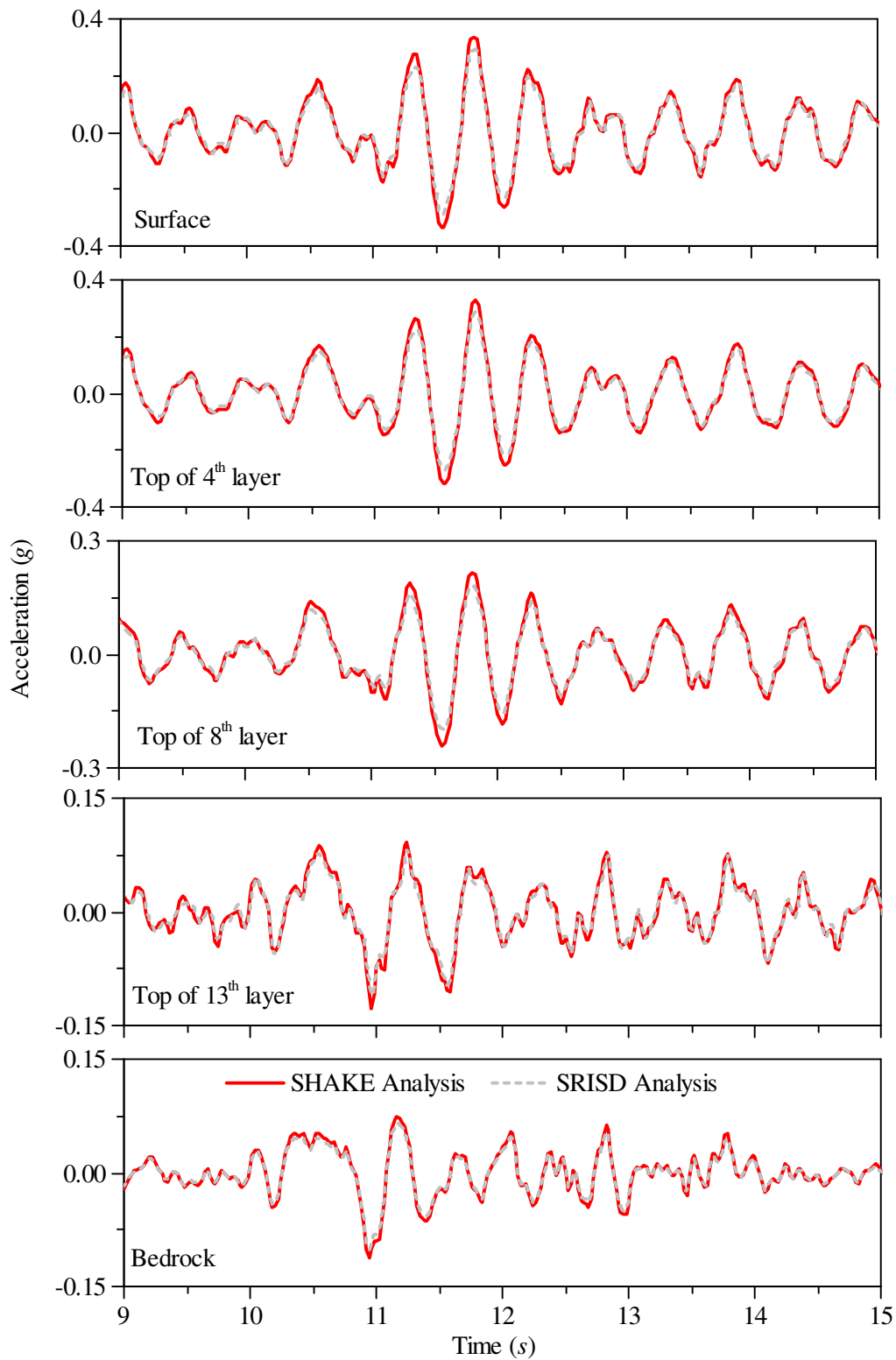
Figure 4.11: Comparison of acceleration time history responses at different depths between SHAKE91 and SRISD for the example profile (Figure 4.8). Response computed for the input motion given at bedrock.
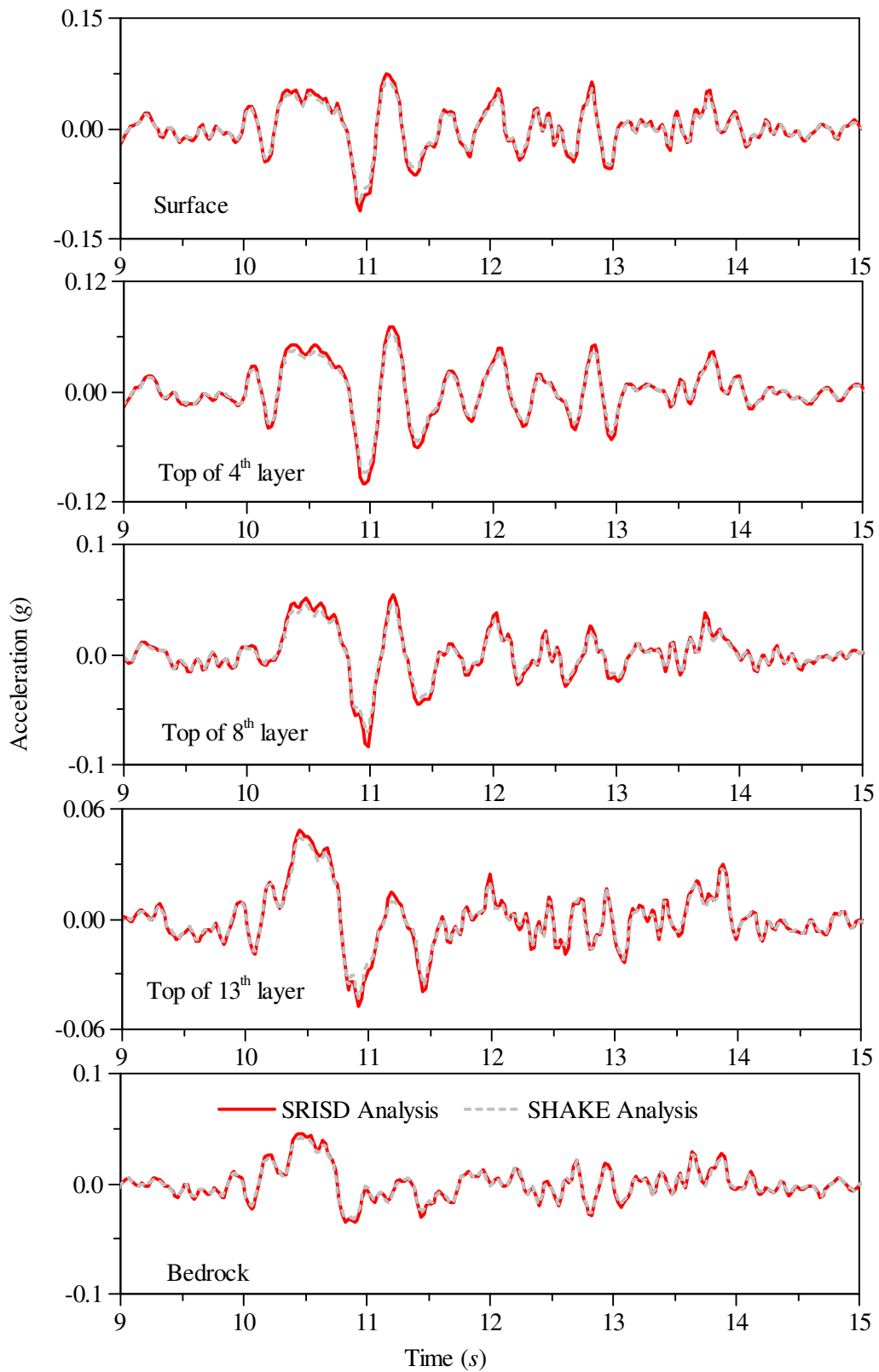
Figure 4.12: Comparison of acceleration time history responses at different depths between SHAKE91 and SRISD for the example profile (Figure 4.8). Response computed for the input motion given at surface.

189

4.7.2 Results and comparison

For example problem considered, the output obtained from SHAKE91 and SRISD were compiled and compared with respect to amplification between surface and bedrock motions. This comparative study clearly demonstrates the good agreement between the results obtained from SHAKE91 and SRISD with almost negligible differences. Amplification ratio between surface layer and bedrock motions is shown in Figure 4.10. It can be observed that the first mode amplitude and frequency are very much comparable. However, in higher modes negligible differences have resulted in values of modal frequencies but the amplification ratio is almost identical. This negligible difference may be attributed to different frequency resolutions used for computation of amplification function.
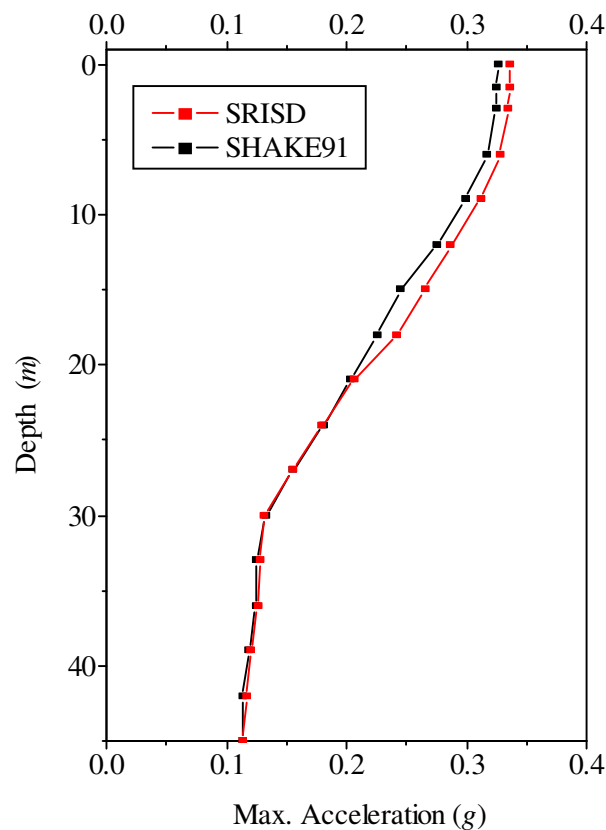
Figure 4.13: Computed maximum acceleration response along the depth of the soil deposit for input motion at the base (Comparison between SHAKE91 and SRISD for the example profile in Figure 4.8).

Most importantly in SHAKE91 the amplification function is computed using the analytical expression for layered profile using the damping and shear modulus

corresponding to converged values of strains obtained after last iteration while in case of SRISD the amplification is computed directly from the computed acceleration time history at the surface and the input motion at the bedrock.

Apart from comparison of amplification results, comparisons made with respect to acceleration time history responses at different depths are shown in Figure 4.11 and Figure 4.12. For the case of input motion at top of the bed rock level, comparison of acceleration time histories between SHAKE91 and SRISD at top of the surface layer, 4th layer, 8th layer and 13th layer along with input motion at the top of bedrock are shown in Figure 4.11, while Figure 4.12 presents the comparison of the responses computed at the top of these layers for the case of input motion being prescribed at surface layer. Finally, SRISD output is satisfactorily validated by comparing the maximum acceleration response as obtained from SRISD and SHAKE91 in Figure 4.13. From the results presented here with regard to computed responses using SHAKE91 and SRISD computer programs it can be concluded that testing of the program SRISD is successful in reproducing the results of SHAKE91.

4.7.3   Comparison with analytical results

Finally, for the purpose of verifying the output of the computer program SRISD, the analytical results obtained in the previous chapter are compared with the SRISD output. Amplification results pertaining to a continuously inhomogeneous soil deposit of 50 m thickness overlying rigid bedrock is taken for the purpose of comparison. The analytical results used here are those obtained for parametric study in the previous chapter. The inhomogeneity function defining the continuous variation of shear modulus along the depth is as given by Eq. 3.24 $\left[G(z) = \Lambda (z + z_0)^m \right]$ of the preceding chapter. The comparison is shown in Figure 4.14. In Figure 4.14a the exact solution is obtained for the case of $m = 4$ with $v_{s0} / v_{sH} = 0.50$ which corresponds to $\Lambda = 3.3912 \times 10^{-4}$ and $z_0 = 120.71$. In Figure 4.14b and 4.14c, same value of $m = 0.4$ is used while the velocity ratios of $v_{s0} / v_{sH} = 0.20$ and $v_{s0} / v_{sH} = 0.50$ are used respectively. In all the cases the density $\rho = 1800 \ kg / m^3$ and damping ratio

$\zeta = 5\%$ are employed. As it can be observed from these figures, the amplification transfer functions computed using the program SRISD exactly simulate the trends of the amplification transfer functions obtained analytically (Eq. 3.36 and 3.41).
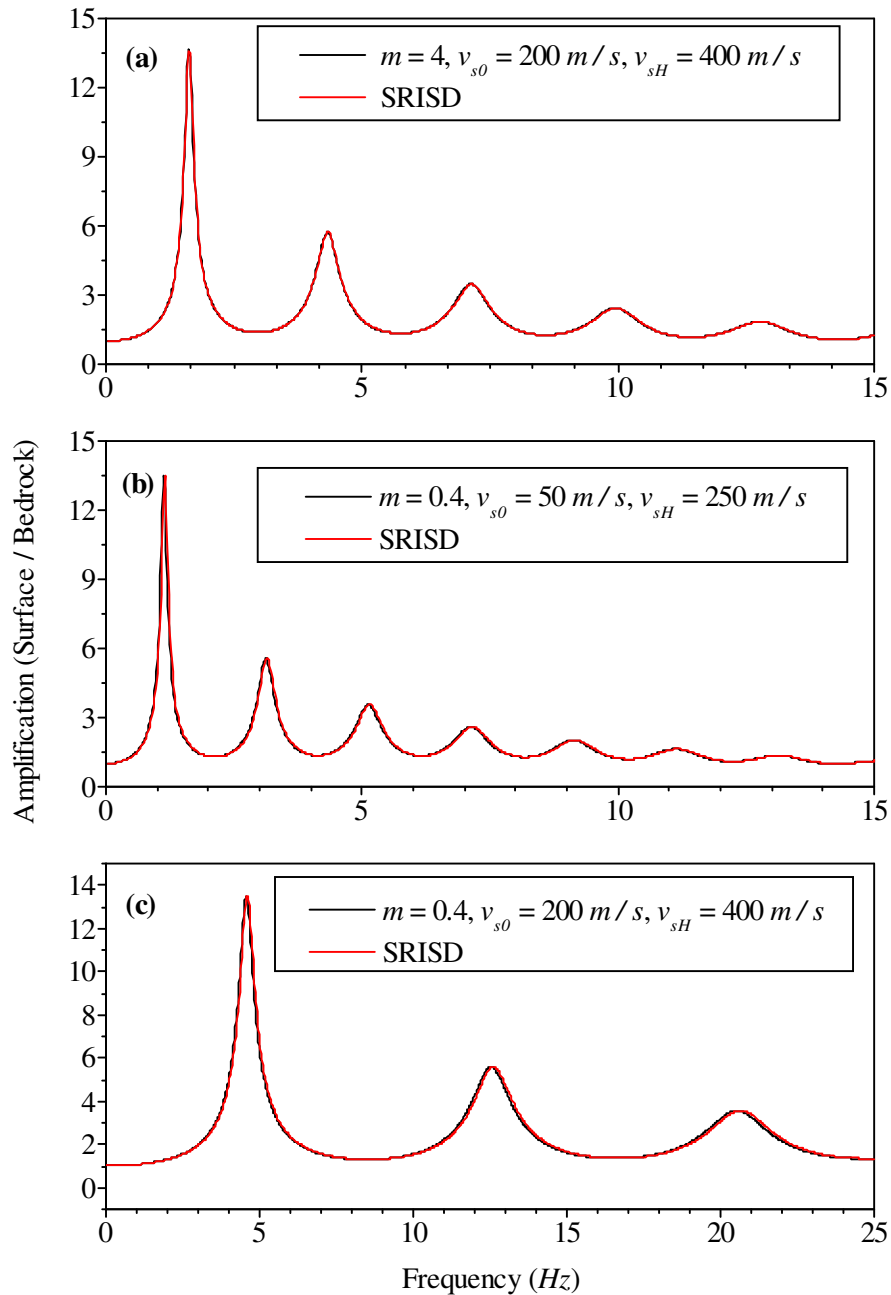
Figure 4.14: Comparison of amplification results between analytical solution and SRISD – Soil deposit overlying rigid bed rock; Damping ratio $\zeta = 5\%$;
(a) $v_{s0}/v_{sH} = 0.50$ & $m = 4.0$, (b) $v_{s0}/v_{sH} = 0.20$ & $m = 0.4$ **and (c)**
$v_{s0}/v_{sH} = 0.50$ & $m = 0.4$
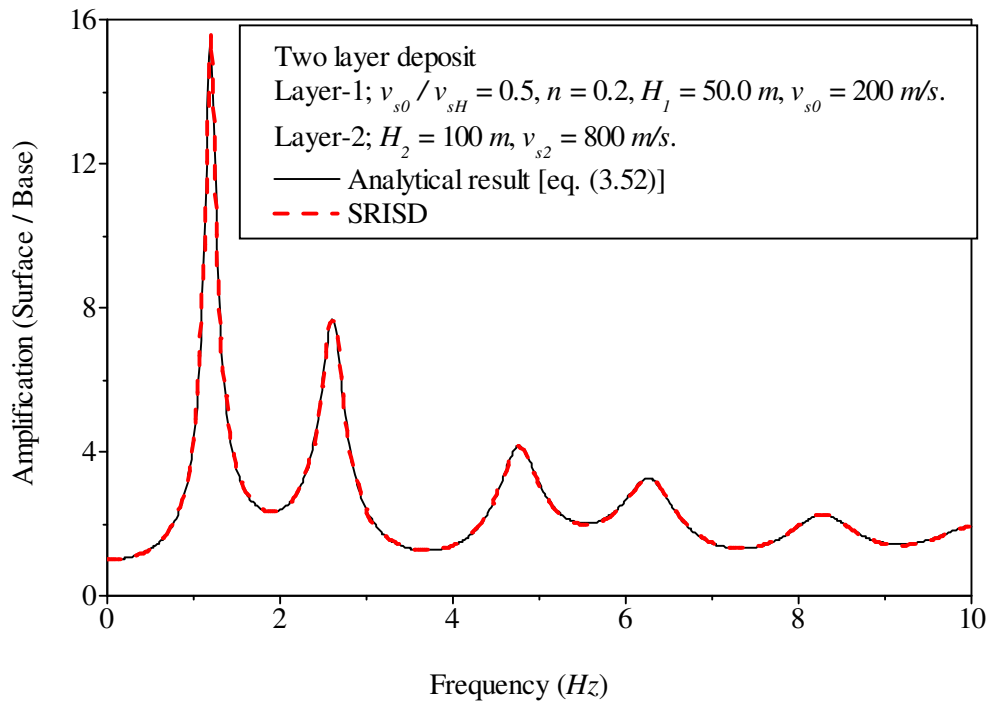
Figure 4.15: Comparison of amplification results for two layer soil profile between analytical solution and SRISD. The inhomogeneity factors of top layer are $v_{s0} / v_{sH} = 0.50$ & $n = 0.20$ ($v_{s0} = 200$ m/s). Shear wave velocity and depth of homogeneous layer considered are $v_{s2} = 800$ m/s and $H_2 = 100$ m respectively.

Finally in order to ascertain the computational ability of SRISD, the results obtained using this computer program are compared with analytical solution of complex two layered soil deposit. Figure 4.15 compares the result obtained for the case of soil deposit with top layer of thickness $H_1 = 50m$ and having inhomogeneity factors $v_{s0} / v_{sH} = 0.50$ and $n = 0.20 (m = 0.4)$ with $v_{s0} = 200$ m/s overlying homogeneous deposit with $v_{s2} = 800$ m/s and $H_2 = 100$ m with usual notations (Figure 3.20). The analytical solution of deposit considered is obtained using Eq. (3.52) and reproduced from Figure 3.21b. As in the case of single layer, it can be observed from this figure that the amplification transfer function computed using the program SRISD exactly simulates the trend of the amplification transfer function obtained analytically. For the purpose of comparative study the soil deposit is discretised at an interval of 0.10 m while using the computer program SRISD. This spatial discrete interval appears to be good enough to ensure stability and accuracy of the results at all frequencies of the input motion.

4.8 PARAMETRIC STUDIES ON AMPLIFICATION USING COMPUTER PROGRAM SRISD

The analytical results presented in the previous chapter are capable of giving amplification for limited cases. While formulating the solution it is assumed that the layer densities and shear wave velocity for the underlying deposit are constant for the case of two layered soil deposit. However, in reality these assumptions are seldom valid. This aspect has been discussed in detail in the preceding chapter along with relevant literature available in this regard.

Along with continuous variation of shear wave velocity the density of the bottom layer is also considered to vary linearly keeping mean density same as in the earlier analyses. The bottom layer is modeled as inhomogeneous layer with shear wave velocity varying linearly and having mean value equal to constant shear wave velocity used for the homogeneous deposit in the earlier analyses. These two cases of density and shear wave velocity variations along the depth have been treated independently.
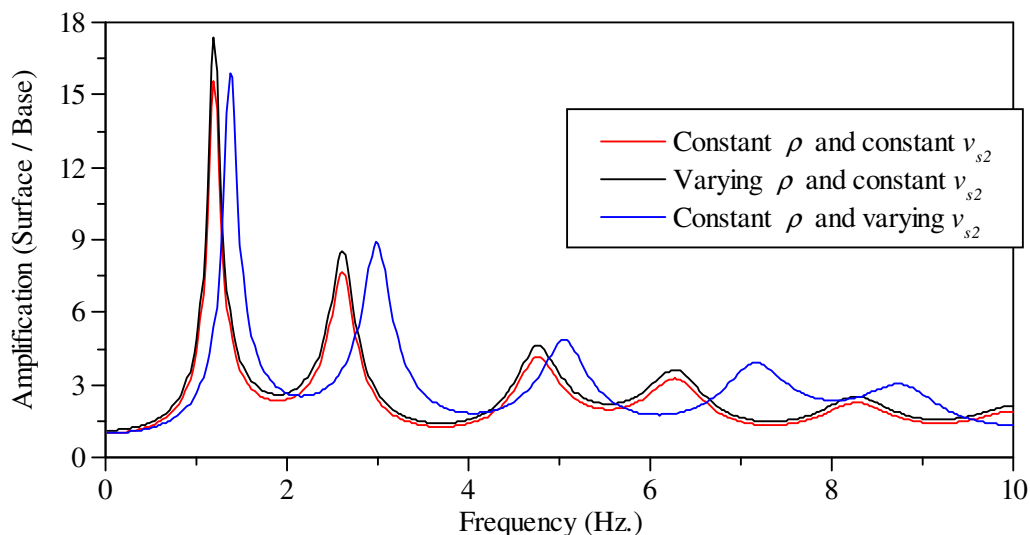
Figure 4.16: Comparison of amplification results for two layer soil profile having continuous variation of density in the top layer and continuous linear variation of shear wave velocity in the bottom layer using SRISD.

194
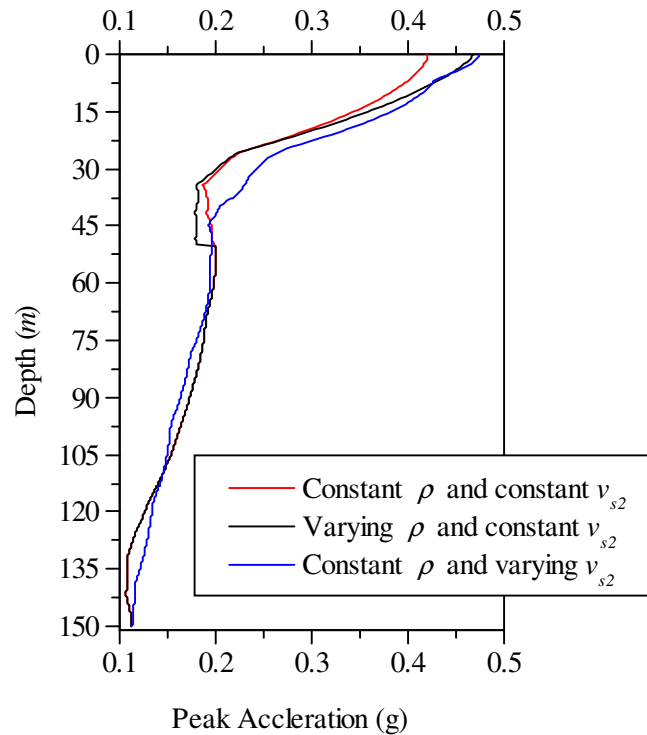
Figure 4.17: Comparison of variation of peak acceleration response along the depth of the profile for two layer soil profile having continuous variation of density in the top layer and continuous linear variation of shear wave velocity in the bottom layer using SRISD.

The results of this study are presented in Figure 4.16 and Figure 4.17 respectively for amplification characteristics and peak acceleration response along the depth. The input motion used for the analysis is Diamond Heights record of 1989 Loma-Prieta (USA) earthquake (Figure 4.11). From these figures it is evident that variation of density along the depth has significant effect on the amplification as well as acceleration response of the computed motion. In all the analytical studies discussed earlier only the variation of stiffness along the depth is considered and density of the deposit is assumed to be constant. The modal frequencies are significantly altered with the variation of density compared to those obtained from the analysis carried out keeping the density constant. Though the study is carried out for a limited case of linear variation of density, SRISD can handle any type of inhomogeneity with respect to density of the soil deposit. The other option included in the program SRISD is the variation of damping along the depth of the soil deposit.

4.9 COMPARISON OF EQUIVALENT LINEAR ANALYSIS RESPONSE COMPUTED USING DIFFERENT SOIL MODELS

In the previous chapter amplification characteristics of soil deposit with continuous distribution of stiffness properties is discussed. However, the results presented there was limited to linear analysis disregarding strain dependency of stiffness and damping properties. In this section, effect of nonlinearity on the estimated response quantities is presented. The results presented here are obtained using SRISD program. Main purpose of this study is to examine the effect of strain dependent G/G_{max} and ζ curves on the predicted response. The results of the analyses carried out using three different soil models namely Vucetic and Dobry (1991), Darendeli (2001) and Zhang et al. (2005) are compared. For the purpose of comparison amplification of surface motion with respect to bedrock motion and variation of maximum acceleration along the depth are considered.

Soil deposit of thickness $30m$ with continuous variation of shear wave velocity defined by $v_{s0} = 100m/s$, $v_{sH} = 300m/s$ and $n = 0.35$ is considered, which corresponds to $v_s(z) = 100(1+0.736z)^{0.35}$ in terms of Eq. 3.6 or its equivalence to Eq. 3.24 may be expressed in terms of shear modulus as $G(z) = 14521.75(1.359+z)^{0.7}$. The density of the soil is $\rho = 1.8 \ t/m^3$ which is considered to be constant throughout the depth. The analysis with Darendeli (2001) and Zhang et al. (2005) are carried out including the effect of mean confining stress but effect of loading frequency is ignored. While Darendeli (2001) curves were obtained for constant value of frequency of $f = 1Hz$ Initial low strain damping is taken as 1.5% while using Vucetic and Dobry (1991) curves while it is calculated using corresponding equations of the other two models.

The equivalent homogeneous deposit having uniform distribution as a substitute to inhomogeneous deposit is also used in this comparative study. The equivalent homogeneous deposit is represented by average shear wave velocity $(v_{s,ave})$ of the continuous velocity distribution. Among several options [Rovithis et al. (2011);

Mylonakis et al. (2011, 2013)] to calculate representative uniform velocity of proxy homogeneous deposit, the following equation is used

$$v_{s,ave} = \frac{1}{H} \int_0^H v_s(z) \, dz \qquad (4.45)$$

Using above equation the average shear wave velocity of an equivalent homogeneous deposit is calculated as 228.93 *m/s*. Input motion used in the analysis is EQ3 accelerogram scaled to give $a_{max} = 0.2g$. Details pertaining to this earthquake record are given in Chapter 2.
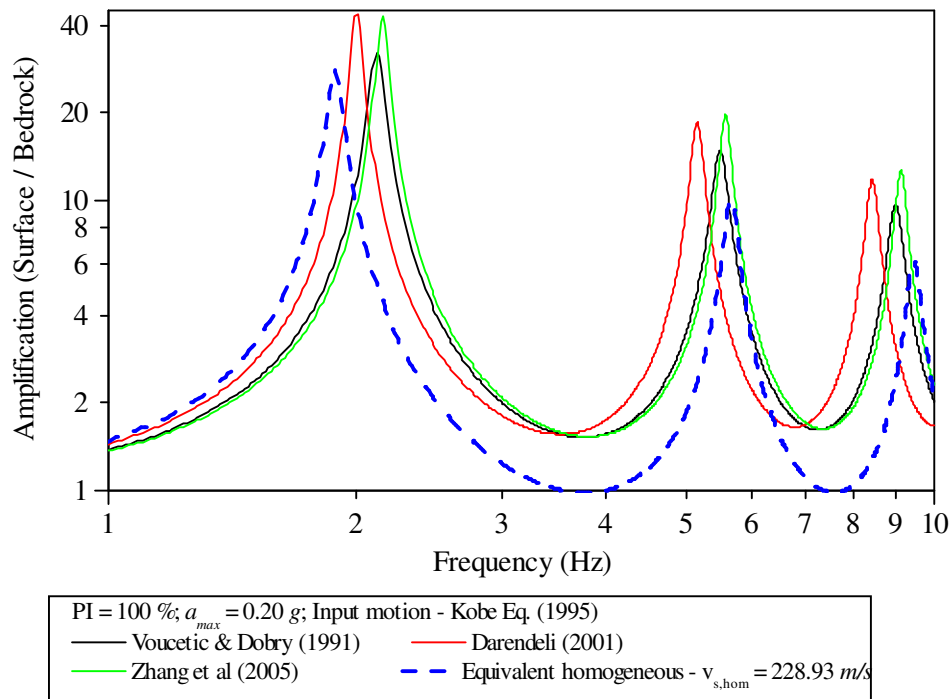
Figure 4.18: Comparison of surface motion amplification computed using different strain dependent shear modulus and damping models (Maximum acceleration = 0.20 *g* and PI = 100 %)

Figure 4.18 presents the amplification ratio of surface to bedrock motions for all three cases of soil models with $PI = 100\%$ from EQL analysis using SRISD program with continuous profile option. The amplification at different resonant frequencies obtained using Darendeli (2001) and Zhang et al. (2005) are almost same with marginal difference in frequencies corresponding to peak amplification. While Vucetic and Dobry (1991) curves yielded significantly lower amplification with resonant

frequencies almost identical to Zhang et al. (2005) results. The equivalent homogeneous deposit exhibits much more stiffness degradation behaviour, despite its shear wave velocity $(v_s = 228.93 m/s)$ value is much larger than inhomogeneous deposit $(v_{s0} = 100 m/s)$ near the surface. This is contradictory to what has been observed earlier in the previous chapter using linear analysis. In case of homogeneous deposit the EQL analysis is carried out using Vucetic and Dobry (1991) curves. Also, the maximum amplification in case homogeneous deposit at fundamental frequency (first peak) is more or less equal to corresponding result obtained for inhomogeneous deposit using Vucetic and Dobry (1991) curves.

Figures 4.19a and 4.19b show the maximum acceleration variation obtained using EQL analysis with different strain dependent shear modulus and damping models respectively for $PI = 30\%$ and $PI = 100\%$. The results presented here are obtained under the EQ3 input motion scaled to give $a_{max} = 0.05g$, i.e. relatively weak excitation. The computed peak surface accelerations for $PI = 30\%$ and $PI = 100\%$ is almost same using Zhang et al. (2005) model while in case of other two models the peak response for $PI = 30\%$ is lesser than that for $PI = 100\%$. Obviously, the homogeneous deposit has significantly less peak acceleration at the surface than continuously inhomogeneous deposit. The maximum acceleration response below 15 m is almost identical irrespective of soil model and profile configuration.

Figures 4.20a and 4.20b show the maximum acceleration response through the depth of the deposit. The results presented are obtained for the case of relatively strong input motion with EQ3 accelerogram being scaled to give $a_{max} = 0.2g$. To some extent the observations made in the previous case are valid in this case too. However, the difference in response estimated using three different soil models is noticeable clearly for the case of $PI = 100\%$ (Figure 4.20b). Equivalent homogeneous deposit and continuously inhomogeneous deposit cases analysed using strain dependent soil properties proposed by Vucetic and Dobry (1991) have resulted in similar kind of maximum acceleration response throughout the depth of the deposit for the case of $PI = 100\%$. But, in case of $PI = 30\%$ the results are distinctly different for all cases particularly nearer to surface.
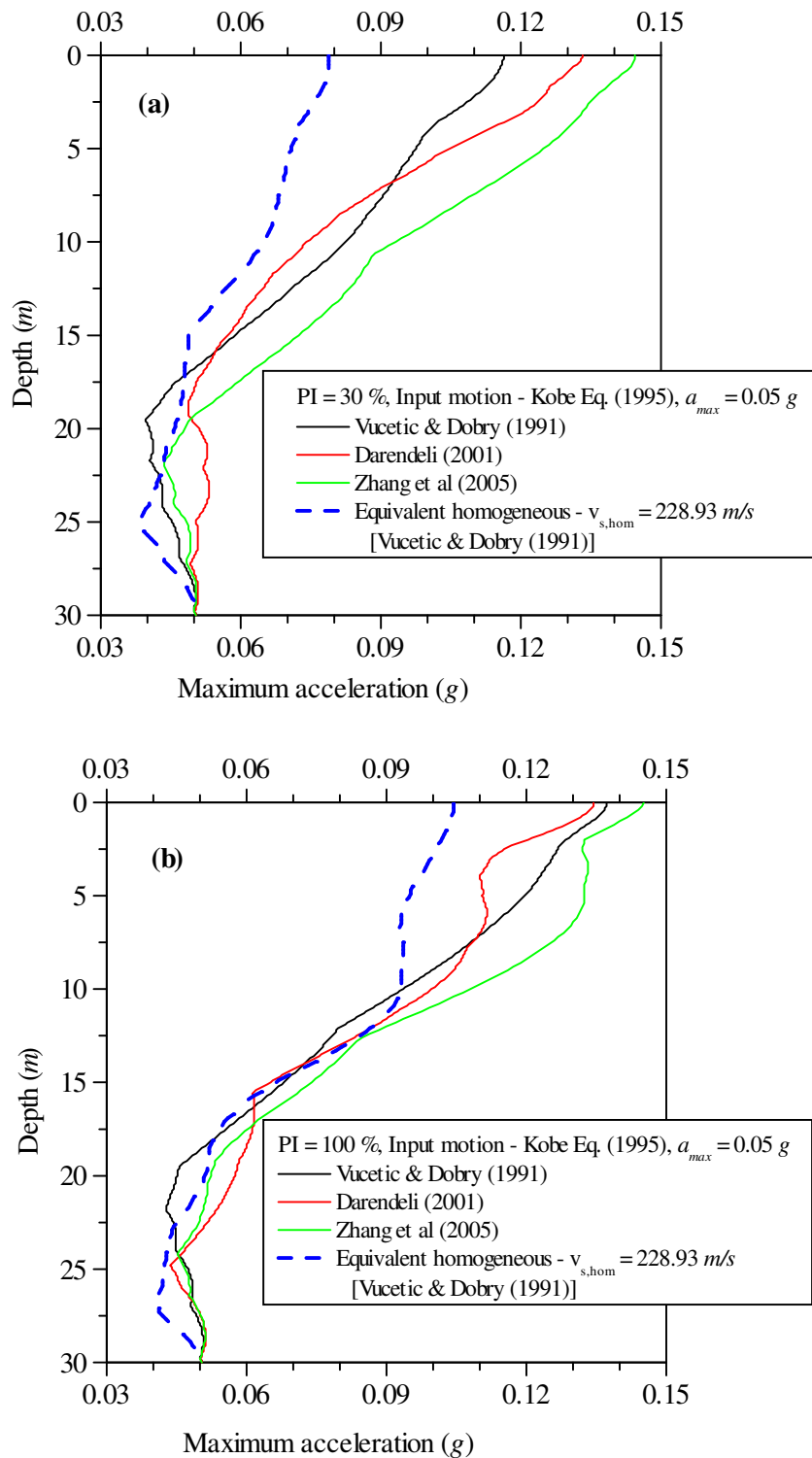
Figure 4.19: Comparison of variation of maximum acceleration along the depth of the soil deposit computed using different models of strain dependent shear modulus and damping properties of soil (Input motion: maximum acceleration = 0.05 *g*) (a) PI = 30 % and (b) PI = 100 %
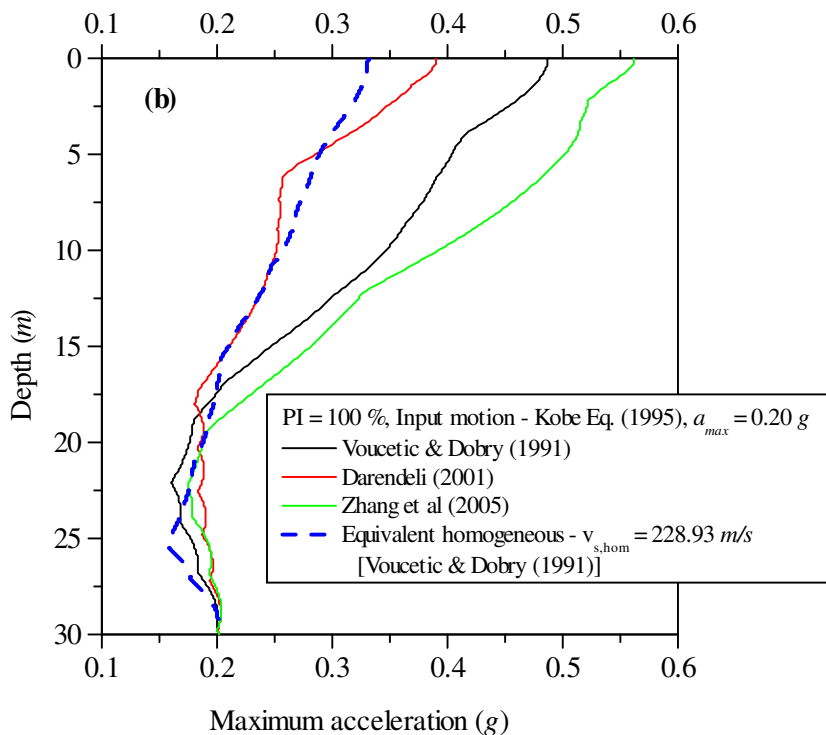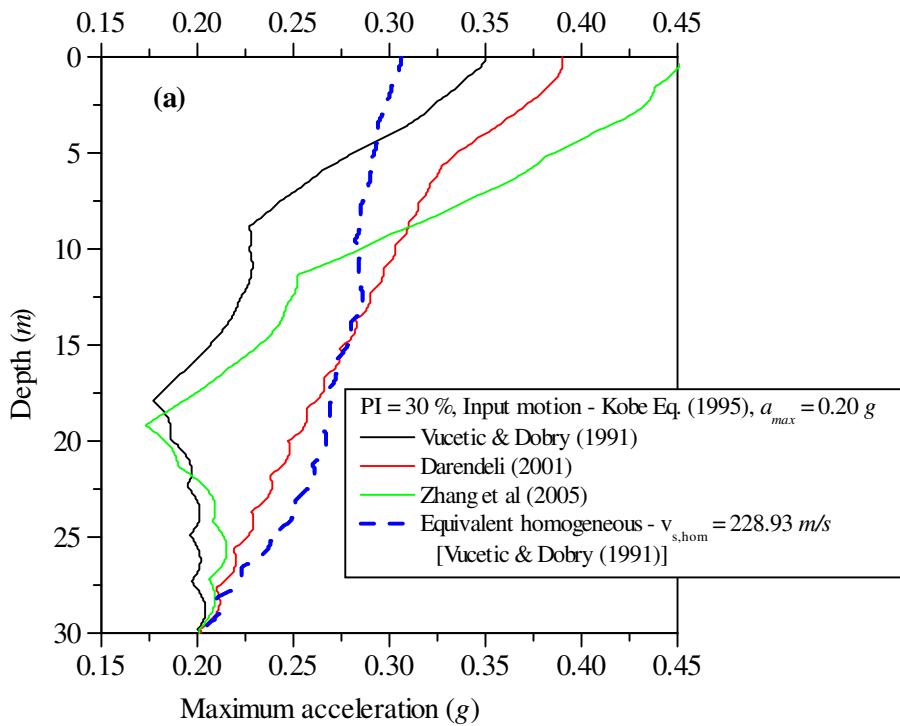
Figure 4.20: Comparison of variation of maximum acceleration along the depth of the soil deposit computed using different models of strain dependent shear modulus and damping properties of soil (Input motion: maximum acceleration = 0.20 *g*) (a) PI = 30 % and (b) PI = 100 %

200
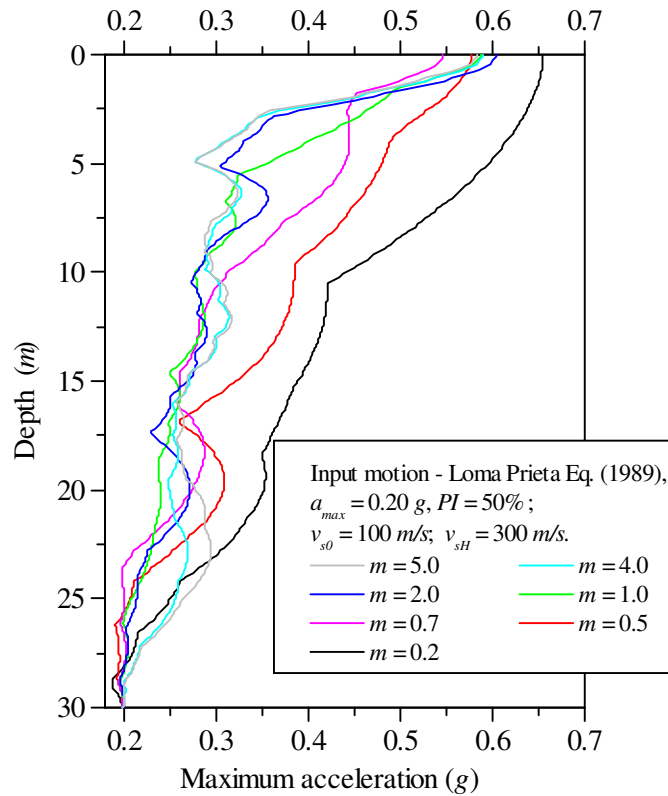
Figure 4.21: Comparison of variation of maximum shear stress along the depth of the soil deposit computed for different values of inhomogeneity parameter *m*; Input motion: maximum acceleration = 0.20 *g* and *PI* = 50 %
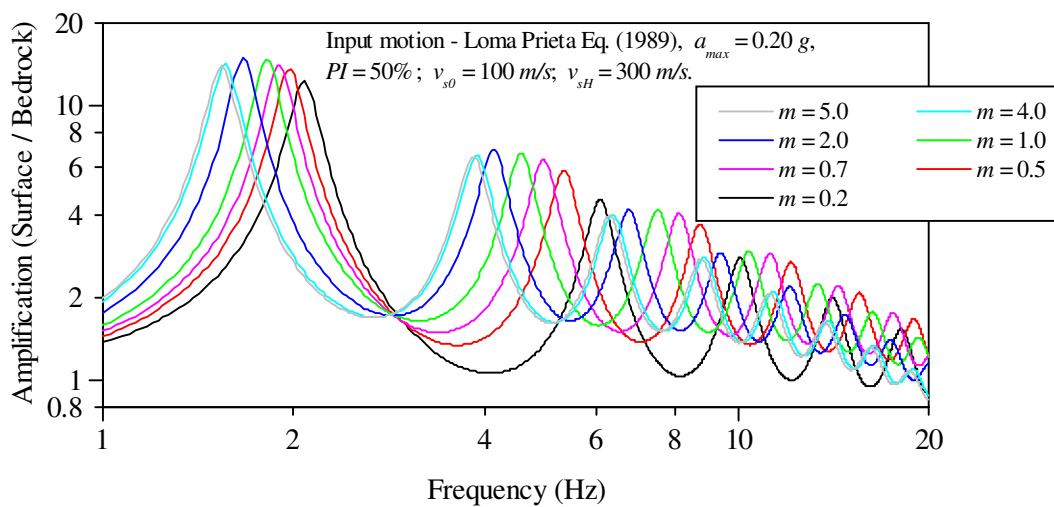
Figure 4.22: Comparison of surface amplification of input motion at bedrock level soil deposit computed for different values of inhomogeneity parameter *m*; Input motion: maximum acceleration = 0.20 *g* and *PI* = 50 %

Finally, the parametric study is carried out to recognize the effect of degree of inhomogeneity on computed response using EQL analysis. For this purpose, the same soil deposit considered in the previous analysis is used here with different degrees of inhomogeneity defined by the value of m which is varied between 0.2 and 5.0. Input motion EQ1 scaled to $a_{max} = 0.2g$ is used in this parametric study. The plasticity index of the soil deposit is taken to be 50%. Surface and base shear wave velocities of the deposit are kept constant with $v_{s0} = 100 m/s$ and $v_{sH} = 300 m/s$ respectively. Figure 4.21 shows variation of maximum acceleration computed for different values of m. The increase in maximum acceleration along the depth is significant as m decreases, particularly when $m < 1.0$. For the values of $m > 1$ the difference in peak acceleration response is barely noticeable and interestingly for $m > 4$ even these minor differences vanishes at all depths. In Figure 4.22 the amplification between surface and bedrock is presented for various values of m. As in case of linear analysis results, the equivalent linear analysis carried out for a particular soil type also shows shift in amplification peaks to lower frequencies. However, for any two values of m, the difference in corresponding frequencies appears to be lesser than that under linear analysis indicating that the stiffness degradation with respect to strains depends on type and degree of inhomogeneity.

4.10   EFFECT OF STEP SIZE USED FOR SPATIAL DISCRETIZATION - STABILITY AND ACCURACY

It is important to ensure stability and accuracy of numerical scheme used to compute response. Establishing reliable and consistent criteria to get accurate and bounded solution for the problem of wave propagation through soil deposit having complex velocity profile combined with nonlinearity is difficult. However, the essential conditions specified for the case of linear response analysis would serve as general guideline. Simplest condition to be satisfied in this regard is minimum step size that should be adopted is governed by minimum shear wave velocity in the soil deposit and maximum frequency of interest. These two factors are related by minimum wave length that should propagate through the medium.
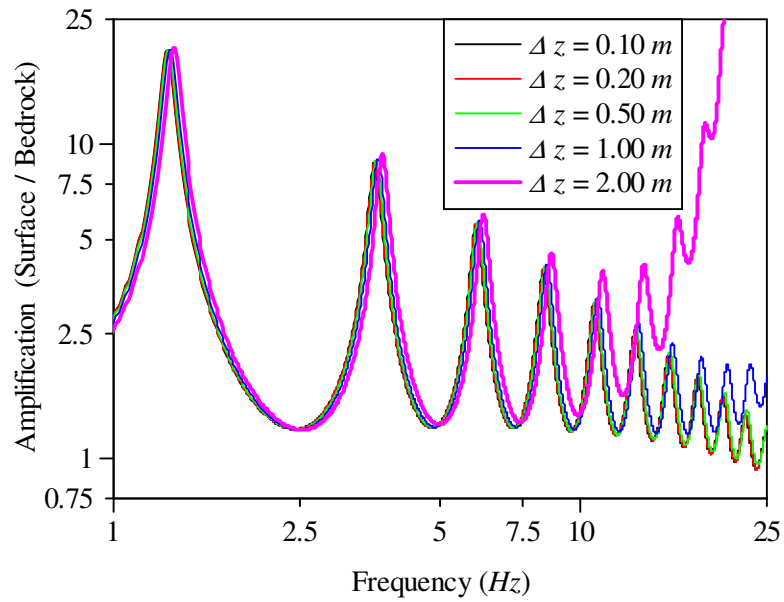
Figure 4.23: Amplification between surface and bedrock motions computed for different step sizes (Δz) used for discretization of the soil deposit; Input motion: Kobe Earthquake (EQ3) normalized to a_{max} = 0.05g
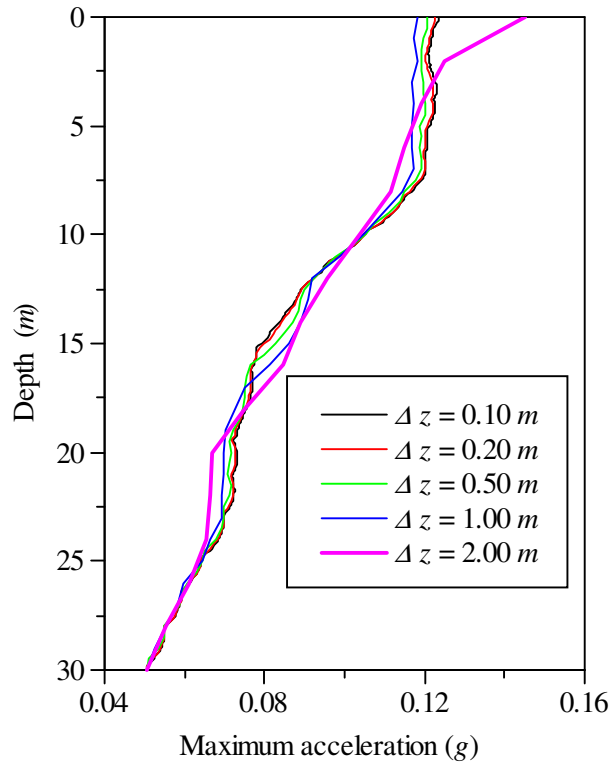
Figure 4.24: Variation of maximum acceleration along the depth computed for different step sizes (Δz) used for discretization of the soil deposit; Input motion: Kobe Earthquake (EQ3) normalized to a_{max} = 0.05g
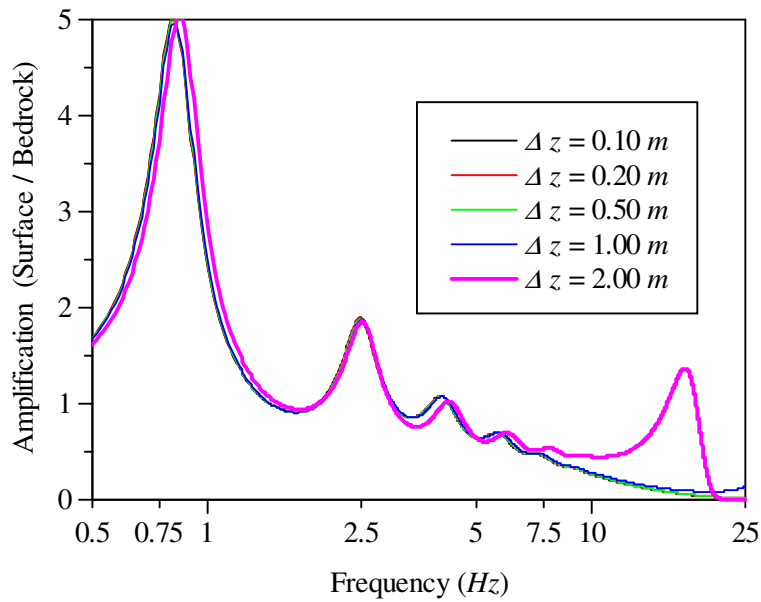
Figure 4.25: Amplification between surface and bedrock motions computed for different step sizes (Δz) used for discretization of the soil deposit; Input motion: Kobe Earthquake (EQ3) normalized to 0.5*g*
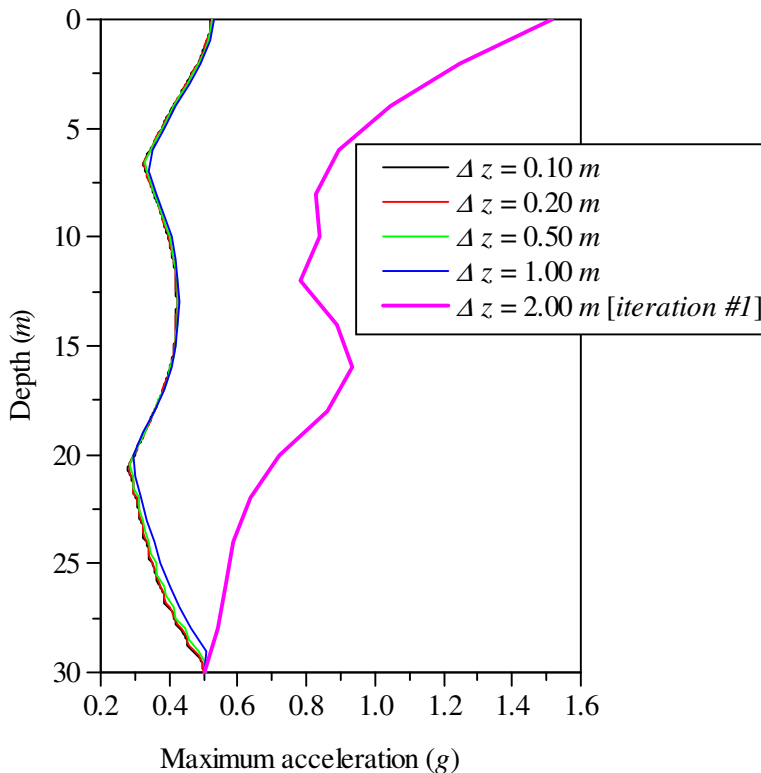
Figure 4.26: Variation of maximum acceleration along the depth computed for different step sizes (Δz) used for discretization of the soil deposit; Input motion: Kobe Earthquake (EQ3) normalized to 0.5*g*

Thus step size that is required to satisfy the above requirement is given by,

$$\Delta z = \frac{v_{s,min}}{4 f_{max}} \qquad\qquad (4.46)$$

Many of the computer programs, for example DEEPSOIL use this criterion to introduce additional sub-layers to ensure layer thickness is sufficiently small to sample frequencies up to $f_{\max}$. However, an example analysis is carried out to study the effect of step size used for discretization of continuously inhomogeneous soil deposit on the computed response. The soil deposit with $v_s(z) = 100(1+0.5z)^{0.25}$ is employed in this study. EQ3 accelerogram scaled to $a_{max} = 0.05g$ and $a_{max} = 0.5g$ are used as input motion at the base of the deposit. The 30 m soil deposit discretised with different step sizes ranging from $0.1m$ to $2.0m$ that correspond to maximum frequency range of 250 to 12.5 Hz. The results of the analysis carried out with input motion of $a_{max} = 0.05g$ are presented for amplification and maximum acceleration in Figures 4.23 and 4.24 respectively. The degradation of stiffness has resulted in the response to grow out of bounds for the case of $\Delta z = 2.0m$ in the frequency range beyond $\approx 10Hz$ and for the case of $\Delta z = 1.0m$ frequency response shows deviation at about 15 Hz even though induced strains are small. The maximum acceleration does not indicate these observations clearly. For the case of input motion with $a_{max} = 0.5g$, the equivalent linear analysis response has attenuated significantly beyond about 6 Hz as shown in Figure 4.25. However, for $\Delta z = 2.0m$ wayward deviation in computed response compared to other cases can be noticed. The amplification results presented here are after 10 iterations of EQL analysis. Figure 4.26 shows maximum acceleration response profiles for different Δz. values. The out of bound peak response for the case of $\Delta z = 2.0m$ is evident in the first iteration. From these results it is obvious that the criterion to ensure accuracy is governed by the reduction in stiffness with increase in induced strain level. It is not sufficient to satisfy the maximum frequency criterion at beginning of the EQL process. It is essential to keep track of stiffness degradation and accordingly vary the step size after successive iterations particularly under strong shaking.

4.11 EXAMPLE ANALYSIS: LA-OBREGON PARK GEOTECHNICAL ARRAY

An example problem is considered to illustrate features of the program SRISD. In this example analysis data pertaining to a geotechnical downhole array of La-Obregon Park site, USA is considered. The soil deposit considered is instrumented at surface and at 70 m depth. The data recorded at this downhole array site during Chino Hills earthquake of 29th July, 2008 are used. The analysis is carried out for all the three cases of shear wave velocity profile idealisations, i.e., layered, discrete data points and continuous variation. These are the three options made available in SRISD program. The main objective of this investigation is to study the feasibility of representing layered profile with a continuously distributed shear wave velocity profile. Considering the extent of reliable soil profile data available for La-Obregon site, it is chosen for this case study. The details of La-Obregon site, its shear wave velocity profile and earthquake data are given in the Appendix II. For the different cases of analysis, the SRISD input data files and the corresponding results of all these analyses cases are comparatively presented in the Appendix II.

These results demonstrate that, for the case of layered deposit analysis with routine method of computing effective strain in EQL iteration process, the results of EERA and SRISD are almost identical. Though approximated continuously varying shear wave velocity profile has low value of regression coefficient ($r^2 = 0.338$), it could estimate all the responses as accurately as that obtained for layered deposit. Moreover, the analysis carried with continuous shear wave velocity profile has better agreement with the recorded response particularly in the high frequency range beyond fundamental resonant frequency. When the analysis carried out using the raw data of shear wave velocity distribution along the depth as inferred from PS-logging survey, the estimated responses are very well in agreement with results of layered analysis.

4.12 SUMMARY

One of the objectives this research study is to develop a computer program to address some of the lacunae of the routine EQL analysis as explained in the previous chapters.

One dimensional site response analysis based on equivalent linear approach as employed in SHAKE considers the soil deposit as finite number of homogeneous layers. However, in reality often soil deposits exhibit continuous inhomogeneity. Also, as observed in the previous chapter, interpretation of field data to arrive at layered configuration is subjective and always associated with uncertainty. In such situations the concerned soil properties may be approximated with continuously varying trend instead of layered idealisation. Thus it avoids the errors involved in manipulation of bore-log data to arrive at layered configuration and also due to contrasting impedance ratio between layers. Moreover, it has been noticed by observation of field data of some of the instrumented sites, that the site cannot be considered as a deposit consisting of homogeneous layers in order to obtain reliable estimation of response quantities. In view of this drawback and also due to the aforementioned necessity it is imperative to develop a seismic site response analysis computer program which is able to model and analyze the soil deposit with continuous variation of soil properties.

The details of the computer program SRISD (**S**eismic **R**esponse of **I**nhomogeneous **S**oil **D**eposits) are presented in this chapter. The numerical scheme employed in developing the program is presented. Various options provided to model the shear wave velocity of the deposit are discussed. For an example problem, the SRISD results are validated with the results obtained using the program SHAKE91. Also the amplification results computed using SRISD is validated successfully with respect to that obtained from exact analytical solutions. The main features of the program discussed in this chapter include framework of the program, different options to input soil profile data, procedure to prescribe strain dependent shear modulus and damping curves apart from details of the curves provided as built-in data, input specifications for control motion and output options. Finally, general criteria required to satisfy stability and accuracy of the solution is highlighted.

SRISD provides three options to input profile data of the soil deposit. In the first option the profile data can be specified as layered profile as in case of many other currently available (for e.g., SHAKE91, EERA, DEEPSOIL, etc.). The input data for each layer include its thickness, low strain shear modulus or shear wave velocity,

density or unit weight, initial damping, plasticity index, coefficient of earth pressure at rest, geological age and OCR. However, last four data are required only when the strain dependent G/G_{max} and ζ curves used are functions of these factors, otherwise they are treated as redundant data. The second option is capable of taking the data at discrete points at specified depths which include the same set of data as mentioned above except layer thickness. This option is useful from practical point of view where in raw data pertaining to shear wave velocity profile, often obtained from continuous profiling procedures (PS logging, SASW, SPT, SCPT, etc.), may directly be used. Thus uncertainties associated with layer interpretation can be avoided. In the third case shear wave velocity or shear modulus, damping and density of the deposit soil deposit may be given in the form of inhomogeneity parameters of any appropriate function which may be chosen from the built-in functions provided to model continuously inhomogeneous soil deposits. These built-in functions defining the continuous variation physical properties of the soil deposit consist of linear, general power law and exponential distributions along the depth. Using these additional options, the capabilities of the SRISD program are illustrated. For example the analytical solutions discussed in the previous chapter are limited to linear elastic analysis and only stiffness of the soil deposit is considered to vary continuously.

In this chapter, results of a parametric study is reported in which apart from low strain stiffness, density of the soil is also considered to vary continuously and consequential effect of constant and continuous variation in density is brought out. Also, employing strain dependent soil property curve options of SRISD equivalent linear analysis is performed to compute the response of a soil deposit with continuous variation of shear wave velocity and its equivalent constant velocity (homogeneous deposit) profiles. The results of these analyses are compared to ascertain the effect of considering average properties of the soil deposit as a proxy to actual continuously distributed properties. Also the effect of choice of strain dependent curves on the computed response is discussed.

The additional features of the computer program which are incorporated based on the proposed improvements to EQL analysis are discussed in Chapter 5.

CHAPTER 5

EQUIVALENT LINEAR ANALYSIS
- PROPOSED REFINEMENTS

5.1   INTRODUCTION

One dimensional seismic ground response analysis is carried out popularly by modeling the soil deposit as layered system. The important inputs for the analysis consist of layer configurations and dynamic soil properties assigned to each of these layers. The ground response is observed to be nonlinear, particularly when input bedrock motion is due to strong earthquake shaking with high acceleration level. In such cases, analysis requires information about the model to represent nonlinear stress-strain behaviour of soil. Both, equivalent linear analysis in frequency domain and true nonlinear analysis in time domain, require strain dependent shear modulus reduction curve and damping curve as input assigned to each layer depending on its soil characteristics.

In equivalent linear analysis the concept of effective strain is used to update shear modulus and damping that is compatible with current level of strain. Majority of the computer programs that are developed for ground response analysis using equivalent linear approach uses a constant value to convert maximum strain to effective strain in an ambiguous manner. This process is iteratively carried out till convergence in maximum strain is achieved. As explained in chapter two of this dissertation, inherently equivalent linear approach has several limitations which directly influence the computed response to diverge from response quantities that are observed during an earthquake or computed using true nonlinear analysis. These discrepancies of equivalent linear approach have been clearly identified by several studies as detailed in chapter two. Also in that chapter, some of these issues were demonstrated by comparative study carried out with regard to time domain nonlinear and frequency domain equivalent linear analysis. Two major issues of primary concern are over prediction of response at frequency range close to fundamental frequency and under

prediction of response at high frequency ranges compared to time domain nonlinear analysis. Apart from these disagreements, strategic issue related to equivalent linear approach which is required to be resolved is ambiguity in computation of effective strain.

The focus of this chapter is to deal with these two issues. An attempt is made to propose alternative strategies to improve capabilities of equivalent linear analysis procedure. Firstly, in order to understand the effect of soil properties on the computed response a parametric analysis is carried out. A rational method for computation of effective strain is proposed based on intensity of shaking. Finally, frequency dependent equivalent linear analysis schemes are proposed which accounts for frequency dependent radiation (geometrical) damping. These proposed improvements to routine equivalent linear analyses have been verified to satisfactorily improve the computed frequency response.

5.2   LIMITATIONS OF EQUIVALENT LINEAR APPROACH

Though equivalent linear method is deficient with regard to accuracy of results compared to truly nonlinear time domain method, it is more often preferred method of analysis. Equivalent linear method (EQL) as implemented in most of the popularly used ground response analysis computer codes was outlined in section 2.7.1 of chapter two. The implementation procedure is depicted in Figures 2.9 and associated flowchart is shown in Figure 2.10. The key parameter in EQL method analysis is the effective strain employed to obtain strain dependent mechanical properties of the soil to use in subsequent iteration. On the other hand in time domain nonlinear analysis properties of the soil deposit are updated based on actual current strain level at the beginning of each time increment. Hence nonlinear analysis in time domain is more appropriate to accurately simulate the ground motion than equivalent linear method provided nonlinearity parameters are accurately evaluated in laboratory and used in the analysis. However dilemmas persist among practicing engineers about the reliability of the constitutive soil model and obtaining the parameters required to define the model apart from stability and error issues associated with numerical integration schemes adopted for solving the equation of motion.

Among other studies, Yoshida et al. (2002) have discussed major deficiencies of equivalent linear method compared to nonlinear methods. Equivalent linear method utilizes effective strain (γ_{eff}) to update soil properties after each of the iterations and these updated shear modulus and damping values are employed in the next iteration. Throughout particular iteration these values remain constant. There is no technically rational procedure available to convert the computed maximum strain (γ_{max}) to equivalent effective strain. Schnabel et al. (1972) and Idriss and Sun (1992) have proposed an empirical relationship to compute effective strain as given by $\gamma_{eff} = R\gamma_{max}$ where R is an empirical parameter which depends on magnitude of the earthquake (M) as $R = (M-1)/10$. However, initially when equivalent linear approach was proposed, Seed and Idriss (1969) recommended a value for effective strain which is equal to two-third of maximum strain. Later, Schnabel et al. (1972) in their manual for SHAKE program they recommended the effective strain value related to magnitude of the earthquake that is used as input motion in the analysis. Obviously, the choice of value of R in the analysis is intended to roughly represent intensity of shaking. This relationship used to establish value of R has no rational reasoning and it is obtained by trial and error process to match the computed response with that of observed record. It is observed that single value of parameter R is not capable of reproducing the entire response history at all the ranges of frequencies i.e., from low to high frequency ranges. As indicated earlier, equivalent linear method (computer code SHAKE) over estimates the responses around fundamental resonant frequency range and underestimates in the high frequency range. Researchers have attributed pseudo resonance as the primary cause for the observed discrepancy.

However, Yoshida et al. (2002) point out that, employing constant value of R always overestimates the maximum strain and this overestimation is larger at high strain levels as it is depicted schematically in Figure 5.1. Curve OC represents the stress-strain model in EQL analysis which corresponds to maximum shear stress versus maximum shear strain relation. On the other hand, curve OBA represents true stress-strain curve. Hence stress is always overestimated in EQL analysis by a magnitude equal to AC i.e., the difference in stress $\left(AC = \tau_{EQL} - \tau_{actual}\right)$ between these two curves.
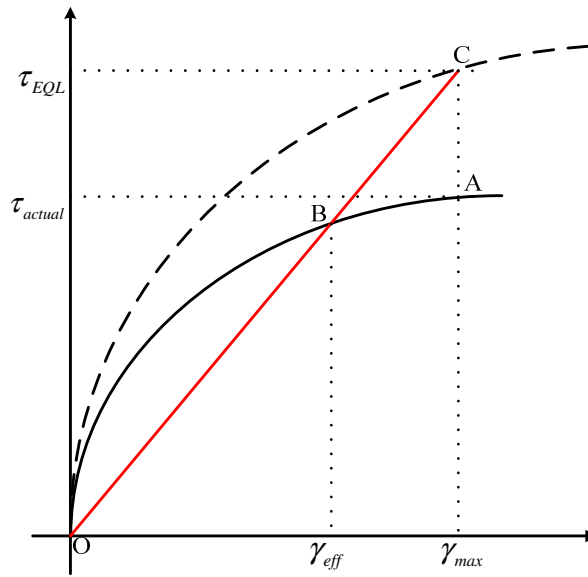
Figure 5.1: Schematic diagram depicting the reason for overestimation of shear stress by the equivalent linear method [reproduced from Yoshida et al. (2002)]

In addition to the above, the concept of evaluating effective strain based on *R* value and eventually using it in computation of modulus and damping for next iteration yields larger damping and smaller modulus particularly at high frequencies. Hence amplification computed from equivalent linear method is always much less than observed. As an example for this deficiency in computation, Yoshida et al. (2002) presented amplification results computed using EQL analysis for a site in Tokyo Bay, Japan, wherein equivalent linear analysis yields amplification much less than amplification computed from actual records. This major shortcoming of EQL analysis was also demonstrated earlier in chapter two of this dissertation. One advantage of the equivalent linear analysis is that we can perform deconvolution i.e., surface motion is transformed to bedrock motion; however bedrock peak acceleration is overestimated for the reason explained above.

5.3   EFFECT OF *R*-VALUE ON COMPUTED RESPONSE USING EQUIVALENT LINEAR ANALYSIS

To study the effect of ratio of effective to maximum strain (*R*-value) on the overall response of the soil deposit, a soil deposit of 30.0 *m* thick with continuous variation of stiffness given by $G(z) = A(z_0 + z)^m$ with shear modulus varying from 18000 *kPa* at

the surface $(G_{z=0})$ to 162000 kPa at the base $(G_{z=30})$ and $m = 4$ is considered. For the case of layered analysis the deposit is divided into 30 layers of 1.0 m thickness.
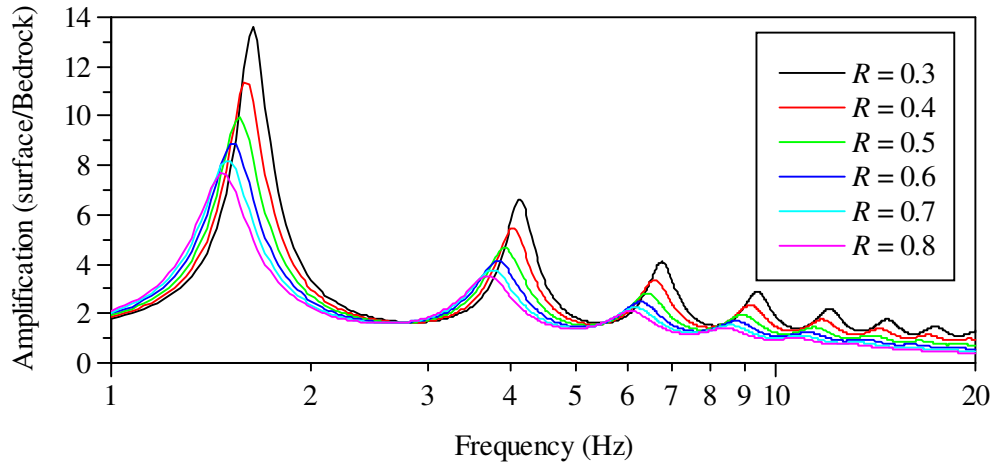
Figure 5.2: Effect of R value on Amplification between surface and bedrock (After eight iterations)
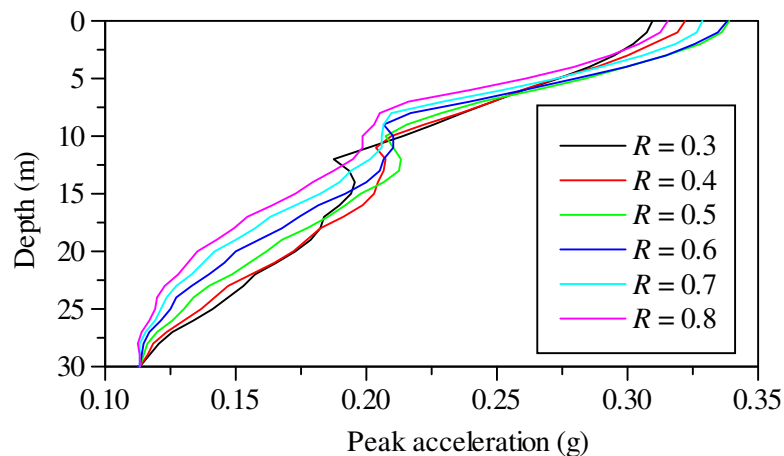
Figure 5.3: Effect of R value on variation of maximum acceleration along the depth (After eight iterations)

Initially, the effect of R-value on the predicted response of the deposit is studied with respect to surface to base amplification and peak acceleration response profile along the depth of the soil deposit. Many studies have recommended an arbitrary value of R equal to 0.65 [Bolisetti et al (2014), Kaklamanos et al (2013), etc.]. However, as mentioned earlier it is recommended to set the value of R based on magnitude of

earthquake as $R = (M - 1)/10$. For the earthquake magnitude ranging between 4 and 9, according to above relationship R value would vary from 0.3 to 0.8.
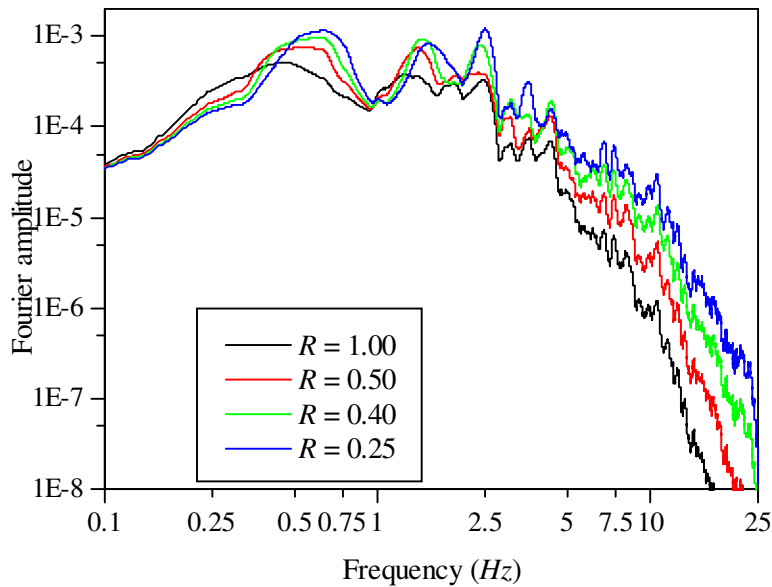
Figure 5.4: Effect of R value on frequency characteristics of computed surface acceleration time history

Figure 5.2 shows the amplification transfer function between surface and base of the deposit considered above. The shear modulus degradation and increase in damping with increase in R is clearly seen in the trends of amplification results. With increase in R, the resonant frequencies are significantly shifted to lower values and amplification peaks are decreased. Figure 5.3 shows variation in maximum acceleration along the depth for various values of R. Thus it can be concluded that, the value of ratio of effective strain to maximum strain has considerable effect on the computed response quantities at all the depths of the deposit. Figure 5.4 shows Fourier spectra of the predicted surface acceleration time history from equivalent linear analysis using different R values for computation of effective strain. This figure evidently brings out effect of R value adopted in EQL analysis on the frequency characteristics of the computed response. As R value increases the high frequency amplitudes are noticeably attenuated. This is because as R value increases the effective strain increases resulting in overestimation of damping from strain dependent damping curves. In chapter two comparative study carried out to relatively evaluate time and frequency domain analyses confirmed the under prediction of high

frequency response by EQL analysis compared to nonlinear time domain analysis. Hence, apart from well understood reasons stated earlier, inappropriate R value may also induce discrepancies in high frequency responses estimated using EQL analysis. Therefore, it is imperative to develop an alternative method to obtain an appropriate R value which is unambiguous and rational. The currently adopted method of computing R value based on the magnitude of the earthquake of input motion has ambiguity associated with it; particularly under following situations,

➢ Input motions derived from the two earthquakes, such as small magnitude near source (small epicentral distance) earthquake and relatively large magnitude far source (large epicentral distance) earthquake may have to be assigned with contradictory low and high values of R despite near source low magnitude earthquake may cause high intensity of shaking compared to high magnitude far-off event.

➢ In case of routine parametric studies, in which any particular accelerogram is scaled to lower or higher maximum values depending on the requirement of intensity of shaking or when an artificial accelerogram is used as input motion, for such requirements the magnitude of the earthquake associated with input motion is difficult to assign. Conceivably, uncertainty associated with the computed responses using arbitrary value of R is difficult to quantify.

5.4   PROPOSED ALTERNATIVE METHODS TO COMPUTE EFFECTIVE STRAIN

5.4.1   Method based on maximum acceleration

In this study a new method is proposed which is based on the level of shaking a particular layer experiences in each of the iteration. The intensity of shaking soil deposit undergoes depends on the intensity of bedrock motion. As discussed previously, in equivalent linear approach it is customary to assume value of R based on intensity of shaking. However intensity of shaking at the bed rock level for given magnitude depend many factors such as fault source mechanism, distance from the site, path effects, etc. Hence traditionally employed empirical method of assigning a

value for *R* based on magnitude of earthquake is inappropriate. Recognizing this fact some of the studies have suggested a particular value for *R* based on experience. These suggested values vary from 0.5 to 0.7 without any rational reasons supporting these recommendations.

In the past several popular relationships relating Peak Ground Acceleration (PGA) and Modified Mercalli Intensity (*MMI*) have been developed. Some of these are site specific while others can be used universally. Compilation of such relationships between PGA and *MMI* are given by Linkimer (2008). These prediction equations are reproduced and given in Table 5.1.

Table 5.1: Correlations between PGA and MMI [Compiled by Linkimer (2008)]

Eq. No.	Correlations	Validity range	Region	Reference
T5.1a	$MMI = \log PGA_{ave}^{3.0} - 1.50$	-	Western USA	Richter (1958); Guttenberg and Richter (1956)
T5.1b	$MMI = \log PGA_{ave}^{2.33} + 1.50$	-	Western USA	Hershberger (1956)
T5.1c	$MMI = \log PGA_{ave}^{3.33} - 0.47$	*IV < MMI < X*	Western USA	Trifunac and Bardy (1975)
T5.1d	$MMI = \log PGA_{max}^{4.0} - 1.0$	*IV < MMI < VIII*	Western USA, Japan and Southern Europe	Murphy and O'Brian (1977)
T5.1e	$MMI = \log PGA_{ave}^{2.86} + 1.24$	*IV < MMI < X*	Western USA, Japan and Southern Europe	Murphy and O'Brian (1977)
T5.1f	$MMI = \log PGA_{max}^{2.20} + 1.0$	*MMI < V*	California, USA	Wald et al (1999)
T5.1g	$MMI = \log PGA_{max}^{3.66} - 1.66$	*V < MMI < VIII*		
T5.1h	$MMI = \log PGA_{max}^{2.30} + 0.92$	*II < MMI < V*	Costa Rica	Linkimer (2008)
T5.1i	$MMI = \log PGA_{max}^{3.82} - 1.78$	*V < MMI < VII*		
T51j	$MMI = \log PGA_{ave}^{2.33} + 0.76$	*II < MMI < V*		
T5.1k	$MMI = \log PGA_{ave}^{4.60} - 3.38$	*V < MMI < VII*		
PGA_{ave} is the average PGA and PGA_{max} is the maximum PGA of the two horizontal components				

These equations are plotted in Figure 5.5 and its mean trend is shown in Figure 5.6. It can be observed in Figure 5.6 that mean trend of the above equations almost exactly

match with the most popular equation proposed by Trifunac and Bardy (1975). Hence, the intensity of shaking at any depth of soil deposit may approximately be related to corresponding peak acceleration by the following (same as Eq. T5.1c in Table 5.1),

$$MMI = 3.33 \times \log(PGA) - 0.47 \tag{5.1a}$$

$$R = (MMI - 1)/10 \tag{5.1b}$$

Knowing peak acceleration at a layer during any iteration we can estimate *MMI* from Eq. (5.1a) which in turn can be used to arrive at the value *R* from Eq. (5.1b).
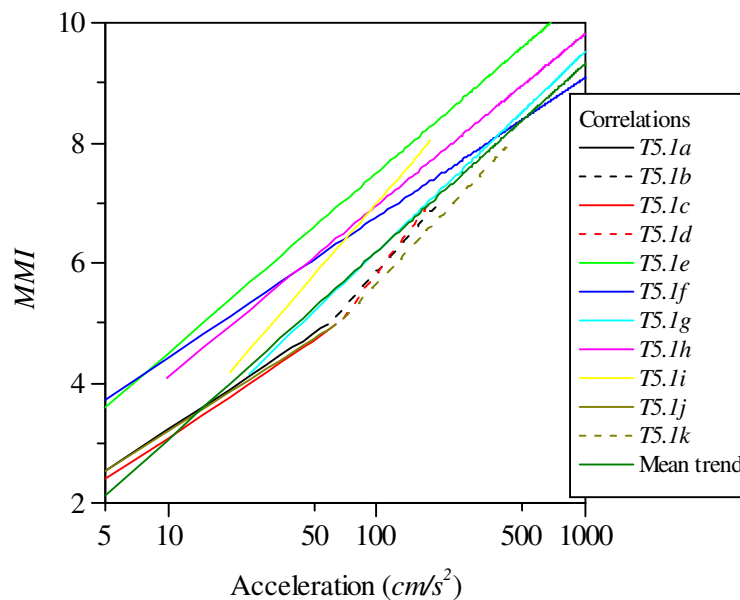
Figure 5.5: Peak Ground Acceleration (PGA) **and Modified Mercalli Intensity** (MMI) **correlations**

The method proposed here is more realistic in the sense that the *R* value to be used is computed automatically based on the intensity of shaking characterised by maximum acceleration. Thus different values of *R* are computed for each of the iterations in equivalent linear analysis. Also the value of *R* is uniquely assigned to each of the layer or node based on computed maximum acceleration at that layer or node in the previous iteration. Hence effective strain corresponding to a layer or node of the soil deposit is computed using allocated *R* value in order to update shear modulus and damping properties of that particular soil layer or node.
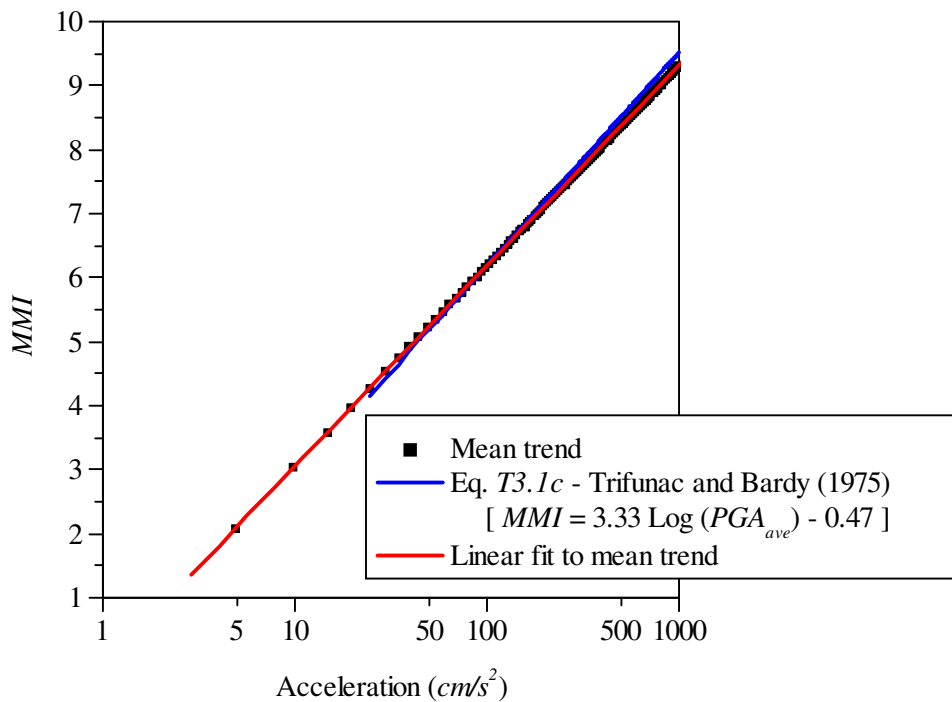
Figure 5.6: Comparison of mean trend of empirical correlations and Trifunac and Bardy (1975) correlation.

5.4.2. Method based on average strain

The other option which was suggested by Roësset (1977) to compute effective strain in equivalent linear analysis is based on average strain calculated from the strain time history. For this purpose Roësset (1977) suggested that average of the largest ten peak strain values may be used. However, the efficiency of this approach has not been investigated. Again, in this approach too it is difficult to assign number of peak values that need to be considered in computing the average strain to yield effective strain. However, option to compute effective strain based on average strain is also provided in SRISD computer program. For this purpose the option is provided in the program to select number of peak values to be considered in strain time history.

5.4.3   Implementation in SRISD program

The proposed alternative method to compute effective strain in the iterative equivalent linear analysis is implemented in SRISD code. The *RMS* values of acceleration and strain time histories are computed for iteration at all discrete nodes in case of

continuously inhomogeneous profile and at mid-depths of layered profile. The flowchart to compute effective strain using different options is shown in Figure 5.7. The options include the methods based on maximum acceleration and average strain apart from routine method using input value of R which is based on the procedure as adopted in SHAKE program. The number of peak strain values, *STNSUM* used to compute γ_{ave} is an input data. However, as recommended in Roësset (1977), default value of ten is used in the absence of this information.
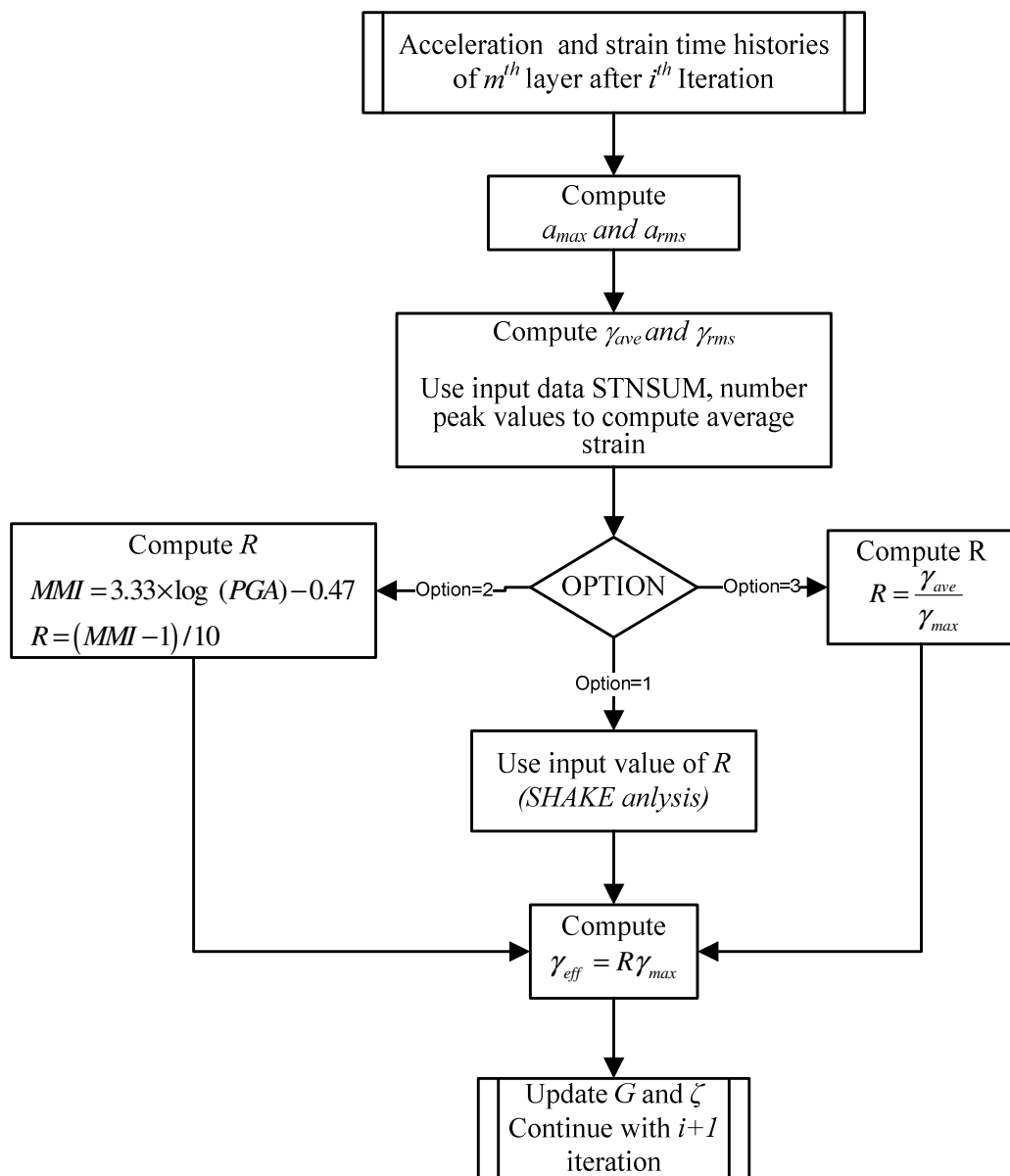
Figure 5.7: Flowchart for computation of effective strain using different options in the computer program SRISD

The three options for computation of *R* are shown in flowchart: *Option1-* Routine analysis option based on magnitude of the earthquake (SHAKE) which remain same for all layer during all iterations of EQL analysis; *Option2-* this is pertaining to newly proposed method in which calculation is based intensity of shaking, different values are assigned to each of the layers and they are updated after every iteration of EQL analysis (Section 5.4.1); *Option3-* this is based on average strain calculated from sum of *STNSUM* peak strains of the strain time history of each of the layers after every iteration (Section 5.4.2).

5.4.4 Comparative study between proposed method and routine analysis.

The equivalent linear analysis is carried using the proposed method for computation of ratio of effective to maximum strain at each layer of the deposit. The continuously inhomogeneous 30 *m* thick soil deposit considered previously (section 5.3) is used in this comparative study.
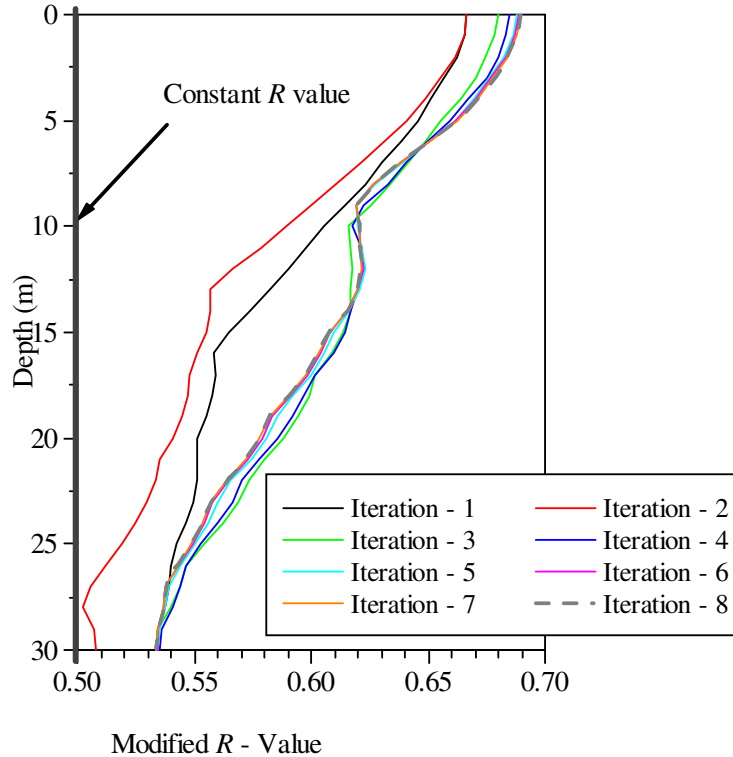
Figure 5.8: Variation of *R* value over each of the eight iterations and thick line represents the constant *R* value used in routine equivalent linear method

The nonlinear soil properties are modeled using strain dependent G/G_{max} and damping curves for sand proposed by Seed and Idriss (1970). The analysis carried out for three cases namely, layered analysis with constant value of $R = 0.50$, continuous analysis with constant value of $R = 0.50$ and continuous profile analysis by computing R value using the proposed method. That is, the value of R is updated after completing particular iteration for every layer unlike traditional method wherein R value remains constant during all iterations for all the layers. These analyses results are presented in Figures 5.8, 5.9, 5.10 and 5.11. Furthermore, the comparative study results are also presented in the Appendix-B for a case of La-Obregon geotechnical array.
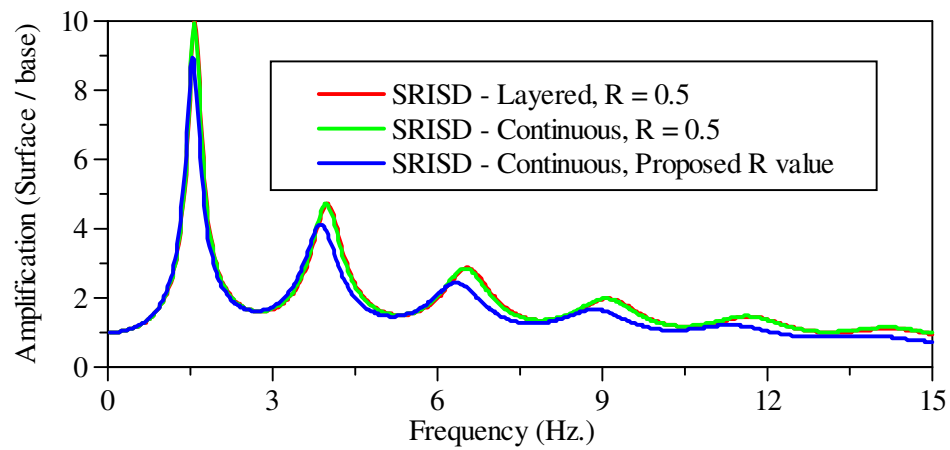
Figure 5.9 Comparison of amplification between surface and base for all the three cases of analysis.
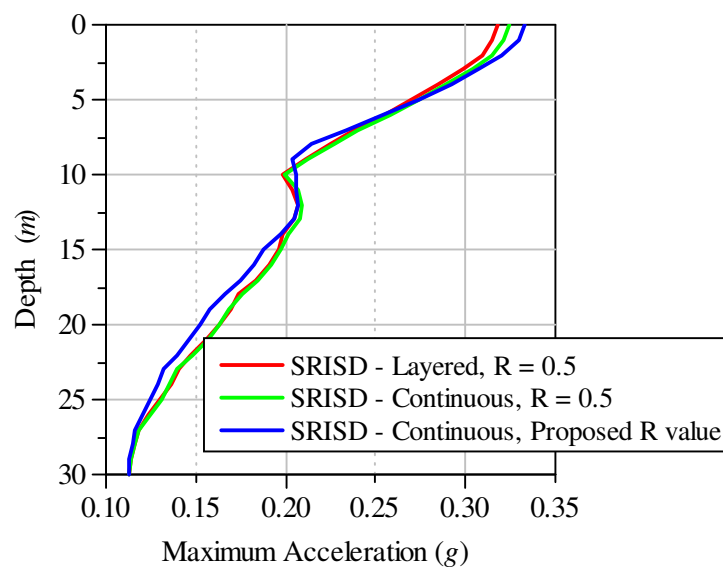
Figure 5.10 Comparison of variation peak acceleration profile along the depth of the deposit for all three cases of analysis (After eight iterations)

221
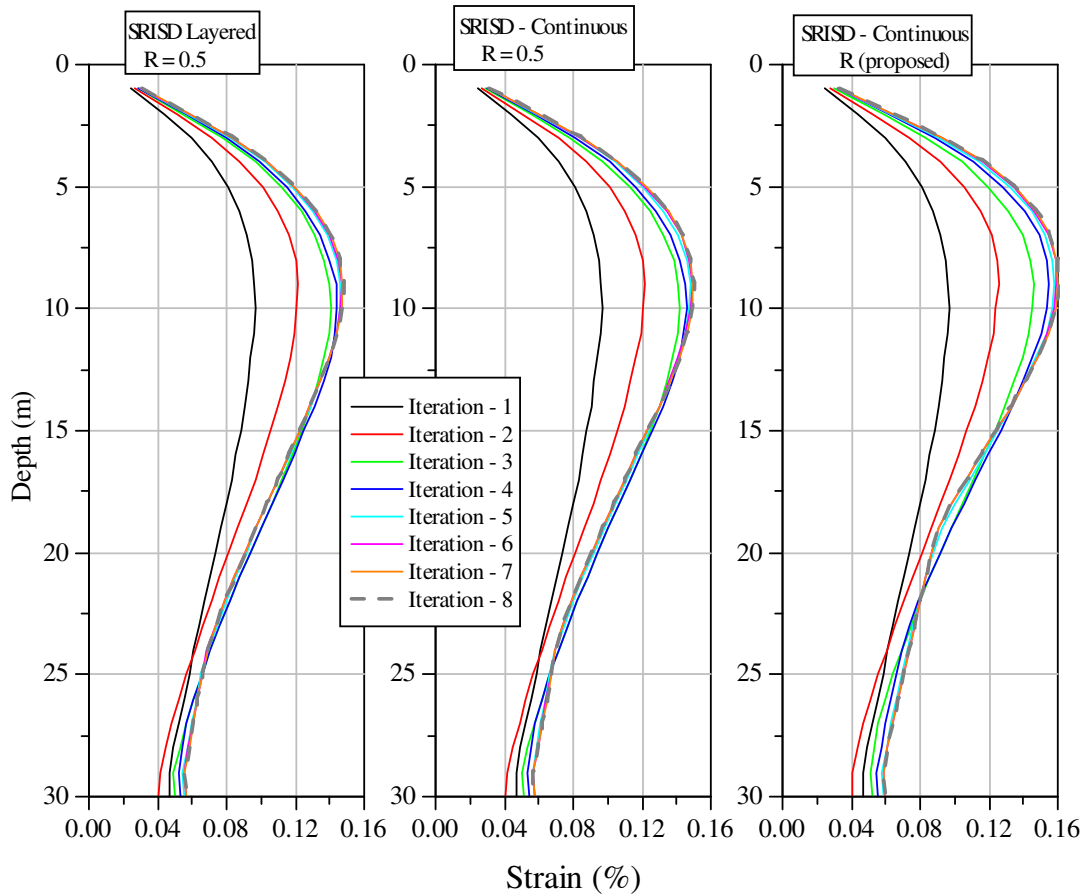
Figure 5.11: Convergence of strain over eight iterations for all the three cases of analysis.

5.5 FREQUENCY DEPENDENT EQUIVALENT LINEAR ANALYSIS

It has been observed that equivalent linear analysis fails to simulate the measured ground motions and in general the analysis doesn't yield consistent results under weak and strong ground shaking. As discussed in Chapter 2. Generally, the response obtained from EQL analysis is overestimated in the vicinity of fundamental resonant frequencies and attenuated response at higher frequencies. Equivalent linear analysis is iteratively employed with the help of strain dependent modulus degradation and damping curves. These curves for particular type of soil are essentially obtained from laboratory tests. Earlier methods of laboratory procedures had several limitations which lead to disputable understanding of frequency dependence of dynamic soil properties. In recent times some researchers have succeeded in recognizing the effect of loading frequency on dynamic soil properties. However, many issues are yet to be

addressed in this regard; particularly, range of frequency and its quantitative effect on energy dissipation characteristics of soil.

5.5.1 Frequency dependency of dynamic soil properties

The routine laboratory methods of determining dynamic soil properties have indicated that dynamic deformation characteristics were observed to be almost insensitive to loading frequency within the frequency range that is vital in seismic response analysis. Determination of dynamic soil properties in the laboratory usually conducted using sinusoidal excitation of soil specimen. Hence, very often the investigator has limited scope to simulate the actual field conditions, particularly the seismic event. In case of earthquake loading soil is excited by multiple frequencies which are very much difficult to reproduce in routine laboratory setups.

Among others, resonant column and cyclic triaxial tests are the most popular means of determining dynamic soil properties in the laboratory. These tests are performed at contrastingly different strain amplitudes and frequencies [Woods (1978)]. Thus, the comparison between the results from resonant column and cyclic triaxial tests should be done at similar frequencies. In resonant column tests the resonant frequency of the specimen is used to evaluate its dynamic properties. Also, conventionally, in case of resonant column test the analysis of test results is carried out by assuming the test specimen is an undamped elastic system to evaluate shear modulus. Then, independently using shear modulus, damping ratio is computed from free vibration or half-power bandwidth method or transfer function method. Hence it is impossible to evaluate frequency dependent dynamic properties using conventional resonance tests.

Owing to reasons cited above with regard to routine laboratory testing procedures, results presented by many researchers indicated that loading frequency in the range of 0.1 – 250 Hz had no significant effect on the shear modulus of both clayey and sandy soils [Hardin and Drenvich (1972a)]. On the other hand, some have [e.g., Richart (1978)] concluded that strain rate or loading frequency significantly affects the dynamic properties of clays but its effect is potentially insignificant in case of sandy soils. An important contribution concerning frequency dependent dynamic soil properties published by Isenhower and Stokoe (1981) questioned the internal

consistency of resonant column tests results under variable strain rates used to measure the stiffness of the soil at prescribed strain level. Their results obtained using cyclic torsional shear tests clearly indicated that, for medium plasticity silty clay, measured shear modulus increases with increase in strain rates.

Several researchers, through experimental evidences, discuss the effect of frequency/strain rate on the dynamic properties of the soil [Dobry and Vucetic (1987); Vucetic and Dobry (1991); Zovoral and campanella (1994); Shibuya et al.,(1995); Malagnini (1996); Lin and Huang (1996); Vucetic et al., (1998); Bray et al.,(1999); Vankov and Sassa (1999); Matesic and Vucetic (2003) and others]. According to Shibuya et al. (1995), the damping ratio decreases in the low frequency range, increases in the high frequency range and it is almost constant in the medium range of frequency as conceptually represented in Figure 5.12. Zovoral and Campanella (1994), using the results of limited number of tests with resonant column and torsional cyclic tests, indicated that the increase in stiffness with strain rate/frequency is significant in case of plastic soils, while in sands it is much smaller. They concluded that frequency dependence of damping property is negligible for both cohesive and cohesionless soils.
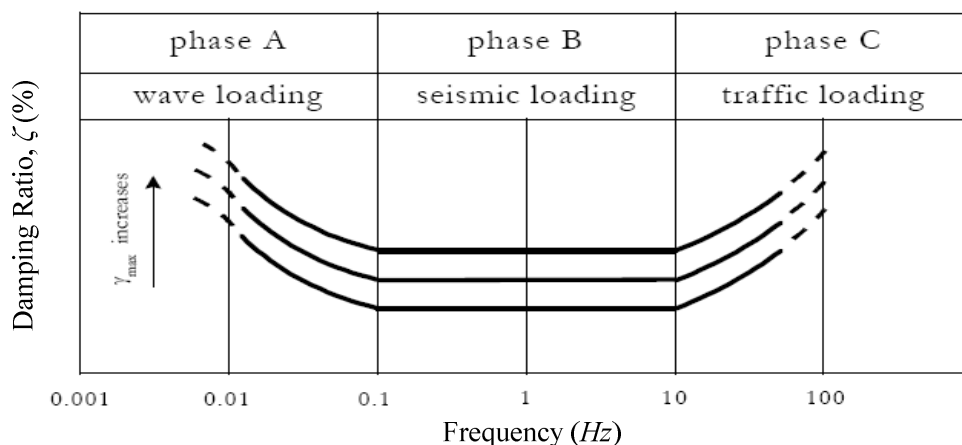
Figure 5.12: Frequency dependence of energy dissipated within a soil mass [Shibuya et al. (1995)]

Laboratory investigation regarding effect rate of strain on dynamic soil properties by Matesic and Vucetic (2003) corroborated the results of Zovoral and Campanella (1994) through more detailed and systematic study. They reported that stiffness at

very small strains does not seem to be affected by the strain rate in low-plasticity soils. However, in case of medium to high plastic soils an increase of the stiffness at very small strain with increasing strain-rate is observed. Also their results clearly indicated that, at higher strain levels, the stiffness reduction curves are affected by the strain rate, soil stiffness generally increases with increasing strain rate. It is important to note that all these tests were conducted at relatively small strain levels in the order of less than $0.1\% / s$. Their main objective was to evaluate shear strain modulus factor, α_G defined as ratio of increase in shear modulus and increase in logarithm of rate of strain ($\dot{\gamma}$) that is, $\alpha_G = (\Delta G) / (\Delta \log \dot{\gamma})$ as discussed in Isenhower and Stokoe (1981).

Effect of loading frequency or strain rate on damping ratio is yet to be ascertained clearly. However, as mentioned earlier, Shibuya et al. (1995) have confirmed that effect of loading frequency on damping ratio is evident. But, the researchers are still debating about general trend that can model dependency of damping property with respect to loading frequency. Rix (2004), through experimental study and followed by analytical verification, reaffirmed the general trend of effect of frequency on damping suggested by Shibuya et al. (1995) which is shown Figure 5.12. Results presented by Rix (2004) with respect to shear modulus agree well with that of other published results, that is shear modulus increases with frequency of loading at all strain levels.

According to Bray et al. (1999) and Gookin et al. (1999) the damping ratio systematically decreases with increasing frequency. On the other hand, the data from a series of cyclic torsional shear tests on Ottawa sand conducted by Lin and Huang (1996), the internal damping of the soil at various strain levels were increased linearly between 2.5 and 8% in the frequency range of 0.1 to 20 Hz. Khan (2008) reported that there is increase in damping in low frequency range $(< 60 Hz)$, while it decreases in frequency range of $60 - 150 Hz$ and it becomes independent for frequencies greater than 150 Hz. Hence, in the studies reported in literature, the trend of dependency of damping on frequency is put up with contradictory results.

Finally, to substantiate frequency effect on dynamic properties of soil, Carvajal et al. (2002) described a procedure of estimating the error between measured and computed

ground response using system identification procedure. The error thus estimated is attributed to frequency dependence of shear modulus and damping. Accordingly these properties are adjusted as frequency dependent properties so as to match the measured response. The trend is shear modulus increases with increase in frequency and no such particular trend is observed for damping but it is observed that, damping ratio generally has a decreasing trend with increase in frequency.

5.5.2 Frequency dependency of observed ground motions

In order to show that both nonlinear and frequency effects are significant in ground motion prediction, Idriss (1991) considered the difference in site amplification of soft soil profile subjected to ground motions of different magnitude ($M = 5.5$ and $M = 7$) earthquakes scaled to same peak ground accelerations. The difference in ground response for the input motions of same PGA but derived from earthquakes of different magnitude, is mainly attributed to frequency content of the ground motions.

Cameron and Green (2004) studied the effect of near field and far field earthquakes at the same location on site amplification. Using the data available they separated the sites into groups namely, near field and far field based on hypocentral distances of less than and greater than 50 km respectively. The near field motions are considerably more erratic and richer in high frequencies than far field motions. From their study Cameron and Green (2004) observed that, in case of near-field sites site amplification is considerably less than site amplification in case of far field sites. Hence they concluded that frequency effect on site amplification is significant.

In equivalent linear method of analysis, damping is kept independent of frequency of excitation. This has serious consequence on the computed results, even though computed response closely matches with that of observed data in case of convolution process (case of input motion being prescribed at base of the soil deposit), the high frequency response at the free surface results in unrealistically low spectral values. In case of de-convolution process (i.e. case of prescribing input motion at the surface) the response solutions of equivalent linear model diverges when the input motion is of high amplitude or rich in high frequencies [Kausel and Assimaki (2002)]

5.5.3 Available methods for frequency dependent analysis

5.5.3.1 Sugito et al. (1994)

Earliest attempt to consider the frequency effect in ground response analysis is Sugito et al. (1994) and Sugito (1995). In their method, the effect of frequency on the ground response is attributed to spectral characteristics of ground motion. The constant, R used to calculate effective strain ($\gamma_{eff} = R\gamma_{max}$) in SHAKE is modified in Sugito's method. In this method the effective strain is considered to be function of Fourier strain spectrum and it is defined as,

$$\gamma_{eff} = R\gamma_{max} \frac{F_\gamma(\omega)}{F_{\gamma_{max}}} \tag{5.2}$$

Here $F_\gamma(\omega)$ is Fourier spectrum of shear strain time history and $F_{\gamma_{max}} = \left[F_\gamma(\omega)\right]_{max}$. Rest of the algorithm is same as in SHAKE except for that the convergence of strain is checked separately for low $(<1 Hz)$, medium $(1 \text{ to } 5\ Hz)$ and high $(>5 Hz)$ frequency ranges. For an example case study, Sugito et al. (1994) illustrated the improvement achieved in the computation of amplification ratio using this method particularly at high frequencies. Furumoto et al., (1999), Furumoto et al., (2000), Yashima et al., (2000) and Ueshima (2000) are some of the additional references related to implementation of this method. To implement this algorithm, Fourier strain spectrum requires smoothening to avoid spurious peaks in Fourier strain amplitudes. This method doesn't take into account the frequency dependency of soil stiffness and damping properties directly.

5.5.3.2 Yoshida et al. (2002)

This study is particularly directed towards overcoming the inherent drawbacks of SHAKE with respect to underestimation of high frequency responses and accommodating rational method of effective strain calculation. Unlike previously explained method [Sugito (1995)] herein the effective strain for the current iteration is calculated as,

$$\gamma_{eff} = \gamma_{max} \qquad (\omega_p > \omega)$$

$$\gamma_{eff} = \gamma_{max} \left\{ 1 - \left(\frac{\log \omega - \log \omega_p}{\log \omega_e - \log \omega_p} \right)^m \right\} \qquad (\omega_p < \omega) \qquad (5.3)$$

$$\gamma_{eff} = 0 \qquad (\omega > \omega_p)$$

where ω_p is frequency corresponding to maximum shear strain, ω_e is the frequency above which nonlinear behavior need not be considered. Thus effective strain is expressed as the mth order polynomial equation (no experimental evidence) of $\log \omega$ between ω_p and ω_e, and γ_{eff} is constant outside this frequency range. It is suggested that $m = 2$ and $\omega_e = 95 \ rad / s \ (\cong 15 Hz)$ results in good prediction of ground response. All these relationships and parametric values are based on experience gained through comparison with measured ground responses. The comments made for sugito`s method is valid for this method too.

In order to verify the efficacy of their method, Yoshida et al. (2002) conducted ground response analyses for three different sites using their modified frequency dependent equivalent linear method. The results obtained from frequency dependent analysis computer codes DYNEQ [Yoshida et al (2002)], FDEL [Sugito (1995)] with routine equivalent linear analysis using SHAKE were compared. Finally, Yoshida et al. (2002) concluded that in case of convolution analysis DYNEQ yields much closer to observed peak acceleration value compared to FDEL and SHAKE. Peak stress and peak strain profiles estimated along the depth of the deposit from all these codes are almost identical. Predictions of deconvolution analyses using frequency dependent analyses computer codes (both DYNEQ and FDEL) are much more realistic compared to observed values and results from both the codes are almost identical. However, results from SHAKE analysis deviates from observed record, that is peak acceleration values are unacceptably overestimated.

5.5.3.3 Kausel and Assimaki (2002)

In this study Kausel and Assimaki (2002) gave different reasoning in support of incorporating frequency parameter in calculation of effective strain. They analysed

normalized Fourier strain amplitude spectra of five different earthquakes and observed that a unique relationship could be established between Fourier strain amplitude and frequency for all the earthquakes under consideration. Deriving Fourier spectra of strain time histories from velocity time histories, they observed that the spectral strain values follow a similar trend in which they decrease with frequency. A smoothened strain spectrum corresponding to this observed trend is represented by,

$$
\begin{aligned}
\gamma(\omega) &= \gamma_0 \left\{ \frac{\exp\left(-\lambda_1 \dfrac{\omega}{\omega_0}\right)}{\left(\dfrac{\omega}{\omega_0}\right)^{\lambda_2}} \right\} \; for(\omega > \omega_0) \\
\gamma(\omega) &= \gamma_0 \qquad\qquad\qquad\; for(\omega \le \omega_0)
\end{aligned}
\tag{5.4}
$$

wherein mean frequency ω_0 of the strain spectrum as well as the least-squares best-fit parameters λ_1 and λ_2 are obtained. An elaborate algorithm is proposed based on Eq. (5.4) to incorporate frequency dependent analysis. The procedure involves finding values of ω_0, λ_1 and λ_2 from spectrum of strain time history for each layer and in successive iterations. Then using Eq. (5.4) smoothened strain spectrum is obtained from which frequency dependent modulus and damping properties are extracted to use in next iteration.

Kausel and Assimaki (2002) implemented their frequency dependent model for ground response analysis of two hypothetical sites representing shallow and deep profiles. Their objective was to test the efficiency of their proposed method which not only model the frequency dependency but also pressure dependency of soil characteristics as the depth of the soil deposit overlying the bedrock increases. Since the main objective of the present research is to study frequency dependent characteristics, here the results of the study pertaining to shallow deposit are highlighted. The shallow deposit considered is of 25 *m* thick with constant mass density and shear wave velocity of 2000 *kg/m³* and 200 *m/s* respectively. The fundamental frequency of the deposit considered works out to be 2.0 *Hz*. Pressure dependent modulus reduction and damping curves proposed by Assimaki et al (2000)

were employed. The prescribed input motion at the base is the record of 1995 Kobe earthquake scaled to maximum of 0.5 *g* and its mean frequency is about 1.7 *Hz*. The surface acceleration responses predicted using both the frequency-dependent and the true nonlinear models were compared and observed that frequency dependent analysis proposed by Kausel and Assimaki (2002) compares very well with true nonlinear analysis particularly with respect to phase of peak values. However, magnitude of acceleration in the strong motion portion it comparatively over predicted while peak acceleration values at the later part is marginally smaller than nonlinear analysis.

5.5.3.4 Darendeli (2001)

In the previous chapter expressions for strain dependent shear modulus and damping proposed by Darendeli (2001) was presented (Eq. 4.36 to 4.41).These generalized expressions are incorporated in SRISD soil properties database. Based on limited experimental data Darendeli (2001) concluded that the effect of loading frequency is insignificant on shear modulus but its effect on the small strain damping property is significant particularly at high frequency. The expression for small strain damping as a function of loading frequency, mean effective confining stress $\left(\sigma_m'\right)$, *OCR* and *PI* is obtained by normalizing its value with respect to frequency of 1 *Hz* as given below (Eq. 4.39, Chapter 4),

$$\zeta_{min} = \left(\frac{\sigma_m'}{p}\right)^{-0.2889} \left[0.8005 + \left(0.0129PI \times OCR^{-0.1069}\right)\right] \times \left(1 + 0.2919\ln f\right) \quad (4.39)$$

The option for using this expression is provided in SRISD in which ζ_{min} is calculated at every increment of loading frequency and added to strain dependent material damping obtained after successive iteration of the analysis. Provision is also made to use this value of ζ_{min} with any other strain dependent material damping curve that is employed in the analysis.

Based on Eq. 4.39, Figures 5.13 and 5.14 summarize the effect of two important parameters, plasticity index and effective confining pressure on frequency dependent small strain damping property of the soil.
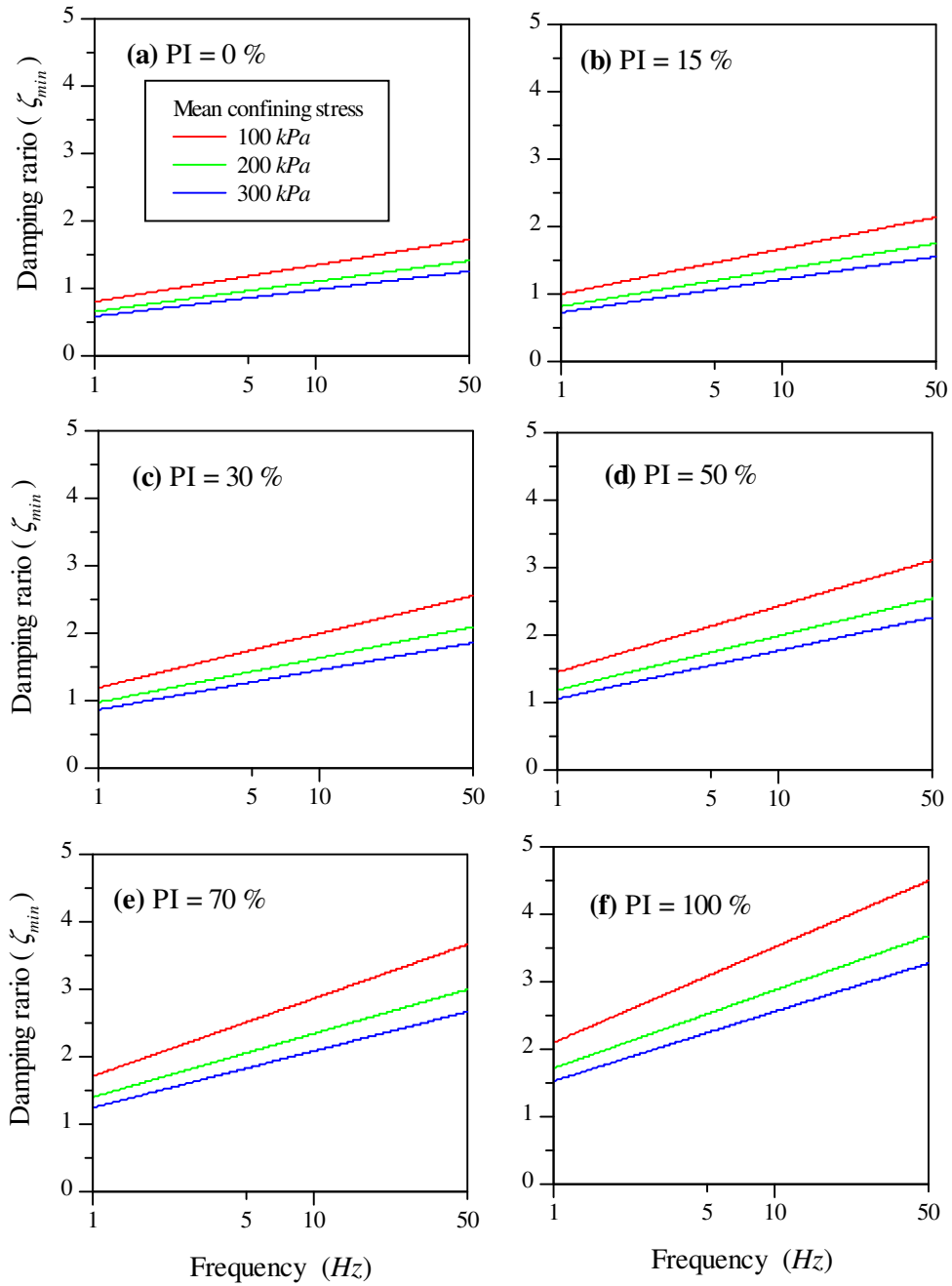
Figure 5.13: Effect of effective confining stress on frequency dependent small strain damping property of soil for different values of plasticity index.

From these figures it can be observed that, small strain damping increases almost by twofold over the frequency range of 1 to 60 Hz for all values $PI > 0$. With increase in loading frequency the rate of increase in material damping is almost same particularly for plastic soils. However, highly plastic soils exhibit larger frequency effect compared to low plastic soils. The minimum damping ratio at 1 Hz frequency is also

higher for a soil with large *PI*. Also, in range of frequency considered the damping decreases with increase in confining stress. This is in confirmation with the variation of damping along the depth of the deposit [Park and Hashash (2005)]. This model is employed in the computer program DEEPSOIL of Hashash (2011).
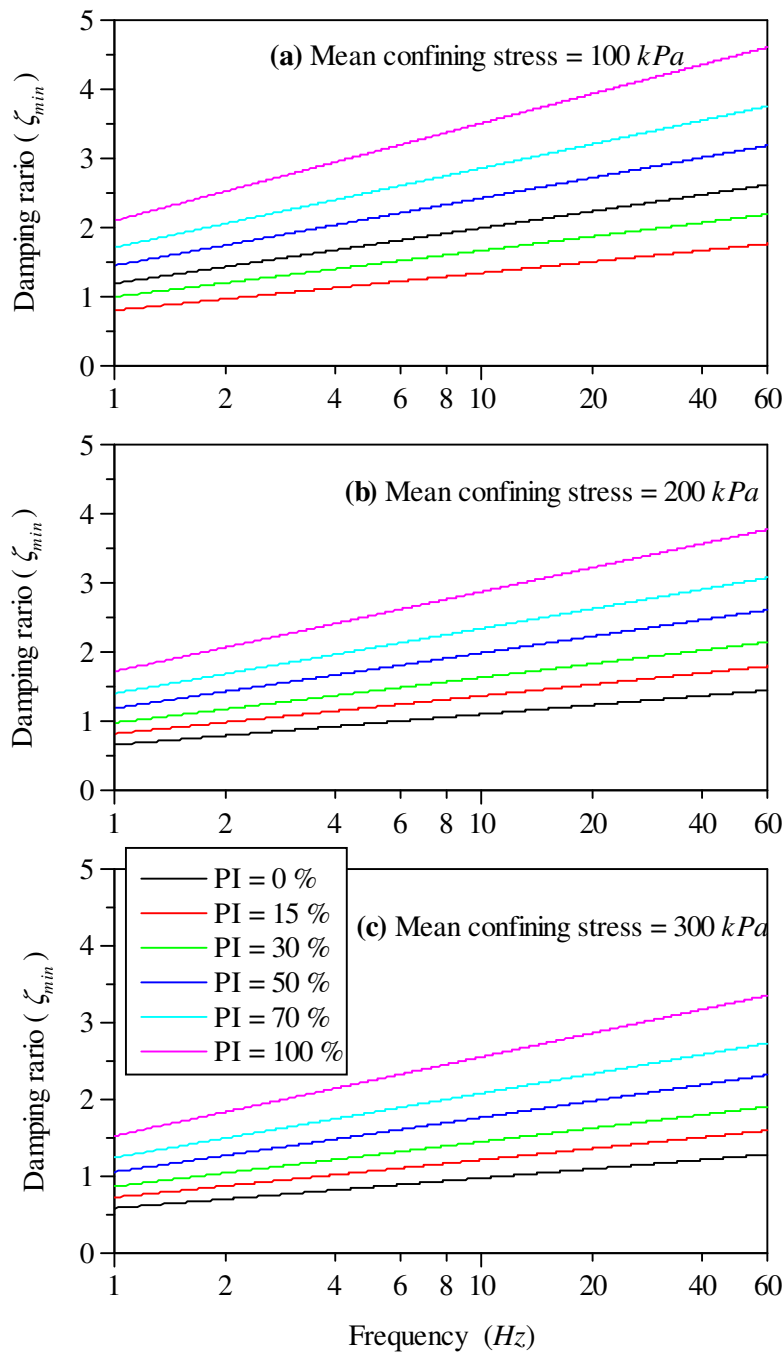
Figure 5.14: Effect of effective plasticity index on frequency dependent small strain damping property of soil for different values of confining pressure.

Although, frequency dependent expression of damping proposed by Darendeli (2001) can be conveniently implemented in EQL analysis scheme, it may not be helpful to overcome major discrepancy in high frequency response of EQL result. Obviously increase in damping with frequency will further dampen out high frequency response but it will aid in reducing the resonant frequency response to some extent provided fundamental frequency of the deposit is well above 1 *Hz*.

5.5.3.5 Park and Hashash (2008); Jeong et al. (2008)

All the methods, except Darendeli (2001), discussed above are formulated without considering effect of frequency on shear modulus and damping properties of soil. Park and Hashash (2008) and Jeong et al. (2008) proposed a method in which the effect of loading frequency on soil properties is incorporated. In order to model strain rate dependent damping, three well documented damping models proposed by Rix and Meng (2005) [also Rix (2004)], Kim et al. (1991) and Darendeli (2001) are employed by Park and Hashash (2008) and Jeong et al. (2008). The procedure developed by them to implement strain rate dependent shear modulus is as follows,

- Determine the maximum shear modulus at the reference frequency, $G_{\text{max[Ref. freq.]}}$,calculated using the equation,

$$G_{\text{max[Ref. Freq.]}} = \frac{[G/G(0.5 \ Hz)]_{\text{Ref. Freq.}}}{[G/G(0.5 \ Hz)]_{\text{f(V}_s)}} \times G_{\text{max[f(V}_s)]} \tag{5.5}$$

in which, $G_{\text{max}[f(v_s)]}$ is the shear modulus determined from the shear wave velocity measured at frequency $f(v_s)$ and $[G/G(0.5 \ Hz)]$ represents the relationship between the normalized shear modulus i.e., rate dependent shear modulus normalized to the modulus obtained at a frequency of 0.5 *Hz*.

- Based on modulus reduction reference curve at a particular reference frequency, the shear modulus reduction curve at a given loading frequency is calculated. The reference shear modulus reduction curve represents the ratio of *G* obtained at the reference frequency $\left(G_{\text{Ref.Freq.}}\right)$ to the G_{max} also measured at the reference frequency

$\left(G_{\max[\text{Ref}.\text{freq.}]}\right)$. By using the normalized rate-dependent function, the shear modulus $\left(G_f\right)$ at a given loading frequency f can be calculated from the $G_{\text{Ref}.\text{Freq.}}$ using the equation:

$$\frac{G_f(\gamma)}{G_{\max[\text{Ref. Freq.}]}} = \frac{[G/G(0.5\ Hz)]_f}{[G/G(0.5\ Hz)]_{\text{Ref. Freq.}}} \times \frac{[G]_{\text{Ref. Freq.}}(\gamma)}{G_{\max[\text{Ref. Freq.}]}} \qquad (5.6)$$

Here, $\dfrac{[G]_{\text{Ref. Freq.}}(\gamma)}{G_{\max[\text{Ref. Freq.}]}}$ is the strain dependent reference shear modulus reduction curve.

- Combining Eq. (5.5) and Eq. (5.6), the following equation is obtained

$$G_f(\gamma) = \frac{[G/G(0.5\ Hz)]_f}{[G/G(0.5\ Hz)]_{f(V_s)}} \times \frac{[G]_{\text{Ref. Freq.}}(\gamma)}{G_{\max[\text{Ref. Freq.}]}} \times G_{\max[f(V_s)]} \qquad (5.7)$$

Above equation represents the frequency dependent shear modulus which is not affected by the reference frequency. Its effect cancels out because successive multiplication of the results of earlier steps. Thus shear modulus is influenced only by the frequency at which the shear wave velocity is measured i.e., $f(v_s)$ and the loading frequency of the input ground motion.
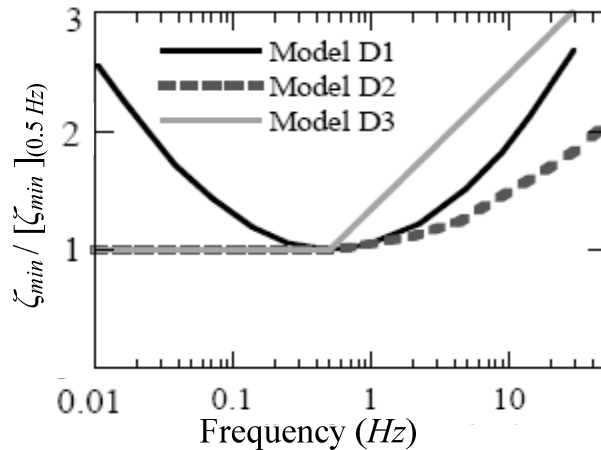
Figure 5.15: Three frequency depending damping models used in frequency dependent equivalent linear analysis of Park and Hashash (2008) and Jeong et al. (2008)

234

The above algorithm was incorporated in their equivalent linear analysis computer program DEEPSOIL. Park and Hashash (2008) and Jeong et al. (2008) carried out a parametric study using the method explained above along with three different frequency dependent damping models. These three models are represented in Figure 5.15. These frequency dependent damping models referred to as D1, D2 and D3 represent the models proposed by Rix and Meng (2005), Kim et al. (1991) and Darendeli (2001) respectively.

From their study they concluded that, when reference frequency is considered to be 0.5 *Hz*, small strain damping in all the cases of damping models considered is larger than that of frequency independent analysis. Hence, the response spectrum obtained using these damping models show decreased amplification. If the reference frequency is fixed at 25 *Hz*, small strain damping in all the cases is smaller than that of frequency independent analysis. Therefore in this case, the response spectrum obtained using strain rate dependent damping models yield increased amplification ratio. Since strain rate effect on damping is larger in case of model D3 compared to D1 and D2 models, the influence of D3 model on the response is observed to be more significant than other two models particularly in case of reference frequency of 0.5 *Hz*. However, this difference is comparatively small when reference frequency 25 *Hz*.

5.5.4   Comparison of methods of frequency dependent ground response analysis

The procedures which deal with the frequency dependent equivalent linear analysis are presented above. Among these procedures, schemes proposed by Yoshida et al. (2002) and Kausel and Assimaki (2002) have been relatively compared and assessed for their efficiency by Kwak et al. (2008). The method proposed by Yoshida et al. (2002), compared to routine equivalent linear analysis, resulted in lower peak ground acceleration at higher frequencies. Whereas, the method proposed by Kausel and Assimaki (2002) is aimed at reducing damping at high frequencies, hence it resulted in better comparison with the nonlinear analysis.

The acceleration response spectra of the predicted surface acceleration time histories for recorded and synthetic input motions are shown in Figure 5.16. In case of synthetic record, which is predominantly high frequency motion, response computed

using the procedure of Yoshida et al. (2002) is grossly overestimated particularly in the 0.01 to 0.4 seconds period range when compared to frequency independent equivalent linear analysis and nonlinear analysis. But in case Park field earthquake record, the results are similar to that of routine equivalent linear analysis. It is clear from the Figure 5.16 that, the frequency dependent analysis of Kausel and Assimaki (2002) significantly overestimates the response in both cases of input motions particularly at high frequency range.
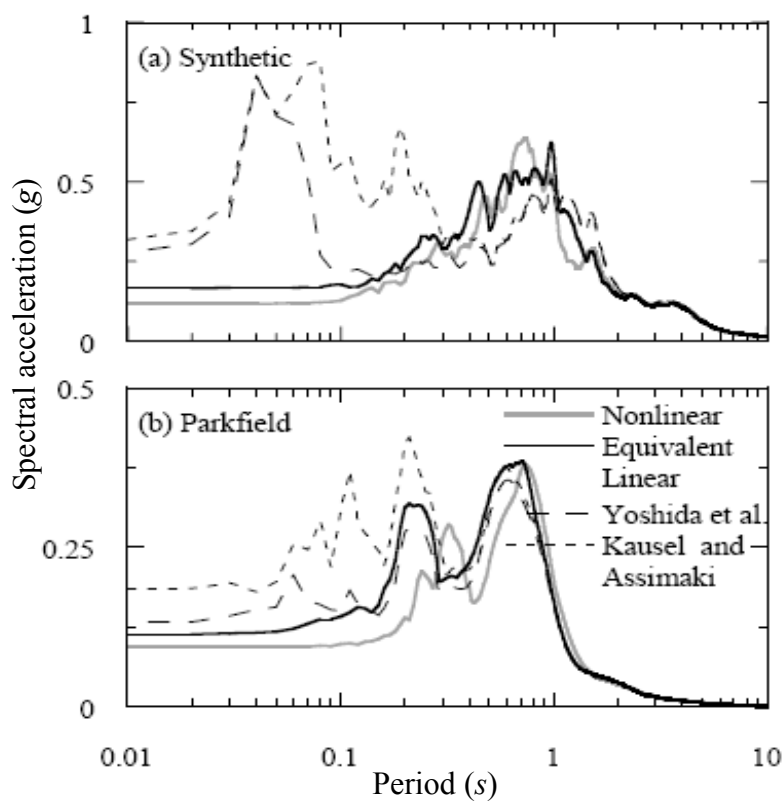
Figure 5.16: Comparison of response spectrums of computed surface motions using frequency dependent analysis procedures with that from equivalent linear and nonlinear analyses [Kwok et al. (2008)].

5.6   PROPOSED METHOD FOR FREQUENCY DEPENDENT ANALYSIS

5.6.1   Preamble to proposed model

In chapter 2, the inconsistencies associated with responses at different frequency ranges computed using routine EQL analysis are discussed. In the previous section, studies with respect to different methods proposed to overcome this intrinsic

discrepancy of EQL approach are reviewed. The literature survey about frequency dependency of soil properties indicates that the experimental data available with regard to strain rate dependent damping is scattered and obscure. Besides, other parameters required to characterize the strain rate dependency of shear modulus and damping ratio are difficult to incorporate because these parameters are yet to be well established. Hence, except Jeong et al. (2008) and Park and Hashash (2008), in all the other methods cited above frequency dependent equivalent linear analyses is formulated without giving due consideration to the effect of loading frequency on soil dynamic properties. Essentially, these methods attempted to model the response in such a way that overestimation of response in low frequency range and underestimation in high frequency range are circumvented. The procedures proposed by Jeong et al. (2008) accounts for frequency dependent characteristics of damping and shear modulus, while procedure proposed by Kausel and Assimaki (2002) is based on field observations. However, both these methods appear to be complex and needs to be provided with additional input data.

The reasons for unrealistic frequency response of EQL analysis is mainly attributed to employing constant values of shear modulus and damping throughout a particular iteration for all frequency ranges. Since the amplitudes of strain associated with low and high frequency responses are distinctly different, apparently far from actual values of G and ζ are assigned when they are obtained for single value of effective strain. Following reasons elucidate the cause for these discrepancies,

➤ The maximum acceleration response is the contribution of high frequency response hence the displacement and thus strain at these frequencies is smaller.

➤ The effective strain computed using constant R value is lower than the strains resulting from low frequency response and higher than the strain level corresponding to high frequency oscillations. Hence higher value of G and small value of ζ are assigned to compute response at low frequency range.

➤ In the high frequency range the strains are smaller than effective strain used to obtain updated soil properties from their reference curves, obviously G is underestimated and ζ is overestimated.

➢ Although, high value of G is expected to result in stiff response of low magnitudes of strain and vice versa is anticipated in high frequency range, the effect of damping in frequency response is significant to give enhanced and attenuated responses at low and high frequency ranges respectively.

Therefore, in order to obtain more realistic responses at different ranges of frequencies, the damping values must be altered pragmatically. Incorporating frequency dependent damping and shear modulus may not resolve the problem at hand because, the studies reviewed in this aspect have clearly indicated that the damping increases in the frequency region of concern. Though studies have indicated that there is significant effect of loading frequency on these properties, the database is too limited to accommodate it in routine EQL analysis. Hence, in this study an attempt has been made to evolve a semi-rational approach wherein damping values are computed and assigned as a function of frequency of excitation. The entire procedure is accommodated in the same framework of EQL analysis with few modifications.

5.6.2 Effect of damping on soil amplification characteristics

In order to bring out the effects of variation in damping and stiffness properties on the amplification response at different modal frequencies, a parametric study is carried out. A homogeneous deposit of 30 m is considered for this purpose. The shear velocity of the deposit is varied to alter the fundamental resonant frequency of the deposit. The amplification transfer function between surface and rigid base is computed using expression obtained in Chapter 2 (Eq.2.33). Figure 5.17 shows the result of this parametric study. The maximum amplification at first four modes (correspond to first four peaks of amplification transfer function) obtained for different values of damping is normalized with respect to corresponding values for undamped case. The fundamental frequencies $\left(f_{n1}\right)$ of the deposit considered are, 0.5, 1.0, 2.0, 4.0 and 10 $Hz.$ which correspond to shear wave velocities of 60, 120, 240, 480 and 1200 m/s.

From this study following conclusions can be drawn. Decrease in amplification at higher modes with increase in fundamental frequency is evident for all values of damping ratios. Also, the higher mode responses are almost insignificant for damping values of about 16% and 10% respectively for Mode-III and Mode-IV irrespective of fundamental frequency of the deposit. The rate of decrease in amplification with increase in fundamental period is dependent on mode of oscillation. The decrease is significantly higher for higher modes particularly for damping ratio less than 2%. The effect of fundamental frequency i.e., the shear wave velocity of the deposit, on amplification characteristics is dominant in relatively long period deposits compared to stiffer deposits. Also effect of stiffness becomes almost consistent after second mode without much difference in maximum amplification at higher modes. Therefore, it is evident that, the effect of damping on amplification characteristics is significant at all modes compared to effect of shear modulus.
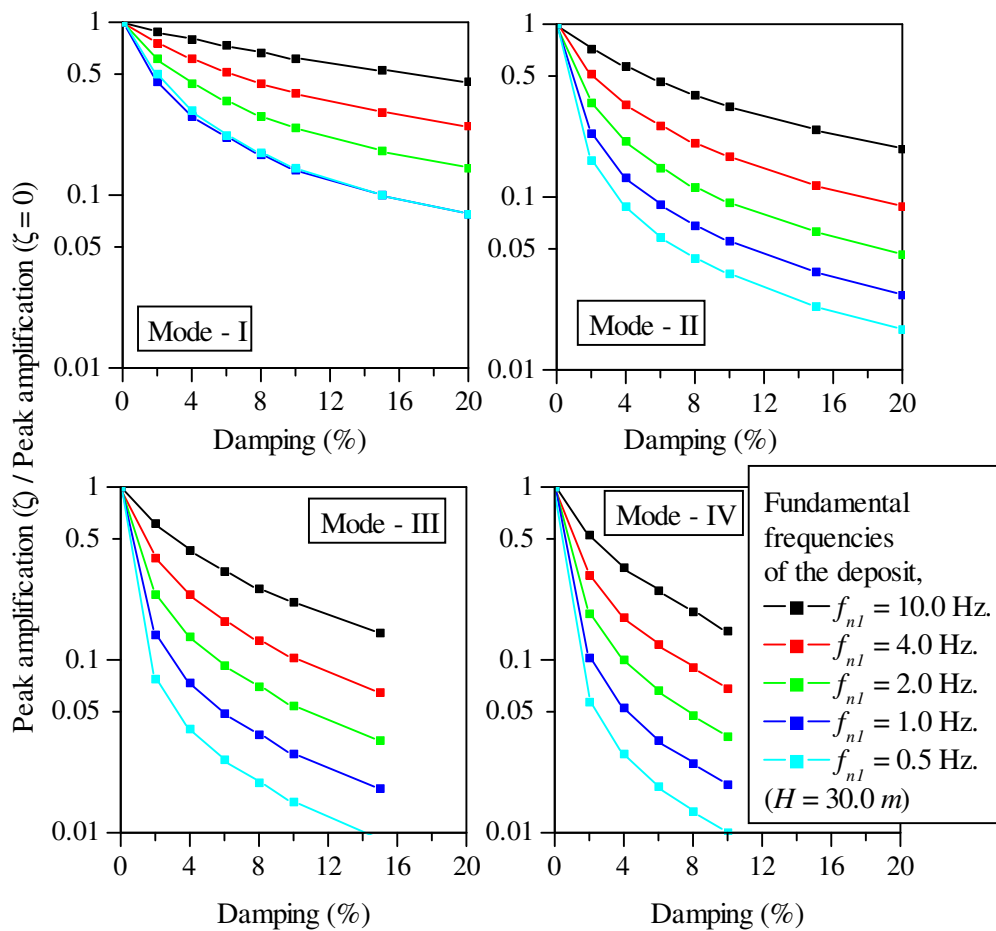
Figure 5.17: Effect of damping on maximum amplification at different modes

5.6.3 Effect of damping on spectral characteristics of the response

In view of significant effect of damping on the response at different frequency ranges, equivalent linear analysis is carried out to confirm these observations. The shear wave velocity profile shown in Figure 4.8 (Chapter 4) is considered for this purpose. The input motion used for this analysis is same as the one used in the analysis carried out to test SRISD program i.e., earthquake motion recorded at Diamond Heights during Loma-Prieta earthquake of 1989. The input motion is prescribed at the base of the deposit. In order to study the effect of damping on the predicted response, the analysis is carried out keeping damping value constant through out the analysis while degradation of shear modulus has been considered. Shear modulus degradation curve of Vucetic and Dobry (1991) recommended for PI=30% is used. As discussed in the previous chapter, this option is unique to SRISD and by opting for this provision analysis can be performed by varying either damping or shear modulus or both. Primarily this option is helpful in assessing the quantitative effect of these two properties independently.
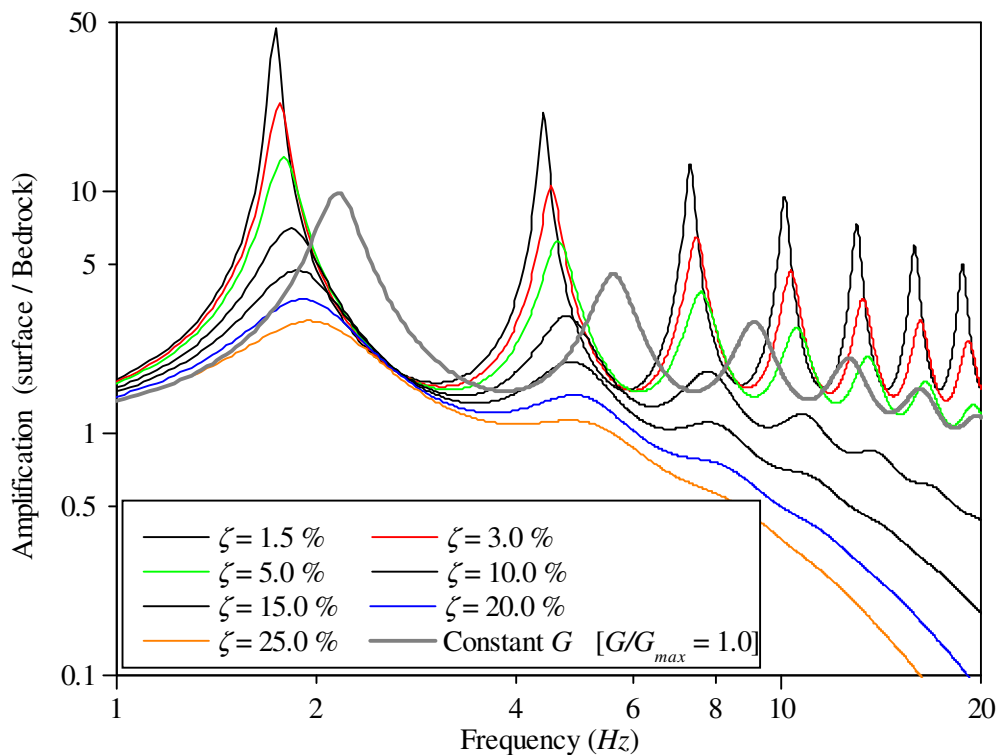
Figure 5.18: Amplification between surface and bedrock computed from EQL analysis carried out using SRISD program.
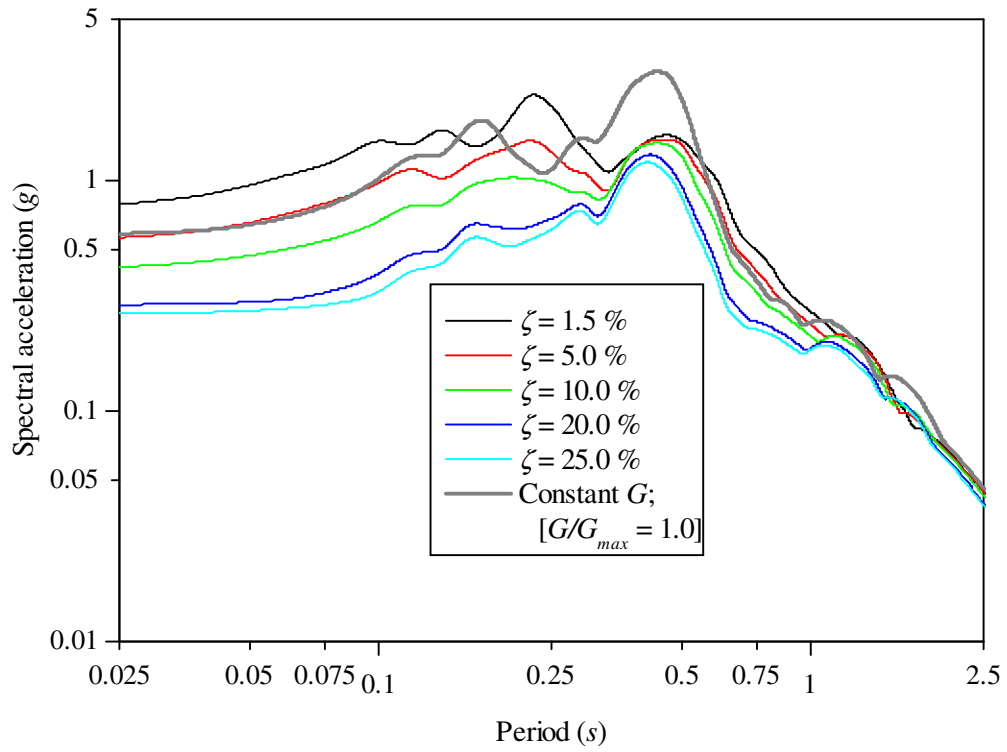
Figure 5.19: Response spectrum of surface motion computed from EQL analysis carried out using SRISD program.
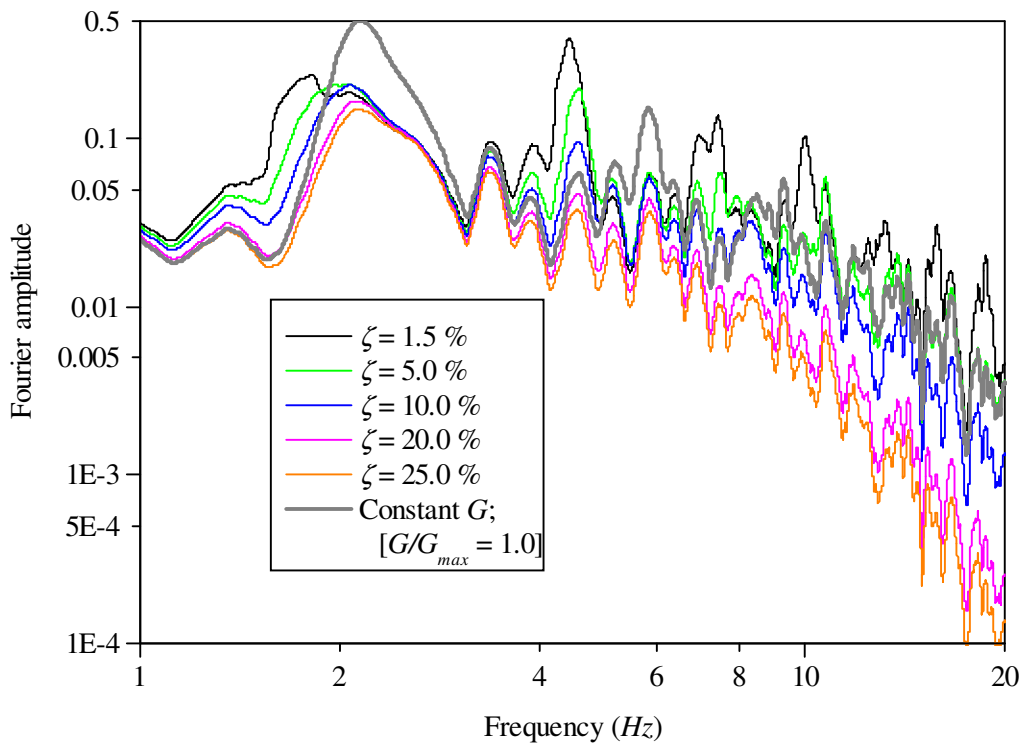
Figure 5.20: Fourier spectrum of surface motion computed from EQL analysis carried out using SRISD program.

241

The results of this analysis are represented in terms of amplification of surface motion with respect to base motion and response spectrum of predicted surface acceleration time history. The analysis is performed by varying the damping ratio from 1.5% to 25%. The amplification results of these analyses are shown in Figure 5.18, also shown is the result of the analysis in which shear modulus is maintained constant while damping is updated depending on strain level using same reference curve [Vucetic and Dobry (1991)]. Figure 5.19 and Figure 5.20 show the response spectrum for 5% damping and Fourier spectrum of the computed surface accelerograms respectively.

All the three figures clearly exhibit the effect of magnitude of damping on the responses at different frequency ranges. From amplification plot (Figure 5.18) it can be observed that, in the low frequency range the effect of damping is relatively less significant compared to its effect in the high frequency ranges. This aspect is even more obvious for higher values of damping compared to its variation in the lower range. Spectral acceleration values are almost unaffected in the low frequency (long period) range. Nevertheless, spectral accelerations (Figure 5.19) as well as Fourier amplitudes (Figure 5.20) are significantly affected at frequencies beyond first resonant frequency ($(\cong 2Hz)$. The analysis carried out ignoring degradation of shear modulus will obviously enhance the high frequency response because stiffer response will induce relatively small strain which result in assignment of low damping value. Therefore, even in this case probably damping is responsible for enhanced high frequency response.

5.6.4 Proposed method for frequency dependent equivalent linear analysis

Earlier in this chapter one of the basic issues related to computation of effective strain was addressed i.e., estimating R value which establishes relation between effective and maximum strains. However, this R value is constant throughout the iteration; consequentially the stiffness and damping properties also remain constant. In this study a new method is proposed in which directly the material damping values are updated in each of the frequency increments of the frequency domain solution

scheme. This procedure is unlike previously proposed procedures [Sugito (1994); Yoshida et al. (2002)] wherein *R*-value is modified in certain frequency ranges.

The main objective of this proposed method is to resolve the issue related to inconsistencies in the response of EQL analysis. As observed, over amplified response near the fundamental frequency of the deposit and attenuated response in higher frequency ranges are the major contradictions in the results of EQL analysis compared to observed data particularly recorded during a strong motion earthquake event. As explained in the previous sections, the probable reasons for these shortcomings are inherent to equivalent linear analysis. In order to overcome these two shortcomings of EQL analysis, development of an appropriate frequency dependent damping formulation can be considered as the remedial strategy.

The proposed method is devised to increase the damping in the vicinity of fundamental mode and decrease the damping at higher frequencies beyond certain target frequency (f_T). The strain dependent material damping used in the iterative EQL analysis procedure is an approximation to actual damping present in the soil, particularly when it is used to solve wave propagation problems. In case of damping associated with wave propagation problems, it consists of two parts; material damping and radiation or geometrical damping [Dobry (2013; 2014), Sarma (1994)]. The strain dependent damping reference curves developed from routine laboratory tests is based on the assumption that energy dissipation is only due to material damping present in the soil and completely ignores frequency dependent radiation damping. The radiation damping is a function of frequency of oscillation. When the soil layer is oscillating in the fundamental mode the contribution of radiation damping (ζ_{RAD}) can be approximated as [Roësset (1977)],

$$\zeta_{RAD}^{(1)} = \frac{2\alpha}{\pi}$$

(5.8)

Here, $\alpha(\leq 1)$ as defined in Chapter 2, is the impedance ratio between soil layer and relatively stiff underlying elastic half-space.

In order account for contribution of radiation damping in the higher modes of oscillations, Zhao (1997) proposed the relationship to estimate $\zeta_{RAD}^{(k)}$, of kth mode using that of first mode (fundamental mode), $\zeta_{RAD}^{(1)}$ as follows,

$$\zeta_{RAD}^{(k)} = \zeta_{RAD}^{(1)} \frac{f_{n1}}{f_{nk}} \tag{5.9}$$

Therefore, the total damping ζ', at the frequency corresponding to k^{th} mode, including material damping may be expressed as,

$$\zeta'\left(f^{(k)}\right) = \zeta + \zeta_{RAD}^{(k)} \tag{5.10}$$

The above expression may be used to compute damping, which results in increased damping value at the mode of vibration under consideration. It is important note that the contribution of radiation damping to total damping decreases with increase in frequency. In the higher modes of vibration its effects almost vanishes. Hence in the computer program SRISD, this equation is used to compute contribution of radiation damping beyond fundamental mode at all the frequencies including intermediate frequencies between the modal frequencies.
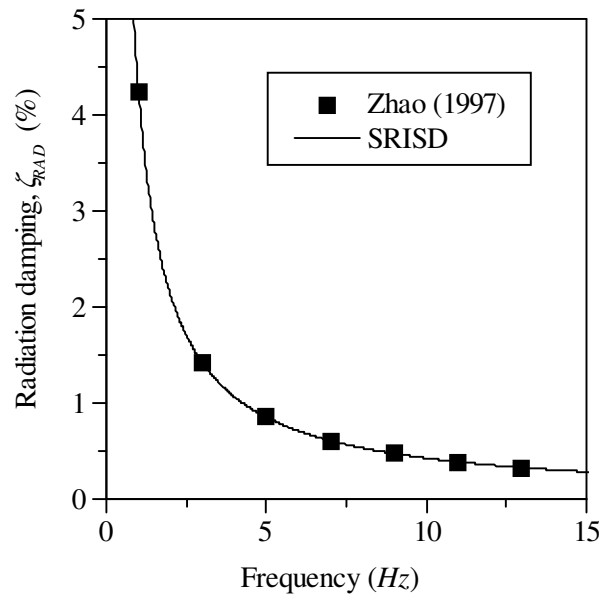
Figure 5.21: Frequency dependent radiation damping implemented in SRISD program and proposed by Zhao (1997)]

In order to illustrate the contribution of radiation damping $30m$ thick homogeneous deposit of shear wave velocity, $v_s = 120m/s$ overlying elastic bedrock of $v_{sr} = 1800m/s$ is considered. The undamped natural frequencies of the deposit are given by $f_{nk} = (2k-1)v_s/4H$ (i.e., $f_{nk} = 1,3,5.....Hz$) for the kth mode. The radiation damping corresponding to these frequencies are computed from Eq. (5.9). Also using the same expression radiation damping in the intermediate frequencies as implemented SRISD program are computed. The impedance ratio, $(\alpha = v_s/v_{sr})$ for this deposit is equal to 1/15. Figure 5.21 shows the decrease in radiation damping with increase in frequency.

In Chapter 2, the example analysis considered to compare nonlinear and EQL methods of analyses, it was noticed that the over estimation of spectral acceleration to some extent persists even in higher modes of vibration. Therefore, the target frequency (f_T) up to which the effect of radiation damping is significant may be ascertained based on the fundamental frequency of the deposit and predominant frequency range of the input motion. As stated earlier, the large value of effective strain ratio is responsible for increase in damping. For the frequencies greater than target modal frequency (f_T) the damping value needs to be reduced to increase the response. In case of viscous damping, the damping ratio is logarithmically related to harmonic amplitudes. Hence to increase the displacement amplitude in the high frequency range damping is assumed to reduce in logarithmic trend. Therefore, the reduced damping (ζ_f) at any given frequency f beyond target frequency (f_T), is calculated by reducing the material damping (ζ_{new}) obtained based on effective strain level as,

$$\zeta_f = \left(1 + \log \frac{f_T}{f}\right) \times \zeta_{new} \qquad \text{for, } f_T \leq f \qquad (5.11)$$

In the above equation, ζ_{new} obtained at end of the previous iteration is used to compute frequency dependent damping in the current iteration.
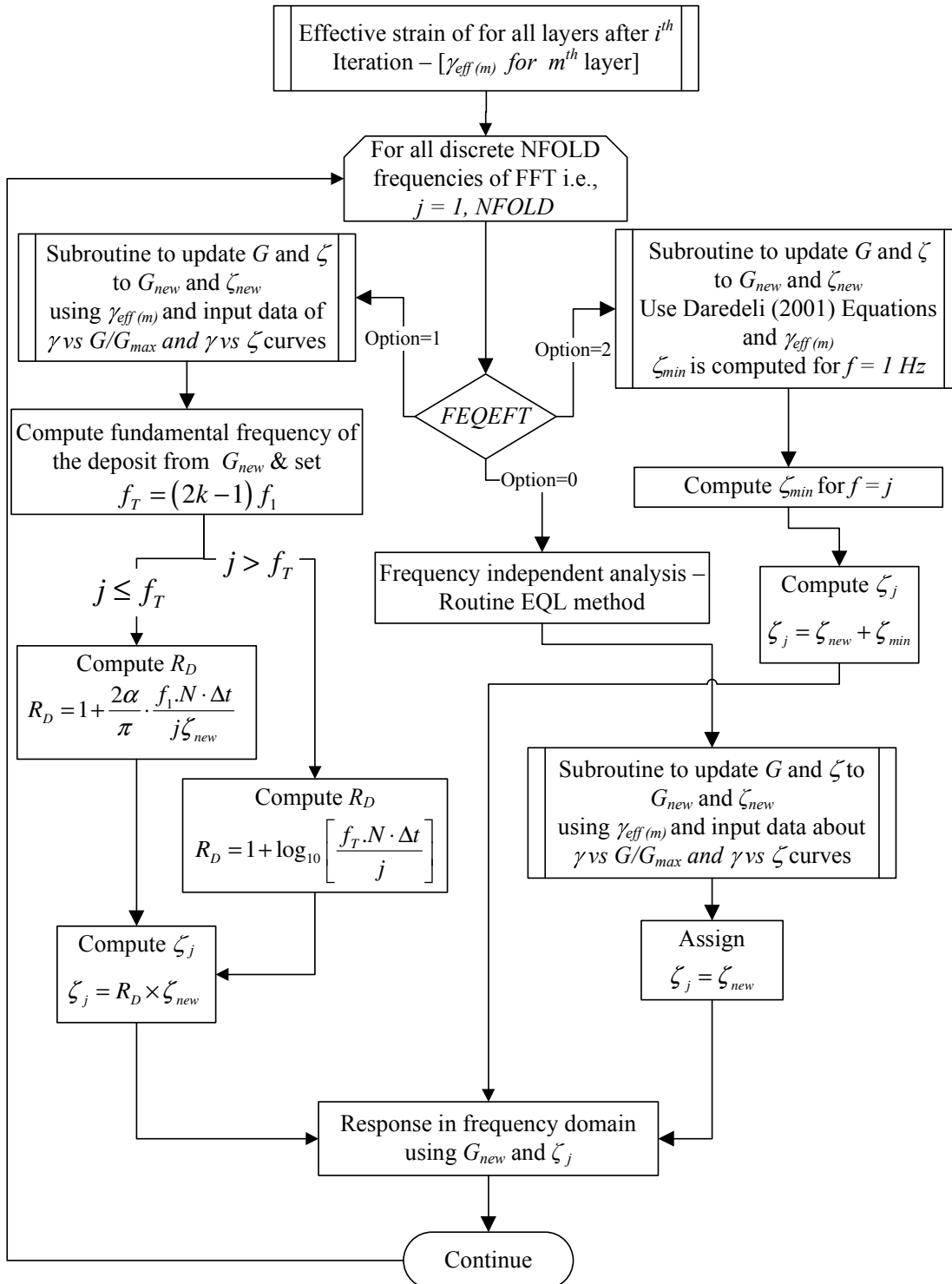
Figure 5.22: Flowchart for equivalent linear analysis with proposed frequency dependent damping formulation as implemented in the computer program SRISD

As explained earlier, for the frequencies less than target frequency (f_T) but greater than fundamental frequency (f_{n1}) the damping ratio is computed by combining Eq. (5.9) and Eq. (5.10) as,

$$\left.\begin{aligned} \zeta_f &= \left(1 + \frac{2\alpha}{\pi}\frac{f_{n1}}{f\zeta_{new}}\right)\times\zeta_{new} && \text{for, } f_{n1} \le f < f_T \\ \zeta_f &= \zeta_{new} && \text{for, } f < f_{n1} \end{aligned}\right\} \tag{5.12}$$

Figure 5.22 shows the flowchart for the proposed procedure as implemented in program SRISD to carry out equivalent linear analysis using frequency dependent damping scheme explained above.

As shown in the flowchart the impedance ratio of the deposit is calculated based on the reduced average shear wave velocity of the deposit after successive iterations. Also fundamental period of the deposit is calculated using this reduced shear modulus. Thus, impedance ratio and fundamental frequency (as well as higher mode natural frequencies) both are altered after each of the successive iterations. Therefore, the proposed method is not only modeling frequency dependent damping but also considering strain dependent stiffness degradation of the deposit in damping calculation. In any case, material damping computation based on strain dependent soil properties reference curves is also taking account of this aspect. Apart from the proposed method, as indicated in the flowchart, Darendeli (2001) expression for computing frequency dependent small strain damping is also included to choose as an option to implement along with any strain dependent damping curve.

5.6.5 Comparative study

In order to ascertain the efficacy of the proposed method a comparative study is carried out. The detail of the soil deposit and input motion considered in this comparative study is same as those considered in Section 5.6.3 (The shear wave velocity profile of Figure 4.8 and input motion is the record of Diamond Heights during Loma-Prieta earthquake of 1989). Using SRISD program the equivalent linear analysis is carried out with and without considering frequency dependent damping

option using SRISD program. The results obtained are compared with corresponding output of nonlinear time domain analysis using DEEPSOIL program.
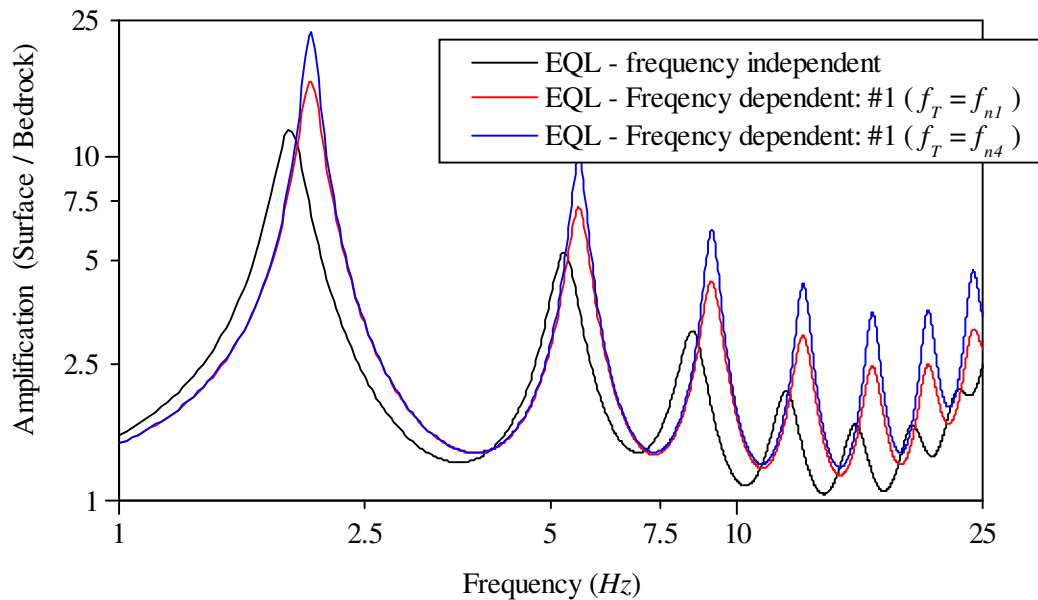
Figure 5.23: Comparison of amplification between surface and base of the soil deposit as computed from routine EQL analysis and proposed method for frequency dependent analysis. Frequency dependent analysis for two cases of target frequencies, i.e., $f_T = f_{n1}$ and $f_T = f_{n4}$ corresponding to first and fourth mode natural frequencies.
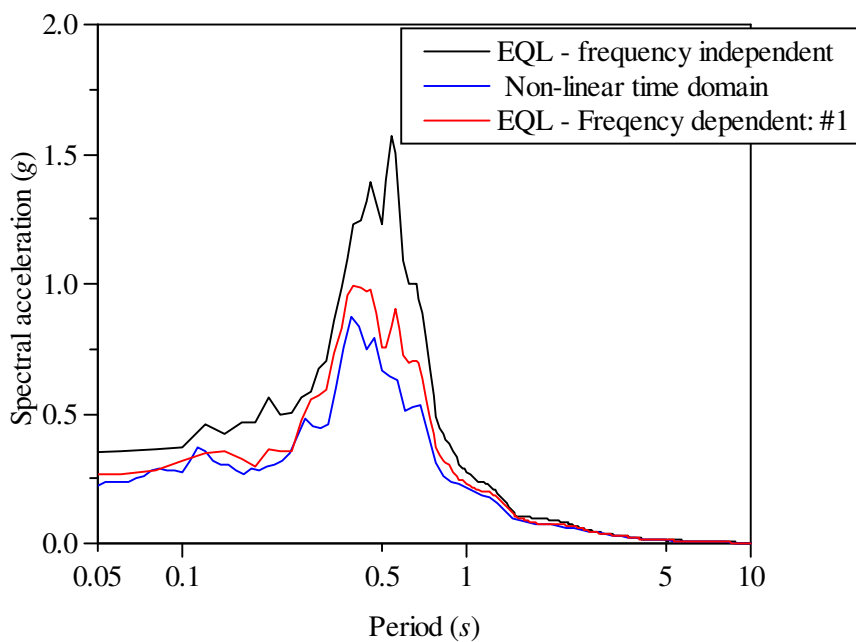
Figure 5.24: Comparison of response spectra of the estimated surface motions from routine EQL analysis, frequency dependent EQL analysis $(f_T = f_{n4})$ and time domain nonlinear analysis.

Figure 5.23 compares the results of amplification ratios between surface and base of the soil deposit obtained from routine EQL analysis and frequency dependent analysis. For frequency dependent analysis two cases of target frequencies are considered; one corresponding to first natural frequency and the other corresponding to fourth mode natural frequency. Below these frequencies radiation damping contribution resulting from contrasting impedances of soil and bedrock is added to effective strain dependent material damping. The peaks of the amplification ratio are higher for frequency dependent analysis than those from routine analysis.
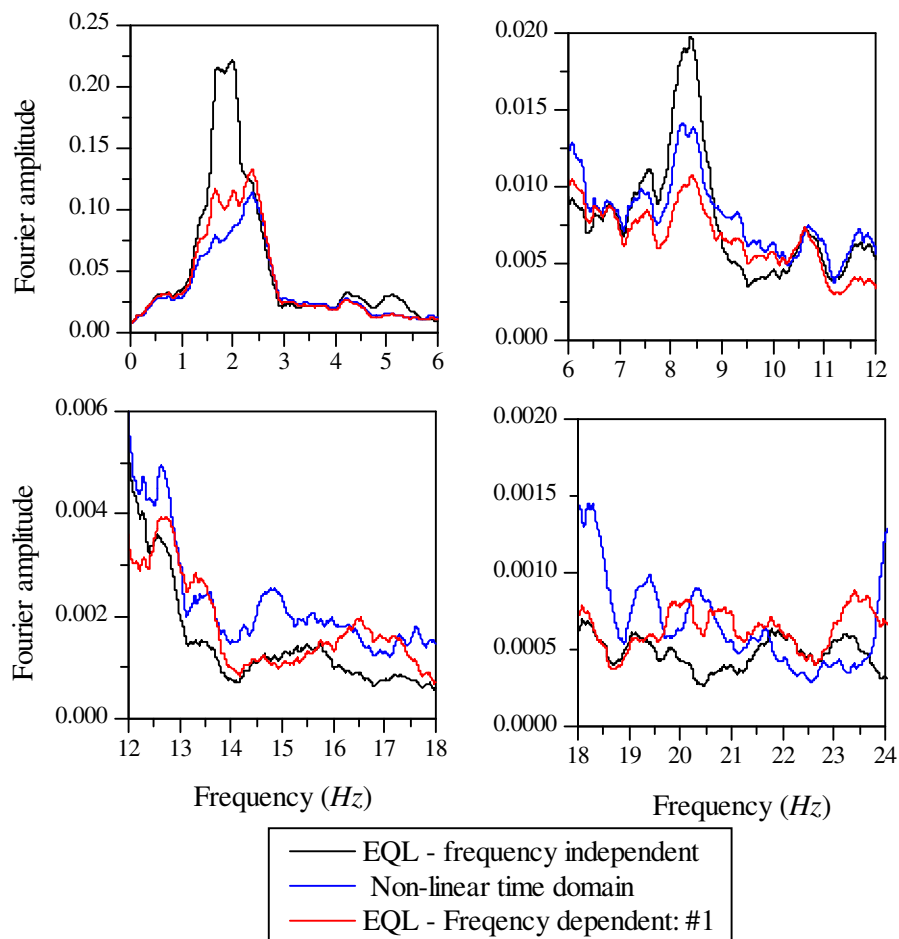
Figure 5.25: Comparison of Fourier spectra of the estimated surface motions from routine EQL analysis, frequency dependent EQL analysis and time domain nonlinear analysis.

Figure 5.24 compares the pseudo spectral acceleration of computed surface motion from routine EQL analysis, frequency dependent EQL analysis and nonlinear time domain analysis. Evidently, the effect of introducing frequency dependent radiation

damping in the EQL analysis has yielded improved resonant response which is abnormally overestimated in the routine EQL analysis when compared to true nonlinear analysis in time domain. Also frequency dependent analysis shows improvement in estimation of low period (high frequency) response that is as good as time domain analysis. Frequency dependent analysis results presented here are obtained by setting the target frequency to fourth mode natural frequency. However, it was noticed that the effect of target frequency on the computed results is almost negligible beyond fourth mode natural frequency which is approximately equal to 15 *Hz* in the first iteration.

In Figure 5.25 the comparison is made with respect to Fourier spectra of the surface motion. For the purpose of clarity the Fourier spectrum is plotted in separate frequency windows. Up to 12 *Hz* frequency dependent EQL analysis compares favorably with time domain analysis relative to routine EQL analysis. However beyond 12 *Hz* the spectrum of frequency dependent analysis matches very well at certain frequencies but deviates significantly in 14 to 19 *Hz* range. It is important note that the target frequency f_T of frequency dependent EQL analysis is reduced to less than 12 *Hz* after eight iterations due to degradation in shear modulus. However, overall performance of the proposed method of EQL analysis based on frequency dependent damping model is satisfactory particularly with respect to its ability in simulating the response at resonant frequency when compared to routine equivalent linear analysis.

5.7   CASE STUDY – TKCH08

5.7.1   Details of TKCH08 Geotechnical array

In order to verify and validate the efficiency of the proposed refinements to equivalent linear method of analysis a case study is presented. Also, the suitability of idealizing the soil deposit with continuous variation of shear wave velocity is investigated. The case study is concerned with evaluation of site response estimated by means of proposed alternative methods with respect to routine method of analysis and comparing with observed field data. For this purpose data pertaining to a geotechnical

array site of Kiban-Kyoshin network (KiK-net) is selected. The TKCH08 downhole array site of KiK-net in Hokkaido of Japan recorded the magnitude 8.0 Tokachi-Oki earthquake of 26th September, 2003. The geotechnical data provided at KiK-net as well as additional information available in Kaklamanos et al. (2011) are used for further interpretation. The details of the TKCH08 downhole array site and of the earthquake considered are given in Table 5.2. The soil deposit consist of 78 *m* deep quaternary sandy gravel deposit of average shear wave velocity of top 30 *m* equal to $v_{s(30m)} = 353.0 m/s$ overlying sandstone bedrock of shear wave velocity 2800 *m/s*.

Table 5.2: Details of TKCH08 site; Geotechnical and Earthquake data used in the case study

Geotechnical data				Earthquake data	
Location	Taiki (Hokkaido Prfecture – Japan)			Event name	Tokachi-Oki
Site code	TKCH08			Date	26th September, 2003
Latitude	42.49N			Magnitude	8.0
Longitude	143.15E			Latitude	4.78N
Instrumentation Depths	0.0 *m* and 100 *m*			Longitude	144.08E
Soil deposit	78 *m* Quaternary sandy gravel (*Q*)overlying Cretaceous sandstone bedrock (*K*)			Epicentral distance	109.44 *km*
Average shear wave velocity	$v_{s(30m)} = 353.0 m/s$ Kaklamanos (2012)			Focal depth	42.0 *km*
Shear wave velocity profile $v_{s(78m,ave)} = 521.28 m/s$ $v_{p(78m,ave)} = 1770.52 m/s$	Depth (*m*) [Density (*t/m³*)]	v_s (*m/s*)	v_p (*m/s*)	$a_{max}(EW)$ - surface	0.5094*g*
	0 – 4 [$\rho = 1.93$]	130	300		
	4 – 36 [$\rho = 2.0$]	480	1850	$a_{max}(NS)$ - surface	0.4241*g*
	36 – 78 [$\rho = 2.0$]	590	1850	$a_{max}(EW)$ - 100*m*	0.130*g*
	78 – 100 [$\rho = 2.6$]	2800	5000	$a_{max}(NS)$ - 100*m*	0.1056*g*

5.7.2   Shear wave velocity profile

The shear wave velocity for the site taken from KiK-net web site is shown in Figure 5.26. Kaklamanos et al. (2011) have reported the shear wave velocity profiles obtained using SASW survey at the sites located adjacent to TKCH08 site. The shear wave velocity profiles these adjacent sites, along with TKCH08 data are shown in Figure 5.26.
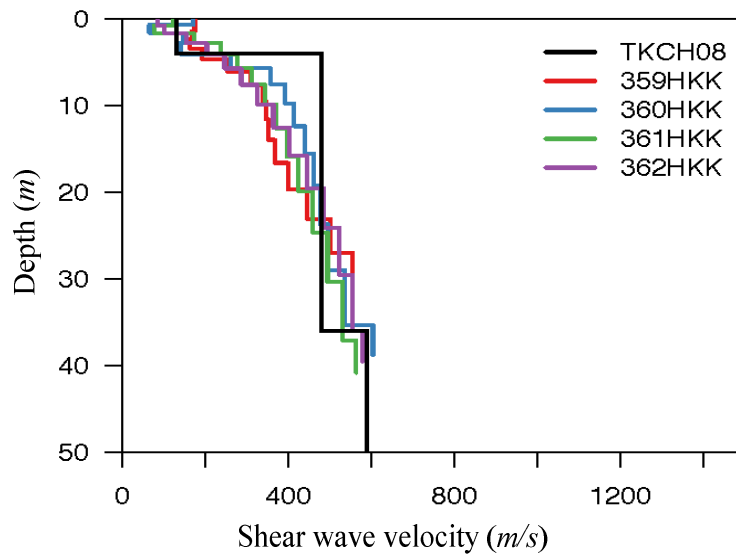
Figure 5.26: Shear wave velocity profiles interpreted from SASW survey adjacent to TKCH08 site [Kaklamanos et al. (2011)]

As can be observed from these shear wave velocity profiles of deposit in the vicinity of TKCH08 site, the profile shows gradually varying trend up to about 40 *m* depth and approaches a constant value of 590 *m/s* beyond 40 *m* and remains constant up to 78 *m*. The bedrock of shear wave velocity 2800 *m/s* is encountered at 78 *m*. Based on these profiles a best fit continuously distributed proxy shear wave velocity profile is obtained as an alternative to TKCH08 layered idealization. For this purpose exponential function is considered to obtain best fit rather than power law functions because in which case the velocity increases with depth instead of converging to constant value as required in the present case. For such situations, wherein the rigidity of the soil attains constant value at larger depth, Vrettos (2013) has recommended an inhomogeneity function of the form $G(z) = G_0 + (G_\infty - G_0)e^{-mz}$ where G_∞ is defining the rigidity at infinite depth. Using the above mentioned exponential form of equation,

that is, $v_s(z) = v_{s0} + (v_{s\infty} - v_{s0})e^{-mz}$, curve fitting parameter $(m = 0.0826)$ is obtained for best fit to represent the variation of shear wave velocity for TKCH08 site. For the soil deposit under consideration v_{s0} and $v_{s\infty}$ are set to 130 *m/s* and 590 *m/s* respectively. Therefore continuous function of shear wave velocity profile which approximates the layered profile is given by $v_s(z) = 560 - 460e^{-0.0826z}$. The layered profile and its approximate continuous profile are shown in Figure 5.27.
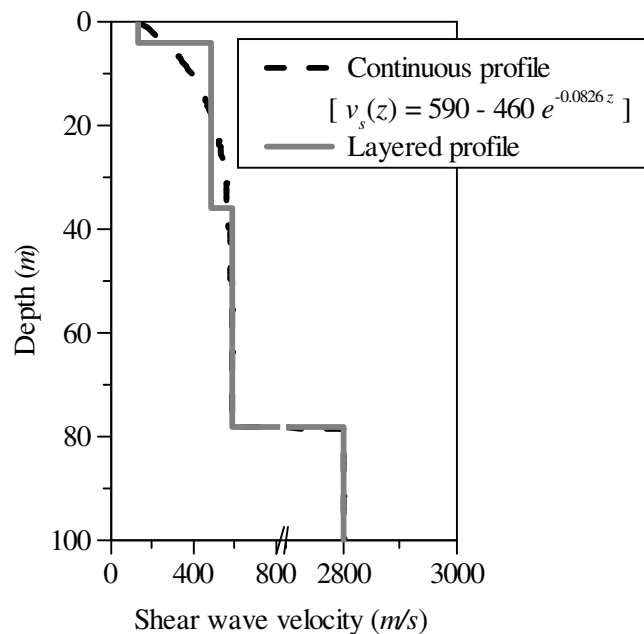
Figure 5.27: Layered shear wave velocity profile (KiK-net) and its approximated continuous profile idealisation.

5.7.3 Earthquake data

The records of Tokachi-Oki earthquake considered in this case study consist of NS and EW horizontal components of the event recorded at the surface and at depth of 100 *m* of the soil deposit. These accelerograms are shown in Figure 5.28. Pseudo acceleration response spectra (5% damping) of these accelerograms are shown in Figure 5.29. The downhole records at 100*m* depth are used as input motions to predict surface response from SRISD program. The peak accelerations corresponding to input motions are 0.13*g* and 0.1056*g* respectively for EW and NS horizontal components. The predominant periods of EW and NS components of input motions as obtained from SeismoSignal-V4.0 (SEISMOSOFT) are 0.16*s* and 0.24*s* respectively. The EW

components of the earthquake show an additional peak at around 4 *s* period compared to NS component. Apart from this observation both the horizontal components of the earthquake exhibit almost similar spectral characteristics. The acceleration time histories computed at the surface (0.0 *m*) using different options of SRISD program are compared with that of recorded data.
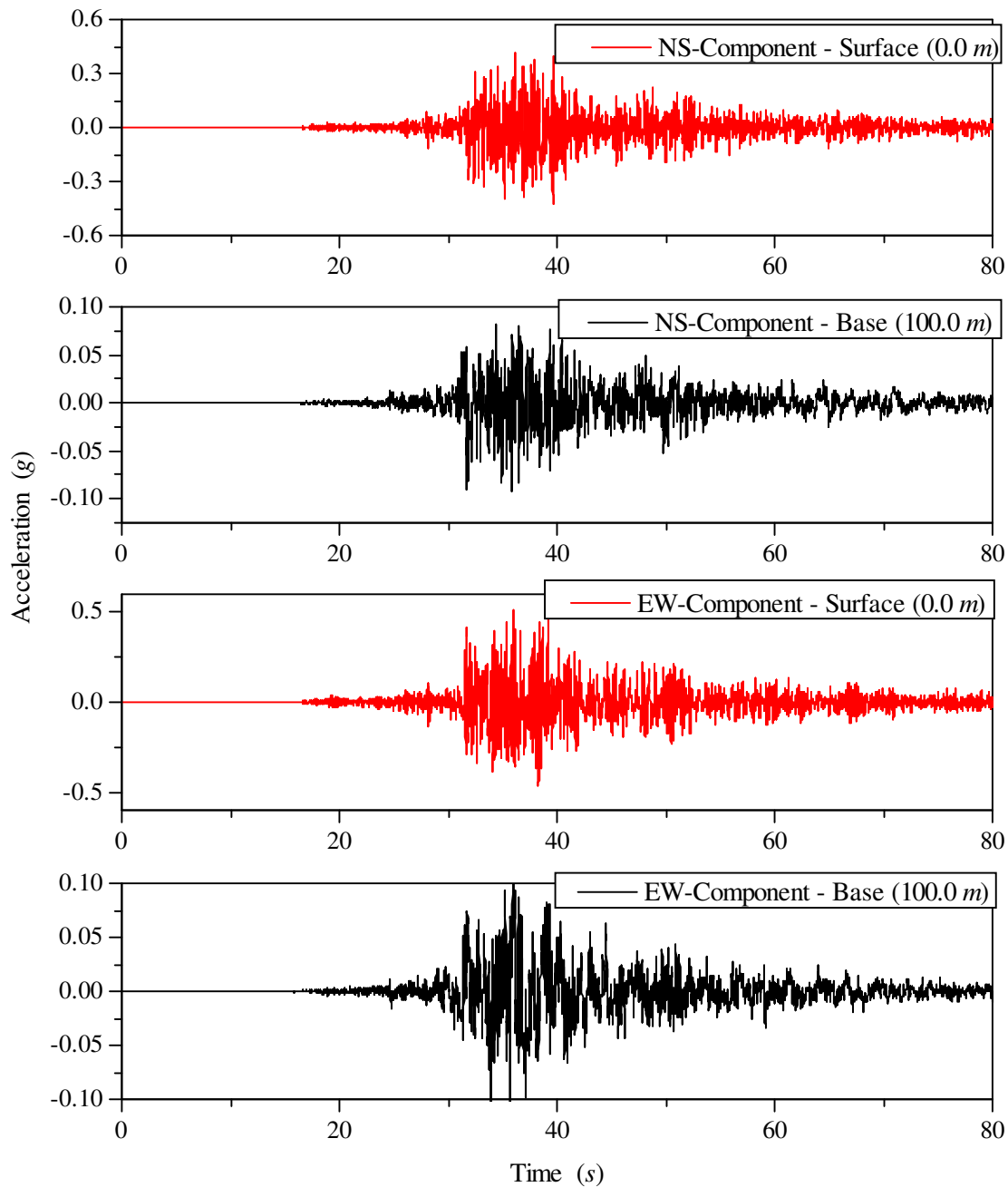
Figure 5.28: Horizontal components of accelerograms recorded at base and surface of the soil deposit of TKCH08 site during 2003 Tokachi-Oki earthquake.
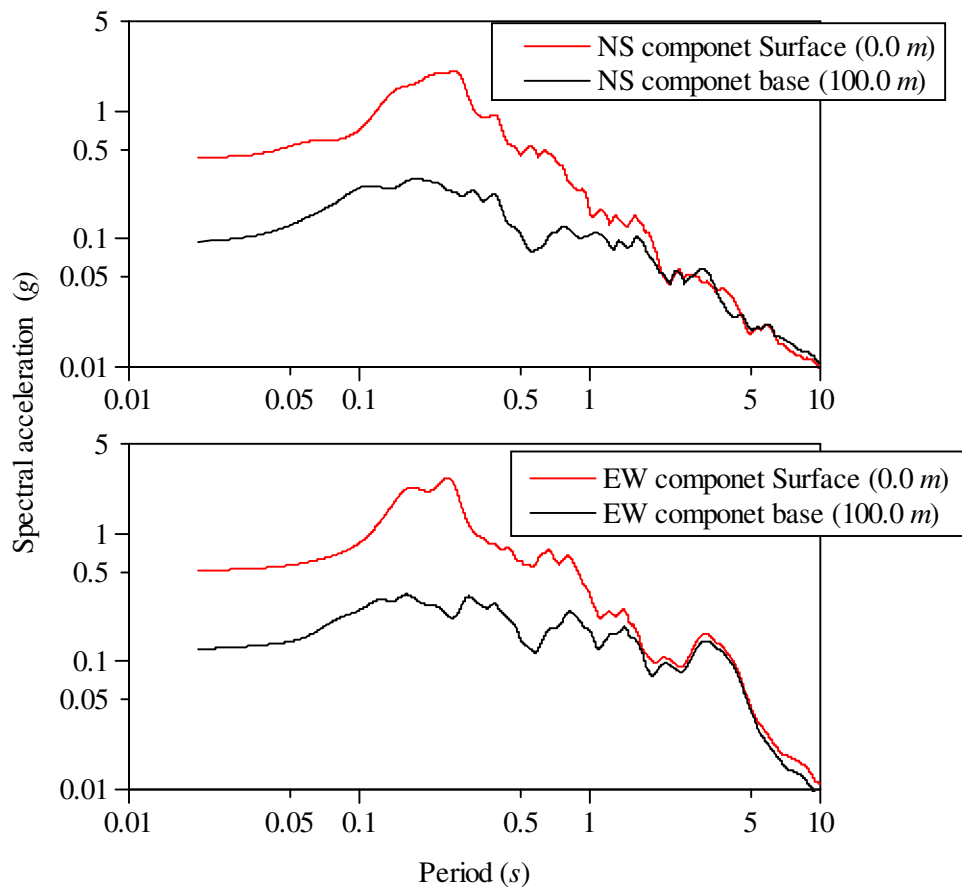
Figure 5.29: Response spectrum of the horizontal components of accelerograms recorded at base and surface of the soil deposit of TKCH08 site during 2003 Tokachi-Oki earthquake.

5.7.4 Different options considered for the case study

The analyses using the program SRISD are carried out with the following options,

➢ Analysis of layered profile by employing routine option to compute effective strain, which is based on magnitude of the earthquake of the input motion as suggested in SHAKE program

➢ Analysis of layered profile by incorporating proposed method for computation of effective strain, which is based on maximum acceleration obtained after successive iteration at every node in the soil profile

➢ Analysis using shear wave velocity profile idealized as continuously varying along the depth with effective strain in consecutive iterations being computed using proposed method

> ➢ All the above analyses are carried out with and without proposed frequency dependent EQL analysis.

Considering the bore-log information of TKCH08 soil deposit provided in KiK-net website, the strain dependent shear modulus and damping curves proposed by Zhang et al. (2005) are used to model nonlinear response of the soil deposit. The details of this model and the equations are presented in Chapter 4. In this model the strain dependent stiffness and damping properties are defined as function of mean confining pressure, OCR, geological age and plasticity index of the soil. Mean effective confining stress (σ'_m) is calculated at required depth from the computed vertical effective stress (σ'_z) as,

$$\sigma'_m = \sigma'_z \left(\frac{1 + 2K_0}{3} \right) \tag{5.13}$$

Here coefficient of lateral pressure at rest (K_0) is obtained from the following equation,

$$K_0 = \frac{v}{1 - v} \tag{5.14}$$

Poisson's ratio, v is calculated using longitudinal and transverse wave velocity (v_p and v_s) profile data of the soil deposit,

$$v = \frac{v_p^2 - 2v_s^2}{2 \left(v_p^2 - v_s^2 \right)} \tag{5.15}$$

For the purpose of calculating Poisson's ratio average values computed from the available TKCH08 site velocity profile data is used. The average values of v_p and v_s calculated for top 78 m of the soil deposit are $v_p = 1770.52 m / s$ and $v_s = 521.28 m / s$ respectively as shown in Table 5.1. Using these values in Eq. (5.15) the Poisson's ratio is obtained as $v = 0.45$, therefore from Eq. (5.14) K_0 is calculated as 0.82. For all the analyses carried out here $K_0 = 0.80$ is used to compute mean confining stress at desired depths using the EFFSTS subroutine of SRISD program.

5.7.5 Validation of proposed method for effective strain computation

SRISD analyses are carried out for two options of effective strain computation independently. Firstly using the R-value based on magnitude of input earthquake motion as suggested in SHAKE which is incorporated in most of the site response analysis programs. The other option provided in SRISD is the newly proposed method based on intensity of shaking as detailed in earlier section of this chapter. Results of these two separate analyses are compared to assess the reliability of the proposed method. In the traditional method based on magnitude of the input earthquake motion the constant R-value used in the analysis is 0.7 for $M = 8$. While for the proposed method R-value need not be assigned because the program itself will assign appropriate R-value depending on intensity of shaking characterised by resulting maximum acceleration in the previous iteration. That is R-value is calculated using Eq. (5.1a and 5.1b) and updated for each of the successive iterations at every node (or layer) of the soil deposit. The comparison of results are made with respect to amplification between surface and base motions, acceleration time histories at the surface, variation of maximum acceleration along the depth and response spectra obtained for the surface acceleration time histories. The analysis is carried out for both, EW and NS components of horizontal motions recorded at TKCH08 site (Figure 5.28). The layered configuration shown in Figure 5.26 is used to model shear wave velocity profile of the soil deposit in both the cases of analyses.

Figure 5.30 conceptually shows the difference in the analysis procedures as a consequence of employing routine and proposed methods for computation of R-value and subsequently used to obtain effective strain after successive iterations. In the routine method the value of R remains constant while it is altered after the completion of particular iteration all along the depth of the soil deposit in case of proposed method. For the purpose of illustration only the variation in R-value that is used for 2nd and final (11th) iterations are shown in the figure. Thus it can be concluded that the R-value used in both the cases are distinctly different. Hence it is interesting to compare the responses that are computed using these two distinctly different methods.
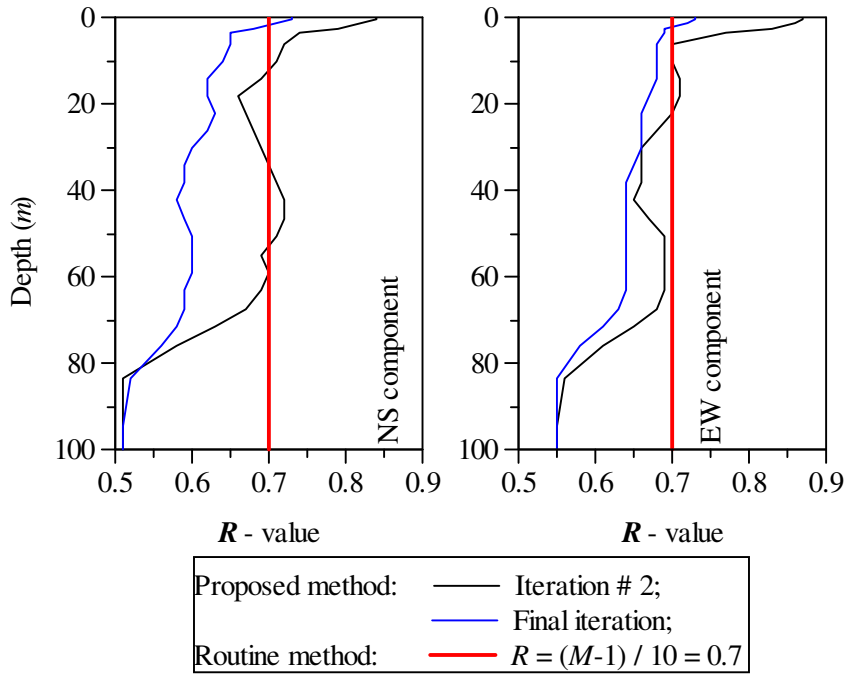
Figure 5.30: Variation of *R* – value along the depth used for calculation of effective strain in each of the successive iterations of EQL analysis
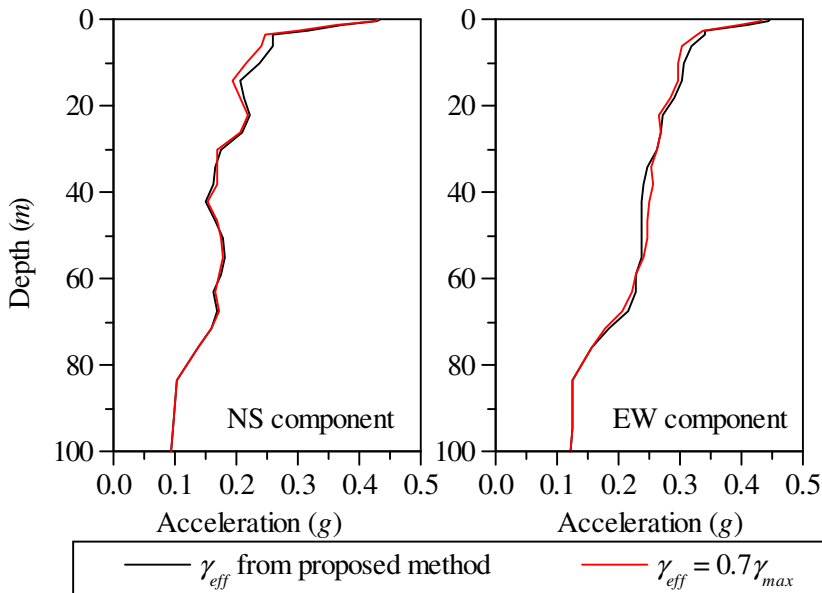
Figure 5.31: Computed variation of maximum acceleration along the depth of the soil deposit using proposed method and routine method for calculation of effective strain in successive iterations of EQL analysis (SRISD)
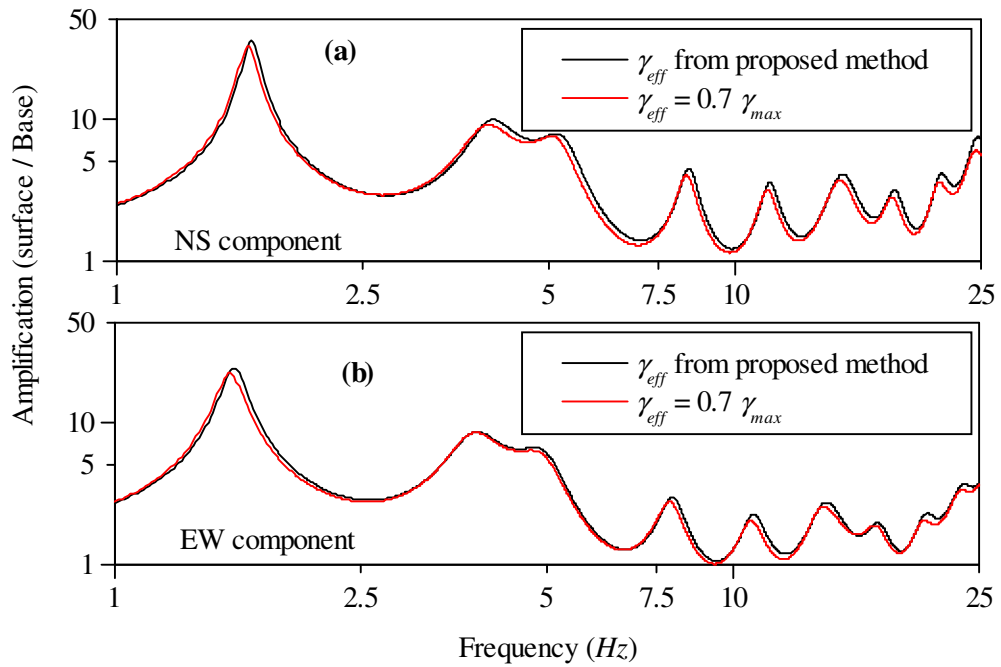
Figure 5.32: Amplification of surface motion with respect to base motion computed using routine and proposed methods for calculation of effective strain in each of the successive iterations of EQL analysis (SRISD) – (a) NS component (b) EW component
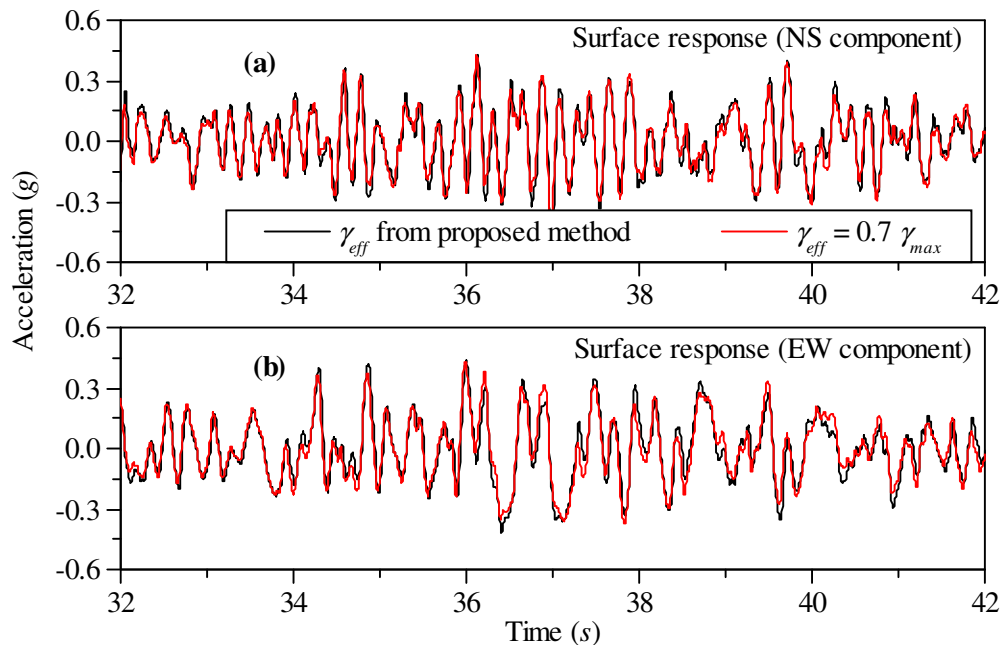
Figure 5.33: Acceleration time histories at the surface of the soil deposit computed using routine and proposed methods for calculation of effective strain in each of the successive iterations of EQL analysis (SRISD) – (a) NS component (b) EW component
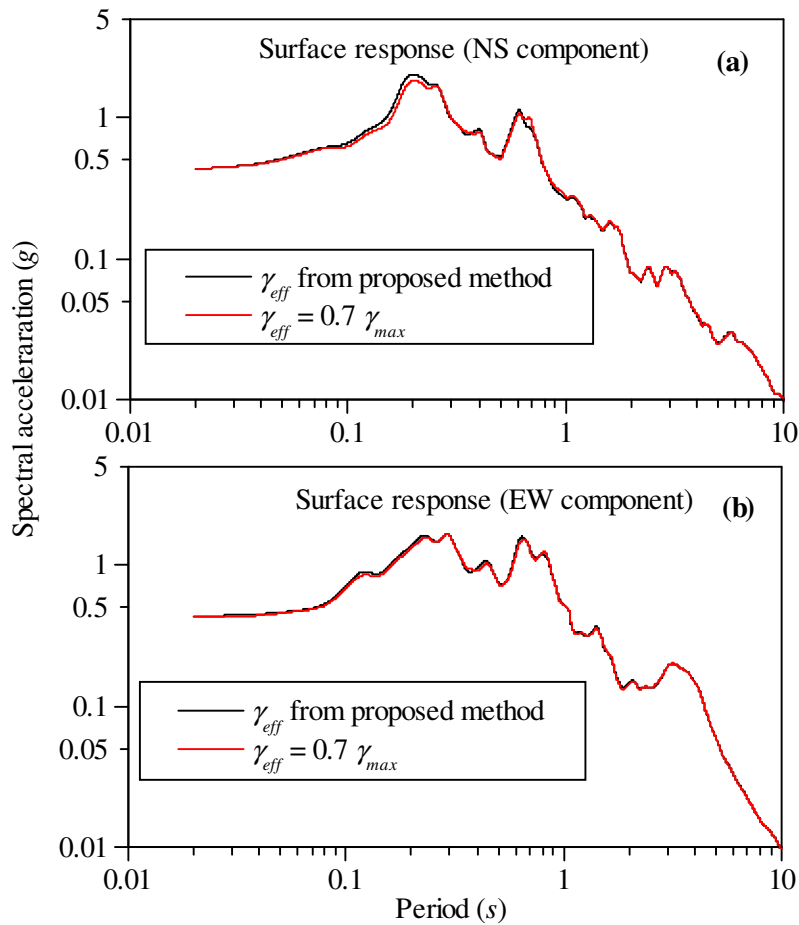
Figure 5.34: Response spectra of predicted acceleration time histories at the surface of the soil deposit using routine and proposed method for calculation of effective strain in each of the successive iterations of EQL analysis (SRISD) – (a) NS component (b) EW component

Figure 5.31 compares variation of maximum acceleration response computed along the depth of the soil deposit from these two methods. Amplification ratio between surface and base of the deposit as obtained from these two options are compared in Figure 5.32. The surface acceleration time histories and their corresponding response spectra are compared in Figures 5.33 and 5.34 respectively. From all these figures it can be concluded that, despite conceptually different methods are used to compute effective strains after each iteration, the converged strain magnitude after their final iterations is same. All the response quantities used in the comparative study establishes that the proposed method is capable of reproducing the results that are obtained from routine method of analysis.

5.7.6 Comparison of results of layered and continuous shear wave velocity profile idealizations – Frequency independent EQL analysis (SRISD)

Apart from proposing an unambiguous procedure to compute effective strain during iterative process of EQL approach, the other main objective addressed in this research study is concerned with overcoming the ambiguities associated with idealizing the soil deposit as layered profile. For this purpose, the variation in shear wave velocity profile data is approximated as continuously inhomogeneous profile. Here the results of the comparative analysis performed using frequency independent EQL analysis are presented. Primarily the study presented here focuses on evaluation of idealizing the deposit with continuous variation of shear wave velocity against layered profile idealisation without opting for frequency dependent EQL analysis. As it was shown in the previous section, that the proposed and routine methods of computation of effective strain will result in almost identical response, the proposed method for computation of effective strain is opted to update soil properties in the successive iterations of EQL analysis.

The layered and approximated continuous shear wave velocity profiles considered to model the soil deposit are shown in Figure 5.28. Soil deposit is discretised into 24 layers such that the natural frequency of the layers is within 20 *Hz.* The continuous approximation of layered shear wave velocity profile significantly decreases the contrasting impedance $(1/\alpha = 3.7)$ between $4m$ deep near surface layer of shear wave velocity, $v_s = 130m/s$ and 32 m deep underlying layer of $v_s = 480m/s$.

The comparison of results obtained for layered and continuous shear wave velocity profile data is made with respect to amplification ratio between surface motion and base input motion, surface acceleration time histories and their corresponding Fourier spectra and response spectra. All the results presented for the case of layered profile is same as that obtained in the comparative study made in the previous section pertaining to analysis carried out with effective strain computed using the method proposed in this research study. Figure 5.35 compares the amplification ratio for both cases of horizontal components of input motions. The peaks corresponding to first

two modes of the amplification transfer functions obtained for both the idealizations of shear wave velocity profiles are more or less same. For the higher modes up to about fifth mode continuous profile shows marginally higher peaks than that for layered profile. Further layered profile exhibits significant increase in the amplification while that obtained for continuous profile gradually decreases. Most importantly, the troughs of the amplification ratio are lifted upwards for the case of continuous profile compared to that of layered profile. This aspect signifies the effect of relatively rigid bedrock on the response of the surface deposit which is poorly reflected in case of layered shear wave velocity profile. All the observations compiled here are valid for the cases of horizontal earthquake components. Beyond 20 *Hz* frequency, the layered profile exhibits poor simulation demonstrating degradation of soil stiffness to such an extent wherein the depth of the layer is large enough to trap high frequency waves leading to building up of wave amplitudes.
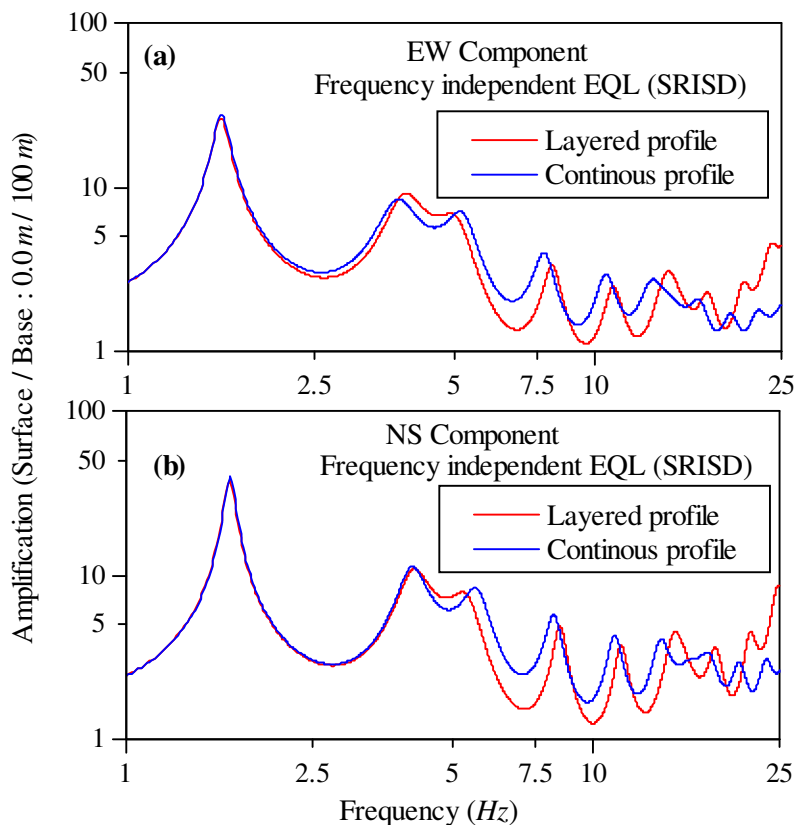
Figure 5.35: Comparison of computed amplification ratio between surface and base motions for the cases of layered and continuous shear wave velocity profiles of TKCH08 site using frequency independent EQL analysis (SRISD). (a) EW component; (b) NS component

262
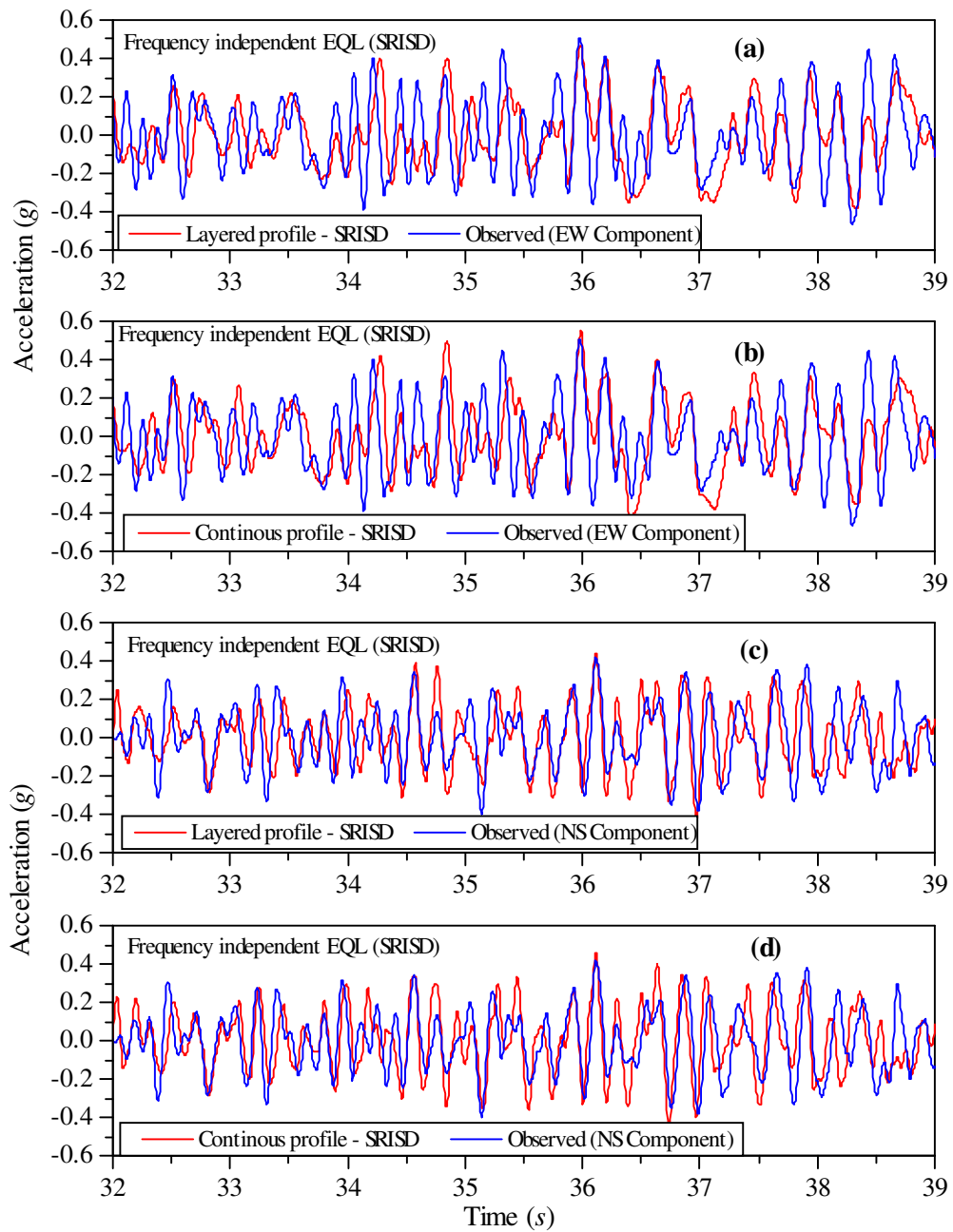
Figure 5.36: Comparison of computed acceleration time history response for the cases of layered and continuous shear wave velocity profiles of TKCH08 site using frequency independent EQL analysis (SRISD) with observed surface motion during 2003 Tokachi-Oki earthquake; (a) Layered profile EW component; (b) Continuous profile EW component; (c) Layered profile NS component and (d) Continuous profile NS component.
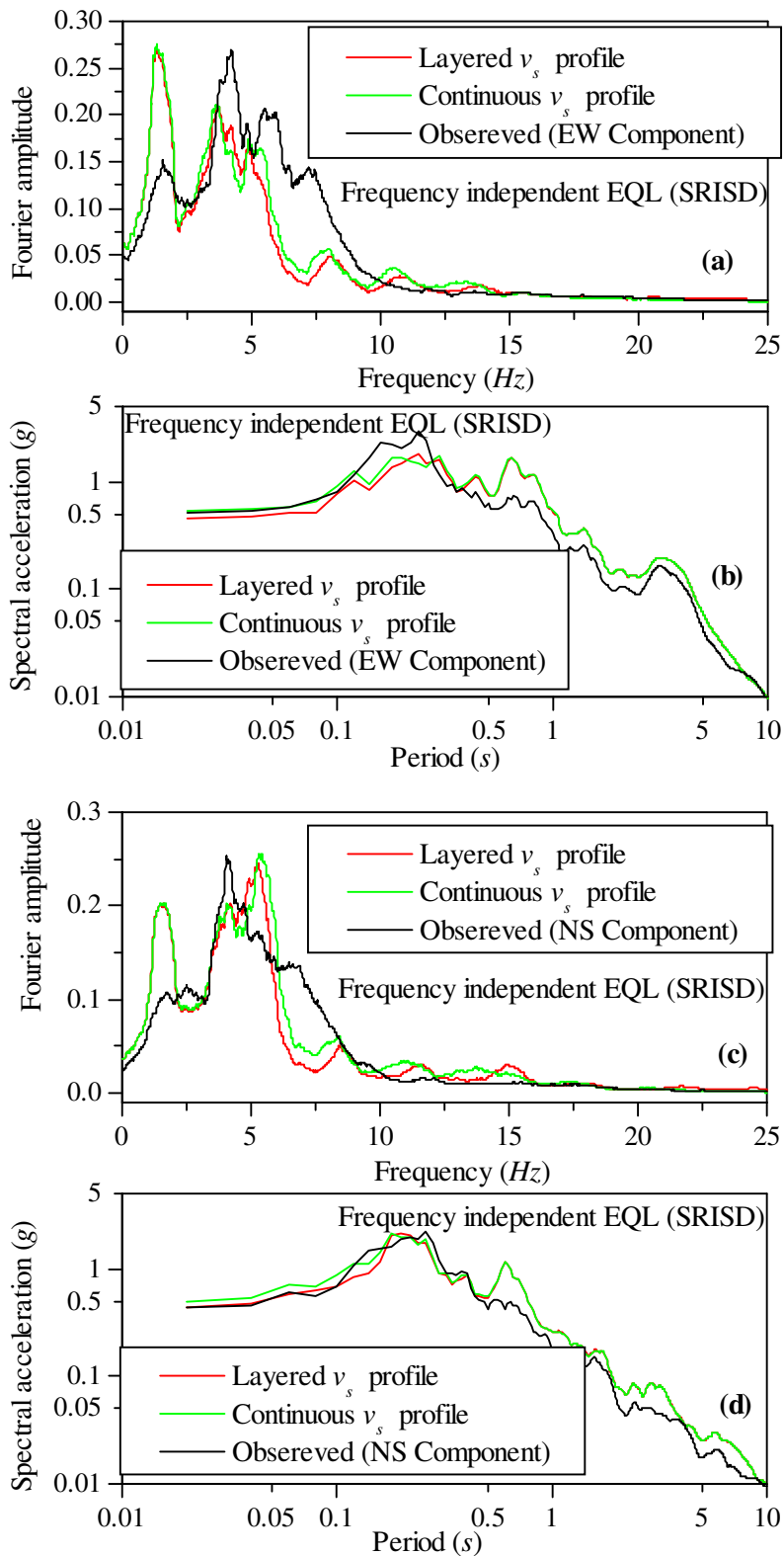
Figure 5.37: Comparison of Fourier spectra and response spectra of the computed acceleration time histories at the surface of the deposit (Figure 5.36); (a and b) EW component; (c and d) NS component

Figures 5.36a and 5.36b compare the surface acceleration time histories corresponding to EW component obtained for layered and continuous idealizations of shear wave velocity profiles respectively, while Figures 5.36c and 5.36d compare those of NW component responses. For the purpose of clarity the time window is selected to represent strong motion region in the neighborhood of maximum acceleration. It can be observed that the peak acceleration response is satisfactorily estimated in both the cases of layered and continuous shear wave velocity profile idealizations. However, continuous idealization has been able to show overall better agreement with the observed record compared to layered deposit though the difference is negligible.

In order to assess relative efficiency of these two idealizations the Fourier amplitude spectra and response spectra of the predicted surface accelerograms corresponding to these two cases are compared. Figures 5.37a and 5.37b respectively present these results for EW component while Figures 5.37c and 5.37d for NS component input motions respectively. The frequency content of the response obtained for continuous shear wave velocity profile has marginally enhanced concurrence with that of observed motion compared to response obtained for layered profile. Nevertheless, the response obtained for both these cases have shown poor agreement with the observed record particularly in the vicinity of lower resonant frequencies. For both EW and NS components the response is overestimated in the frequency range less than about 2 *Hz*. This observation is evident in response spectrum representation also. In the 4 *Hz* to 10 *Hz* frequency range the response is underestimated in case of EW component response. In this range of frequencies the predicted response for the NS component has distinctly different characteristics. Though the response spectra of NS component responses have shown good agreement with that of corresponding recorded motion in the high frequency range (low period), the differences in the Fourier amplitudes in this frequency range is evident. However, it can be noted that overall trend of the response predicted by employing continuous shear wave velocity profile is comparatively better than that corresponding to response obtained using layered profile. The overestimation and underestimation of response respectively at low and high frequency ranges are in accordance with the observations made in the Chapter 2.

5.7.7 Comparison of results of layered and continuous shear wave velocity profile idealizations – Frequency dependent EQL analysis (SRISD)

In order to improve the observed discrepancies with respect to predicted responses for the cases considered in the previous section, proposed frequency dependent EQL analysis is carried out. The proposed method described in Section-5.6.4 and implemented in the program SRISD is opted with all the other data being same. The target frequency required for this analysis is fixed based on the observations made in the frequency independent EQL analysis carried out in the previous section. For the cases of EW and NS component input motions target frequency f_T, up to which additional geometrical damping is to be considered, is set to $2f_1$ and $3f_1$ respectively where f_1 is the fundamental frequency of the deposit.
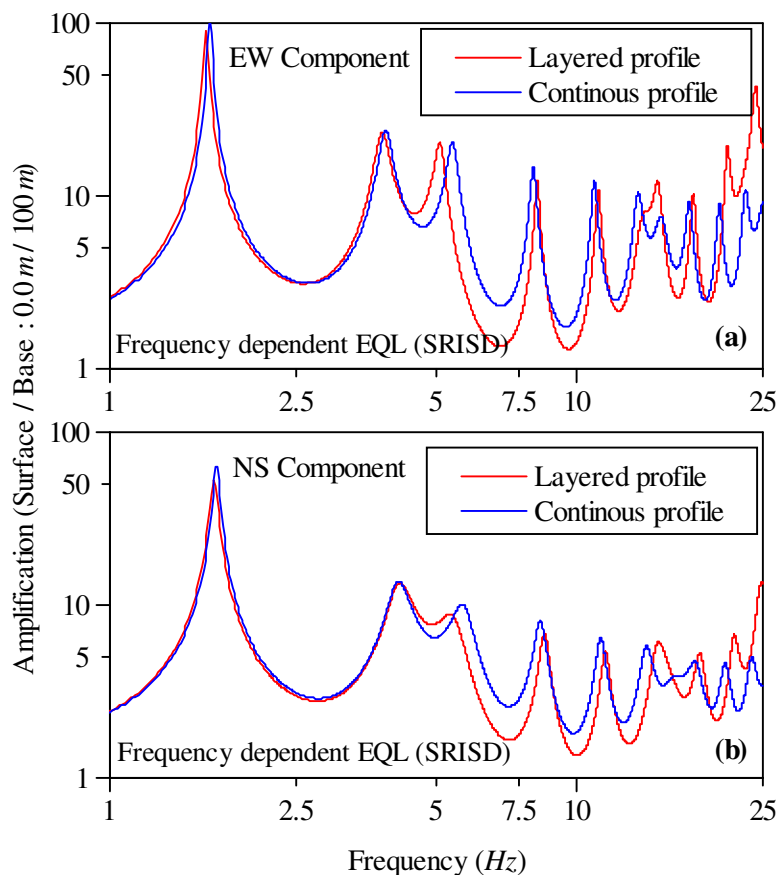
Figure 5.38: Comparison of computed amplification ratio between surface and base motions for the cases of layered and continuous shear wave velocity profiles of TKCH08 site using frequency dependent EQL analysis (SRISD); (a) EW component; (b) NS component

In the proposed method for frequency dependent EQL analysis, the fundamental frequency of the deposit is updated after successive iterations based on updated average shear modulus of the soil deposit. Thus both f_1 and therefore f_T are updated for subsequent iteration.
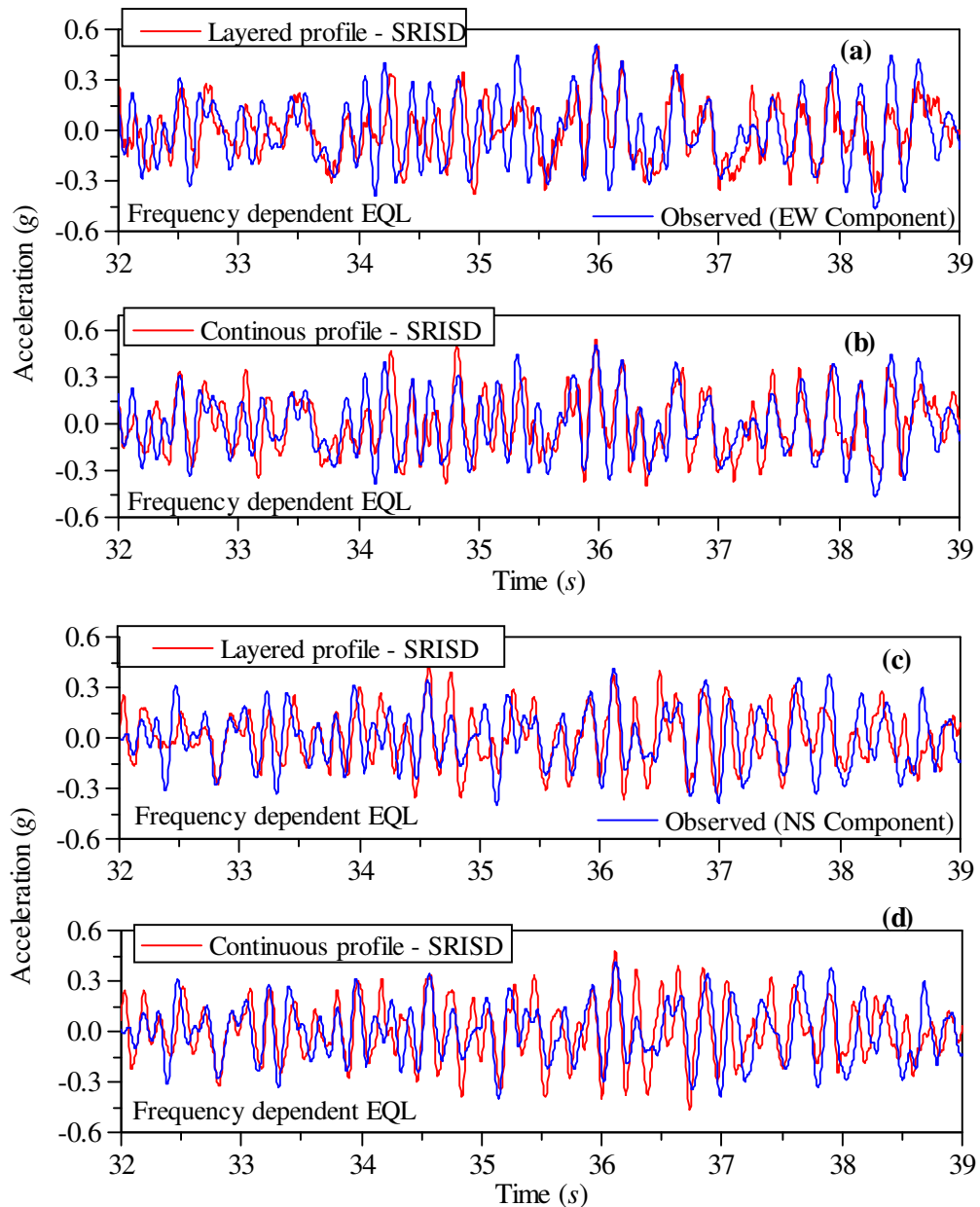
Figure 5.39: Comparison of computed acceleration time history responses for the cases of layered and continuous shear wave velocity profiles of TKCH08 site using frequency dependent EQL analysis (SRISD) with observed surface motion during 2003 Tokachi-Oki earthquake. (a) Layered profile EW component; (b) Continuous profile EW component; (c) Layered profile NS component; and (d) Continuous profile NS component
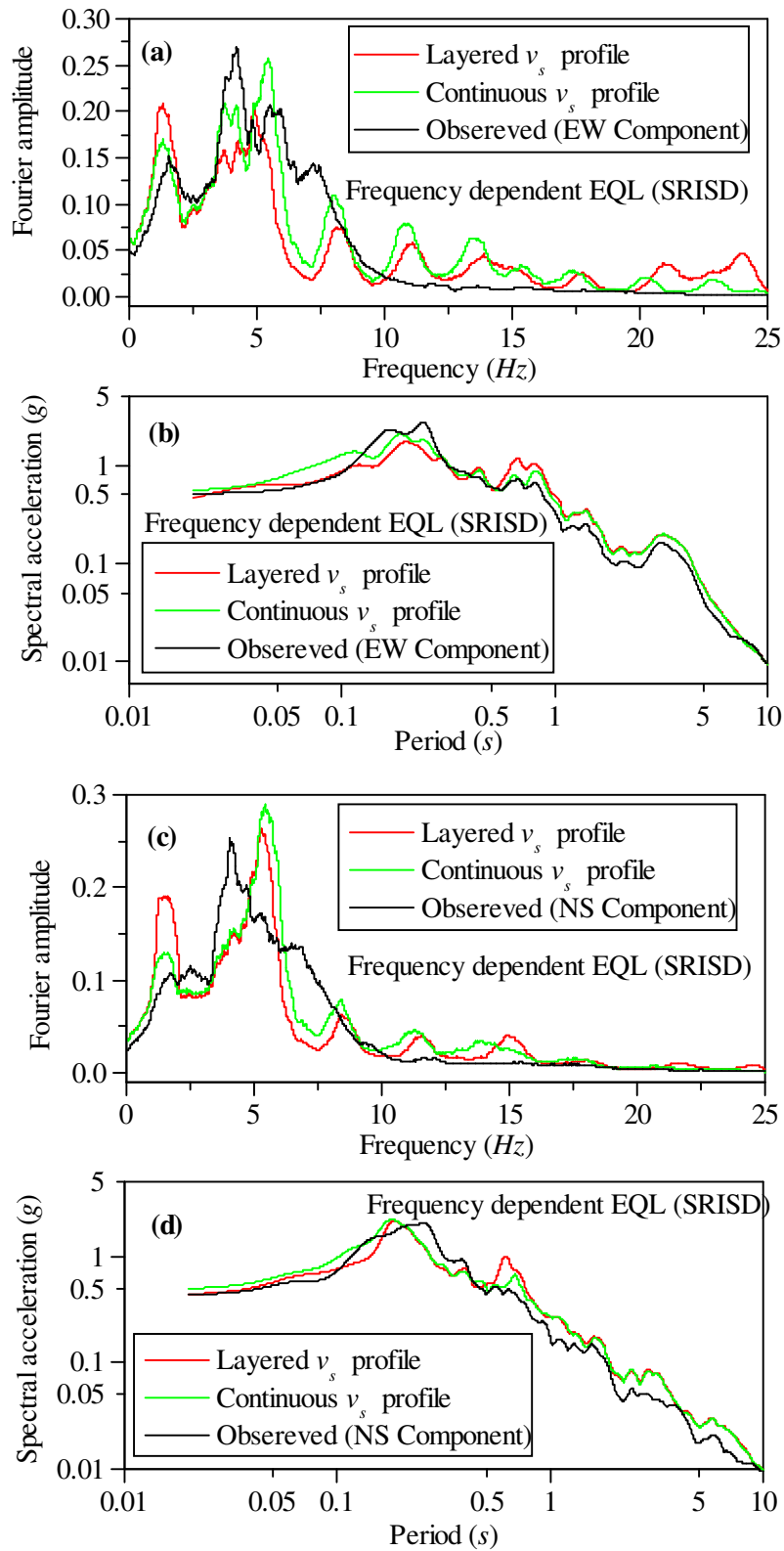
Figure 5.40: Comparison of Fourier spectra and response spectra of the computed acceleration time histories at the surface of the deposit (Figure 5.39); (a and b) EW component; (c and d) NS component

Figures 5.38a and 5.38b present the amplification ratio between computed surface motion and input base motion respectively for EW and NS components of the input earthquake motion. Compared to frequency independent analysis there is increase in maximum amplification in all the modes. Also, the maximum values obtained for layered and continuous profile closely agrees with each other though there is noticeable difference in corresponding modal frequencies.

Acceleration time histories of the predicted surface responses corresponding to EW component motion are presented in Figures 5.39a, and 5.39b respectively for layered and continuous idealization of shear wave velocity profile, while that of NS component are presented in Figures 5.39c and 5.39d. Relative comparison of responses obtained for layered and continuous idealizations can be clearly seen in the Figures 5.40. Figures 5.40a and 5.40c present the Fourier spectra of the predicted surface accelerogram of EW and NS component motions respectively for layered and continuous shear wave velocity profile cases. In both the cases the improvement in predicted motions is evident compared to frequency independent EQL analysis results presented in the previous section. Also analysis carried out for the case of shear wave velocity profile idealized with continuous variation has resulted in comparatively better agreement with the measured data than the results obtained for the case of layered idealization.

5.7.8   Results and discussion

In this section the results obtained for the case study presented above is analysed statistically. In order to ascertain the efficiency of the proposed refinements of this research study relative to routine analysis procedure three statistical parameters are used to obtain goodness of fit between predicted and observed data. Though customarily the peak accelerations of the predicted and observed responses are compared in most of the cases to asses the efficiency of the prediction, it may not be complete evaluation of the predicted response in view of complex nature of variation in acceleration time history and its frequency components. To overcome this inadequacy, Kaklamanos et al. (2011) suggested following statistical measures for the purpose of quantitative validation.

> *Pearson's correlation coefficient*:

The goodness of fit is quantified using the correlation coefficient r, given by

$$r = \frac{\sum_{i=1}^{n}(O_i - \bar{O})(P_i - \bar{P})}{\sqrt{\sum_{i=1}^{n}(O_i - \bar{O})^2 \sum_{i=1}^{n}(P_i - \bar{P})^2}}$$ (5.16)

Here, O_i and P_i respectively represent observed and predicted response quantities at the ith instant, while $\bar{O}$ and $\bar{P}$ represent corresponding arithmetic mean values.

> *Efficiency coefficient*:

Nash-Sutcliffe model efficiency coefficient E, is given by

$$E = 1 - \frac{\sum_{i=1}^{n}(O_i - P_i)^2}{\sum_{i=1}^{n}(O_i - \bar{O})^2}$$ (5.17)

This method, commonly used in the analysis of hydrological data, is explained in Legates and McCabe (1999). Higher the efficiency coefficient implies better agreement between predicted (P_i) and observed (O_i) responses. This assessment is considered to be superior because E is sensitive to differences in means and variances of observed and predicted responses [Legates and McCabe (1999)].

> *Root mean square error*:

The root mean square of the error $RMS_{(error)}$ in predicted values with respect to observed values is expressed as

$$RMS_{(error)} = \sqrt{\frac{1}{n}\sum_{i=1}^{n}(O_i - P_i)^2}$$ (5.18)

The units (g) of the acceleration response is retained in $RMS_{(error)}$

Using all the above three statistical parameters, the responses computed from different analyses cases are evaluated with respect to observed acceleration data. For the acceleration time histories shown in Figures 5.36 and 5.39, Pearson's correlation coefficient, efficiency coefficient and root mean square error are computed and

tabulated in Table 5.3. Also these coefficients for the respective response spectra are tabulated in Table 5.4.

Table 5.3: Results of the statistical analyses for goodness-of fit of the acceleration response at the surface computed from SRISD with respect to observed record

Type of analysis	Shear wave velocity profile	Statistical parameters	Earthquake component considered for the analysis	
			NS component	EW component
Frequency independent EQL analysis (SRISD)	Layered profile	r	0.623	0.594
		E	0.453	0.466
		$RMS_{(error)}$	0.050	0.059
	Continuous profile	r	0.629	0.588
		E	0.426	0.438
		$RMS_{(error)}$	0.052	0.058
Frequency dependent EQL analysis (SRISD)	Layered profile	r	0.578	0.585
		E	0.403	0.491
		$RMS_{(error)}$	0.053	0.056
	Continuous profile	r	0.637	0.643
		E	0.472	0.512
		$RMS_{(error)}$	0.050	0.055

Table 5.4: Results of the statistical analyses for goodness-of fit of the response spectra of computed surface response with respect to that of observed record

Type of analysis	Shear wave velocity profile	Statistical parameters	Earthquake component considered for the analysis	
			NS component	EW component
Frequency independent EQL analysis (SRISD)	Layered profile	r	0.948	0.868
		E	0.888	0.724
		$RMS_{(error)}$	0.016	0.030
	Continuous profile	r	0.956	0.866
		E	0.900	0.705
		$RMS_{(error)}$	0.015	0.031
Frequency dependent EQL analysis (SRISD)	Layered profile	r	0.928	0.902
		E	0.859	0.808
		$RMS_{(error)}$	0.018	0.025
	Continuous profile	r	0.950	0.955
		E	0.900	0.906
		$RMS_{(error)}$	0.015	0.017

NS - Component

EW - Component

Legend:
- Layered profile - Frequency independent analysis
- Continuous profile - Frequency independent analysis
- Layered profile - Frequency dependent analysis
- Continuous profile - Frequency dependent analysis
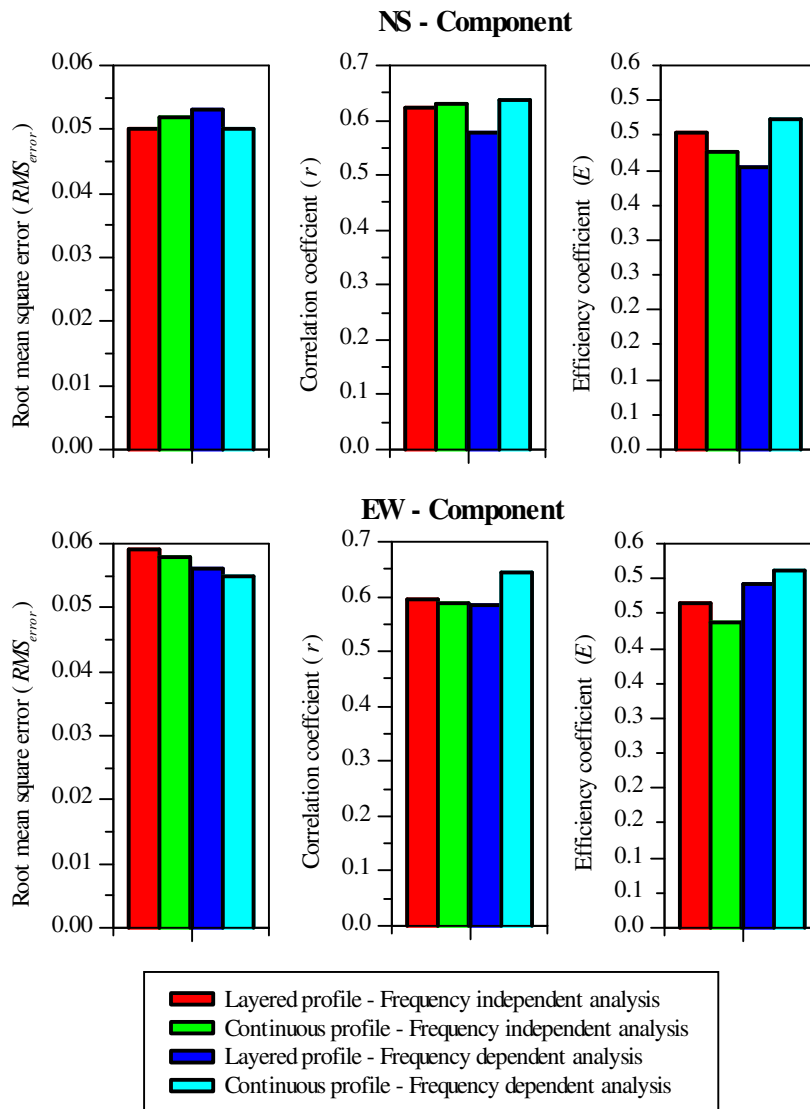
Figure 5.41: Comparison of goodness-fit parameters obtained for computed acceleration responses at the surface of the TKCH08 soil deposit with different cases of analysis. NS – component (top row) and EW – component (bottom row)

The statistical quantities representing goodness-of-fit of computed responses with respect to observed response tabulated in Table 5.3 are presented with separate bar charts for each of the different cases of analyses in Figure 5.41. The error associated with predicted response is quantified by RMS_{error} and is observed to be least for the response computed using frequency dependent analysis with soil deposit is modeled by means of continuous shear wave velocity profile, while, same kind of analysis carried out with layered shear wave velocity profile under NS-component input motion has resulted in response with relatively large RMS_{error} value compared to

results of other analysis cases. In fact RMS_{error} associated with EW and NS horizontal components of earthquake input motions show different trends particularly with respect to frequency dependent analysis of layered deposit. On the other hand, RMS_{error} associated with EW-component motion is least for the frequency dependent analysis compared to frequency independent analysis and for continuous soil profile compared to layered profile.
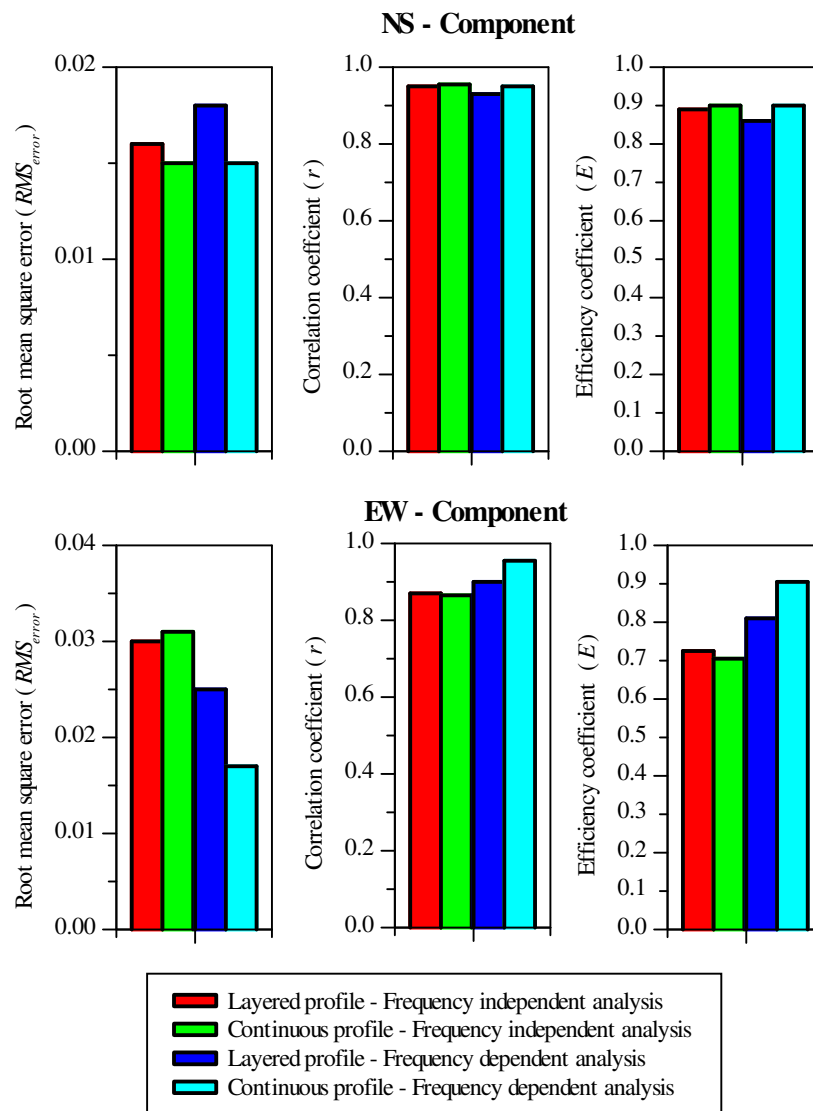
Figure 5.42: Comparison of goodness-fit parameters obtained for response spectra of computed acceleration responses at the surface of the TKCH08 soil deposit with different cases of analysis. NS – component (top row) and EW – component (bottom row)

From Figure 5.41 it can be observed that both, Pearson's correlation coefficient (r) and efficiency coefficient (E) are higher for frequency dependent analysis with continuous variation of shear wave velocity profile compared to response obtained under the case of layered profile and frequency independent analysis. However, frequency independent analysis with continuous velocity profile has resulted in marginally poor agreement with observed record compared to that for layered profile. All these observation are also in confirmation with the bar charts presented in Figure 5.42 which are obtained for response spectra of computed acceleration time histories and corresponding observed records. In conclusion, responses computed using frequency dependent analysis proposed in this study has shown better agreement with observed response compared to routine frequency independent analysis. Also, approximating the layered deposit of contrasting layer impedances with continuous variation of shear wave velocity will favorably improve predictability of response using EQL analysis, particularly at resonant frequencies.

5.8   SUMMARY

In the previous chapter, details about the computer program developed for the purpose seismic site response analysis was presented. The main feature of this program is that it can accommodate different idealisations of soil profile including continuous distribution of soil properties along the depth. Apart from fulfilling this main purpose of the present study, it is intended to look into other limitations of routine one-dimensional equivalent linear analysis to improve its response prediction capabilities. The two major issues of concern identified in Chapter 2 of this thesis and well recognized in the literature are addressed. The major issue is related to ambiguity in the method used for calculation of effective strain during the EQL iterations. The other issue of concern in frequency domain EQL analysis is its inconsistency in simulation of response in the regions of fundamental resonant frequency and at high frequency regime. Proposed alternative methods that are reported in the literature to circumvent these two lacunae of routine site response analysis procedure are reviewed and alternative methods are proposed to overcome these deficiencies. Finally a case study is presented in detail, in which the responses computed with and without using

all these proposed options are compared with the well documented observed data during an earthquake. For this purpose data pertaining to a geotechnical downhole array site of Japan is selected. The results of this comparative study are presented and analysed using statistical tools.

Almost all the programs currently available for equivalent linear analysis in frequency domain recommend constant value for effective to maximum strain ratio (R-value) which is calculated based on magnitude of the earthquake input motion used for the analysis. Also this ratio remains unaltered for all iterations and at all depths of the soil deposit though temporal and spatial variation of computed strain time history in successive iterations is obvious. Currently employed method for computing effective strain was initially proposed in the SHAKE91 program manual and it has been verified to give satisfactory results. However, in this chapter, the circumstances in which it is impossible to assign this value without ambiguity are emphasized. Two options are incorporated in SRISD as alternative methods to compute unique value of effective strain for each of the successive iterations.

The first method is based on peak acceleration obtained in the previous iteration is used to calculate Modified Mercalli Intensity (MMI) and same kind of well established relationship is used to calculate R-value $[R = (MMI - 1)/10]$ except that MMI is used instead of magnitude. For this purpose well established empirical relationship between peak acceleration and MMI is used. The advantage of this method is that user intervention is completely avoided in the calculation of effective strain because program itself updates the value of R by assigning appropriate value at every node in each of the successive iterations based on corresponding maximum acceleration computed in the previous iteration. In the second method the average strain is calculated and used as effective strain. However this option is kept open ended because user can give the value of number of peaks that should be considered to calculate average strain.

In order to improve the response prediction capability of EQL analysis at resonant frequencies, based on the observation made, a semi empirical scheme is proposed. Usually the response is overestimated at resonant frequencies, particularly at lower

modes; and high frequency responses are underestimated. To enhance the response at lower resonant frequencies, in addition to material damping energy dissipation due to radiation of wave energy in the elastic half-space is considered. Also the material damping is reduced logarithmically to amplify the response in higher frequency range beyond target frequency f_T.

As mentioned earlier, owing to indistinct approach of computing effective strain, most often selection of R-value is biased. Widely accepted choice of R-value ranges from 0.5 to 0.7. For an example problem with arbitrarily selected earthquake input motion and analyses are carried out for different R-values. It has been shown that, the maximum acceleration response, amplification transfer function and Fourier amplitude spectra of the computed surface accelerogram are sensitive to chosen value of R. This illustrative example evidently emphasizes the need for an alternative rational approach to compute R-value in order to overcome inconsistencies in frequency domain EQL analysis. Also it has been verified, the proposed alternative method for computation of R-value is as reliable as present method in satisfying the convergence criteria of the EQL analysis. The proposed method, as illustrated in accompanying flowchart, can be easily accommodated within the framework of frequency domain equivalent linear analysis computer programs.

The response computed using frequency dependent EQL analysis proposed in the present study is compared with the results of routine EQL analysis and time domain nonlinear analysis. This comparative study clearly establishes the efficacy of the proposed method in improving spectral characteristics of the predicted response. It has been observed that, accounting for the effect of radiation damping has considerably enhanced the quality of the predicted response at the fundamental resonant frequency of the deposit in agreement with that of time domain nonlinear response.

Finally, a case study is presented to verify all the proposed improvements to frequency domain equivalent linear analysis. The downhole geotechnical array TKCH08 (KIK-net) of Japan is selected for this purpose. This array site is selected because, as reported in the cited literature, it perfectly qualifies for one dimensional

analysis. Also additional shear velocity profile data obtained independently in the vicinity of this site and well documented in the literature enabled to idealize the profile quantitatively with continuous variation of shear wave velocity along the depth. Among the earthquakes recorded at this site, 2003 Tokachi-Oki event of magnitude 8.0 is recognized to have resulted in nonlinear response of the soil deposit. Thus TKCH08 is considered as an ideal site for validation of all the proposed alternatives of this research study.

Various options of SRISD program that are exercised in this case study include, layered and its equivalent continuous shear wave velocity profiles, frequency independent and frequency dependent EQL analyses and analyses are performed for input motions consisting of both NS and EW horizontal components. The response quantities obtained from SRISD analyses are compared with the corresponding observed data. Results of the statistical analysis are presented to compare predicted and observed responses quantitatively.

The three statistical parameters, such as Pearson's correlation coefficient (r), Efficiency coefficient (E) and Root mean square of the error (RMS_{error}) are used to compare the responses predicted using different options of SRISD with the observed response quantities. All the analyses pertaining to this case study are carried out by using the option of proposed method for computing effective strain in the iterations of EQL analysis.

For both the case of input motions the proposed frequency dependent equivalent analysis with approximated continuous shear wave profile predicted the response which closely matched with observed response compared to that of routine EQL analysis with layered profile. The comparisons are presented with respect to surface acceleration responses as well as their response spectra. The abstract of these results are tabulated in the Table shown below. From the results presented in the table it is evident that both correlation coefficient (r) and efficiency coefficient (E) are more for frequency dependent EQL analysis with shear wave velocity profile being idealised with a continuous function compared to results obtained for routine EQL analysis

with layered shear wave velocity profile. Root mean square of the error of the predicted response with respect to observed response also supports this observation. Hence it can be concluded that, proposed recommendations of this study can effectively improve the predictability of frequency domain equivalent linear analysis.

Acceleration time history response at the surface of the soil deposit						
Input motion	NS – horizontal component			EW – horizontal component		
Analysis	r	E	RMS_{error}	r	E	RMS_{error}
Layered profile – Frequency independent routine EQL analysis	0.623	0.453	0.050	0.594	0.466	0.059
Continuous profile – Frequency dependent EQL analysis	0.637	0.472	0.050	0.643	0.512	0.055
Response spectra of acceleration time history response						
Layered profile – Frequency independent routine EQL analysis	0.948	0.888	0.016	0.868	0.724	0.030
Continuous profile – Frequency dependent EQL analysis	0.950	0.900	0.015	0.955	0.906	0.017

CHAPTER 6

AN ALTERNATIVE METHOD FOR ESTIMATION OF FUNDAMENTAL PERIOD OF LAYERED SOIL DEPOSITS

6.1   INTRODUCTION

It has been well established that the damage caused during an earthquake is directly related to local geological conditions of the site. During an earthquake, seismic waves propagate through heterogeneous soil deposit above engineering bedrock. This alters wave characteristics usually resulting in amplification or attenuation of wave amplitudes in addition to change in its frequency characteristics. This phenomenon is primarily dependent on modal characteristics of the soil deposit overlying engineering bedrock. Particularly, amplification is dominant in the vicinity of the fundamental frequency of the soil deposit. Through several post earthquake geotechnical studies [for e.g., Seed et al. (1972)], it has long been recognized that the intensity of structural damage and its distribution are closely dependent on dynamic characteristics of the underlying soil deposit, particularly the depth, stiffness and amplification characteristics. 1985 Mexico earthquake [Seed et al. (1988); Singh et al. (1988)], 2001 Bhuj (Gujarat) earthquake [Prasad et al. (2001); Sitharam and Govindaraju (2004); Kumar (2006)], 1989 Loma Prieta and 1994 Northridge earthquakes [Seed et al. (1990); Benuska (1990); Borcherdt and Glassmoyer (1992); Holzer (1994) and others] and other earthquakes elsewhere have clearly demonstrated the importance of considering local site effects in the design of earthquake resistant structures, particularly to avoid their eventual resonant state.

The current state of research in the field of earthquake engineering mainly focuses on modeling the seismic site effects in an appropriate and simplest possible manner. Hence in the recent past, evolving reliable method of assessing site effects has been the primary task of earthquake geotechnical engineering research throughout the world. One of the simplest analytical methods of assessing the site effects, in terms of amplification corresponding to fundamental frequency of the soil deposit overlying

bedrock, is to consider the heterogeneous layered soil deposit overlying the bedrock as one dimensional homogeneous layer having equivalent constant shear wave velocity.

As discussed in Chapter 2, very often in practice, one dimensional seismic response analysis of inhomogeneous soil deposit is carried out for the case of vertically incident shear waves propagating through horizontally layered soil deposit. Through several studies on free vibration characteristics of two dimensional soil deposits, it has been recognized that the fundamental period computed from one dimensional analysis fairly represents the fundamental period of wide and shallow sediment filled valleys of low shape factor (ratio of depth of the valley to its half width, is about less than 0.3) [Paolucci (1999)]. Moreover it has been established by Bard and Bouchon (1985) that the fundamental period of two dimensional soil deposit may be approximately related to one dimensional fundamental period of the deposit at the valley center and its shape factor.

Most of the international code of practices prescribe average shear wave velocity of top 30 m of soil deposit (v_{s30}) as parameter for site classification [Eurocode-EC8 (2004); FEMA-P-749 (2010)]. On the other hand, some of the seismic design codes such as, building laws of Japan adopt natural period of soil deposit as the criteria for seismic site classification [Marino et al. (2005)]. Essentially, based on these site classification data, codes will provide soil amplification or attenuation factors (scaling factors) to arrive at scaled elastic design response spectra which are compatible with local soil conditions. In this regard, some related studies have indicated that fundamental natural period of the surface layer above the bedrock is more appropriate parameter to predict amplification ratios than v_{s30} criteria particularly for long period deposits [Zhao (2011) and McVerry ((2011)]. Apart from its application in general site classification based on amplification ratio, fundamental natural period is also an essential input parameter in the analysis of underground structures [Sawada (2004)]. It may be pointed out that such a rational method of computing design forces by appropriately accounting for local soil condition is absent in Indian code of practice IS-1893 (2002). Currently, Indian code classifies foundation soil into three categories

namely soft, medium and hard (rock) soils depending on range of SPT-N values. There is immediate need for updating Indian seismic design codes commensurate with other national codes by incorporating local site effects in computation of design forces [Khose et al. (2010)]. For this purpose, fundamental natural period of the soil deposit may be used as key parameter because it accounts for both stiffness and depth of the surface soil deposit above the bed rock. Hence reliable assessment of fundamental period of the soil deposit is an important primary step in seismic site characterisation particularly in the process of microzonation of urban area.

Perceiving its importance in seismic site characterisation tasks, many methods have been formulated and proposed to estimate reliably the fundamental period of one dimensional horizontally layered soil deposit. Some of these methods are briefly described. While implementing these methods, it is essential to idealize the soil deposit as a layered profile as far as possible closely representing the actual shear wave velocity distribution.

Uncertainty is evident in idealizing the actual profile into an equivalent layered system because of complex variability of soil properties along the depth. As pointed out in Chapter 3, the soil deposit may exhibit distinct continuous variation of soil properties depending upon its genesis, stress history and other related process. However, questionably, even such deposits displaying distinct continuous variation soil properties are approximated as layered system. In such situations, employing the methods derived for layered profiles may be inappropriate for estimation of fundamental period.

Firstly, methods available for the estimation of fundamental period of layered soil deposits are reviewed. Methods based on weighted average of shear wave velocities of the layered soil profile are most widely employed in practice. There are methods which are accurate and more reliable than weighted average methods, but they are iterative in procedure and hence tedious. Consequently, they are unpopular for quick estimation of fundamental period of soil deposits. A new method, which is simple and comparatively reliable, for computing fundamental period is proposed and presented in this chapter. The proposed method primarily involves approximating the layered

shear wave velocity profile with an equivalent linearly varying shear wave velocity profile. The closed form exact analytical solution is used to compute the fundamental period of the deposit of linearly varying shear wave velocity profile. The efficiency of the proposed method and other available methods is verified by comparing their results with values computed from recorded earthquake accelerograms of instrumented geotechnical downhole arrays.

6.2   FUNDAMENTAL PERIOD OF INHOMOGENEOUS SOIL DEPOSIT

Since shear wave velocity and fundamental period are directly interrelated, many empirical relationships have been proposed to compute average shear wave velocity as an equivalent substitute to complex shear wave velocity profile of inhomogeneous layered deposit. Summary and relative comparison of all empirical methods available till then are given in the paper by Dobry et al. (1976). In addition to these empirical methods, Dobry et al. (1976) have discussed about other comparatively accurate methods based on closed form solutions like successive application of exact solution for two layer system proposed by Madera (1971) and method based on linear approximation of fundamental mode shape. Procedure to implement Madera's two layer solution to multiple layers deposit is discussed later in this chapter.

Among the analytical methods available to compute fundamental period of the layered deposit Rayleigh's method is most accurate. The general iterative procedure to implement Rayleigh's method in case of horizontally layered soil deposits is detailed in Dobry et al. (1976). Period corresponding to first peak of amplification transfer function computed using the theory of multiple reflections of waves is an alternative reliable and accurate method for computing fundamental period of layered deposits. For this purpose, one can use the expression derived in Chapter 2 (Eq. 2.33) or computer program such as SHAKE which directly computes the amplification transfer function from Haskell-Thompson transformation matrix. Dobry et al. (1976) compared fundamental period computed from both exact Rayleigh's iterative method and transfer function of SHAKE program for several profiles of different velocity structures and concluded that they yield almost same result. Hence, fundamental period computed from amplification transfer function can be considered as exact

value. In case of almost all approximate methods for computation of fundamental period of the horizontally layered soil deposit, it is assumed that the soil deposit is overlying the rigid bedrock. However, Sawada (2004) derived an approximate relationship for fundamental period of layered soil deposit overlying elastic bedrock. But, in the presence of any intermediate relatively stiff layer, this method yields imaginary value for natural period. In such cases the method becomes cumbersome as it ceases to be a closed form equation and involves further trial and error process. Therefore, it may be appropriate to compute the fundamental period considering the total depth of soil deposit above the bedrock and ignore the relatively large shear wave velocity associated with the underlying bed rock. Rigid bedrock assumption is justified when the objective of the analysis is estimation of fundamental period of the deposit, not the associated amplification, because effect of rigidity of bedrock on the fundamental period is negligible [Jiang and Kuribayashi (1988)].

6.2.1   Method-1: Weighted average of shear wave velocity $\left(T^{(1)}\right)$

For a homogeneous soil deposit of total thickness H and constant shear velocity v_s, the fundamental period (T) is given by,

$$T = \frac{4H}{v_s} \tag{6.1}$$

In case of layered soil deposit, average shear wave velocity, $\overline{v}_s$ is obtained to compute fundamental period. Usually, for a soil deposit of N layers with shear wave velocities v_{si}, and corresponding layer thicknesses H_i, $\overline{v}_s$ is calculated as weighted average of the layer shear wave velocities from,

$$\overline{v}_s = \frac{1}{H} \sum_{i=1}^{N} v_{si} H_i \tag{6.2a}$$

Then fundamental period is computed from Eq. (6.1) using $\overline{v}_s$ instead of v_s. Thus,

$$T = T^{(1)} = \frac{4H^2}{\sum\limits_{i=1}^{N} v_{si} H_i}$$
(6.2b)

6.2.2   Method-2: Sum of layer periods $\left(T^{(2)}\right)$

Alternatively, if weighted average velocity of the layered deposit is computed using,

$$\frac{1}{\overline{v}_s} = \frac{1}{H} \sum\limits_{i=1}^{N} \frac{H_i}{v_{si}}$$
(6.3a)

then, substituting (6.3a) in (6.1), the fundamental period is given by,

$$T = T^{(2)} = \sum\limits_{i=1}^{N} \frac{4H_i}{v_{si}} = \sum\limits_{i=1}^{N} T_i$$
(6.3b)

$T_i (i = 1, 2, \ldots N)$ are natural periods of each of the individual layers in the deposit. Hence, fundamental period of the layered deposit is nothing but sum of the fundamental periods of its individual layers [Zeevaert (1972)]. According to Dobry et al. (1976), the order of error in fundamental period computed from these two methods is about 20% and it could be as large as 50% in some cases where large velocity gradient exists between any two layers of the deposit.

6.2.3   Method-3: Simplified Rayleigh's Method $\left(T^{(3)}\right)$

Dobry et al. (1976) have proposed a non-iterative alternative approach basically derived from exact Rayleigh's procedure. For the profiles considered in their study they noted that Rayleigh's iterative procedure usually converges, within acceptable error range (within ± 3 %), to fundamental period in the first iteration itself. Based on this observation, a set of closed form equations was formulated for computation of the fundamental period as obtained in the first iteration of Rayleigh's equation. The fundamental period using this method is computed from the following equations,

$$X_{i+1} = X_i + \frac{H - z_{mi}}{v_{si}^2} H_i \tag{6.4a}$$

$$T = T^{(3)} = \pi \sqrt{\frac{\sum_{i=1}^{N} (X_i + X_{i+1})^2 H_i}{\sum_{i=1}^{N} \frac{(X_{i+1} - X_i)^2}{H_i} v_{si}^2}} \tag{6.4b}$$

X_i and X_{i+1} are the estimated fundamental mode shapes at the bottom and top of the ith layer. At the lower boundary of the bottommost layer, X_i is taken as zero i.e., $X_i = X_1 = 0$ and Eq. (6.4a) is used to estimate X_i at all other layer boundaries. z_{mi}, is the depth of midpoint measured from top of the deposit. Thus $(H - z_{mi})$ represents depth of midpoint of ith layer measured from bottom of the deposit. All other quantities of Eq. (6.4a & 6.4b) are same as defined earlier. It may be noted that the computations are carried out considering layers starting from the bottommost layer ($i = 1$) to surface layer at the top (i.e., $i = N$).

6.2.4 Method-4: Linear fundamental mode shape $\left(T^{(4)} \right)$

Another modification to Rayleigh's method as proposed by Dobry et al. (1976) is based on the assumption of linear fundamental mode shape. Assuming X_1 to X_N to vary linearly from 0 to 1 over the total depth of the soil deposit and accordingly substituting in Eq. (6.4b) for X_i and X_{i+1} we get closed form relationship as given in Eq. (6.5)

$$T = T^{(4)} = 2\pi \sqrt{\frac{H^3}{3 \sum_{i=1}^{N} v_{si}^2 H_i}} \tag{6.5}$$

6.2.5 Method-5: Successive application of two layer solution $(T^{(5)})$

Madera (1971) proposed an alternative method in which fundamental period solution obtained for two-layered system overlying bedrock is used repeatedly to analyse

multilayered soil deposit. Though this procedure is reliable, it is tedious compared to simple average shear wave velocity method.

Figure 6.1 shows two adjacent homogeneous layers of thicknesses H_a and H_b; densities ρ_a and ρ_b; and having individual fundamental periods T_a and T_b respectively. The combined fundamental period of set of these two layers T_{a-b}, is obtained by satisfying the boundary conditions such as, shear stress is zero at the top of the first layer, relative displacement at the of bottom of second layer with respect to underlying rigid bedrock is zero and at the interface of two layers, stresses and displacements are continuous.
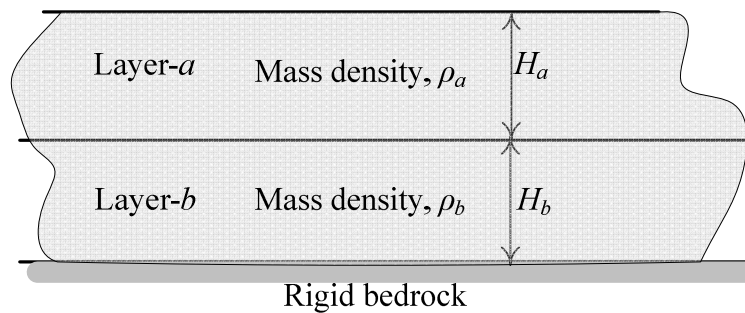
Figure 6.1: Two layers soil deposit overlying rigid bedrock considered in Madera's approach.

Finally, the combined natural period T_{a-b} of two layered system is obtained by solving following equation,

$$\tan\left(\frac{\pi}{2}\frac{T_a}{T_{a-b}}\right)\tan\left(\frac{\pi}{2}\frac{T_b}{T_{a-b}}\right)=\frac{T_a}{T_b}\frac{H_b\rho_b}{H_a\rho_a} \tag{6.6}$$

Dobry et al. (1976) have graphically represented the solution (i.e., for T_{a-b}) of the above transcendental equation for a range of values of $H_a\rho_a/H_b\rho_b$ and T_b/T_a using which one can approximately ascertain the value of T_{a-b}. If the densities of the layers are assumed to be constant then Eq. (6.6) reduces to,

$$\tan\left(\frac{\pi}{2}\frac{T_a}{T_{a-b}}\right)\tan\left(\frac{\pi}{2}\frac{T_b}{T_{a-b}}\right)=\frac{T_aH_b}{T_bH_a} \tag{6.7}$$

The fundamental period of a soil deposit made up of several layers can be computed by successive application of Eq. (6.7) by considering two layers, having individual fundamental periods T_1 and T_2 respectively, at a time. In the first instant, combined period, $T_{1-2} = T_{a-b}$ of top two layers is computed using $T_a = T_1$ and $T_b = T_2$ in Eq. (6.7). Then these two layers are treated as equivalent single layer with equivalent values of depth, density and period T_{1-2} to represent it as Layer-a in the next instant and third layer is treated as Layer-b. Again, $T_{1,2-3}$ (natural period of top three layers together) is computed by using T_{1-2} for T_a and T_3 for T_b in Eq. (6.7). This process of successively computing the natural period is continued till the last layer (lowermost layer is the layer immediately above the bedrock) is reached. Final result represents the combined natural period, $T^{(5)} = T_{1-N}$ of all layers. The equivalent depth of the layer-a above m^{th} layer is a simple summation of depths of all layers up to m^{th} layer i.e.,

$$H_a = \sum_{i=1}^{m-1} H_i \tag{6.8}$$

The main drawback of the above mentioned procedure is obtaining solution for Eq. (6.7) manually. Although charts are developed for this purpose, it is cumbersome to implement this procedure in every successive step. Also, for any intermediate value other than the range of values used in charts, interpolation is necessary. In order to eliminate these shortcomings in implementation of this procedure, Hadjian (2002) approximated the solution of Eq. (6.7) by transforming the equation into cosine function form.

6.3 PROPOSED METHOD FOR ESTIMATION OF FUNDAMENTAL PERIOD OF SOIL DEPOSITS $\left(T^{(New)} \right)$

The new method proposed in this study essentially involves idealisation of layered soil profile with an equivalent soil deposit having continuous shear wave velocity profile of linearly variation. For this purpose, an equation for fundamental period of the deposit with linearly varying shear wave velocity profile is derived. For any

layered profile with distinct shear wave velocity for each layer, curve fitting process using regression analysis can be employed to get an equivalent linear fit. Thus obtained curve fitting constants, consisting of non-zero shear wave velocity at the surface and rate of change of shear wave velocity along the depth, are used to estimate the fundamental period of the layered profile.

6.3.1   Deposit with continuous variation of shear wave velocity

Here, the objective is to approximate the layered profile with an equivalent profile having continuous variation of shear wave velocity. Simple case of linear variation of shear wave velocity has been considered to find free vibration response of the soil deposit for vertically propagating transverse waves. Earlier, earthquake response of linearly non-homogeneous soil deposits has been presented in Chapter 3. Wave equation describing one dimensional shear wave propagation in a soil deposit of constant density ρ, and continuously varying shear modulus $G(z)$, along the depth z, is represented by

$$\frac{\partial^2 u}{\partial t^2} = \frac{1}{\rho}\frac{\partial}{\partial z}\left(G(z)\frac{\partial u}{\partial z}\right) \tag{3.4}$$

$G(z)$, is related to depth dependent shear wave velocity $v_s(z)$ as, $G(z) = \rho v_s^{\,2}$. Linear distribution of shear wave velocity (shown in Figure 3.5 of Chapter 3) may be represented by, $v_s(z) = v_0 + \overline{a}z$ (Eq. 3.12 of Chapter 3). The solution of Eq. (3.4) is obtained in Chapter 3 as,

$$U(z) = \frac{1}{\sqrt{(v_{s0} + \overline{a}z)}}\left\{A_1 e^{i\sqrt{\left(\omega/\overline{a}\right)^2 - (0.5)^2}\,\ln(v_{s0}+\overline{a}z)} + A_2 e^{-i\sqrt{\left(\omega/\overline{a}\right)^2 - (0.5)^2}\,\ln(v_{s0}+\overline{a}z)}\right\} \tag{3.12}$$

Here, $i = \sqrt{-1}$, A_1 and A_2 are constants evaluated by satisfying boundary conditions; zero shear stress at the surface (at $z = 0$) and zero relative displacement at the base (at $z = H$) in (3.12) yield characteristic eigen values equation as,

$$2\eta\cos\eta + \ln(\mu)\sin\eta = 0 \tag{6.9}$$

Here, $\mu = v_{sH} / v_{s0}$ is the ratio of base to surface shear wave velocities. v_{sH} is the shear wave velocity at the bottom (i.e., $z = H$) of the deposit ($v_{sH} = v_{s0} + \overline{a}H$). The solution of Eq. (6.9), η is the dimensionless quantity related to μ and ω (modal frequencies) as,

$$\eta = \frac{\ln(\mu)}{\overline{a}} \sqrt{\omega^2 - (0.5\overline{a})^2} \qquad (6.10)$$

Thus, for a soil deposit having linearly varying shear wave velocity profile, knowing the values of v_{s0} and v_{sH} Eq. (6.9) can be solved. Hence, the fundamental frequency, ω (or fundamental period, $T = 2\pi / \omega$) of the deposit with linearly varying shear wave velocity profile is function of smallest root (η) of Eq. (6.9). Therefore, using $\overline{a} = v_{s0}(\mu - 1) / H$ in (6.10), we get ω as

$$\frac{\omega H}{v_{s0}} = \frac{\mu - 1}{\ln \mu} \sqrt{\eta^2 + \left\{ \ln \sqrt{\mu} \right\}^2} \qquad (6.11)$$

6.3.2 Linear regression analysis

In the proposed method, in order to compute fundamental period of the layer deposit, it is essential to get equivalent linear distribution of shear wave velocity representing layer deposit with distinct shear wave velocity for each of the layer. The equivalent linear distribution of shear wave velocity is obtained in the form of Eq. (3.12). Using linear regression analysis by method of least squares, fitting parameters v_{s0} and $\overline{a}$ of Eq. (3.12) are obtained. Substituting H, μ and v_{s0} along with smallest root η of Eq. (6.9), into Eq. (6.11) fundamental frequency ω can be estimated.

If N data points corresponding to shear wave velocities and depths represent the layered configuration of shear wave velocity profile, then linear regression using method of least squares [Johnson (2000)] may be employed to obtain parameters v_{s0} and $\overline{a}$ for linearly varying shear wave velocity profile. Let i^{th} layer shear wave velocity and corresponding mid-depth be represented by v_{si} and $z_{i(mid)}$

$(i = 1, 2, 3, ...N)$ respectively. Then, following equations are used to get least square estimate of v_{s0} and k,

$$\left.\begin{array}{l} S_{zz} = \sum_{i=1}^{N} z_{i(mid)}^2 - \left[\left(\sum_{i=1}^{N} z_{i(mid)}\right)^2 \Big/ N\right] \\[4mm] S_{vv} = \sum_{i=1}^{N} v_{si}^2 - \left[\left(\sum_{i=1}^{N} v_{si}\right)^2 \Big/ N\right] \\[4mm] S_{zv} = \sum_{i=1}^{N} z_{i(mid)} v_{si} - \left(\sum_{i=1}^{N} z_{i(mid)} \sum_{i=1}^{N} v_{si} \Big/ N\right) \end{array}\right\} \qquad (6.12)$$

Then,

$$\left.\begin{array}{l} \overline{a} = \dfrac{S_{zv}}{S_{zz}} \\[4mm] v_{s0} = \left(\sum_{i=1}^{N} v_{si} \Big/ N\right) - \left(\overline{a} \sum_{i=1}^{N} z_{i(mid)} \Big/ N\right) \end{array}\right\} \qquad (6.13)$$

Finally, in order to ascertain the inherent variability in shear wave velocity profile defined by the original data set corresponding to layered idealisation with respect to assumed linear trend, coefficient of variation (*COV*) and correlation coefficient (*r*) are calculated. Normalization of standard deviation (*SD*) with respect to the mean shear wave velocity of the assumed linear variation (mean of the trend, $\overline{t}$) gives *COV* [Phoon and Kulhawy (1999)]. Thus,

$$SD = \sqrt{\frac{1}{N-1}\left[S_{vv} - \left(S_{zv}^2 / S_{zz}\right)\right]} \qquad (6.14)$$

$$COV = \frac{SD}{\overline{t}} = \frac{\sqrt{\dfrac{1}{N-1}\left[S_{vv} - \left(S_{zv}^2 / S_{zz}\right)\right]}}{\dfrac{1}{N}\sum_{i=1}^{N}\left(v_{s0} + \overline{a} z_{i(mid)}\right)} \qquad (6.15)$$

And correlation coefficient is,

$$r = \frac{S_{zv}}{\sqrt{S_{zz}S_{vv}}} \qquad\qquad (6.16)$$

COV and *r* are useful indicators of goodness of linear fit for layered profile. If the linear fit manifests in high value of *COV*, then it is an indication of increase in variability of the shear wave velocity profile [Chenari et al. (2012)]. On the other hand low value of *r* is representing the case of highly scattered shear wave velocity profile along the depth. This may be the case of profiles with large shear wave velocity contrasts between layers or in case of large fluctuations in depth of individual layers.

6.3.3 Approximation of fundamental period

In Eq. (6.11) the LHS represents the dimensionless frequency dependent term while RHS is a function of μ and η. As can be seen in Eq. (6.9), η is function of μ alone. Therefore, it is possible to establish a relationship between μ and $\omega H/v_0$ by computing η for different values of μ. Varying the values of μ in the range $1.0 \le \mu \le 10.0$, the smallest root of Eq. (6.9), η is computed and then using this in Eq. (6.11), $\omega D/v_0$ is obtained. Figure 6.2 shows μ ($1.0 \le \mu \le 10.0$) versus $\omega H/v_0$ plot. Also, the regression curve for the equation of the form $\left(\omega H/v_0\right) = a + b\mu^c$ is shown. The values of the curve fitting constants *a*, *b* and *c* that provide best fit are 0.324, 1.254 and 0.853 respectively. Thus, the relationship between μ and $\omega H/v_0$ is expressed as,

$$\frac{\omega H}{v_0} = 0.324 + 1.254\mu^{0.853} \qquad\qquad (6.17)$$

The error in estimated value of $\omega H/v_{s0}$ using the above equation compared to its actual value as obtained using Eq. (6.9) and Eq. (6.11) for varying values of μ is also shown in Figure 6.2. As it can be seen the error (dashed line) is acceptably low (that is, less than 0.2%), except in the small range of values around $\mu \approx 2$ where error is about 0.25%. Hence, instead of solving the transcendental equation (Eq. 6.9),

approximated relationship given in Eq. (6.17) can be directly employed to compute $\omega H/v_0$.
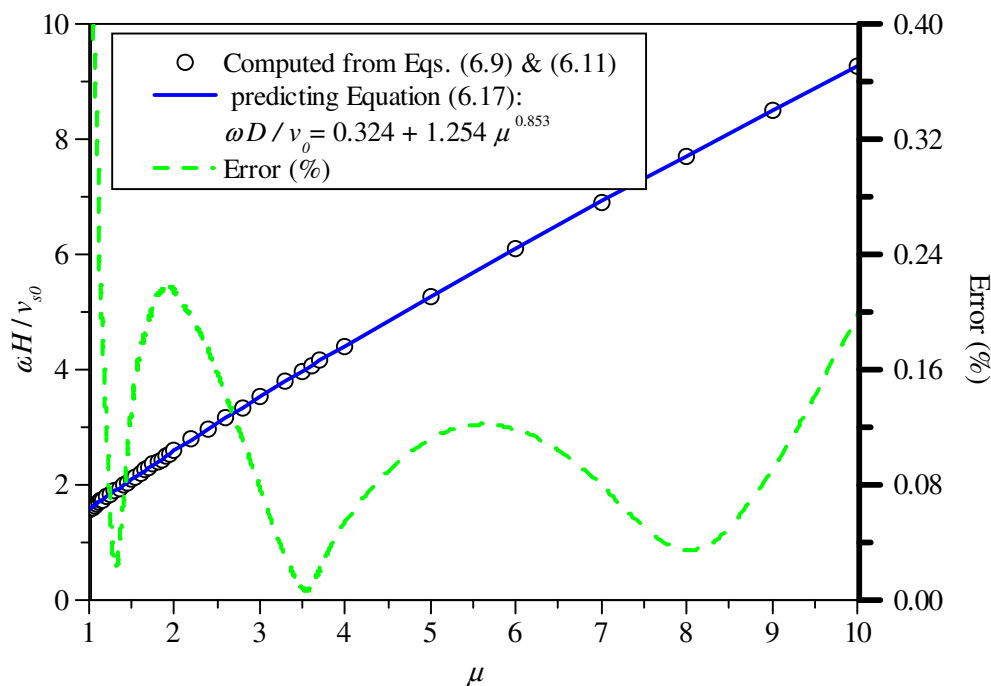
Figure 6.2: Relationship between μ **and** $\dfrac{\omega H}{v_{s0}}$ $\left(\text{for, } 1 \leq \mu \leq 10\right)$

Knowing the depth H, shear wave velocities v_{s0} and v_{sH}, the fundamental period can be computed using Eq. (6.17) and $T = 2\pi/\omega$ as,

$$T^{(New)} = \frac{2\pi H}{v_{s0}(0.324 + 1.254\mu^{0.853})} \tag{6.18}$$

It can be verified that, in case of a homogeneous soil deposit of total thickness H and constant shear velocity v_{s0}, the error in the fundamental period computed using Eq. (6.18) is less than 0.5% compared to exact value obtained from Eq. (6.1).

6.3.4 Step by step procedure of the proposed method

The method proposed in this study for estimating the fundamental period of a layered soil deposit involves simple procedure requiring fewer steps like weighted average shear wave velocity or simplified Rayleigh's methods in which no iterative process is

required unlike Madera's or exact Rayleigh's methods. Following are the steps of the proposed method:

i. The data v_{si} and mid depth of the corresponding layer ($z_{i(mid)}$) of layered shear wave velocity profile are tabulated.

ii. The sums $S_{\bullet\bullet}$ (S_{zz}, S_{vv} and S_{zv}) are computed using Eq. (6.12)

iii. Fitting parameters v_{s0} and $\bar{a}$ are computed from Eq. (6.13)

iv. Shear wave velocity ratio $\mu = v_{sH} / v_{s0}$ is computed where, $v_{sH} = v_{s0} + \bar{a}H$

v. The fundamental period $T^{(New)}$ is computed using Eq. (6.18)

6.4   VERIFICATION OF THE PROPOSED METHOD

One of the most reliable methods of ascertaining fundamental period of a site is by analyzing its downhole array data of earthquake accelerograms recorded at that site. The recorded earthquake data pertaining to an instrumented downhole array provide vital information for seismic site characterisation. The new method proposed here is validated by comparing the fundamental period computed with that obtained from actual earthquake data recorded in some of the instrumented geotechnical arrays.

6.4.1   Geotechnical arrays

Table 6.1 presents the details of the four instrumented geotechnical downhole arrays employed in this study to validate the proposed alternative procedure for computing fundamental period of the layered profile. These geotechnical downhole arrays were established as part of a project on site amplification studies by the California Strong Motion Instrumentation Program (CSMIP) in California, USA. Geotechnical data available at these stations include suspension logging shear-wave velocity profiles. The data related to shear wave velocity profile and earthquakes recorded by these instrumented sites are available in CSMIP website. More details about these arrays are given in Graizer et al. (2000) and references cited therein.

Table 6.1: Strong motion geotechnical array stations

Downhole Geotechnical Array	Agency	Station No.	Latitude/ Longitude	Sensor depths, m
La-Obregon Park Geotechnical array	CSMIP	24400	34.037N 118.178W	**0, 70**
La-Cienega Geotechnical Array	CSMIP	24703	34.036N 118.378W	**0**, 18, **100**, 252
Eureka Somoa Geotechnical Array	CSMIP	89734	40.819N 124.165W	**0**, 19, 33, 56, **136**
El Centro - Meloland Geotechnical Array	CSMIP	01794	32.773N 115.447W	**0**, 30, 100, **195**

Table 6.2: Layer data of shear wave velocity profiles considered for the analysis

Array	Obregon Park		La-Cienega		El-Centro Meloland		Eureka Somoa	
Layer No.	Layer Depth (m)	v_s (m/s)	Layer Depth (m)	v_s (m/s)	Layer Depth (m)	v_s (m/s)	Layer Depth (m)	v_s (m/s)
1.	1.22	399.29	2.13	139.90	2.44	185.01	10.06	149.96
2.	3.66	487.68	1.83	179.83	4.57	114.91	4.88	180.14
3.	2.13	420.62	3.05	210.01	3.05	224.94	5.18	230.12
4.	3.66	478.54	3.05	239.88	4.88	164.90	11.89	259.99
5.	3.66	539.50	3.05	279.81	5.18	199.95	10.06	220.07
6.	1.52	420.62	4.88	309.68	7.93	249.94	10.06	239.88
7.	1.22	548.64	2.13	289.86	1.83	309.98	12.80	289.87
8.	1.83	429.77	1.83	349.91	6.10	355.09	24.99	320.04
9.	2.13	350.52	2.13	369.72	11.89	299.92	14.94	359.97
10.	1.83	469.39	1.83	339.85	17.07	420.01	45.11	409.96
11.	1.22	539.50	3.96	313.94	24.99	480.06	24.99	459.94
12.	3.05	460.25	9.75	472.44	17.07	549.86	14.94	600.15
13.	8.84	429.77	21.34	411.48	17.98	459.94	5.11	449.89
14.	7.93	478.54	12.19	624.84	10.97	600.15		
15.	4.88	600.46	26.85	518.16				
16.	6.10	499.87						
17.	2.13	670.56						
18.	13.11	530.35						

In these arrays, apart from triaxial accelerometers at the surface and engineering bedrock levels, sensors are installed at several intermediate depths except in case of La-Obregon Park Geotechnical array. The highlighted (boldfaced) depths in the Table 6.1 against an array indicate the total depth (H) of the soil column considered for analysis. The accelerograms recorded by the sensors located at these corresponding depths are used for computing the fundamental period of the soil column. These instrumented sites are chosen to represent wide range of soil column depths ranging from 70 m to 195 m and exhibiting significant variability with respect to shear wave velocity profile along the considered depths. These factors associated with the chosen

soil deposits amply ascertain the efficacy of the proposed method compared to other approximate methods for estimation of the fundamental period.

The shear wave velocity profiles idealised into layered soil deposits are inferred from continuous PS logging and SASW data. The layer configurations considered in this study are adopted from Graizer et al. (2000) and also from the website of Pacific Earthquake Engineering Research Center (PEER) sponsored research project on Calibration Sites for Validation of Nonlinear Geotechnical Models [Stewart (2002)]. Layer depths and their corresponding shear wave velocities used in the present study are given in Table 6.2.

6.4.2   Fundamental period using earthquake data

Acceleration time histories recorded during an earthquake at two depths can be used to determine dynamic characteristics, such as fundamental period and amplification transfer function of soil deposit included between these two depths [Roësset (1977)]. For this purpose response spectrum for low damping value is obtained for both these records, and ratio between these response spectra is obtained. Fundamental period for the deposit is determined as period corresponding to peak of the response spectrum ratio between ground surface and bottom of the soil deposit. To determine the fundamental periods of the soil deposits of geotechnical arrays considered in this analysis, earthquake accelerograms recorded by these instrumented geotechnical arrays are selected as indicated in Table 6.3. For this purpose, earthquake accelerograms of both the horizontal components are considered. All the earthquakes considered are of weak ground motions with low peak ground accelerations of less than 0.02g.

For the recorded motion at a particular array the response spectrum of 2% damping is obtained at two depths, one for the recorded surface motion and another for the motion recorded at the depth considered for defining the depth of soil deposit. These response spectra are smoothened and spectral ratio is obtained. Period corresponding to peak of the response spectrum ratio is taken as the fundamental period of the deposit included between ground surface and the considered depth of the deposit.

Figures 6.3(a) to Figure 6.3(d) show ratio of response spectra between selected depths obtained for the soil deposits of four geotechnical arrays considered. The periods corresponding to peaks of the spectra of both the horizontal components of the earthquake along with their average curve are also given.

Table 6.3: Details of earthquake events considered in the analysis

Geotechnical Array	Earthquake event	Epicentral distance (km)	Components of the event	PGA (g) (Horizontal)
Obregon Park Geotechnical array	Calexico area eq. M_w=7.2 April 4th 2010	348.30	90°	0.011
			360°	0.013
La Cienega Geotechnical array	Calexico area eq. M_w=7.2 April 4th 2010	349.30	90°	0.010
			180°	0.009
Eureka Somoa Geotechnical Array	Eureka Offshore eq. M_L=4.4 September 22nd 2000	24.40	90°	0.010
			180°	0.011
El Centro Meloland Geotechnical array	Borrego Springs Area Eq. M_L=5.4 July 7th 2010	120.70	270°	0.008
			360$^{°}$	0.011

The results obtained from the above analysis using the earthquake data is summarized in Table 6.4. For each of the soil deposit considered for verification of the proposed method, only one of the seismic events recorded by the downhole instruments of these sites is selected. However, Graizer et al. (2000) have analysed several events recorded by some of these downhole arrays and obtained mean trend of spectral amplification ratio between surface and bedrock. Periods corresponding to peak spectral ratio shown in Table 6.4 for La-Cienega deposit compares very well with range of period of peak amplification under weak motions presented by Graizer et al. (2000). In addition, spectral ratios obtained for weak and strong motion separately have indicated reduction in amplification under strong ground motions compared to weak motions and decrease in period corresponding to peak amplification due to strong ground motion. In order to eliminate these effects on computed fundamental period, only the records of weak motions are selected for this analysis.
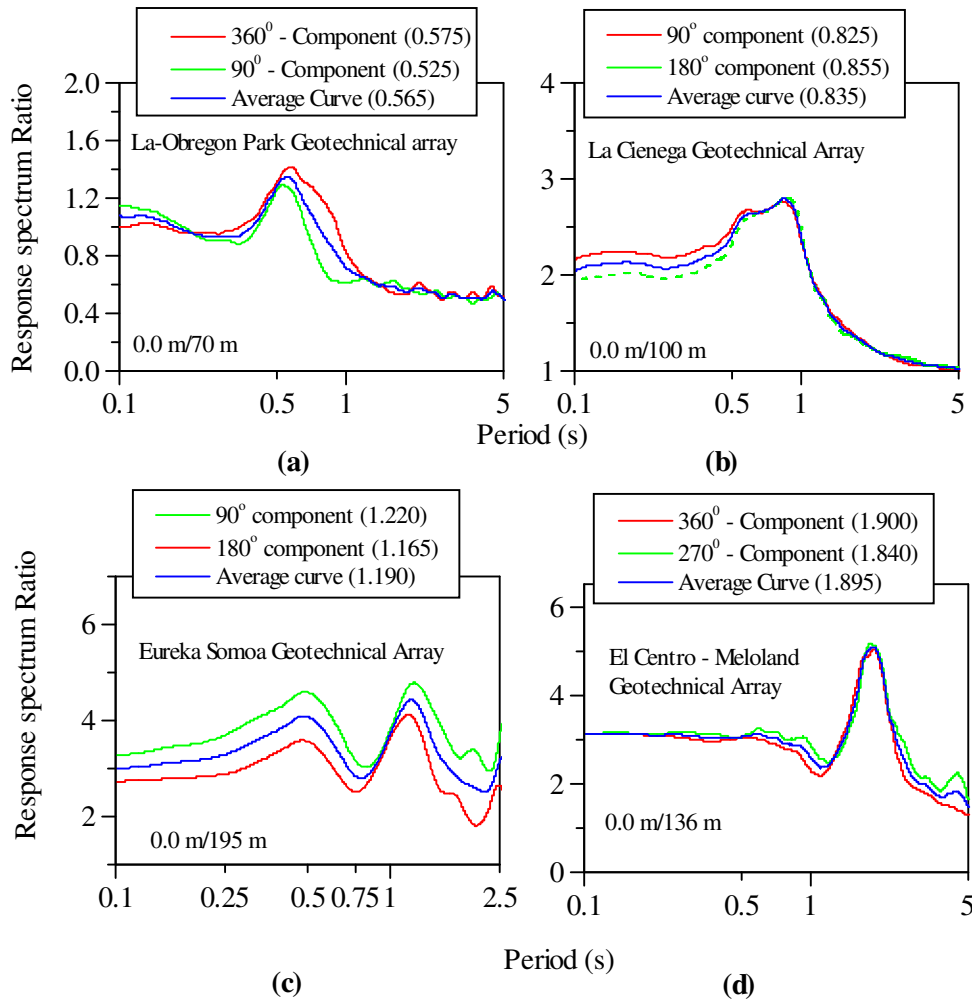
Figure 6.3: Computation of Fundamental periods from response spectrum ratio method (a) La-Obregon Park (surface/70 m) (b) La Cienega (surface/100 m) (c) Eureka Somoa (surface/136 m) and (d) El Centro Meloland (surface/195 m)

Table 6.4: Fundamental periods computed from response spectrum ratio method and SHAKE analysis

Geotechnical Array	Component	T (s) [RS ratio method]	$T^{(EQR)}$ (s) [Average curve]	$T^{(SHAKE)}$ (s) [SHAKE analysis]	% difference
Obregon Park	90°	0.525	0.565	0.555	1.80%
	360°	0.575			
La Cienega	90°	0.825	0.835	0.834	0.12%
	180°	0.855			
El Centro Meloland	270°	1.840	1.895	1.956	3.12%
	360°	1.900			
Eureka Somoa	90°	1.220	1.190	1.188	0.17%
	180°	1.165			

The fundamental period computed from representative earthquake data recorded at each of these four arrays is reaffirmed by comparing these results with periods corresponding to first peak of the amplification transfer function obtained for the corresponding site using SHAKE. As noted earlier, the natural period computed from theory of multiple reflections of waves employed in SHAKE is almost same as the exact solution of Rayleigh's iterative method. Amplification transfer function between surface and depth H is obtained for low damping value of 2% for all four sites and is as shown in Figure 6.4. For this purpose, computer program EERA [Bardet et al (2000)] is used. Also shown are the periods corresponding to peaks representing fundamental period of the particular soil deposit. The amplification shown in Figure 6.4 is normalized using respective maximum values such that amplification ratio is one for all the cases. The fundamental periods computed from earthquake data and SHAKE analysis $T^{(EQR)}$ and $T^{(SHAKE)}$ respectively are presented in Table 6.4. The percentage difference $T^{(EQR)}$ and $T^{(SHAKE)}$ is given in last column of the Table 6.4. There is a good agreement between results obtained from these two methods confirming the accuracy of average range of site periods obtained from spectral ratio of recorded data.
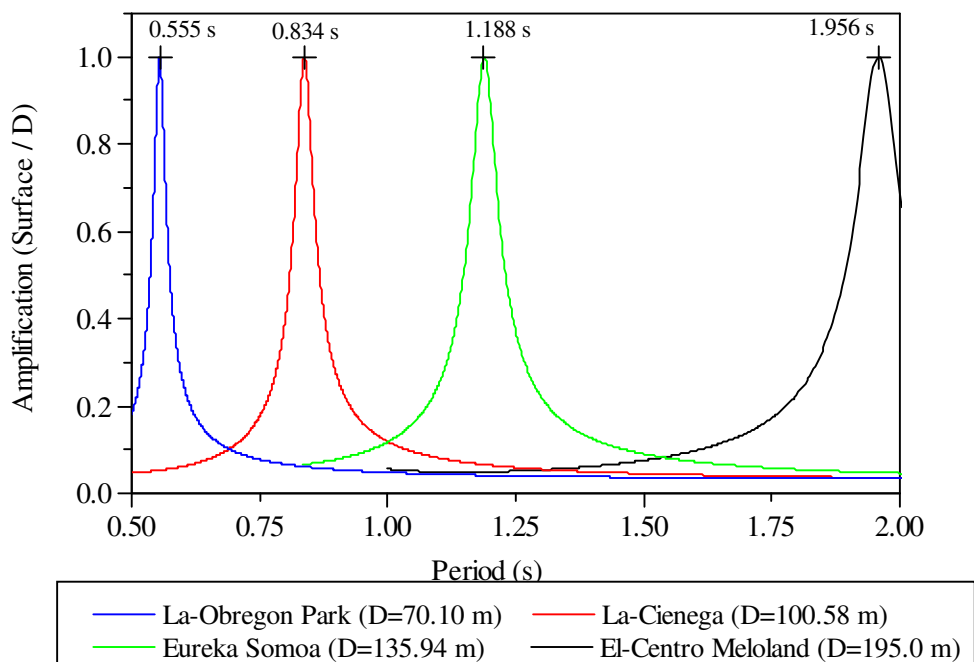
Figure 6.4 Fundamental period computed from amplification transfer function of SHAKE Program

6.4.3 Fundamental period using proposed method

In order to validate the proposed method, the fundamental periods of four soil deposits (Table 6.1) considered above are computed using the proposed method as well as from other analytical methods discussed earlier. The computed fundamental period results are relatively compared with those obtained using actual earthquake data summarized in Table 6.4. Firstly, the proposed method is implemented using the procedure as described earlier (Section 6.3.4). The layer-wise shear velocity data given in Table 6.2 are tabulated with shear wave velocities and corresponding layer mid-depths measured from surface. Summations required to be used in Eq. (6.12) are calculated for all the four soil deposits as shown in Table 6.5. Also, in continuation, Table 6.5 gives the values of summations of Eq. (6.12), linear trend fitting constants v_{s0} and $\bar{a}$ (Eq. 6.13) and statistical quantities of the linear trend (Eq. 6.14 and 6.15).

Instead of calculating manually, it is also possible to obtain curve fitting parameters v_{s0} and $\bar{a}$ using any graph plotting software tool. In that case, data of a particular deposit tabulated in Table 6.5 may directly be used to plot the shear wave velocity profile and implement curve fitting tool by selecting linear fit option. Such a plot of layered profile along with equivalent linearly varying shear wave profiles for all the four cases of soil deposits considered are shown in Figure 6.5(a) to Figure 6.5(d).

Parameters v_{s0} and $\bar{a}$ obtained in Table 6.5 and shown in Figures 6.5(a) to 6.5(d) are identical. In all cases the equivalent linear shear wave velocity profile is found to represent the actual layered profile with *COV* less than 0.20. The *r* value for La-Obregon Park deposit is as low as 0.581 indicating highly scattered distribution of shear wave velocities along the depth compared to other deposits as in those cases *r* value is around 0.90. Low *COV* indicate that fluctuation of discrete shear wave velocity values along the depth is uniform with respect to its linear trend. The curve fitting results are tabulated for all the soil profile cases in Table 6.5 along with computed value of their fundamental period $T^{(New)}$ using Eq. (6.18).

Table 6.5: Calculation of fundamental period using proposed method

Soil Deposit	La-Obregon Park		La-Cienega		Eureka Somoa		El Centro Meloland	
No. (i)	$z_{i(mid)}$	v_{si}	$z_{i(mid)}$	v_{si}	$z_{i(mid)}$	v_{si}	$z_{i(mid)}$	v_{si}
1	0.00	399.29	0.00	139.90	0.00	185.01	0.00	149.96
2	0.61	399.29	1.07	139.90	1.22	185.01	5.03	149.96
3	3.05	487.68	3.05	179.83	4.72	114.91	12.50	180.14
4	5.94	420.62	5.49	210.01	8.53	224.94	17.53	230.12
5	8.84	478.54	8.53	239.88	12.50	164.90	26.06	259.99
6	12.50	539.50	11.58	279.81	17.53	199.95	37.03	220.07
7	15.09	420.62	15.54	309.68	24.08	249.94	47.09	239.88
8	16.46	548.64	19.05	289.86	28.96	309.98	58.52	289.87
9	17.98	429.77	21.03	349.91	32.92	355.09	77.42	320.04
10	19.96	350.52	23.01	369.72	41.91	299.92	97.38	359.97
11	21.95	469.39	24.99	339.85	56.39	420.01	127.41	409.96
12	23.47	539.50	27.89	313.94	77.42	480.06	162.46	459.94
13	25.60	460.25	34.75	472.44	98.45	549.86	182.42	600.15
14	31.55	429.77	50.29	411.48	115.98	459.94	192.45	449.89
15	39.93	478.54	67.06	624.84	130.45	600.15	195.00	449.89
16	46.33	600.46	86.87	518.16	135.94	600.15		
17	51.82	499.87	100.58	518.16				
18	55.93	670.56						
19	63.55	530.35						
20	70.10	530.35						
N	20		17		16		15	
$\sum z_{i(mid)}$	530.66		500.79		786.99		1238.293	
$\sum z^2_{i(mid)}$	22690.14		29122.78		72632.96		174622.1	
$\sum v_{si}$	9683.496		5707.38		5399.84		4769.817	
$\sum v^2_{si}$	4798692.85		2224454.69		2215159.47		1764561.71	
$\sum z_{i(mid)} v_{si}$	274825.9		226729.92		375709.34		520794.89	
S_{zz} (Eq. 6.12)	8610.298		14370.603		33923.135		72397.420	
S_{vv} (Eq. 6.12)	110188.115		308326.074		392769.490		247818.097	
S_{zv} (Eq. 6.12)	17895.168		58601.781		110107.389		127032.821	
$\bar{a}$ (Eq. 6.13)	2.078		4.078		3.246		1.755	
v_{s0} (Eq. 6.13)	429.030		215.602		177.839		173.136	
$v_{sH} = v_{s0} + kH$	574.698		625.767		619.100		515.361	
$\mu = v_{sH} / v_0$	1.340		2.902		3.481		2.977	
$T^{(New)}(s)$ (Eq. 6.18)	**0.531**		**0.853**		**1.213**		**2.020**	
SD (Eq. 6.14)	61.983		65.838		48.569		36.215	
COV (Eq. 6.15)	0.128		0.196		0.144		0.114	
r^2 (Eq. 6.16)	0.338		0.775		0.910		0.899	
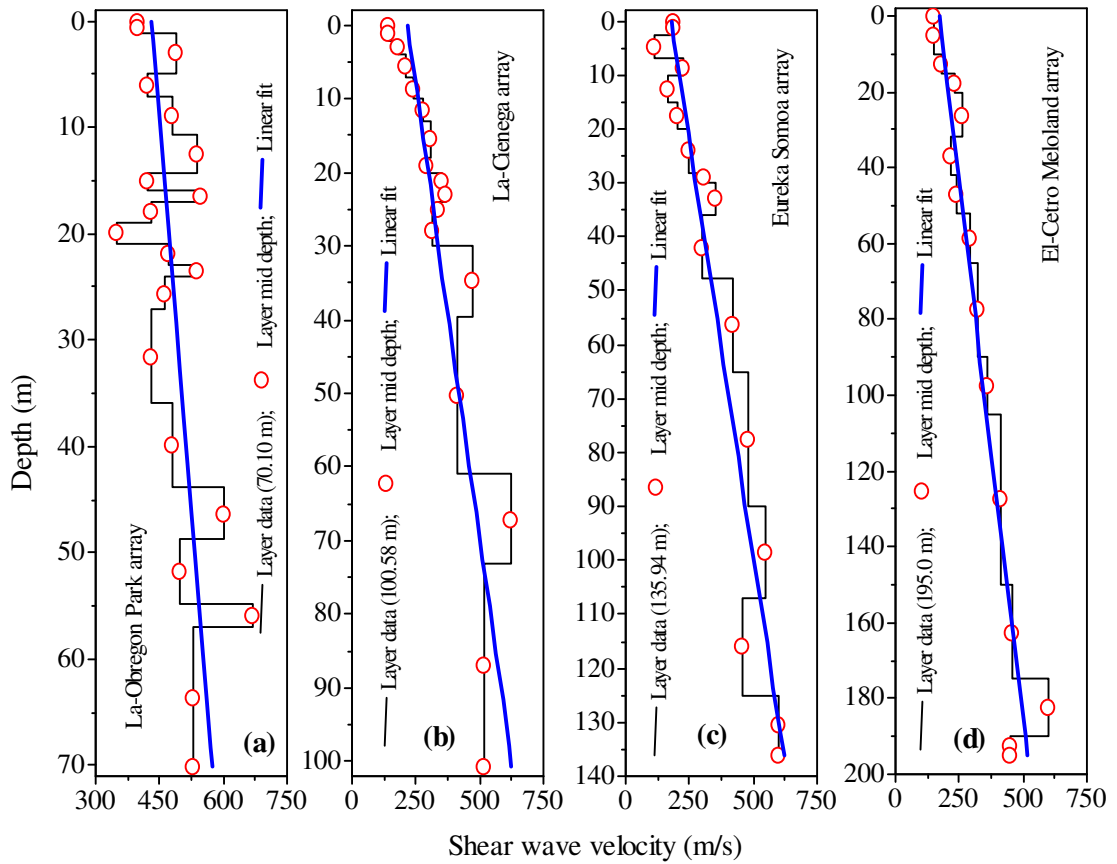
Figure 6.5: Equivalent linear shear wave velocity profile for the layered soil deposits (a) $v_{s0} = 429.03; \bar{a} = 2.078$ **, (b)** $v_{s0} = 215.601; \bar{a} = 4.078$ **, (c)** $v_{s0} = 177.839;$ $\bar{a} = 3.246$ **and (d)** $v_{s0} = 173.136; \bar{a} = 1.755$

6.4.4 Fundamental period using other methods

Fundamental periods of the four soil deposits considered above are also estimated from other five methods, discussed in sections 6.2.1 to 6.2.5 above and the results are presented here. The specimen calculations for implementation of these methods, except simplified Rayleigh's method, are illustrated in Table 6.6 for the case of La Cienega deposit. In Column (4) of Table 6.6, fundamental period is computed using average shear wave velocity of the deposit, i.e. using Eq. (6.2b) and Eq. (6.3b) respectively. In Col. (5), values computed are fundamental periods of the respective individual layer of thickness H_i and velocity v_{si}. In Column (6), summation required for Method-4 is computed. Cumulative depth up to bottom of a particular layer, i.e. sum of all individual layer thickness (H_i) up to and including i^{th} layer is computed in

301

Column (7). In Column (8 and 9), fundamental period of the deposit is computed using Madera's approach by obtaining the solution of transcendental equation (Eq. 6.6) for every layer. The values of H_a and H_b (representing thicknesses of top and bottom layers of a two layer system) are replaced with $\sum H_{i-1}$ and H_i respectively. i.e, in Eq. (6.6) the ratio H_a / H_b is replaced by $\sum H_{i-1} / H_i$ given in Column (8) against each layer starting from second layer to compute $T_{1-(i)}$ which represents the fundamental period of the deposit consisting of all layers up to and including i^{th} layer. Hence, the fundamental natural period ($T^{(5)} = T_{1-15} = 0.850$ s) of the entire soil deposit as computed from Madera's approach is mentioned at the bottom of Column (9). Summary of results of $T^{(1)}, T^{(2)}, T^{(4)}$ and $T^{(5)}$ respectively corresponding to Methods 1, 2, 4 & 5 are tabulated in last column of Table 6.6. Implementation of simplified Rayleigh's procedure is demonstrated for the case of La Cienega deposit in Table 6.7.

6.5   RESULTS AND DISCUSSION

In order to ascertain the efficiency of the proposed method over other methods, fundamental period computed from proposed method is compared with that obtained by approximate methods $[T^{(1)}, T^{(2)}, T^{(3)} \& T^{(4)}]$ and with more rigorous Madera's approach $[T^{(5)}]$. Table 6.8 summarizes results obtained from all the procedures including proposed method $[T^{(new)}]$. For the purpose of comparing these estimated results with realistic values, fundamental periods obtained from response spectrum ratio of recorded earthquake data $[T^{(EQR)}]$ and period corresponding to first peak of amplification transfer function obtained from SHAKE $[T^{(SHAKE)}]$ analysis are tabulated. Figure 6.6 compares the results obtained from different methods including proposed method with respect to fundamental period computed from recorded earthquake data as well as from SHAKE analysis. Percentage error in the fundamental period computed using approximate methods, including proposed method of the present study, with respect to $T^{(SHAKE)}$ is presented using bar graph in Figure 6.7.

Table 6.6: Specimen calculation for La-Cienega profile using methods 1, 2, 3 and 4

(1) Layer (i)	(2) depth (H_i)	(3) v_{si}	(4) $v_{si} \times H_i$	(5) $4H_i / v_{si}$ (T_i)	(6) $v_{si}^2 \times H_i$	(7) $\sum H_i$	(8) $\dfrac{\sum H_{i-1}}{H_i}$	(9) Madera (1971) (Eq. 6.7)	Summary of results of Methods 1, 2, 4 & 5
1	2.13	139.90	298.50	0.061	41760.75	2.13		$T_1 = 0.061$	Method – 1, $\left(\dfrac{4H^2}{\sum_{i=1}^{N} v_{si} H_i} \right)$ $T^{(1)} = \mathbf{0.93\ s}$
2	1.83	179.83	328.88	0.041	59142.57	3.96	1.17	$T_{1-2} = 0.095$	
3	3.05	210.01	640.10	0.058	134426.02	7.01	1.30	$T_{1-3} = 0.143$	
4	3.05	239.88	731.15	0.051	175385.77	10.06	2.30	$T_{1-4} = 0.186$	
5	3.05	279.81	852.85	0.044	238632.86	13.11	3.30	$T_{1-5} = 0.220$	
6	4.88	309.68	1510.23	0.063	467683.76	17.98	2.69	$T_{1-6} = 0.269$	Method – 2, $\left(\sum T_i \right)$ $T^{(2)} = \mathbf{1.042\ s}$
7	2.13	289.86	618.46	0.029	179268.49	20.12	8.43	$T_{1-7} = 0.296$	
8	1.83	349.91	639.92	0.021	223913.31	21.95	11.00	$T_{1-8} = 0.313$	
9	2.13	369.72	788.84	0.023	291651.71	24.08	10.29	$T_{1-9} = 0.330$	Method – 4, $\left(2\pi \sqrt{\dfrac{H^3}{3\sum_{i=1}^{N} v_{si}^2 H_i}} \right)$ $T^{(4)} = \mathbf{0.812\ s}$
10	1.83	339.85	621.52	0.022	211225.27	25.91	13.17	$T_{1-10} = 0.349$	
11	3.96	313.94	1243.97	0.050	390537.45	29.87	6.54	$T_{1-11} = 0.397$	
12	9.75	472.44	4607.99	0.083	2176999.17	39.62	3.06	$T_{1-12} = 0.429$	
13	21.34	411.48	8779.34	0.207	3612521.70	60.96	1.86	$T_{1-13} = 0.618$	
14	12.19	624.84	7618.05	0.078	4760061.91	73.15	5.00	$T_{1-10} = 0.668$	Method – 5, $\left(T_{1-15} \right)$ $T^{(5)} = \mathbf{0.850\ s}$
$N = 15$	27.43	518.16	14214.17	0.212	7365211.80	100.58	2.67	$T_{1-15} = \mathbf{0.850}$	
Sum →	**100.58**		**43493.97**	**1.042**	**20328422.54**				

303

Table 6.7: Specimen calculation for La-Cienega profile using method - 3

Layer	H_i	$H - z_{mi}$	v_{si}	$X_{i+1} = X_i + \dfrac{H - z_{mi}}{v_{si}^2}$	$(X_i + X_{i+1})^2 H_i$	$\dfrac{(X_{i+1} - X_i)^2}{H_i} v_{si}^2$
15	27.43	86.87	518.16	0.009	0.002	0.771
14	12.19	67.06	624.84	0.011	0.005	0.140
13	21.34	50.29	411.48	0.017	0.017	0.319
12	9.75	34.75	472.44	0.019	0.013	0.053
11	3.96	27.89	313.94	0.020	0.006	0.031
10	1.83	24.99	339.85	0.020	0.003	0.010
9	2.13	23.01	369.72	0.021	0.004	0.008
8	1.83	21.03	349.91	0.021	0.003	0.007
7	2.13	19.05	289.86	0.021	0.004	0.009
6	4.88	15.54	309.68	0.022	0.009	0.012
5	3.05	11.58	279.81	0.023	0.006	0.005
4	3.05	8.53	239.88	0.023	0.006	0.004
3	3.05	5.49	210.01	0.024	0.007	0.002
2	1.83	3.05	179.83	0.024	0.004	0.001
1	2.13	1.07	139.90	0.024	0.005	0.000
Σ	100.58				0.094	1.372

$$\text{Method} - 3,\ T = T^{(3)} = \pi \sqrt{\dfrac{\sum_{i=1}^{N}(X_i + X_{i+1})^2 H_i}{\sum_{i=1}^{N}\dfrac{(X_{i+1} - X_i)^2}{H_i} v_{si}^2}} = 0.822$$

Table 6.8: The fundamental periods computed from different methods

Profiles $(\rightarrow)$ / Periods $(\downarrow)$	La-Obregon Park	La-Cienega	Eureka Somoa	El-cento Meloland
$T^{(1)}$	0.568	0.930	1.341	2.184
$T^{(2)}$	0.577	1.042	1.590	2.458
$T^{(3)}$	0.559	0.822	1.248	2.011
$T^{(4)}$	0.511	0.812	1.154	1.888
$T^{(5)}$	0.548	0.850	1.136	2.597
$T^{(New)}$	0.531	0.853	1.213	2.020
$T^{(SHAKE)}$	0.555	0.834	1.188	1.956
$T^{(EQR)}$	0.565	0.835	1.190	1.895

In case of La Obregon Park deposit, shallowest deposit$(H = 70m)$ among the cases considered, the fundamental period computed from approximate methods agree closely with that of exact value [$T^{(SHAKE)} = 0.555\ s$] However, for this soil deposit the error in estimated value is largest in case of Method-4 which is close to about 8%,

whereas for all other methods, the error is less than 5%. In case of La Cienega and Eureka Somoa soil deposits ($H = 100m$ and $H = 136m$ respectively), except for Methods 1 and 2 ($T^{(1)} \& T^{(2)}$) the computed fundamental periods all other methods have yielded the results with error less than around 5%. For these two soil deposits the error associated with weighted average shear wave velocity method ($T^{(1)}$) is about 12% while it is more than 25% in case of sum layer periods method ($T^{(2)}$).
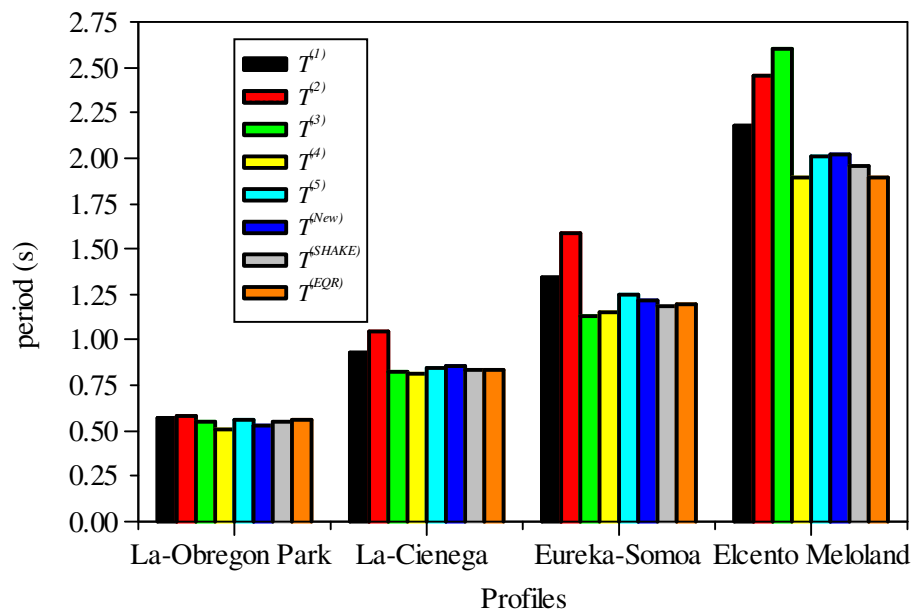
Figure 6.6: Comparison of fundamental periods computed from different methods
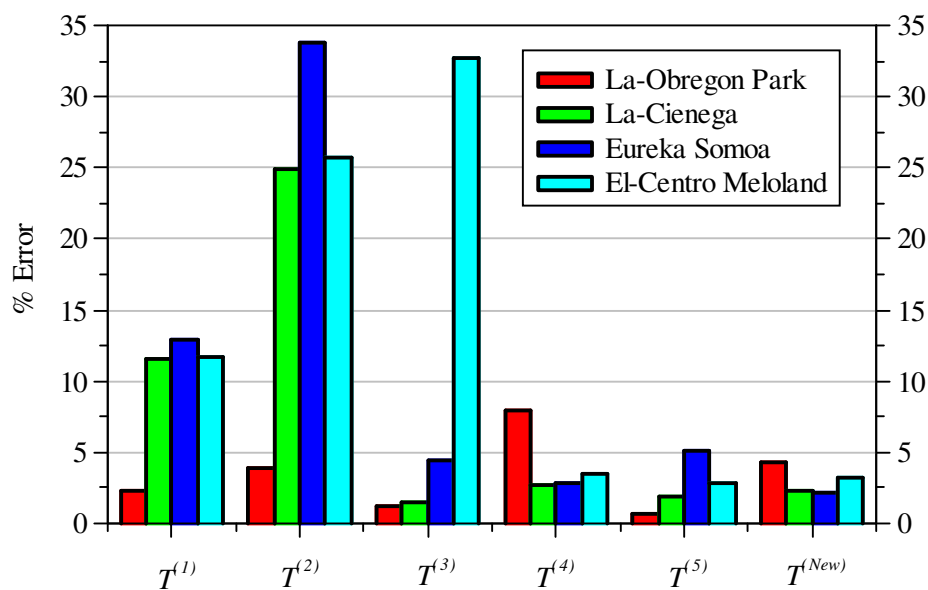
Figure 6.7: Percentage error in fundamental periods computed from different methods

The deepest soil deposit among the cases considered is El-Centro Meloland $(H = 195m)$. For this case, the error in estimated fundamental period using simplified Rayleigh's Method ($T^{(3)}$) is about 33%. It is interesting note that the fundamental period estimated using this method was close to exact value with less than 5% error in case of other three comparatively shallower soil deposits considered in this study. Hence this method appears to be inconsistent for deeper soil deposits, because mode shape resulting from first iteration of Rayleigh's method could be far from exact mode shape as depth of the soil deposit increases. Method based on assumption of linear mode shape (Method-4) is much simpler to implement and has estimated the fundamental period with better accuracy than Method-3. However, in case of La Obregon Park, the fundamental period computed using Method-4 ($T^{(4)}$) is comparatively more erroneous than other approximate methods.

Method based on successive application of exact solution for two layered system (Method-5) has predicted the fundamental period ($T^{(5)}$) within acceptable error range of about 5%. However, implementation of this method is tedious and becomes more cumbersome as number of layers associated with the soil deposit increase.

The newly proposed alternative method presented here has been able to estimate the fundamental period [$T^{(New)}$] which closely agrees with the exact values in case of all the four deposits considered in this study. The error associated with $T^{(New)}$ compared to exact value [$T^{(SHAKE)}$] are 4.32%, 2.28%, 2.10% and 3.27% respectively for La Obregon Park, La Cienega, Eureka Somoa and El Centro Meloland soil deposits. Thus, it can be concluded that the proposed method appears to be both consistent and accurate than other approximate methods yet simpler to implement than reliable but tedious procedures such as method based on successive application of two layer solution proposed by Madera (1971).

6.6   SUMMARY

Considering the importance of the fundamental period in seismic site characterisation, a simplified alternative method is proposed to estimate the fundamental period of

layered soil deposit on rigid bedrock. In this new method, the layered shear wave velocity profile of the soil deposit is approximated with an equivalent linearly varying shear wave velocity profile. An equation for the fundamental period is proposed based on closed form solution obtained for linearly varying shear wave velocity profile. The proposed method is validated by comparing its results with that of exact solution and as well as with the results computed from actual earthquake data.

The fundamental periods computed from popularly used approximate methods based on average shear wave velocity of the deposit is found to be inconsistent for relatively deeper deposits and also in case of large fluctuation in shear wave velocities along depth. The proposed method is seen to be more reliable and accurate for estimating the fundamental period of the layered soil deposits particularly for deeper deposits with significant variation in shear wave velocity profile. Further, it is observed that successive use of two layered solution is comparatively accurate but tedious to implement than the proposed method.

CHAPTER 7

CONCLUSIONS AND SCOPE FOR FUTURE STUDY

7.1   CONCLUSIONS

7.1.1 General

Reliable and consistent site response prediction for expected seismic forces is an important issue in earthquake disaster mitigation tasks. Also free-field response analysis is an integral part of the study concerned with soil structure interaction problem. Routine seismic ground response analysis in engineering practice is usually performed by modeling the ground as one-dimensional horizontally layered deposit and analysis is carried out in frequency domain. Equivalent linear (EQL) approach is used in order to account for nonlinear behaviour of soil deposit under strong seismic excitation. In most of the situations, seismic site response analysis is accomplished by employing standard curves developed and readily available in literature. Popularity of computer programs implementing EQL method is evident primarily because of its ease in implementation and interpretation of results as compared to true non-linear analysis. Though non-linear time domain method has ability to simulate dynamic response of ground, complexities involved in obtaining the realistic parameters of non-linear models makes it unpopular in routine engineering practice. The present study contributes to enhance the scope of seismic site response analysis using EQL approach by addressing the following issues.

- In the routine analysis the soil deposit is idealised as layered system though most often variations in soil properties along the depth of a soil deposit is either continuous or discretely random. Thus, within the framework of currently used popular programs, a computer program for one dimensional seismic site response analysis is developed, which can adequately model continuously or discretely inhomogeneous soil deposits instead of usual layer approximation.

- The method to compute effective strain in turn used to get strain compatible shear modulus and damping properties during the iteration process of EQL approach is ambiguous and lacks rational reasoning. Thus, an unambiguous and rational method which accounts for resulting intensity of shaking in each of the successive iterations it evolved.

- The major inconsistency of EQL approach is discrepancies in the computed response at certain frequency ranges. Major cause for this is unrealistic damping values assigned at these frequency ranges disregarding magnitude of strain associated with these frequencies. Accordingly, a scheme is proposed in which the damping value of the soil is appropriately assigned to overcome these consistencies.

- Estimation of fundamental period of soil deposit is an important prerequisite in seismic site characterisation. Hence, the possibility of extending the concept of idealizing the shear wave velocity profile as continuously varying profile to assess fundamental period of layered soil deposit is investigated. This extended study has resulted in an alternative method to estimate fundamental period of layered soil deposit.

The conclusions of the study carried out are summarized in the following sections.

7.1.2 Seismic response analysis of layered soil deposits

- Under the excitation of relatively weak input motion, the results of frequency domain and time domain linear analyses are in good agreement. Spectral characteristics of the computed response clearly reveal the effect of frequency content of the input motion.

- Spectral characteristics of the responses computed for relatively strong input motion indicate that the high frequency response from EQL analysis is always underestimated compared to that of time domain nonlinear analysis. Frequency range at which underestimation of response sets off appears to be consistently associated with the frequency content of the input motion and modal characteristics of the soil deposit.

- The response of the soil deposit excited by means of two input motions with distinctly different frequency characteristics but normalized to same relatively low maximum acceleration is equally sensitive to spectral characteristics of the input motion and plasticity index (PI) of the soil. Though large difference is observed in computed peak surface acceleration for different PI values, spectral amplitudes of their corresponding response spectra appears to be having negligible difference.

7.1.3   Seismic response of continuously inhomogeneous soil deposit

- As the impedance of the layer decreases, wave energy dissipated in that layer increases. However, the wave amplitude increases as the impedance of a layer decreases relative to base layer. Since amplification of wave amplitude is sensitive to layer impedances, the importance of appropriate idealization of the shear wave velocity profile of the soil deposit becomes evident.

- The decrease in contrasting impedance ratio tends to be insignificant after certain limiting number of layers used to approximate the continuously varying shear wave velocity profile.

- As impedance ratio between inhomogeneous soil deposit and underlying bedrock increases, the maximum amplification decreases. The troughs of the amplification transfer function are shifted upward signifying much of the energy is reflected back into the flexible half-space.

- In rigid bedrock underlying an inhomogeneous deposit, irrespective of degree of inhomogeneity the maximum amplification is unaltered. However, the modal frequencies of the deposit are dependent on degree of inhomogeneity. Thus, the current practice of modeling the bedrock as rigid when input motion is prescribed at the base of the deposit (within motion) not only overestimates the response at resonant frequencies but also affects the spectral characteristics of the computed response.

- The response of continuously inhomogeneous deposits is sensitive to impedance ratio between surface layer and bedrock, damping ratio, inhomogeneity parameters such as shear wave velocity ratio $\left(v_{sH} / v_{s0} \text{ or } G_H / G_0 \right)$ and degree of inhomogeneity defined by power $(m \text{ or } n)$ of the inhomogeneity function.

- The parametric study carried out indicates that the prediction of high frequency response can be improved without affecting much of the lower mode responses. The appropriate configuration of Gibson layers can be effectively used to represent continuously inhomogeneous soil deposits instead of approximating them with a stack of homogeneous layers.

- In order to compare the implications of idealizing the deposit with continuous and layered profiles, soil deposit and recoded earthquake data of La-Cienega and El-Centro Meloland geotechnical array sites (USA) are considered. Results of idealisation with more number of layers indicating continuous variation in soil properties is found to be closer to reality than those with less number of layers. The results clearly demonstrate that the high frequency response characteristics are very much sensitive to layer configuration particularly contrasting impedance ratios between the layers.

7.1.4 Computer program SRISD

- The computer program SRISD developed is tested and validated by comparing its output with analytical closed form solutions of continuously inhomogeneous soil deposits and layered deposits responses computed using SHAKE analysis. The unique features of SRISD are:

  – Three options are provided to input profile data of the soil deposit.

  – An option may be chosen to vary either shear modulus and/or damping in successive iterations.

  – Refined options for selecting the method for computing effective strain are incorporated.

312

- The frequency dependent equivalent linear analysis can be chosen by opting either frequency dependent damping model proposed by Darendeli (2001) or frequency dependent analysis model proposed in this study.

7.1.5 Refinements to equivalent linear analysis

- It has been shown that the maximum acceleration response, amplification transfer function and Fourier amplitude spectra of the computed surface accelerogram all these response quantities are sensitive to chosen value of R.

- The advantage of the proposed method for computing effective strain is that, the user intervention is completely avoided in the calculation of effective strain because program itself updates the value of R by assigning appropriate value at every node in successive iterations based on intensity of shaking in the previous iteration.

- The proposed alternative method for computation of R-value is as reliable as routine method in satisfying the convergence criteria of the EQL analysis. It can be easily accommodated within the framework of frequency domain equivalent linear analysis computer programs.

- Accounting for the effect of radiation damping considerably enhances the quality of the predicted response at the fundamental frequency of the deposit comparing well with that of time domain nonlinear response.

- In order to verify all the proposed improvements, a case study related to a downhole geotechnical array [TKCH08 (KIK-net)] of Japan is presented. It is evident that both correlation coefficient (r) and efficiency coefficient (E) are more for frequency dependent EQL analysis with shear wave velocity profile being idealised with a continuous function compared to results obtained for routine EQL analysis with layered shear wave velocity profile as presented in the table below. Hence it can be concluded that, proposed recommendations are able to effectively improve the predictability of frequency domain EQL analysis.

313

Acceleration time history response at the surface of the soil deposit from the downhole geotechnical array TKCH08 (KIK-net) of Japan				
Input motion	NS – horizontal component		EW – horizontal component	
Analysis	r	E	r	E
Layered profile – Frequency independent routine EQL analysis	0.623	0.453	0.594	0.466
Continuous profile – Frequency dependent EQL analysis	0.637	0.472	0.643	0.512
Response spectra of acceleration time history response				
Layered profile – Frequency independent routine EQL analysis	0.948	0.888	0.868	0.724
Continuous profile – Frequency dependent EQL analysis	0.950	0.900	0.955	0.906

7.1.6   Fundamental period layered soil deposit

- Considering the importance of the fundamental period in seismic site characterisation, an alternative method is proposed to estimate the fundamental period of layered soil deposit on rigid bedrock. The proposed method is validated by comparing its results with exact values of fundamental periods of four natural soil deposits and it is shown to be acceptable for a wide range of depths of soil profiles ranging from 70 m to 195 m, however the other approximate methods show wide scatter in the fundamental period with increase in depth of deposit.

7.2   SCOPE FOR FUTURE STUDY

The concept of approximating the randomly inhomogeneous soil deposit as continuously inhomogeneous deposit in seismic response analysis seems to be promising in overcoming uncertainties in the predicted response particularly with respect to idealization of shear wave velocity profile. However the present study is limited to frequency domain equivalent linear analysis, hence this concept may be extended to time domain nonlinear analysis.

In the present study frequency dependent damping is modeled by incorporating radiation damping to reduce the response near fundamental frequency of the deposit. The number of modes to be considered is arrived based on the observations of limited parametric study. Elaborate parametric study may be carried out to relate radiation damping to modal frequencies of the deposit and frequency characteristics of the input motion. Thus one may propose an unbiased method to assign the frequency range for which radiation damping effect is to be considered in the analysis.

In the present study the radiation damping accounting for energy dissipation only in the half-space (elastic bedrock) underlying the soil deposit is considered. The magnitude of damping additionally introduced is in proportional to fundamental frequency of the deposit, which is computed based average shear wave velocity of the soil deposit. However further investigation needs to be taken up to consider the radiation damping effect more realistically with due consideration to energy dissipated at the interfaces of all the layers due to reflection of waves depending upon corresponding impedance ratio at the interface.

Currently available data with respect to frequency dependency of shear modulus and damping ratio is widely scattered and contradictory. Once the effect of excitation frequency on dynamic soil properties is clearly established more rational frequency dependent equivalent linear analysis schemes can be incorporated into the computer program developed in this study.

The concept of equivalent linear shear wave velocity idealisation appears to be efficient in estimating the modal characteristics of layered soil profile. Application of this concept to estimate amplification characteristics of the layered soil deposit may be explored to develop empirical ground motion prediction equations to incorporate in code of practice, thus overcoming the unrealistic modeling of discontinuity at layer interfaces leading to contrasting layer impedances.

REFERENCES

- Ambraseys N. N. (1959) "A Note on the Response of an Elastic Overburden of Varying Rigidity to an Arbitrary Ground Motion", Bulletin of the Seismological Society of America, vol.49, No. 3, pp 211-220

- Andrus, R. D., Mohanan, N. P., Piratheepan, P., Ellis, B. S., and Holzer, T. L. (2007), "Predicting shear-wave velocity from cone penetration resistance", 4th International Conference on Earthquake Geotechnical Engineering, Greece, June 25-28, Paper No. 1454.

- Ansal, A., İyisan, R. and Yildirim, H. (2001) "The cyclic behaviour of soils and effects of geotechnical factors in microzonation", Soil Dynamics and Earthquake Engineering, Vol. 21, pp. 445-452.

- Ansal, A., Kurtulus, A. and Tönük, G. (2010), "Seismic microzonation and earthquake damage scenarios for urban areas", Soil Dynamics and Earthquake Engineering, Vol. 30, pp. 1319-1328

- Afra, H. and Pecker, A. (2002), "Calculation of free field response spectrum of a non-homogeneous soil deposit from bedrock response spectrum", Soil Dynamics and Earthquake Engineering, Vol. 22, pp. 157-165.

- Arulanandan, K., Li, X. S., and Sivathasan, K. (2000), "Numerical simulation of liquefaction-induced deformation", Journal of Geotechnical and Geo-environmental Engineering, ASCE, Vol. 126, pp. 657-666

- Assimaki, D., Kausel, E. and Whittle, A. (2000) "Model for dynamic shear modulus and damping for granular soils", Journal of Geotechnical and Geo-environmental Engineering, ASCE, Vol. 126, No. 10, pp 859-869.

- Atkinson K. (1984), "Elementary numerical analysis", John Wiley & Sons Inc, New York, USA.

- Bard P.Y. and M. Bouchon (1985), "The two-dimensional resonance of sediment filled valleys", Bulletin of Seismological Society of America, Vol. 75, pp. 519-541.

- Bardet J. P., K. Ichii, and C. H. Lin (2000), "EERA - A Computer Program for Equivalent-linear Earthquake site Response Analyses of Layered Soil Deposits", Department of Civil Engineering, University of Southern California, Los Angeles, USA.

- Bardet J.P. and Tobita T. (2001) "NERA - A Computer Program for Nonlinear Earthquake Response Analysis of Layered Soils Deposits", Report prepared at Department of Civil Engineering, University of Southern California, Los Angeles, USA.

- Bathe K. J., and Wilson E. L. (1987), "Numerical methods in finite element analysis", Prentice-Hall of India Pvt. Ltd., New Delhi.

- Benuska, L. (editor), (1990). "Loma Prieta Earthquake Reconnaissance Report: Chap. 4, Geotechnical aspects", EERI, Earthquake Spectra, Supplement to Vol. 6, pp 81-125.

- Beresnev, I. A. and Wen K. L (1996), "Nonlinear soil response--A reality?", Bulletin of Seismological Society of America, Vol. 6, pp. 1964-1978.

- Berrill, J.B. (1977), "Site effects during the San Fernando, California, earthquake", Proceedings of the Sixth World Conference on Earthquake Engineering, India, pp. 432-438.

- Bertero, V. (1989) "The 19 September 1985 Mexico earthquake: Building behavior", Report No. UCB/EERC 86-08, Earthquake Engineering Research Center, University of California, Berkeley.

- Bielak, J., Hisada, Y., Bao, H., Xu, J. N., and Ghattas, O. (2000) "One- vs. Two- or Three-Dimensional Effects in Sedimentary Valleys", 12th World Conference Earthquake Engineering, New Zealand, paper no. 2689.

- Bolisetti, C., Whittaker, A. S., Mason, H. B., Almufti, I. and Willford, M. (2014), "Equivalent linear and nonlinear site response analysis for design and risk assessment of safety-related nuclear structures", Nuclear Engineering and Design, Vol. 275, Elsevier, pp. 107-121.

- Boore D. M. (2003), "A compendium of P- and S-wave velocities from surface-to-borehole logging: Summary and reanalysis of previously published data and analysis of unpublished data", U.S. Geological Survey Open-File Report 03 -191. http://geopubs.wr.usgs.gov/open-file/of03-191/ (Accessed on April, 2010)

- Boore D. M., J. F. Gibbs, W. B. Joyner, J. C. Tinsley, and D. J. Ponti (2003), "Estimated ground motion from the 1994 Northridge, California, earthquake at the site of the interstate 10 and La Cienega boulevard bridge collapse, West Los Angeles, California", Bulletin of the Seismological Society of America, Vol. 93, No. 6, pp. 2737–2751.

- Boore D.M. (2004) "Can Site Response be Predicted?", Journal of Earthquake Engineering, Imperial College Press Vol. 8, Special Issue 1 (2004), pp. 1–41.

- Boore D.M. (2006), "Determining subsurface shear-wave velocities: A review", Third International Symposium on the Effects of Surface Geology on Seismic Motion, Grenoble, France, 30 August - 1 September 2006, Paper No. 103

- Borcherdt, R. D. and Gibbs, J. F. (1976). "Effects of local geologic conditions in the San Francisco Bay region on ground motions and the intensities of the 1906 earthquake", Bulletin of Seismological Society of America, Vol. 66, pp. 467-500.

- Borcherdt, R. D., and Glassmoyer, D. (1992), "On the characteristics of local geology and their influence on ground motions generated by the Loma Prieta earthquake in the San Francisco Bay region.", Bulletin of Seismological Society of America, Vol. 82, pp. 603-641.

- Bray, J. D., Gookin, W. B. and Riemer, M. F. (1999) "On the dynamic characterization of soils", Earthquake Geotechnical Engineering, by Sêco e Pinto (Editor), Balkema, Rotterdam.

- Brown L T., Boore, D. M. and Stokoe K. H. (2002), "Comparison of shear-wave slowness profiles at 10 strong-motion sites from noninvasive SASW measurements and measurements made in boreholes", Bulletin of the Seismological Society of America, Vol. 92, No. 8, pp. 3116–3133.

- California Strong Motion Instrumentation Program (CSMIP), Website: //ftp.consrv.ca.gov/_pub/dmg/csmip/GeotechnicalArrayData (Accessed on 27th April, 2012)

- Cameron, W. L. and Green, R. A. (2004) "Soil nonlinearity versus frequency effects", Opinion Paper, International Workshop on the Uncertainties in Nonlinear Soil Properties and their Impact on Modeling Dynamic Response, March 18-19, PEER Headquarters, UC Berkeley.

- Carvajal, J. C., Taboada-Urtuzuástegui, V. M. and Romo, M. P. (2002), "Influence of earthquake frequency content on soil dynamic properties at CAO site", Soil Dynamics and Earthquake Engineering, Vol. 22, pp 297-308.

- Center for Engineering Strong Motion Data (CESMD), Website: http://www.strongmationcenter.org/cgi-bin/CESMD/ (Accessed on, 22th May, 2012)

- Chang, D. W., Roesset, J. M. and Wen, C. H. (2000), "Time-domain viscous damping model based on frequency-dependent damping ratios", Soil Dynamics and Earthquake Engineering, Vol. 19, pp. 551-558.

- Chapra, S. C and Canale, R. P. (1998), "Numerical Methods for Engineers: with Programming and Software applications", 3rd Edition, McGraw-Hill Book Co., Singapore.

- Chen, X. and Chandra, N. (2004), "The effect of heterogeneity on plane wave propagation through layered composites", Composites Science and Technology, Vol. 64, No. 10-11, pp. 1477-1493.

- Chenari J. R., Taheri A. A. and Davoodi M. (2012), "Uncertainty in fundamental natural frequency estimation for alluvial deposits", Computational methods in Civil Engineering, Vol. 3, No. 1, pp. 77-94.

- Cherry, S. (1974), "Estimating underground motions from surface accelerograms", in Engineering Seismology and Earthquake Engineering by Solnes, J. (Editor)), NATO Advanced study institute series, Applied sciences, No.3, pp. 125-150.

- Chin, B. and Aki, K. (1991), "Simultaneous study of the source, path, and site effects on strong ground motion during the 1989 Loma Prieta earthquake: A preliminary result on pervasive nonlinear site effects", Bulletin of Seismological Society of America, vol. 81, 1859-1884.

- Ching, J. Y. and Glaser, S. D. (2001), "1D Time-domain solution for seismic ground motion prediction", Journal of Geotechnical and Geo-environmental Engineering, ASCE, Vol. 127, pp. 36-47.

- Chopra, A. K. (1995), "Dynamics of Structures: Theory and Applications to Earthquake Engineering", Prentice Hall of India Pvt. Ltd., New Delhi.

- Clough, R. W and Penzien, J. (1993), "Dynamics of Structures", 2nd Edition, McGraw-Hill Book Co., Singapore.

- Constantopoulos, I. V., Roësset, J. M. and Christian, J. T. (1973), "A comparison of linear and exact nonlinear analysis of soil amplification", Fifth World Conference on Earthquake Engineering., Rome, Session No. 5B, Paper No. 225.

- Dakoulas, P. and Gazetas, G. (1985), "A class of inhomogeneous shear models for seismic response of dams and embankments", Soil Dynamics and Earthquake Engineering, Vol. 4 (4), pp. 166-182.

- Darendeli, M. B. (2001), "Development of a new family of normalized modulus reduction and material damping curves." PhD dissertation, Univ. of Texas at Austin, Austin, USA.

- Davis R. O. (1994), "Effects of weathering on site amplification calculations", Proceedings of 8th International conference on computer methods and advances in Geomechanics, (Eds. Siriwardane H.J. and M. M. Zaman) May, 1994, USA, pp. 117-123

- Davis, R. O. (1995), "Effects of weathering on site response", Earthquake Engineering and Structural Dynamics, Vol. 24, 1995, pp. 301-309.

- Davis, R. O. and Hunt, B. (1994), "Amplification of vertically propagating SH waves by multiple layers of Gibson soil", International Journal for Numerical & Analytical Methods in Geomechanics, Vol. 18, 1994, pp. 205-212.

- Davis, R. O. and J. B. Berrill (1998), "Rational approximation of stress and strain based on downhole acceleration measurements", International Journal for Numerical and Analytical Methods in Geomechanics, Vol. 22, pp. 603-619.

- Dickenson, S. E., Ferritto, J., Kaldveer, P. and Soydemir, C. (1998), "Seismic and geologic hazards", in Seismic guidelines for ports, by S.D. Werner (Editor), ASCE, Technical council on lifeline earthquake engineering, Monograph No. 12, pp. 4.1-4.64.

- Dickenson, S. E., Seed, R. B., Lysmer, J. and Mok, C. M. (1991), "Response of soft soils during the 1989 Loma Prieta earthquake and implications for seismic design criteria", Proceedings of the 4th Pacific conference on Earthquake Engineering, Vol. 3, pp 191-204.

- Dobry, R, I., Oweis, I. and Urzua A. (1976), "Simplified procedures for estimating the fundamental period of a soil profile", Bulletin of Seismological Society of America, Vol. 66, pp 1293 – 1321.

- Dobry, R. (2013), "Radiation damping in the context of one-dimensional wave propagation: A teaching perspective", Soil Dynamics and Earthquake Engineering, Vol. 47, pp 51-61.

- Dobry, R. (2014), "Simplified methods in soil dynamics", Soil Dynamics and Earthquake Engineering, Vol. 61-62, pp 246-268.

- Dobry, R. and Vucetic, M. (1987). "Dynamic properties and seismic response of soft clay deposits.", Proceedings, International Symposium on Geotechnical Engineering of Soft Soils, Mexico City, Vol.2, pp.51-87.

- Dobry, R., Martin, G. R., Parra, E. and Bhattacharyya, A. (1994) "Development of site-dependent ratios of elastic response spectra (RRS) and site categories for building seismic codes", Proceedings of the1992 NCEER/SEAOC/BSSC Workshop on Site Response During Earthquakes and Seismic Code Provisions, G.R. Martin, (Editor)., University of Southern California, Los Angeles, November 18-20, 1992, Special Publication NCEER-94-SP01, Buffalo, NY.

- Douglas, J. F, Gasiorek, J. M. and Swaffield, J. A. (2003), "Fluid mechanics", 4th Edition (II Indian reprint), Pearson Education Pvt. Ltd. (Singapore), New Delhi, India.

- Drosos, V. A., Gerolymos, N. and Gazetas, G. (2012), "Constitutive model for soil amplification of ground shaking: Parameter calibration, comparison, validation", Soil Dynamics and Earthquake Engineering, Vol. 42, pp 255-274.

- Elgamal, A. W., Zeghal, M., Tang H. T. and Stepp J. C. (1995), "Lotung downhole array. I: Evaluation of site dynamic properties", Journal of Geotechnical Engineering Division, ASCE, Vol. 121, pp. 350-362.

- EPRI (1993), "Guidelines for determining design basis ground motions", Electric Power Research Institute, Palo Alto, California , Report No. TR-102293, Vol.2.

- Erdik, M. O. (1987), "Site response analysis", in Strong Ground Motion Seismology by M. O. Erdik and M. N. Toksöz (Editors), D. Reidel Publishing Company, Dordrecht, 479-534.

- Eurocode-EC8 (2004), "BS EN 1998-1: Design of structures for earthquake resistance- Part 1: General rules, seismic actions and rules for buildings", British Standard (BS), UK.

- FEMA-P-749 (2010), "Earthquake-resistant design concepts - An introduction to the NEHRP recommended seismic provisions for new buildings and other structures", Federal Emergency Management Agency Report, By the National Institute of Building Sciences Building Seismic Safety Council, Washington DC, USA

- Ferritto, J., Dickenson, S., Priestley, N., Werner, S. and Taylor, C. (1999), "Characterization of regional seismicity and ground shaking", Chapter-1 in Technical Report TR-2103-SHR (Vol. 1), Naval Facilities Engineering Service Center, California, USA, pp 1-47.

- Field, E. H., Johnson, P. A., Beresnev, I. A., and Zeng, Y. (1997). "Nonlinear ground motion amplification by sediments during the 1994 Northridge earthquake." Nature, Vol. 390, pp. 599-602.

- Finn, W. D. L. (1988), "Dynamic analysis in geotechnical engineering", in Earthquake Engineering Soil Dynamics II: Recent Advances in Ground – Motion Evaluation, Lawrence Von Thun J. (Editor), ASCE, Geotechnical Special Publication, 20, pp. 523-591.

- Finn, W. D. L. (1999), "Evolution of dynamic analysis in geotechnical earthquake engineering", Workshop on New Approaches to Liquefaction Analysis, Fhwa-RD-99-165, http://ntl.bts.gov/lib/7000/7500/7518/finn.pdf (Accessed on 16-Aug-2008).

- Finn, W. D. L., Lee, M. K. W. and Martin, G. R. (1977), "An effective stress model for liquefaction", Journal of Geotechnical Engineering Division, ASCE, Vol. 103, pp. 517-553.

- Finn, W. D. L., Martin, G. R. and Lee, M. K. W (1978), "comparison of dynamic analysis for saturated sands", ASCE Geotechnical Engineering Division Specialty Conference, Pasadena, California, June 1978, pp. 472-491.

- Frankel A. (1993) "Three-dimensional simulations of ground motions in the San Bernardino Valley, California, for hypothetic earthquakes on the San Andreas fault", Bulletin of Seismological Society of America, Vol. 83, pp. 1020-1041.

- Frankel, A. and Vidale, J.E. (1992) "A three dimensional simulation of seismic waves in the Santa Clara Valley, California from a Loma Prieta aftershock", Bulletin of Seismological Society of America, Vol. 82, pp. 2045-2074.

- Furumoto, Y., Sugito, M. and Yashima A. (2000) "Frequency-dependent equivalent linearized technique for FEM response analysis of ground" , 12th WCEE (2000), Auckland, New Zealand, paper no. 1806/5/A (CD-ROM)

- Furumoto, Y., Sugito, M., Yashima, A. and Fukagawa Y. (1999) "Time dependent ground motion amplification due to liquefaction on man-made island", 7th US-Japan Workshop on Earthquake Resistant Design of life Line Facilities and Constructions against Liquefaction, Seatle, USA 1999.

- Gazetas, G. (1981), "Torsional displacements and stresses in non-homogeneous soils", Géotechnique, Vol. 31, No.4, pp. 487-496.

- Gazetas, G. (1982), "Vibrational characteristics of soil deposits with variable wave velocity", International Journal for Numerical & Analytical Methods in Geomechanics, Vol. 6, 1982, pp. 1-20

- Gibson, R. E. (1974), "The analytical method in soil mechanics", 14th Rankine lecture, Geotechnique, Vol. 24, No.2, pp. 115-140

- Gookin, W. B., Bray, J. and Riemer, M. (1999) "The Combined Effects of Loading Frequency and other Parameters on Dynamic Properties of Reconstituted Cohesive Soils", UC Berkeley Geotechnical Engineering Report No. GT/99-14.

- Graizer, V., Shakal, A. and Hipley, P. (2000), "Recent data recorded from downhole geotechnical arrays", Proceedings of SMIP2000 Seminar on Utilization of Strong-Motion Data, Sept. 12, California, pp. 23-38.

- Guttenberg, B. and Richter, C. F. (1956), "Earthquake magnitude, intensity, energy and acceleration", Bulletin of the Seismological Society of America, Vol. 32, pp 163-191.

- Hadid, M. and Arfa, H. (2000), "Sensitivity analysis of site effects on response of pipelines", Soil Dynamics and Earthquake Engineering, Vol. 20, pp. 249-260.

- Hadjian A.H. (2002), "Fundamental period and mode shape of layered soil profiles", Soil Dynamics and Earthquake Engineering, Vol. 22, pp 885 – 891.

- Hardin, B. O. and Drnevich, V. P. (1972a), "Shear modulus and damping in soils: Measurement and parameter effects", Journal of Soil Mechanics and Foundation Engineering Division, ASCE, Vol. 98 No. SM6, pp 603-624.

- Hardin, B. O. and Drnevich, V. P. (1972b), "Shear modulus and damping in soils: Design equations and curves", Journal of Soil Mechanics and Foundations Division, ASCE, Vol. 98, No. SM7, pp. 667-692.

- Hardin, B.O. and Richart, F.E. (1963) "Elastic Wave Velocities in Granular soils", Journal of Soil Mechanics & Foundations Division, ASCE, Vol. 89, February, pp 33-65.

- Hashash, Y. M. A. (2011), "DEEPSOIL V 5.0, Tutorial and User Manual", University of Illinois at Urbana-Champaign, Urbana, Illinois.

- Hashash, Y. M. A. and Park, D. (2001), "Non-linear one dimensional seismic ground motion propagation in the Mississippi embayment", Engineering Geology, Vol. 62, pp 185-206.

- Hashash, Y. M. A. and Park, D. (2002), "Viscous damping formulation and high frequency motion propagation in non-linear site response analysis", Soil Dynamics and Earthquake Engineering, Vol. 22, pp. 611–624.

- Hashash, Y. M. A., Phillips, C. and Groholski, D. R. (2010), "Recent advances in non-linear site response analysis", Paper No. OSP 4, Fifth International Conference on Geotechnical Earthquake Engineering and Soil Dynamics, May 24-29, 2010, San Diego, California, USA.

- Haskel, N. A. (1953), "The dispersion of surface waves on multilayered media", Bulletin of Seismological Society of America, Vol. 43, No. 1, pp. 17-34.

- Haskel, N. A. (1960), "Crustal reflections of plane SH waves", Journal of Geophysics research, Vol. 65, pp. 4147-4150.

- Hershberger, J. (1956), "A comparison of earthquake accelerations with intensity ratings", Bulletin of the Seismological Society of America, Vol. 46, pp 317-320.

- Holzer, T. L. (1994), "Loma Prieta damage largely attributed to enhanced ground shaking." American Geophysical Union (EOS), Vol. 75, pp. 299-301.

- Hŕyeiw, R. D. (1989), "Ray-path curvature in shallow seismic investigations", Journal Geotechnical Engineering, ASCE, Vol. 115, No. 9, pp. 1258-1284.

- Idriss, I. M. (1990), "Response of soft soil sites during earthquakes", Proceedings of H.B. Seed Memorial Symposium at UCB California, USA, Vol. 2, pp. 273-289.

- Idriss, I. M. (1991) "Earthquake Ground Motions at Soft Soil Sites", Proceedings, 2nd International Conference on Recent Advances in Geotechnical Earthquake Engineering and Soil Dynamics, March 11-15, St. Louis, Missouri, pp 2265-2272.

- Idriss, I. M. and Seed, H. B. (1967), "Response of horizontal soil layers during earthquakes", Report no. UCB-GT-67-01, Soil mechanics and bituminous materials laboratory, Department of Civil Engineering, University of California, Berkeley. USA. p.88.

- Idriss, I. M. and Seed, H. B. (1968), "Seismic response of horizontal soil layers", Proceedings of the ASCE, Journal of Soil Mechanics and Foundation Division, Vol. 94, pp 1003-1031.

- Idriss, I. M. and Sun, J. I. (1992), "Users manual for SHAKE91: A computer program for conducting equivalent linear seismic response analyses of horizontally layered soil deposits", Center for Geotechnical Modeling, Department of Civil & Environmental Engineering, University of California, Davis, California, USA.

- Idriss, I. M., Lysmer, J., Hwang, R. and Seed, H. B. (1973), "QUAD-4: A computer program for evaluating seismic response of soil-structures variable finite element procedures", Report No. UCB/EERC 73-16, Earthquake Engineering Research Center, University of California, Berkeley.

- Inaudi, J. A. and Kelly, J. M. (1995), "Linear hysteretic damping and the Hilbert transform", ASCE, Journal of Engineering Mechanics Division, ASCE, Vol. 121, pp. 626-632.

- Inaudi, J. A. and Markis, N. (1996), "Time-domain analysis of linear hysteretic damping", Earthquake Engineering and Structural Dynamics, Vol. 25, pp. 529-545.

- IS 1893 - Part 1 (2002), "Criteria for earthquake resistant design of structures: General provisions and buildings", Bureau of Indian Standards (BIS), New Delhi, India.

- Isenhower W. M. and Stokoe K. H. (1981), "Strain rate dependent shear modulus of San Francisco bay mud", Proceedings of International Conference on Recent Advances in Geotechnical Earthquake Engineering and Soil Dynamics, St. Louis, Missouri, Vol. 2, pp 182-191.

- Ishibashi, I. and Zhang, X. (1993). "Unified Dynamic Shear Moduli and Damping Ratios of Sand and Clay," Soils and Foundations, Vol. 33, No. 1, pp.182-191.

- Ishihara, K. (1996), "Soil Behaviour in Earthquake Geotechnics", Clarendon press, Oxford.

- Ishihara, K. and Towhata, I. (1982), "Dynamic response analysis of level ground based on the effective stress method", in Pande, G. N. and Zienkiewicz, O. C. (Editors), Soil mechanics – transient and cyclic loads, Wiley, New York, pp 133–172.

- Jeong, C. G., Park, D. and Hashash, Y. M. A. (2008), "Simulation of rate dependent soil behavior in one-dimensional seismic wave propagation", Proceedings, 15th International Congress on Sound and Vibration, 6-10 July, Daejeon, Korea, pp. 1275-1282.

- Jiang, T. and Kuribayashi, E. (1988), "The three-dimensional resonance of axi-symmetric sediment-filled valleys", Soils and Foundations, No.4, Vol. 28, pp 130-146.

- Johnson, R. A. (2000) "Probability and Statistics for Engineers", 6th Edition, Pearson Education, Inc. India.

- Joyner, W. B. (1975) "A method for calculating nonlinear seismic response in two dimensions", Bulletin of Seismological Society of America, Vol. 65, pp. 1337-1357.

- Joyner, W. B. and Boore, D. M. (1988), "Measurement, characterization, and prediction of strong ground motion", Earthquake Engineering and Soil Dynamics II – Recent Advances in Ground Motion Evaluation, *Geotechnical Special Pub.-20*, ASCE, pp. 43-102.

- Joyner, W. B. and Chen, A. T. F. (1975), "Calculation of nonlinear ground response in earthquakes", Bulletin of Seismological Society of America, Vol. 65, pp. 1315-1336.

- Kaklamanos, J. (2012), "Quantifying uncertainty in earthquake site response models using the KiK-net database", Ph.D. dissertation submitted to Department of Civil and Environmental Engineering, Tufts University, USA.

- Kaklamanos, J., Bradley, B. A., Thompson, E. M. and Baise L. G. (2013), "Critical parameters affecting bias and variability in site-response analyses using KIK-net downhole array data", Bulletin of the Seismological Society of America, Vol. 103, No. 3, pp. 1733–1749

- Kaklamanos, J., Thompson, E. M., Baise, L. G. and Dorfmann, L. (2011), "Identifying and modeling complex site response behavior: Objectives, preliminary results, and future directions", Proceedings of the NSF Engineering Research and Innovation Conference, Atlanta, Georgia. 4-7 Jan 2001.

- Kaufman, H. (1953), "Velocity functions in seismic prospecting", Geophysics, Vol. 18, pp 289-297.

- Kausel, E. and Assimaki, D. (2002) "Seismic simulation of inelastic soils via frequency-dependent moduli and damping", Journal of Engineering Mechanics Division, ASCE, 128, pp 34-47.

- Khan, Z., G., Cascante, M. H., El Naggar, and Lai, C. G. (2008), "Measurement of frequency dependent dynamic properties of soils using the resonant column device" Journal of Geotechnical and Geo-environmental Engineering, ACSE Vol. 134, No. 9, pp 1319–1326.

- Khose, V. N., Singh, Y. and Lang, D. (2010), "Limitations of Indian seismic design codes for RC buildings", Proceedings of 14th Symposium on Earthquake Engineering, *D*ecember 17-19, Indian Institute of Technology – Roorkee, India, pp. 1416-1423.

- Kiban – Kyoshin network (KiK-Net), National Research Institute for Earth Science and Disaster Prevention, Japan, *http://www.kyoshin.bosai.go.jp/,* (Accessed on 14th August, 2014)

- Kim D. S., Stokoe K. H., and Hudson W. R. (1991), "Deformational characteristics of soils at small to intermediate strains from cyclic tests", Research Rep. No. 1177-3, Center for Transportation Research, Bureau of Engineering Research, University of Texas at Austin, pp 1-42.

- King, J. L. and Tucker, B. E. (1984) "Observed variations of earthquake motions across a sediment-filled valley", Bulletin of Seismological Society of America, Vol. 74, No. 1, pp.137-151.

- Kokusho, T. and Yoshida, Y. (1997) "SPT-N value and S-wave velocity for gravelly soils with different grain size distribution," Soils and Foundations, JSSMFE, Vol. 37 (4), pp. 105-113.

- Kokusho, T., Tohma, J., Yajima, H., Tanaka, Y., Kanatani, M. and Yasuda, N. (1992), "Seismic response of soil layer and its dynamic properties", Proceedings of the Tenth World Conference on Earthquake Engineering, Madrid, Spain, Vol. XI, pp. 6671-6680.

- Kottke, A. R. and Rathje, E. M. (2008), "Technical Manual for Strata", Report No. 2008/10 Pacific Earthquake Engineering Research Center, College of Engineering, University of California, Berkeley, p. 81.

- Krahn, J. and Fredlund, D. G. (1983), "Variability in the engineering properties of natural soil deposits", Fourth International Conference on Application of Statistics and Probability in Soil and Structural Engineering, 13-17, June 1983, Florence, Italy.

- Kramer, S. L. (1996), "Geotechnical earthquake engineering", Prentice Hall International Publication, 1996.

- Kramer, S. L. and Paulsen, S. B. (2004), "Practical Use of Geotechnical Site Response Models", International Workshop on Uncertainties in Nonlinear Soil Properties and their Impact on Modeling Dynamic Soil Response, PEER, UC, Berkeley, http://peer.berkeley.edu/lifelines/Workshop304/pdf/p_Kramer.pdf (Accessed on July, 2009)

- Kumar. J. (2006), "Ground response of Ahmedabad city during Bhuj earthquake: a case study", EJGE, Paper No. 0657.

- Kwak D. Y., Jeong, C. G., Park, D. and Park, S. (2008), "Comparison of frequency dependent equivalent linear analysis methods", Proceedings of 14th World Conference on Earthquake Engineering October 12-17, Beijing, China, Paper No. 14-04-01-0087.

- Kwok, A. O. L., Stewart, J. P., Hashash, Y. M. A., Matasovic, N., Pyke, R. M., Wang, Z. and Yang, Z. (2007), "Use of exact solutions of wave propagation problems to guide implementation of nonlinear seismic ground response analysis procedures", Journal of Geotechnical and Geo-environmental Engineering, ASCE, Vol. 133, pp. 1385–1398.

- Lade, P. V. (2005), "Overview of constitutive models for soils", in Calibration of constitutive models, by Yamamuro, J. A and Kaliakin V. N., (Editors), Geo-Frontiers Congress, ASCE, pp. 1-34.

- Lambe, W. T. and Whitman, R.V. (1979), "Soil Mechanics (SI Version)" John Wiley & Sons, New York, 1979, pp 553.

- Lee, M. K. W. and Finn, W. D. L. (1978), "DESRA-2, Dynamic effective stress response analysis of soil deposits with energy transmitting boundary including assessment of liquefaction potential." Soil Mechanics Series, No. 36, Department of Civil Engineering, University of British Columbia, Vancouver, Canada.

- Lee, M. K. W. and Finn, W. D. L. (1991), "DESRA-2C: Dynamic Effective Stress Response Analysis of Soil deposits with energy transmitting boundary including assessment of liquefaction potential", University of British Columbia, Faculty of Applied Science.

- Legates, D. R., and McCabe, Jr. G. J. (1999), "Evaluating the use of "goodness-of-fit" measures in hydrologic and hydro-climatic model validation", Water Resources Research, Vol. 35, pp 233–241.

- Li, W. and Assimaki, D. (2010), "Simulating soil stiffness degradation in transient site response predictions", Soil Dynamics and Earthquake Engineering, Vol. 30, pp. 299-309.

- Liao, T., McGillivray, A., Mayne, P. W., Zavala, G., and Elhakim, A. (2002), "Seismic Ground Deformation Modeling", Project Report MAE HD-7A, School of Civil & Environemental Engineering, Georgia Institute of Technology, Atlanta, GA. USA.

- Lin, M.L and Huang, T.H (1996) "The effects of frequency on damping properties of sand", Soil Dynamics and Earthquake Engineering, 15, pp 269-278.

- Linkimer, L (2008), "Relationship between peak ground acceleration and Modified Mercalli Intensity in Costa Rica", Revista Geólogica de América Central, Vol. 38, pp. 81-94.

- Lo Presti, D., Lai, C. and Foti, S. (2004) "Geophysical and geotechnical investigations for ground response analysis", Chapter 4 in Recent Advances in Geotechnical Earthquake Engineering and Microzonation, by A. Ansal (Editor), Kluwer Academic Pub. Netherlands, pp.101-138

- Lojelo, L. and Sano, T. (1988), "Seismic response of a soil deposit with a linear variation of the V_s profile", Proceedings of the IX world conference on Earthquake Engineering, Tokyo-Kyoto, Japan, Vol. II, pp. 417-422.

- Lysmer, J. (1978) "Analytical Procedures in Soil Dynamics", Report No. EERC-UBC 78-29, Earthquake Engineering Research Centre, Univ. of Calif., Berkeley 1978.

- Lysmer, J., Udaka, T., Seed, H. B. and Hwang, R. (1974), "LUSH: A computer program for complex response analysis of soil-structure systems", Report No. UCB/EERC 74-4, Earthquake Engineering Research Center, University of California, Berkeley.

- Lysmer, J., Udaka, T., Tsou, C. F. and Seed, H. B. (1975), "FLUSH: A computer program for approximate 3-D analysis of soil-structure interaction problems", Report No. UCB/EERC 75-30, Earthquake Engineering Research Center, University of California, Berkeley.

- Macari, E.J. and Hoyos, jr. L. (1996), "Effect of degree of weathering on dynamic properties of residual soils", Journal Geotechnical Engineering Division, ASCE, Vol. 122, No. 12, pp. 988-997.

- Madera G. A. (1971), "Fundamental period and peak accelerations in layered systems", Research report R70-37, Department of Civil Engineering, MIT, Cambridge, Massachusetts USA.

- Malagnini, L. (1996), "Velocity and attenuation structure of very shallow soils: evidence for frequency-dependent Q." Bulletin of the Seismological Society of America, 86(5), pp 1471-1486.

- Marino, E. M., Nakashima, M. and Mosalam, K. M. (2005), "Comparison of European and Japanese seismic design of steel building structures", Engineering Structures, Vol. 27, pp 827-840.

- Marsh, E. J. (1992), "Two dimensional nonlinear seismic ground response studies", Ph.D. thesis, submitted to School of Engineering University of Auckland, New Zealand.

- Martin, P. P. and Seed, H. B. (1978), "MASH: a computer program for the non-linear analysis of vertically propagating shear waves in horizontally layered deposits" Report No. UCB/EERC-78-23, Earthquake Engineering Research Center, University of California, Berkeley.

- Martin, P. P. and Seed, H. B. (1982), "One dimensional dynamic ground response analysis", Journal Geotechnical Engineering Division, ASCE, Vol.108, GT7, pp 935-952.

- Matasovic, N. (1993), "Seismic response of composite horizontally-layered soil deposits", Ph.D. Thesis, University of California, Los Angeles.

- Matasovic, N. and Hashash, Y. M. A (2012), "Practices and procedures for site-specific evaluations of earthquake ground motions - *A Synthesis of Highway Practice*", Report: NCHRP Synthesis 428, National Cooperative Highway Research Program, Transportation Research Board, Washington, D.C. USA.

- Matesic, L. and Vucetic, M. (2003), "Strain-rate effect of soil secant shear modulus at small cyclic strains", Journal Geotechnical and Geo-environmental Engineering, ASCE, 129, No. 6, pp 536-549.

- Mayne, P.W. and Rix, G (1995) "Correlations between shear wave velocity and cone tip resistance in natural clays", *Soils and Foundations*, JSSMFE, Vol. 35(2), pp. 107-110, 1995.

- McVerry, G. H. (2011), "Site-effect terms as continuous functions of site period and v_{s30}", Proceedings of the Ninth Pacific Conference on Earthquake Engineering Building an Earthquake-Resilient Society, 14-16 April, Auckland, New Zealand.

- Murphy J.R. and O'Brian L. J. (1977), "The correlation of peak ground acceleration amplitude with seismic intensity and other physical parameters", Bulletin of the Seismological Society of America, Vol. 67, pp 877-915.

- Mylonakis G.E., Rovithis E., and Parashakis H. (2011), "1D seismic response of soil: continuously inhomogeneous vs equivalent homogeneous soil", COMPDYN 2011, III ECCOMAS Thematic Conference on Computational Methods in Structural Dynamics and Earthquake Engineering, M. Papadrakakis, M. Fragiadakis and V. Plevris (Editors), Corfu, Greece, 25–28 May.

- Mylonakis, G. E., Rovithis, E. and Parashakis H. (2013), "1D harmonic response of layered inhomogeneous soil: exact and approximate analytical solutions", in Computational Methods in Earthquake Engineering, M. Papadrakakis et al. (editor), Computational Methods in Applied Sciences 30, DOI 10.1007/978-94-007-6573-3_1.

- Newmark N. M., and Rosenblueth E. (1971), "Fundamentals of Earthquake Engineering", Prentice Hall, Inc., Englewood Cliffs, N.J. 1971, p 640.

- Newmark, N. M. (1968), "Problems in Wave Propagation in Soil and Rock", Symposium on Wave Propagation and Dynamic Properties of Earth Materials, University of New Mexico, Albuquerque, pp 7-26.

- Ohta, Y. and Goto, N. (1978), "Empirical shear wave velocity equations in terms of characteristic soil indexes," Earthquake Engineering and Structural Dynamics, Vol. 6, pp. 167-187, 1978.

- Okamoto, S. (1984), "Introduction to earthquake engineering", Univ. of Tokyo press, Japan.

- Pande, G. N. and Zienkiewicz, O. C. (Editors) (1982), "Soil Mechanics – Transient and cyclic loads", John Wiley & Sons, New York.

- Paolucci, R. (1999), "Shear resonance frequencies of alluvial valleys by Rayleigh's method", Earthquake Spectra, Vol. 15, No. 3, pp. 503-521

- Papadakis, C., Streeter, V. L. and Wylie, E. B. (1974), "Bedrock Motions Computed from Surface Seismograms", Journal Geotechnical Engineering Division, ASCE, Vol.100, pp 1091-1106.

- Park, D. and Hashash, Y. M. A. (2004), "Soil damping formulation in nonlinear time domain site response analysis", Journal of Earthquake Engineering, Vol. 8, pp. 249-274.

- Park, D. and Hashash, Y. M. A. (2005), "Evaluation of seismic site factors in the Mississippi Embayment – I, Estimation of dynamic properties", Soil Dynamics and Earthquake Engineering, Vol. 25, pp 134-144.

- Park, D. and Hashash, Y. M. A. (2008), "Rate-dependent soil behavior in seismic site response analysis", Canadian Geotechnical Journal, Vol. 45, No. 4, pp 454-469.

- Phoon, K. K. and F. H. Kulhawy (1999), "Characterization of geotechnical variability", Canadian Journal of Geotechnical Engineering, Vol. 36, pp. 612-624.

- Pitilakis, K. (2004), "Site effects", Chapter 5 in Recent Advances in Geotechnical Earthquake Engineering and Microzonation, by A. Ansal (Editor), Kluwer Academic Pub. Netherlands, pp.139-197

- Prasad S.K. (1996), "Evaluation Of Deformation Characteristics Of 1-G Model Ground during Shaking using a Laminar Box", Doctoral thesis submitted to Department of civil engineering, Univ. of Tokyo, Japan, 1996.

- Prasad, S. K., Chandradhara, G. P. and Vijayendra, K. V. (2001), "Seismic ground response at Ahmedabad during Gujarat earthquake of 2001", Proceedings of Indian Geotechnical conference, IGC - 2001, Indore, India, 14th – 16th Dec., Vol. 1, pp. 336-339.

- ProShake (Version-1.1) – Computer Program for One-dimensional Ground Response Analysis, EduPro Civil Systems Inc., USA, http://www.proshake.com/ (Accessed on April 24, 2012).

- Pyke, R. M. (2000), "TESS – A Computer program for nonlinear ground response analysis", TAGA Engineering Software Services, Lafayette, California, USA.

- Pyke, R., Laird, J. and North, J. (2007), "Evaluation of uncertainties in dynamic properties", 4th International Conference on Earthquake Geotechnical Engineering, June 25-28, 2007, Paper No. 1359.

- Ralston, A. and Rabinowitz, P. (1978), "A first course in numerical analysis", 2nd Edition, McGraw-Hill Inc, New York, USA.

- Ramirez, R. W. (1985) "The FFT – Fundamentals and Concepts", Prentice-Hall Inc, Englewood Cliffs, New Jersey, USA.

- Richart, F. E. (1975), "Some effects of dynamic soil properties on soil-structure interaction", Journal Geotechnical Engineering Division, ASCE, vol. 101, pp. 1197-1240.

- Richart, F. E. (1978), "Field and laboratory measurement of dynamic soil properties", Proceedings, International Symposium on Dynamical Measurements in Soil and Rock Mechanics, Karlsruhe, Rotterdam, Vol. 1, pp 3-36.

- Richter, C. F. (1958), "Elementary seismology", W. H. Freeman and Co., San Francisco, USA.

- Rix, G. J. (2004) "Frequency Dependence of Dynamic Soil Properties", Opinion Paper, International Workshop on the Uncertainties in Nonlinear Soil Properties and their Impact on Modeling Dynamic Response, March 18-19, PEER, UC Berkeley, USA.

- Rix, G. J. and Meng, J. W. (2005), "A non-resonance method for measuring dynamic soil properties", Geotechnical Testing Journal, ASTM, Vol. 28, No. 1, pp 1-8.

- Roësset, J. M. and Whitman, R. V. (1969), "Theoretical background for amplification studies", Research report R69-15, Soil publication no. 231, School of Engineering, Massachusetts Institute of Technology, Cambridge USA.

- Roësset, J. M. (1977), "Soil Amplification of Earthquakes", Chap. 19 - Numerical Methods in Geotechnical Engineering by C.S.Desai and J.T.Christian (Editors), McGraw-Hill Pub., New York, 1977, pp 639-682.

- Rovithis, E. N., Parashakis, H. and Mylonakis, G. E. (2011), "1D harmonic response of layered inhomogeneous soil: Analytical investigation", Soil Dynamics and Earthquake Engineering, Vol. 31, pp. 879-890.

- Salt, P. E. (1974), "Seismic site response", Bulletin of the New Zealand National Society of Earthquake Engineering, Vol. 7, No2, pp. 62-77.

- Sarma, S. K. (1994), "Analytical solution to the seismic response of visco-elasitic soil layers", Geotechnique, Vol. 44, No. 2, pp. 265-275.

- Sawada, S. (2004), "A simplified equation to approximate natural period of layered ground on the elastic bedrock for seismic design of structures", 13th World Conference on Earthquake Engineering, August 1-6, Vancouver, B.C., Canada, Paper No. 1100.

- Scherbaum, F., Palme, C. and Langer, H. (1994), "Model parameter optimization for site dependent simulation of ground motion by simulated annealing – re-evaluation of the Ashigara valley prediction experiment," Natural Hazards, Vol. 10, pp. 275–296.

- ScheThis, M., Lombaert, G., Degrande, G., Degrauwe, D. and Schoors, B. (2007), "The Green's functions of a vertically inhomogeneous soil with a random dynamic shear modulus", Probabilistic Engineering Mechanics, Vol. 22, pp. 100-111

- Schilling, R. J. and Harris, S. L. (2002) "Applied Numerical Methods for Engineers using MATLAB and C", Thomson Asia Pvt. Ltd., Singapore.

- Schmertmann, J. H. (1991), "The Mechanical Aging of Soils", Journal of Geotechnical Engineering Division, ASCE, Vol. 117, No. 9, pp 1288-1330.

- Schnabel, P. B., Lysmer, J. L. and Seed, H. B. (1972), "SHAKE: A Computer Program for Earthquake Response Analysis of Horizontally Layered Sites", Report No. UCB/EERC – 72/12, Earthquake Engineering Research Center, University of California, Berkeley.

- Schneider, J. F., Silva, W. J. and Stark, C. L. (1993), "Ground motion model for the 1989 M6.9 Loma Prieta earthquake including effects of source, path, and site," Earthquake Spectra, 9(2), pp. 251-287.

- Schreyer, H. L. (1977), "One-dimensional elastic waves in inhomogeneous media", Journal of Engineering Mechanics Division, ASCE, Vol. 103, EM5, pp 979-990

- Seed, H. B. and Idriss, I. M. (1969), "The influence of soil conditions on ground motions during earthquakes", Journal of Soil Mechanics and Foundation Engineering Division, ASCE, Vol. 95, No. SM1, pp 99-137.

- Seed, H. B. and Idriss, I. M. (1970), "Soil moduli and damping factors for dynamic response analyses", Report No. UCB/EERC – 70/10, Earthquake Engineering Research Center, University of California, Berkeley.

- Seed, H. B., Romo, M. P., Sun, J. I., Jaime, A. and Lysmer, J. (1988), "The Mexico earthquake of September 19, 1985-Relationships between soil conditions and earthquake ground motions", Earthquake Spectra, Vol. 4, No. 4, pp. 687-729

- Seed, H. B., Whitman, R. V., Dezfulian, H., Dobry, R., and Idriss, I. M. (1972), "Soil conditions and building damage in 1967 Caracas Earthquake", Journal of Soil Mechanics and Foundations, ASCE, Vol. 98, No. SM8, pp. 787-806.

- Seed, R. B., Dickenson, S. E., Rau, G. A., White, R. K. and Mok, C. M. (1994), "Observations regarding seismic response analyses for soft and deep clay sites, Proceedings of the 1992 NCEER/SEAOC/BSSC Workshop on Site Response During Earthquakes and Seismic Code Provisions, G.R. Martin (Editor), University of Southern California, Los Angeles, November 18-20, 1992, National Center for Earthquake Engineering Research Special Publication NCEER-94-SP01, Buffalo, NY.

- Seed, R. B., Dickenson, S. E., Riemer, M. F., Bray, J. D., Sitar, N., Mitchell, J. K., Idriss, I. M., Kayen, R. E., Kropp, A. K., Harder, L. F., and Power, M. S. (1990), "Preliminary report on the principle geotechnical aspects of the October 17, 1989 Loma Prieta earthquake", Report No. UCB/EERC-90/05, Earthquake Engineering Research Center, University of California, Berkeley.

- SeismoSignal-Version 4.0, SEISMOSOFT – Earthquake Engineering Software Solutions, http://www.seismosoft.com/en/seismosignal.aspx (Accessed on February 12, 2014).

- Semblat, J. F. (2011), "modeling seismic wave propagation and amplification in 1D/2D/3D linear and nonlinear unbounded media", International Journal of Geomechanics, ASCE, Vol. 11, No. 6, pp. 440-448.

- Shibuya, S., Mitachi, T., Fukuda, F. and Degoshi, T. (1995), "Strain rate effects on shear modulus and damping of normally consolidated clay", Geotechnical Testing Journal, Vol. 18, No. 3, pp 365-375.

- Silva W.J. (1976), "Body waves in a layered anelastic solid", Bulletin of Seismological Society of America, Vol. 66, pp. 1539-1554.

- Silva W.J. and Lee K. (1987), "WES RASCAL code for synthesizing earthquake ground motions" State of the Art for Assessing Earthquake Hazards in the United States, Rep. 24, U.S. Army Engineers, WES, Paper no. S-73-1.

- Singh S K., Lermo J., Dominguez T., Ordaz M., Espianoza J M., Mena E. and Quass R. (1988), "A study of amplification of seismic waves in the valley of Mexico City with respect to a hill zone site.", Earthquake Spectra, 4, 1988, pp 653-673.

- Sitharam, T. G. and Govindaraju, L. (2004) "Geotechnical aspects and ground response studies in Bhuj earthquake, India", Geotechnical and Geological Engineering, Vol. 22, pp 439–455.

- Sitharam, T.G. and Anbazhagan, P., (2008), "Seismic microzonation: Principles, practices and experiments", EJGE Special Volume Bouquet 08, http://www.ejge.com/Bouquet08/Preface.htm (accessed on 22-April-2012)

- Sojka R. E., Busscher, W. J. and Lehrsch, G. A. (2001), "In situ strength, bulk density, and water content relationships of a durinodic xeric haplocalcid soil", *Soil Science*, Vol. 166, No. 6, pp. 520-529.

- Stewart, J. (2002), "Calibration Sites for Validation of Nonlinear Geotechnical Models", Website: http://seas.ucla.edu/~jstewart/CalibrationSites/Engineering Model / (accessed on 26-July-2010)

- Stewart, J. P. and Kwok, A. O. L. (2008), "Nonlinear seismic ground response analysis: code usage protocols and verification against vertical array data", In Proceedings of the Geotechnical Engineering and Soil Dynamics IV, Sacramento, CA, May 18–22.

- Streeter, V. L., Wylie, E. B. and Bedford, K. W. (1998), "Fluid Mechanics", 9th International Edition, McGraw-Hill Book Co., Singapore.

- Streeter, V. L., Wylie, E. B. and Richart, F. E. (1974), "Soil motion computations by characteristics method", ASCE, Journal Geotechnical Engineering Division, Vol. 100, pp. 247-263.

- Sugito, M. (1995), "Frequency-dependent equivalent strain for equi-linearized technique", Proc. of the First International Conference on Earthquake Geotechnical Engineering, Vol. 1, A. A. Balkena, Rotterdam, the Netherlands, pp. 655-660.

- Sugito, M., Goda G. and Masuda T. (1994), "Frequency dependent equi-linearized technique for seismic response analysis of multi-layered ground", Journal of Geotechnical Engineering, Proceedings of JSCE, 493, 49-58 (in Japanese with English abstract).

- Sun J.I., Golesorkhi R. and Seed H.B. (1988), "Dynamic moduli and damping ratios for cohesive soils", Report No. UCB/EERC – 88/15, Earthquake Engineering Research Center, University of California, Berkeley.

- Suwal, S., Pagliaroli, A. and Lanzo, G. (2014), "Comparative study of 1D codes for site response analyses", International Journal of Landslide and Environment, Vol. 2, No. 1 (November), pp. 24-31.

- Taylor P. W. and Larkin T. J. (1978), "Seismic site response of nonlinear soil media", Journal Geotechnical Engineering Division, ASCE, Vol. 104, GT3 pp. 369-383.

- Terzaghi I. (1955), "Influence of geologic factors on the engineering properties of sediments", Economic Geology, Fiftieth Anniversary Volume, 1955, pp. 557-618.

- Thomson, W. T. (1935), "Transmission of elastic waves through a stratified solid medium", Journal of Applied Physics, Vol. 21, pp. 89-93.

- Toki, K. and S. Cherry (1972), "Inference of subsurface acceleration and strain from accelerograms recorded at ground surface", Proceedings of 4th European Conference on Earthquake Engineering, London.

- Toki, K. and S. Cherry (1974), "Inference of underground seismic motions from surface accelerograph records", Proceedings of 5th World Conference on Earthquake Engineering, Rome, Vol. 1, pp. 745-754.

- Towhata, I. (1996), "Seismic wave propagation in elastic soil with continuous variation of shear modulus in the vertical direction", Soils and Foundations, Vol. 36, No. 1, pp. 61-72.

- Towhata, I. (2008), "Geotechnical earthquake engineering", Springer Series in Geomechanics and Geoengineering, Springer-Verlag, Berlin.

- Travasarou T. and G. Gazetas (2004), "On the linear seismic response of soils with modulus varying as a power of depth – The Maliakos marine clay", Soils and Foundations, Vol. 44, No. 5, 2004, pp. 85-93.

- Trifunac M. D. and Brady A. G. (1975), "On the correlations of seismic intensity scale with peaks of recorded strong ground motion", Bulletin of the Seismological Society of America, Vol. 65, pp 139–162.

- Tsai, N. C. and Housner, G. W. (1970), "Calculation of Surface Motions of a layered Half-space", Bulletin of Seismological Society of America, Vol. 60, pp. 1625-1651.

- Tucker, B. E. and King, J. L. (1984), "Dependence of sediment-filled valley response on input amplitude and valley properties", Bulletin of Seismological Society of America, Vol. 74, No. 1, pp. 153-165.

- Ueshima T (2000), "Application of equivalent linear analysis method taking account of frequency dependent characteristics of ground strain to seismic data from Lotung, Taiwan", EM2000, 14th Engineering Mechanics Conference, ASCE, May 2000, Dept. of Civil Engineering, Univ. of Texas, Austin,USA.

- US Army Corps of Engineers (USAE), Computer program WESHAKE5 Manual http://geoscience.wes.army.mil/Software.htm (Last accessed, August, 2010)

- Vankov D.A. and Sassa K. (1999) "Dependence of pore pressure on frequency of loading at sliding surface", Slope Stability Engineering by Yagi, Yamagami and Jiang (Editors), Balkema, Rotterdam. pp 601-606

- Vijayendra, K. V. and Prasad, S. K. (2001), "Prediction of dynamic soil properties of soil from In-situ SPT test", Proceedings of International Conference in Civil Engineering, ICCE – 2001, July, IISc, Bangalore.

- Visone C., Santucci de Magistris, F. and Bilotta, E. (2010), "Comparative study on frequency and time domain analyses for seismic site response", EJGE (Electronic Journal), Vol. 15, Bundle – A, pp. 1-20.

- Vrettos C. (2013), "Dynamic response of soil deposits to vertical SH waves for different rigidity depth-gradients", Soil Dynamics and Earthquake Engineering, Vol. 47(4), pp. 41-50.

- Vucetic M, and Dobry R. (1991). "Effect of soil plasticity on cyclic response", Journal Geotechnical Engineering Division, ASCE, 117(1), pp 89-107.

- Vucetic M., Lanzo G. and Doroudian M. (1998), "Damping at small strains in cyclic simple shear tests", Journal Geotechnical Engineering Division, ASCE, 124(7), pp 585-594.

- Wair, B. R., DeJong, J. T. and Shantz, T. (2012), "Guidelines for estimation of shear wave velocity profiles", PEER Report 2012/08, Pacific Earthquake Engineering Research Center, University of California, USA, pp. 68

- Wald, D. J., Quintoriano V., Heaton T. H. and Kanamori H. (1999), "Relationship between peak ground acceleration, peak ground velocity and Modified Mercalli intensity in California", Earthquake Spectra, Vol. 15, pp 557-564.

- Wood, M. D. (2004), "Geotechnical modeling", E & FN Spon, London

- Woods, R. D. (1978), "Measurement of dynamic soil properties", Proceedings of Conference on Earthquake Engineering and Soil Dynamics, Specialty conference ASCE I, pp 91-178.

- Yashima, A., Sugito, M. and Okada, H. (2000), "Evaluation of liquefaction potential by frequency dependent equivalent linearized technique", 13 WCEE (2004), Vancouver BC, Canada, paper no. 200.

- Yoshida, N. (2014), "Comparison of seismic ground response analyses under large earthquakes", Indian Geotechnical Journal, Vol. 44, No. 2, pp. 119–131.

- Yoshida, N., Kobayashi, S., Suetomi, I. and Miura, K. (2002), "Equivalent Linear Method considering Frequency Dependent Characteristics of Stiffness and Damping", Soil Dynamics and Earthquake Engineering, Vol. 22, pp 205-222.

- Yu, G., Anderson, J. G. and Siddhartan, R. (1993), "On the characteristics of nonlinear soil response", Bulletin of Seismological Society of America, Vol. 83, pp. 218-244.

- Zeevaert L. (1972), "Foundation Engineering for Difficult Subsoil Conditions", Van Nostrand Pub., New York.

- Zeghal, M., Elgamal, A. W., Tang, H. T. and Stepp, J. C. (1995), "Lotung downhole array. II: Evaluation of soil nonlinear properties", Journal of Geotechnical Engineering Division, ASCE, Vol. 121, pp. 363-378.

- Zeng, Y. and Anderson J.G. (1996) "A composite source model of the 1994 Northridge earthquake using genetic algorithms", Bulletin of Seismological Society of America, Vol. 86(1B), pp. S71-S83.

- Zhang, J, Andrus, R. D. and Hsein Juang, C. (2005), "Normalized shear modulus and material damping ratio relationships", Journal of Geotechnical and Geo-environmental Engineering, ASCE, Vol. 131, No. 4, pp. 453-464.

- Zhang, J, Andrus, R. D. and Hsein Juang, C. (2008), "Model Uncertainty in Normalized Shear Modulus and Damping Relationships", Journal of Geotechnical and Geo-environmental Engineering, ASCE, Vol. 134, No. 1, pp. 24-36.

- Zhao, J. X. (1996), "Estimating modal parameters for a soft-soil site having a linear distribution of shear wave velocity with depth", Earthquake Engineering and Structural Dynamics, Vol. 25, 1996, pp. 163-178.

- Zhao, J. X. (1997), "Modal analysis of soft-soil sites including radiation damping", Earthquake Engineering and Structural Dynamics, Vol. 26, pp 93-113.

- Zhao, J. X. (2011), "Comparison between v_{s30} and site period as site parameters in ground-motion prediction equations for response spectra", 4th IASPEI / IAEE International Symposium on Effects of Surface Geology on Seismic Motion, August 23–26, University of California Santa Barbara, USA

- Zhou, J. and Gong, X. (2001), "Strain degradation of saturated clay under cyclic loading", Canadian Geotechnical Journal, Vol. 38, pp 208-212.

- Zovoral, D. Z. and Campanella, R. G. (1994) "Frequency effects on damping/modulus of cohesive soils", ASTM Special Technical Publication No. 1213, Dynamic Geotechnical Testing II, by Ebelhar R. J., Drenvich, V. P. and Kutter, B. L. (Editors), pp 191-201.

APPENDIX – I

MATLAB PROGRAMS TO COMPUTE AMPLIFICATION FUNCTION OF INHOMOGENEOUS SOIL DEPOSITS USING ANALYTICAL SOLUTION

AI.1 Program for Amplification of Continuously Inhomogeneous Soil Deposits

```
%************************************************************************
%************************************************************************
% program inhomocontinuous.m
%************************************************************************
%************************************************************************
%
% Program to compute Amplification function between free surface motion and
% bedrock motion for continuously inhomogeneous soil deposit
% Input motion is Harmonic Excitation
%
%************************************************************************
%
% Depth dependent Shear wave velocity function is vs(z)=vs0*(1+az)^(n/2)
% Continuous varation of shear wave velocity considered is G(z)=A(z0+z)^n
%
%************************************************************************
%
%Amplification Surface to outcrop rock (Elastic bedrock – Amp2 of CHAPTER-3
%Amplification Surface to Base (Rigid bedrock) – Amp1 of CHAPTER-3
%Amplification for n<1; n=1; and n>1 or m<2; m=2; and m>2 [Towhata (1996)]
%For linear shear wave velocity distribution enter n=2
%Amplification is computed for constant density throughout the depth
%z = Depth coordinate; z0 and A are inhomogeinity parameters
%
%************************************************************************
%
% Brock = 1 when bedrock is considered to be rigid
% Brock = 2 when bedrock is considered to be elastic (flexible)
%
%************************************************************************
%************************************************************************
%************************************************************************
%************************************************************************
```

```
clear all;
Brock=input('input bedrock option: [rigid (1) or flexible (2)] Brock:');
n=input('input value of inhomogeneity factor (n):');
v0=input('input value of surface velocity (v0):');
vH=input('input value of base velocity (vH):');
H=input('input total depth of the deposit (H):');
rho=input('input density (rho):');
fmax = input('enter max. frequency (rad/s) for amplification (fmax):');
if (Brock == 2)
vr=input('input value of bedrock velocity velocity (vr):');
rbr=input('input bedrock density (rbr):');
end;
damp=input('input damping factor in % (damp):');
damp=damp/100;
VRn=(v0/vH)^(2/n);
z0=H*VRn/(1-VRn);
A=(rho*v0*v0*complex(1,(2*damp)))/(z0^n);
disp(z0);disp(VRn);disp(A);
lam=(2/(2-n))*sqrt(rho/A);
ztH=lam*((H+z0)^((2-n)/2));
zt0=lam*((z0)^((2-n)/2));
zt=ztH*(2-n)/2;
nu=1/(2-n);
%
%-Linear distribution of shear wave velocity
%
if (n == 2)
    damc=sqrt(complex(1,2*damp));
    v0c=v0*damc;
    vHc=vH*damc;
    mu=vHc/v0c;
    a=(vHc-v0c)/H;
    omg=0;
  for dd=0.1:0.1:fmax;
    omg=omg+1;
    k=sqrt((dd/a)^2-0.25);
    theta=k*log(mu);
    A1=(2*k*cos(theta)+sin(theta))/(2*k*sqrt(mu));
    if (Brock==1)
      AA(omg)=1/A1;  %#ok<AGROW>
    else
      A2=(vH*rho/(vr*rbr))*dd*sin(theta)/(k*a*sqrt(mu));
      AA(omg)=1/(A1+(complex(0,1)*A2)); %#ok<AGROW>
```

340

```matlab
        end;
        omg1(omg)=dd/(2*3.1415926);  %#ok<AGROW>
    end;
end;
%
%-Non-Linear distribution of shear wave velocity with n<2
%
if (n<2 && Brock == 2)
    nu1=nu+1;
    b=(n-2)/(sqrt(z0)*3.141592654*rho);
    omg=0;
for dd=0.1:0.1:fmax;
    omg=omg+1;
    A1=(bessely(nu,zt0*dd)*(besselj(nu,ztH*dd)-zt*dd*besselj(nu1,ztH*dd))));
    A2=(besselj(nu,zt0*dd)*(bessely(nu,ztH*dd)-zt*dd*bessely(nu1,ztH*dd))));
    A3=(1/(rho*dd*dd*sqrt(z0+H)))*(A1-A2);
    A41=(bessely(nu,ztH*dd)*besselj(nu,zt0*dd));
    A42=(bessely(nu,zt0*dd)*besselj(nu,ztH*dd));
    A4=(A41-A42)*(sqrt(H+z0)/(complex(0,1)*rbr*vr*dd));
    A5=A3+A4;
    AA(omg)=(b/(dd*dd))/(A5);  %#ok<AGROW>
    omg1(omg)=dd/(2*3.141592654);  %#ok<AGROW>
end;
elseif (n<2 && Brock == 1)
    nu1=nu+1;
    b=(sqrt((z0+H)/z0))*(n-2)/3.141592654;
    omg=0;
for dd=0.1:0.1:fmax;
    omg=omg+1;
    A1=(bessely(nu,zt0*dd)*(besselj(nu,ztH*dd)-zt*dd*besselj(nu1,ztH*dd))));
    A2=(besselj(nu,zt0*dd)*(bessely(nu,ztH*dd)-zt*dd*bessely(nu1,ztH*dd))));
    AA(omg)=(b)/(A1-A2);  %#ok<AGROW>
    omg1(omg)=dd/(2*3.141592654);  %#ok<AGROW>
end;
%
%-Non-Linear distribution of shear wave velocity with n>2
%
elseif (n>2 && Brock == 2)
    nu1=-nu+1;
    b=(n-2)/(sqrt(z0)*3.141592654*rho);
    omg=0;
for dd=0.1:0.1:fmax;
    omg=omg+1;
```

341

```
    A1=((bessely(-nu,-zt0*dd))*(besselj(nu1,-ztH*dd)));
    A2=((besselj(-nu,-zt0*dd))*(bessely(nu1,-ztH*dd)));
    A12=(A1-A2)*(1/(sqrt(A*rho*dd*dd)*((H+z0)^((n-1)/2))));
    A3=((besselj(-nu,-zt0*dd))*(bessely(-nu,-ztH*dd)));
    A4=((bessely(-nu,-zt0*dd))*(besselj(-nu,-ztH*dd)));
    A34=(A3-A4)*(sqrt(H+z0)/(complex(0,1)*rbr*vr*dd));
    AA(omg)=(b/(dd*dd))/(A12+A34); %#ok<AGROW>
    omg1(omg)=dd/(2*3.141592654); %#ok<AGROW>
end;
elseif (n>2 && Brock == 1)
   nu1=-nu+1;
   b=(n-2)*(sqrt(((z0+H)^(n-1))*A))/((sqrt(z0*rho))*3.141592654);
  omg=0;
for dd=0.1:0.1:fmax;
    omg=omg+1;
    A1=((bessely(-nu,-zt0*dd))*(besselj(nu1,-ztH*dd)));
    A2=((besselj(-nu,-zt0*dd))*(bessely(nu1,-ztH*dd)));
    AA(omg)=(b/dd)/(A1-A2); %#ok<AGROW>
    omg1(omg)=dd/(2*3.141592654); %#ok<AGROW>
end;
end;
plot(omg1,abs(AA));
xlabel('Frequency (Hz)');
if(Brock == 1)
    ylabel('Amp1-amplification (surface/rigid bedrock)');
else
    ylabel('Amp2-amplification (surface/elastic bedrock)');
end;
%*******************************************************************
%*******************************************************************
```

342

AI.2 Program for Amplification of Soil Deposit with Stack of Gibson Layers or Homogeneous Layers

```
%***********************************************************************
%***********************************************************************
% program inhomogibsonlay.m
%***********************************************************************
%***********************************************************************
%
% Program to compute Amplification function between free surface motion and
% bedrock motion for soil deposit consists of stack of gibson layers
% Input motion is Harmonic Excitation; Davis and Hunt (1994)
%
%***********************************************************************
%
% Shear modulus for each layer is linearly distributed along the depth
% Continuous varation of shear modulus in each layer is G(z)=a + b*z
% z = Depth coordinate; a and b are inhomogeinity parameters
% For stack of homogeneous layers b=0 i.e., G is constant   [CHAPTER-2]
%
%***********************************************************************
%
%Amplification Surface to outcrop rock (Elastic bedrock - Amp2 of CHAPTER-3
%Amplification Surface to Base (Rigid bedrock) - Amp1 of CHAPTER-3
%Amplification is computed for constant layer density
%Thompson-Haskel Transformation matrix is formulated for each of the layer
%
%***********************************************************************
%
% Brock = 1 when bedrock is considered to be rigid
% Brock = 2 when bedrock is considered to be elastic (flexible)
%
%***********************************************************************
% array data of v0[..], vb[..], h[..], rho[..] and damp[..]
%***********************************************************************
%***********************************************************************
%***********************************************************************
%***********************************************************************
clear all;
lay=input('input number of layers (lay):');
%
%Following arrays contain "lay" number of data for each of the layer
%
```

343

```
v0=[300;400];  %shear wave velocity at the top of the layer
vb=[200;500];  %shear wave velocity at the bottom of the layer
h=[50;50];     %depth of the layer
rho=[1.8;1.8]; %density of the layer
damp=[5;5];    %damping ratio of the layer in percentage
for m=1:lay
    damc(m)=sqrt(complex(1,2*damp(m)/100)); %#ok<AGROW>
    disp(damc(m));
    g0(m)=(v0(m)*damc(m))^2*rho(m); %#ok<AGROW>
    gb(m)=(vb(m)*damc(m))^2*rho(m); %#ok<AGROW>
    if ((v0(m)-vb(m))<0.0001)
        gbar(m)=g0(m); %#ok<AGROW>
    else
        gbar(m)=(gb(m)-g0(m))/g0(m); %#ok<AGROW>
    end;
end;
fmax = input('enter max. frequency (rad/s) for amplification (fmax):');
Brock=input('input bedrock option: [rigid (1) or flexible (2)] Brock:');
if (Brock == 2)
vr=input('input value of bedrock velocity velocity (vr):');
rbr=input('input bedrock density (rbr):');
gr=vr^2*rbr;
end;
omg=0;
for dd=0.1:0.1:fmax;
    omg=omg+1;
    H=[1 0;0 1]; %Intialize Thompson-Haskel matrix
    A(omg)=[0];T=0;t11=0;t12=0;t21=0;t22=0;zt1=0;zt2=0; %#ok<AGROW>
    for k=lay:-1:1
        if (v0(k)== vb(k))
            kk(k)=1/(v0(k)*damc(m)); %#ok<AGROW>
            gc(k)=(v0(k)*damc(k))^2*rho(k); %#ok<AGROW>
            kh=kk(k)*h(k)*dd; %#ok<AGROW>
            kg=kk(k)*gc(k)*dd;
            t11=cos(kh);t12=sin(kh)/kg;t21=-kg*sin(kh);t22=cos(kh);
            %
            T=[t11 t12;t21 t22];%compute Thompson-Haskel matrix of the layer
            %
        else
        zt1(k)=(2*dd*h(k))/(gbar(k)*sqrt(g0(k)/rho(k))); %#ok<AGROW>
        zt2(k)=zt1(k)*sqrt(1+gbar(k)); %#ok<AGROW>
        t111=(-bessely(1,zt1(k))*besselj(0,zt2(k)));
        t112=(besselj(1,zt1(k))*bessely(0,zt2(k)));
```

344

```matlab
        t11=((pi/2)*zt1(k))*(t111+t112);
        t121=(-bessely(0,zt1(k)).*besselj(0,zt2(k)));
        t122=(besselj(0,zt1(k)).*bessely(0,zt2(k)));
        t12=(((pi/2)*zt1(k))/(dd*sqrt(g0(k)*rho(k))))*(t121+t122);
        t211=(bessely(1,zt1(k))*besselj(1,zt2(k)));
        t212=(besselj(1,zt1(k))*bessely(1,zt2(k)));
        t21=(((pi/2)*zt2(k))*(dd*sqrt(g0(k)*rho(k))))*(t211-t212);
        t221=(bessely(0,zt1(k))*besselj(1,zt2(k)));
        t222=(besselj(0,zt1(k))*bessely(1,zt2(k)));
        t22=((pi/2)*zt2(k))*(t221-t222);
        T=[t11 t12;t21 t22];
        end;
        H=H*T;          %update Thompson-Haskel matrix
    end;
    if (Brock == 2)
        AAN=((complex(0,1)*dd*rbr*vr*H(1,1))+H(2,1));
        AA(omg)=(complex(0,1)*dd*rbr*vr)/AAN; %#ok<AGROW>
    else
        AA(omg)=1.0/(H(1,1)); %#ok<AGROW>
    end
omg1(omg)=dd/(2*3.141592654); %#ok<AGROW>
end;
plot(omg1,abs(AA));
xlabel('Frequency (Hz)');
if(Brock == 1)
    ylabel('Amp1-amplification (surface/rigid bedrock)');
else
    ylabel('Amp2-amplification (surface/elastic bedrock)');
end;
```

345

APPENDIX II

ILLUSTRATIVE EXAMPLE OF ANALYSIS USING
SRISD (Seismic Response of Inhomogeneous Soil Deposits)

AII.1 INTRODUCTION

This appendix outlines the input and output features of SRISD program using different options available for idealisation of shear wave velocity of the deposit. Details of these options are explained in Chapter 4. In addition to routine SHAKE kind of analysis, an example run is carried out using the proposed option to calculate effective strain in the iterative process of equivalent linear analysis. Theoretical background of the proposed method for this purpose is presented in Chapter 5. The example problem considered here is related to La-Obregon Park geotechnical array. The data of Chino Hills Earthquake recorded at this site is used for this purpose.

AII.2 LA-OBREGON PARK GEOTECHNICAL ARRAY

The details about La-Obregon Park geotechnical array are presented Chapter 6. This geotechnical downhole array was established by California Strong Motion Instrumentation Program (CSMIP), USA. Soil deposit details consisting of PS-logging data and its layered idealisation are taken from the website associated with the research project on Calibration Sites for Validation of Nonlinear Geotechnical Models of University of California, Berkeley [Stewart (2002)]. The strain dependent nonlinear behaviour of the soil deposit is modeled using suggested shear modulus and damping curves as suggested in this website. The raw data of shear wave velocity profile obtained from PS-logging survey and its layered idealisation as given in the website are shown in Figure AII.1. The approximated equivalent linear variation of the shear wave velocity distribution is also shown in this figure. The details for this linear fit is given in Chapter 6 (Table 6.5). The strain dependent soil properties used in the analysis are shown in Figure AII.2. The average curves of shear modulus and damping shown in the same figure are used in the analysis in which continuously distributed shear wave velocity profile is considered.

347
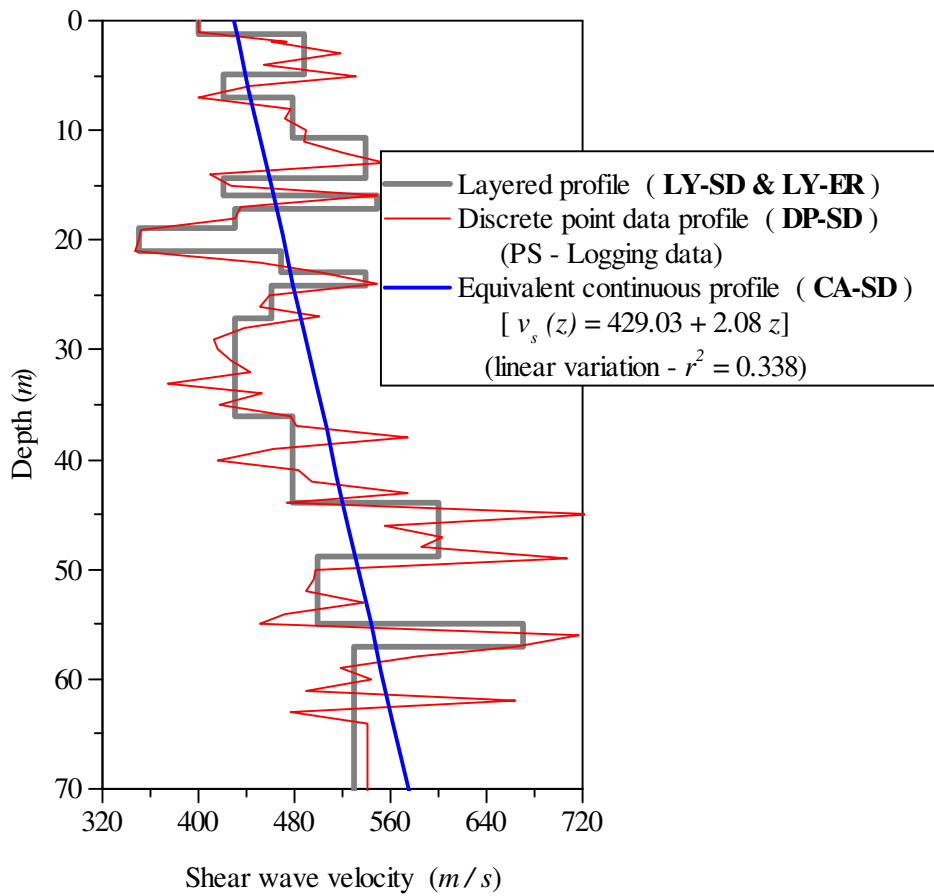
Figure AII.1: Shear wave velocity profiles data of La-Obregon Park geotechnical array soil deposit used in the analysis.
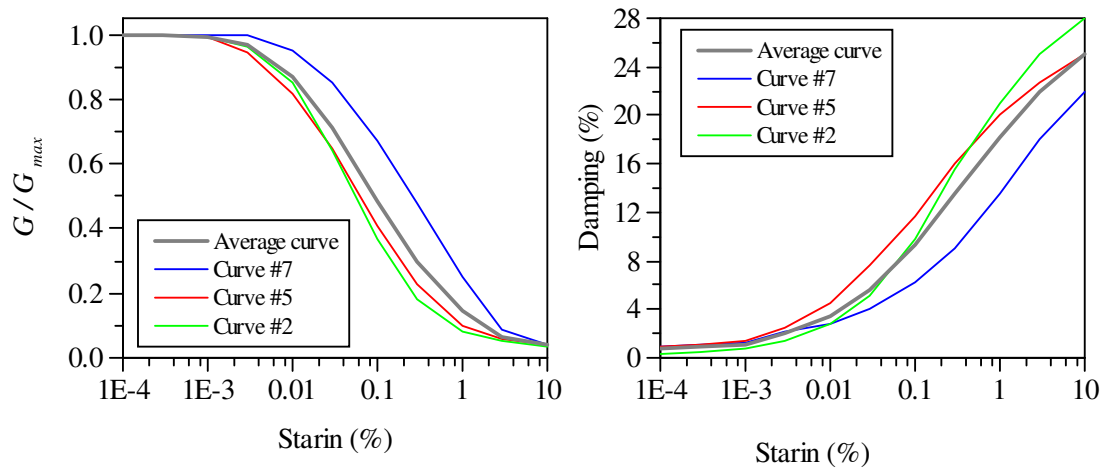
Figure AII.2: Strain dependent soil property curves (G/G_{max} and ζ) used in the analysis. Average curve used for the case of analysis carried out with approximated continuously varying shear wave velocity profile.

AII.3   EARTHQUAKE DATA

La-Obregon downhole geotechnical array is instrumented to record all the three component acceleration time history at the surface and at the depth of 70.0 m from the surface. The horizontal components are designated as 90 and 360 degree components. Data used for this example study is earthquake record of July 29, 2008 Chino Hills earthquake. The details of this earthquake event are tabulated in Table AII.1. The 360 degree component of this event recorded at 0 m and -70.0 m are shown in Figure AII.3. The acceleration time history recorded at 70.0 m is used as base input motion in this illustrative example.

Table AII.1: Details of Chino Hills Earthquake of 2008, recorded at La-Obregon Park site

Moment magnitude	5.4
Epicentral distance	39.2 km
Focal depth	13.6 km
Latitude	33.95N
Longitude	117.77W
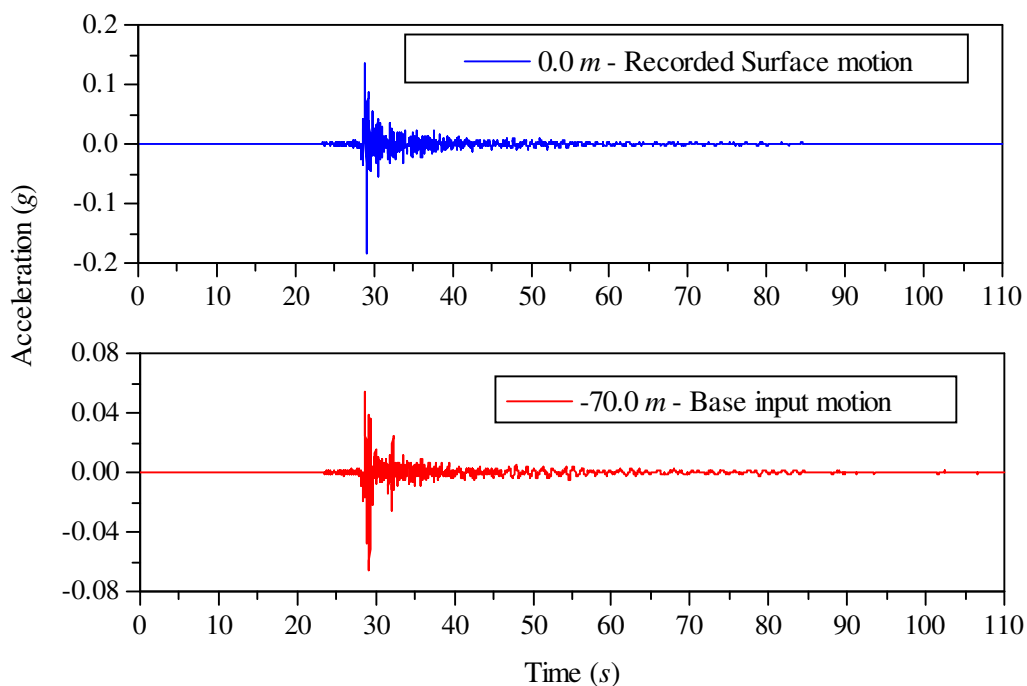
Figure AII.3: Earthquake accelerograms recorded at La-Obregon Park site at the surface and at depth 70.0 m.

AII.4 ANALYSIS CASES

As shown in Figure AII.1 three cases of shear wave velocity profiles are analysed. The designations of problem cases analysed are shown in Table AII.2.

Table AII.2: Designations used for different input cases considered

Case details	Designation
SRISD Analysis for layered shear wave profile with constant R-value (0.44 for $M_w = 5.4$)	**LY-SD**
SRISD Analysis for layered shear wave profile with R-value as proposed in this study (Chapter 5).	**LY-SD-R**
SHAKE Analysis (using EERA program) for layered shear wave profile with constant R-value (0.44 for $M_w = 5.4$)	**LY-ER**
SRISD Analysis for shear wave profile defined by discrete data points (PS-Logging data) with R-value as proposed in this study (Chapter 5)	**DP-SD**
SRISD Analysis for shear wave profile defined by linear function of depth (Continuous variation) with R-value as proposed in this study (Chapter 5). The strain dependent soil properties are those corresponding to average curves of Figure AII.2	**CA-SD**
SRISD Analysis for shear wave profile defined by linear function of depth (Continuous variation) with R-value as proposed in this study (Chapter 5). The strain dependent soil properties are those obtained using normalized equations proposed by Zhang et al. (2005)	**CZ-SD**

In Table AII.2, **LY** represents layered deposit, **DP** represents profile for which data are given at discrete points and **C** represents continuous profile. the average curve is designated by **A** and Zhang et al (2005) model is represented by **Z.** Hence **CA** and **CZ** are representing the soil deposit of continuous shear wave velocity profile and soil properties being modeled using average G/G_{max} and ζ curves (Figure AII.2) and Zhang et al (2005) model respectively. **SD** and **ER** are indicating the programs used for the analysis that is SRISD and EERA respectively. Strain dependent soil properties curves shown in Figure AII.2 are designated by curve numbers which refers to number assigned to these curves in SRISD built-in data. Actually Curve #5 and #7 are representing Vucetic and Dobry (1991) proposed curves for clay of plasticity index 15% and 50% respectively. While Curve #2 represents Seed and

Idriss (1970) average curve for sand. Zhang et al (2005) normalized soil property model is represented by Curve #22.

AII.5   INPUT DATA FILES

Input data files for SRISD program for the cases of shear wave velocity profiles are described here. In all the three cases the input files mainly consists of three parts. In the first part problem definition and input motion file are specified. In the second part the soil deposit properties are given. In the third part various options for the analysis and output specifications are instructed to the program. Thus only second part of the input file differs depending upon the option selected to model the shear wave velocity profile of the soil deposit. Input data file for the analysis case of **LY-SD-R** is presented in Table AII.3. In this table, for the sake of clarity, these three parts of the input file are shown separately.

The soil deposit data include; layer depth (*m*), soil type, unit weight (kN/m^3), shear wave velocity (m/s) low strain damping, (%), plasticity index (%), OCR and geological age. If the soil type is chosen from the models available in SRISD built-in data, then soil type is given in terms numbers assigned in the program. To input new data procedure explained Chapter 4 may be adopted and the coefficients of the polynomial representing data are entered. Plasticity index, OCR and geological age data are used only when the selected soil model is function of these factors [for e.g., Ishibashi and Zhang (1993), Darendeli (2001), Zhang et al. (2005) etc.]. When the chosen soil model is capable of calculating initial damping ratio, then the corresponding data given as input is considered to be redundant. During the iterations of equivalent linear analysis, the magnitudes of shear modulus or damping can be kept constant independently by exercising this option during program execution.

Tables AII.4 and AII.5 list the input files of the analyses cases **DP-SD** and **CZ-SD** respectively. The explanatory notes appended to these tables give details about input data to be given in order to exercise different options of SRISD program. Background details of these options are discussed in Chapters 4 and 5. Results obtained for all these analyses cases are presented in the following sections.

Table AII.3: Input data file for LY-SD-R analysis case

Line no	Input file	Comments	Line no
1	INPUT FILE LY-SD-R ANALYSIS LA–OBREBON SITE (38 LAYERS)	Title of the problem	1
2	CH36070.ACC	Input motion file	2
3	LOL381.OUT	Out file #1	3
4	LOL382.OUT	Out file #2	4
5	70.0	Total depth of the deposit	5
6	1	Type of shear wave velocity profile	6
7	38	Number of layers	7
8	1.22 5 16.50 399.29 2 15 1 2	Line #8 to Line #45	8
9	1.22 5 16.50 487.68 2 15 1 2	Layer details are entered in the following	9
10	1.22 5 16.50 487.68 2 15 1 2	sequence	10
11	1.22 5 16.50 487.68 2 15 1 2		11
12	0.91 2 16.83 420.62 2 0 1 2	Column #1 – layer depth	12
13	1.22 5 16.77 420.62 2 15 1 2	Column #2 – soil type (as given in SRISD)	13
14	0.61 2 16.92 478.54 2 0 1 2	Column #3 – unit wt (kN / m^3)	14
•	• • • • • • • •	Column #4 – shear wave velocity (m / s)	•
		Column #5 – initial damping	
•	• • • • • • • •	Column #6 – plasticity index	•
43	2.74 2 17.17 530.35 2 0 1 2	Column #7 – OCR	43
44	2.74 2 17.23 530.35 2 0 1 2	Column #8 – Geological age	44
45	2.67 2 17.29 530.35 2 0 1 2		45
46	70.0	Depth at which input motion is to be given	46
47	0, 0.72	Depth of water table & K$_0$– (only used in calculation of effective confining stress)	47
48	0 17.29 530.35 2	Bedrock properties (Type, unit wt., Shear wave velocity, damping)	48
49	1 0.44 20	Choice of R, R-value, No. of iterations	49
50	0	Choice of frequency dependent analysis	50
51	Y	Output of accn time histories required?	51
52	1	No. of required depths	52
53	0	Depths (as many as indicated previously)	53
54	Y	Out stress-strain time histories required?	54
55	1	No. of required depths	55
56	0.6	Depths (as many as indicated previously)	56
57	Y	Amplification ratios required?	57
58	1	No. of required depths	58
59	0.0,70.0	Depths (as many as indicated previously)	59

Note-1: In line# 6; For selecting layered profile analysis, input 1(present case); For soil deposit with continuous variation of shear wave velocity, input 2; For profile of discrete data points, input 3.

Note-2: In line# 8 to 45; Plasticity index, OCR and Geological age data are used only when soil type is 20 [Darendeli (2001)] or 21 [Ishibashi and Zhang (1993)] or 22 [Zhang et al (2005)] otherwise these data are ignored.

Note-3: In line# 47; These data (depth of GWT and K$_0$) are used to calculate effective confining pressure (σ'_m) by default. However σ'_m is further used only when strain dependent soil properties are function of σ'_m (i.e., soil type is 20 or 21 or 22 as mentioned in the previous note).

Note-4: In line# 49; For routine analysis, input choice as 1 and specify R-value (0.44 in this case). If R is calculated internally based intensity of shaking after successive iterations as in case of proposed method input 2 and need not specify R-value or input 3, if R is to be calculated based on average specified number of peak values of strain history then input 3 and followed by number of peak strain values to be considered for calculating the average (Default 10). Details are given in flowchart of Chapter 5 (Figure 5.7)

Note-5: In line# 50; For routine analysis (Frequency independent), input choice as 0, if the frequency dependent analysis is desired using the method proposed in this study then input 1 the followed by the frequency (Target frequency, f_T) up to which radiation damping need to be incorporated beyond which damping is logarithmically decreased; when soil type is 20 [Darendeli (2001) model] frequency dependent analysis can be invoked by input 2, then damping is calculated using the excitation frequency.). Details are given in flowchart of Chapter 5 (Figure 5.22).

Table AII.4: Input data file for DP-SD analysis case

Line no	Input file	Comments	Line no
1	INPUT FILE – Vs profile by Discrète data set (70 pts)-LA-OBREBON	Title of the problem	1
2	CH36070.ACC	Input motion file	2
3	LA0DC1.OUT	Out file #1	3
4	LA0DC2.OUT	Out file #2	4
5	70	Total depth of the deposit	5
6	3	Type of shear wave velocity profile	6
7	70	Number of layers	7
8	0.00 5 16.50 400.0 2 15 1 2	Line #8 to Line #77	8
9	1.00 5 16.50 400.0 2 15 1 2	Data at desired depth are entered in the	9
10	2.00 5 16.50 473.9 2 15 1 2	following sequence	10
11	3.00 5 16.50 518.1 2 15 1 2		11
12	4.00 5 16.50 454.5 2 15 1 2	Column #1 – depth at which the data are	12
13	5.00 5 16.50 531.9 2 15 1 2	specified	13
14	6.00 2 16.83 442.5 2 0 1 2	Column #2 – soil type (as given in SRISD)	14
•	• • • • • • • •	Column #3 – unit wt (kN / m³)	•
•	• • • • • • • •	Column #4 – shear wave velocity (m / s) Column #5 – initial damping	•
75	67.00 2 17.23 540.5 2 0 1 2	Column #6 – plasticity index	75
76	68.00 2 17.23 540.5 2 0 1 2	Column #7 – OCR	76
77	69.00 2 17.23 540.5 2 0 1 2	Column #8 – Geological age	77
78	70	Depth at which input motion is to be given	78
79	0 0.72	Depth of water table & K_0– (only used in calculation of effective confining stress)	79
80	2 17.23 540.5 2	Bedrock properties (Type, unit wt., Shear wave velocity, damping)	80
81	50	Step size for R-K scheme (cm)	81
82	2 20	Choice of R, R-value, No. of iterations	82
83	0	Choice of frequency dependent analysis	83
84	Y	Output of accn. time histories required?	84
85	1	No. of required depths	85
86	0	Depths (as many as indicated previously)	86
87	Y	Out stress-strain time histories required?	87
88	1	No. of required depths	88
89	0.5	Depths (as many as indicated previously)	89
90	Y	Amplification ratios required?	90
91	1	No. of required depths	91
92	0.0,70.0	Depths (as many as indicated previously)	92

Note-1: In line# 6, for selecting layered profile analysis, input 1; For soil deposit with continuous variation of shear wave velocity, input 2; For profile of discrete data points, input 3 (present case).

Note-2: In line# 8 to 77; Plasticity index, OCR and Geological age data are used only when soil type is 20 [Darendeli (2001)] or 21 [Ishibashi and Zhang (1993)] or 22 [Zhang et al (2005)] otherwise these data are ignored.

Note-3: In line# 79 these data (depth of GWT and K_0) are used to calculate effective confining pressure (σ'_m) by default. However σ'_m is further used only when strain dependent soil properties are function of σ'_m (i.e., soil type is 20 or 21 or 22 as mentioned in the previous note).

Note-4: In line# 81 for routine analysis, input choice as 1 and specify R-value (blank in this case). If R is calculated internally based intensity of shaking after successive iterations as in case of proposed method input 2 (as in this case) and need not specify R-value or input 3, if R is to be calculated based on average specified number of peak values of strain history then input 3 and followed by number of peak strain values to be considered for calculating the average (Default 10). Details are given in flowchart of Chapter 5 (Figure 5.7)

Note-5: In line# 83; For routine analysis (Frequency independent), input choice as 0, if the frequency dependent analysis is desired using the method proposed in this study then input 1 the followed by the frequency (Target frequency, f_T) up to which radiation damping need to be incorporated beyond which damping is logarithmically decreased; when soil type is 20 [Darendeli (2001) model] frequency dependent analysis can be invoked by input 2, then damping is calculated using the excitation frequency.). Details are given in flowchart of Chapter 5 (Figure 5.22).

Table AII.5: Input data file for CZ-SD analysis case

Line no	Input file	Comments	Line no
1	INPUT FILE CA-SD ANALYSIS LA–OBREBON SITE (linear variation)	Title of the problem	1
2	CH36070.ACC	Input motion file	2
3	LA0F0CZ1.OUT	Out file #1	3
4	LA0F0CZ2.OUT	Out file #2	4
5	70.0	Total depth of the deposit	5
6	2	Type of shear wave velocity profile	6
7	1	Number of layers	7
8	70.0 1 22 2 0 1 2	Layer details are entered in the following sequence; Layer depth, type of continuous variation, soil type, initial damping, plasticity index, OCR, Geological age	8
9	429.03 574.70 16.93 17.19	Vs0, VsH, unit wt. at the surface and at the base	9
10	1.0	Value of b in the power law function $Vs=Vs0 (1+az)^b$ (b=1 for linear variation)	10
11	0 17.19 574.70 2	Bedrock properties (Type, unit wt., Shear wave velocity, damping)	11
12	70.0	Depth at which input motion is to be given	12
13	0.0 0.72	Depth of water table & K_0– (only used in calculation of effective confining stress)	13
14	50 50	Step size for R-K scheme (cm)	14
15	2 20	Choice of R, R-value, No. of iterations	15
16	0	Choice of frequency dependent analysis	16
17	Y	Out acceleration time histories required?	17
18	1	No. of required depths	18
19	0.0	Depths (as many as indicated previously)	19
20	Y	Out stress-strain time histories required?	20
21	1	No. of required depths	21
22	0.5	Depths (as many as indicated previously)	22
23	Y	Amplification ratios required?	23
24	1	No. of required depths	24
25	0.0 70.0	Depths (as many as indicated previously)	25

Note-1: In line# 6; For selecting layered profile analysis, input 1; For soil deposit with continuous variation of shear wave velocity, input 2 (present case); For profile of discrete data points, input 3.

Note-2: In line# 8; Plasticity index, OCR and Geological age data are used only when soil type is 20 [Darendeli (2001)] or 21 [Ishibashi and Zhang (1993)] or 22 [Zhang et al (2005)] otherwise these data are ignored. In the present case soil type is 22. Initial damping is ignored if soil type is 20 or 22 and calculates it by the respective equations.

Note-3: In line# 13; These data (depth of GWT and K_0) are used to calculate effective confining pressure (σ'_m) by default. However σ'_m is further used only when strain dependent soil properties are function of σ'_m (i.e., soil type is 20 or 21 or 22 as mentioned in the previous note)

Note-4: In line# 14; the step sizes used here represent the nodes at which soil properties are updated after successive iteration and second value is a dummy node at which response is calculated but soil properties at these nodes are not updated using the curves of strain dependent properties. However at these nodes soil properties are interpolated from updated properties of the adjacent nodes. In the present case 0.5 m is used for both, i.e., no intermediate nodes are considered.

Note-5: In line# 15; for routine analysis, input choice as 1 and specify R-value. If R is calculated internally based intensity of shaking after successive iterations as in case of proposed method input 2 (present case) and need not specify R-value or input 3, if R is to be calculated based on average specified number of peak values of strain history then input 3 and followed by number of peak strain values to be considered for calculating the average (Default 10). Details are given in flowchart of Chapter 5 (Figure 5.7)

Note-6: In line# 16; For routine analysis (Frequency independent), input choice as 0, if the frequency dependent analysis is desired using the method proposed in this study then input 1 the followed by the frequency (Target frequency, f_T) up to which radiation damping need to be incorporated beyond which damping is logarithmically decreased; when soil type is 20 [Darendeli (2001) model] frequency dependent analysis can be invoked by input 2, then damping is calculated using the excitation frequency.). Details are given in flowchart of Chapter 5 (Figure 5.22).
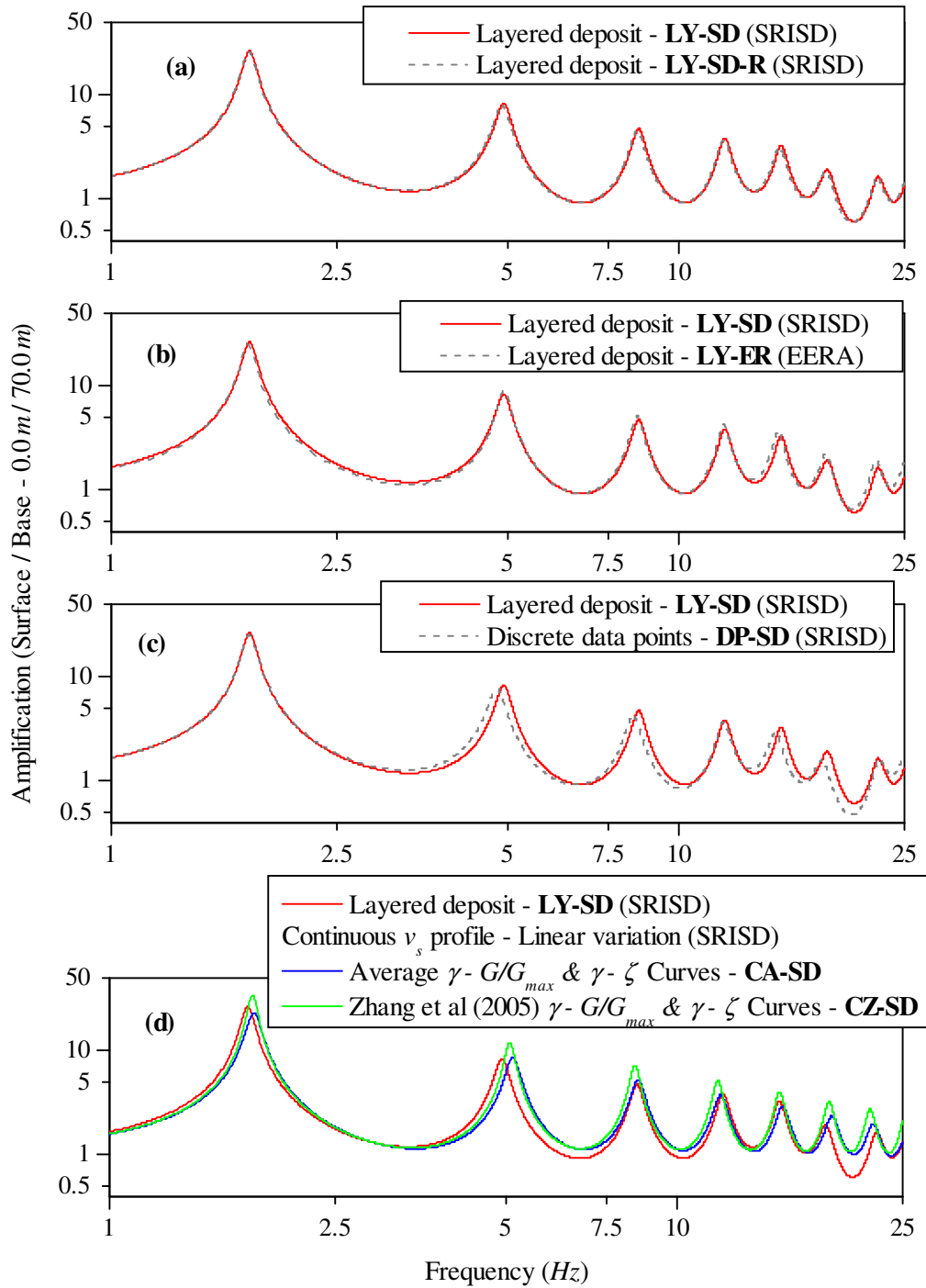
Figure AII.4: Amplification ratio between surface and base input motions (0.0*m*/70.0*m*) computed for different idealisations of shear wave profiles from SRISD analysis [(c) and (d)]. Comparison of amplification ratio results from SRISD and EERA for the case of layered profile [(b)]. Comparison of amplification ratio results from SRISD using routine and proposed methods of computing effective strain for the case of layered profile [(a)].
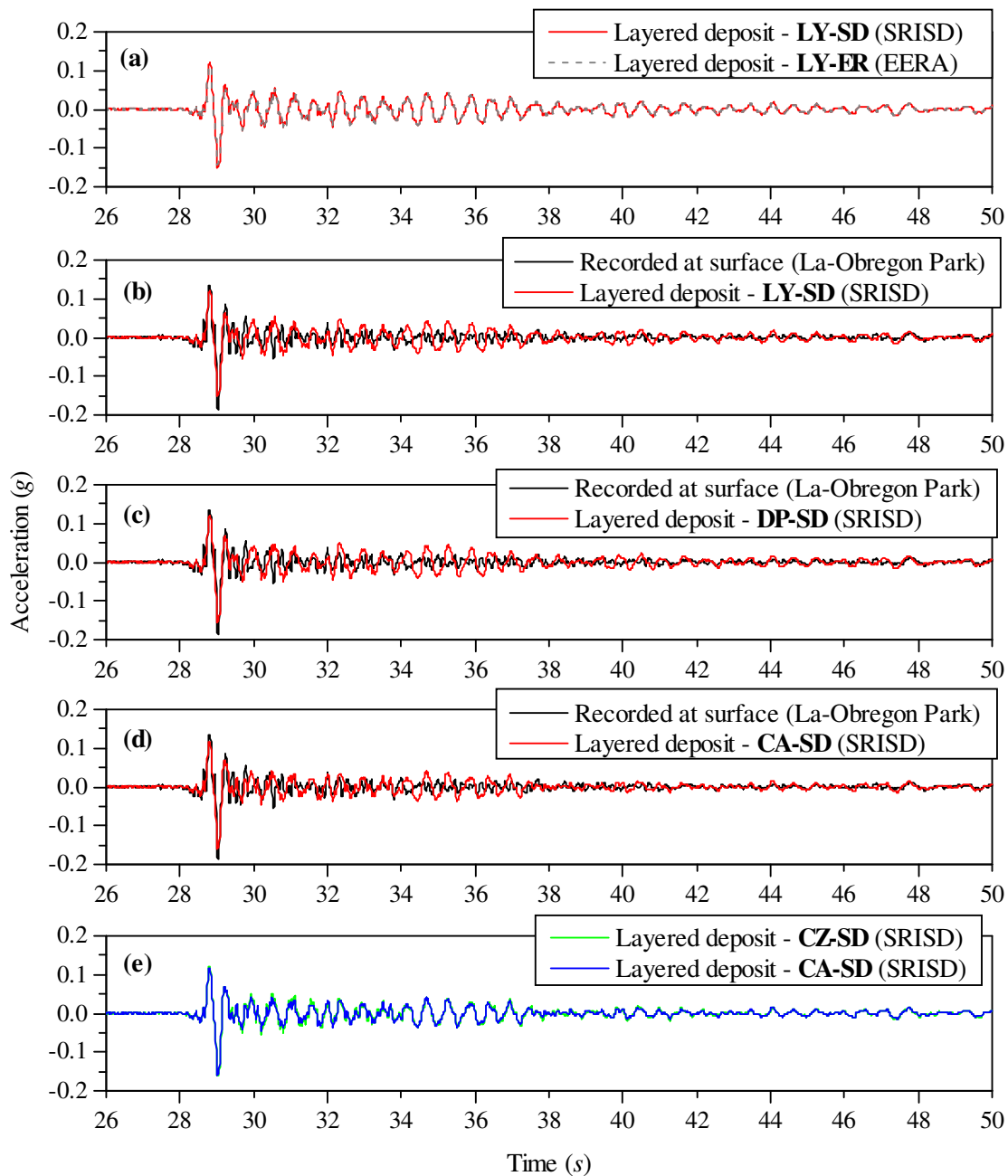
Figure AII.5: Surface acceleration responses computed for different idealisations of shear wave profiles from SRISD analysis [(b) (c) and (d)]. Comparison of surface acceleration response results from SRISD and EERA for the case of layered profile [(a)]. Comparison of surface acceleration response results from SRISD analysis using average curves to represent strain dependent soil properties and normalized model for strain dependent soil properties of Zhang et al (2005) [(e)] with continuous variation approximation of shear wave velocity profile.
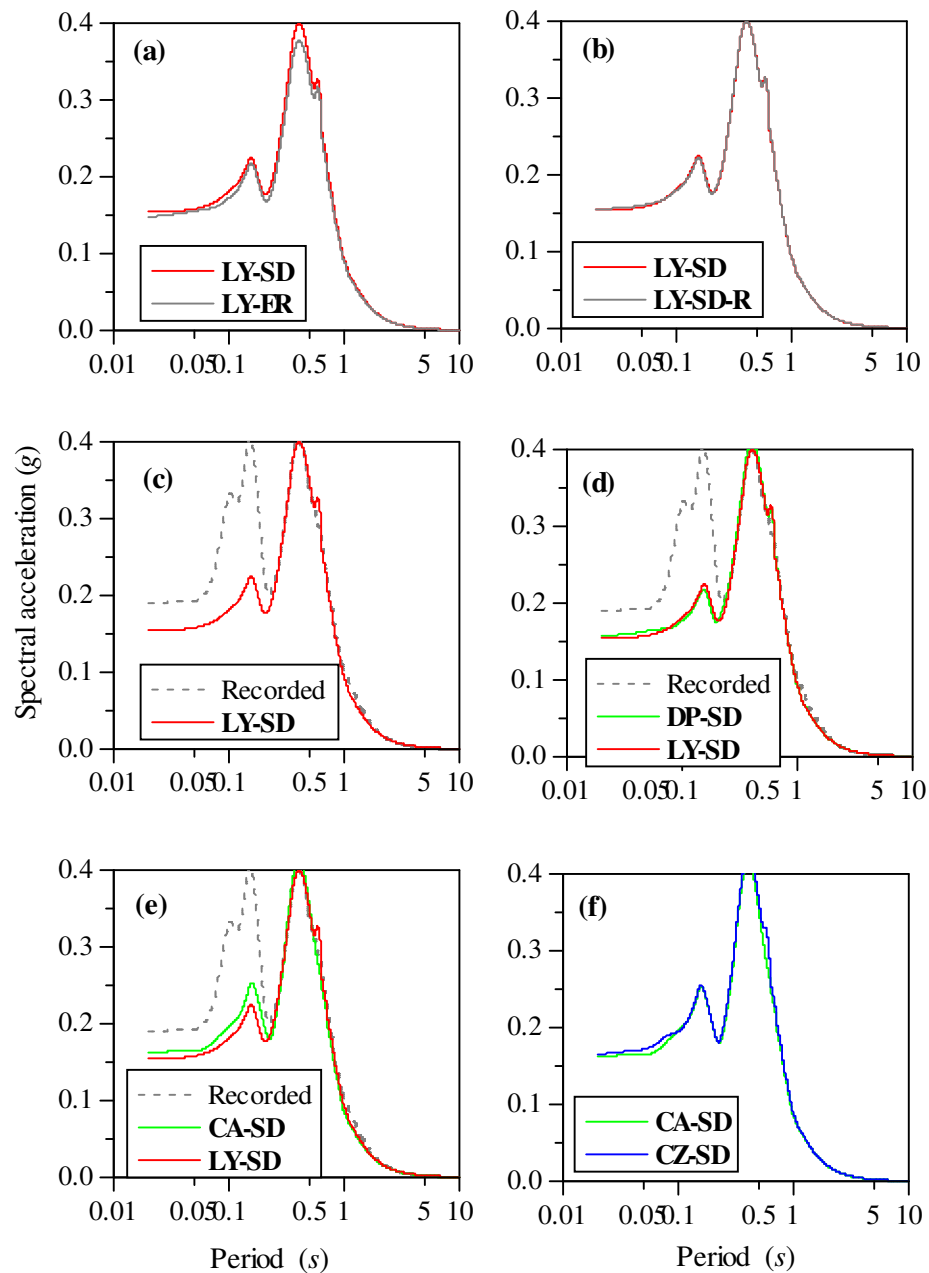
Figure AII.6: Response spectra of computed acceleration responses at the surface of the soil deposit idealised with different shear wave profiles; Comparison of results of SRISD analyses with that of recorded motion [(c) (d) and (e)]; Comparison of results of SRISD and EERA for the case of layered profile [(a)]; Comparison of results of SRISD using routine and proposed methods of computing effective strain for the case of layered profile [(b)]; Comparison of response spectra of SRISD analysis using average curves to represent strain dependent soil properties and normalized model for strain dependent soil properties of Zhang et al (2005) with continuous variation approximation of shear wave velocity profile [(f)].
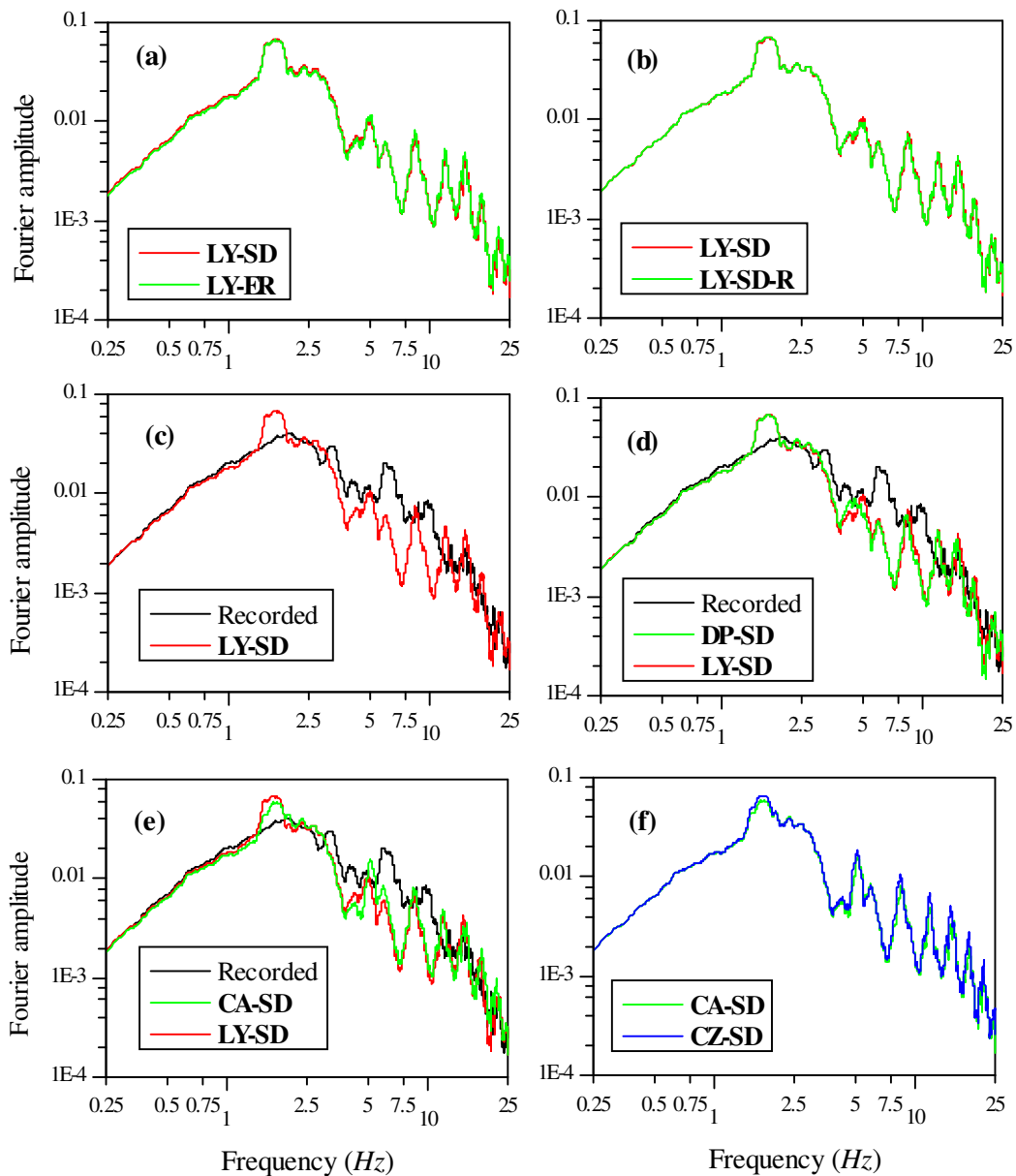
357

Figure AII.7: Fourier spectra of computed acceleration responses at the surface of the soil deposit idealised with different shear wave profiles; Comparison of results of SRISD analyses with that of recorded motion [(c) (d) and (e)]; Comparison of results of SRISD and EERA for the case of layered profile [(a)]; Comparison of results of SRISD using routine and proposed methods of computing effective strain for the case of layered profile [(b)]; Comparison of response spectra of SRISD analysis using average curves to represent strain dependent soil properties and normalized model for strain dependent soil properties of Zhang et al (2005) with continuous variation approximation of shear wave velocity profile [(f)].
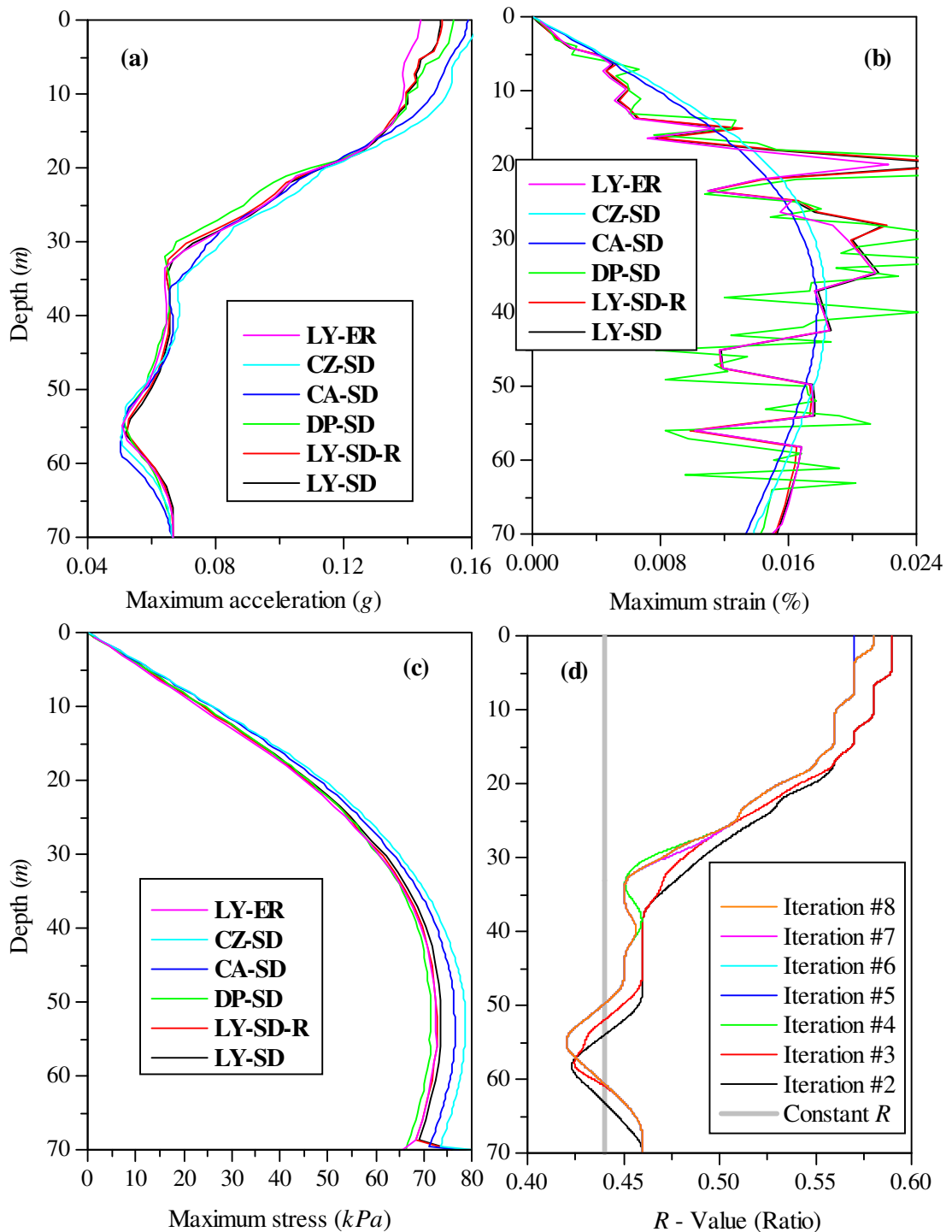
Figure AII.8: Variation of maximum responses along the depth of the soil deposit computed for different cases of analyses; (a) Maximum acceleration, (b) maximum strain and (c) Maximum shear stress; (d) Variation of ratio of effective to maximum strain at different depths as obtained from proposed method of analysis in comparison with its constant value as in case of routine analysis.

AII.6 RESULTS

Figure AII.4 compares the results of amplification ratio as obtained for different cases of analyses listed in Table AII.2. Also the results of SRISD are compared with that of EERA. The acceleration time history at the surface of the deposit under these cases is shown comparatively in Figure AII.5. The response spectra and Fourier amplitude spectra of the predicted surface acceleration response from these analyses are presented in Figure AII.6 and Figure AII.7 respectively. Figure AII.8 comparatively show the variation of maximum responses of acceleration, shear strain and shear stress along the depth as obtained for different cases of analyses. Also to illustrate the essential difference between newly proposed and routine methods for computation of effective strain, R-value obtained for each of the iterations is plotted against constant value of $R = 0.44$ that is used in the routine analysis.

PUBLICATIONS BASED ON PRESENT RESEARCH WORK

<u>Journal Paper</u>

• Vijayendra K.V., Sitaram Nayak, S.K. Prasad (2015), "An Alternative Method to Estimate Fundamental Period of Layered Soil Deposit", Indian Geotechnical Journal, Volume 45, Issue 2, pp 192-199.

<u>Conference Papers</u>

• Vijayendra K.V., Prasad SK., and Sitaram Nayak (2012), "Effect of Layer Impedances on the Frequency Characteristics of Predicted Surface Motion", *Indian Geotechnical Conference – 2012*, New Delhi, India. December 13 – 15, 2012. *Theme-Geotechnical Earthquake Engineering, Paper No. H 822*

• Vijayendra K.V., Prasad SK., and Sitaram Nayak (2011), "Importance of Continuous Variation in Soil Properties Instead of Layered Idealization in Seismic Response Study of Ground", *Indian Geotechnical Conference – 2011*, Kochi, India. December 15 – 17, 2011. *Theme-Geotechnical Earthquake Engineering, Paper No. 361.*

• Vijayendra K.V., Prasad SK., and Sitaram Nayak (2010), "Computation of Fundamental Period of Soil Deposit – A Comparative Study" *Indian Geotechnical Conference – 2010*, Mumbai, India. December 16th – 18th, 2010. *Theme-T4, Geotechnical Earthquake Engineering, Paper No. 314.*

• Prasad, S. K., Sitharam Nayak, Vijayendra, K. V. and Satish Reddy (2010), "Site Specific Ground Motion for Seismic Design of Structures", *4th CUSAT National Conference on Recent Advances in Civil Engineering*, Cochin, September, 16-18, 2010

• Prasad S.K., Vijayendra K.V., Sitaram Nayak and G. P. Chandradhara (2010), "Requirements of Site Investigation for Seismic Design of Geotechnical Structures", *National Workshop on Soil Exploration and Foundation Design*, Vadodara, India. June 25-26, 2010.

BIO-DATA

Name: K. V. Vijayendra

Date of Birth: 14th February, 1962

Residence address: # 204/17, 4th Main road,

                         Ganganagar,

                         Bangalore – 560032

Institute address: Department of Civil Engineering,

                         Bangalore Institute of Technology,

                         K. R. Road, V. V. Puram

                         Bangalore – 560004

Contact Number: +91 – 9945488198

Email: vijayendra.kv@gmail.com

Academic qualification:

- Bachelor of Engineering (B.E.) – Civil Engineering
  University Visveswaraya College of Engineering (UVCE)
  Bangalore University, Jnana Bharathi, Bangalore - 560056

- Master of Engineering (M.E.) - Geotechnical Engineering
  University Visveswaraya College of Engineering (UVCE)
  Bangalore University, Jnana Bharathi, Bangalore - 560056

Professional and Teaching Experience:

Year	Institution	Designation
July, 1985 – May, 1986	Engineering cell, Department of Sericulture, Government of Karnataka.	Assistant Engineer
Sept,1988 - Oct, 1991	Department of Civil Engineering, Dayanand Sagar College of Engineering, Bangalore.	Lecturer
Nov, 1991 – Mar, 1998	Department of Civil Engineering, Bangalore Institute of Technology, Bangalore.	Lecturer
Apr, 1998 – Mar, 2003	Department of Civil Engineering, Bangalore Institute of Technology, Bangalore.	Senior Lecturer
Apr, 2003 – till to date	Department of Civil Engineering, Bangalore Institute of Technology, Bangalore.	Associate Professor